P
2 mlf

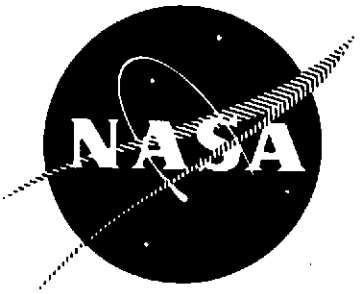

NASA CR-121236

R-9269

ADVANCED SPACE ENGINE

PRELIMINARY DESIGN

By

A. T. Zachary

ROCKETDYNE DIVISION
ROCKWELL INTERNATIONAL

Prepared for

NATIONAL AERONAUTICS AND SPACE ADMINISTRATION

NASA-Lewis Research Center
Contract NAS3-16751

1. Report No.	2. Government Accession No.	3. Recipient's Catalog No.
NASA CR-121236		

4. Title and Subtitle	5. Report Date
ADVANCED SPACE ENGINE PRELIMINARY DESIGN	October 1973
	6. Performing Organization Code

7. Author(s)	8. Performing Organization Report No.
A.T. Zachary	R-9269
	10. Work Unit No.

9. Performing Organization Name and Address	11. Contract or Grant No.
Rocketdyne Division, Rockwell International Canoga Park, California, 91304	NAS3-16751
	13. Type of Report and Period Covered
12. Sponsoring Agency Name and Address	Contractor Report
National Aeronautics and Space Administration Washington, D.C., 20546	14. Sponsoring Agency Code

15. Supplementary Notes

Project Manager, D.D. Scheer, NASA-Lewis Research Center, Cleveland, Ohio

16. Abstract

Analysis and design of an optimum LO_2/LH_2, combustion topping cycle, 88,964 N (20,000-pound) thrust, liquid rocket engine was conducted. The design selected is well suited to high-energy, upper-stage engine applications such as the Space Tug and embodies features directed toward optimization of vehicle performance.

A configuration selection was conducted based on prior Air Force Contracts F04611-71-C-0039, F04611-71-C-0040, and F04611-67-C-0016, and additional criteria for optimum stage performance. Following configuration selection, analyses and design of the major components and engine systems were conducted to sufficient depth to provide layout drawings suitable for subsequent detailing. In addition, engine packaging to a common interface and a retractable nozzle concept were defined. Alternative development plans and related costs were also established. The design embodies high-performance, low-weight, low NPSH requirements (saturated propellant inlet conditions at start), idle-mode operation, and autogenous pressurization. The design is the result of the significant past and current LO_2/LH_2 technology efforts of the NASA centers and the Air Force, as well as company-funded programs.

17. Key Words (Suggested by Author(s))	18. Distribution Statement
Hydrogen/Oxygen Engine High Chamber Pressure Regenerative Cooling High Area Ratio Channel Wall Construction	

19. Security Classif. (of this report)	20. Security Classif. (of this page)	21. No. of Pages	22. Price*
Unclassified	Unclassified	504	

* For sale by the National Technical Information Service, Springfield, Virginia 22151

FOREWORD

The work herein was conducted by the Advanced Programs and Engineering personnel of Rocketdyne, a Division of Rockwell International Corporation, under contract NAS3-16751 from July 1972 to April 1973. Mr. Dean D. Scheer, Lewis Research Center, was NASA Project Manager. Mr. Harold G. Diem was Rocketdyne Program Manager, and Mr. A. T. Zachary, as Project Engineer, was responsible for the technical direction of the program.

Important contributions to the conduct of the program and to the preparation of the report material were made by the following Rocketdyne personnel:

Engine System Design	H. E. Marker
Turbomachinery	A. Csomor
Combustion Devices	J. R. Lobitz
Controls	R. L. Goodwin

CONTENTS

ILLUSTRATIONS

TABLES

SUMMARY

The Advanced Space Engine Preliminary Design Program was conducted over a 10-month period of performance to select an optimum configuration for a 88,964 newton (20,000-pound) thrust LO_2/LH_2 combustion topping cycle engine. In addition to configuration selection and design, operational features and development plans were investigated. The program consisted of five working and one reporting tasks. All tasks and milestones were completed on schedule. The initial effort of the study was devoted to configuration selection. Tradeoffs were conducted based on alternatives presented in the Statement of Work and previous studies; specifically, the results of Air Force Contracts F05611-71-C-0039, F04611-71-C-0040, and F04611-67-C00116. The selected engine was baselined as non-throttling; however, the impact of throttling was assessed. The selected engine configuration consisted of a single preburner, GH_2 turbine-driven boost pumps with a 400:1, 90-percent length nozzle.

The primary effort was devoted to engine system and major component analyses and design culminating in the preparation of design layouts. The analyses conducted included engine balance and transient studies, operational modes (idle mode, autogenous pressurization, etc.), and other engine and major component analyses such as performance, heat transfer, and structural. Of significant benefit to these analyses were the results of the Engine Dynamic Model Program (NAS3-16687) and the LO_2/LH_2 Thrust Chamber Design and Analysis Program (NAS3-16774). Layouts of the engine assembly and each major component were prepared in sufficient detail to allow for subsequent detail design. The engine schematic and packaging are presented in Fig. 1, 2, and 3. The results of the analyses and design effort are briefly summarized in Table I.

In the course of the preliminary design study, another task was added to study programmatic and design alternatives required for consideration in vehicle studies concurrently in process. This effort consisted of determination of alternative engine development programs and their related costs and investigation into modification of engine packaging to meet a common vehicle/engine interface. Also, the design of a retractable nozzle was conducted. The program plans were defined and are subsequently presented in this report. The modification of the engine packaging posed no major problem, and design of a suitable retractable nozzle was completed which results in an engine stowed length of only 1.2827 meters (50.5 inches).

The engine design presented fully meets the system requirements and provides the required baseline engine configuration for subsequent study of component interactions and system dynamics prior to beginning full engine development.

Concurrent with the effort conducted for selection of an optimum engine configuration, key technology areas critical in the development of the Advanced Space Engine were identified.

Primary in these considerations was the small, high-pressure turbomachinery required to meet the engine requirements while being lightweight and capable of long life. The multistage, high rotative speed requirements establish the main fuel turbopump as the most critical technology area, followed next by the main oxidizer turbopump.

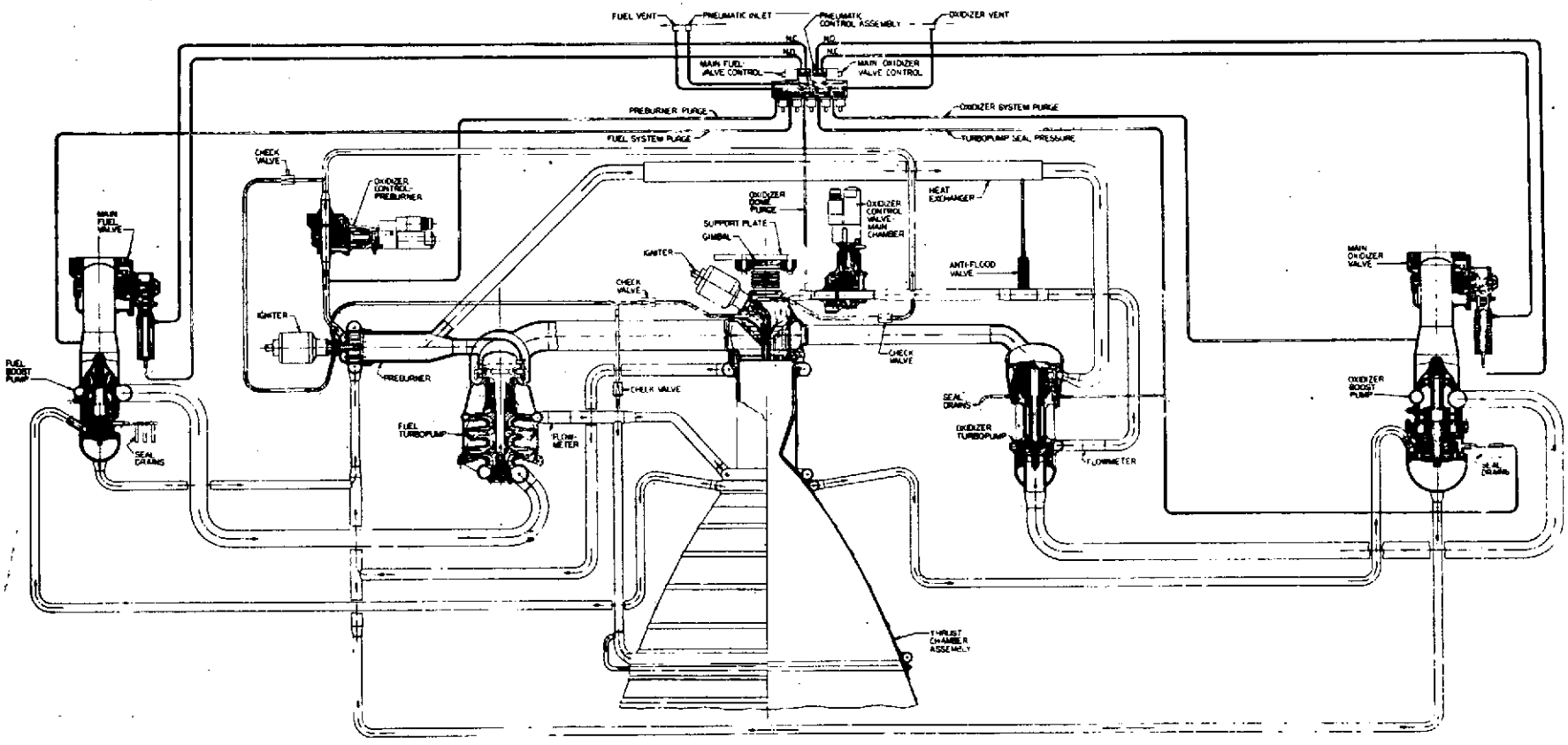

Figure 1. Advanced Space Engine Schematic (88,964 N; 20K)

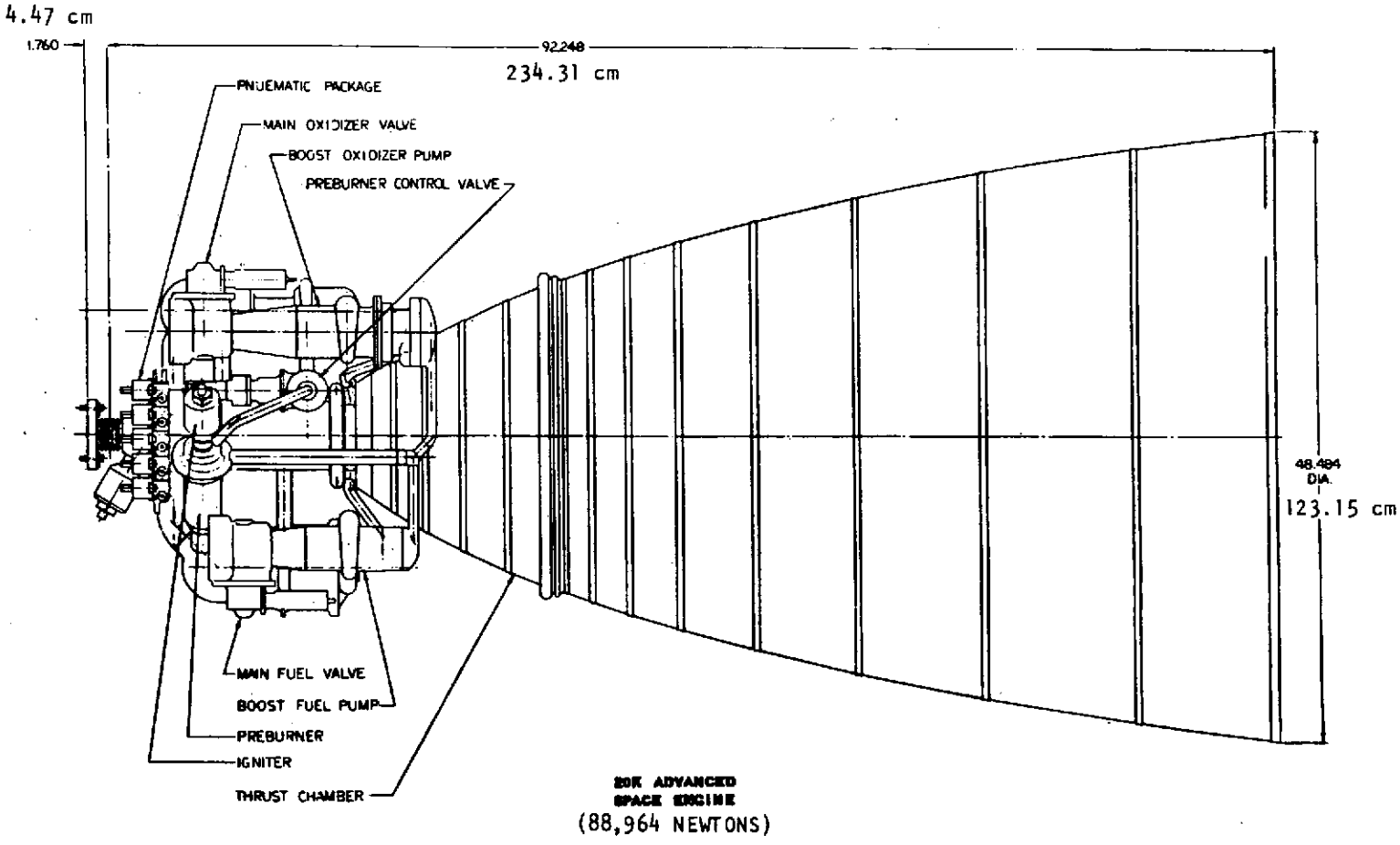

Figure 2. Baseline Engine Package

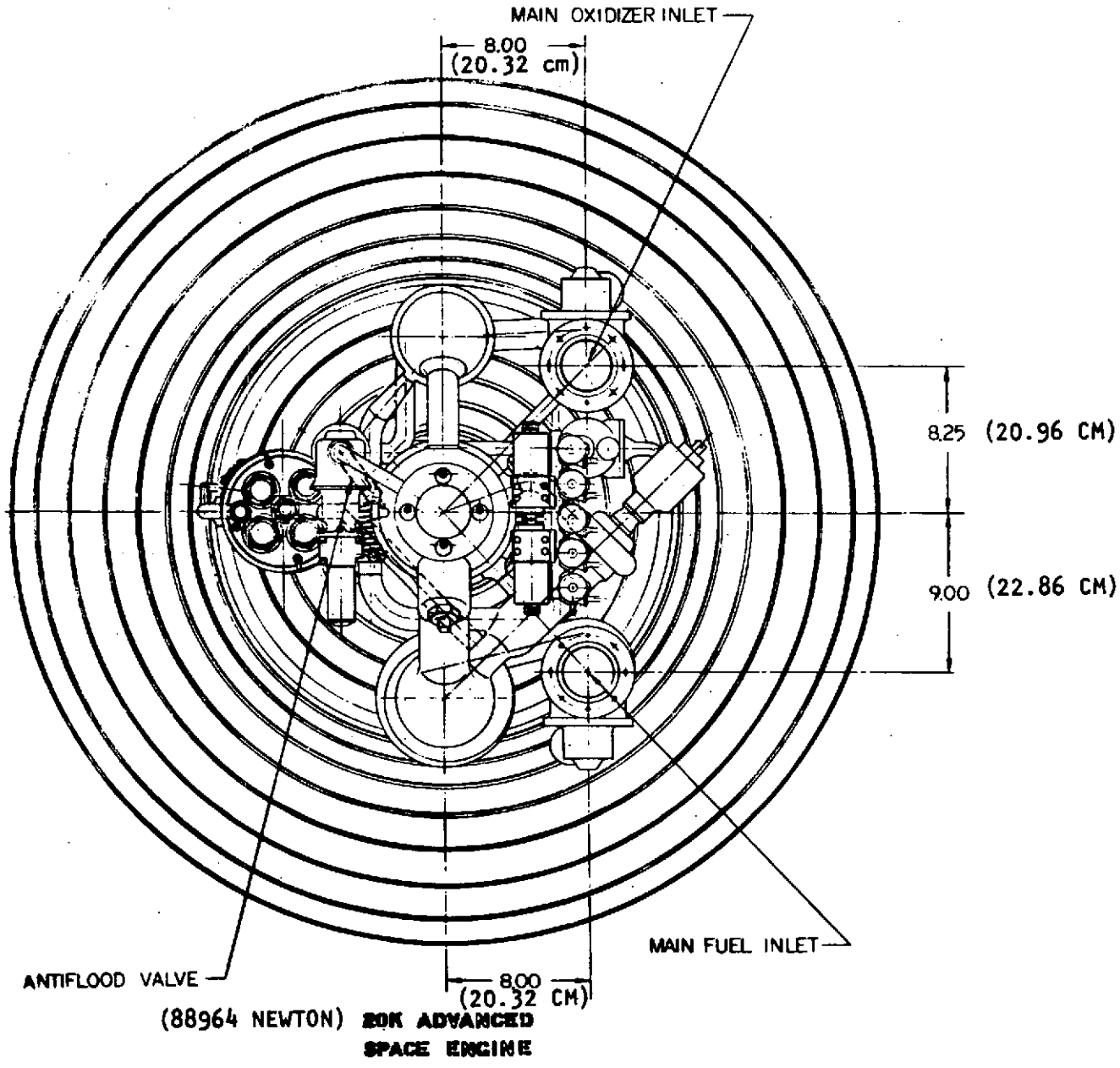

Figure 3. Engine Packaging (End)

TABLE I. POINT DESIGN AND OPERATIONAL DATA

	Tank-Head Idle Mode	Pumped Idle Mode	Mainstage
A. Engine Performance			
Vacuum Thrust, pounds (newton)	60 (267)	1332 (5925)	20,000 (88,964)
Chamber Pressure, psia (N/m^2)	8.5 (58,599)	176 (0.121×10^7)	2233 (1.539×10^7)
Specific Impulse, seconds (N-s/kg)		442.5 (4339)	473.4 (4642)
Mixture Ratio		Fig. 1-74	5.5 to 6.5
GO_2 Bleed Flowrate Capability			Page 109
GH_2 Bleed Flowrate Capability			Page 109
Weight, lbm (kg)			337 (152.9)
Life (minimum number of firings and minimum operating time)			Table 1-1
Start and Shutdown Transients			Fig. 1-71 and 1-73
B. Engine Geometry			
Center of Gravity			*
Maximum Length (fixed and 2-position nozzles), inches (cm)			94 (238.8)
Minimum Length (2-position nozzle), inches (cm)			50.5 (128.3)
Maximum Diameter (fixed and 2-position nozzles), inches (cm)			49 (124.4)
Expansion Ratio			400:1
Dynamic Envelope			70
C. Interface Requirements			
Moment of Inertia			**
NPSH, feet		0/0-start	2' LO_2/15' LH_2-mainstage
Inlet Conditions (Temperature and Pressure)			Table 1-1
Inlet Line Locations			Fig. 7-16
Actuator Attach Location			Fig. 7-16
Chilldown (flowrate vs time during idle mode)			Fig. 1-71
Total Engine Idle Mode Flow During Warm Engine Start		5.4 lb LO_2/5.3 lb LH_2 (2.44 kg) (2.40 kg)	
Electrical Power (peak and steady-state)			Fig. 5-11
Pressurant Requirements			Table 5-1

*Inches from gimbal centerline x = 20.1 (51 cm)
y = 1.1 (2.79 cm)
z = -1.5 (-3.81 cm)

**About gimbal centerline I_y = 65.2 slug ft^2 (87.9 kg m^2)
I_z = 65.5 slug ft^2 (88.3 kg m^2)

About engine center of gravity I_y = 35.6 slug ft^2 (48.0 kg m^2)
I_z = 36.0 slug ft^2 (48.5 kg m^2)

The primary considerations with respect to the combustion devices are their thermal fatigue life and, although similar combustor chambers and injectors have been fabricated and tested, the high-pressure operation of the preburner and high-pressure/high-heat-flux operation of the thrust chamber should be investigated to ensure meeting the long-life requirement of the engine. In addition to the preburner and thrust chamber technology, the development of a suitable igniter will be essential to successful engine operation and, therefore, should be explored.

INTRODUCTION

System studies have been conducted to determine the feasibility of developing a resuable vehicle for performing future NASA and Air Force space maneuvering missions. These studies have shown that over the thrust range of interest high-pressure, staged-combustion cycle engines offer the highest specific impulse and payload capability. A review of the vehicle and engine system study results indicates that a single bell nozzle, staged-combustion cycle engine at a 88,964 newton (20,000-pound) thrust level is near optimum for the DOD and NASA mission requirements. Further, it is clear that some of the advanced features (e.g., pressurized-idle operation and very low NPSH) are attractive from the mission and/or vehicle standpoint.

The objective of this program was to provide the preliminary design of a high-performance, staged-combustion cycle rocket engine with a nominal vacuum thrust of 88,964 newtons (20,000 pounds) using hydrogen/oxygen as propellants.

The purpose of this effort was twofold: (1) to resolve the best approach among the several technical choices made by previous study contracts so that component research may be properly focused and (2) provide a preliminary design for a 88,964 newton (20,000-pound) thrust, staged-combustion cycle research engine which will allow studies of component interaction problems and engine dynamics problems prior to the beginning of any effort on a development engine. This report presents the results of the study defining an optimum engine configuration that fully meets the program objectives and establishes the required baseline design definition required for future technology efforts.

TASK 1: ENGINE SYSTEM PRELIMINARY DESIGN

This task was conducted to select the overall engine configuration and design. The effort included consideration of alternate approaches based on previous studies, engine point and off-design analyses, transient operation studies, engine packaging analysis, and establishment of operational requirements. The engine configuration and operating conditions criteria utilized are presented in Table 1-1. The effort was initiated with analyses necessary to show optimum choice of alternate approaches and culminated in the preparation of engine layout drawings in sufficient detail to enable subsequent preparation of detail drawings.

CONFIGURATION SELECTION

The selection of the engine baseline configuration was initiated with definition of the design alternatives as stipulated in the Statement of Work and shown in Table 1-2. In consideration of the design alternatives, the results of the previous Air Force Contracts (F04611-71-C-0039, F04611-71-C-0040, and F04611-67-C-0116, Ref. [1], [2], and [3]) were considered and are briefly summarized in Table 1-3. In addition design limits based on past studies and experience were also established, as shown in Table 1-4, to guide the configuration selection studies. Combinations of the design alternatives were assessed and in combination with the specific tradeoff of alternatives subsequently presented, culminated in the selection of alternative engine configurations. These configurations were then traded off as to cycle balance (maximization of chamber pressure), performance, transient characteristics, flexibility, complexity, weight, and parametric costs. From these considerations, a baseline nonthrottling engine configuration was selected in accordance with the NASA study requirements. Following the baseline selection, the impact of throttling was also assessed.

TABLE 1-2. DESIGN ALTERNATIVES

Design Configuration	Operational Mode
Boost Pump Drive Methods	Throttling requirements
Gears Hydraulic Turbine Hydrogen Gas Turbines	No throttling 6:1 throttling*
Regenerative Cooling Scheme	Design point net positive suction head (feet) (joules/kg)
Pass and a Half Split	LO_2: 0** 2 (5.98) 16 (47.8)
Preburner Configuration	LH_2: 0** 15 (44.8) 60 (179.3)
Single Preburner	Start mode
Dual Preburner Separately Supplying Combustion Products to Each Turbine	Normal Pressurized idle Tank-head idle

*Perturbation of Baseline Design Only
**Tank-Head Idle-Mode Start Only

TABLE 1-1. ENGINE CONFIGURATION AND OPERATING CONDITIONS

Propellants	Liquid hydrogen Liquid oxygen
Vacuum Thrust, pounds (newtons)	20,000 (88,964)
Vacuum Thrust Throttling Capability	*
Vacuum Specific Impulse	*
Engine Mixture Ratio	6.0 (nominal at full thrust) 5.5 to 6.5 (operating range at full thrust) *(1)
Chamber Pressure	*(2)
Drive Cycle	Staged combustion
Envelope Restrictions Length (maximum) Diameter (maximum)	 * *
Engine System Weight	*
Nozzle Type	Fixed bell
Nozzle Expansion Ratio	400:1
Propellant Inlet Temperature Range, R (K) Hydrogen Oxygen	 36.5 to 40 (20.3 to 22.2) 162 to 172 (90 to 95.6)
NPSP at Pump Inlet at Full Thrust Hydrogen Oxygen	 * *
Engine Temperature Range at Normal Prestart	200 to 560 (111.1 to 311.1)
Service Life Between Overhauls	300 thermal cycles or 10 hours accumulated run time(3)
Service-Free Life	60 thermal cycles or 2 hours accumulated run time
Maximum Single-Run Duration, seconds	2000
Maximum Time Between Firings During Mission, days	14
Minimum Time Between Firings During Mission, minutes	1
Maximum Storage Time in Orbit (dry), weeks	52

*To be determined or selected during contract.

(1) Engine mixture ratio at throttled, pressurized-idle, or tank-head-idle and pumped-idle conditions shall be selected during the contract and shall be at magnitudes that do not compromise the full-thrust design.

(2) Maximum attainable within limits imposed by component performance and/or life

(3) Thermal cycle defined as engine start (to any thrust level) and shutdown

TABLE 1-3. SUMMARY OF PREVIOUS STUDIES

Pratt & Whitney	Aerojet	Rocketdyne
F = 25K (111,206 newtons)	F = 25K (111,206 newtons)	F = 25K (111,206 newtons)
P_c = 1900 psia (1.31 $N/m^2 x10^7$)	P_c = 1800 psia (1.24 $N/m^2 x10^7$)	P_c = 2200 psia (1.517 $N/m^2 x10^7$)
MR = 6.0	MR = 6.0	MR = 6.0
ϵ = 250	ϵ = 290	ϵ = 350
W_T = 375.2 pounds (170.2 kg)	W_T = 459.3 pounds (208.3 kg)	W_T = 367 pounds (166.5 kg)
• Gear-Driven Boost Pumps (Off LO_2 Main Pump Shaft)	• Full-Flow, Hydraulic-Driven Boost Pumps	• GH_2 Turbine-Driven Boost Pumps
• 1-1/2 Pass Thrust Chamber Cooling to ϵ = 100 (Dump-Cooled Nozzle)	• 1-1/2 Pass Thrust Chamber Cooling to ϵ = 290 (Full Regenerative Thrust Chamber)	• Split Flow Thrust Chamber Cooling to ϵ = 350 (Full Regenetive Thrust Chamber
• Single Preburner	• Single Preburner	• Dual Preburner
• 5:1 Throttling	• 5:1 Throttling	• 5:1 Throttling
• 16/60 NPSH (47.8/179.3 joules/kg) (0 NPSH LO_2 Pumping, a Technology Problem)	• 16/60 NPSH (47.8/179.3 joules/kg) (0 NPSH LO_2 Pumping Feasible)	• 16/60 NPSH (47.8/179.3 joules/kg) (0 NPSH LO_2 Pumping Feasible)
• Propellant Bleed, Normal Start	• Propellant Bleed, Normal Start	• Idle Mode

TABLE 1-4. DESIGN GROUND RULES

Thrust Chamber	
Thermal Fatigue Life Data	To be specified
Injector Efficiency	0.995
Curvature Enhancement Factor	1.4
Minimum Injector Pressure Drop	10% of chamber pressure
Preburners	
Temperature Uniformity	±50 R (22.2 K)
Thermal Fatigue Life Data	To be specified
Minimum Injector Pressure Drop	10% of chamber pressure
Pumps	
Bearing DN	Less than 2×10^6
Tip Width	Greater than 0.03 inch (0.762 mm)
Diameter Ratio (hub/tip)	Less than 0.8
Specific Speed	From 600 to 2000 (0.2196 to 0.732; dimensionless)
Seal Leakage	To be determined
Tip Speed	Less than 1650 ft/sec (502.9 m/s)
Turbines	
Tip Speed	Less than 1500 ft/sec (457.2 m/s)
Blade Height	Greater than 0.15 inch (3.81 mm)
AAN^2	Less than 4×10^{10} $in.^2\text{-}rpm^2$
Pitch Diameter	Greater than 2 inches (5.08 cm)
Inlet Temperature	Less than 2000 R (1111 K)
Pressure Ratio	Less than 1.8:1
Hub/Tip Diameter Ratio	Less than 0.9:1
Turbine Pitch/Impeller Diameter Ratio	Less than 3:1
Control Valves	
Pressure Drop	15% of controlled pressure difference minimum
Leakage	To be determined

PRELIMINARY CONFIGURATION SELECTION

Boost Pump Tradeoff Study was initiated with the establishment of pump and drive features and characteristics considered most desirable. The selected criteria are presented in Table 1-5. The alternative boost pump/drive configurations were traded off against the established criteria and those configurations considered most promising were subsequently incorporated into alternative engine configurations for final selection. A summary of the boost pump/drive tradeoff is subsequently presented.

TABLE 1-5. BOOST TURBOPUMP DESIRABLE FEATURES AND REQUIREMENTS

- Provide System Chilldown Benefit and Transient Control During Start
- Maintain NPSH for Main Pump
  - Start
  - Mainstage
  - Off Design
- Life (300 starts and 10 hours minimum)
- Minimize Nonpropulsive Propellant Losses
- Practical Mechanical Design
- Minimize Impact on Power Cycle

Gear-Driven Boost Pumps. The gear-driven LO_2 and LH_2 boost pump configurations considered are shown in Fig. 1-1 and 1-2. The design calls for geared operation off the main oxidizer pump with suitable lubrication of the gears. The operation off the main oxidizer pump is preferable because of the lower speed. The advantages of the gear drive are: (1) positive operation in conjunction with main pump operation and (2) simplicity of design. However, several major disadvantages were identified. The maximum life demonstrated for this approach is 5.56 hours of cumulative operation at a pitch line velocity of 81.28 m/s (16,000 fpm), resulting in badly worn gears (Ref. 1). Assuming improvements capable of providing a pitch line velocity of 101.6 m/s (20,000 fpm), a pitch line velocity of approximately 127 m/s (25,000 fpm) 8378 rad/s (80,000 rpm) would be required to maintain high main pump performance. This would be particularly critical if the drive was off the main LH_2 turbopump where high performance is most essential. This high pitch line velocity (and corresponding high Hertz stress) coupled with a 10-hour cumulative life requirement could result in a significant development problem. In addition, simultaneous boost/main pump startup would prevent use of the boost pumps during the engine chilldown process. Further, mechanical coupling would limit flexibility in packaging. The requirement for gearbox coolant could result in additional nonpropulsive propellant losses and, if the gearbox is hydrogen cooled, an oxidizer boost pump dynamic seal package would be required.

Full-Flow LO_2 and LH_2 Hydraulic Drive. The full-flow hydraulic drive configurations are presented in Fig. 1-3 and 1-4, respectively. The design features consist of placing the boost pump drive turbine in a tandem arrangement between the main pump inducer and stage so that the developed head and flow of

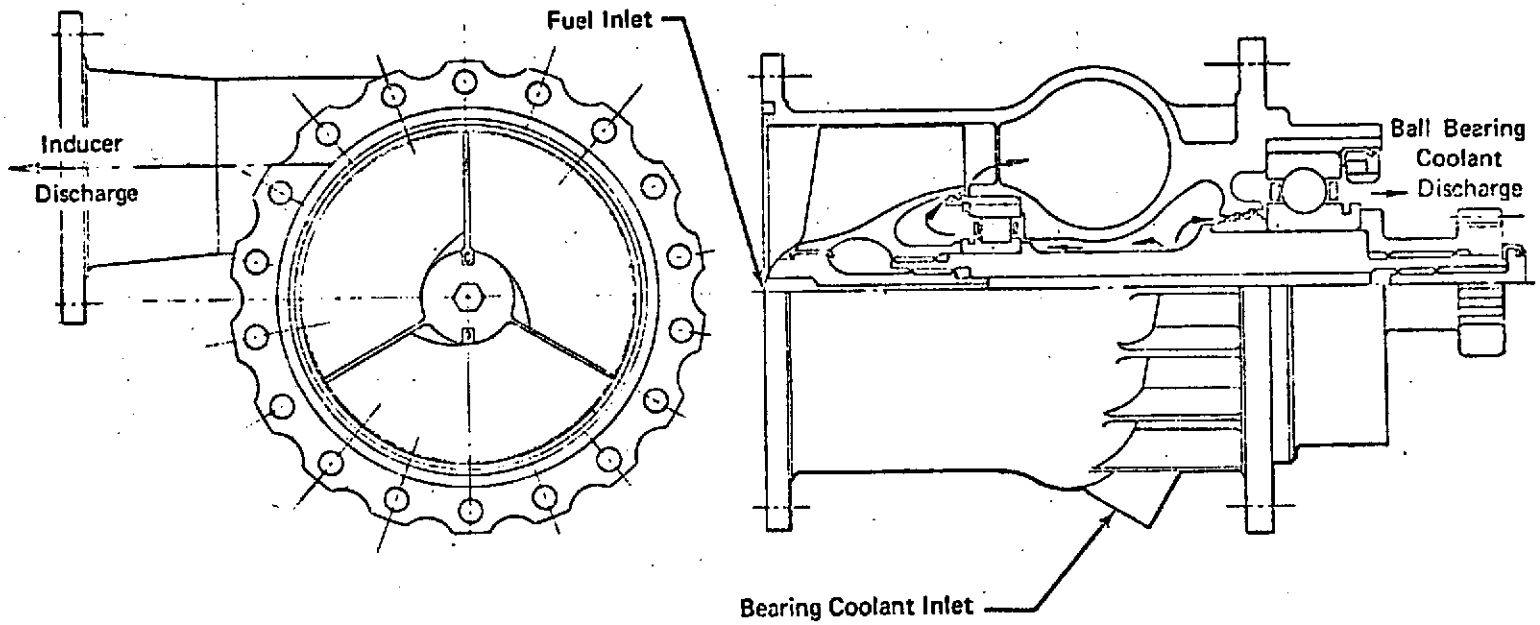

Figure 1-1. Gear-Driven LH_2 Boost Pump Design

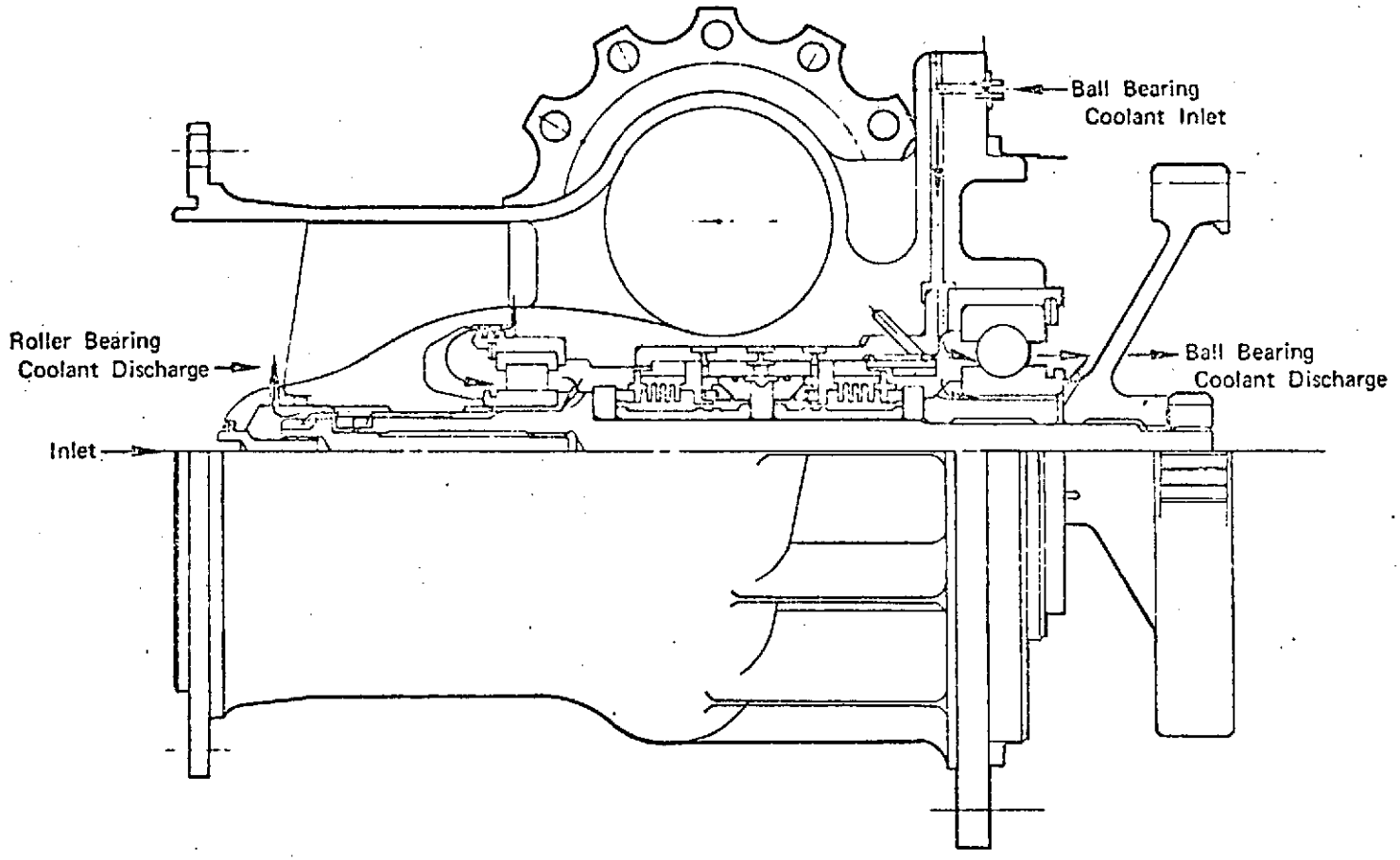

Figure 1-2. Gear-Driven LO_2 Boost Pump Design

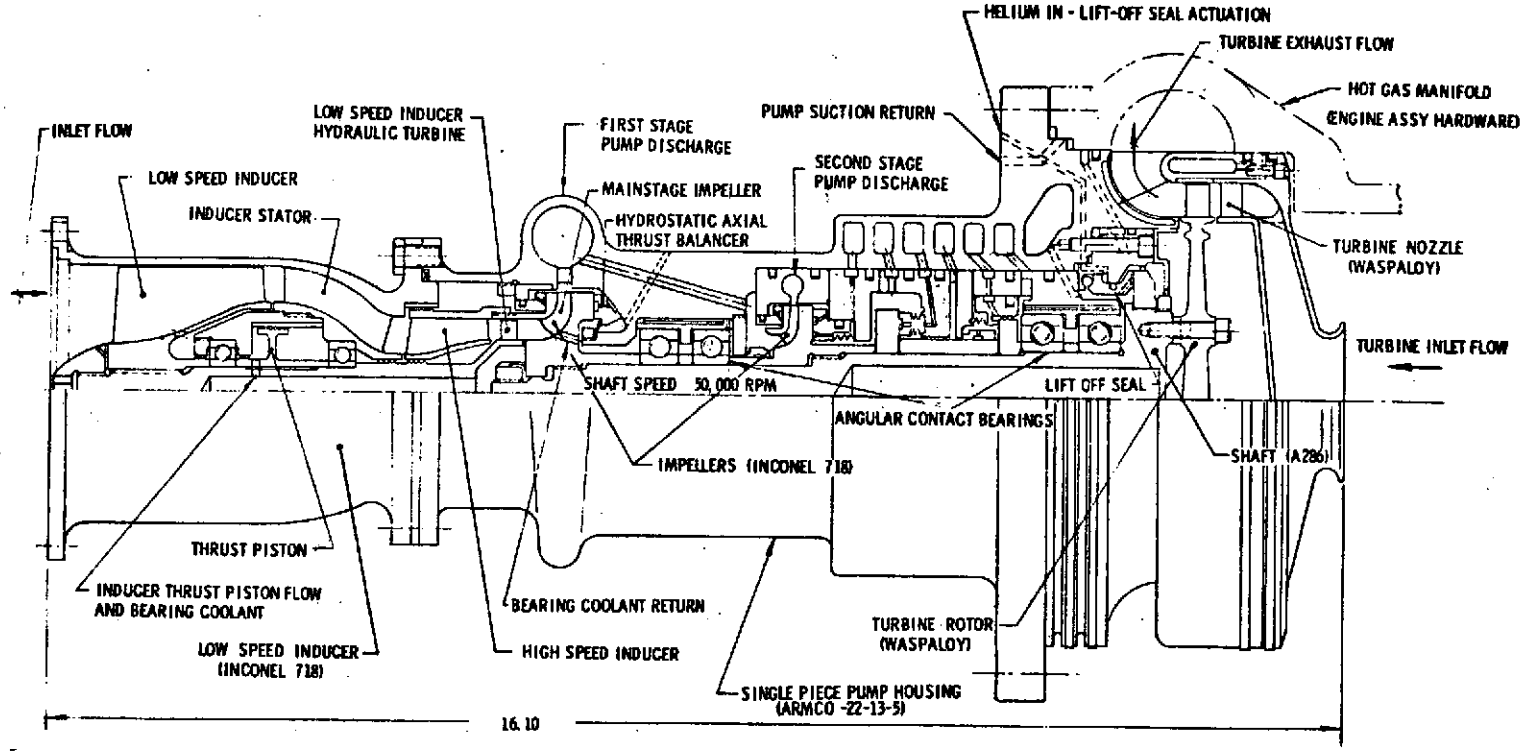

Figure 1-3. Oxidizer Turbopump Concept (Full Flow Hydraulic Boost Pump Drive)

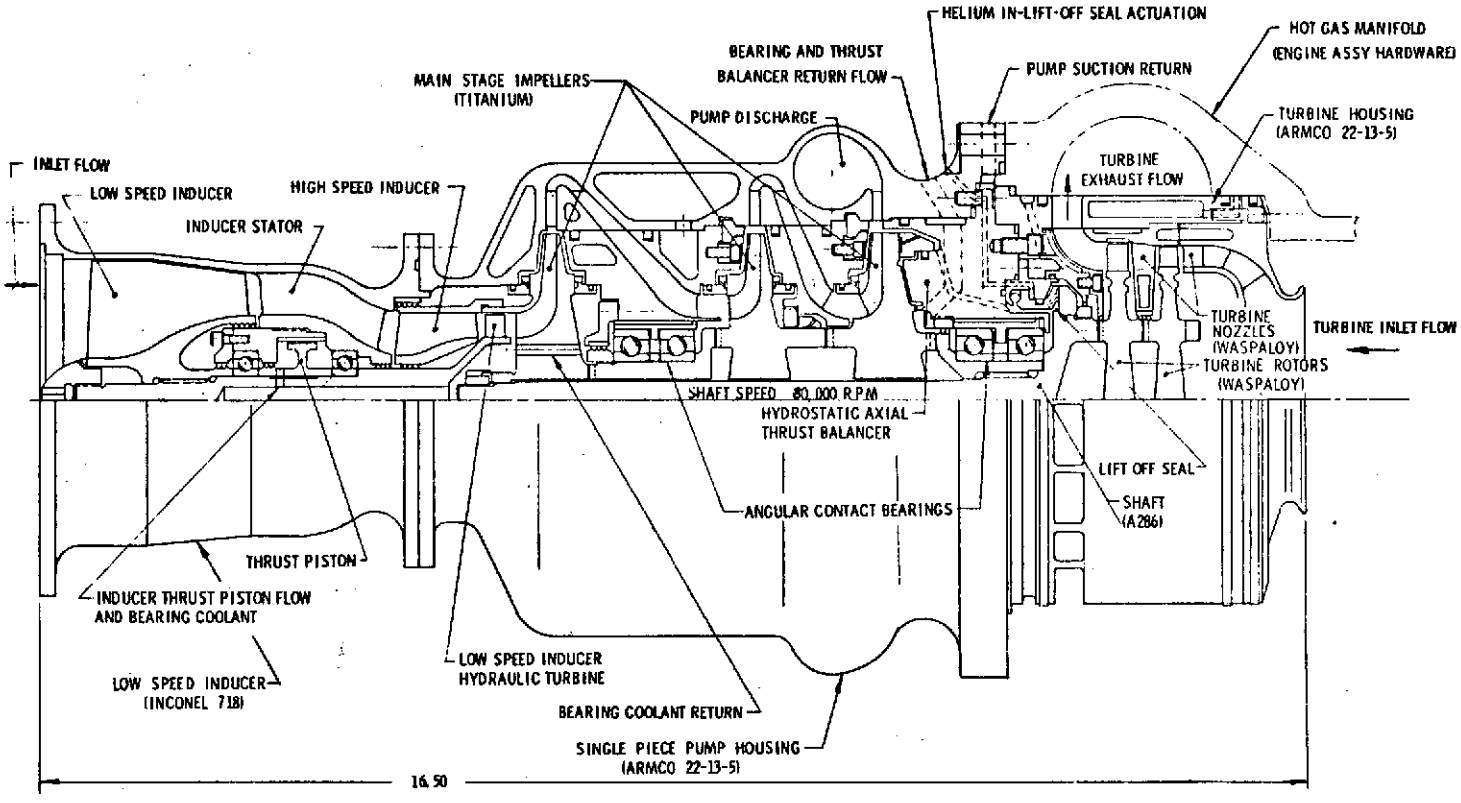

Figure 1-4. Fuel Turbopump Concept (Full Flow Hydraulic Boost Pump Drive)

the main pump inducer provide the energy for boost pump turbine drive. The advantages of this approach are integrated packaging, elimination of all nonpropulsive propellant losses, and good life capability. However, low-required NPSH for the boost pumps and limited turbine diameter (main pump inducer diameter) result in low available horsepower for boost pump drive. To match the boost pump developed head with the required main pump inlet head, particularly in the case of the main LO_2 pump, results in a significant reduction in main pump speed. This required reduction in main pump speed correspondingly results in decreased efficiency and increased weight. In addition, the boost pumps do not start until the main pumps begin rotation and therefore provide no chilldown benefit. Also, the tandem arrangement limits packaging and lacks flexibility in overcoming potential problems.

Partial-Flow Hydraulic Drive. A typical partial-flow hydraulic drive approach is presented in Fig. 1-5. The drive consists of bypassing a portion of the main pump discharge flow through the boost pump hydraulic turbine and returning it to the main pump inlet (as part of the boost pump discharge flow) or a suitable low-pressure location upstream of the main injector.

The advantages of this approach are that nonpropulsive propellant losses are eliminated, there is flexibility in packaging, and there is good life capability. However, in the case of the LH_2 pump, attempts to minimize recirculation flow would result in a large vapor fraction. This large vapor fraction (up to 60 percent for designs assessed) would make the hydraulic turbine design difficult, if not impractical. The startup of the hydraulic turbines would lag the main pump startup and therefore would not provide any benefit during chilldown. In addition, the reintroduction of two-phase flow (from chilldown of hydraulic turbine loop) into the main pump inlet may inhibit main pump operation during the start transient.

GH_2 Turbine Drive. Typical LO_2 and LH_2 boost pump/GH_2 turbine drive configurations are shown in Fig. 1-6 and 1-7. The system utilizes a portion of the thrust chamber coolant flow to drive the boost pump turbines. The hydrogen flow is then directed to the preburner, and rejoins the remainder of the coolant flow. This approach is most effectively utilized in conjunction with the split flow thrust chamber (parallel cooling of fixed nozzle and combustion chamber) configuration. By utilizing the fixed nozzle coolant to drive the turbines and in parallel with the combustion chamber, the impact on the engine cycle is minimized.

The GH_2 turbine drive approach provides the possibility of some degree of control over the start transient, initiates operation early in the sequence of events and thus enhances chilldown, allows for maximum flexibility for packaging, provides flexibility in off-design operation, and has good life capability.

The disadvantages of this approach are the high axial boost pump shaft load, GH_2 leakage into the main fuel pump inlet ($\sim$0.3 percent of mainstage mass flow), the requirement for an LO_2 boost pump dynamic seal package, the small required turbine admission, and low pressure ratio (affecting control during transient operation).

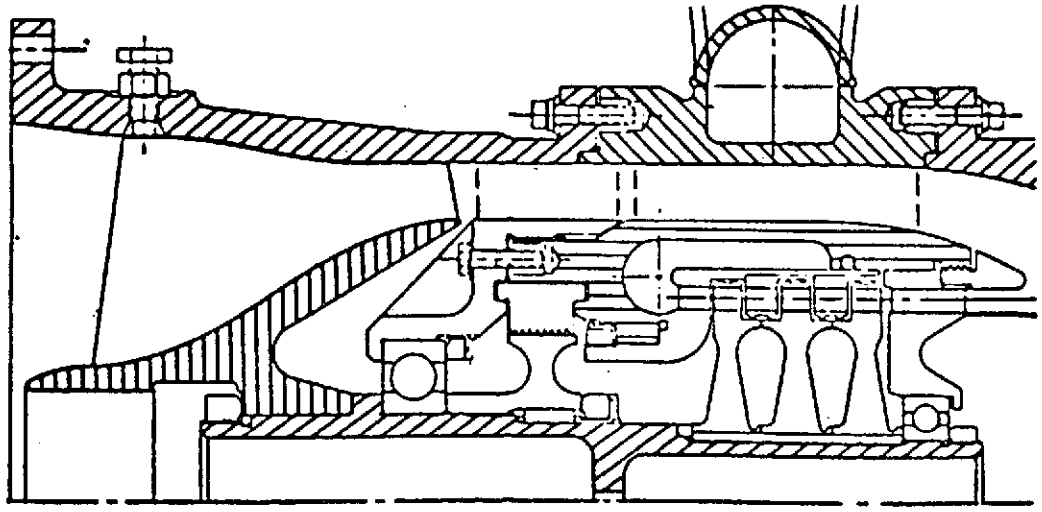

Figure 1-5. Partial Flow Hydraulic Boost Pump Drive

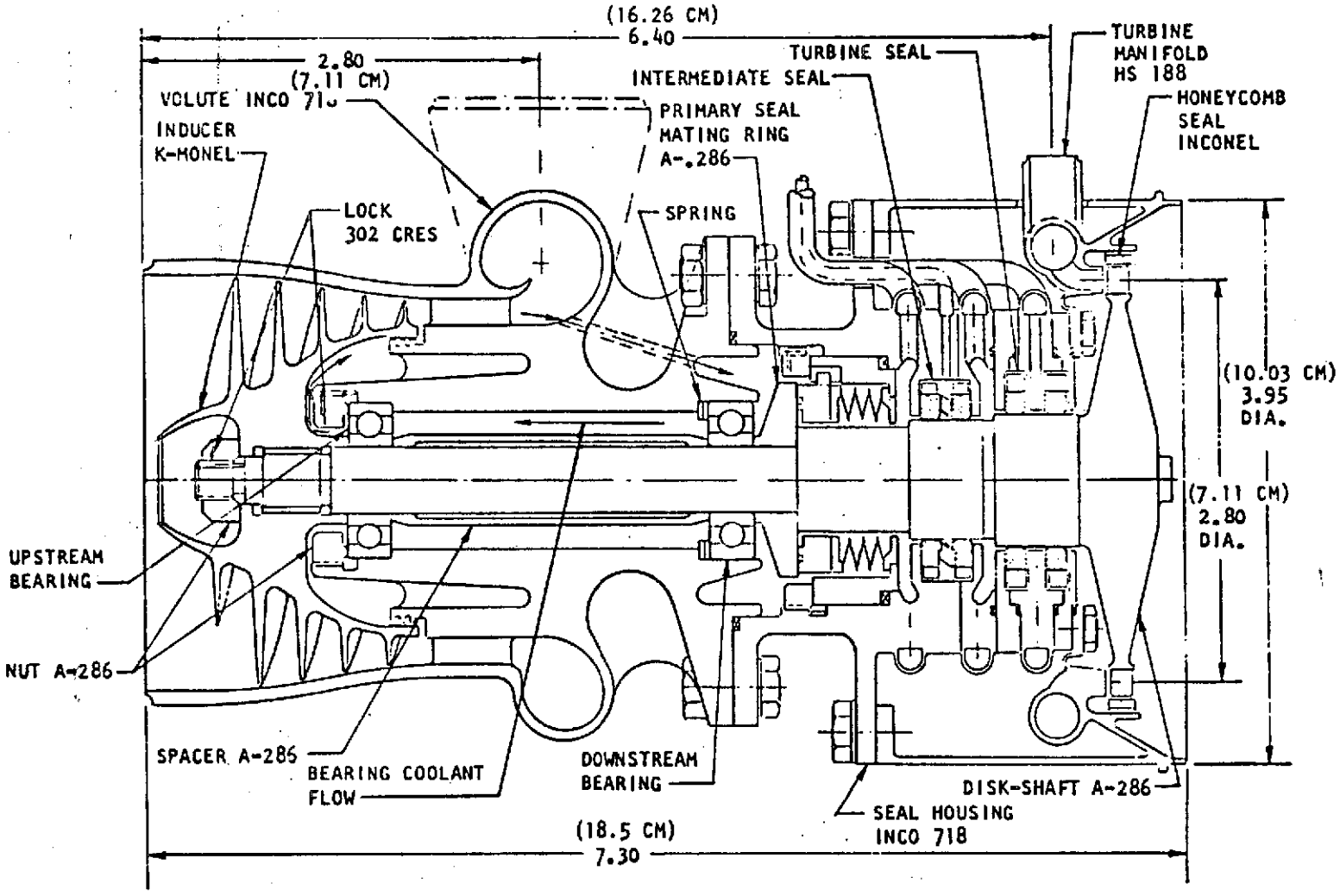

Figure 1-6. LO_2 Boost Pump (GH_2 Turbine Drive)

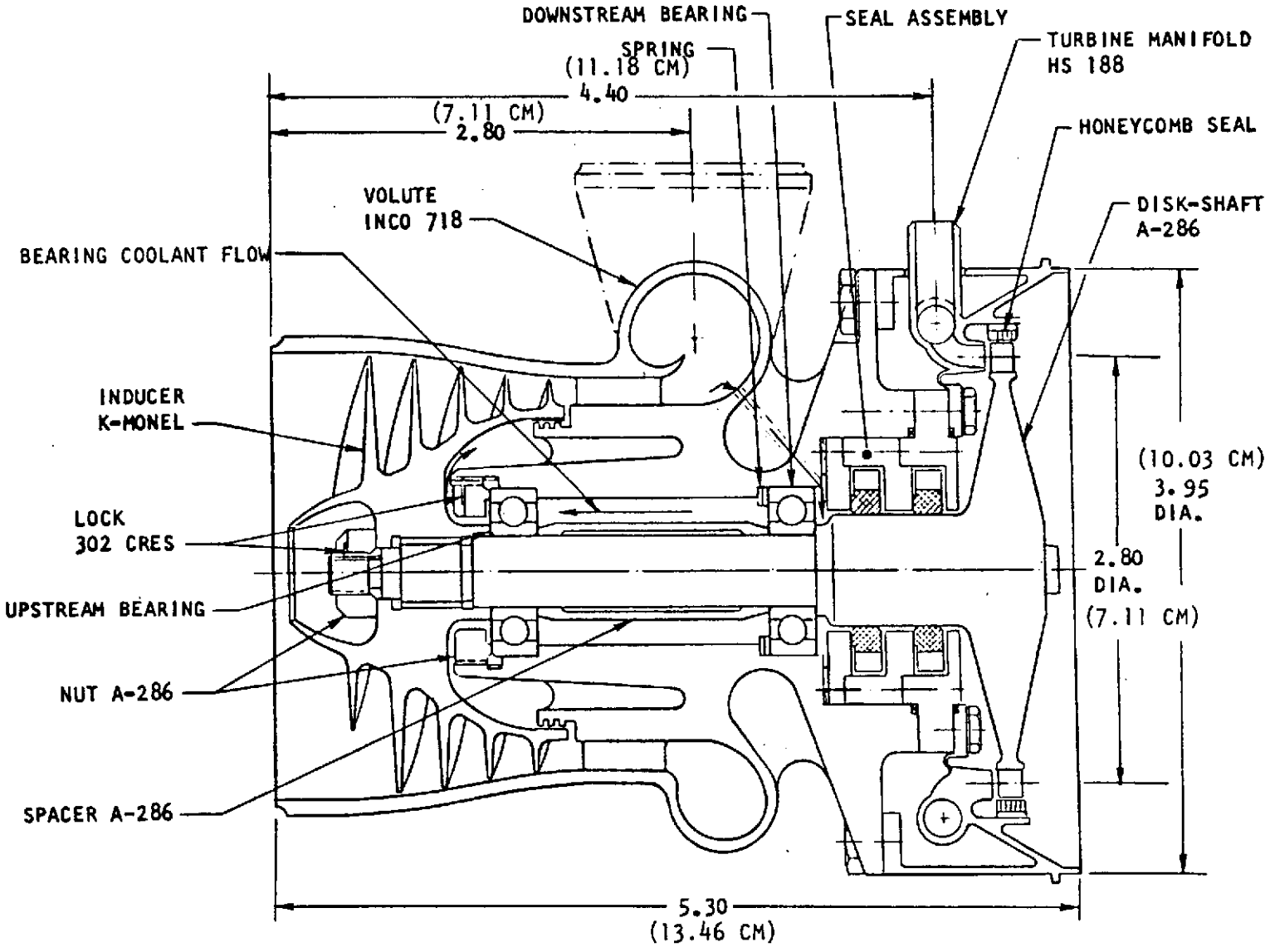

Figure 1-7. LH_2 Boost Pump (GH_2 Turbine Drive)

Boost Pump Drive Selection. The alternative boost pump drive systems were assessed with respect to those features and characteristics considered desirable (previously presented in Table 1-5 and in the order of preference established as shown in Table 1-6). The alternatives presented are in terms of meeting desirable features (yes), problem area (?) and not meeting criteria of desirable features (no). The GH_2 turbine drive approach for the LH_2 boost pump was selected. The GH_2 turbine drive and the partial-flow hydraulic turbine configurations for the LO_2 boost pump were determined to be of sufficient merit to justify their continued study as part of the engine system tradeoff.

Thrust Chamber Configurations

Since an adequate tradeoff of the competing thrust chamber configurations (1-1/2-pass and split-flow cooling circuit, as shown in Fig. 1-8) could not be conducted without consideration of the complete engine, both alternatives were utilized in alternative engine configurations to be subsequently discussed. The essential features of the injector assembly are shown in Fig. 1-9.

Preburner Configurations

The single and dual preburner configurations are shown in Fig. 1-10, 1-11, and 1-12. The side-mounted spark igniter location shown was selected as preliminary for purposes of the study with possible relocation to the center of the injector based on further study. The air-gap igniter configuration was selected because of the wider range of operation than competing designs demonstrated during prior NASA/LeRC technology programs (NAS3-14350 and 14351). Both single and dual preburner configurations were utilized in the engine tradeoff studies.

Selection of Alternative Engine Configurations

Based on the foregoing tradeoffs, eight alternative engine configurations incorporating features presented in Table 1-7, were selected. These configurations were analyzed for final selection of a baseline engine configuration.

TABLE 1-7. PRELIMINARY SELECTION OF ENGINE ALTERNATIVES

Throttling	Preburners	Thrust Chamber Cooling	Boost Pump Drive
None	1	1-1/2 Pass	O_2-Hydrogen/H_2 Gas
None	1	1-1/2 Pass	O_2-Gas/H_2-Gas
None	1	Split	O_2-Hydrogen/H_2-Gas
None	1	Split	O_2-Gas/H_2-Gas
None	2	1-1/2 Pass	O_2-Hydrogen/H_2-Gas
None	2	1-1/2 Pass	O_2-Gas/H_2-Gas
None	2	Split	O_2-Hydrogen/H_2-Gas
None	2	Split	O_2-Gas/H_2-Gas

TABLE 1-6. BOOST PUMP DRIVE TRADEOFF

Drive	Provide Start Control	Provide NPSH			Long Life	No Losses	Packaging Flexibility	Mech Design	Low Potential Eng. Cycle Impact	Order of Preference	
		Start	Mainstage	OffDesign						LH_2	LO_2
Gear	No	Yes	Yes	?(LH_2 Pump)	No	No	No	?(Life)	No	4	4
LH_2 Hyd											
Full	No	Yes	Yes	Yes	Yes	Yes	No	?(Turbine)	No	3	
Partial	No	?(Start Lag)	Yes	Yes	Yes	Yes	Yes	Yes	No	2	
LO_2 Hyd											
Full	No	Yes	Yes	Yes	Yes	Yes	No	?(Turbine)	No		3
Partial	No	?(Start Lag)	Yes	Yes	Yes	Yes	Yes	Yes	No		2
GH_2 Turb.											
LO_2	Yes	Yes	Yes	Yes	Yes	No	Yes	?	Yes		1
LH_2	Yes	Yes	Yes	Yes	Yes	Yes	Yes	?	Yes	1	

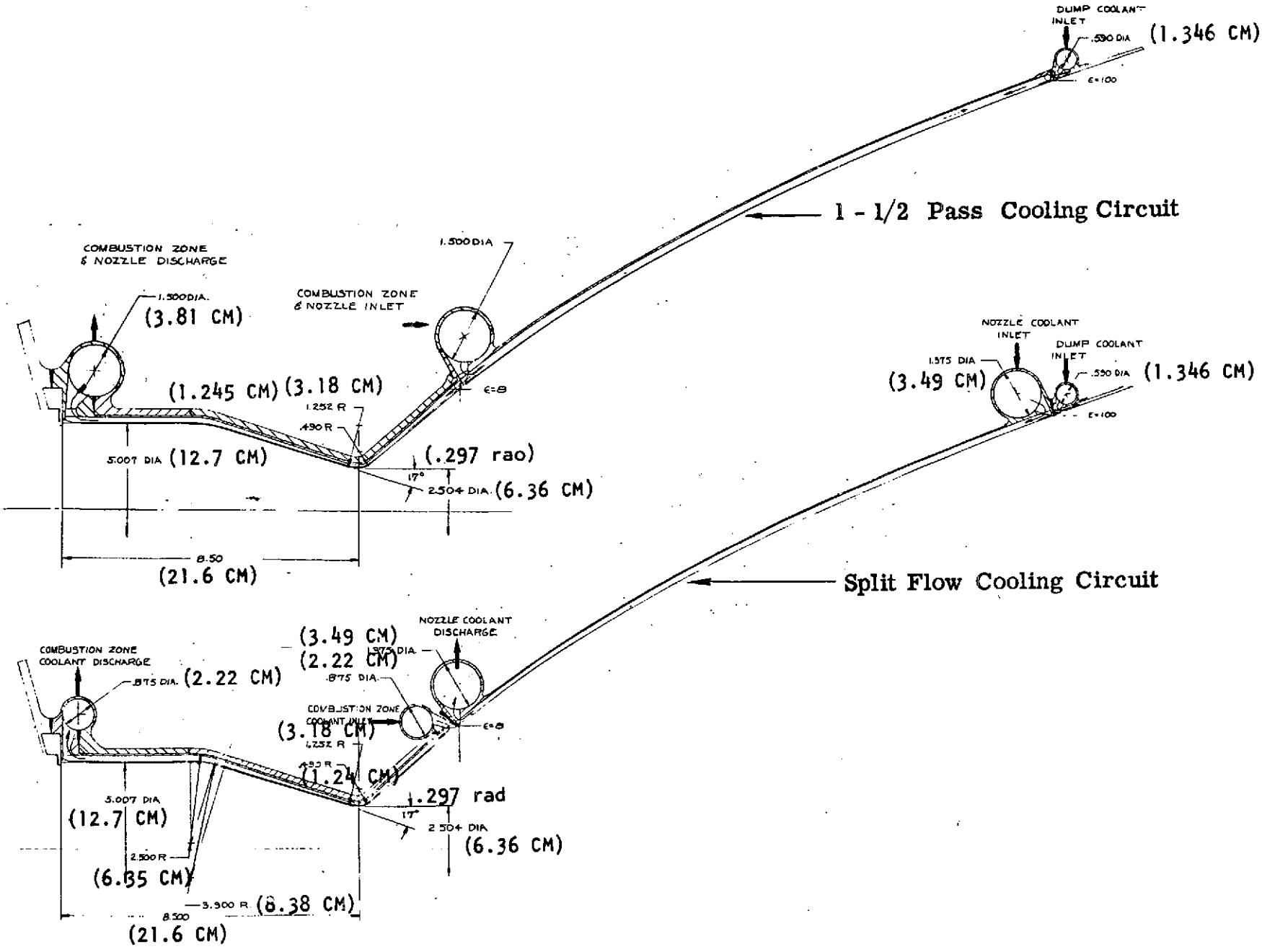

Figure 1-8. Thrust Chamber Configurations

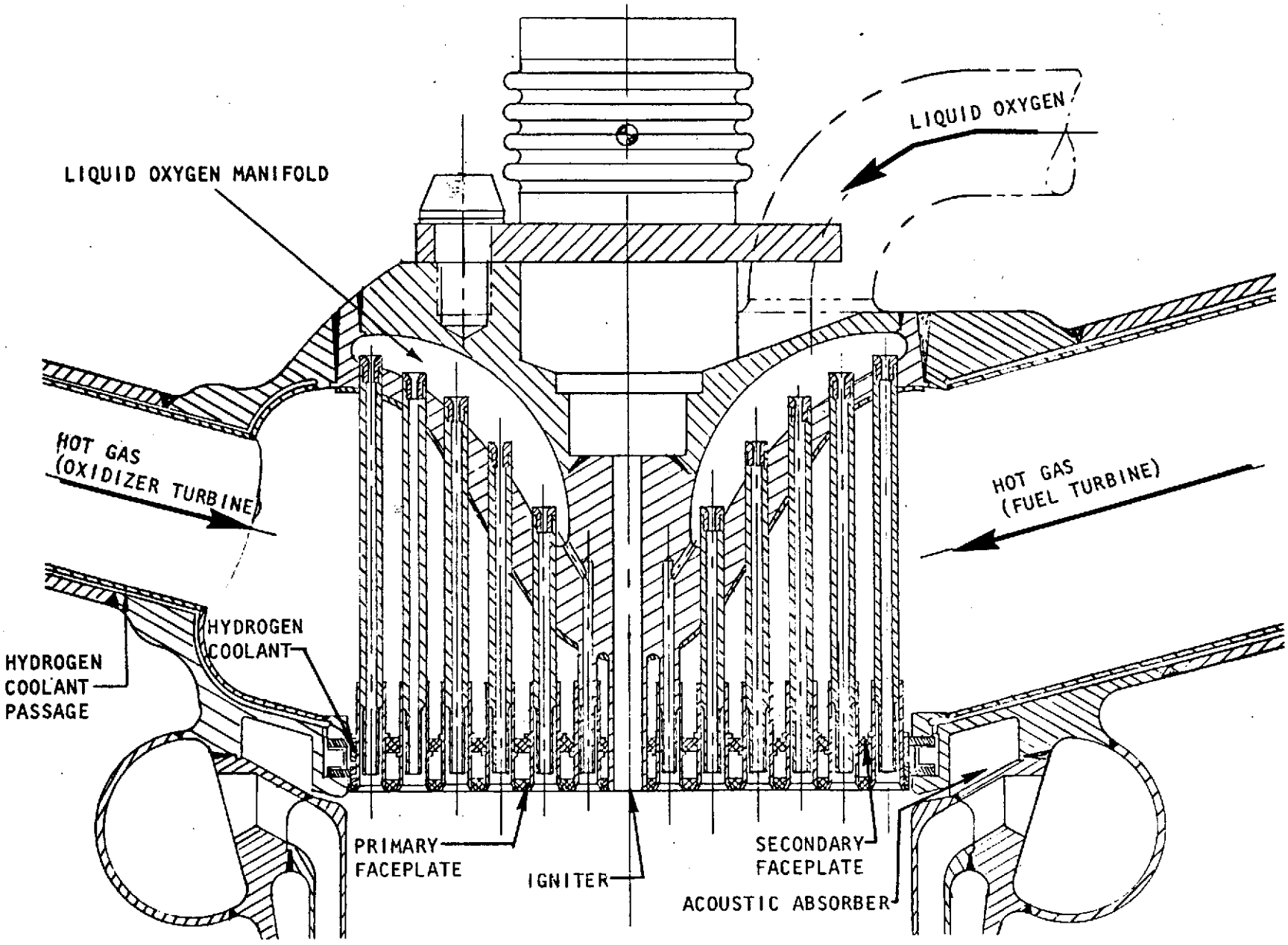

Figure 1-9. Main Injector Assembly

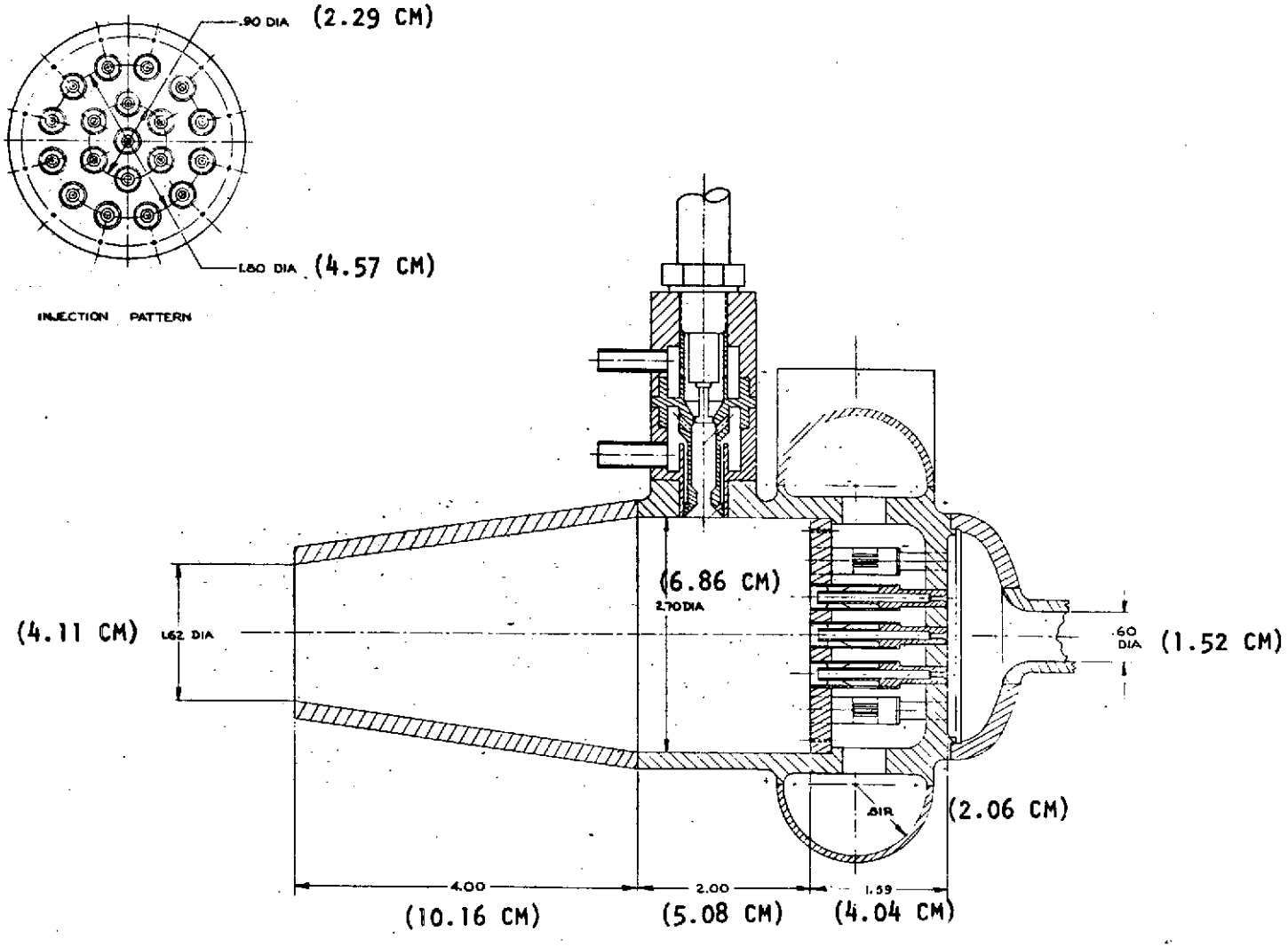

Figure 1-10. Single Preburner Configurations

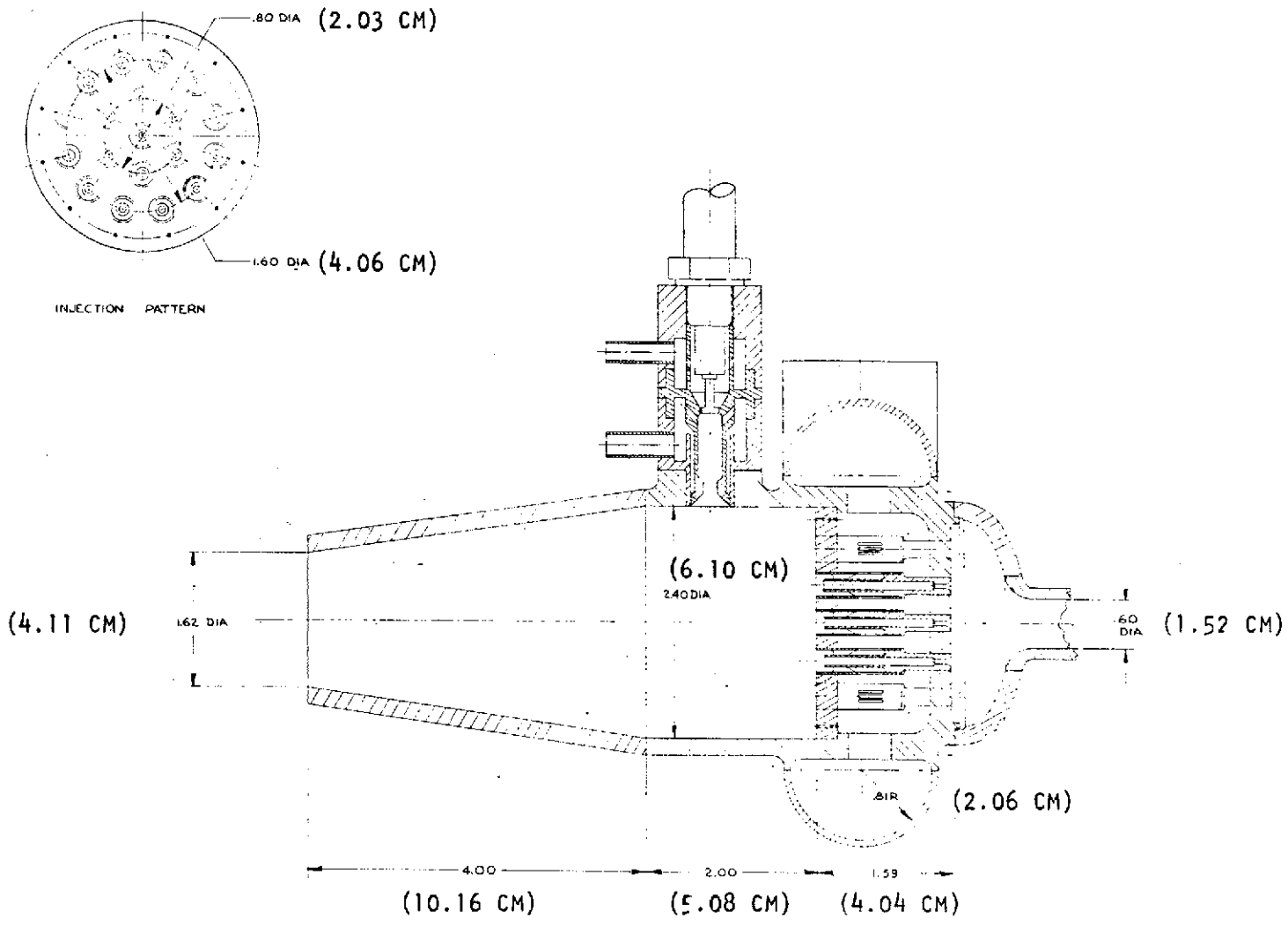

Figure 1-11. Fuel Preburner (Dual Configuration)

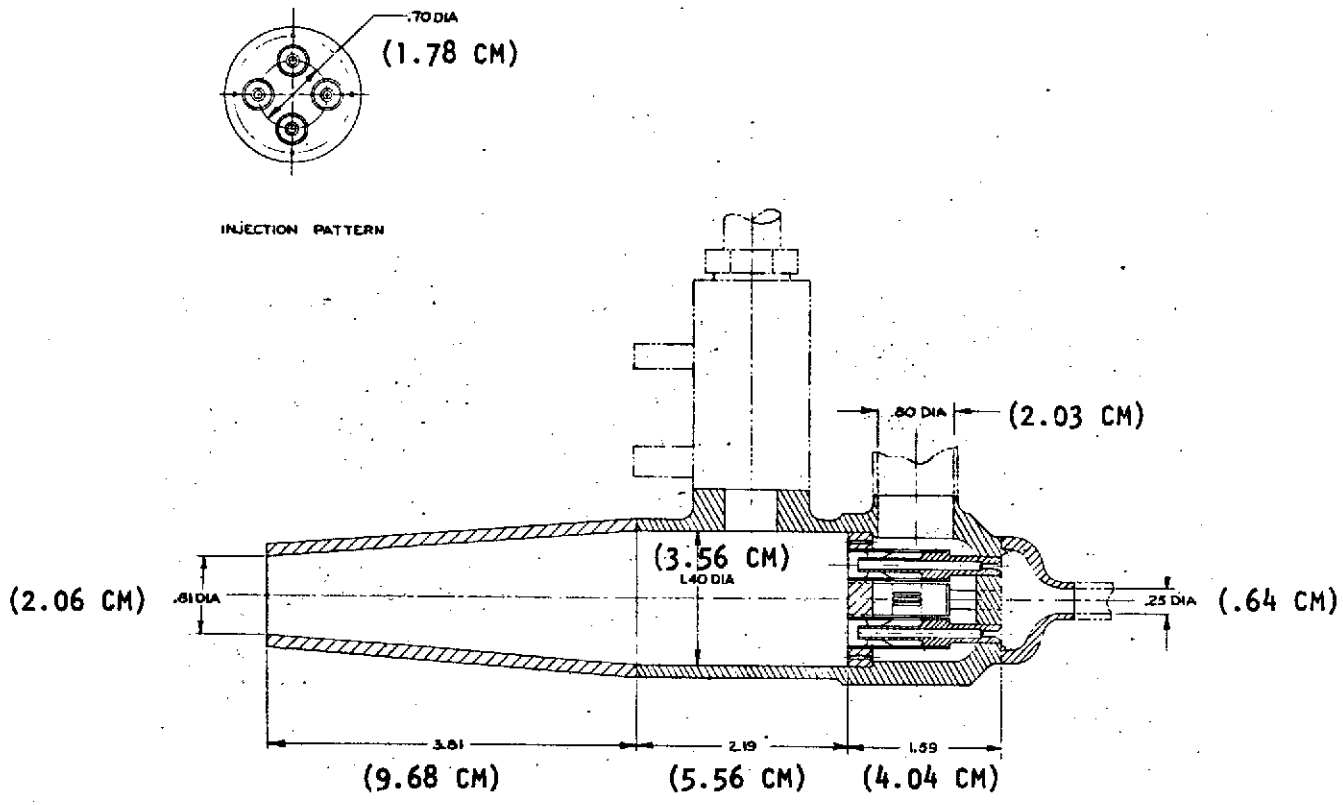

Figure 1-12. Oxidizer Preburner (Dual Configuration)

Typical Other Engine Hardware

To establish complete engine configurations for the purpose of conducting the tradeoff study, typical configurations of the other major engine components were identified and are presented: the main hydrogen and oxygen turbopumps (Fig. 1-13 and 1-14), the engine controller (Fig. 1-15) typical main propellant valve concepts (Fig. 1-16 and 1-17) and the control valve concept (Fig. 1-18).

ENGINE CONFIGURATION TRADEOFF

Utilizing the eight alternative engine configurations previously identified, a tradeoff was conducted for selection of the baseline, nonthrottling engine configuration. The tradeoff included consideration of cycle balance and performance, transient operation, flexibility and complexity, weight, and cost.

Cycle Balance and Performance

To establish a common basis for configuration comparison as well as provide for the required operating margin, an analysis of preburner/turbine temperature margin was conducted, as shown in Fig. 1-19. The baseline preburner temperature of 1033 K (1860 R) was selected. The design margin provided by increasing preburner temperature is presented in Table 1-8.

TABLE 1-8. ENGINE DESIGN MARGIN

- Design Engine for Maximum Stress Conditions
- Operate at Reduced Preburner Temperature
- 60 F (33.3 K) temperature reduction is equivalent to:
  - 0.0758×10^7 N/m^2 (110 psia) in chamber pressure
  - 2 percent in main fuel pump and turbine combined efficiency
  - 7 percent in main oxidizer pump and turbine combined efficiency

The eight alternative configurations to be studied for selection of the baseline nonthrottling configurations are shown schematically in Fig. 1-20 through 1-27. The corresponding operating conditions, selected by optimizing engine chamber pressure at given operating conditions, are presented in Tables 1-9 through 1-16. The specific impulse of each configuration was parametrically determined based on the use of a 400:1 area ratio nozzle (a study ground rule) and 90-percent length nozzle for optimum performance. The results are presented in Table 1-17.

Also as shown, the lengths of the engines were determined. To further assess the impact of high chamber pressure, the performance was determined using a fixed engine length of 208.28 cm (82 inches) (used in previous Air Force studies), 70% length nozzle, and with no limit on area ratio (Table 1-18). It should be noted that those configurations incorporating the LO_2 hydraulic turbine for the LO_2 boost pump drive (configurations 1, 3, 5, 7) have slightly higher performance due to elimination of the boost pump dynamic

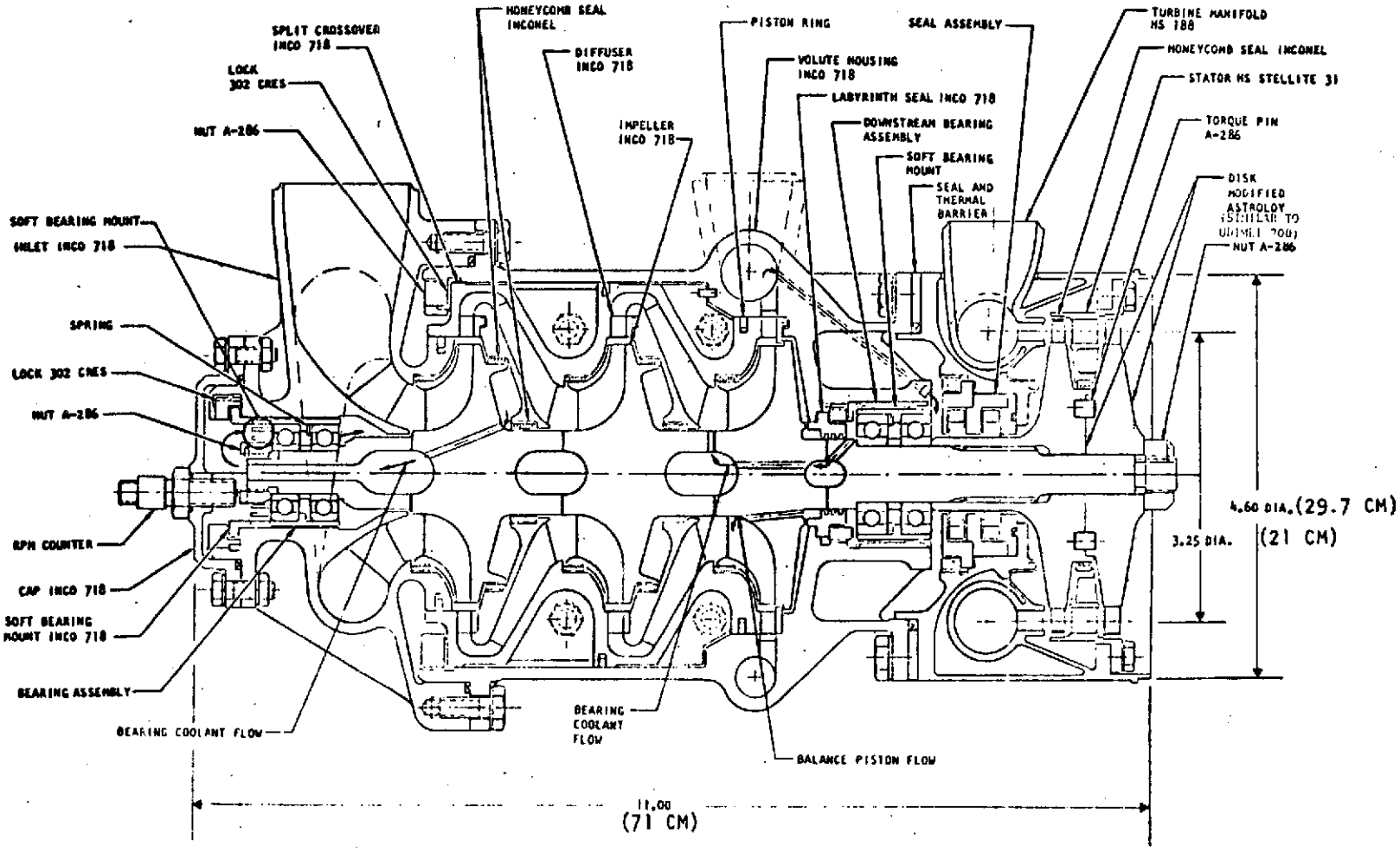

Figure 1-13. LH_2 Main Turbopump

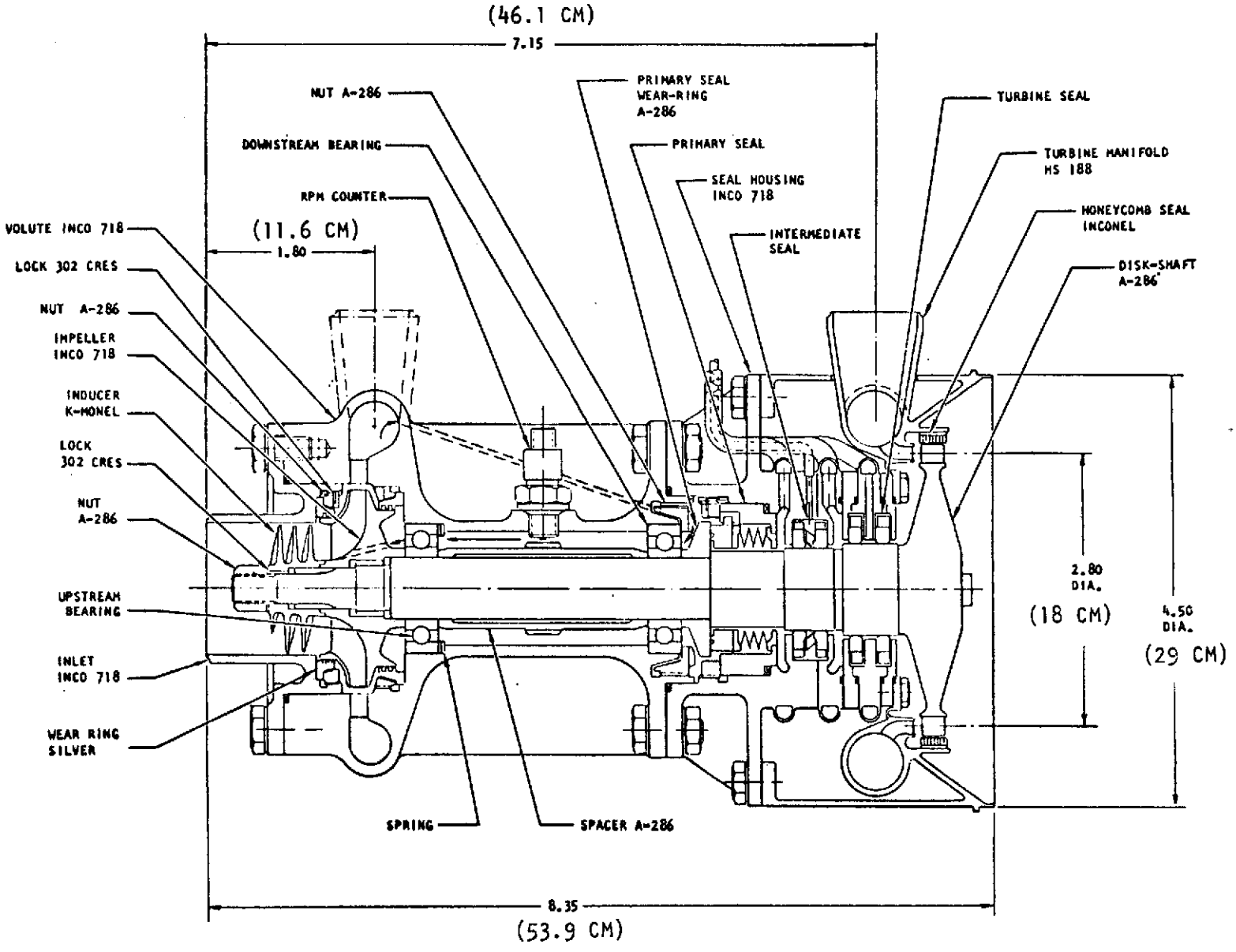

Figure 1-14. LO_2 Main Turbopump

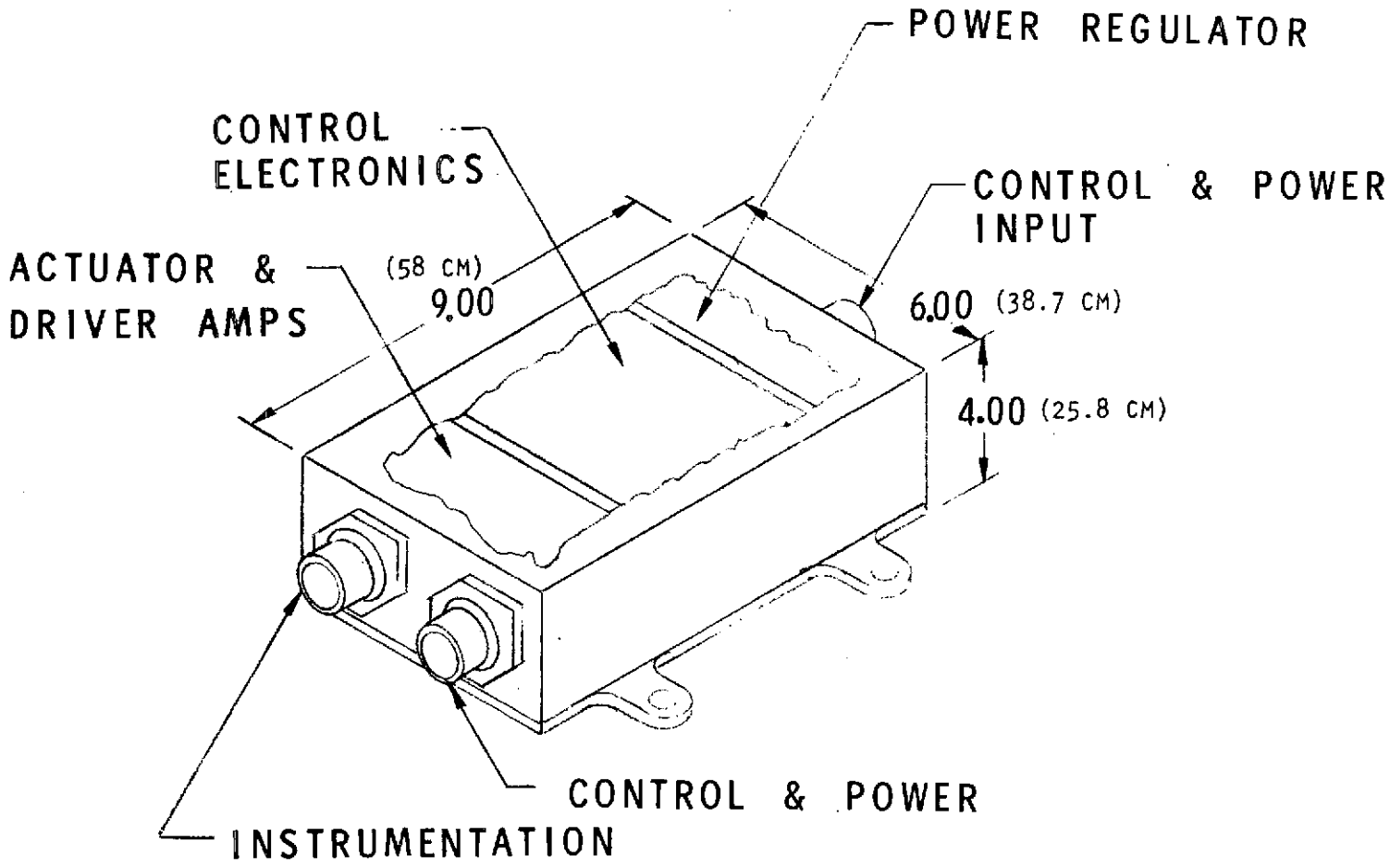

Figure 1-15. Engine Controller

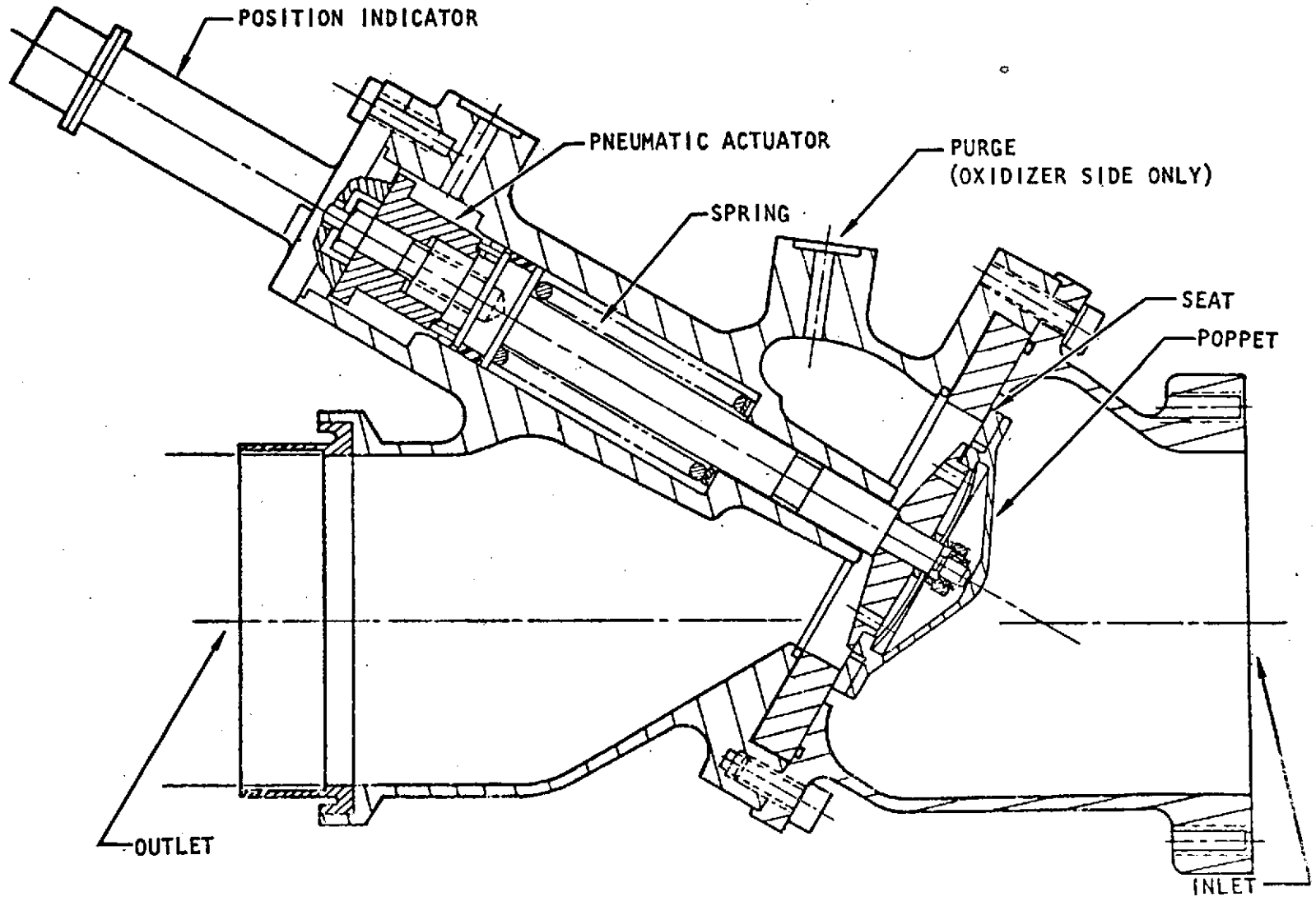

Figure 1-16. Main Valve Assembly

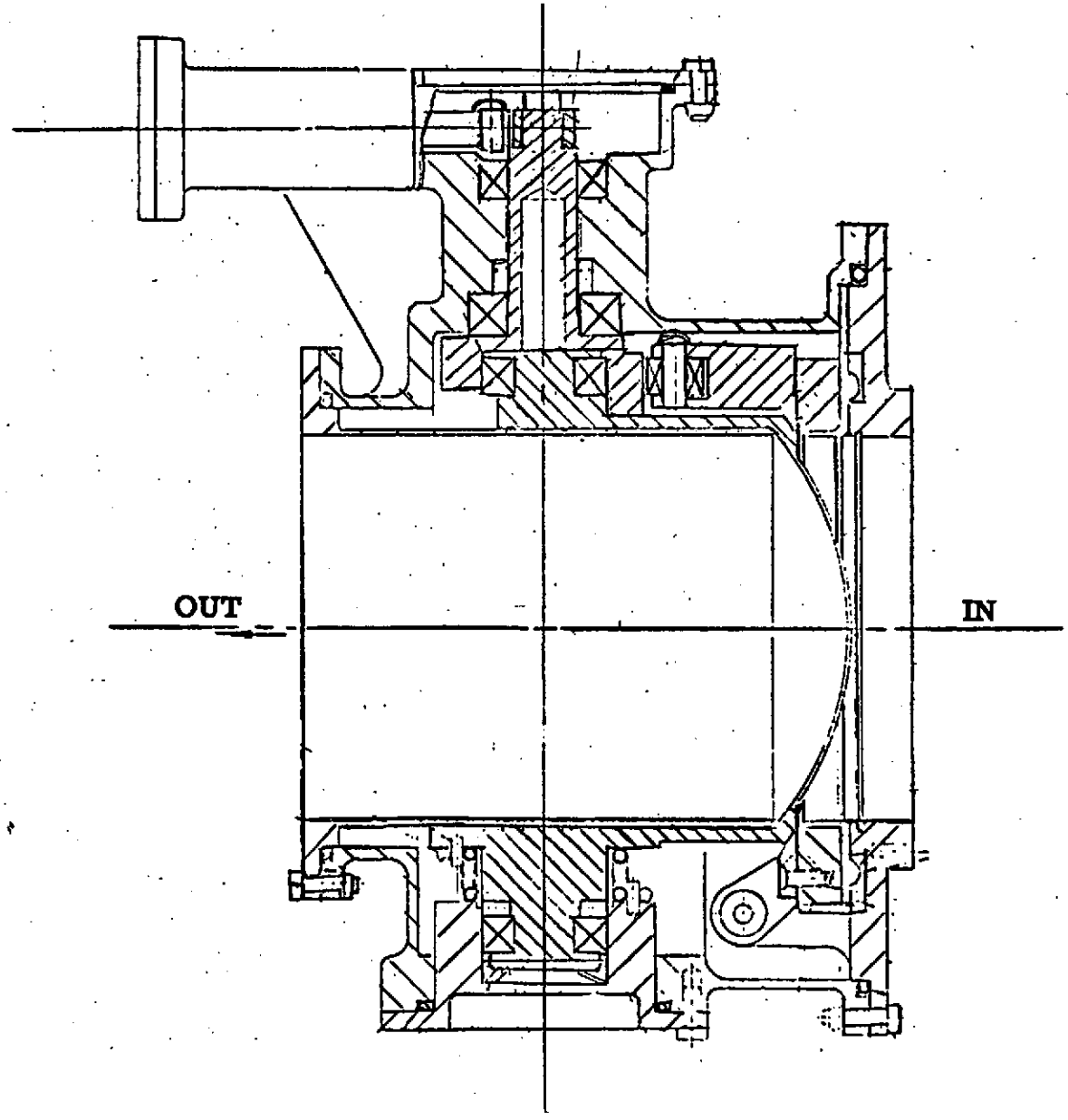

Figure 1-17. Alternate Main Vlave Configuration

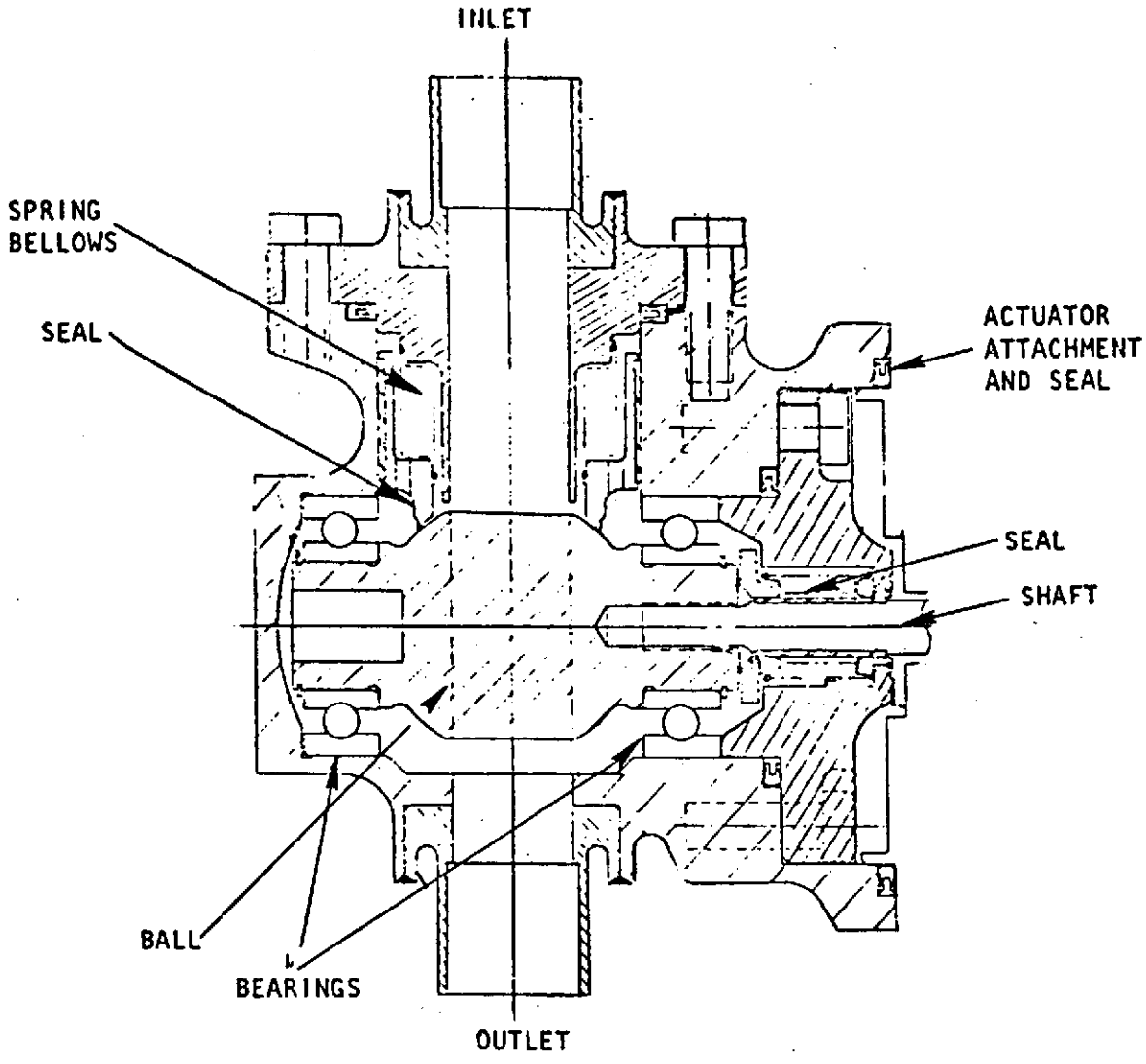

Figure 1-18. Control Valve for Preburner Fuel Inlet and Thrust Chamber Oxidizer Inlet

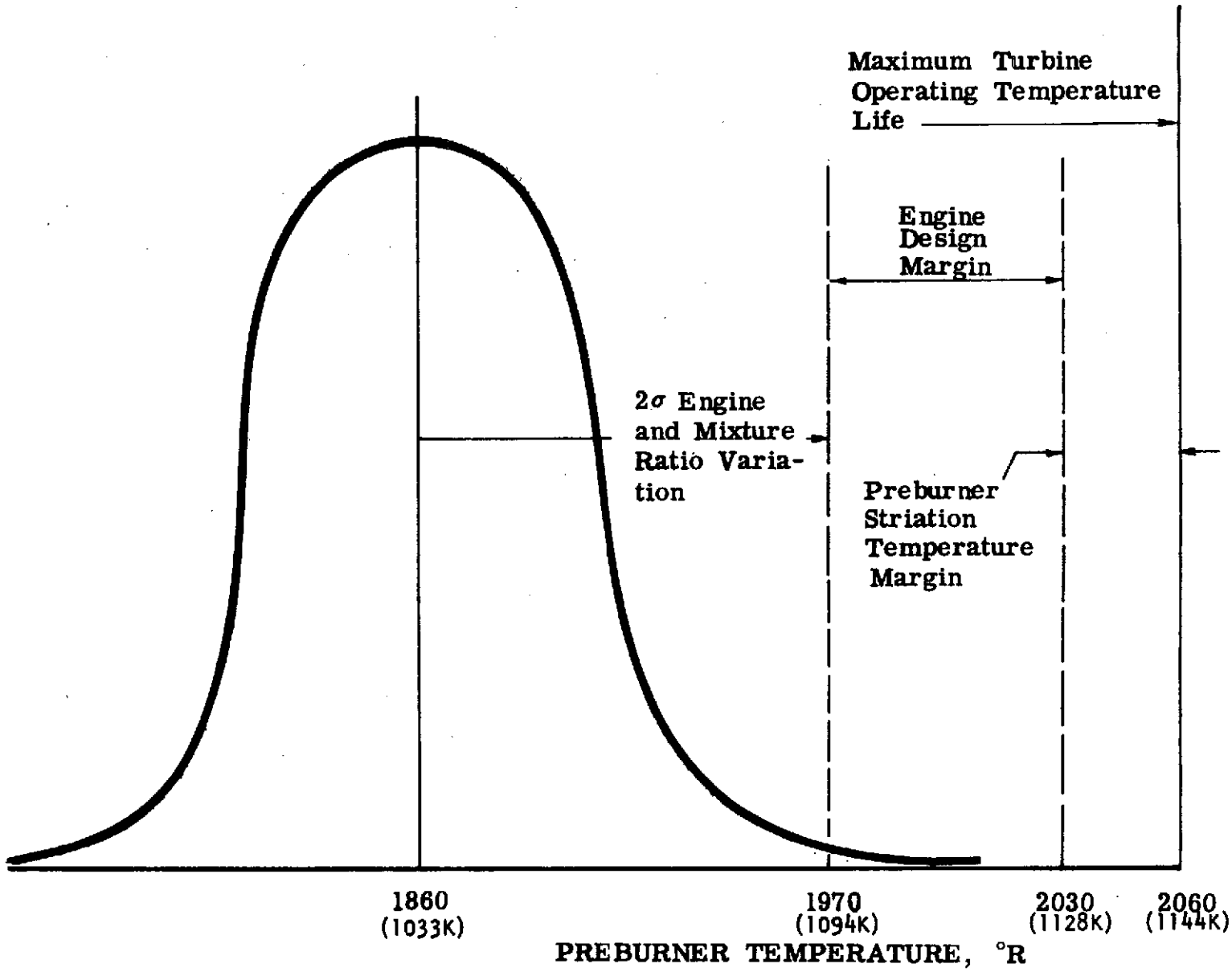

Figure 1-19. Engine Variation and Design Margin

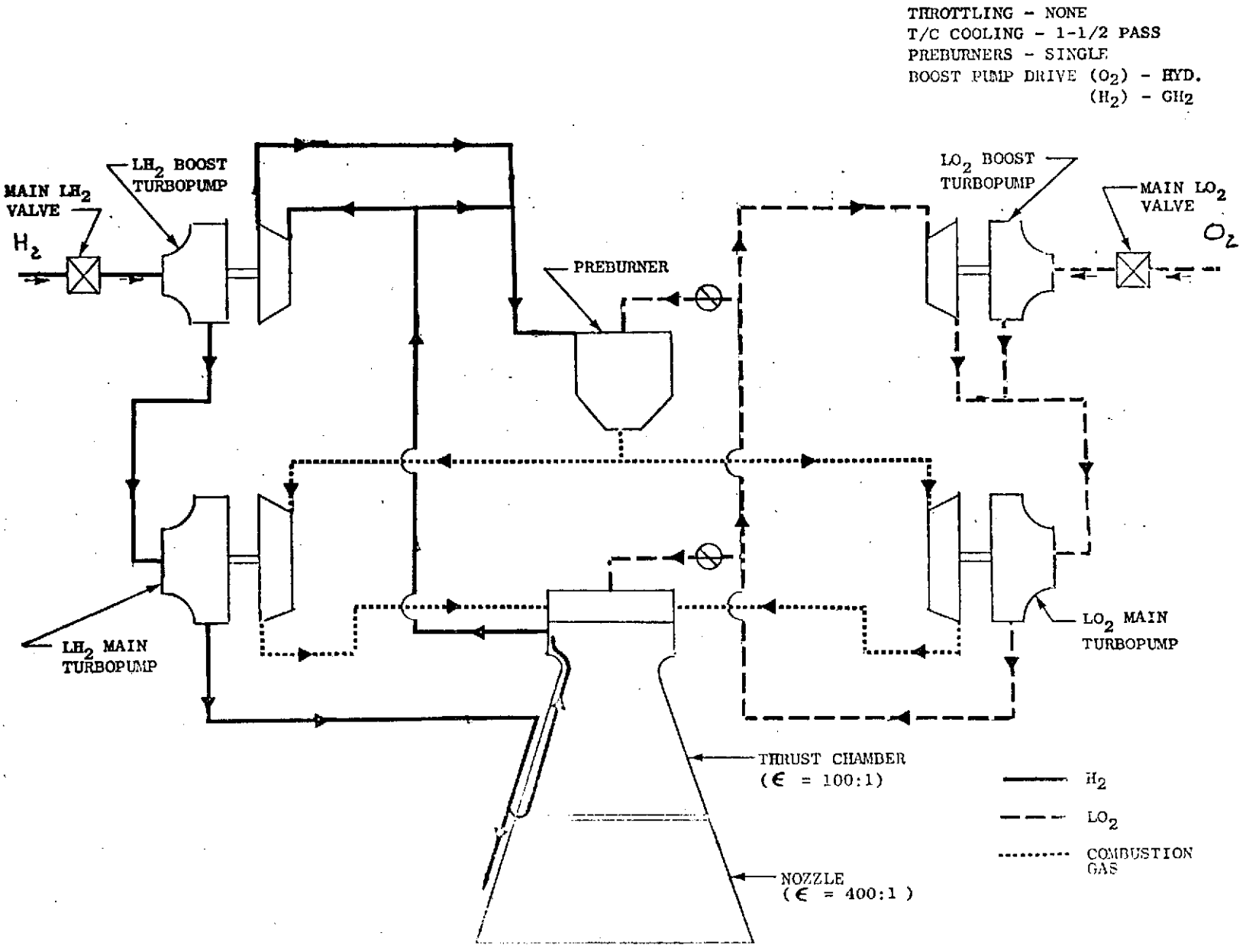

Figure 1-20. Alternate No.1

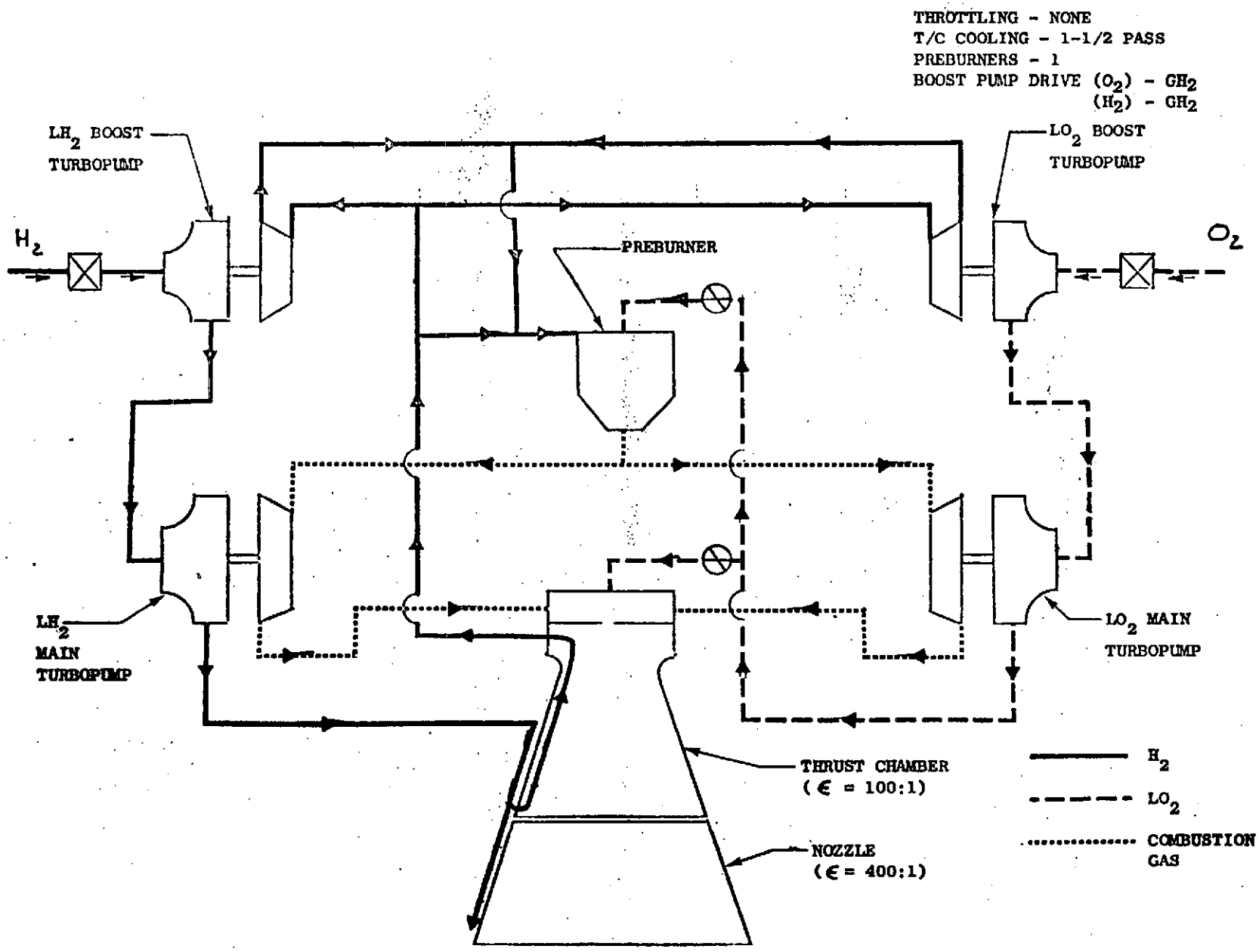

Figure 1-21. Alternate No.2

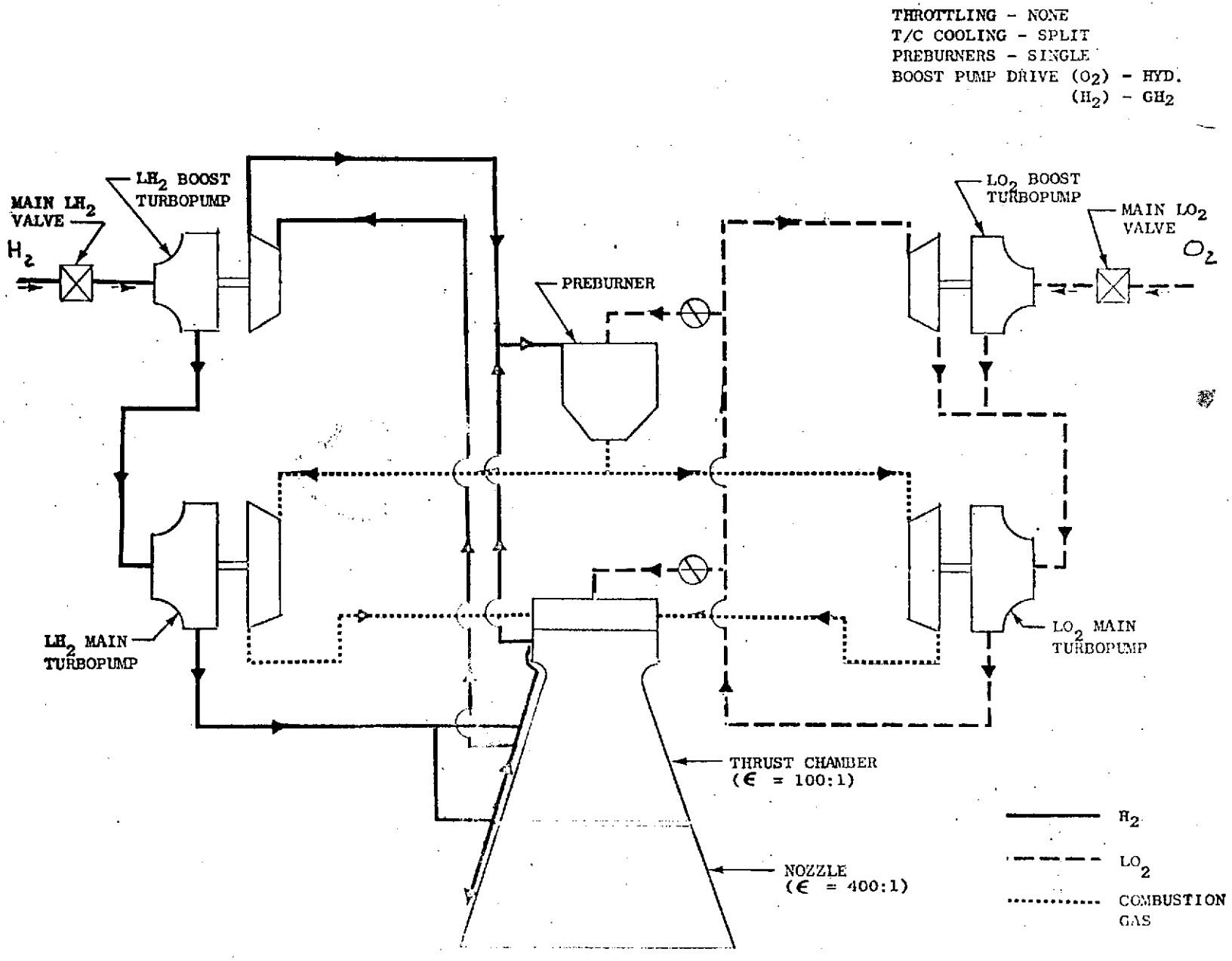

Figure 1-22. Alternate No.3

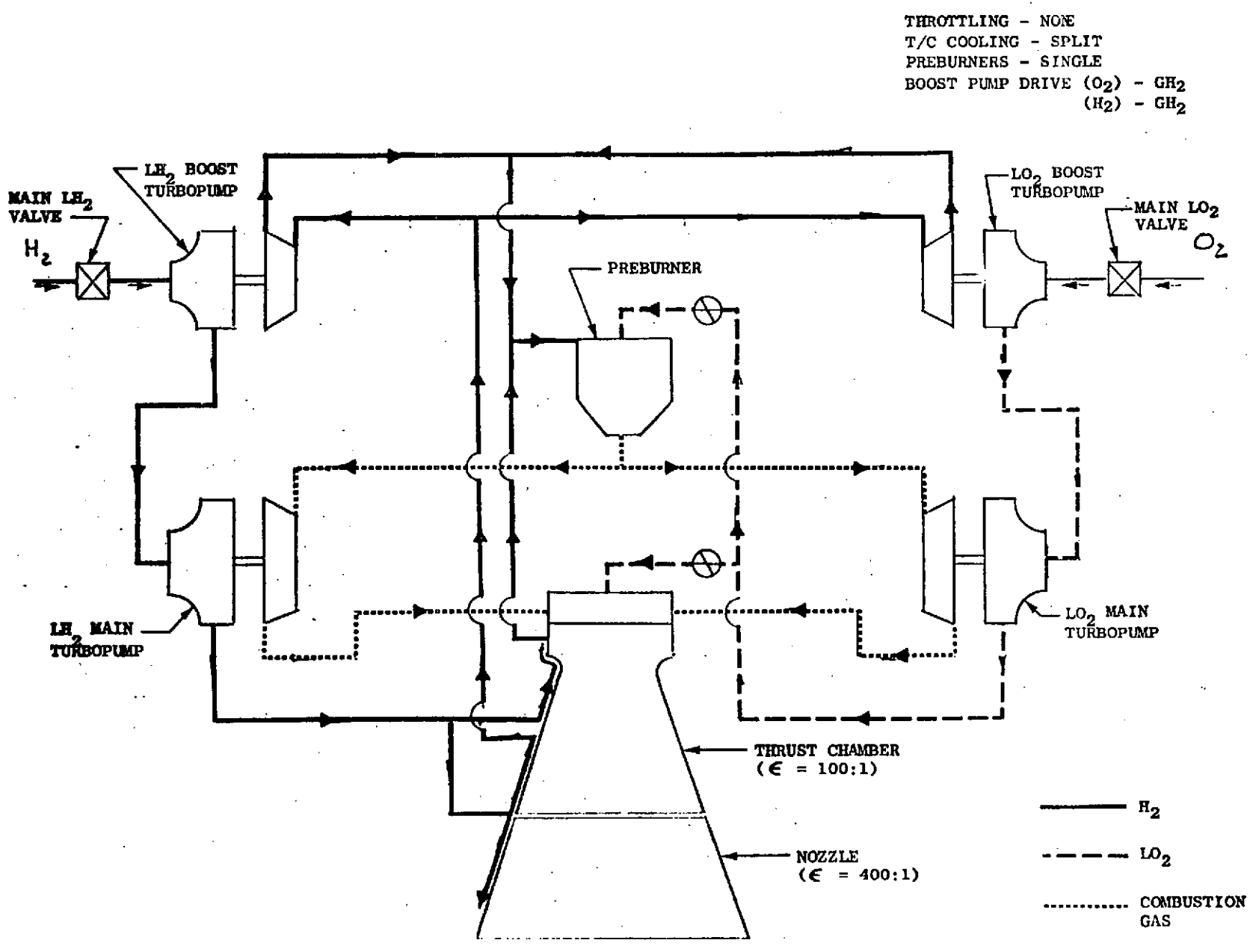

Figure 1-23. Alternate No.4

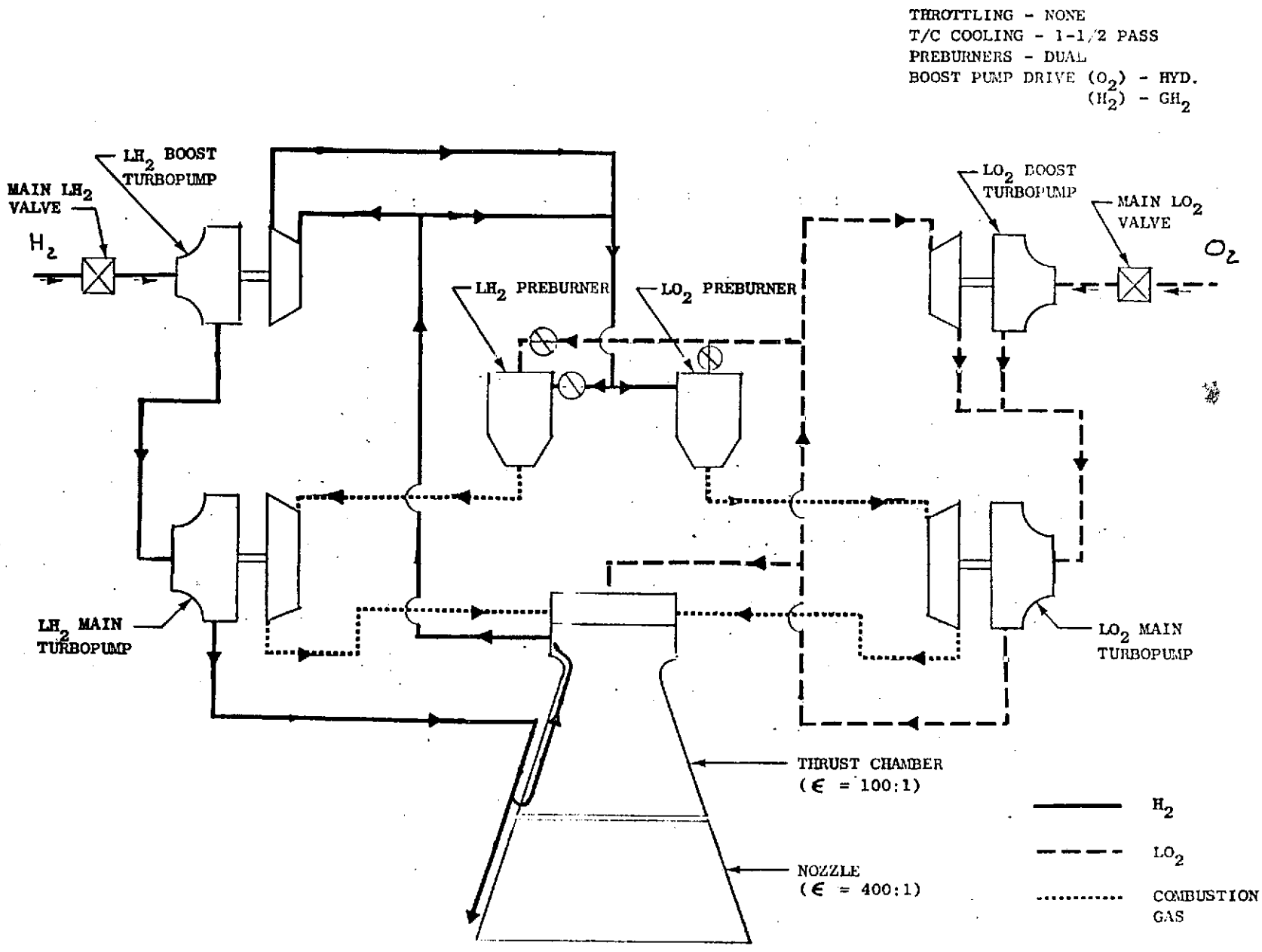

Figure 1-24. Alternate No.5

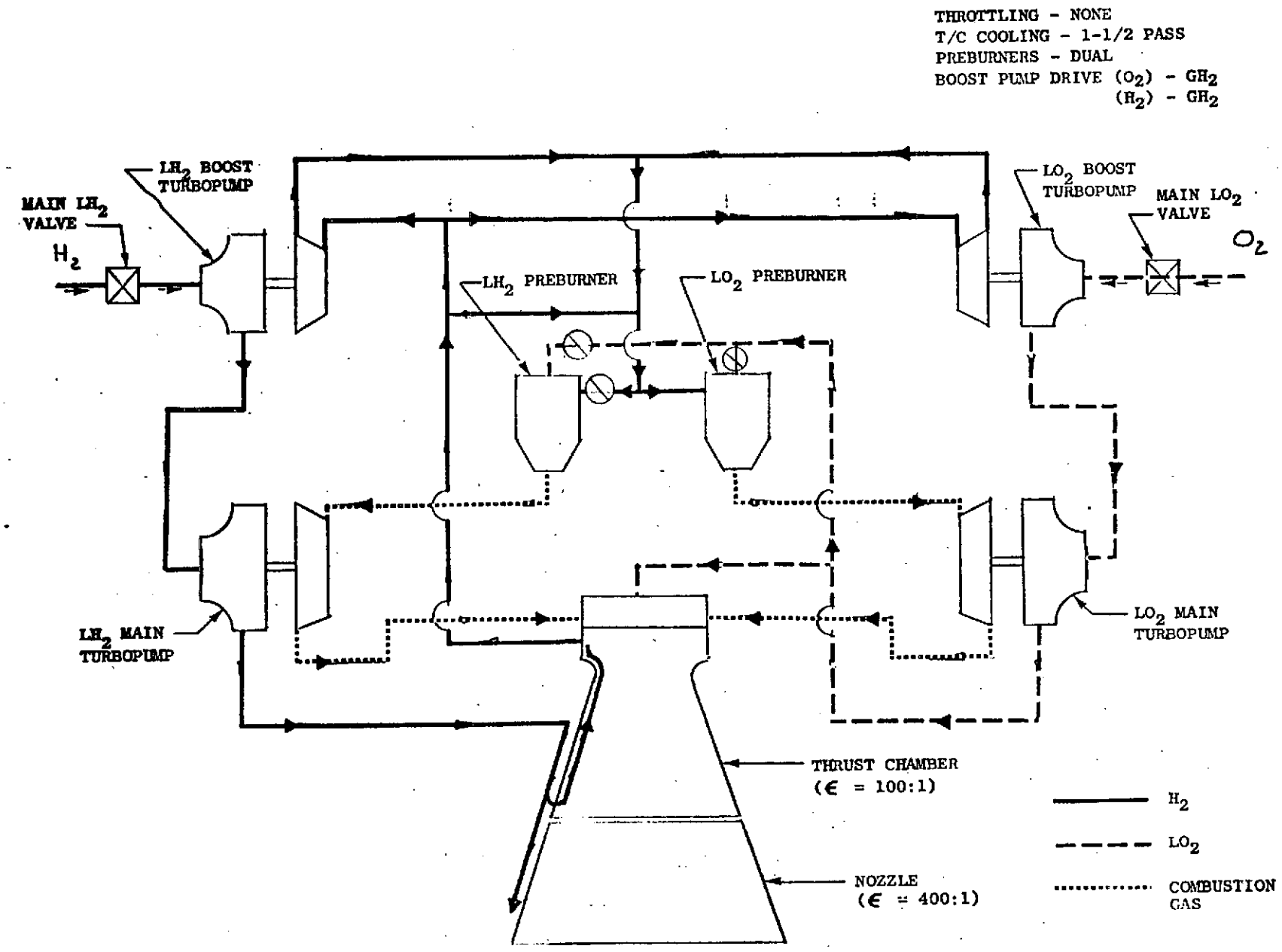

Figure 1-25. Alternate No.6

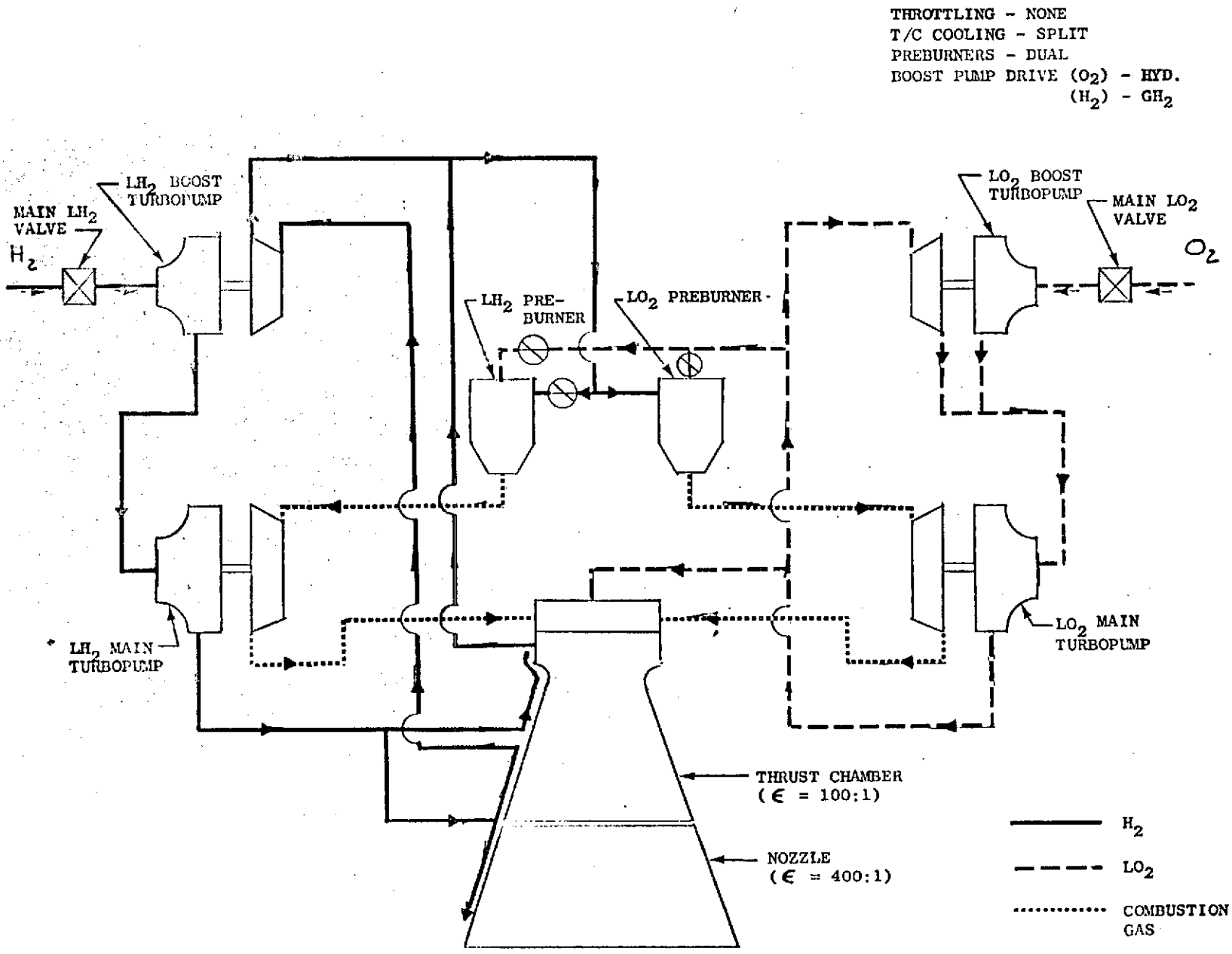

Figure 1-26. Alternate No.7

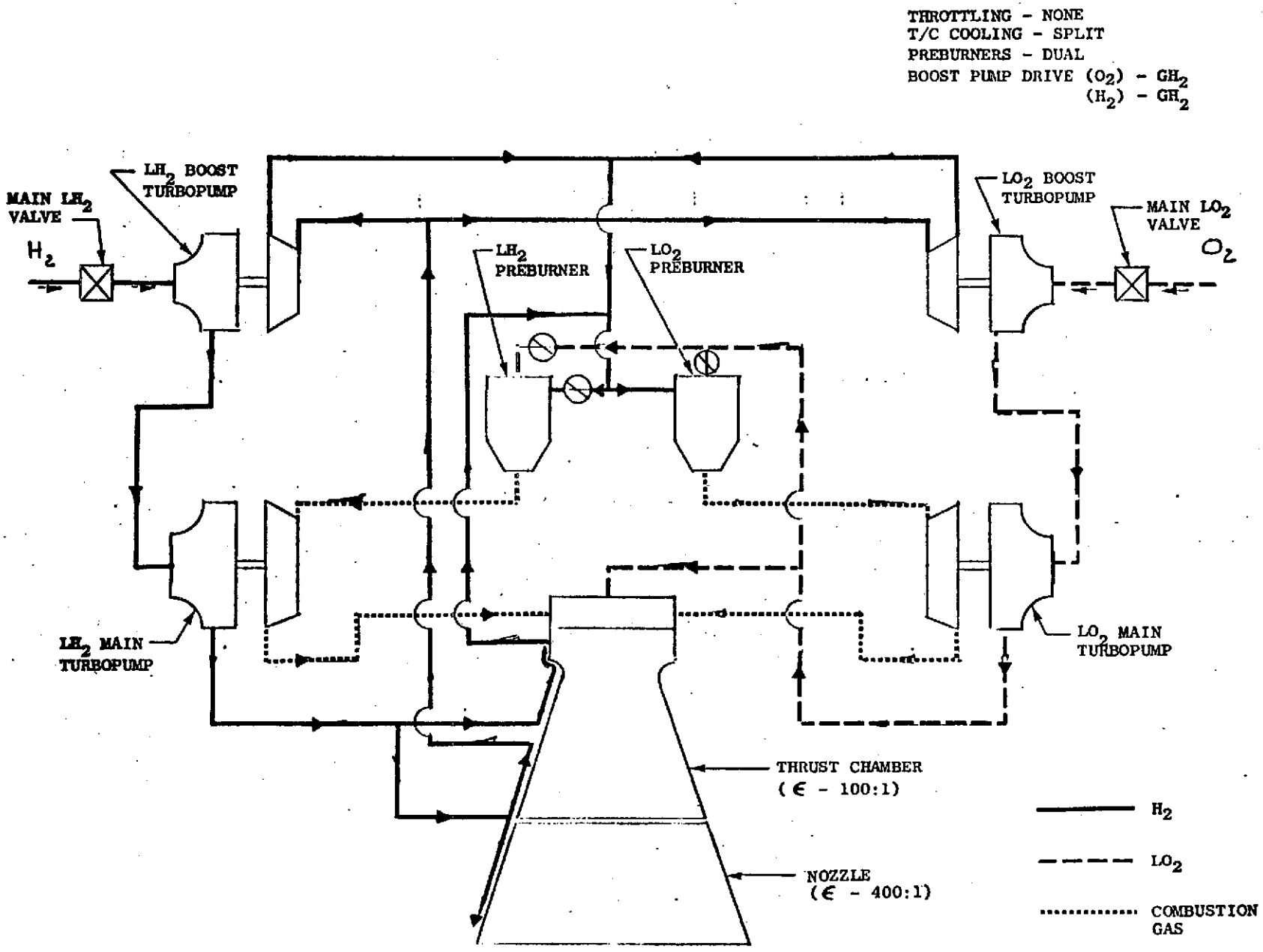

Figure 1-27. Alternate No.8

TABLE 1-9. ALTERNATE NO. 1

P_c, psia	1875 (1.29 $N/m^2 x10^7$)
P_{PB}, psia	2882 (1.98 $N/m^2 x10^7$)
T_{PB}, R	1860 (1033 K)

	Fuel Boost Pump	Fuel Main Pump	Oxidizer Main Pump	Oxidizer Boost Pump
P_D, psia	76.6 (528,138 N/m^2)	4547 (3.135 $N/m^2 x10^7$)	3359 (2.316 $N/m^2 x10^7$)	115.7 (797,723 N/m^2)
$\dot{W}$, lb/sec	6.05 (2.74 kg/s)	6.05 (2.74 kg/s)	46.3 (21 kg/s)	36.3 (16.5 kg/s)
Hp	27.5 (20,515 watts)	2276 (1,697,896 watts)	709.4 (529,212 watts)	17.9 (13,353 watts)
Speed, rpm	27,250 (2854 rad/s)	102,100 (10,692 rad/s)	78,270 (8196 rad/s)	7300 (764.5 rad/s)

TABLE 1-10. ALTERNATE NO. 2

P_c, psia	1900 (1.31 $N/m^2 x10^7$)
P_{PB}, psia	2862 (1.97 $N/m^2 x10^7$)
T_{PB}, R	1860 (1033 K)

	Fuel Boost Pump	Fuel Main Pump	Oxidizer Main Pump	Oxidizer Boost Pump
P_D, psia	76.6 (528,138 N/m^2)	4541 (3.13 $N/m^2 x10^7$)	3345 (2.31 $N/m^2 x10^7$)	115.7 (797,723 N/m^2)
$\dot{W}$, lb/sec	6.05 (2.74 kg/s)	6.05 (2.74 kg/s)	36.3 (16.5 kg/s)	36.3 (16.5 kg/s)
Hp	27.5 (20,515 watts)	2260 (1,685,960 watts)	558.6 (416,716 watts)	17.9 (13,353 watts)
Speed, rpm	27,250 (2854 rad/s)	103,100 (10,797 rad/s)	88,560 (9274 rad/s)	7300 (764.5 rad/s)

TABLE 1-11. ALTERNATE NO. 3

P_c, psia	2134 (1.47 $N/m^2 x10^7$)
P_{PB}, psia	3148 (2.17 $N/m^2 x10^7$)
T_{PB}, R	1860 (1033 K)

	Fuel Boost Pump	Fuel Main Pump	Oxidizer Main Pump	Oxidizer Boost Pump
P_D, psia	76.6 (528,138 N/m^2)	4402 (3.035 $N/m^2 x10^7$)	3691 (2.544 $N/m^2 x10^7$)	115.7 (797,723 N/m^2)
$\dot{W}$, lb/sec	6.05 (2.74 kg/s)	6.05 (2.74 kg/s)	46.3 (21 kg/s)	36.3 (16.5 kg/s)
Hp	27.5 (20,515 watts)	1991 (1,485,286 watts)	787.4 (587,400 watts)	17.9 (13,353 watts)
Speed, rpm	27,250 (2854 rad/s)	126,280 (13,224 rad/s)	78,815 (8253 rad/s)	7300 (764.5 rad/s)

TABLE 1-12. ALTERNATE NO. 4

P_c, psia	2170 (1.50 $N/m^2 x10^7$)
P_{PB}, psia	3189 (2.2 $N/m^2 \times 10^7$)
T_{PB}, R	1860 (1033 R)

	Fuel Boost Pump	Fuel Main Pump	Oxidizer Main Pump	Oxidizer Boost Pump
P_D, psia	76.6 (528,138 N/m^2)	4470 (3.08 $N/m^2 x10^7$)	3743 (2.58 $N/m^2 x10^7$)	115.7 (797,723 N/m^2)
$\dot{W}$, lb/sec	6.05 (2.74 kg/s)	6.05 (2.74 kg/s)	36.3 (16.5 kg/s)	36.3 (16.5 kg/s)
Hp	27.5 (20,515 watts)	2103 (1,568,838 watts)	631 (470,726 watts)	17.9 (13,353 watts)
Speed, rpm	27,250 (2854 rad/s)	114,845 (12,027 rad/s)	92,160 (9651 rad/s)	7300 (764.5 rad/s)

TABLE 1-13. ALTERNATE NO. 5

	P_c, psia	1825 (1.26 N/m^2x10^7)		
	P_{PB}, psia	2663 (FPB)/2912 (OPB) (1.84 N/m^2x10^7/2.01 N/m^2x10^7)		
	T_{PB}, R	1860/1860 (1033 K/1033 K)		
	Fuel Boost Pump	Fuel Main Pump	Oxidizer Main Pump	Oxidizer Boost Pump
P_D, psia	76.6 (528,138 N/m^2)	4547 (3.14 N/m^2x10^7)	3127 (2.16 N/m^2x10^7)	115.7 (797,723 N/m^2)
$\dot{W}$, lb/sec	6.05 (2.74 kg/s)	6.05 (2.74 kg/s)	46.3 (21 kg/s)	36.3 (16.5 kg/s)
Hp	27.5 (20,515 watts)	2278 (1,699,388 watts)	657.8 (490,719 watts)	17.9 (13,353 watts)
Speed, rpm	27,250 (2854 rad/s)	101,980 (10,679 rad/s)	74,280 (7779 rad/s)	7300 (764.5 rad/s)

TABLE 1-14. ALTERNATE NO. 6

	P_c, psia	1850 (1.27 N/m^2x10^7)		
	P_{PB}, psia	2699 (FPB)/2952 (OPB) (1.86 N/m^2x10^7/ 2.04 N/m^2x10^7)		
	T_{PB}, R	1860/1860 (1033 K/1033 K)		
	Fuel Boost Pump	Fuel Main Pump	Oxidizer Main Pump	Oxidizer Boost Pump
P_D, psia	76.6 (528,138 N/m^2)	4608 (3.18 N/m^2x10^7)	3170 (2.19 N/m^2x10^7)	115.7 (797,723 N/m^2)
$\dot{W}$, lb/sec	6.05 (2.74 kg/s)	6.05 (2.74 kg/s)	36.3 (16.5 kg/s)	36.3 (16.5 kg/s)
Hp	27.5 (20,515 watts)	2464 (1,828,144 watts)	527.7 (393,664 watts)	17.9 (13,353 watts)
Speed, rpm	27,250 (2854 rad/s)	91,960 (9630 rad/s)	85,060 (8907 rad/s)	7300 (764.5 rad/s)

TABLE 1-15. ALTERNATE NO. 7

P_c, psia	2050 (1.41 N/m^2x10^7)
P_{PB}, psia	2997 (FPB)/3272 (OPB) (2.07 N/m^2x10^7/ 2.26 N/m^2x10^7)
T_{PB}, R	1860/1860 (1033 K/1033 K)

	Fuel Boost Pump	Fuel Main Pump	Oxidizer Main Pump	Oxidizer Boost Pump
P_D, psia	76.6 (528,138 N/m^2)	4469 (3.08 N/m^2x10^7)	3513 (2.42 N/m^2x10^7)	115.7 (797,723 N/m^2)
$\dot{W}$, lb/sec	6.05 (2.74 kg/s)	6.05 (2.74 kg/s)	46.3 (21 kg/s)	36.3 (16.5 kg/s)
Hp	27.5 (20,515 watts)	2100 (1,566,600 watts)	744 (555,024 watts)	17.9 (13,353 watts)
Speed, rpm	27,250 (2854 rad/s)	115,100 (12,053 rad/s)	81,580 (8543 rad/s)	7300 (764.5 rad/s)

TABLE 1-16. ALTERNATE NO. 8

P_c, psia	2075 (1.43 N/m^2x10^7)
P_{PB}, psia	2038 (FPB)/3311 (OPB) (2.09 N/m^2x10^7/ 2.28 N/m^2x10^7)
T_{PB}, R	1860/1860 (1033 K/1033 K)

	Fuel Boost Pump	Fuel Main Pump	Oxidizer Main Pump	Oxidizer Boost Pump
P_D, psia	76.6 (528,138 N/m^2)	4530 (3.12 N/m^2x10^7)	3556 (2.45 N/m^2x10^7)	115.7 (797,723 N/m^2)
$\dot{W}$, lb/sec	6.05 (2.74 kg/s)	6.05 (2.74 kg/s)	36.3 (16.5 kg/s)	36.3 (16.5 kg/s)
Hp	27.5 (20,515 watts)	2235 (1,667,310 watts)	596 (444,616 watts)	17.9 (13,353 watts)
Speed, rpm	27,250 (2854 rad/s)	104,690 (10,963 rad/s)	92,280 (9664 rad/s)	7300 (764.5 rad/s)

TABLE 1-17 PERFORMANCE SUMMARY

(ε = 400, 90% Thrust Chamber Length; Includes Dynamic Seal Leakage)

Alternative P_c, psia	Engine Length, inches	Specific Impulse, seconds
1 - 1875 (1.29 $N/m^2 x10^7$)	100.1 (2.54 m)	475.1 (4659 newton-s/kg)
2 - 1900 (1.31 $N/m^2 x10^7$)	99.5 (2.53 m)	474.8 (4656 newton-s/kg)
3 - 2135 (1.47 $N/m^2 x10^7$)	94.8 (2.407 m)	475.3 (4661 newton-s/kg)
4 - 2170 (1.50 $N/m^2 x10^7$)	94.0 (2.39 m)	475.0 (4658 newton-s/kg)
5 - 1825 (1.26 $N/m^2 x10^7$)	101.3 (2.573 m)	475.0 (4658 newton-s/kg)
6 - 1850 (1.28 $N/m^2 x10^7$)	100.6 (2.56 m)	474.7 (4655 newton-s/kg)
7 - 2050 (1.41 $N/m^2 x10^7$)	96.4 (2.45 m)	475.3 (4661 newton-s/kg)
8 - 2075 (1.43 $N/m^2 x10^7$)	95.9 (2.44 m)	474.9 (4657 newton-s/kg)

TABLE 1-18 PERFORMANCE SUMMARY

(Engine Length = 208 cm (82 inches), 70% Thrust Chamber Length, No Limit on ε; Includes Dynamic Seal Leakage)

Alternative P_c, psia	Area Ratio	Specific Impulse, seconds
1 - 1875 (1.29 $N/m^2 x10^7$)	409.5	472.8 (4637 newton-s/kg)
2 - 1900 (1.31 $N/m^2 x10^7$)	414.7	472.7 (4636 newton-s/kg)
3 - 2135 (1.47 $N/m^2 x10^7$)	463.5	474.1 (4649 newton-s/kg)
4 - 2170 (1.50 $N/m^2 x10^7$)	470.7	473.8 (4646 newton-s/kg)
5 - 1825 (1.26 $N/m^2 x10^7$)	399.1	472.5 (4634 newton-s/kg)
6 - 1850 (1.276 $N/m^2 x10^7$)	404.3	472.3 (4632 newton-s/kg)
7 - 2050 (1.41 $N/m^2 x10^7$)	445.8	473.8 (4646 newton-s/kg)
8 - 2075 (1.43 $N/m^2 x10^7$)	451.0	473.4 (4642 newton-s/kg)

seal propellant losses than corresponding GH_2 turbine drive configurations. From these analyses, the four most desirable configurations from a performance and engine length standpoint were selected and are presented in Table 1-19.

Start Transient and NPSH

As specified by the Statement of Work, the impact of normal start, pressurized idle start, and tank-head idle-mode start operations were assessed. The specific conditions are presented in Table 1-20. A typical start sequence is shown in Fig. 1-28. The start characteristics of those configurations incorporating the GH_2 turbine boost pump drive were all considered satisfactory (Fig. 1-29 and 1-30). However, the hydraulically driven boost pump lagged the main LO_2 pump startup and, thus would not provide any benefit to engine conditioning during start (Fig. 1-31). Analysis of the engine start conditions indicate that the oxidizer flowrate through the engine was doubled by having the benefit of the LO_2 boost pump operation, as presented in Table 1-21. This factor, in conjunction with the uncertainty of heat transfer effects during hydraulic turbine priming and the potential for faster start with the use of GH_2 turbine drive by raising idle-mode power level, resulted in the selection of the GH_2 turbine for the LO_2 boost pump drive as the most desirable based on engine start considerations.

An analysis was conducted to determine the impact of NPSH requirements on the engine. The specific result was a variation in boost pump size and rotative speed, as summarized in Table 1-22. These results are for mainstage operation. Because of the low flow requirements during start, it was determined that moderate mainstage requirements of 2 feet LO_2 and 15 feet LH_2 (baselined for study) could be met and still provide 0/0 NPSH capability during start. This approach appeared to be the most practical and, therefore, was recommended.

Flexibility and Complexity

As is apparent, flexibility can be considered synonymous with increased complexity and, therefore, there is an inherent tradeoff between these two factors. Those aspects considered as providing greater flexibility are presented in Table 1-23. The design features considered in terms of complexity are presented in Table 1-24. These features were traded off and the results grouped by engine configuration as to least complex to most complex, as presented in Table 1-25.

Weight and Cost

Weight and parametric cost analyses were conducted for the alternative configurations and the results are summarized in Tables 1-26 and 1-27. Also included is the weight impact of the mainstage NPSH requirements as affecting boost pump weight (Table 1-28). The weights presented by subsystems as well as total engine weight were subsequently modified during the engine design phase. However, the relative characteristics remained essentially the same.

TABLE 1-19. CYCLE BALANCE AND PERFORMANCE SUMMARY

Alternatives preferred for performance maximization or length minimization are:

Alternative P_c, psia	Preburners	Thrust Chamber Cooling	Boost Pump Drive
3 - 2135 (1.47 $N/m^2 x10^7$)	1	Split	H_2/GH_2
4 - 2170 (1.50 $N/m^2 x10^7$)	1	Split	GH_2/GH_2
7 - 2050 (1.41 $N/m^2 x10^7$)	2	Split	H_2/GH_2
8 - 2075 (1.43 $N/m^2 x10^7$)	2	Split	GH_2/GH_2

TABLE 1-20. START CONDITIONS

- Normal Start
  - Propellants Settled
  - Engine Thermally Conditioned
  - NPSH's of 2/15 and 16/60 (5.97/44.8 and 47.8/179.3 joules/kg)
- Pressurized Idle
  - Propellants Supplied at Required NPSH
  - Idle Mode Used to Settle Tank Propellants
  - NPSH of 2/15 (5.97/44.8 joules/kg) for Start and Operation
- Tank-Head Idle
  - Propellants Supplied at Saturated Conditions
  - Idle Mode to Settle Propellants and Condition Engine
  - Pump Operation at 0/0 NPSH Provides Autogenous Pressurization of Main Tanks

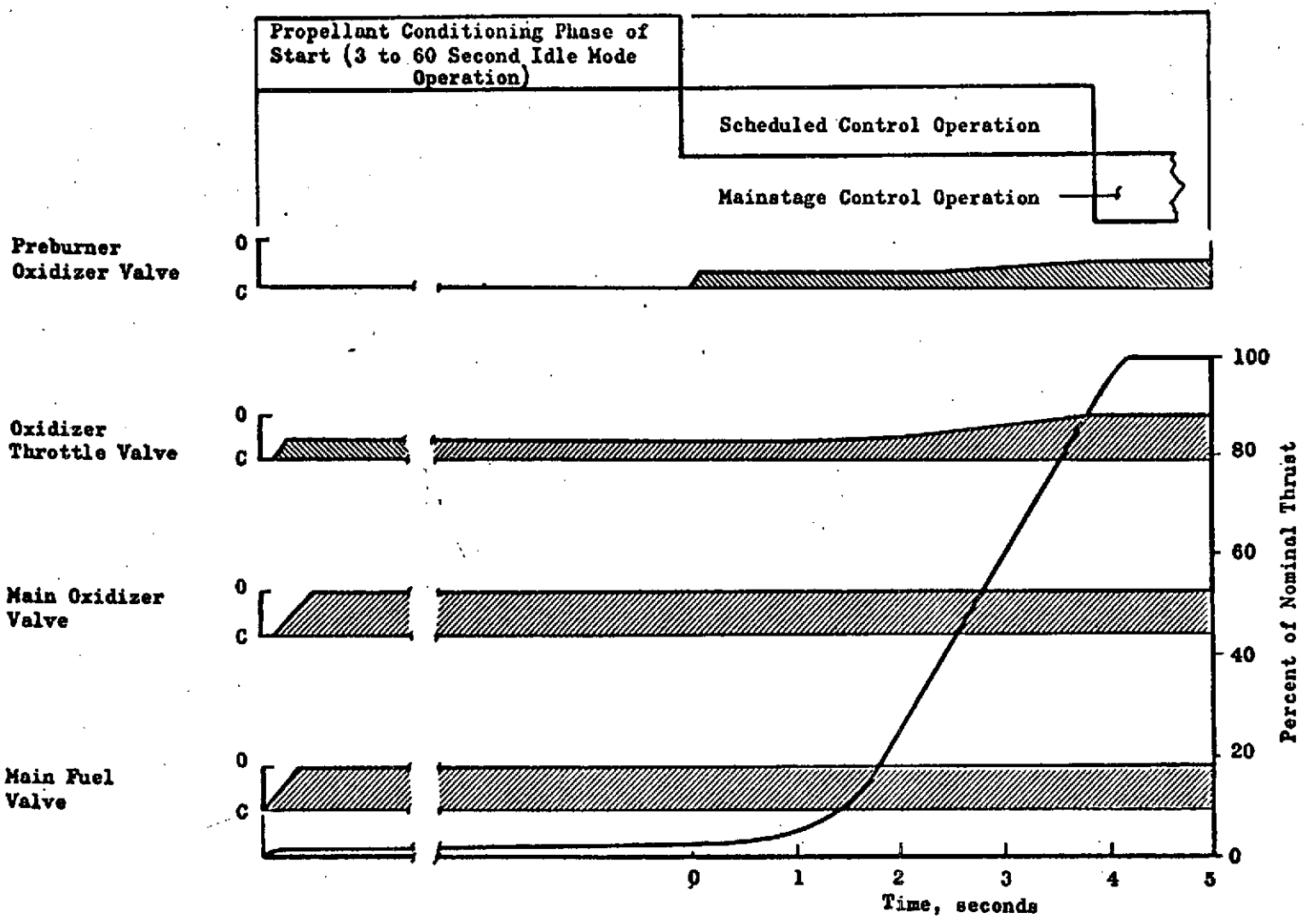

Figure 1-28. Start Transient Sequence Single Preburner (Nonthrottling)

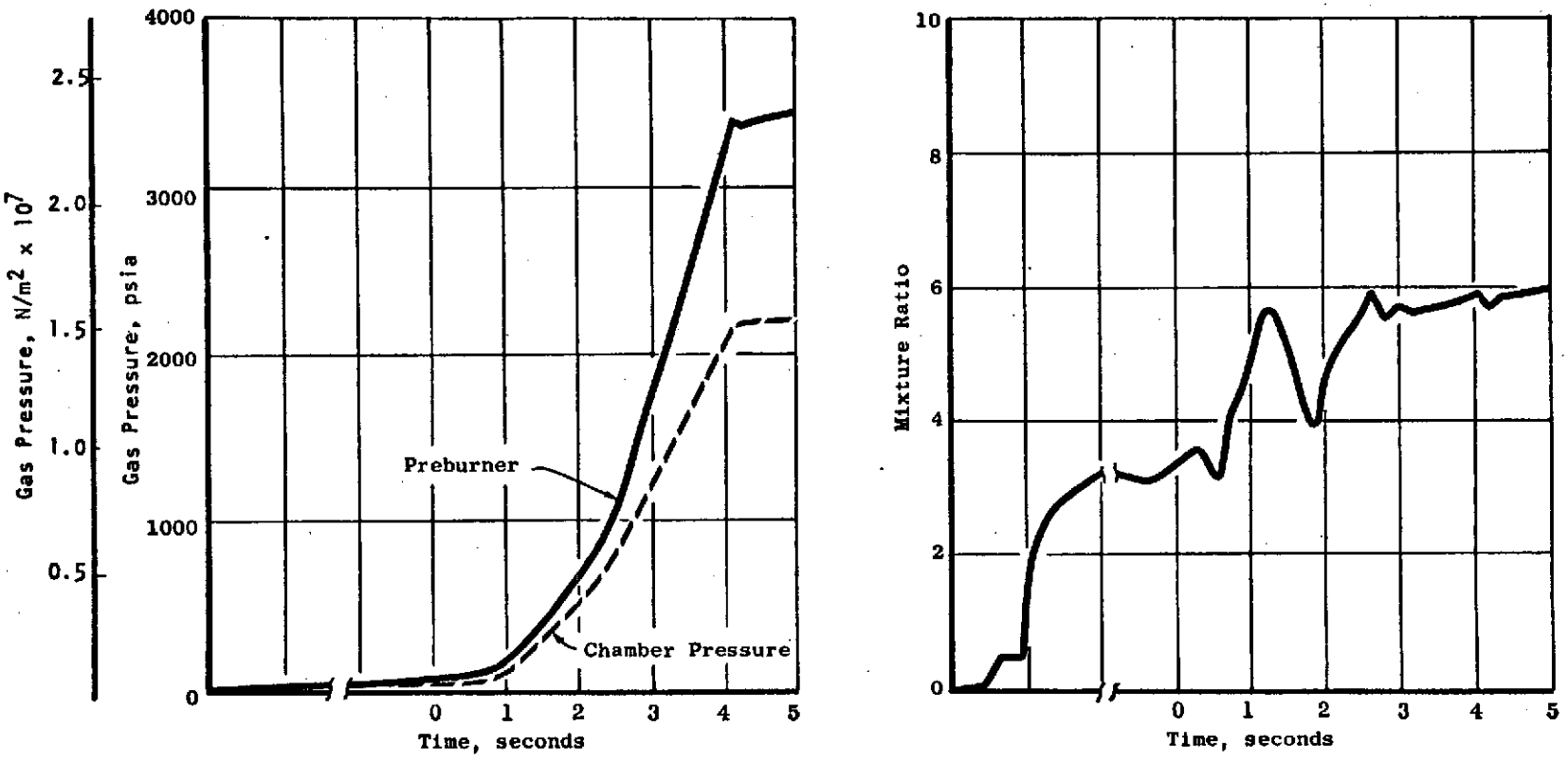

Figure 1-29. Engine Start Characteristics (Dual Preburners, GH_2 Boost Pump Drive, Nonthrottling)

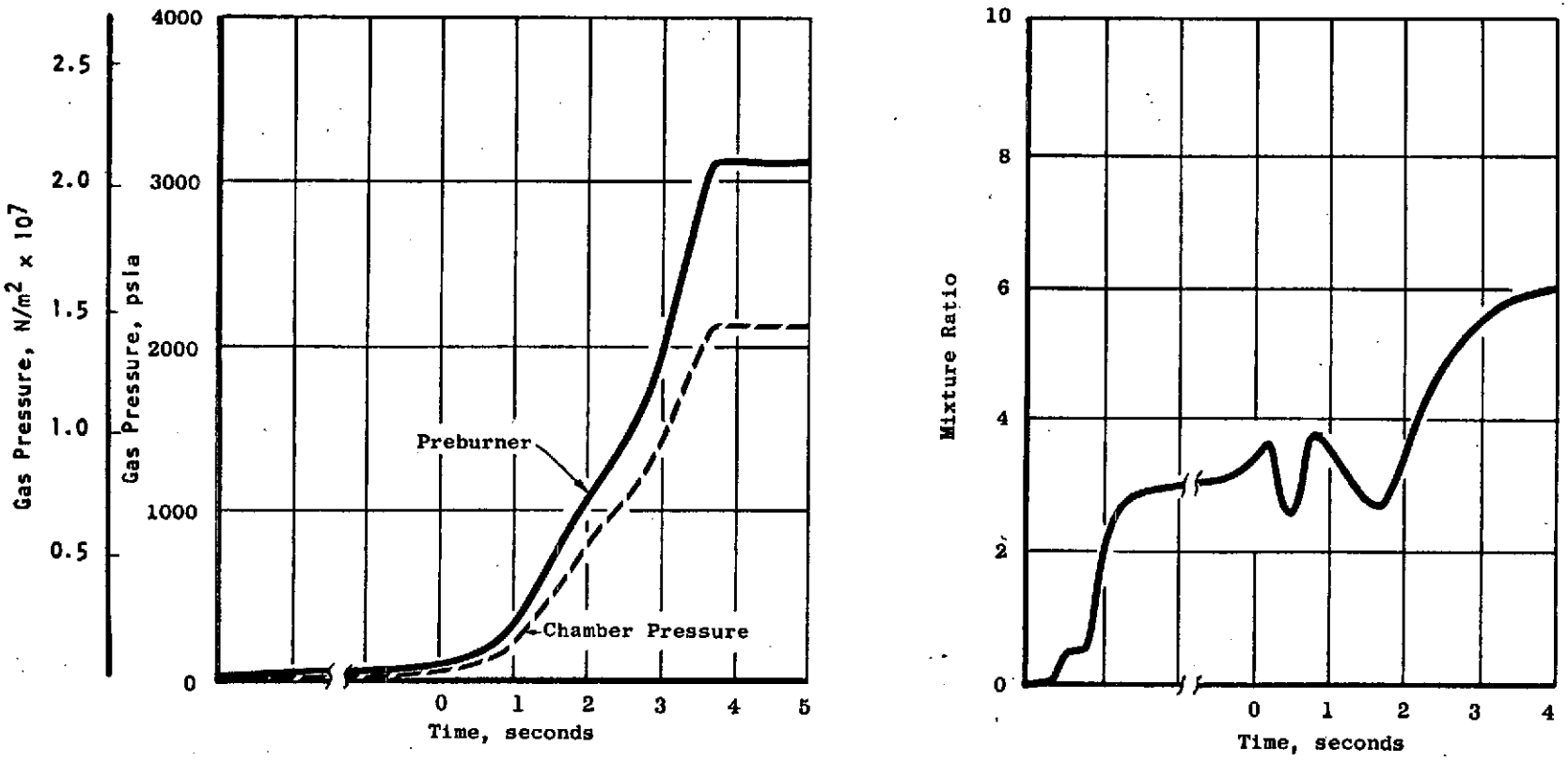

Figure 1-30. Engine Start Characteristics (Single Preburner, GH_2 Boost Pump Drive, Nonthrottling)

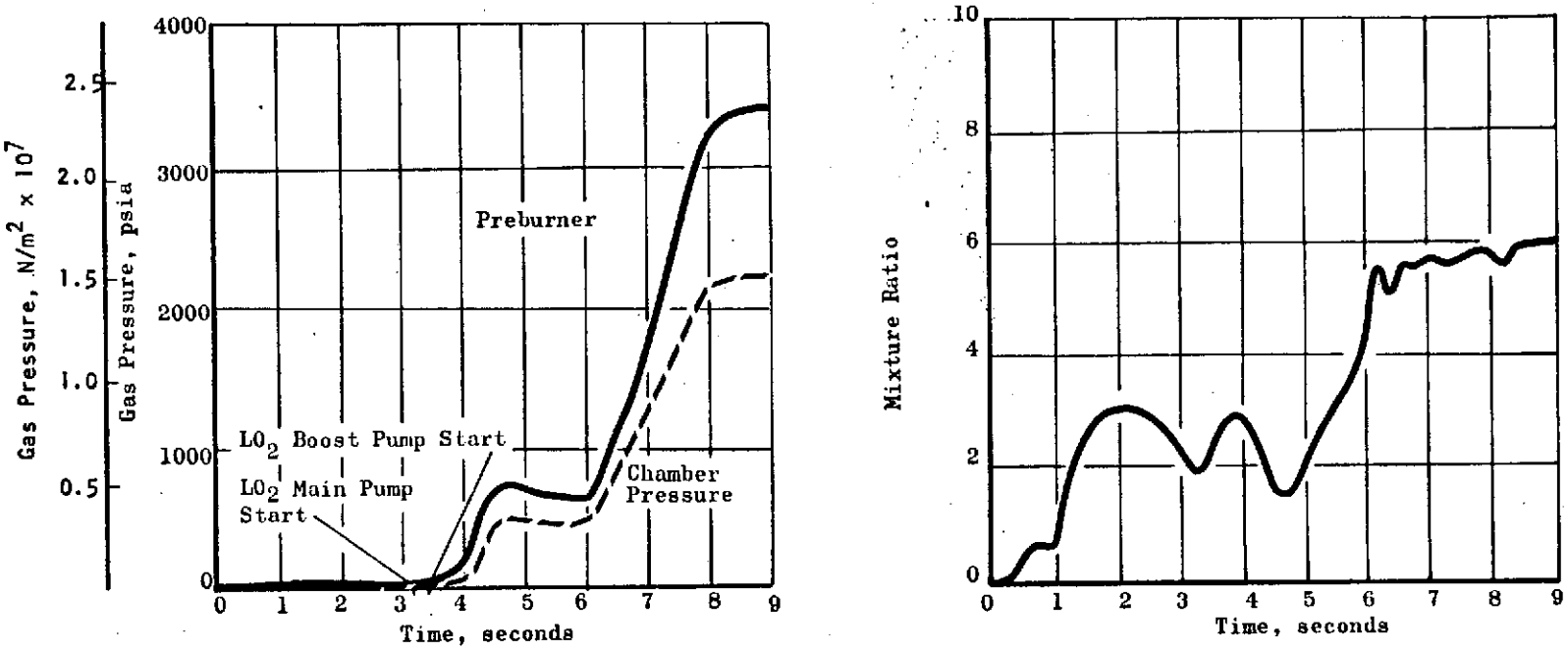

Figure 1-31. Engine Start Characteristics (Hydraulic LO_2 Boost Pump Drive; Engine Thermally Conditioned)

TABLE 1-21. INFLUENCE OF BOOST PUMP OPERATION OF LO_2 FLOW DURING IDLE MODE

	Horsepower	Developed Pressure	Weight Flow	Estimated Chilldown Time (from 430 R, 239 K)
With Boost Pump	0.2 (149.2 watts)	5 psi (34,474 N/m^2)	0.8 lb/sec (0.363 kg/s)	~ 12 seconds
Without Boost Pump	-	-	0.4 lb/sec (0.181 kg/s)	~ 24 seconds

TABLE 1-22. BOOST PUMP CONFIGURATIONS FOR SPECIFIED MAINSTAGE NPSH VALUES

(Assumed inlet line lengths of 5 feet (1.524 m) LO_2 and 16.6 feet (5.08 m) LH_2)

Type	NPSH (joules/kg)	P_1, psia (N/m^2)	P_2, psia (N/m^2)	$\dot{W}$, lb/sec (kg/s)	N, rpm	Tip Diameter, inches (cm)	Eye Diameter, inches (cm)	Hub Diameter inches (cm)
O_2	16 (47.8)	15.7 (108,248)	115.7 (797,723)	36.32 (16.48)	14,566	2.128 (5.4)	2.128 (5.4)	0.638 (1.62)
	2 (5.97)				7,300	3.595 (9.13)	3.585 (6.57)	1.076 (2.73)
	0				2,068	12.641 (32.1)	6.031 (15.3)	1.809 (4.59)
H_2	60 (179.3)	16.6 (114,453)	76.6 (528,138)	6.053 (2.747)	87,663	2.112 (5.36)	2.112 (5.36)	0.634 (1.61)
	15 (44.8)				27,250	3.217 (8.17)	3.217 (8.17)	0.965 (2.45)
	0				27,250	3.217 (8.17)	3.217 (8.17)	0.965 (2.45)

0 NPSH LO_2 is centrifugal - all others are inducers

0 NPSH LO_2 needs a 6-inch line

2 NPSH LO_2 is suitable for 0 NPSH idle-mode start (tanks pressurized during idle mode)

TABLE 1-23. FLEXIBILITY

- GH_2 Turbine Drive for Boost Pumps
  - Power Required
  - Packaging
- Duel Preburners
  - Start
  - System Development
  - System Modification (MR Range, Throttling, etc.)
- Split Flow Thrust Chamber Cooling
  - Coolant Flow Distribution
    - Performance
    - Life

TABLE 1-24. COMPLEXITY CONSIDERATIONS

• Thrust Chamber Assembly	- 1-1/2 pass vs split flow thrust chamber manifold requirements
• Preburners	- single vs dual
• Boost Pump Drive	- turbine configuration, propellant separation requirements
• Main Turbopumps	- speed, developed head
• Ducting	- quality of hot gas or propellant ducting
• Valves and Controls	- number of primary valves
• Ignition System	- number of igniter units

TABLE 1-25. NONTHROTTLING ENGINE COMPLEXITY SUMMARY

Configuration	Areas of Complexity
• Least Complex	
• Alternate 1 - Single Preburner, 1-1/2 Pass Thrust Chamber, Hydraulic LO_2 Boost Pump Drive	Main LO_2 turbopump, hot-gas manifold
• Next Least Complex	
• Alternate 2 - Single Preburner, 1-1/2 Pass Thrust Chamber, GH_2/LO_2 Boost Pump Drive	Main LO_2 turbopump, hot-gas manifold, propellant ducts
• Alternate 5 - Dual Preburner, 1-1/2 Pass Thrust Chamber, Hydraulic LO_2 Boost Pump Drive	Preburners, primary valves, propellant ducts, ignition system
• Moderately Complex	
• Alternate 3 - Single Preburner, Split Flow Thrust Chamber, Hydraulic LO_2 Boost Pump Drive	Main LO_2 and LH_2 turbopumps, TCA, hot-gas manifold
• Alternate 6 - Dual Preburner, 1-1/2 Pass Thrust Chamber, GH_2 Boost Pump Drive	Preburners, main LO_2 turbopumps, primary valves, propellant ducts, ignition system
• Most Complex	
• Alternate 4 - Single Preburner, Split Flow Thrust Chamber, GH_2 Boost Pump Drive	Main LO_2 and LH_2 turbopumps, TCA, hot-gas manifold, propellant ducts
• Alternate 7 - Dual Preburner, Split Flow Thrust Chamber, Hydraulic LO_2 Boost	Main LO_2 and LH_2 turbopumps, preburners, TCA, primary valves, propellant ducts, ignition system
• Alternate 8 - Dual Preburner, Split Flow Thrust Chamber GH_2 Boost Pump Drive	Main LO_2 turbopump, preburners, TCA, primary valves, propellant ducts, ignition system

TABLE 1-26. NONTHROTTLING ENGINE WEIGHT* TRADEOFF

Alternate Engine Configuration	TCA	Preburner	Turbopump	Hot-Gas** Manifold	Control Valves	Propellant Ducts	Ignition System	Controls-Pneumatic, Electric	Gimbal	Total*** Engine
1	133.4 (60.5)	10.1 (4.58)	65.4 (29.7)	17.5 (7.94)	35.1 (15.9)	5.1 (2.31)	7.8 (3.54)	19.5 (8.85)	1.9 (0.862)	325.4 (147.6)
2	131.4 (59.6)	10.0 (4.54)	65.4 (29.7)	17.6 (7.98)	35.1 (15.9)	5.1 (2.31)	7.8 (3.54)	19.5 (8.85)	1.9 (0.862)	323.2 (146.6)
3	133.7 (60.6)	10.1 (4.58)	65.3 (29.6)	18.6 (8.44)	35.1 (15.9)	5.4 (2.45)	7.8 (3.54)	19.2 (8.71)	1.9 (0.862)	326.8 (148.2)
4	132.0 (59.9)	10.1 (4.58)	65.8 (29.8)	18.8 (8.53)	35.1 (15.9)	5.5 (2.49)	7.8 (3.54)	19.1 (8.66)	1.9 (0.862)	325.7 (147.7)
5	136.5 (61.9)	12.7 (5.76)	65.0 (29.5)	15.9 (7.21)	38.9 (17.6)	5.0 (2.27)	9.0 (4.08)	19.6 (8.89)	1.9 (0.862)	334.8 (151.9)
6	134.9 (61.2)	12.8 (5.81)	65.3 (29.6)	16.0 (7.26)	38.9 (17.6)	5.0 (2.27)	9.0 (4.08)	19.5 (8.85)	1.9 (0.862)	333.6 (151.3)
7	138.1 (62.6)	12.9 (5.85)	64.0 (29.03)	16.9 (7.67)	38.9 (17.6)	5.3 (2.40)	9.0 (4.08)	19.3 (8.75)	1.9 (0.862)	336.9 (152.8)
8	136.7 (62.0)	12.9 (5.85)	65.7 (29.8)	17.0 (7.71)	38.9 (17.6)	5.3 (2.40)	9.0 (4.08)	19.2 (8.71)	1.9 (0.862)	337.3 (153.0

* All units in pounds (kilograms)
** Includes hot-gas ducting
*** 10-percent contingency

TABLE 1-27. NONTHROTTLING ENGINE PARAMETRIC COST ANALYSIS

Engine Configuration	DDT&E Cost, millions	Production Cost (First Unit), thousands
1	114.3	787.5
2	112.9	772.6
3	114.2	785.2
4	112.8	771.2
5	117.1	833.9
6	115.8	820.2
7	117.2	834.6
8	115.8	820.6

TABLE 1-28. SIZE IMPACT OF NPSH REQUIREMENTS

	NPSH		
Boost Pump	0/0	2/15 (5.97/44.8 joules/kg)	16/60 (47.8/179.3 joules/kg)
Fuel			
Weight, pounds	8.6 (3.9 kg)	8.6 (3.9 kg)	7.5 (3.4 kg)
Diameter, inches	3.2 (8.128 cm)	3.2 (8.128 cm)	2.1 (5.33 cm)
Oxidizer			
Weight, pounds	55.1 (25 kg)	13.4 (6.08 kg)	8.0 (3.62 kg)
Diameter, inches	12.6 (32 cm)	3.6 (8.128 cm)	2.1 (5.33 cm

Nonthrottling Engine Configuration Selection

The preceding tradeoffs were assessed and summarized for an overall evaluation for selection of the baseline configuration. The summary is presented in Table 1-29. As shown, those factors not lending themselves to quantitative definition were listed in order of preference (A, B, C, etc.) for qualitative evaluation. Also, the significance of chamber pressure, though not apparent from the table, was that high chamber pressure means a shorter engine as well as the implications of high specific impulse and low engine weight already reflected in the table. The shorter length is significant in terms of the limited space available in the space shuttle cargo bay. In summary, the recommended configuration and operating conditions are presented in Table 1-30.

TABLE 1-29. NONTHROTTLING ENGINE RECOMMENDATIONS

- Alternative Configuration No. 4 is Recommended (split flow thrust chamber, single preburner, GH_2 boost pump drive)
- Boost Pumps Sized for 2/15 NPSH (5.97/44.8 joules/kg) With Idle-Mode Start at 0/0 NPSH and Autogenous Tank Pressurization Should be Pursued
- Tank-Head Idle-Mode Start is Recommended

IMPACT OF THROTTLING

Following selection of the baseline configuration, analyses were conducted to determine the impact of throttling with regard to the same factors assessed during the prior engine tradeoff. The effort was initiated with selection of the additional components required to incorporate throttling. The modifications to the single preburner configurations include addition of a main fuel valve and a fuel preburner modulating bypass valve and incorporation of a throttling preburner injector (heat exchange, pintle-type, or dual manifold). The dual-preburner configuration would require addition of a main oxidizer valve and a preburner oxidizer modulating valve. Incorporating of throttling preburner injectors would also be required. Modification of the main injector is not required because it was decided for the baseline design that, in lieu of enduring the complexity of adding a "boost stage" to the main oxidizer pump for providing the preburner oxidizer flow, a single-stage main oxidizer pump would be utilized and, therefore, take a significant pressure drop across the main injector. The loss of cycle efficiency is minimal in comparison to the possible mechanical complexities.

To assess the impact on cycle balance and performance, the three most desirable engine configurations (3, 4, and 8) were studied. The engine operating characteristics, schematics, and performance are shown in Fig. 1-32 through 1-34 and Tables 1-31 through 1-34, respectively.

Start transient analysis was conducted on the alternative configurations. The addition of the throttling controls enhanced engine start capabilities and, therefore, analysis provided no major basis for selection of one configuration over the others. A typical start sequence is presented in Fig. 1-35 and transient characteristics are shown in Fig. 1-36 and 1-37.

TABLE 1-30. ENGINE CONFIGURATION TRADEOFF MATRIX SUMMARY
(Nonthrottling Engines)

Alternate Engine Configuration	Cycle Balance, Chamber Pressure, psi ($N/m^2 x 10^7$)	Performance,* Specific Impulse, seconds (N-s/kg)	Start Transient Characteristics**	Flexibility**	Complexity**	Weight, pounds*	Engine DDT&E and Production Cost
1	1875 (1.29)	475.1 (4659)	B	D	A	325.4 (147.6 kg)	114.3 M 787.5 K
2	1900 (1.31)	474.8 (4656)	A	C	B	323.2 (146.6 kg)	112.9 M 772.6 K
3	2135 (1.47)	475.3 (4661)	B	C	C	326.8 (148.2 kg)	114.2 M 785.2 K
4	2170 (1.5)	475.0 (4658)	A	B	D	325.7 (147.7 kg)	112.8 M 771.2 K
5	1825 (1.26)	475.0 (4658)	B	C	B	334.8 (151.9 kg)	117.1 M 833.9 K
6	1850 (1.28)	474.7 (4655)	A	B	C	333.6 (151.3 kg)	115.8 M 820.2 K
7	2050 (1.41)	475.3 (4661)	B	B	D	336.9 (152.8 kg)	117.2 M 834.6 K
8	2075 (1.43)	474.9 (4657)	A	A	D	337.3 (153 kg)	115.8 M 820.6 K

*Predictated on 400:1 area ratio nozzle and no length limit
**Letter designation indicates order of perference

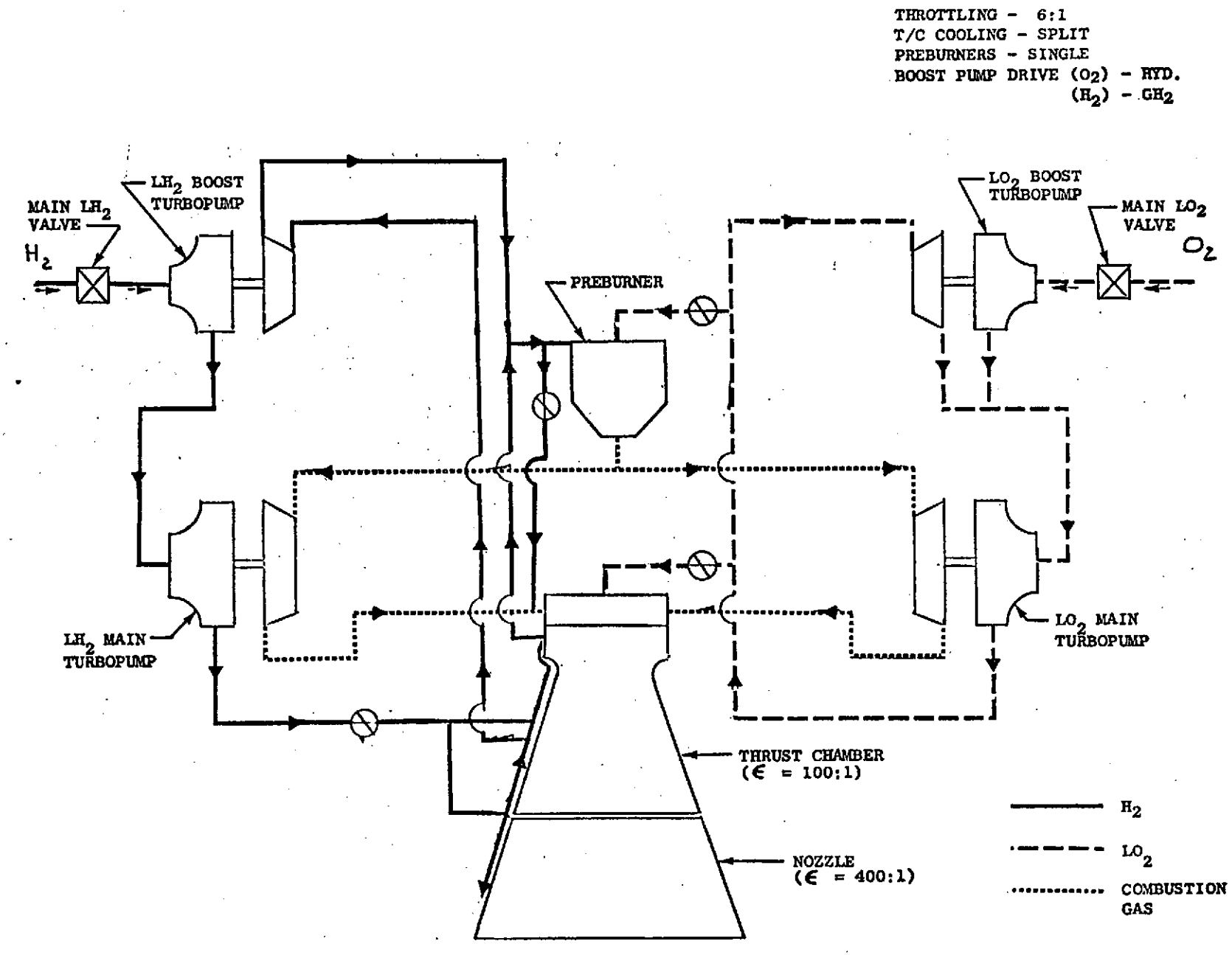

Figure 1-32. Alternate No.3T

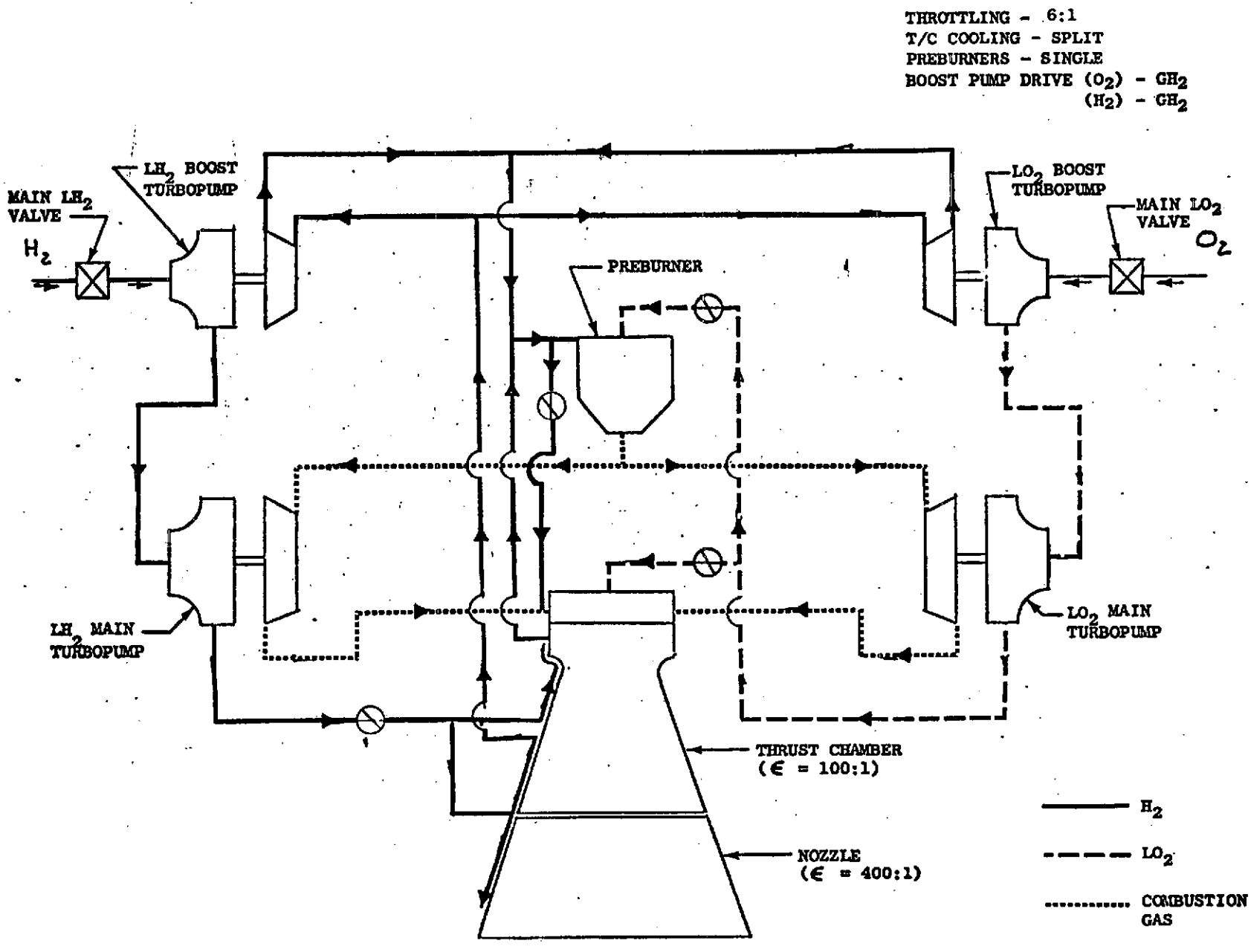

Figure 1-33. Alternate No.4T

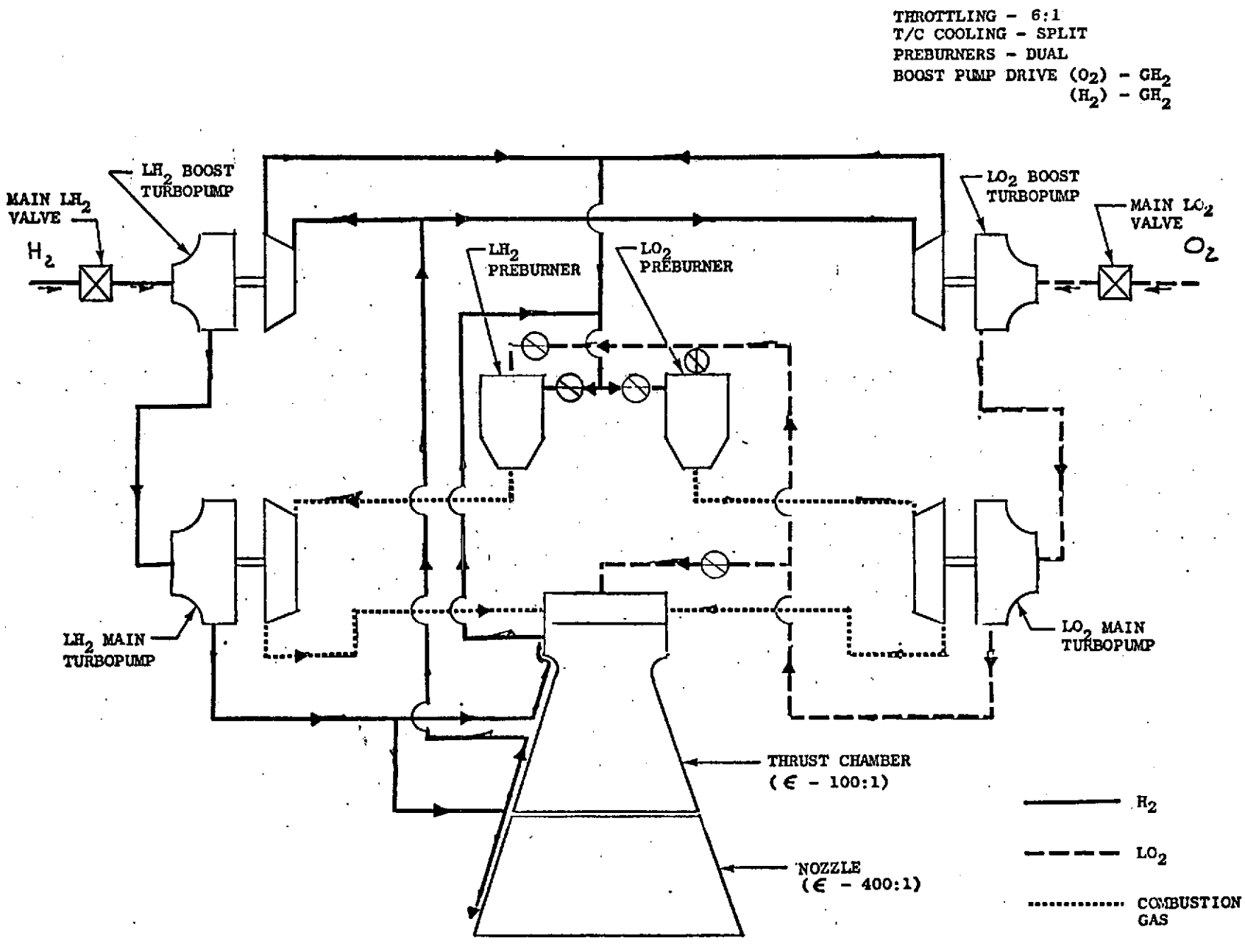

Figure 1-34. Alternate No.8T

TABLE 1-31. ALTERNATE NO. 3T

P_c, psia	1825 (1.26 N/m^2x10^7)
P_{PB}, psia	2766 (1.91 N/m^2x10^7)
T_{PB}, R	1860 (1033 K)

	Fuel Boost Pump	Fuel Main Pump	Oxidizer Main Pump	Oxidizer Boost Pump
P_D, psia	76.6 (528,138 N/m^2)	4493 (3.10 N/m^2x10^7)	3809 (2.63 N/m^2x10^7)	115.7 (797,723 N/m^2)
$\dot{W}$, lb/sec	6.05 (2.74 kg/s)	6.05 (2.74 kg/s)	46.3 (21 kg/s)	36.3 (16.5 kg/s)
Hp	27.5 (20,515 watts)	2149 (1,603,154 watts)	809.5 (603,887 watts)	17.9 (13,353 watts)
Speed, rpm	27,250 (2854 rad/s)	110,990 (11,623 rad/s)	86,220 (9029 rad/s)	7300 (764.5 rad/s)

TABLE 1-32. ALTERNATE NO. 4T

P_c, psia	1850 (1.28 N/m^2x10^7)
P_{PB}, psia	2755 (1.9 N/m^2x10^7)
T_{PB}, R	1860 (1033 K)

	Fuel Boost Pump	Fuel Main Pump	Oxidizer Main Pump	Oxidizer Boost Pump
P_D, psia	76.6 (528,138 N/m^2)	4490 (3.10 N/m^2x10^7)	3798 (2.62 N/m^2x10^7)	115.7 (797,723 N/m^2)
$\dot{W}$, lb/sec	6.05 (2.74 kg/s)	6.05 (2.74 kg/s)	36.3 (16.5 kg/s)	36.3 (16.5 kg/s)
Hp	27.5 (20,515 watts)	2141 (1,597,186 watts)	646.4 (482,214 watts)	17.9 (13,353 watts)
Speed, rpm	27,250 (2854 rad/s)	111,580 (11,685 rad/s)	83,700 (8765 rad/s)	7300 (764.5 rad/s)

TABLE 1-33. ALTERNATE NO. 8T

	P_c, psia	1950 (1.34 N/m^2x10^7)		
	P_{PB}, psia	3062 (FPB)/2725 (OPB) (2.11 N/m^2x10^7/ 1.87 N/m^2x10^7)		
	T_{PB}, R	1860 (1033 K)		
	Fuel Boost Pump	Fuel Main Pump	Oxidizer Main Pump	Oxidizer Boost Pump
P_D, psia	76.6 (528,138 N/m^2)	4564 (3.15 N/m^2x10^7)	3824 (2.64 N/m^2x10^7)	115.7 (797,723 N/m^2)
$\dot{W}$, lb/sec	6.05 (2.74 kg/s)	6.05 (2.74 kg/s)	36.3 (16.5 kg/s)	36.3 (16.5 kg/s)
Hp	27.5 (20,515 watts)	2325 (173,445 watts)	642.8 (479,529 watts)	17.9 (13,353 watts)
Speed, rpm	27,250 (2854 rad/s)	99,140 (10,382 rad/s)	98,250 (10,289 rad/s)	7300 (764.5 rad/s)

TABLE 1-34. PERFORMANCE SUMMARY (Throttling Engine Configurations)

Fixed Area Ratio (ε = 400:1)		
Configuration (P_c), psia (N/m^2x10^7)	Engine Length, inches (m)	Specific Impulse, seconds (N-s/kg)
3T-1825 (1.26)	101.3 (2.57)	475.0 (4658)
4T-1850 (1.28)	100.6 (2.56)	474.7 (4655)
8T-1950 (1.34)	98.4 (2.50)	474.9 (4657)
Fixed Engine Length (L_E = 82 inches; 2.08 m)		
Configuration (P_c), psia (N/m^2x10^7)	Area Ratio	Specific Impulse, seconds (N-s/kg)
3T-1825 (1.26)	399.1	472.5 (4634)
4T-1850 (1.28)	404.3	472.3 (4632)
8T-1950 (1.34)	425.0	472.9 (4638)

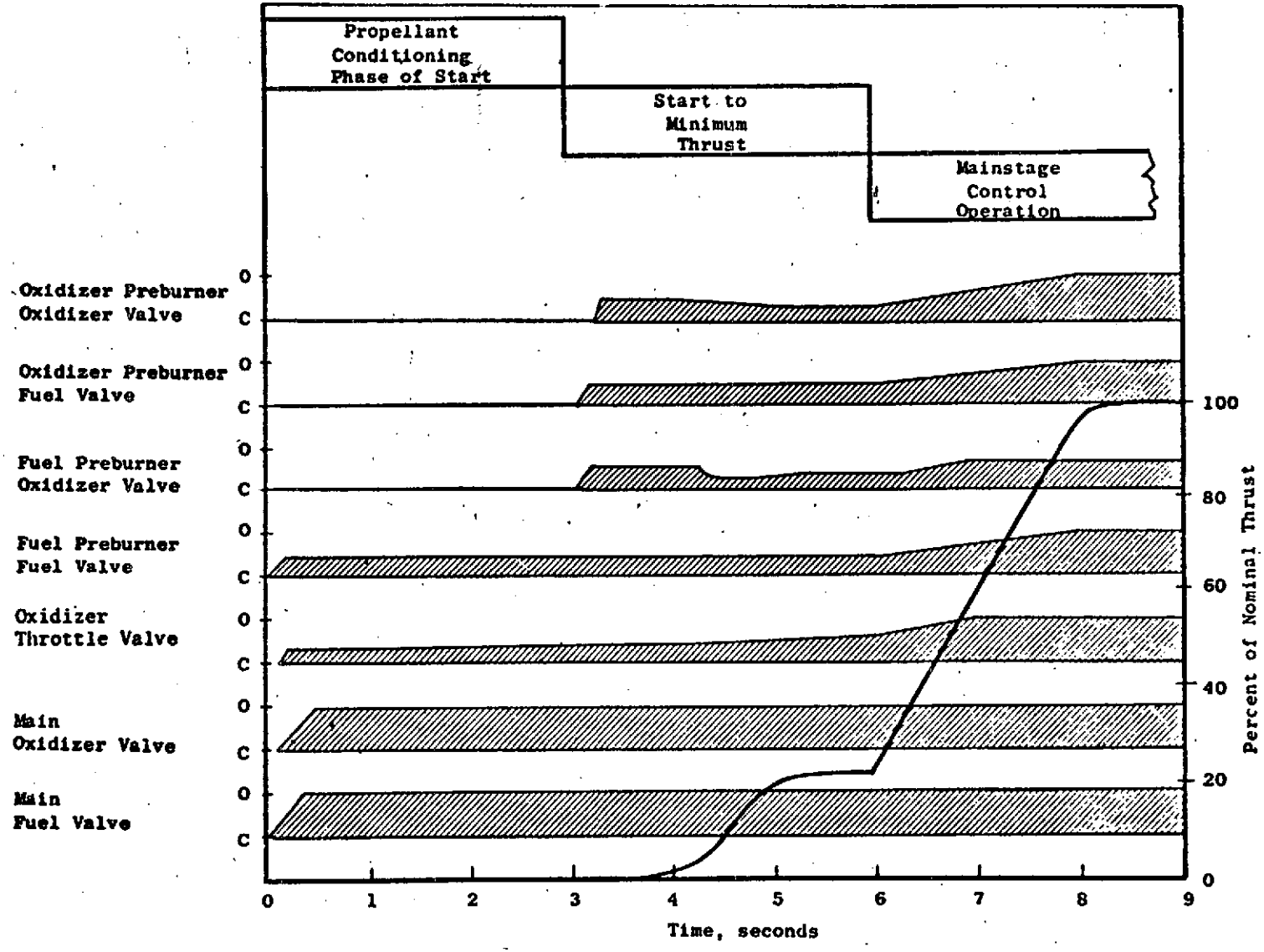

Figure 1-35. Start Transient Sequence

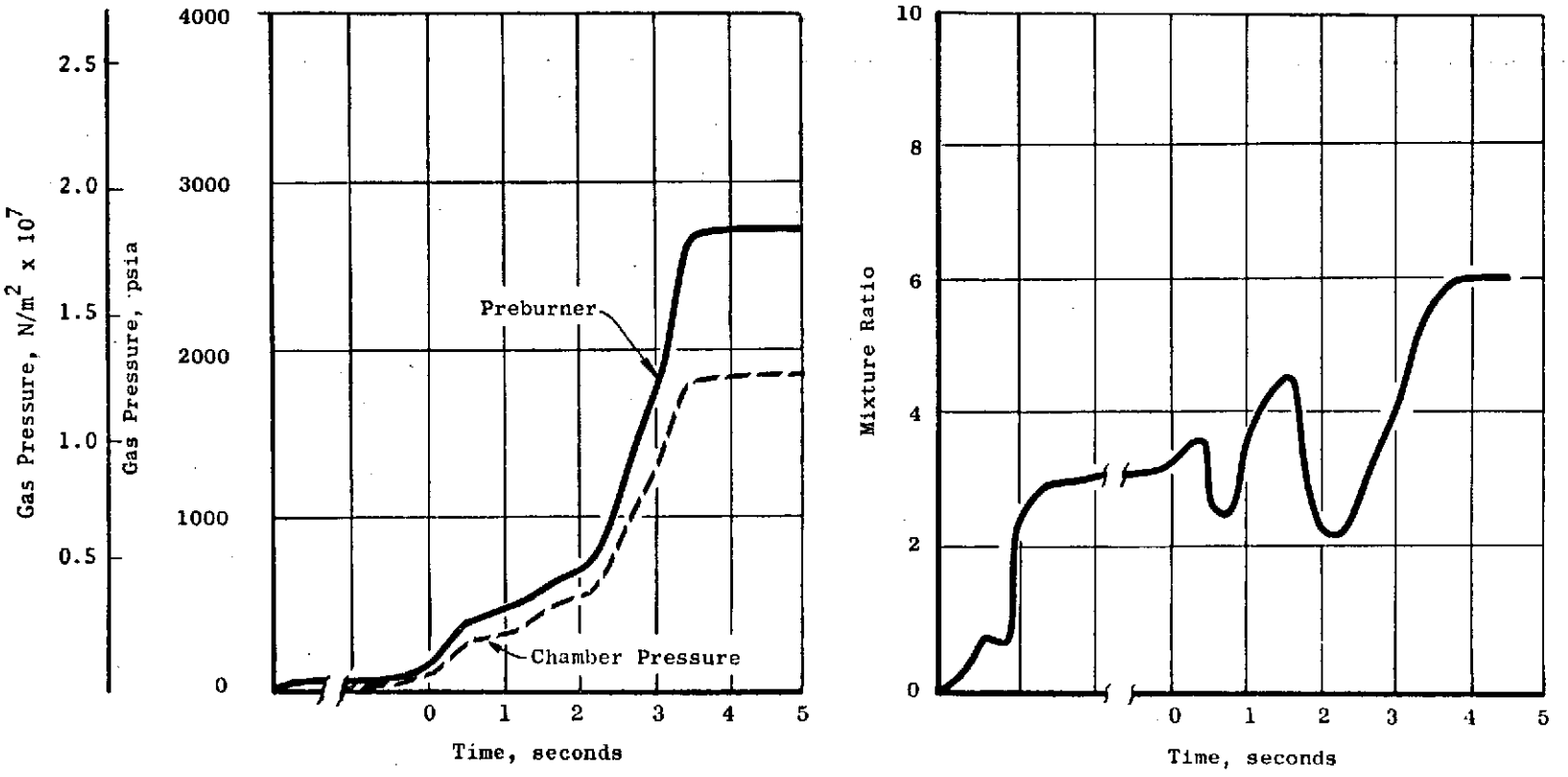

Figure 1-36. Engine Start Characteristics (Single Preburner, GH_2 Boost Pump Drive, Throttling)

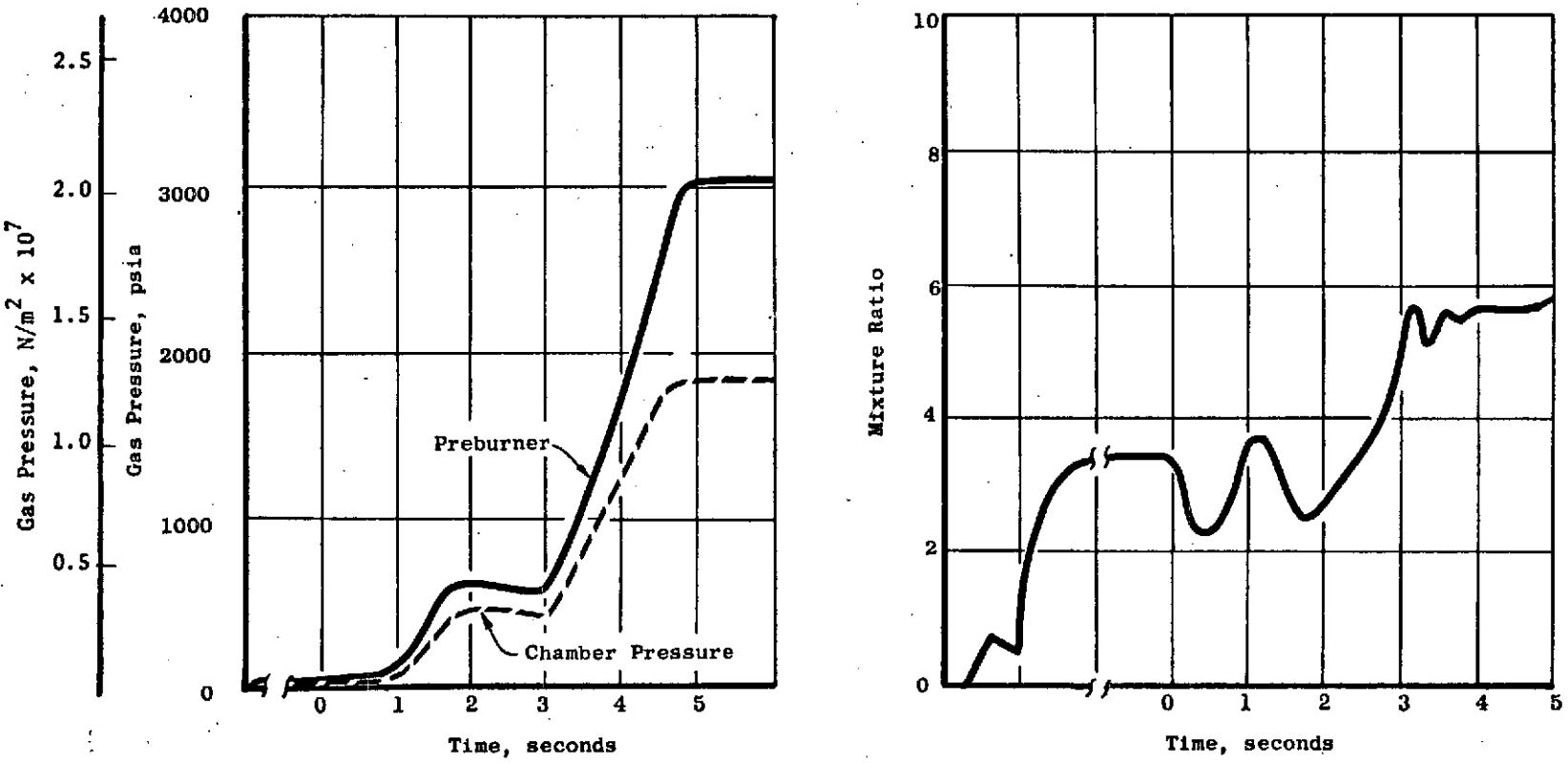

Figure 1-37. Engine Start Characteristics (Dual Preburners, GH_2 Boost Pump Drive, Throttling)

The additional weight and cost resulting from the addition of throttling was established and is presented in Tables 1-35 and 1-36, respectively.

The final assessment of the impact of throttling was conducted and is summarized in Table 1-37. It was concluded that the dual preburner configuration (8T) was the most desirable throttling configuration. The baseline configuration selected during the nonthrottling engine configuration study (4T) and modified for throttling was close to the dual preburner configuration in overall capability.

CONCLUSIONS

It was concluded that the engine configuration consisting of GH_2 turbine-driven boost pumps, a split-flow thrust chamber, and a single preburner (configuration 4) provided the most capability and, therefore, was recommended as the baseline configuration. Though the dual preburner configuration was the most desirable for a throttling engine, the baseline configuration could be modified for throttling without significant penalty. Therefore, even though the baseline was a nonthrottling configuration, it was determined that particular care will be taken during the remainder of the program not to preclude subsequent incorporation of throttling capability. In addition, it was also concluded that incorporation of tank-head idle-mode start and operation with boost pumps sized for 0.6 meters (2 feet) LO_2 and 4.57 meters (15 feet) LH_2 NPSH is feasible and should be pursued as ground rules for the engine design effort.

TABLE 1-35. THROTTLING ENGINE WEIGHT* TRADEOFF

Alternate Engine Configuration	TCA	Preburner	Turbopump	Hot-Gas** Manifold	Control Valves	Propellant Ducts	Ignition System	Controls-Pneumatic, Electric	Gimbal	Total*** Engine
3T	151.5 (68.7)	9.9 (4.49)	66.0 (29.9)	17.2 (7.8)	49.3 (22.4)	5.0 (2.27)	7.8 (3.54)	19.6 (8.89)	1.9 (0.86)	361.0 (163.7)
4T	149.9 (68)	10.0 (4.54)	66.0 (29.9)	17.2 (7.8)	49.3 (22.4)	5.0 (2.27)	7.8 (3.54)	19.5 (8.85)	1.9 (0.86)	359.3 (163)
8T	143.9 (65.3)	12.8 (5.81)	66.4 (30.1)	16.5 (7.48)	53.2 (24.1)	5.2 (2.36)	0.9 (0.408)	19.4 (8.8)	1.9 (4.86)	361.1 (163.8)

*All units in pounds (kilograms)
**Includes hot-gas ducting
***10-percent contingency

TABLE 1-36. THROTTLING ENGINE PARAMETRIC COST ANALYSIS

Engine Configuration	DDT&E Cost, M	Production Cost (First Unit), K
3T	122.5	871.4
4T	121.0	855.8
8T	123.0	898.7

TABLE 1-37. THROTTLING ENGINE CONFIGURATION TRADEOFF MATRIX

Alternate Engine Configuration	Cycle Balance, Chamber Pressure, psi ($N/m^2 x 10^7$)	Performance,* Specific Impulse, seconds (N-s/kg)	Start Transient Characteristics**	Flexibility**	Complexity**	Weight, pounds*	Engine DDT&E and Production Cost
3T	1825 (1.26)	475.0 (4658)	B	C	A	361.0 (163.7)	122.5 M 871.4 K
4T	1850 (1.28)	474.7 (4655)	A	B	B	359.3 (163)	121.0 M 855.8 K
8T	1950 (1.34)	474.9 (4657)	A	A	B	361.1 (163.8)	123.0 M 898.7 K

*Predicated on 400:1 area ratio nozzle and no length limit
**Letter designation indicates order of preference

ENGINE ASSEMBLY PRELIMINARY DESIGN

The engine assembly preliminary design effort consisted of analytical determination of engine operating characteristics, both at design point and off-design conditions, engine assembly and interconnecting component design including the heat exchanger, and supporting analyses such as stress, heat transfer, and fluid dynamics. To provide guidance in the subsequent discussions, the engine schematic is presented in Fig. 1-38. The results of the analyses and design effort are discussed subsequently.

ENGINE BALANCE AND OFF-DESIGN OPERATION

Utilizing the steady-state and dynamic models developed under the Engine Dynamics Computer Programs (NAS3-16687) for the NASA-Lewis Research Center, the steady-state balance and off-design operating conditions were initially determined based on the results of the preliminary configuration selection effort. The preliminary engine balance established was utilized by the various component and subsystem design organizations as the basis for conducting analyses and the required design effort. The specific component and subsystems operating and geometric characteristics were again inputed into the dynamic model for a final engine balance. The final results of this iterative process are presented subsequently in Fig. 1-39 through 1-41 for engine mixture ratios of 6.0, 6.5, and 5.5. The characteristics presented are only a summary, with detail component information presented in subsequent discussions of the major components.

The dynamic model was also utilized to determine engine margin by increasing preburner temperature up to the maximum allowable (and still meet turbine life) and, therefore, determine the potential increase in chamber pressure. This margin can be utilized for overcoming engine hardware variations, development problems, etc., thus minimizing development risk. The impact of increasing preburner temperature on key engine parameters is shown in Fig. 1-42 through 1-67. Performance variation with mixture ratio is shown in Fig. 1-68.

START/SHUTDOWN, IDLE MODE, AND PROPELLANT DUMP OPERATIONS

The engine start, idle mode, and cutoff characteristics were analyzed with the dynamic model prepared for NASA-LeRC under Contract NAS3-16687. Engine control sequences are presented in Fig. 1-69 (definition of abbreviated terms shown in Table 1-38). Characteristics for normal engine start were analyzed under "cold" start conditions such as restart immediately following an engine shutdown (pumps at cryogenic temperatures) and "warm" start conditions resulting from long coast (engine thermally stabilized at 255 K (460 R). A tank-head idle-mode start was analyzed for cold start conditions. It was assumed that saturated propellants existed at boost pump inlets for both warm and cold starts, and that the pressure was increased to the minimum NPSP requirements prior to mainstage. All start sequences (normal, powered idle and tank-head idle) begin with the opening of the inlet valves and the moving of the main oxidizer control valve to an intermediate position. The concurrent initiation of the spark igniters at start results in main chamber idle-mode ignition under tank head. The turbopumps are physically prevented from turning by a

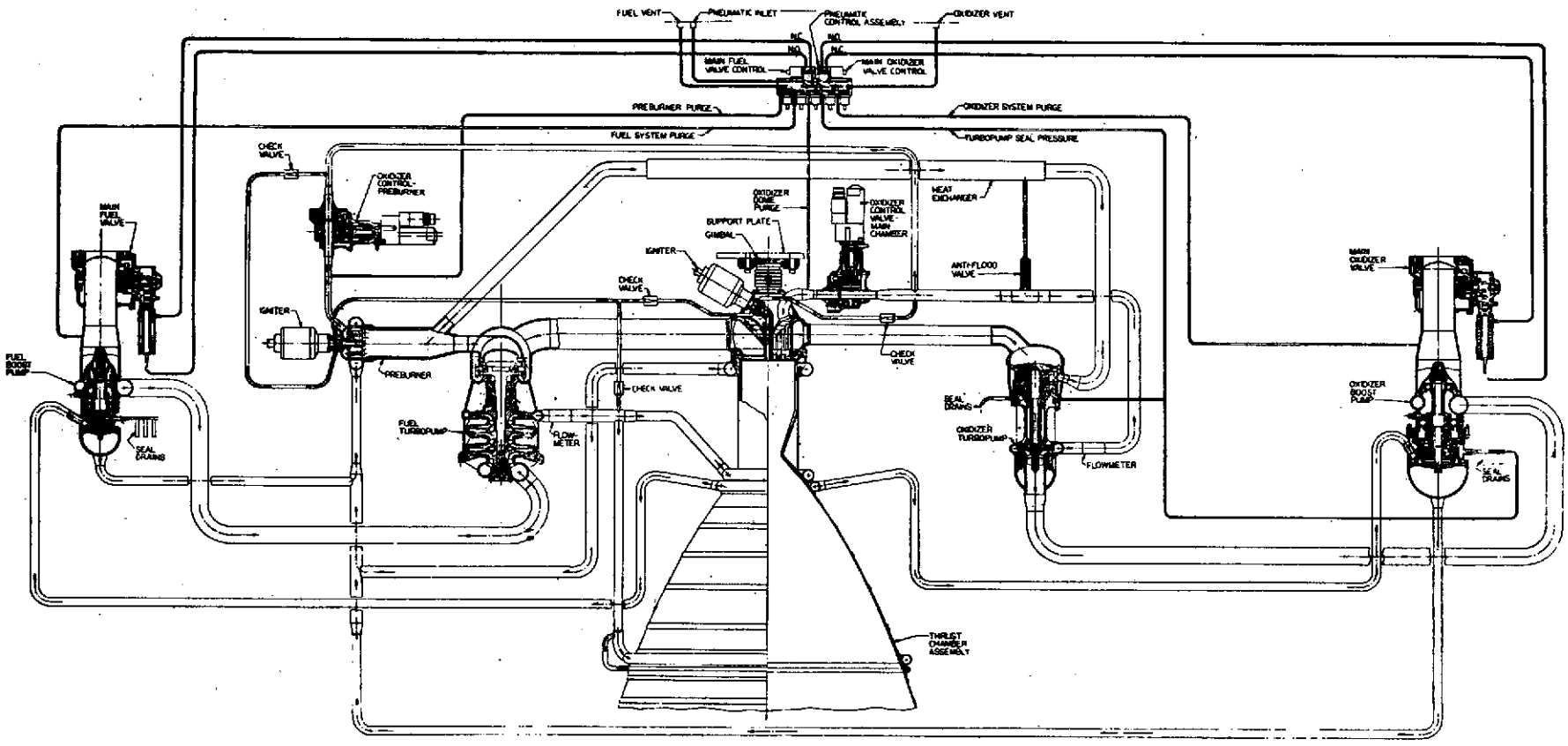

Figure 1-38. Advanced Space Engine Schematic, 88,964 N (20K)

Performance

Thrust, pounds	20000.0 (88964 N)
Chamber Pressure, psia	2233.0 (1.54 $N/m^2 x10^7$)
Engine Mixture Ratio	6.0
Area Ratio	400.0
ODE Specific Impulse, seconds	493.05 (4835 N-s/kg)
ODE Characteristic Velocity, ft/sec	7613.2 (2321 m/s)
Specific Impulse Energy Release Efficiency	0.995
Specific Impulse Reaction Kinetic Efficiency	0.9964
Specific Impulse Divergence Efficiency	0.9955
Specific Impulse Heat Loss Efficiency	1.0
Specific Impulse Boundary Layer Efficiency	0.9740
Effective TDK Specific Impulse, seconds	489.06 (4796 (N-s/kg)
Boundary Layer Specific Impulse Loss, seconds	12.81 (126 N-s/kg)
Delivered Specific Impulse, seconds (includes effect of leakage and dump-cooling flows)	473.43 (4643 N-s/kg)

System Pressures, psia (N/m^2)

	Propellant		Hot-Gas System	
	Oxidizer	Fuel	Oxidizer	Fuel
Engine Inlet Pressure	16.4 (113,074	17.2 (118,590)		
Boost Pump Discharge Pressure	104.0 (717,055)	71.2 (490,907)		
Main Pump Inlet Pressure	104.0 (717,055)	71.2 (490,907)		
Main Pump Discharge Pressure	4440.0 ($3.06x10^7$)	4560 ($3.14x10^7$)		
Combustor Coolant Discharge Pressure				3840.0 ($2.65x10^7$)
Boost Turbine Inlet Pressure			4430.0 ($3.05x10^7$)	4430.0 ($3.05x10^7$)
Boost Turbine Discharge Pressure			3790.0 ($2.61x10^7$)	3790.0 ($2.61x10^7$)
Preburner Pressure			3420.0 ($2.35x10^7$)	
Main Turbine Inlet Pressure			3420.0 ($2.35x10^7$)	3420.0 ($2.35x10^7$)
Chamber Injection Pressure			2450.0 ($1.69x10^7$)	
Chamber Combustion Pressure			2233.0 ($1.54x10^7$)	

Figure 1-39. Operating Characteristics (MR = 6)

Pump Description

	Main Pump		Boost Pump	
	Oxidizer	Fuel	Oxidizer	Fuel
Pump				
Wheel Speed, rpm (rad/s)	81000.0 (8482)	89200.0 (9341)	6710.0 (702.7)	28900.0 (3026)
Inlet Pressure, psia (N/m^2)	104.3 (719,123)	71.2 (490,907)	16.4 (113,074)	17.2 (118,590)
Outlet Pressure, psia (N/m^2)	4440.0 (3.06×10^7)	4560.0 (3.14×10^7)	104.0 (717,055)	71.2 (490,907)
Flowrate, lb/sec (kg/s)	36.21 (1304)	6.04 (217.4)	36.21 (1304)	6.04 (217.4)
Inducer				
ΔP, psid (N/m^2)			87.6 (603,981)	54.0 (372,317)
Turbine Description				
Flowrate, lb/sec (kg/s)	2.55 (91.8)	6.66 (239.8)	0.58 (20.9)	0.70 (25.2)
Admission, fraction	0.26	1.00	0.05	0.05
Inlet Pressure, psia (N/m^2)	3420.0 (2.36×10^7)	3420.0 (2.36×10^7)	4430.0 (3.05×10^7)	4430.0 (3.05×10^7)
Outlet Pressure psia (N/m^2)	2486.3 (1.71×10^7)	2472.7 (1.70×10^7)	3790.0 (2.61×10^7)	3790.0 (2.61×10^7)
Pressure Ratio	1.38	1.38	1.17	1.17
Inlet Temperature, R (K)	1862 (1032)	1862 (1032)	521 (289)	521 (289)

Figure 1-39. (Concluded)

Performance	
Thrust, pounds (N)	20000.0 (88964)
Chamber Pressure, psia ($N/m^2 x10^7$)	2200.0 (1.517)
Engine Mixture Ratio	6.5
Area Ratio	400.0
ODE Specific Impulse, seconds (N-s/kg)	491.35 (4818)
ODE Characteristic Velocity, ft/sec (m/s)	7467.8 (2276)
Specific Impulse Energy Release Efficiency	0.9950
Specific Impulse Reaction Kinetic Efficiency	0.9954
Specific Impulse Divergence Efficiency	0.9955
Specific Impulse Heat Loss Efficiency	1.0
Specific Impulse Boundary Layer Efficiency	0.9740
Effective TDK Specific Impulse, seconds (N-s/kg)	480.44 (4751)
Boundary Layer Loss, seconds (N-s/kg)	12.78 (125)
Delivered Specific Impulse, seconds (N-s/kg) (includes effect of leakage and dump-cooling flows)	471.28 (4622)

System Pressures, psia (N/m^2)

	Propellant		Hot-Gas System	
	Oxidizer	Fuel	Oxidizer	Fuel
Engine Inlet Pressure	15.8 (108,937)	17.6 (121,348)		
Boost Pump Discharge Pressure	90.5 (623,976)	70.7 (487,459)		
Main Pump Inlet Pressure	90.5 (623,976)	70.7 (487,459)		
Main Pump Discharge Pressure	3920.0 ($2.7x10^7$)	4440.0 ($3.06x10^7$)		
Combustor Coolant Discharge Pressure				3760.0 ($2.59x10^7$)
Boost Turbine Inlet Pressure			4320.0 ($2.98x10^7$)	4320.0 ($2.98x10^7$)
Boost Turbine Discharge Pressure			3710.0 ($2.56x10^7$)	3710.0 ($2.56x10^7$)
Preburner Pressure			3360.0 ($2.32x10^7$)	
Main Turbine Inlet Pressure			3360.0 ($2.32x10^7$)	3360.0 ($2.32x10^7$)
Chamber Injection Pressure			2440.0 ($1.68x10^7$)	
Chamber Combustion Pressure			2200.0 ($1.52x10^7$)	

Figure 1-40. Operating Characteristics (MR = 6.5)

Pump Description

	Main Pump		Boost Pump	
	Oxidizer	Fuel	Oxidizer	Fuel
Pump				
Wheel Speed, rpm (rad/s)	77300.0 (8095)	87500.0 (9163)	6390.0 (669.2)	28300.0 (2964)
Efficiency, fraction	0.70	0.57		
Inlet Pressure, psia (N/m^2)	90.5 (623,976)	70.7 (487,459)	15.8 (108,937)	17.6 (121,348)
Outlet Pressure, psia (N/m^2)	3920.0 ($2.7x10^7$)	4440.0 ($3.06x10^7$)	90.5 (623,976)	70.7 (487,459)
Flowrate, lb/sec (kg/s	36.78 (16.7)	5.66 (2.57)	36.78 (16.7)	5.66 (2.57)
Tip Speed, ft/sec (m/s)	800.0	1640.0		
Flow Coefficient		0.10		
Head Coefficient		0.60		
Inducer				
Inlet Flow Velocity, ft/sec (m/s)				
Tip Speed, ft/sec (m/s)	535.0 (163.1)		107.0 (32.6)	
Flow Coefficient	0.12		0.07	
Head Coefficient	0.40		0.42	
ΔP, psid (N/m^2)			74.7 (514,982)	53.1 (366,071)

Turbine Description

Flowrate, lb/sec (kg/s)	2.45 (1.11)	6.41 (2.91)	0.54 (0.245)	0.65 (0.295)
Admission, fraction	0.26	1.00	0.05	0.05
Inlet Pressure, psia (N/m^2)	3360.0 ($2.32x10^7$)	3360.0 ($2.32x10^7$)	4320.0 ($2.98x10^7$)	4320.0 ($2.98x10^7$)
Outlet Pressure, psia (N/m^2)	2473.0 ($1.71x10^7$)	2460.0 ($1.7x10^7$)	3710.0 ($2.56x10^7$)	3710.0 ($2.56x10^7$)
Pressure Ratio	1.36	1.37	1.16	1.16
Inlet Temperature, R (K)	1884 (1047)	1884 (1047)	545 (302.8)	545 (302.8)

Figure 1-40. (Concluded)

Performance

Thrust, pounds (N)	20000.0 (88,964)
Chamber Pressure, psia ($N/m^2 x10^7$)	2267.0 (1.56)
Engine Mixture Ratio	5.5
Area Ratio	400.0
ODE Specific Impulse, seconds (N-s/kg)	493.68 (4841)
ODE Characteristic Velocity, ft/sec (m/s)	7747.0 (2361)
Specific Impulse Energy Release Efficiency	0.9950
Specific Impulse Reaction Kinetic Efficiency	0.9973
Specific Impulse Divergence Efficiency	0.9955
Specific Impulse Heat Loss Efficiency	1.0
Specific Impulse Boundary Layer Efficiency	0.9741
Effective TDK Specific Impulse, seconds (N-s/kg)	490.10 (4806)
Boundary Layer Specific Impulse Loss, seconds N-s/kg)	12.80 (125.5)
Delivered Specific Impulse, seconds (N-s/kg) (includes effect of leakage and dump-cooling flows)	474.43 (4653)

System Pressures, psia (N/m^2)

	Propellant		Hot-Gas System	
	Oxidizer	Fuel	Oxidizer	Fuel
Engine Inlet Pressure	17.1 (117,900)	16.8 (115,832)		
Boost Pump Discharge Pressure	118.0 (813,581)	71.3 (491,596)		
Main Pump Inlet Pressure	118.0 (813,581)	71.3 (491,596)		
Main Pump Discharge Pressure	5020.0 ($3.46x10^7$)	4690 ($3.23x10^7$)		
Combustor Coolant Discharge Pressure				3920.0 ($2.70x10^7$)
Boost Turbine Inlet Pressure			4550.0 ($3.14x10^7$)	4550.0 ($3.14x10^7$)
Boost Turbine Discharge Pressure			3870.0 ($2.67x10^7$)	3870.0 ($2.67x10^7$)
Preburner Pressure			3480.0 ($2.4x10^7$)	
Main Turbine Inlet Pressure			3480.0 ($2.4x10^7$)	3480.0 ($2.4x10^7$)
Chamber Injection Pressure			2470.0 ($1.7x10^7$)	
Chamber Combustion Pressure			2267.0 ($1.56x10^7$)	

Figure 1-41. Operating Characteristics (MR = 5.5)

Pump Description

	Main Pump		Boost Pump	
	Oxidizer	Fuel	Oxidizer	Fuel
Pump				
Wheel Speed, rpm (rad/s)	85000.0 (8901)	91000.0 (9529)	7040.0 (737.2)	29500.0 (3089)
Inlet Pressure, psia (N/m^2)	118.0 (813,581)	71.3 (491,596)	17.1 (117,900)	16.8 (115,832)
Outlet Pressure, psia (N/m^2)	5020.0 ($3.46x10^7$)	4690.0 ($3.23x10^7$)	118.0 (813,581)	71.3 (491,596)
Flowrate, lb/sec (kg/s)	35.67 (16.2)	6.49 (2.94)	35.67 (16.2)	6.49 (2.94)
Inducer				
Inlet Flow Velocity, ft/sec (ms/)				
Tip Speed, ft/sec (m/s)				422.0 (128.6)
Flow Coefficient				0.065
Head Coefficient				0.31
ΔP, psid (N/m^2)			100.9 (695,681)	54.5 (375,764)
Efficiency, fraction				0.70
Turbine Description				
Flowrate, lb/sec (kg/s)	2.65 (1.20)	6.92 (3.14)	0.62 (0.281)	0.74 (0.336)
Admission, Fraction	0.26	1.00	0.05	0.05
Inlet Pressure, psia (N/m^2)	3480.0 ($2.4x10^7$)	3480.0 ($2.4x10^7$)	4550.0 ($3.14x10^7$)	4550.0 ($3.14x10^7$)
Outlet Pressure, psia (N/m^2)	2498.6 ($1.72x10^7$)	2484.7 ($1.71x10^7$)	3870.0 ($2.67x10^7$)	3870.0 ($2.67x10^7$)
Pressure Ratio	1.39	1.40	1.18	1.18
Inlet Temperature, R (K)	1848 (1027)	1848 (1027)	498 (276.7)	498 (276.7)

Figure 1-41. (Concluded)

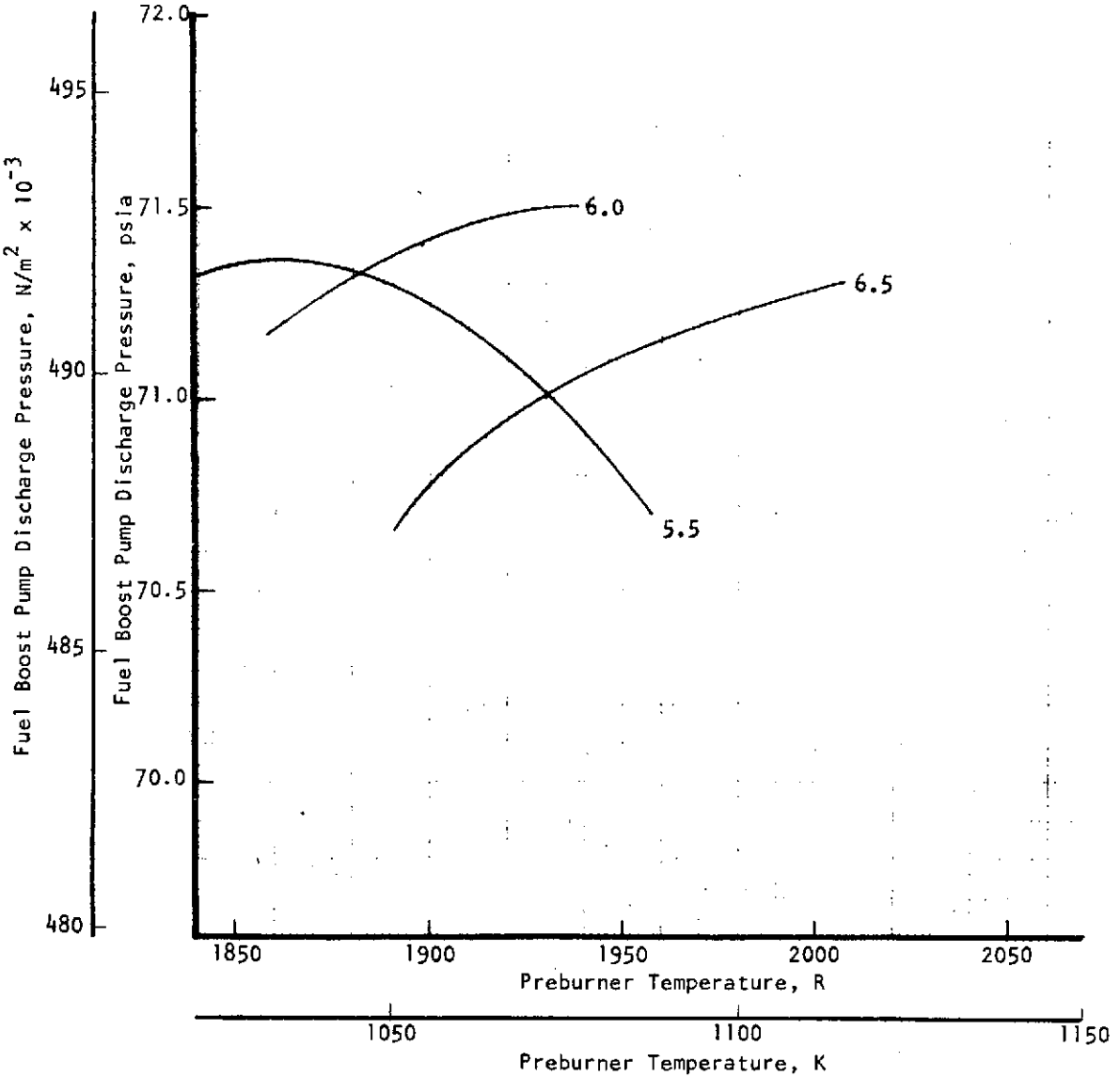

Figure 1-42. Fuel Boost Pump Discharge Pressure vs Preburner Temperature

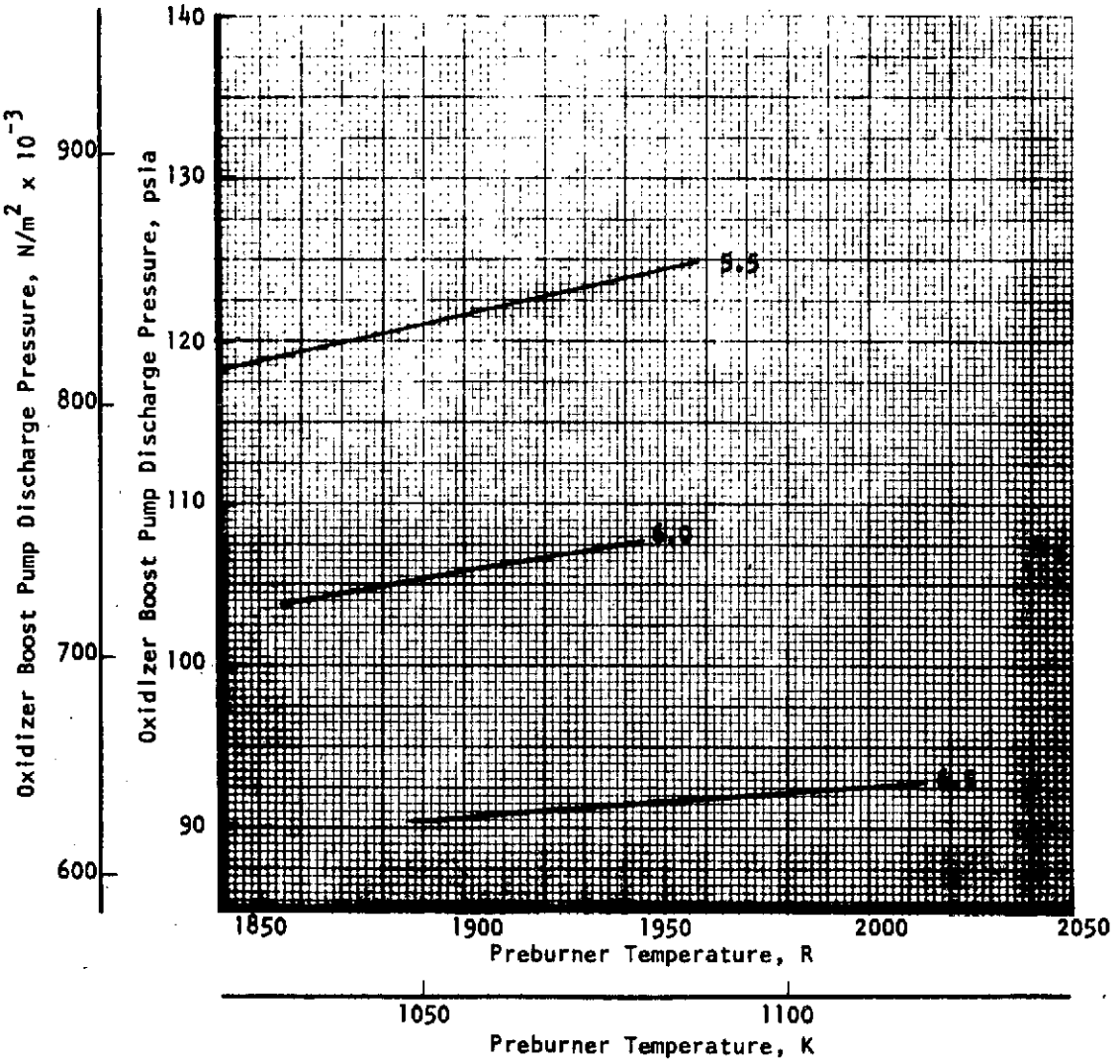

Figure 1-43. Oxidizer Boost Pump Discharge Pressure vs Preburner Temperature

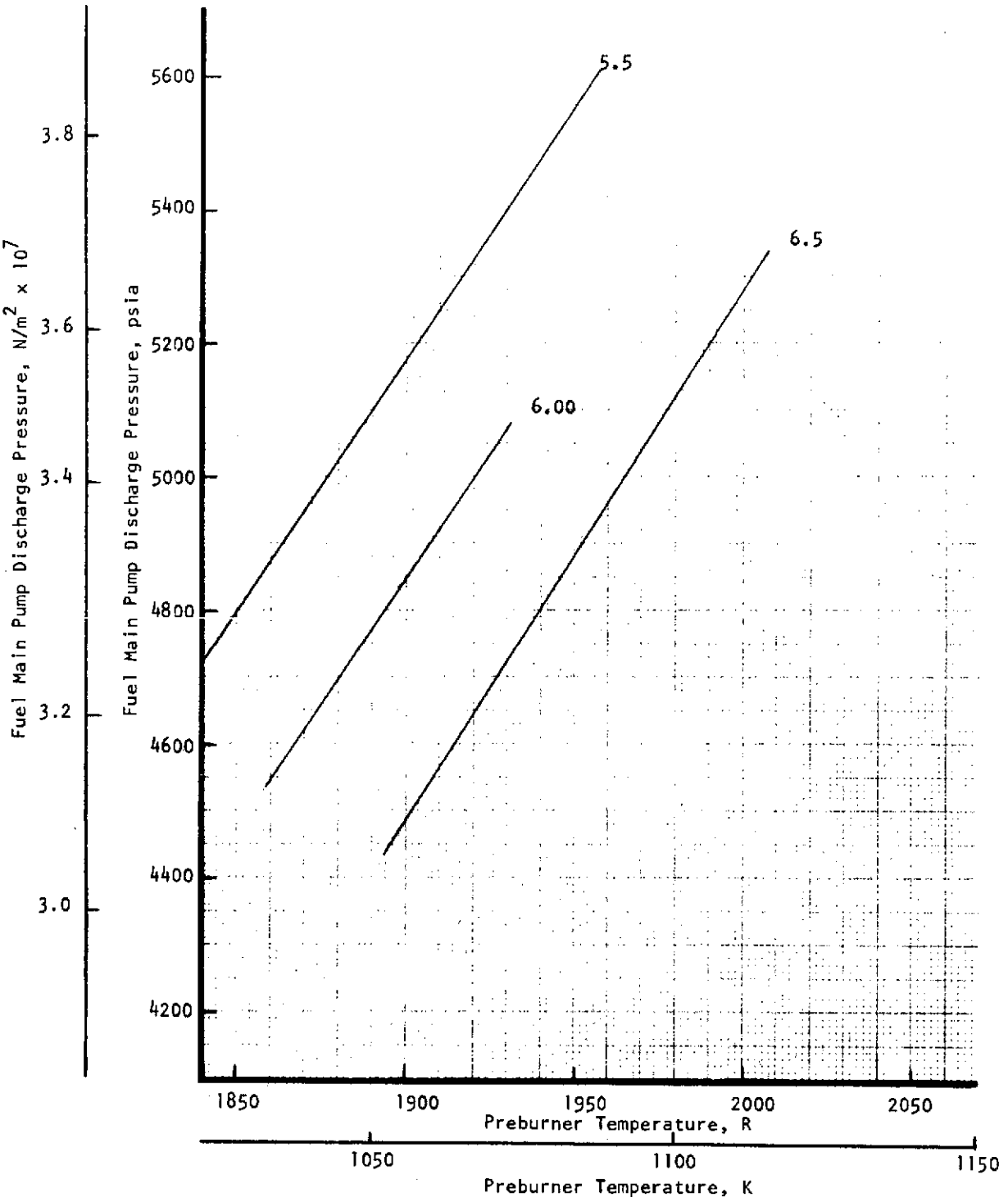

Figure 1-44. Fuel Main Pump Discharge Pressure vs Preburner Temperature

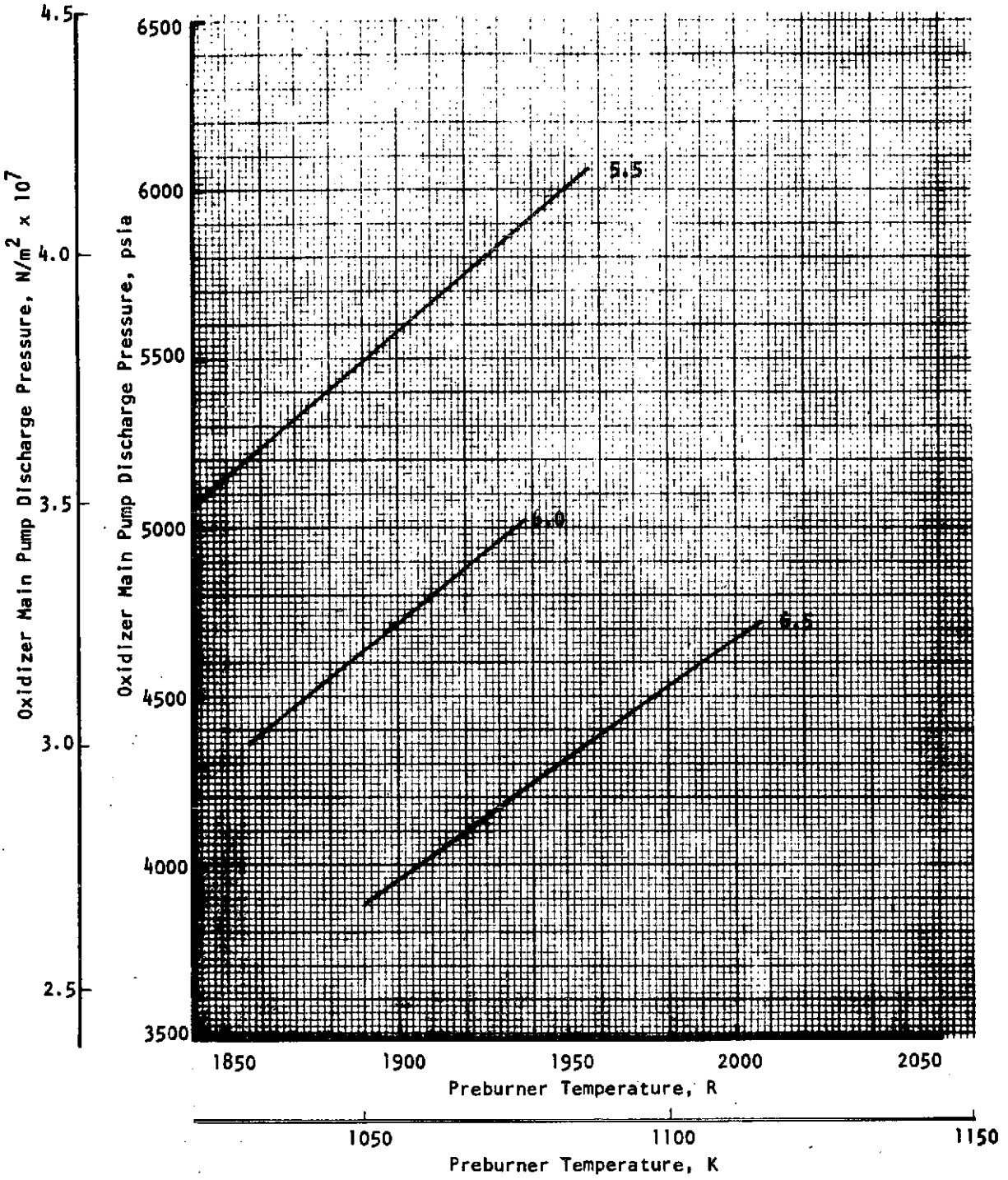

Figure 1-45. Oxidizer Main Pump Discharge Pressure vs Preburner Temperature

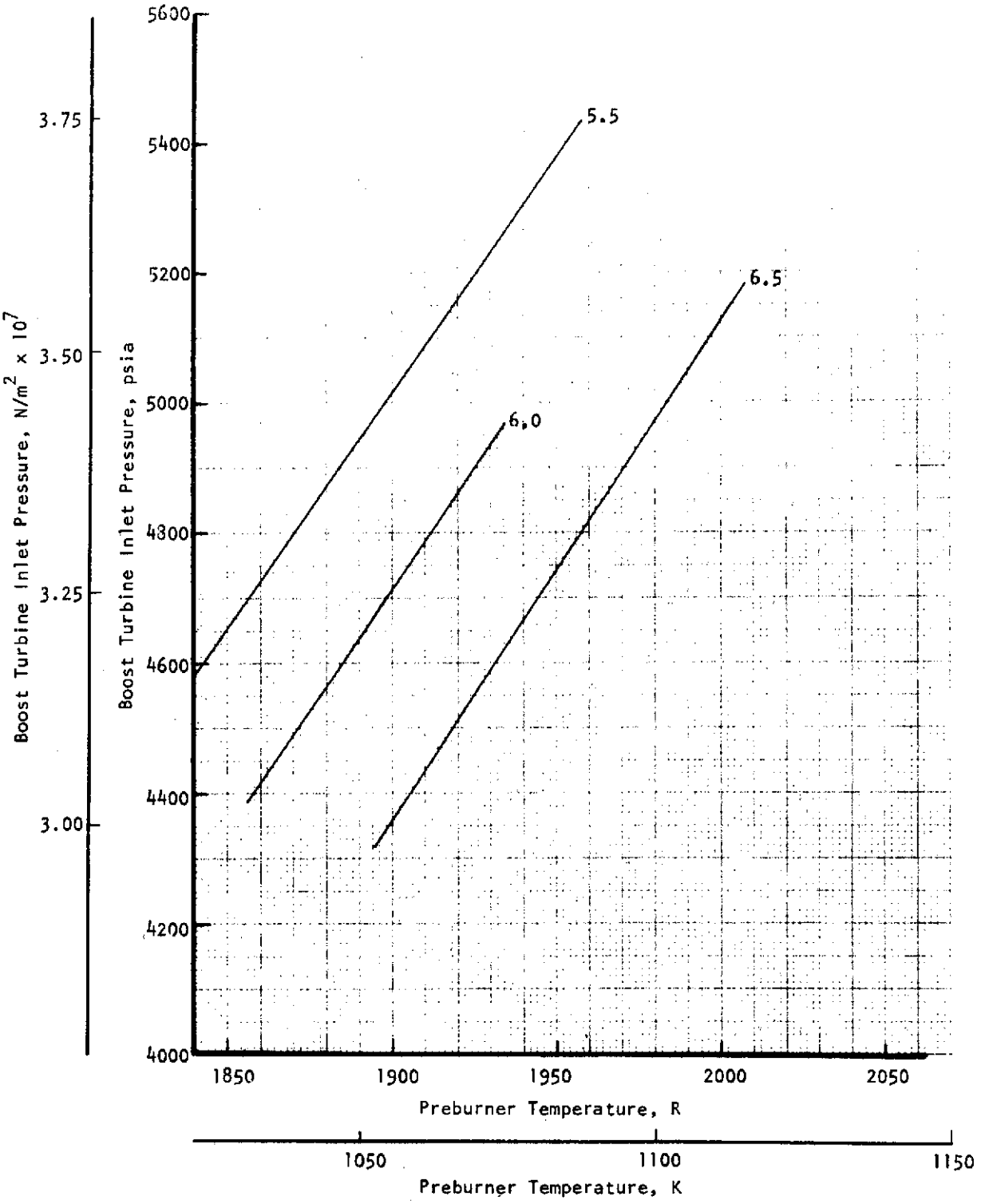

Figure 1-46. Boost Turbine Inlet Pressure vs Preburner Temperature

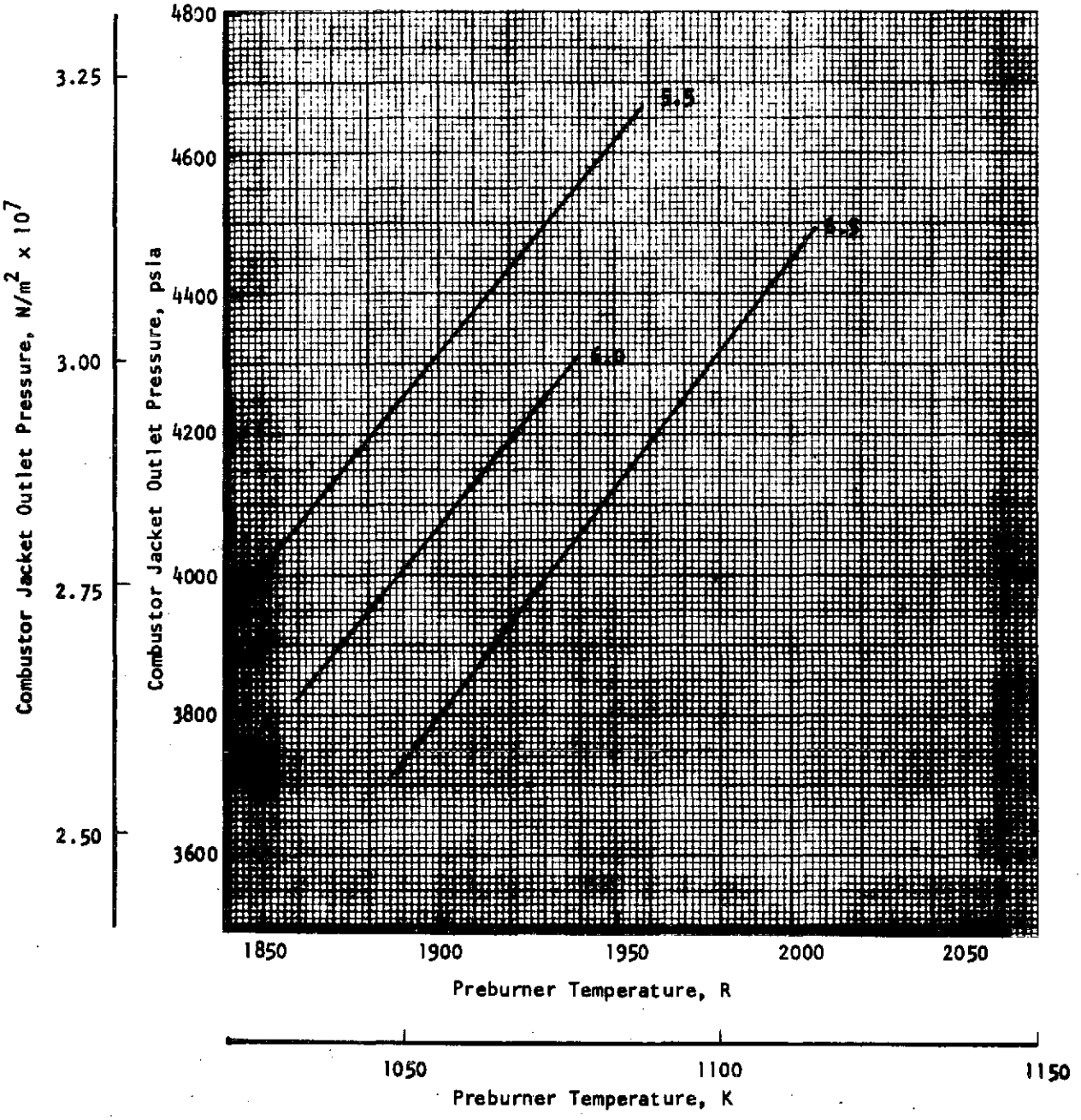

Figure 1-47. Combustor Jacket Outlet Pressure vs Preburner Temperature

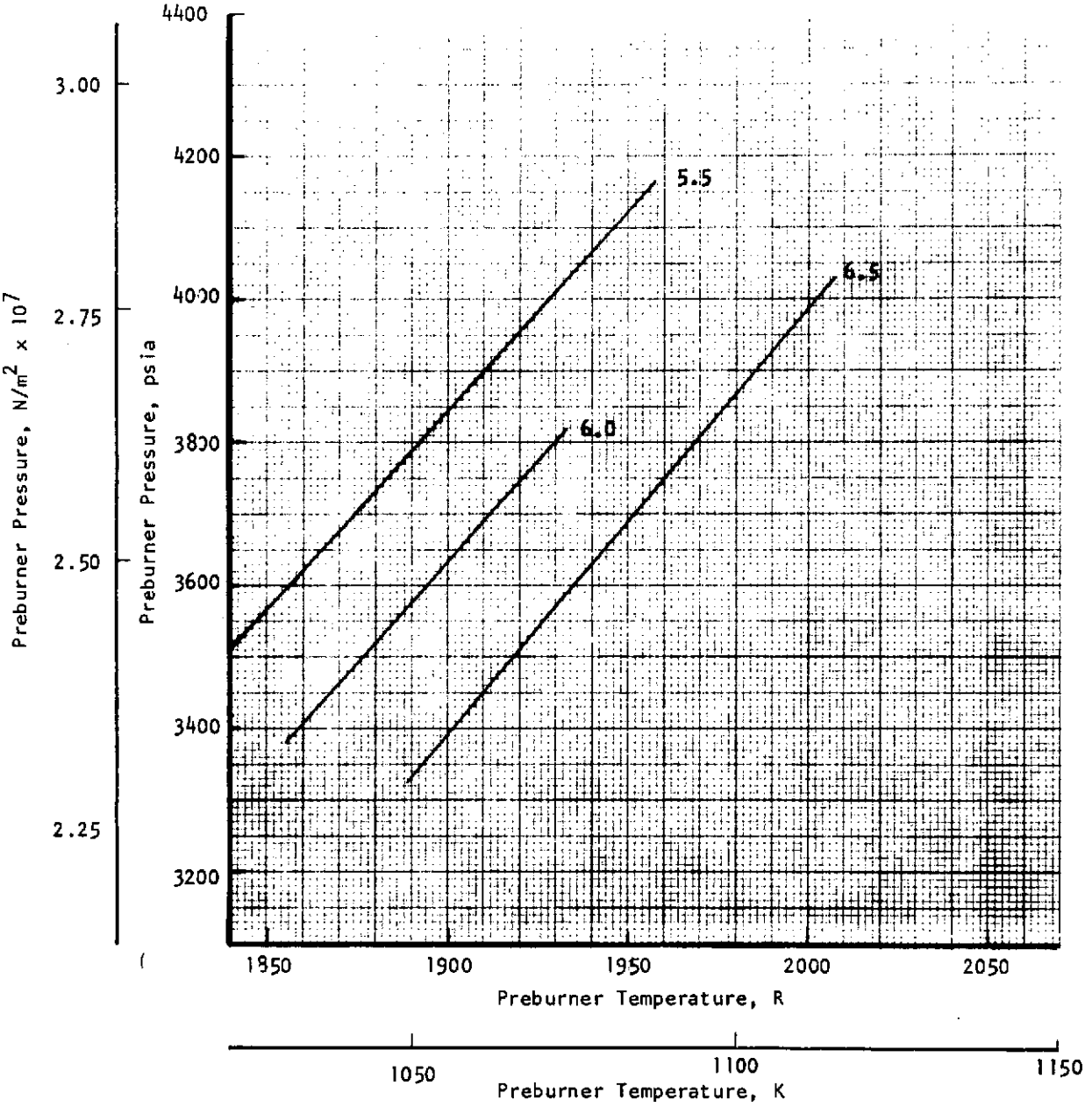

Figure 1-48. Preburner Pressure vs Preburner Temperature

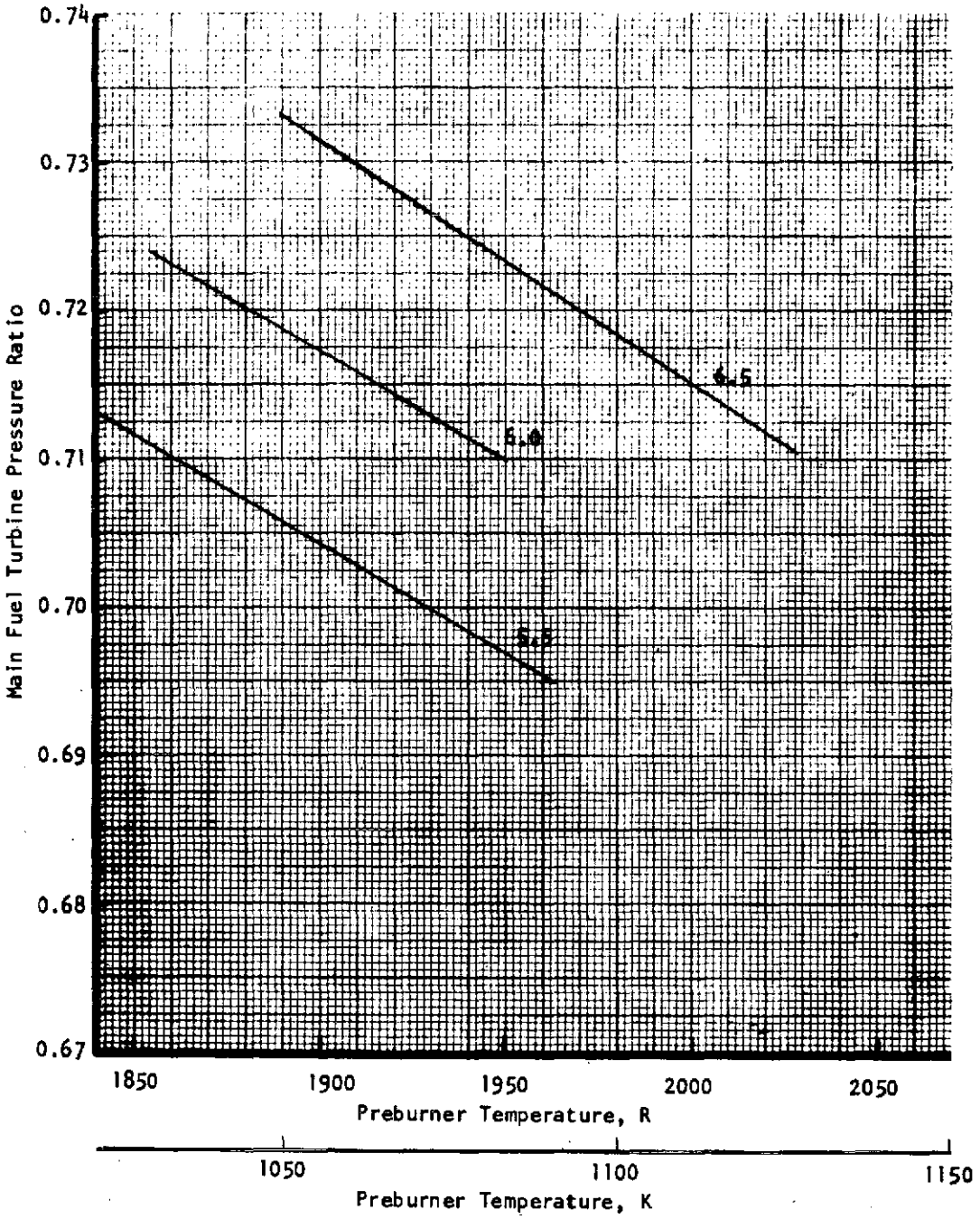

Figure 1-49. Main Oxidizer Turbine Pressure Ratio vs Preburner Temperature

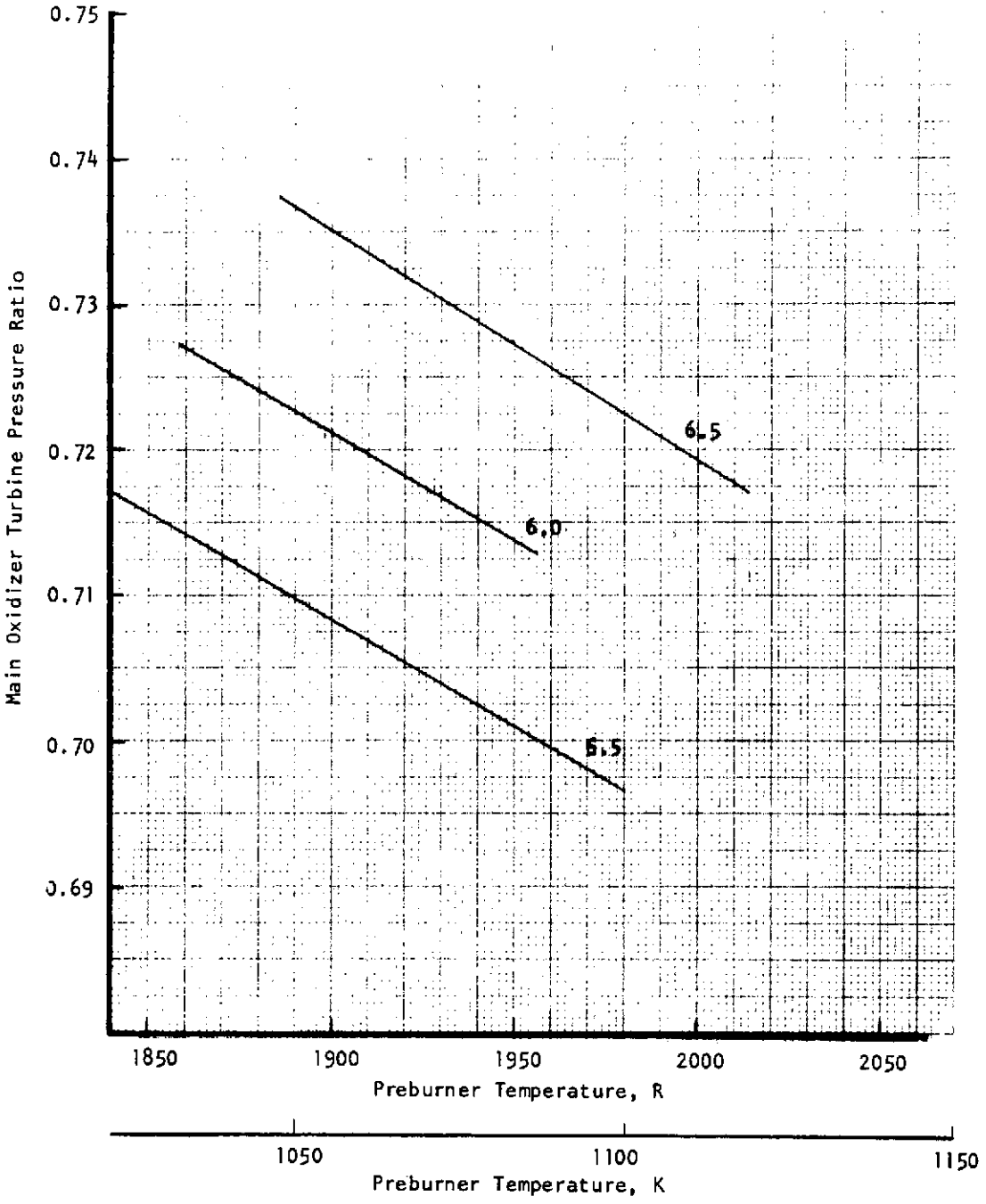

Figure 1-50. Main Oxidizer Turbine Pressure vs Preburner Temperature

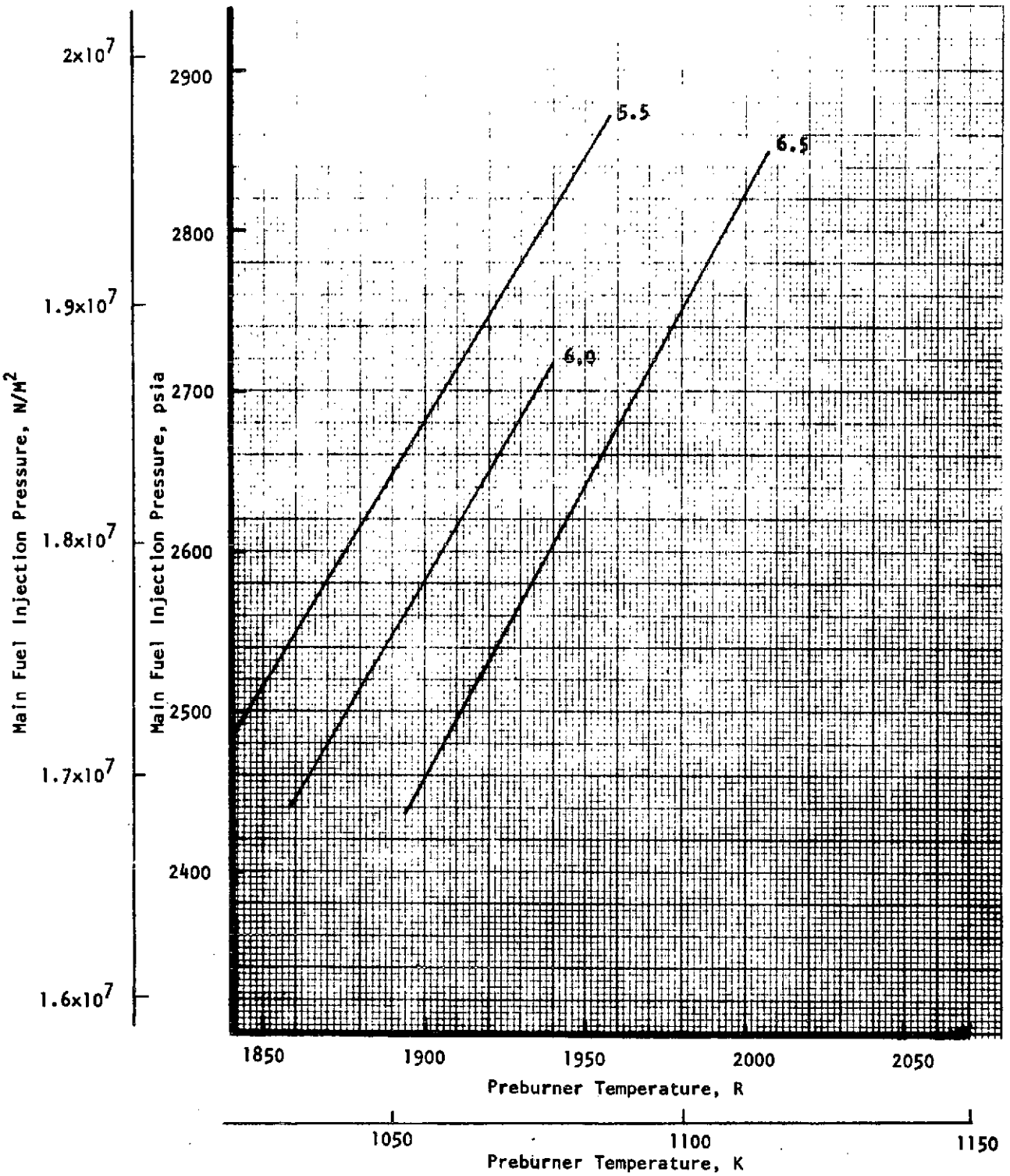

Figure 1-51. Main Fuel Injection Pressure vs Preburner Temperature

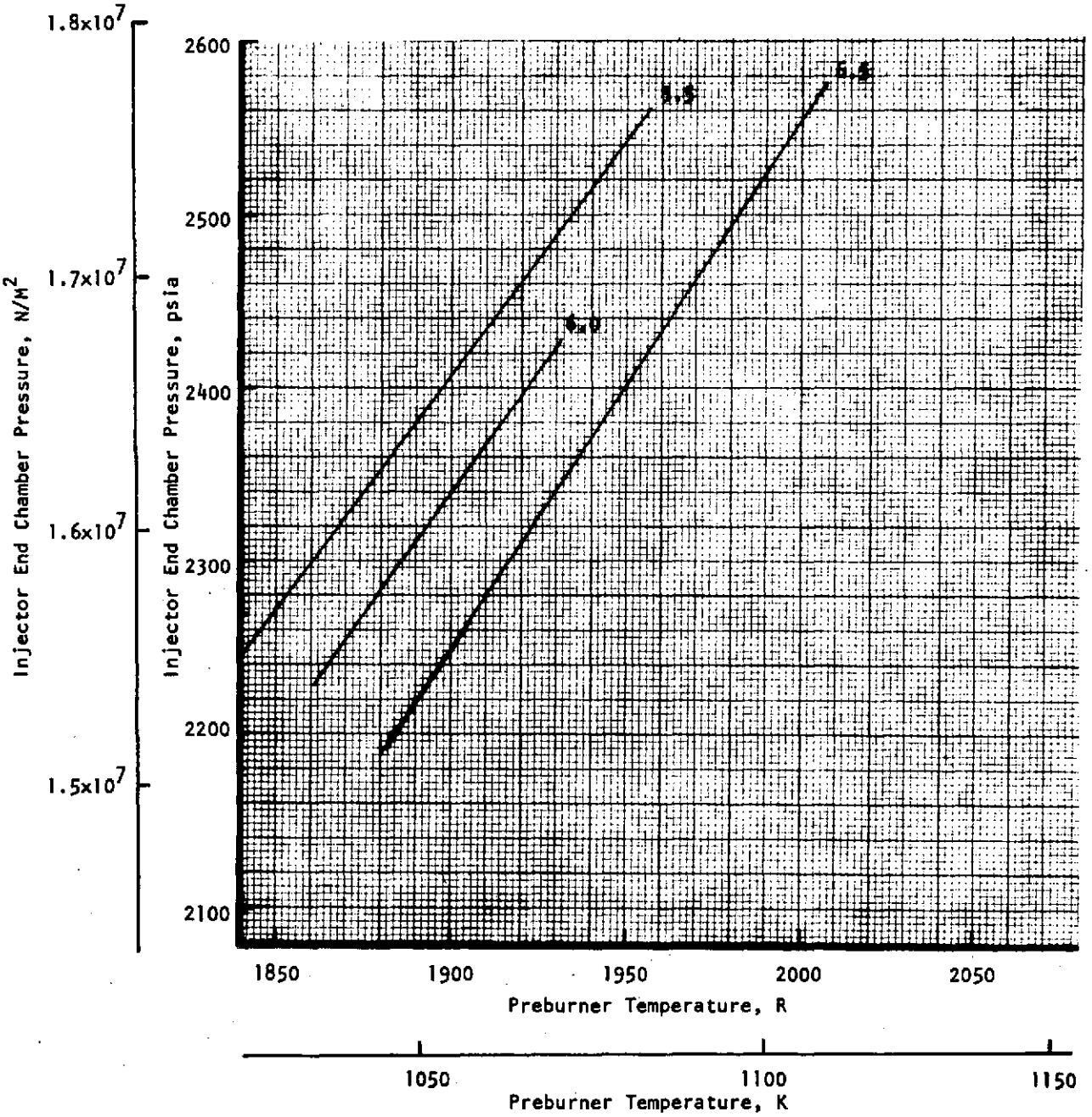

Figure 1-52. Injector End Chamber Pressure vs Preburner Temperature

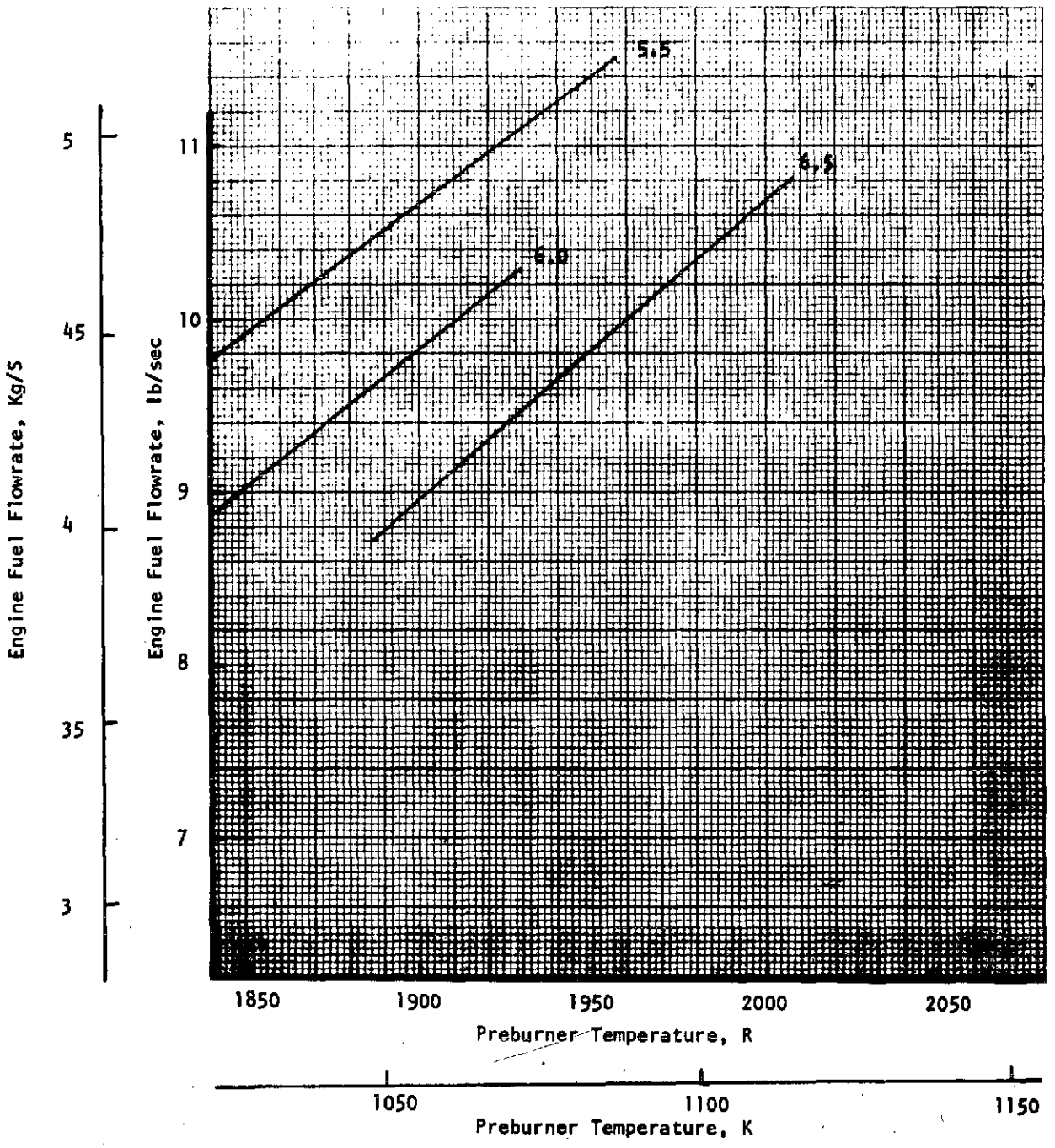

Figure 1-53. Engine Fuel Flowrate vs Preburner Temperature

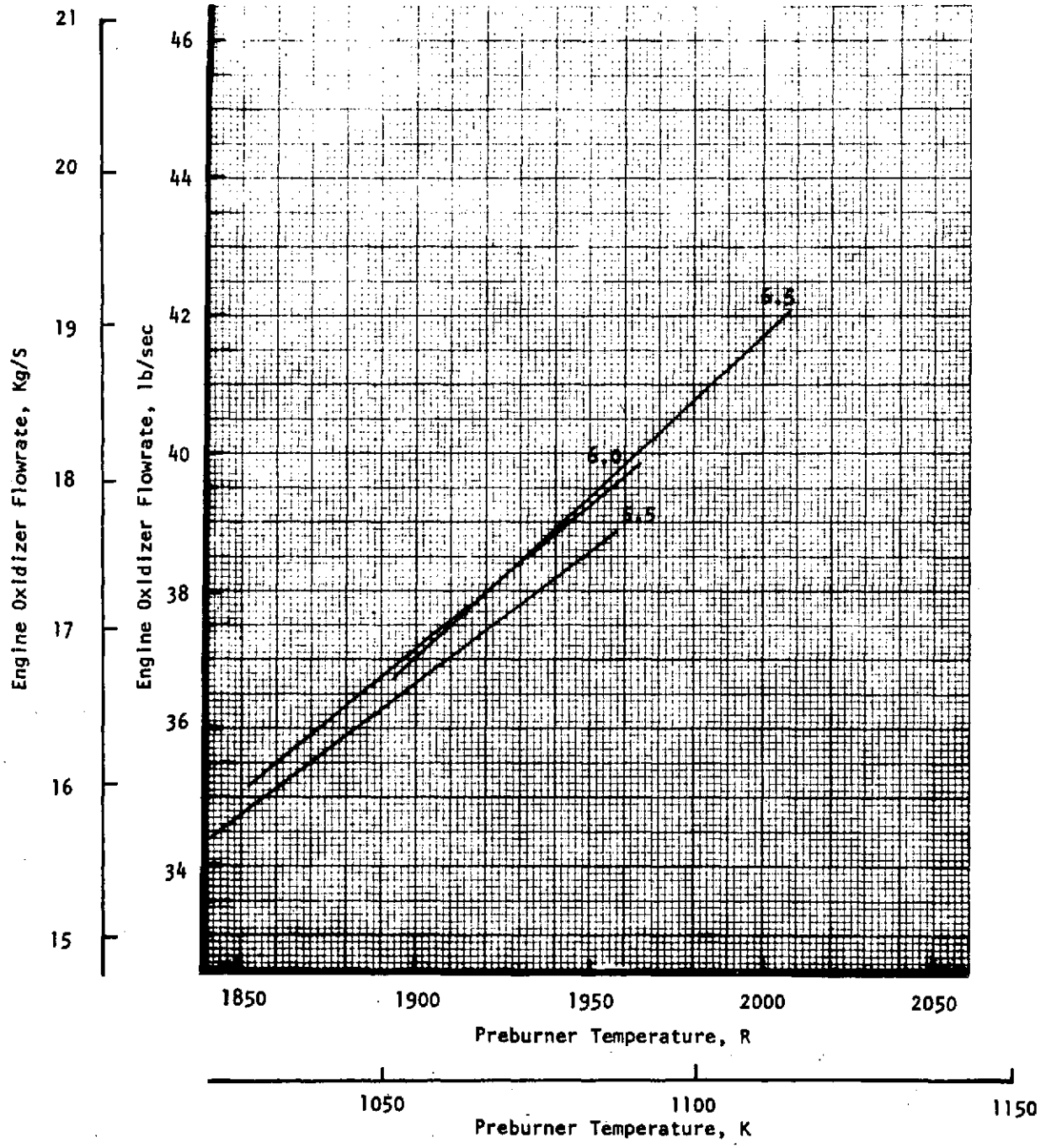

Figure 1-54. Engine Oxidizer Flowrate vs Preburner Temperature

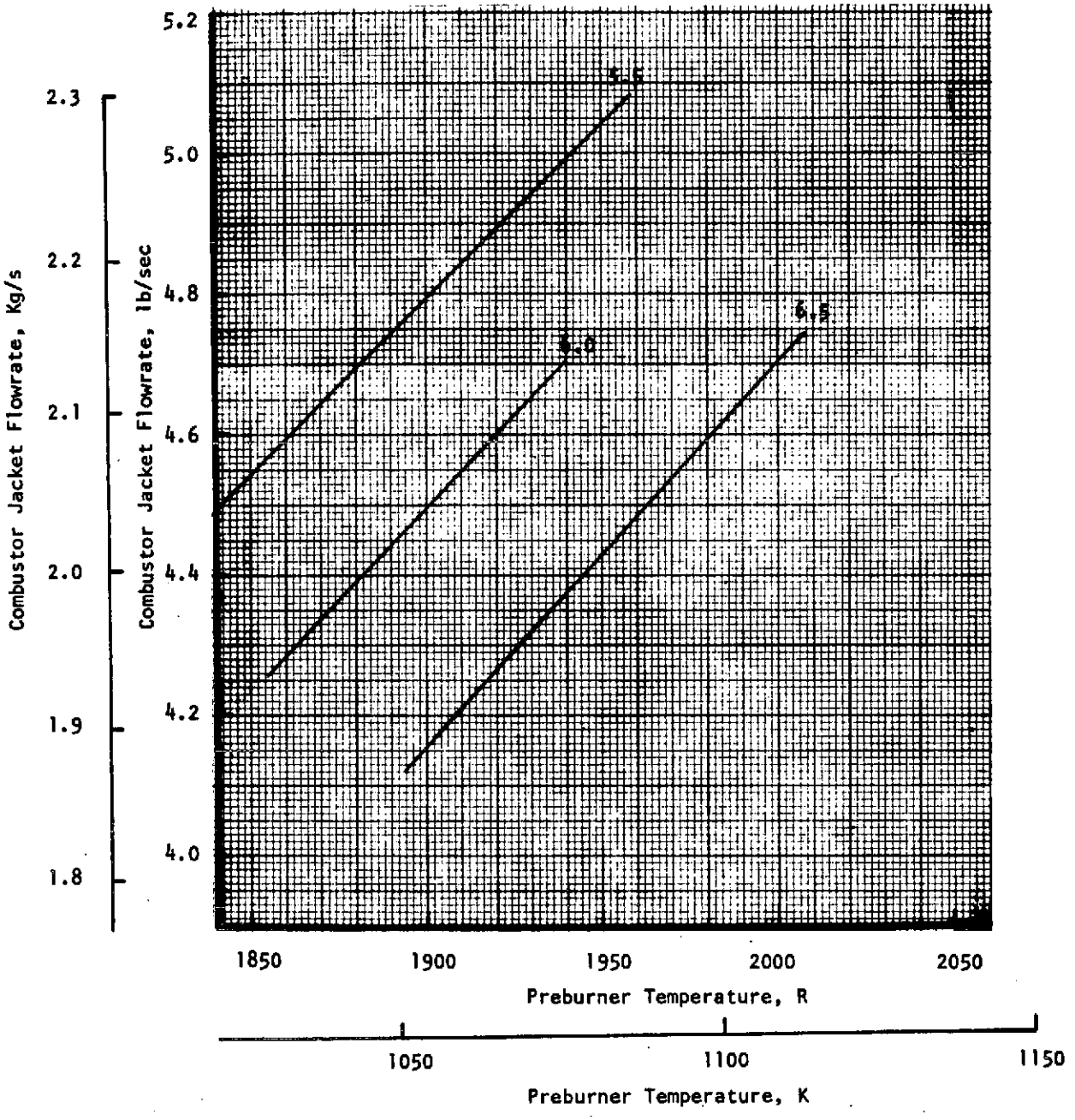

Figure 1-55. Combustor Jacket Flowrate vs Preburner Temperature

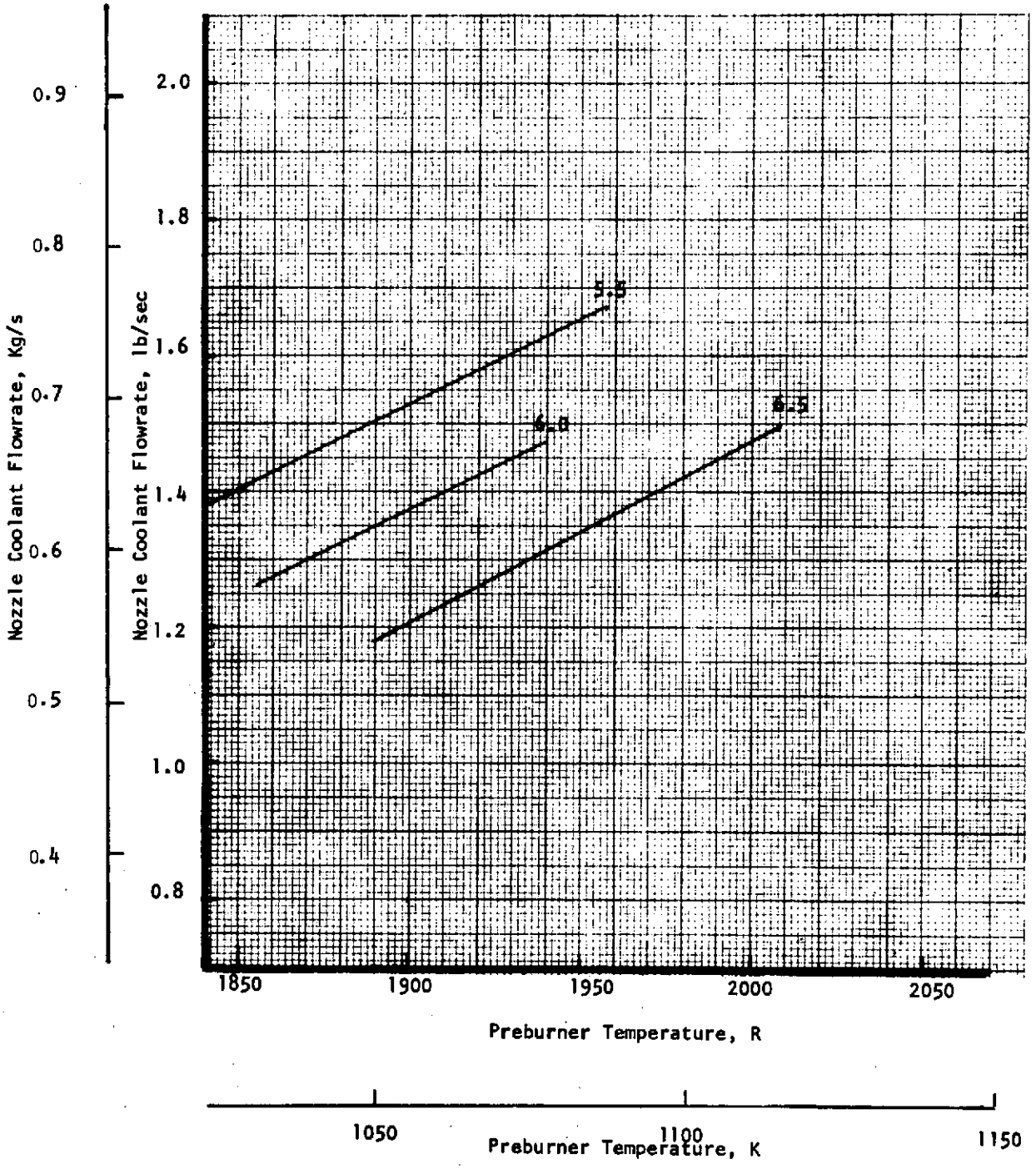

Figure 1-56. Nozzle Coolant Flowrate vs Preburner Temperature

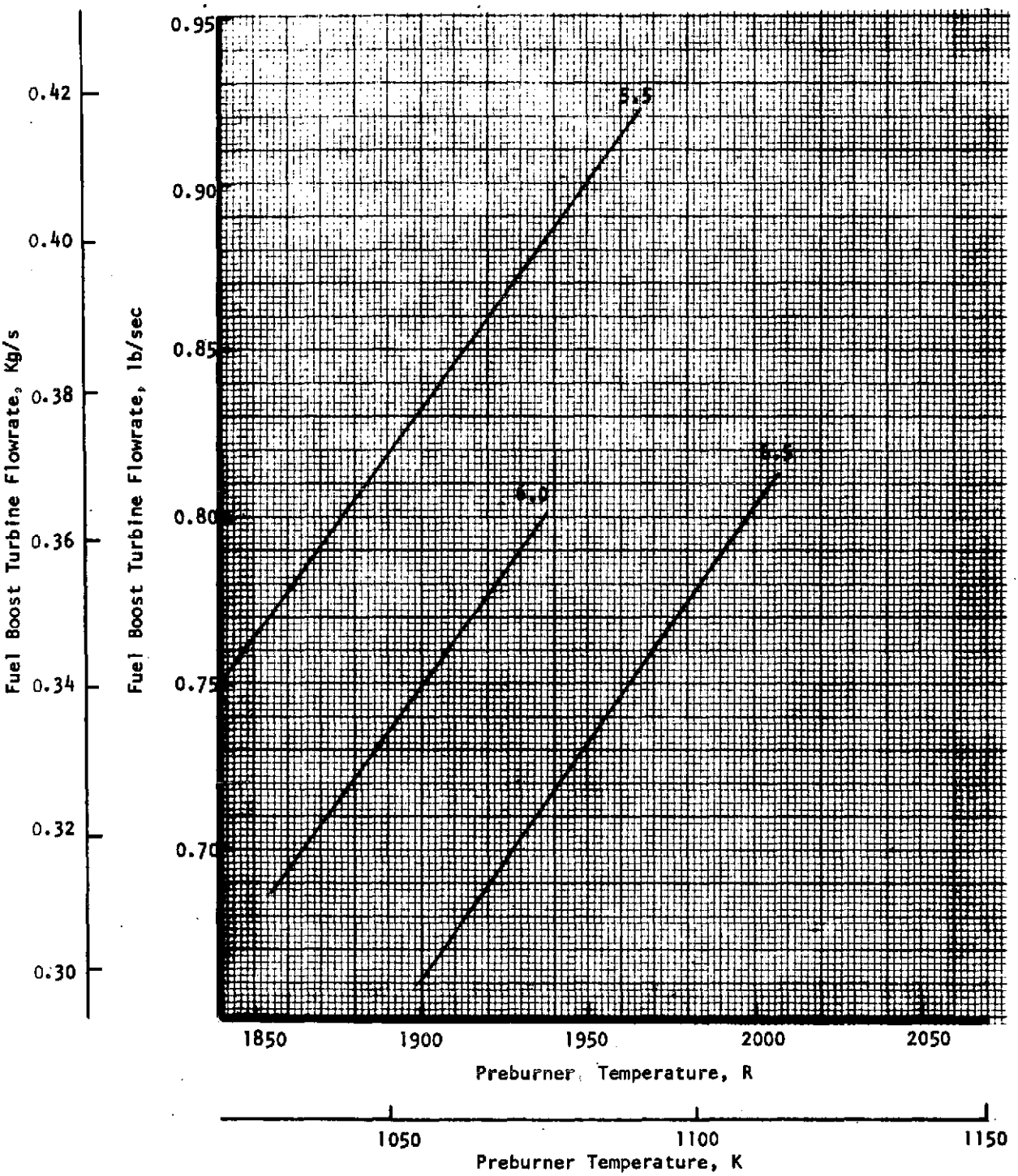

Figure 1-57. Fuel Boost Turbine Flowrate vs Preburner Temperature

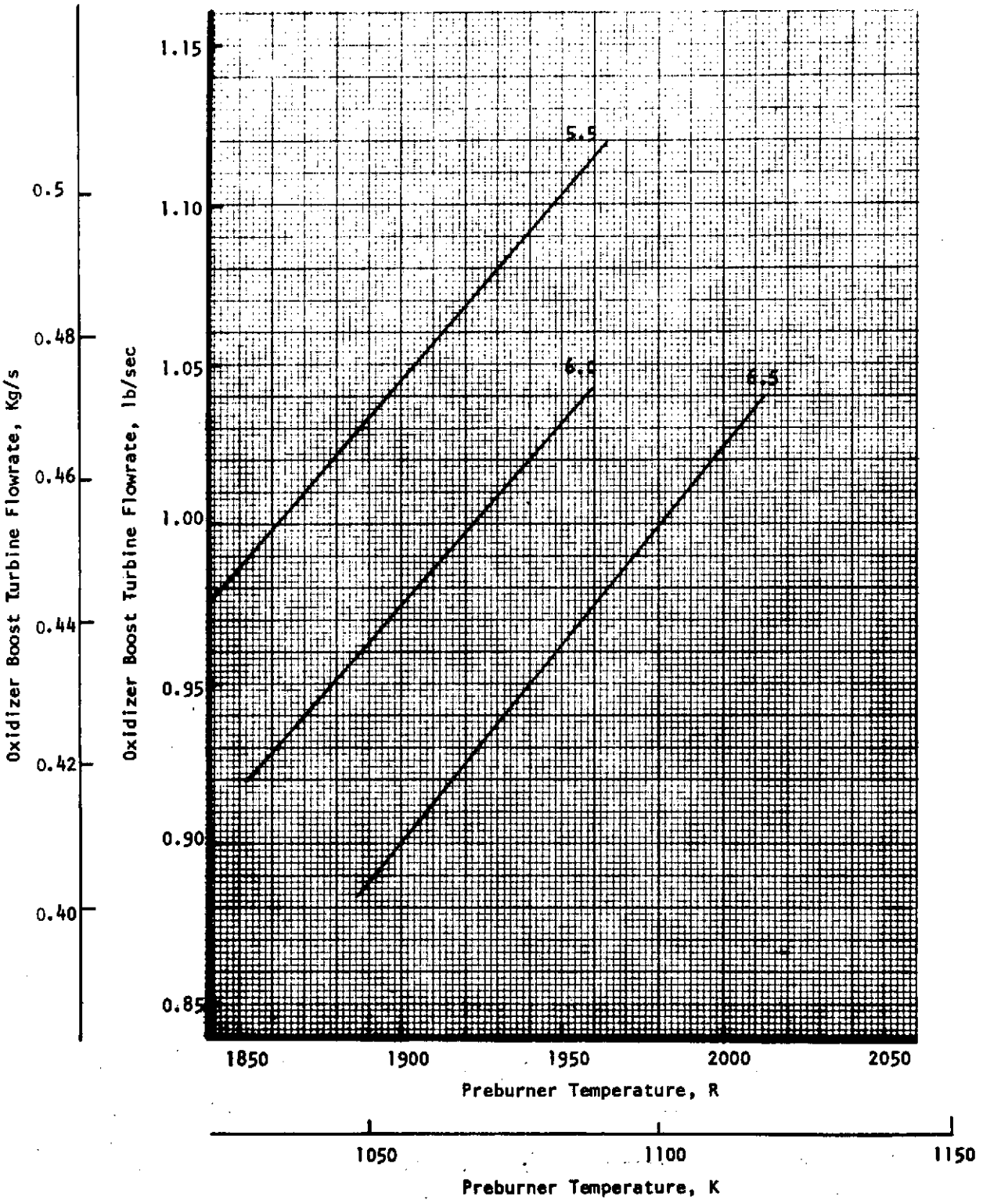

Figure 1-58. Oxidizer Boost Turbine Flowrate vs Preburner Temperature

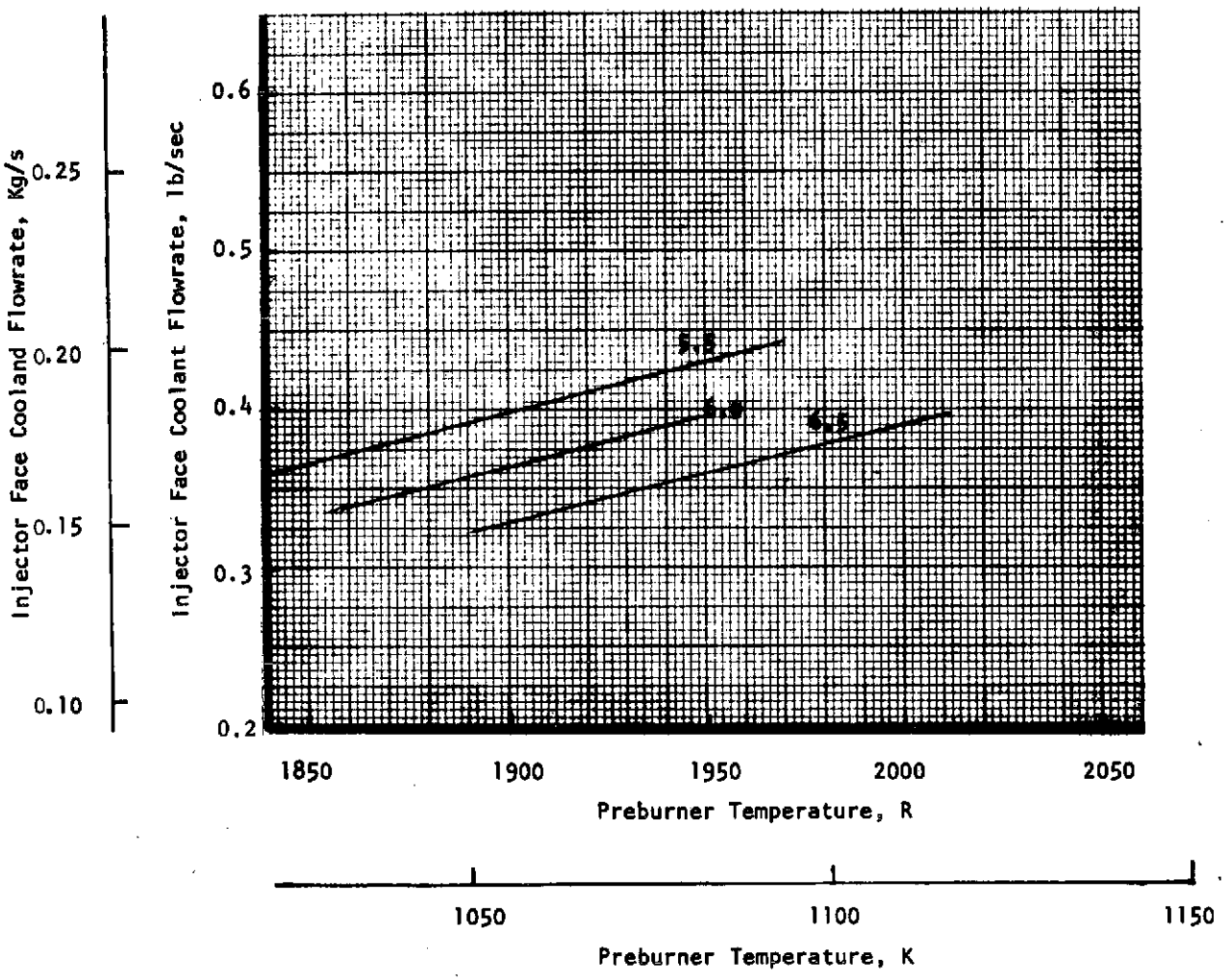

Figure 1-59. Injector Face Coolant Flowrate vs Preburner Temperature

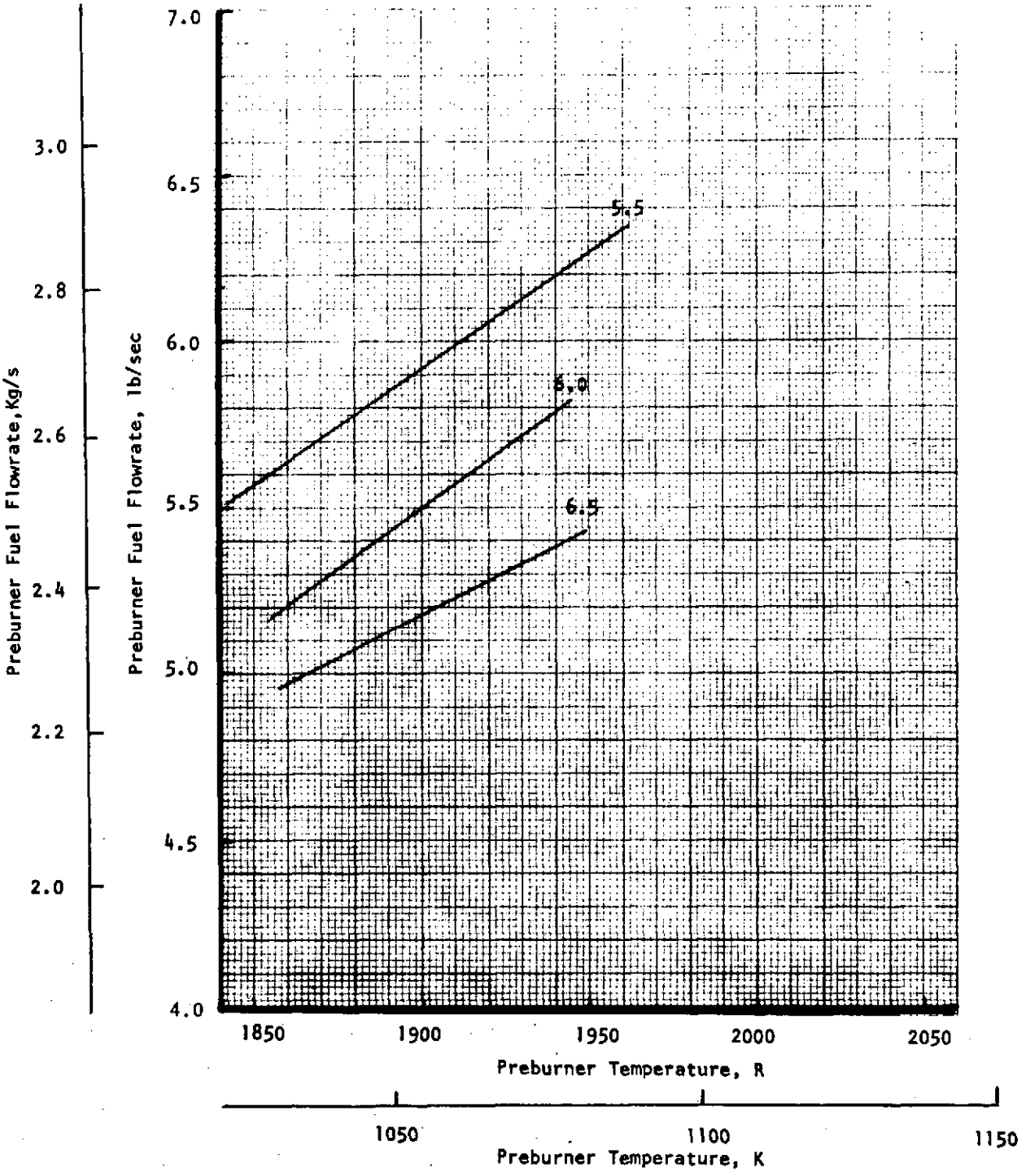

Figure 1-60. Preburner Fuel Flowrate vs Preburner Temperature

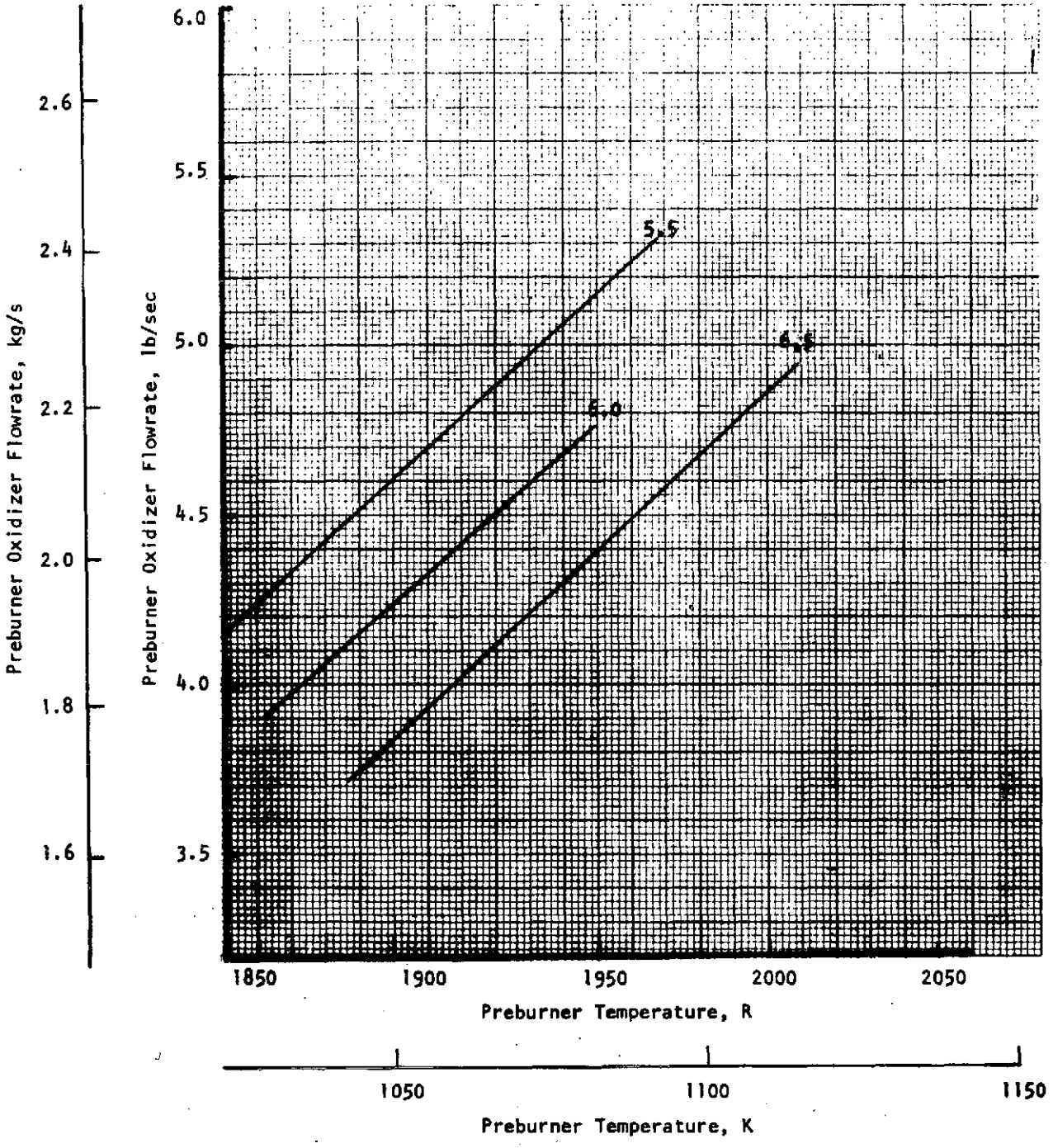

Figure 1-61. Preburner Oxidizer Flowrate vs Preburner Temperature

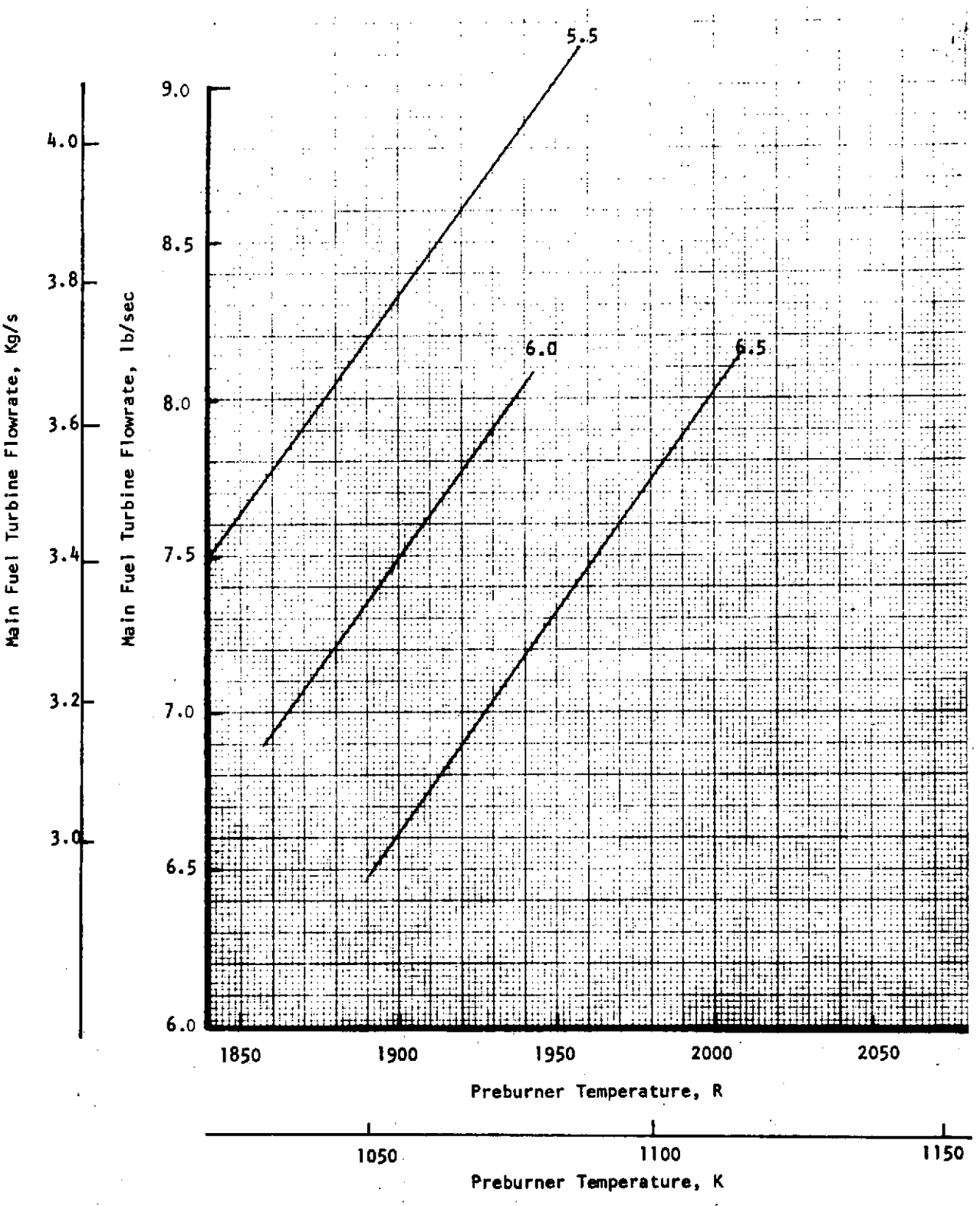

Figure 1-62. Main Fuel Turbine Flowrate vs Preburner Temperature

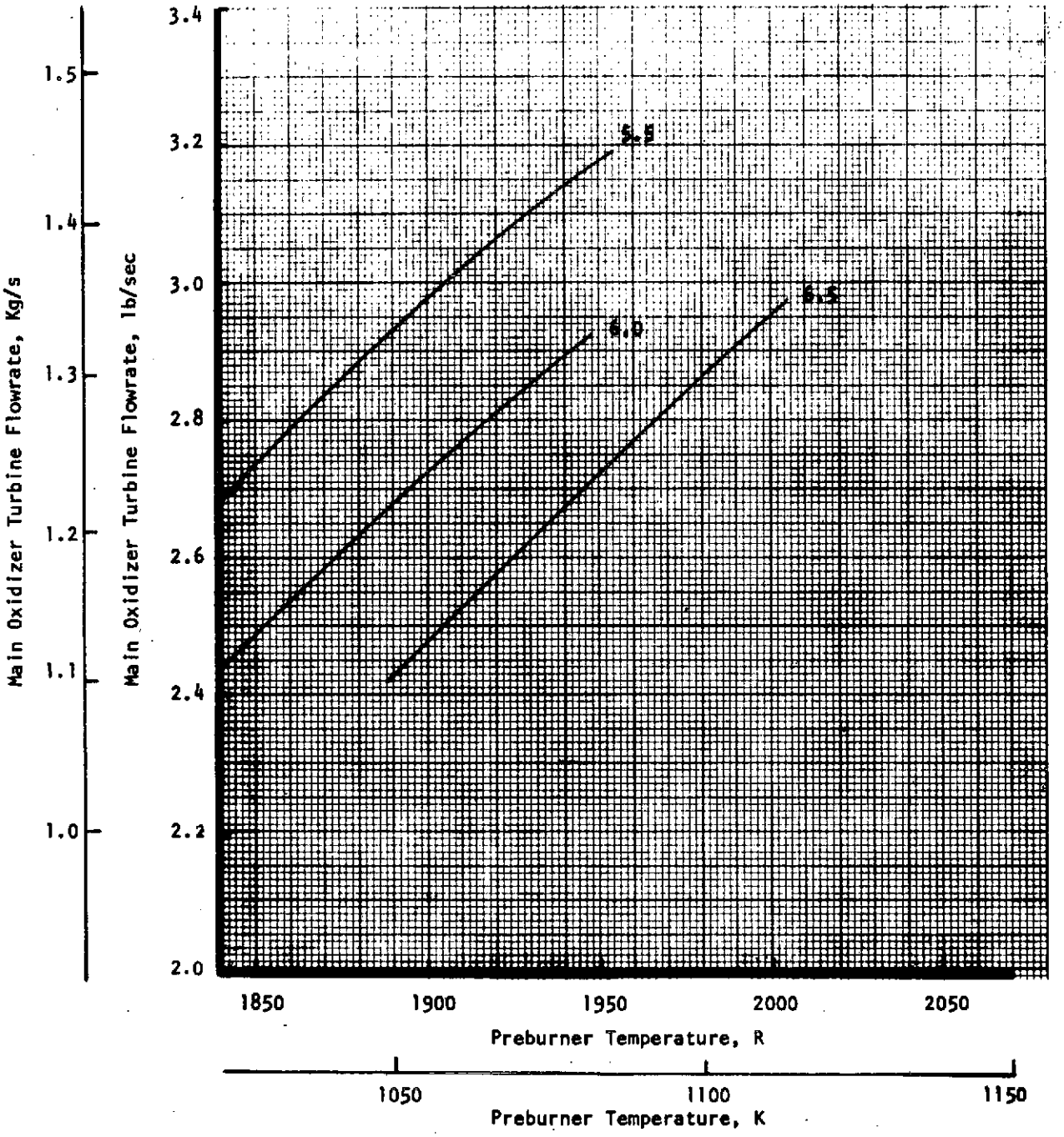

Figure 1-63. Main Oxidizer Turbine Flowrate vs Preburner Temperature

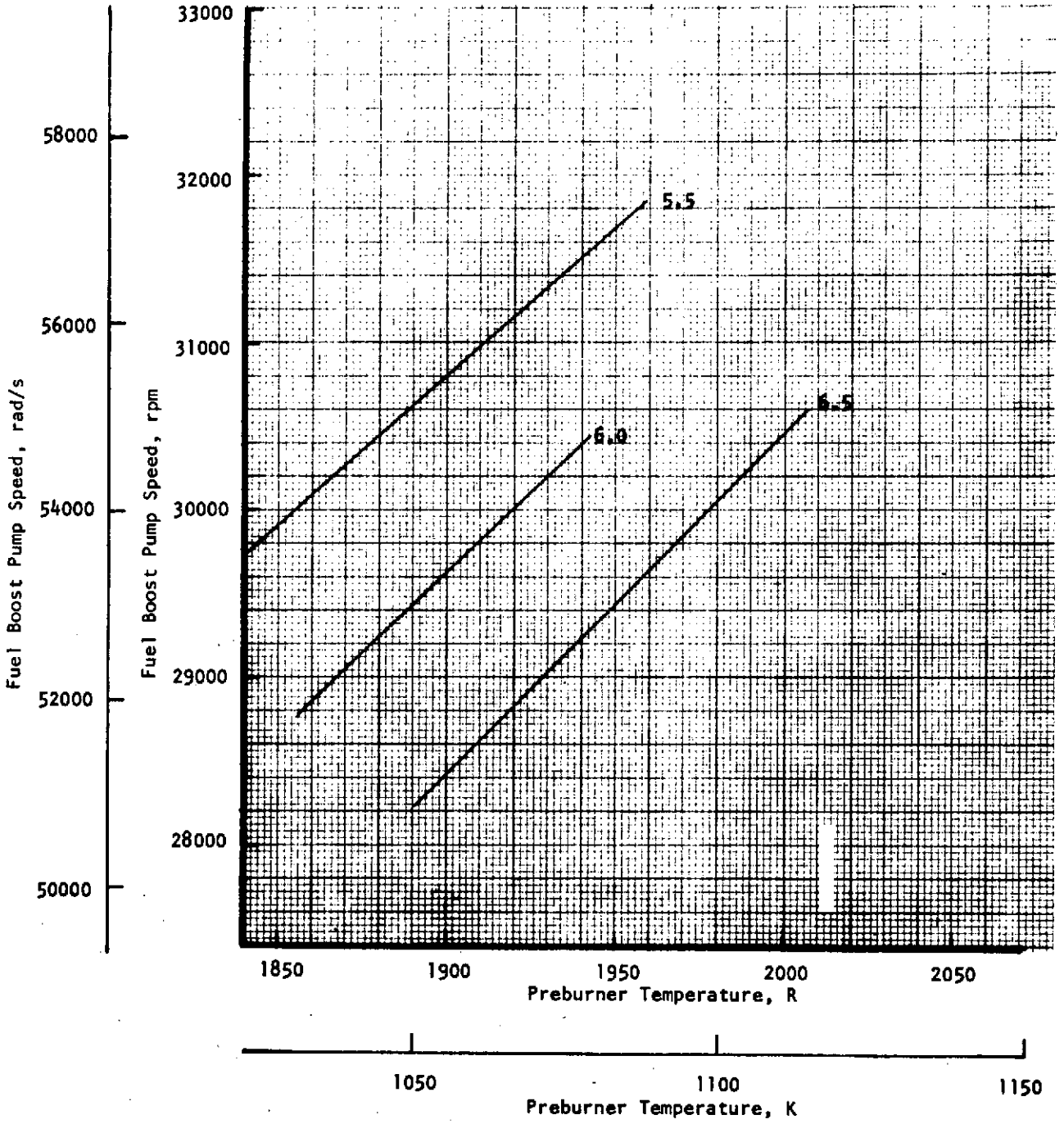

Figure 1-64. Fuel Boost Pump Speed vs Preburner Temperature

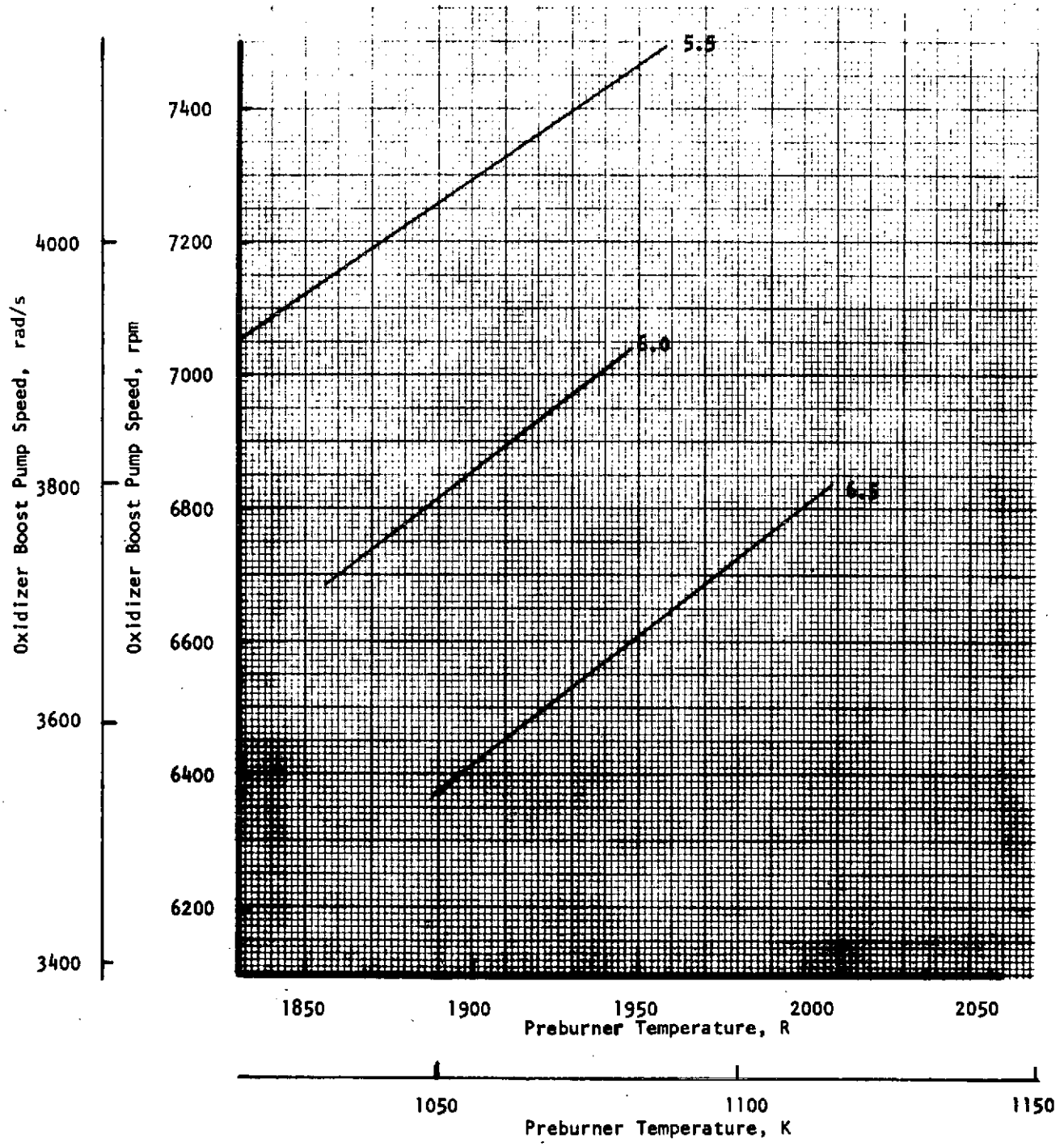

Figure 1-65. Oxidizer Boost Pump Speed vs Preburner Temperature

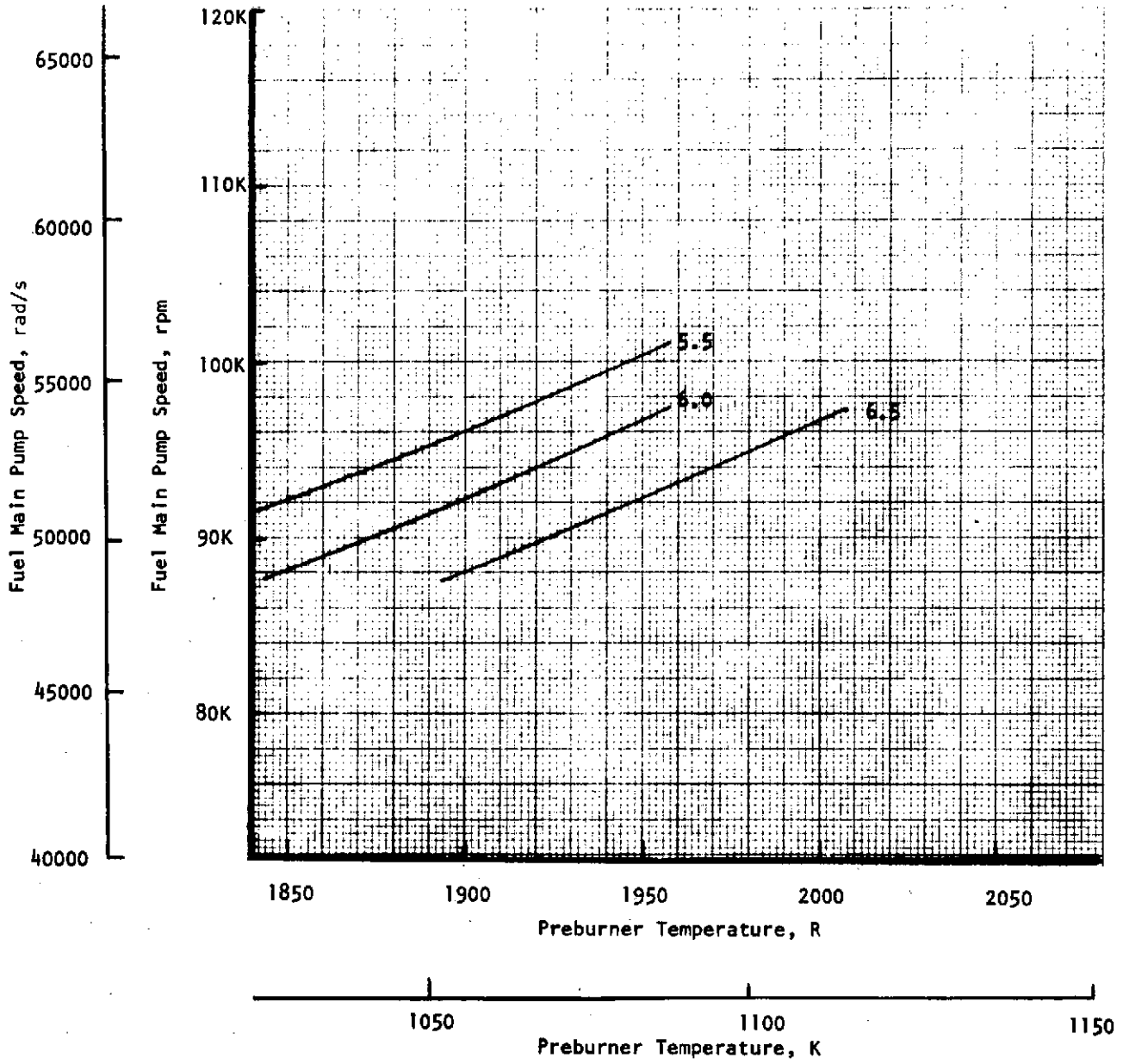

Figure 1-66. Fuel Main Pump Speed vs Preburner Temperature

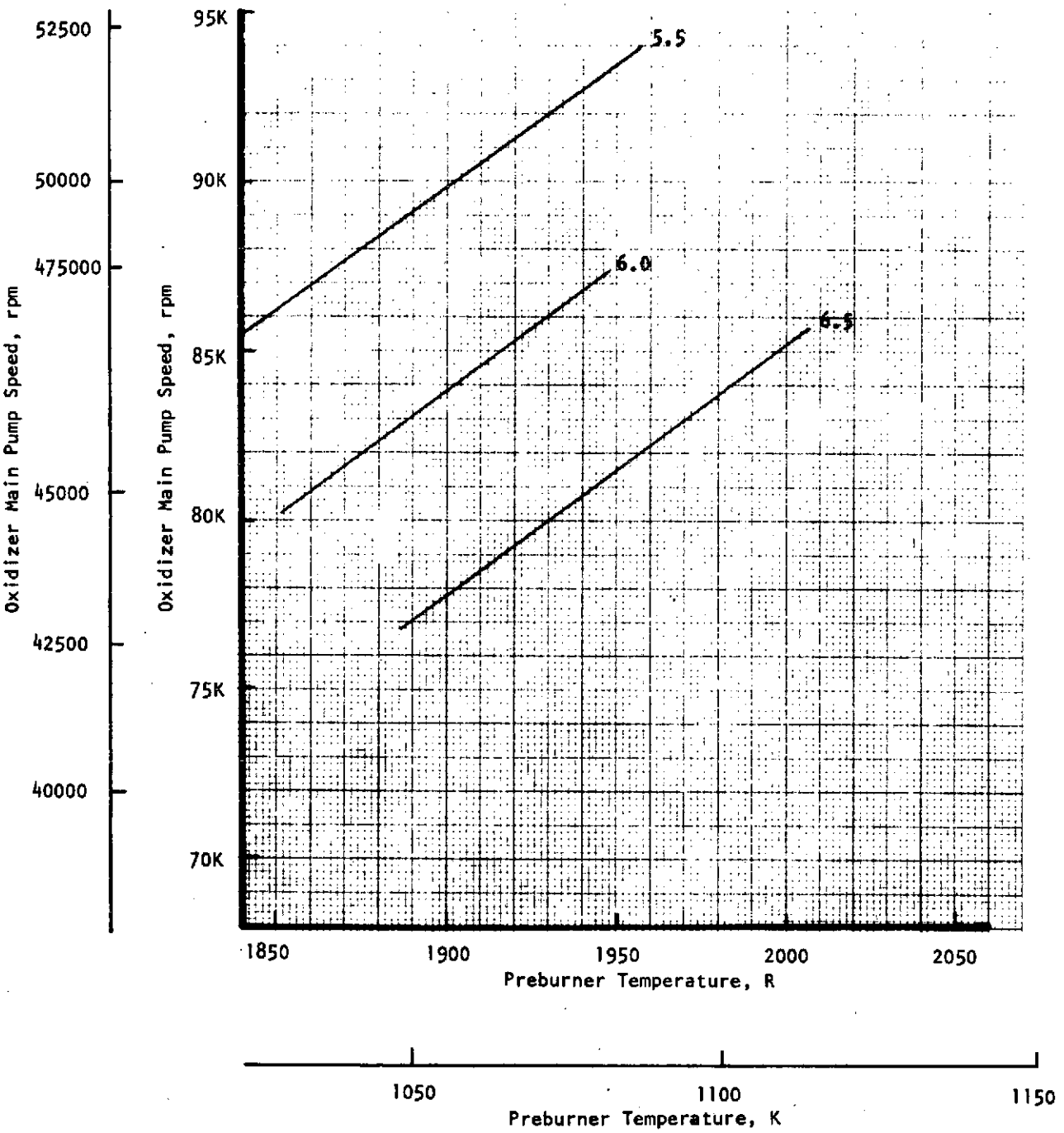

Figure 1-67. Oxidizer Main Pump Speed vs Preburner Temperature

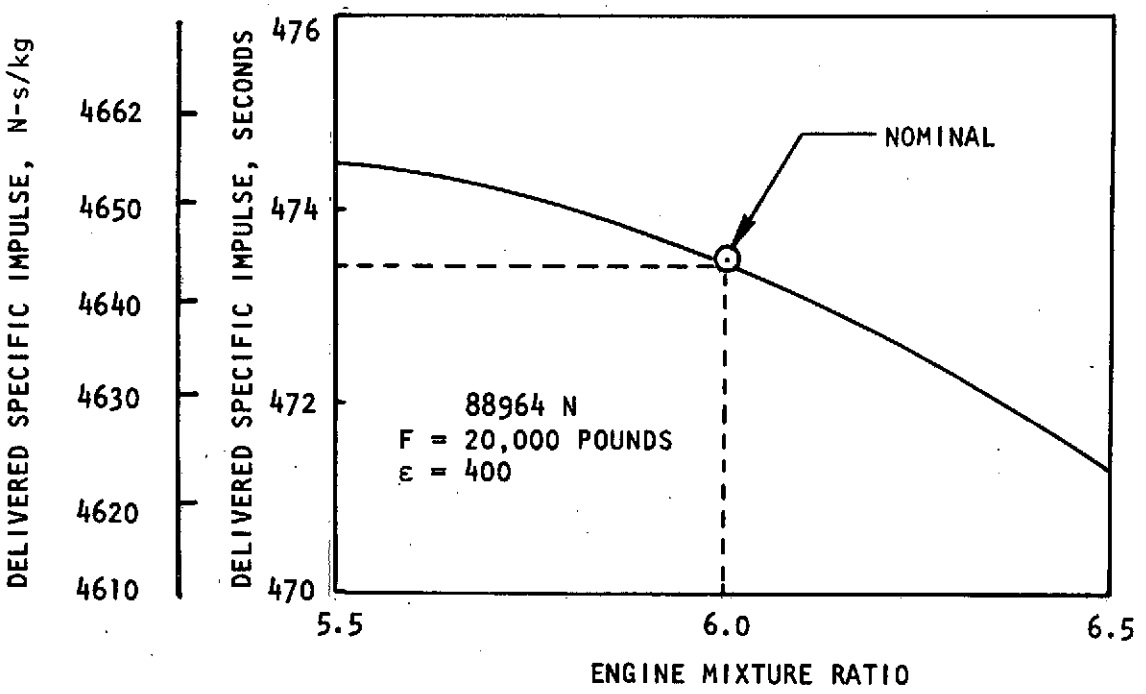

Figure 1-68. Performance Variation with Mixture Ratio

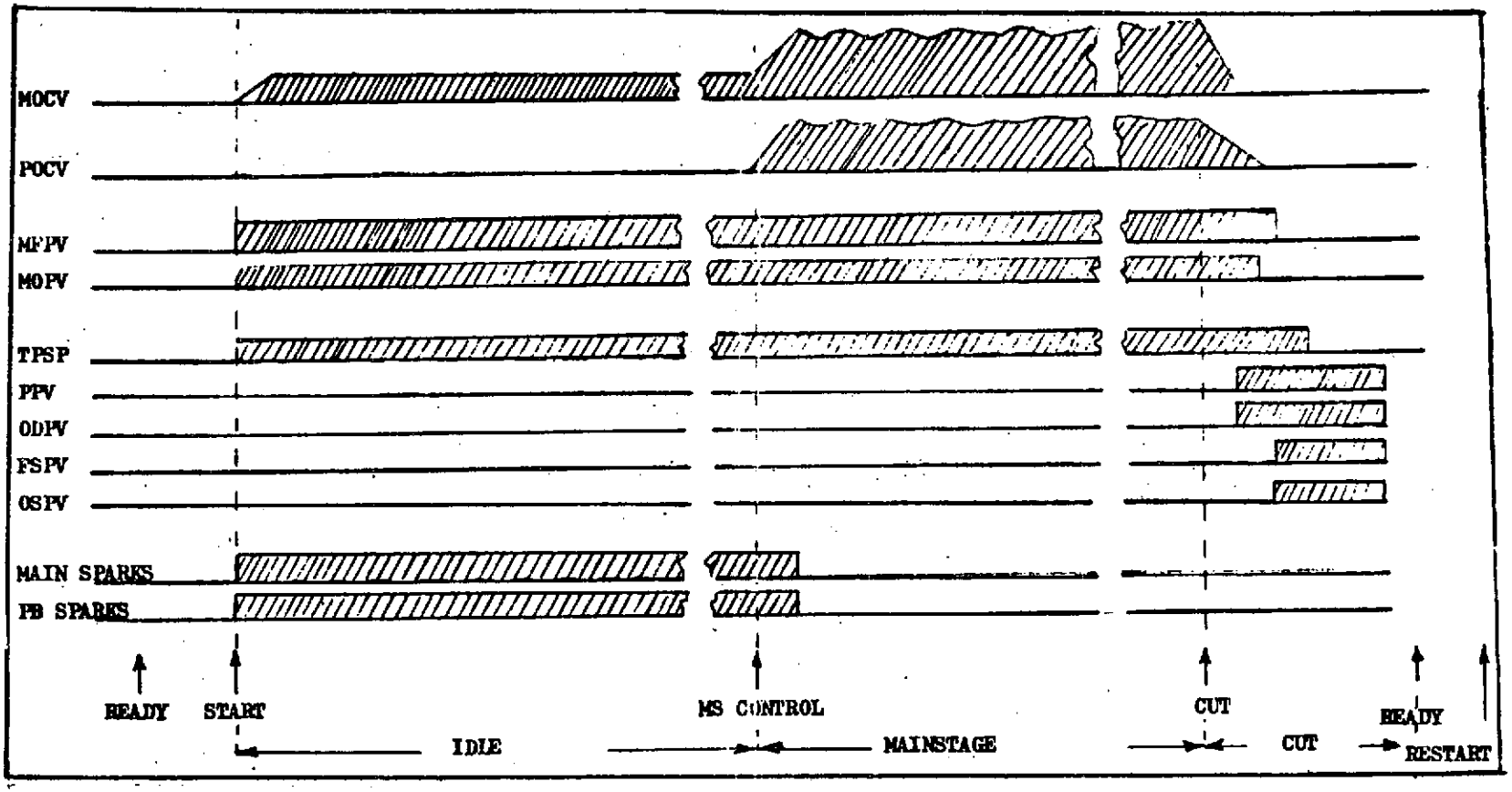

Figure 1-69. Engine Control Valve Sequening

suitable brake (e.g., magnetic or mechanical). A tank-head idle start is shown in Fig. 1-70. Propellant utilization for the tank-head idle start is summarized in Table 1-39 . By allowing the turbopumps to turn, the engine transitions into pump-fed idle as heat input to the thrust chamber coolant provides energy for the low-level operation of the boost pump and main pump turbines. The preburner oxidizer valve is closed for both tank-head and pump-fed idle. The pump-fed idle mode stabilizer for low-level engine operation ($P_c \approx 1{,}213{,}477$ N/m^2; 176 psia), for thermal conditioning prior to mainstage ramping, and for autogenous pressurization of the main propellant tanks. The powered idle mode start sequence is identical to the normal start sequence (shown in Fig. 1-71), except that P_c is stabilized once powered idle conditions are attained. The engine operates under closed-loop control for ramping from powered idle to mainstage. The entire normal start sequence is presented in Fig. 1-71, with the propellant utilization summarized in Table 1-40. Cutoff sequences and cutoff propellant utilization for nominal and tank-head idle are presented in Fig. 1-72 and 1-73, and in Tables 1-41 and 1-42. For cutoff, hydrogen is flowed after the termination of the oxidizer flow to provide a fuel-rich transient. The hydrogen flow time may shorten as long as hardware integrity is not compromised. During tank-head idle, the MOV is open only 1 percent. Since control variations could be large, it is proposed that a small bypass loop carry the idle flow, thus allowing the MOV to remain closed. It is anticipated that dispersions on transient performance will be small since: (1) valve positions are in relatively low gain regimes under open-loop control, and (2) closed-loop control may follow the reference curve arbitrarily close, depending on the quality of the controls.

As part of the dynamic model analyses, a propellant dump analysis was conducted. The time required to expel 408 kg (900 pounds) of liquid oxygen and 68 kg (150 pounds) of liquid hydrogen individually through the engine using tank vapor pressure was completed. Using the dynamic start model with appropriate simulation of propellant dump conditions, the respective LO_2/LH_2 average flowrates were determined to be 1.22 and 0.59 kg/s (2.7 and 1.3 lb/sec). Therefore, the required time to expel the total propellants required are 333 and 115 seconds, respectively

AUTOGENOUS PRESSURIZATION AND HEAT EXCHANGER DESIGN

Main Tank Pressurization

To minimize vehicle weight by eliminating the requirement for separate main tank pressurization, autogenous pressurization has been considered. The mainstage flowrates and temperatures for maintaining propellant tank pressures at levels required to maintain pump inlet NPSH requirements are shown below:

Pressurant	Temperature	Flowrate
Hydrogen	400 R (222 K)	0.034 lb/sec (0.0154 kg/s)
Oxygen	400 R (222 K)	0.134 lb/sec (0.0608 kg/s)

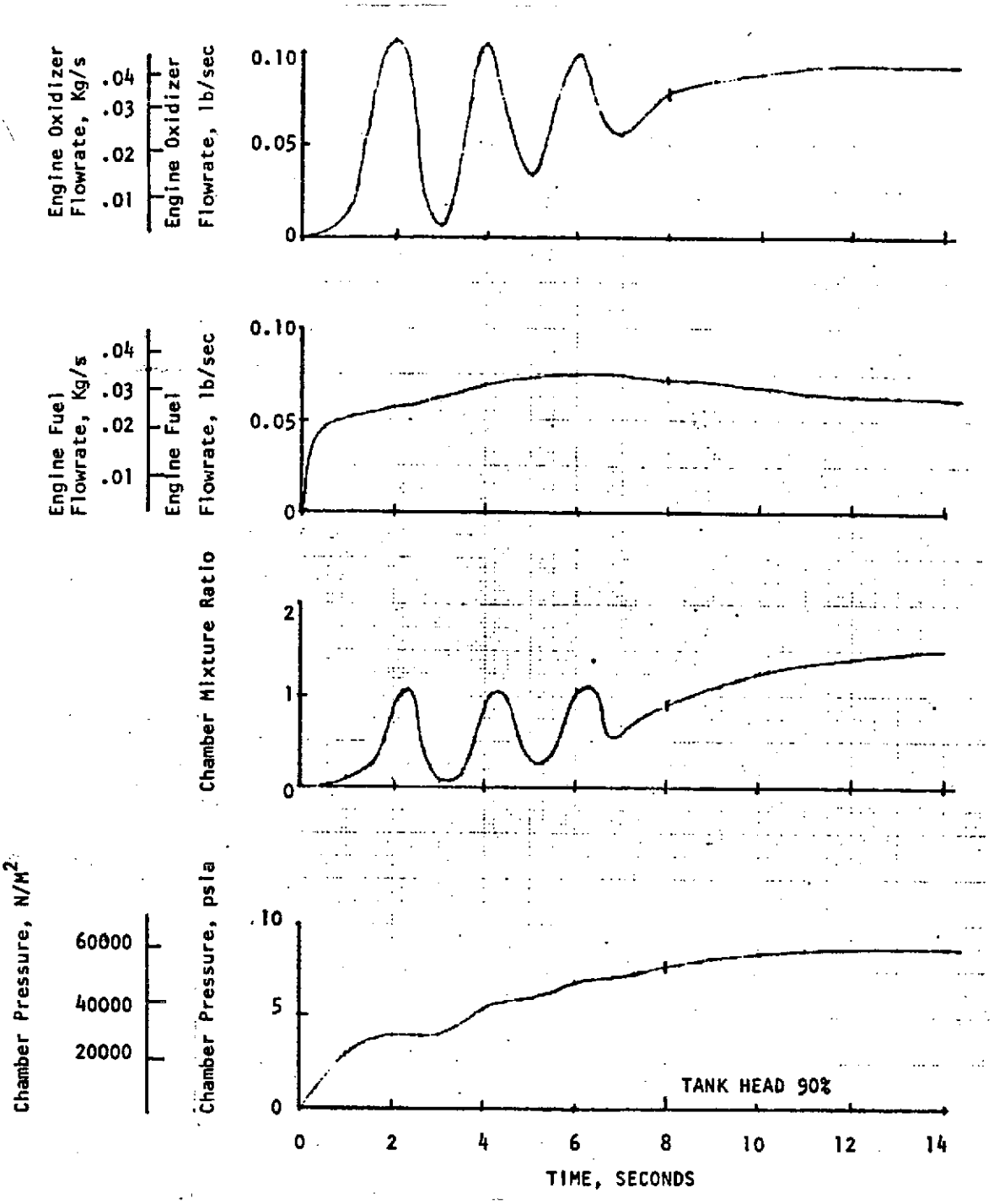

Figure 1-70. Tank-Head Engine Start

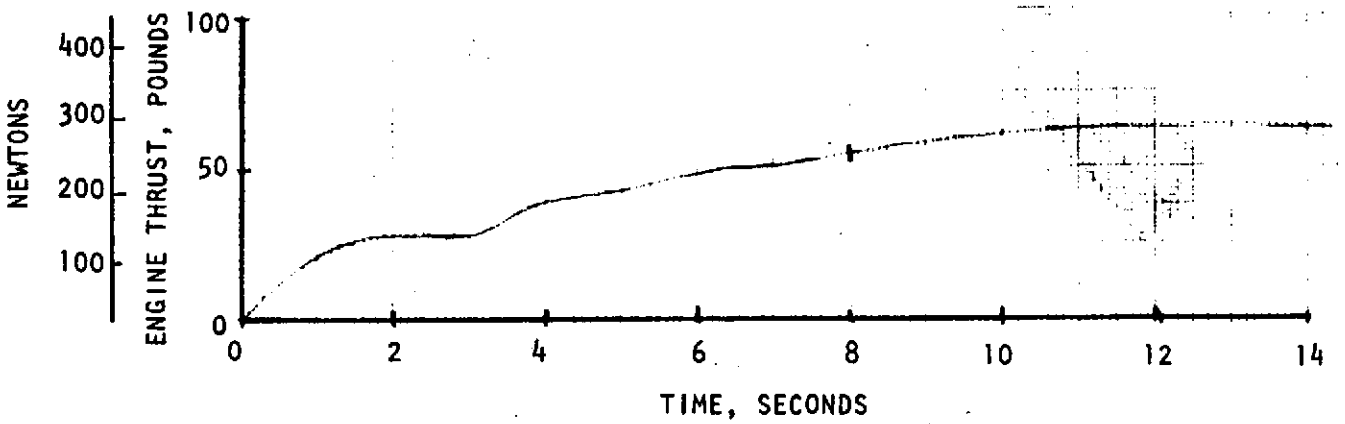

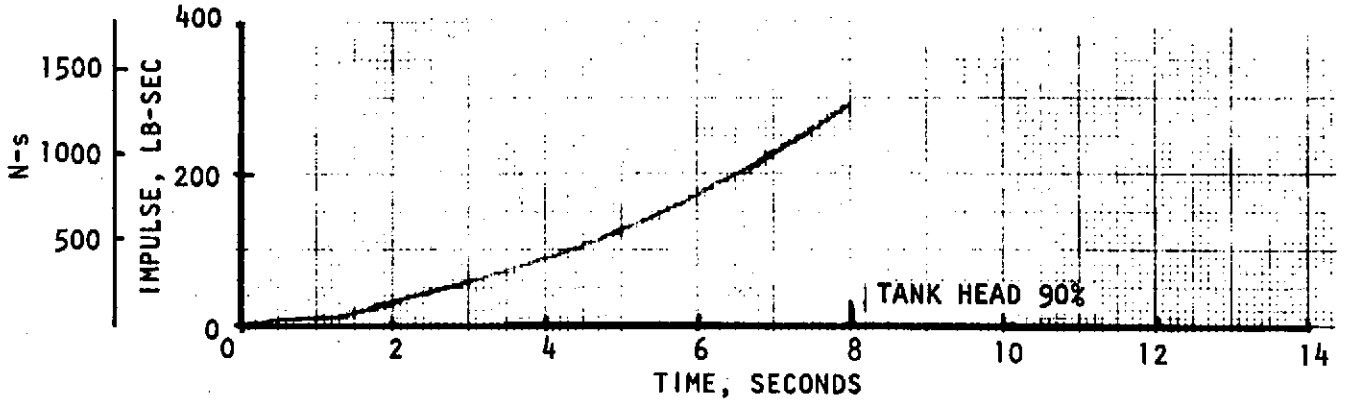

Figure 1-70. (concluded)

TABLE 1-38. CONTROL SYSTEM ABBREVIATIONS

MFPV	-	Main Fuel Pilot Valve
MOPV	-	Main Oxidizer Pilot Valve
MOCV	-	Main Oxidizer Control Valve
POCV	-	Preburner Oxidizer Control Valve
PPV	-	Preburner Purge Valve
ODPV	-	Oxidizer Dome Purge Valve
FSPV	-	Fuel System Purge Valve
OSPV	-	Oxidizer System Purge Valve
PI 1	-	Preburner Igniter No. 1
PI 2	-	Preburner Igniter No. 2
MI 1	-	Main Igniter No. 1
MI 2	-	Main Igniter No. 2
TPSP	-	Turbopump Seal Purge

TABLE 1-39. TANK-HEAD START SEQUENCE PROPELLANT UTILIZATION

Total Impulse		
	Cold Start	294 lb-sec (1308 N-s)
Hydrogen Flow		
	Cold Start	0.51 lb (0.231 kg)
Oxygen Flow		
	Cold Start	0.48 lb (0.218 kg)

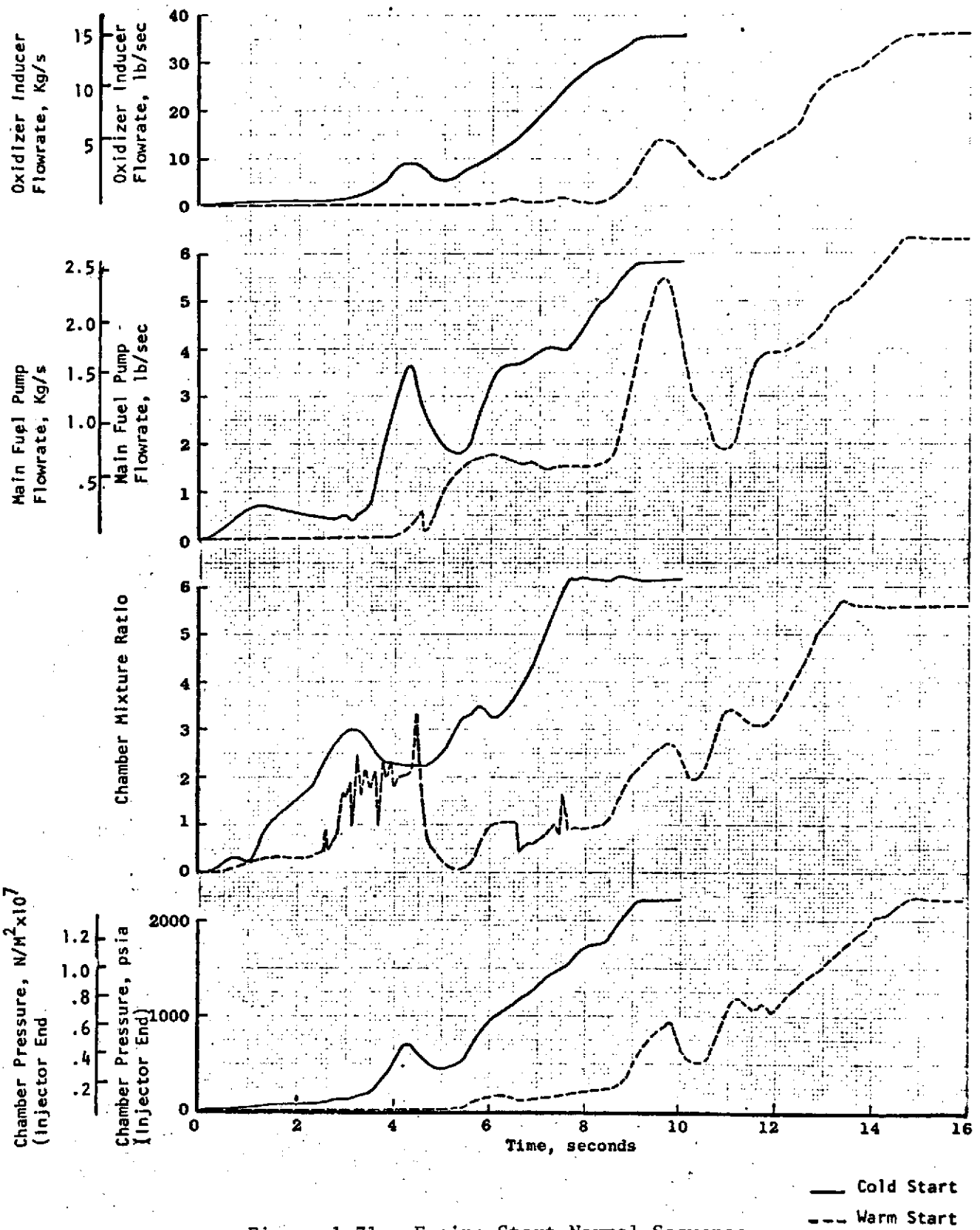

Figure 1-71. Engine Start Normal Sequence

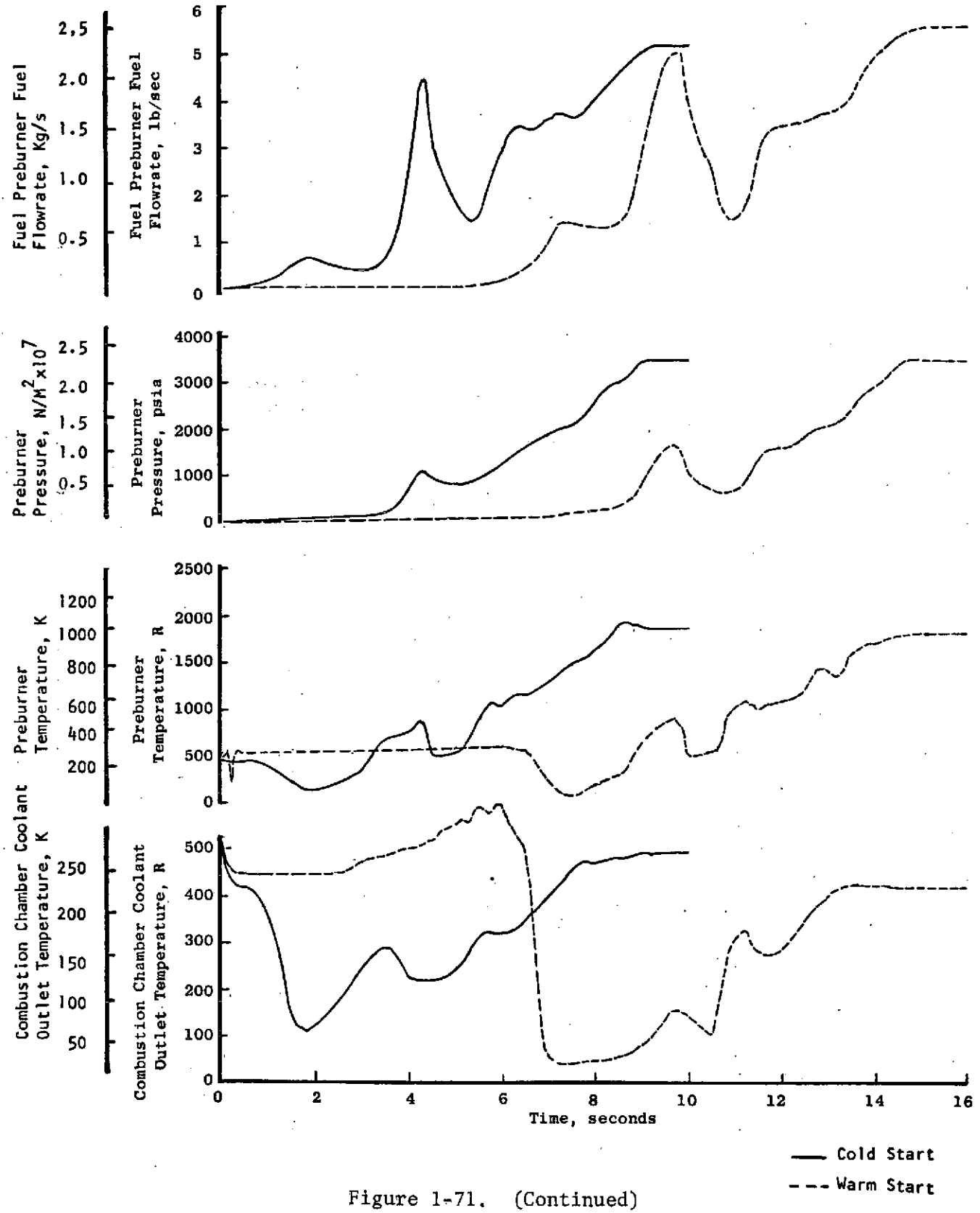

Figure 1-71. (Continued)

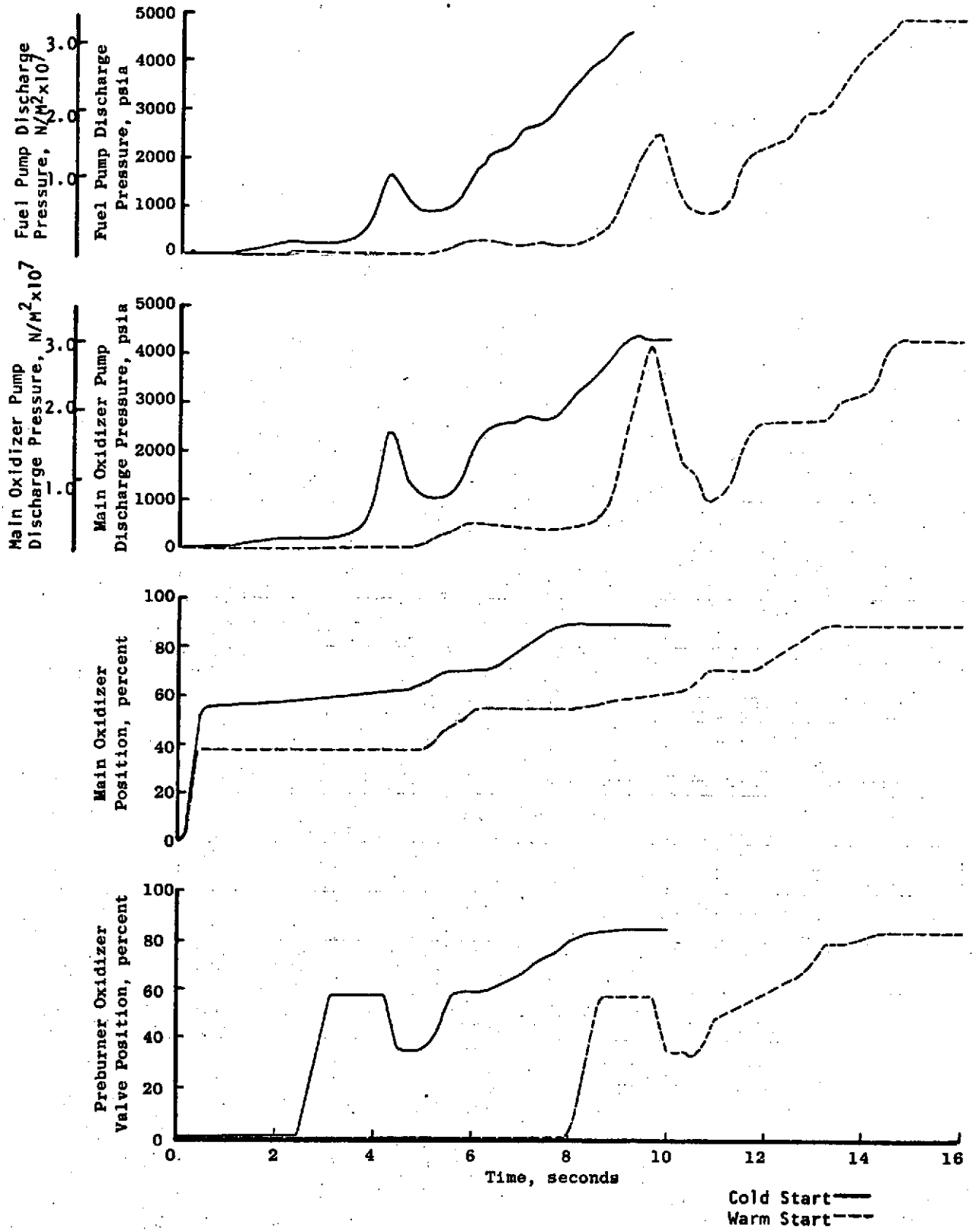

Figure 1-71. (Continued)

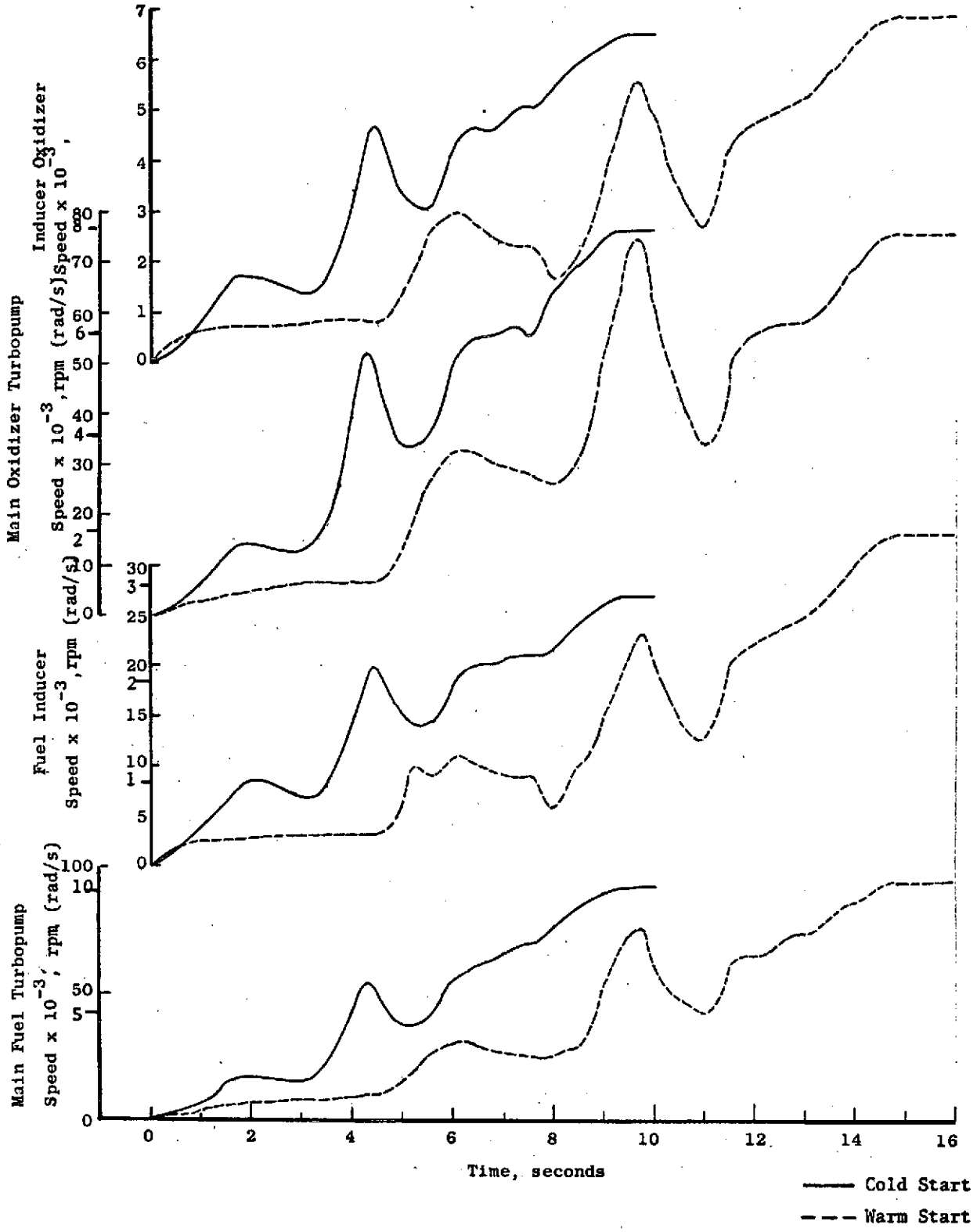

Figure 1-71. (Concluded)

TABLE 1-40. NORMAL START SEQUENCE PROPELLANT UTILIZATION

Total Impulse	
Cold Start	46,500 lb-sec (206,842 N-s)
Warm Start	51,900 lb-sec (230,863 N-s)
Hydrogen Flow	
Cold Start	19.4 lb (8.8 kg)
Warm Start	27.2 lb (12.3 kg)
Oxygen Flow	
Cold Start	80.0 lb (36.3 kg)
Warm Start	83.9 lb (38.1 kg)

TABLE 1-41. TANK-HEAD CUTOFF SEQUENCE PROPELLANT UTILIZATION

Total Impulse	10 lb-sec (44.5 N-s)
Hydrogen Flow	0.01 lb (0.0045 kg)
Oxygen Flow	0.01 lb (0.0045 kg)

TABLE 1-42. NORMAL CUTOFF SEQUENCE PROPELLANT UTILIZATION

Total Impulse	2640 lb-sec (11743 N-s)
Hydrogen Flow	3.65 lb (1.66 kg)
Oxygen Flow	3.72 lb (1.69 kg)

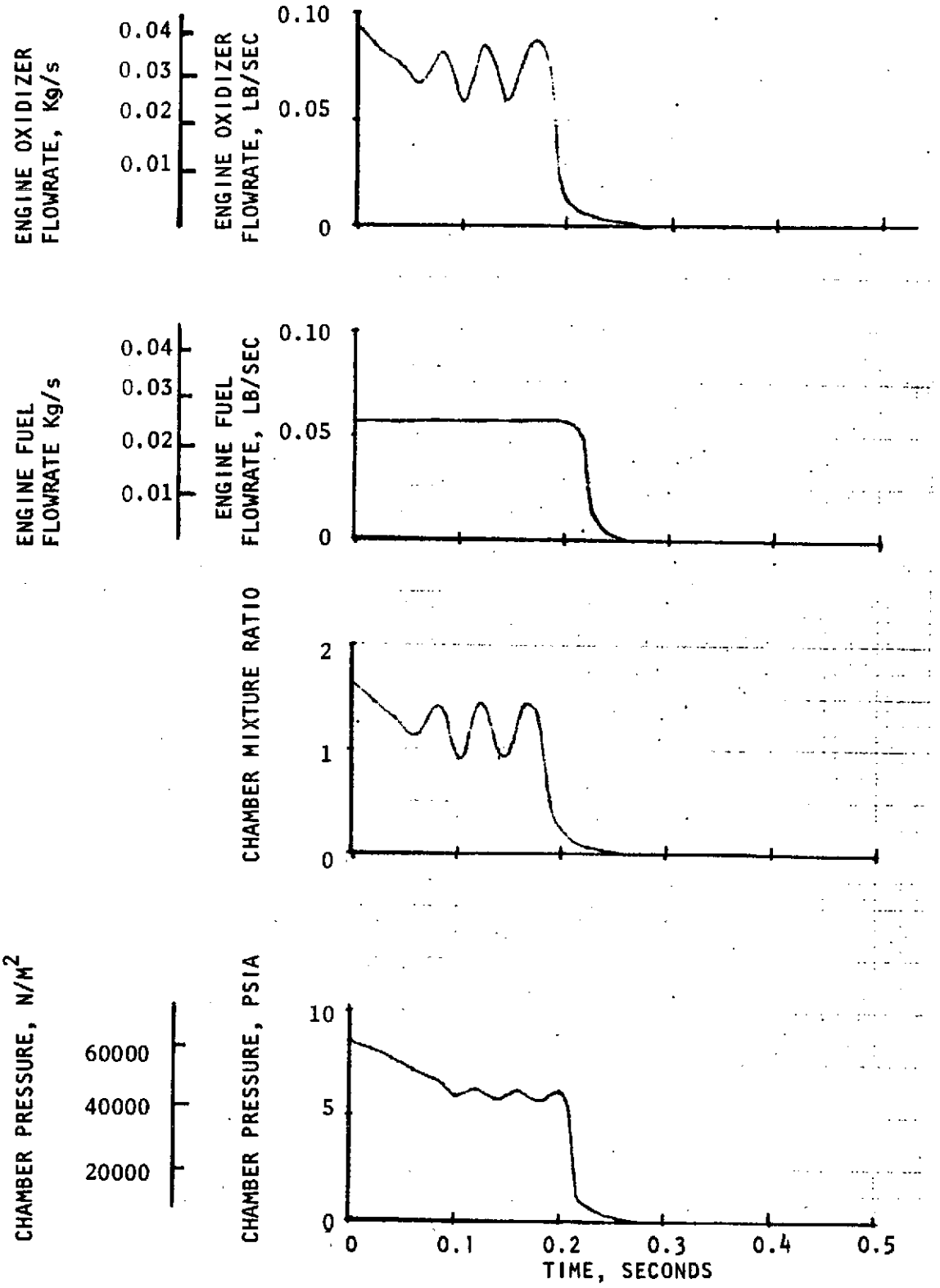

Figure 1-72. Tank-Head Idle Cutoff Sequence

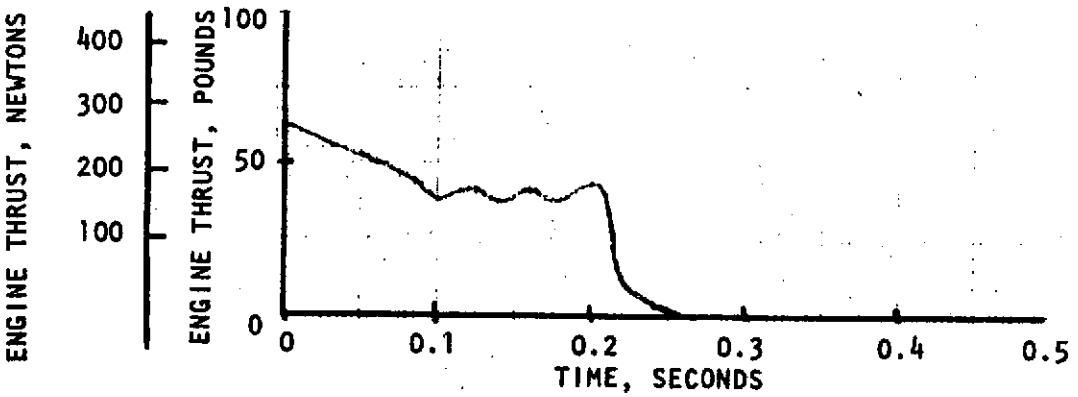

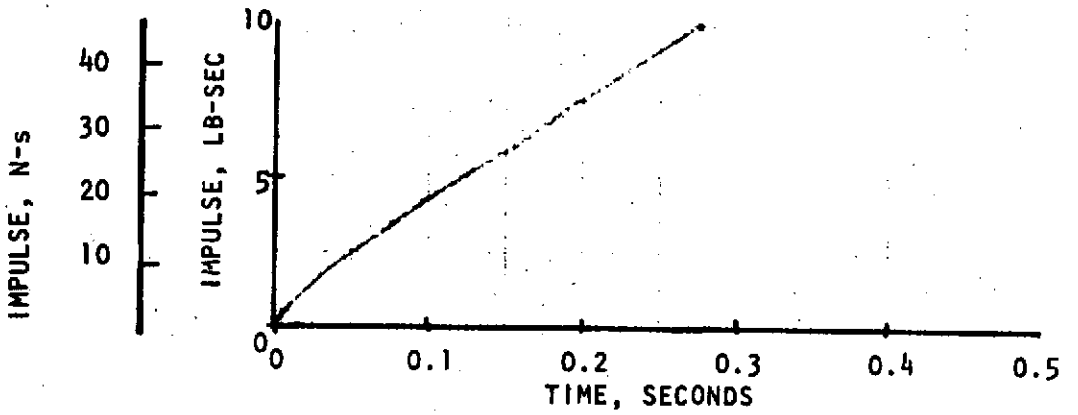

Figure 1-72. (Concluded)

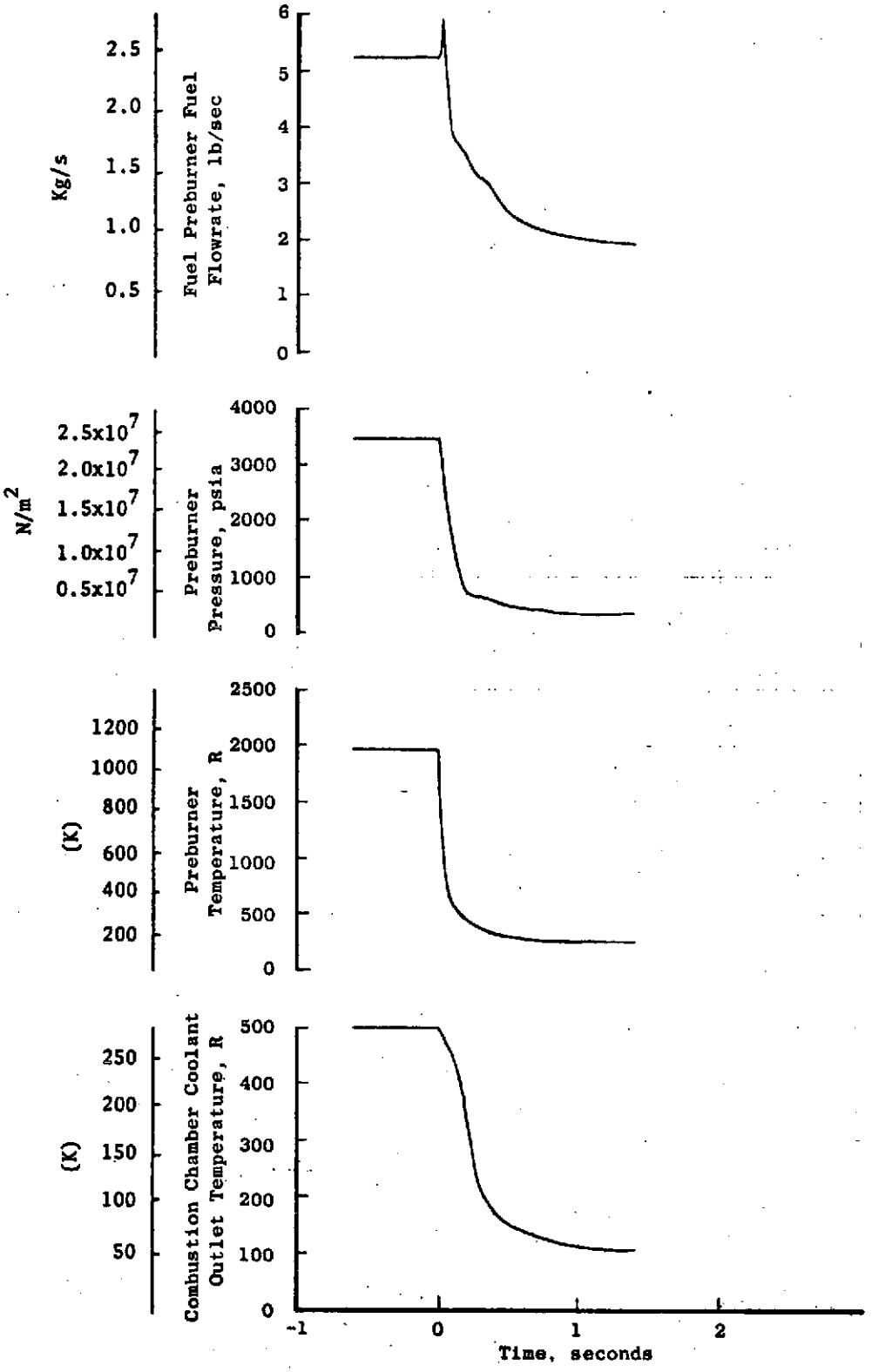

Figure 1-73. Engine Cutoff Normal Sequence

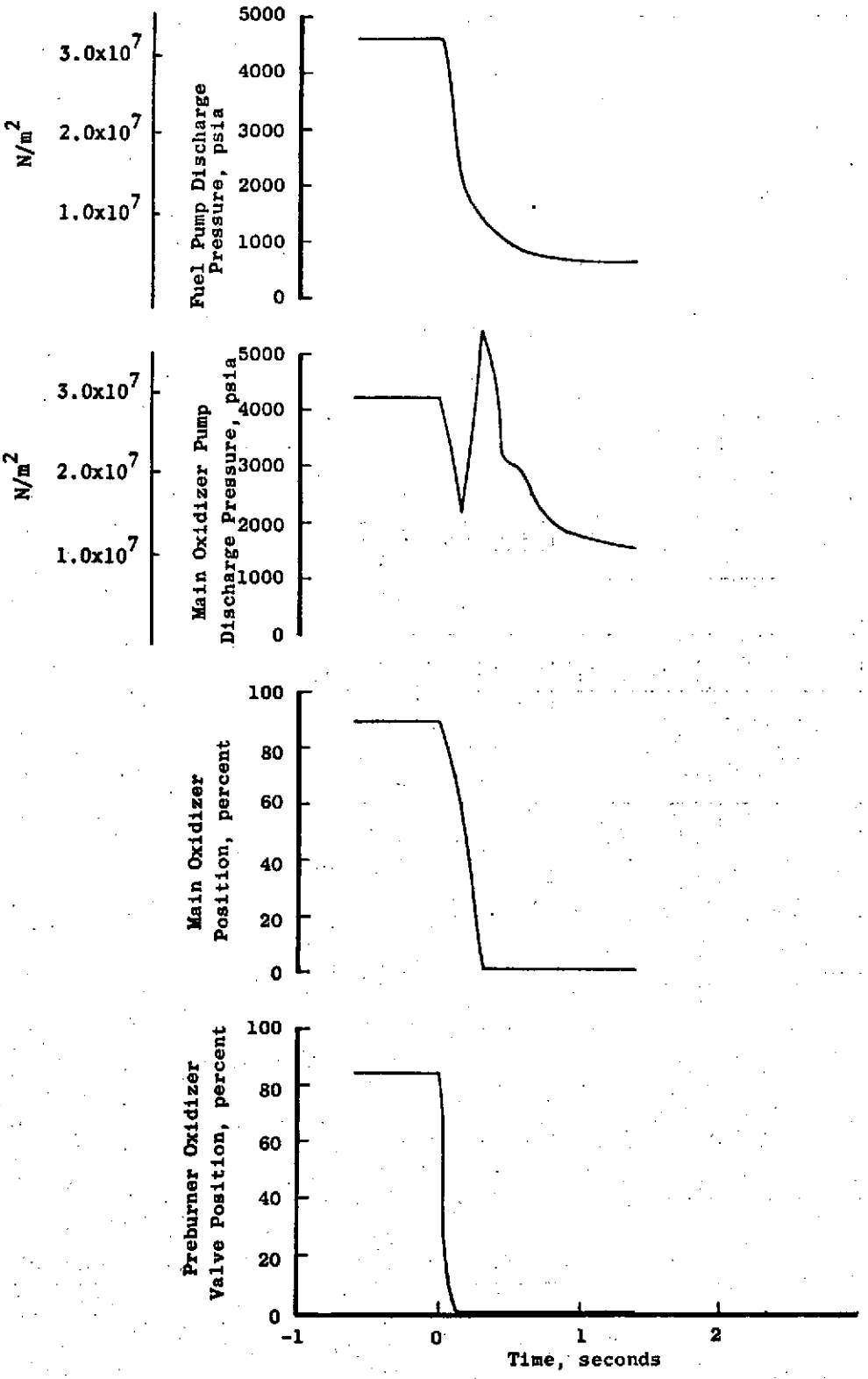

Figure 1-73. (Continued)

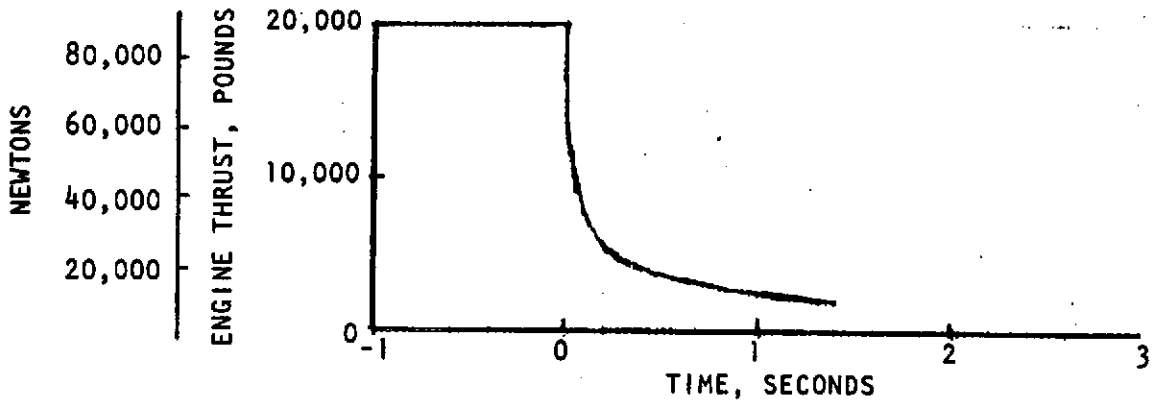

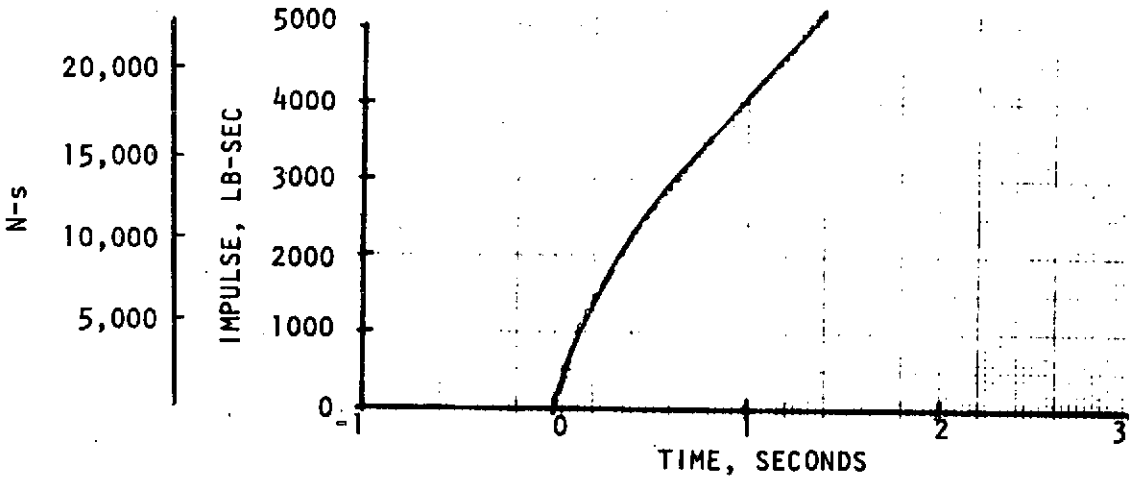

Figure 1-73. (Concluded)

Utilizing hydrogen which has passed through the combustion chamber cooling jacket (278 K; 500 R), the main fuel tank pressurization is readily provided. In addition, by placing a heat exchanger around the main oxidizer turbine inlet hot-gas duct, heating of oxygen bled off the main oxidizer pump discharge can be readily conducted to provide the main oxidizer tank pressurization. The ability of the engine to provide sufficient pressurization at a suitable temperature during idle mode operation will require more investigation. A key factor in determining this capability is the pressurization flowrate requirements that need to be defined. Flowrates of less than 0.0454 kg/s (0.1 lb/sec) appear to be practical in terms of engine operation. The temperature of the hydrogen leaving the cooling jacket during idle mode is a function of main chamber idle mode mixture ratio which, in turn, is controlled by the positioning of the main oxidizer control valve. As shown in Fig. 1-74, the exit temperature of the hydrogen can be controlled but with direct effect on idle mode chamber pressure. This investigation should be extended into experimental testing to demonstrate the feasibility of autogenous pressurization during idle mode operation.

Heat Exchanger

The heat exchanger design shown in Fig. 1-75 consists of a tube wrapped around the oxidizer turbine feed duct. An alternative design initially considered was of a counterflow concentric tube configuration. The coiled tube configuration has a lower pressure drop and, therefore, may be desirable. To finalize the heat exchanger design will require further definition of the autogenous pressurization of the main tanks, particularly during idle mode operation. The coil design currently appears to be the preferable approach. It has nine turns of 0.559 cm (0.220 in.) diameter by 0.081 cm (0.032 in.) wall tube wrapped around and brazed to a section of preburner discharge duct. The duct incorporates annular grooves to enhance surface contact and, therefore, heat transfer. The assembly is welded on the main preburner discharge duct. The external heat exchanger concept provides a significant safety margin as compared to concepts internal to the hot-gas duct. The oxidizer is supplied to the heat exchanger from the oxidizer main turbopump discharge and controlled by the antiflood valve to prevent backflow into the engine. The exit of the coil is located at the customer connect interface. It is anticipated that the actual flow control will be provided by the vehicle tank regulator.

ENGINE PACKAGING

The engine packaging arrangement shown in Fig. 1-76 and 1-77 is based on the close coupling of all components. The result is a small, complete package with a forward center of gravity location, minimizing the gimbaled mass. Physical positioning of components was determined by mounting components of the feed system and exhaust ducting considering thermal expansion/contraction and pressure losses. The main turbopumps are mounted to the thrust chamber and supported by the turbine discharge ducts. The boost turbopumps are mounted by attaching the pump discharge to the main pump inlet, while the propellant feed system lines act as additional supports and help to damp vibrations.

The single preburner is close coupled to the main fuel turbine hot-gas inlet ducting. The other preburner discharge duct is routed around the thrust chamber

POWERED IDLE-MODE WITH P. B. IGNITION

PBOV CLOSED

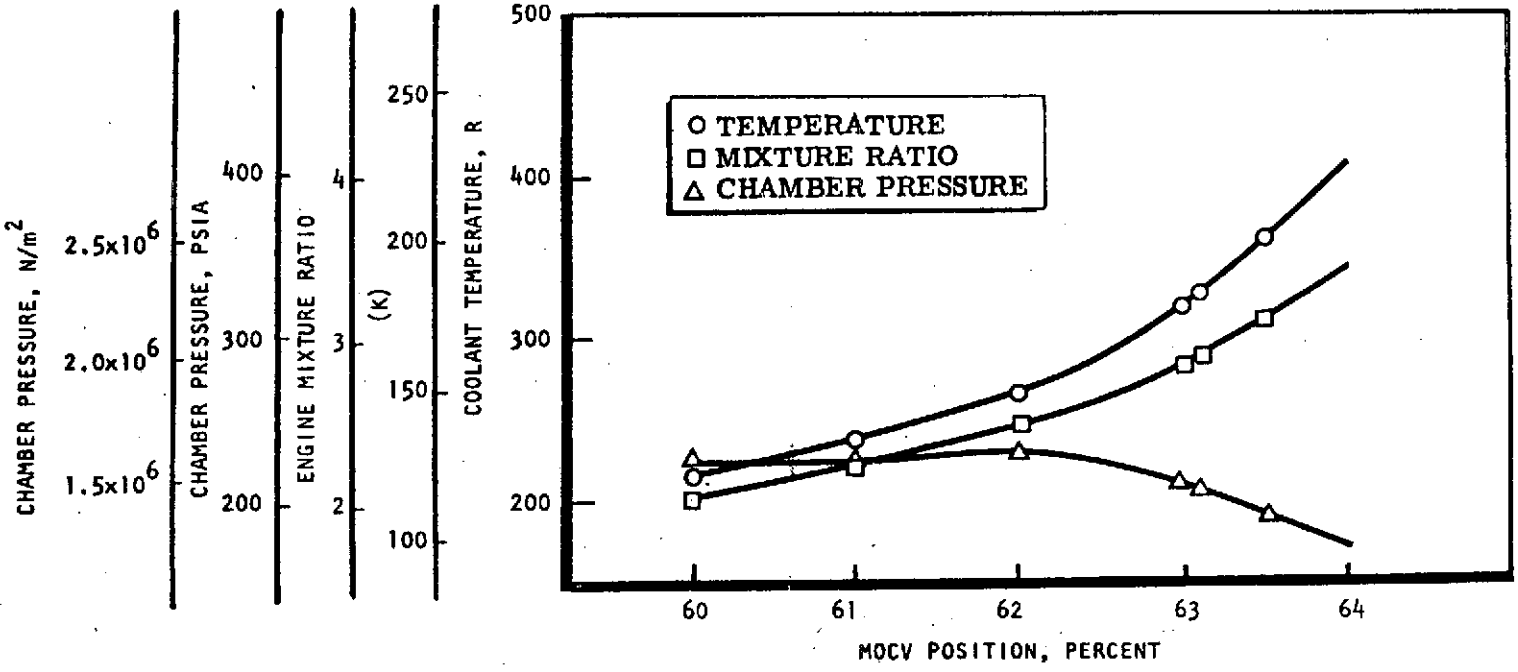

Figure 1-74. Influence of MOCV Position During Idle Mode

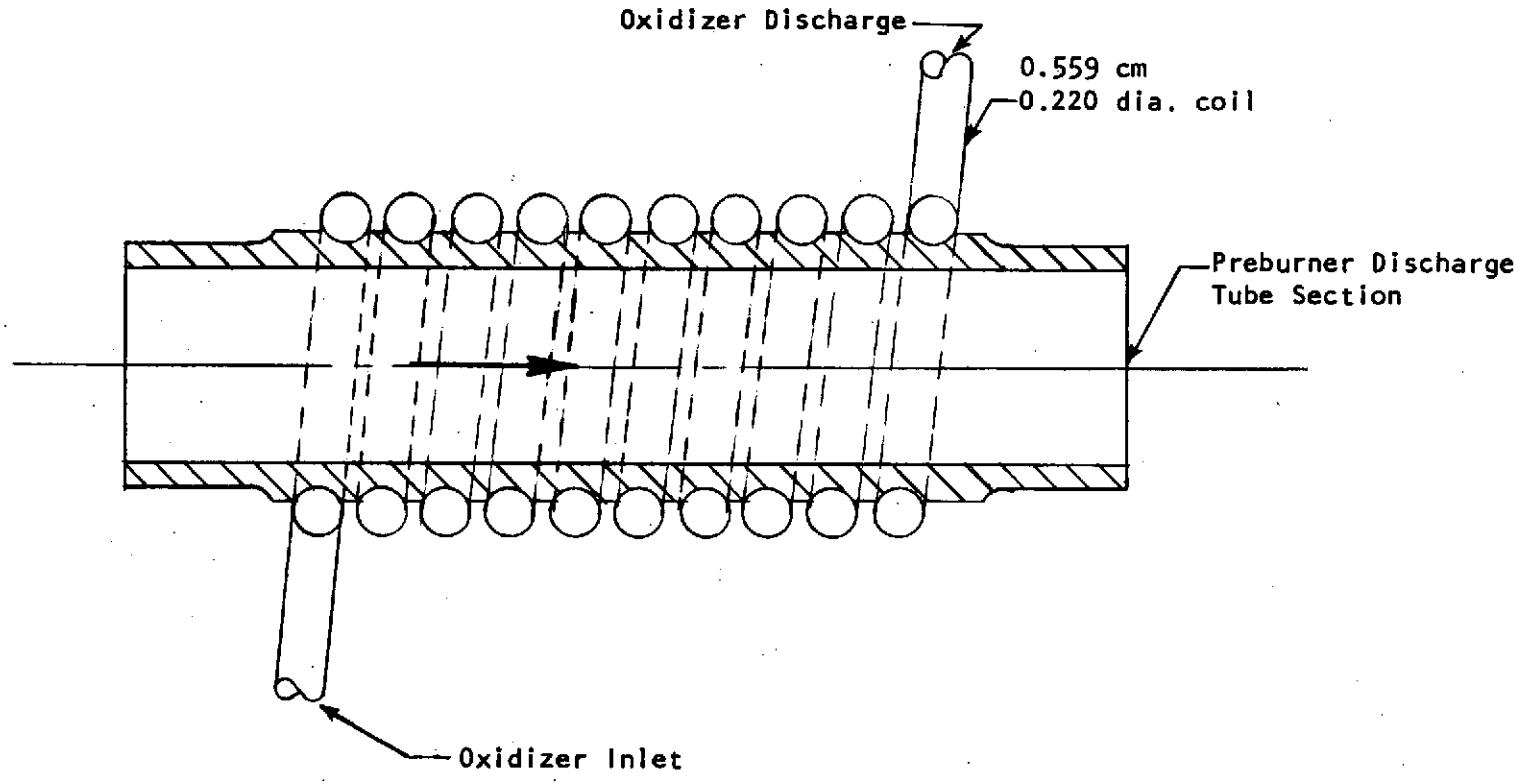

Figure 1-75. LO_2 Heat Exchanger Design

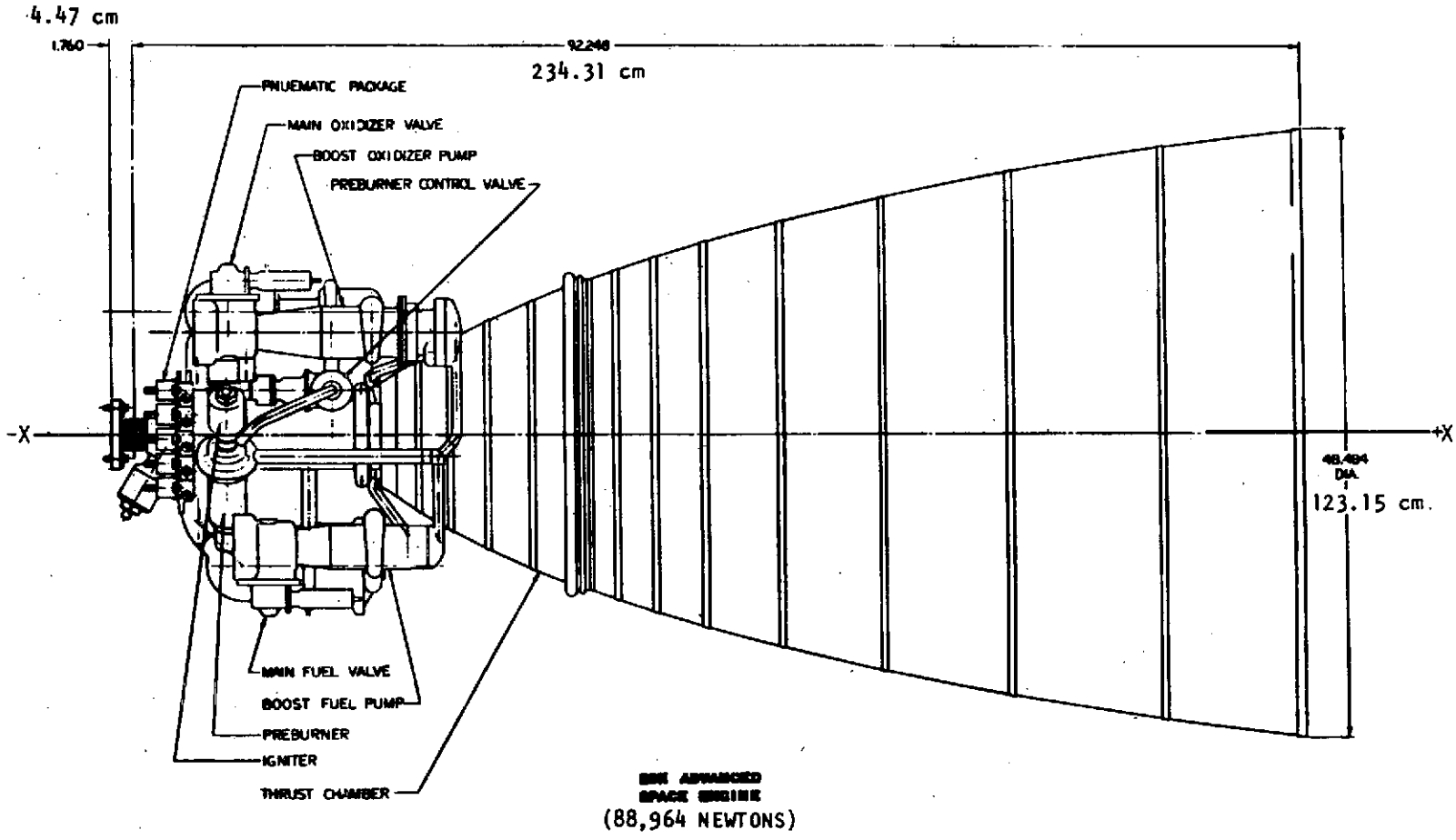

Figure 1-76. Advanced Space Engine Showing X-Axis

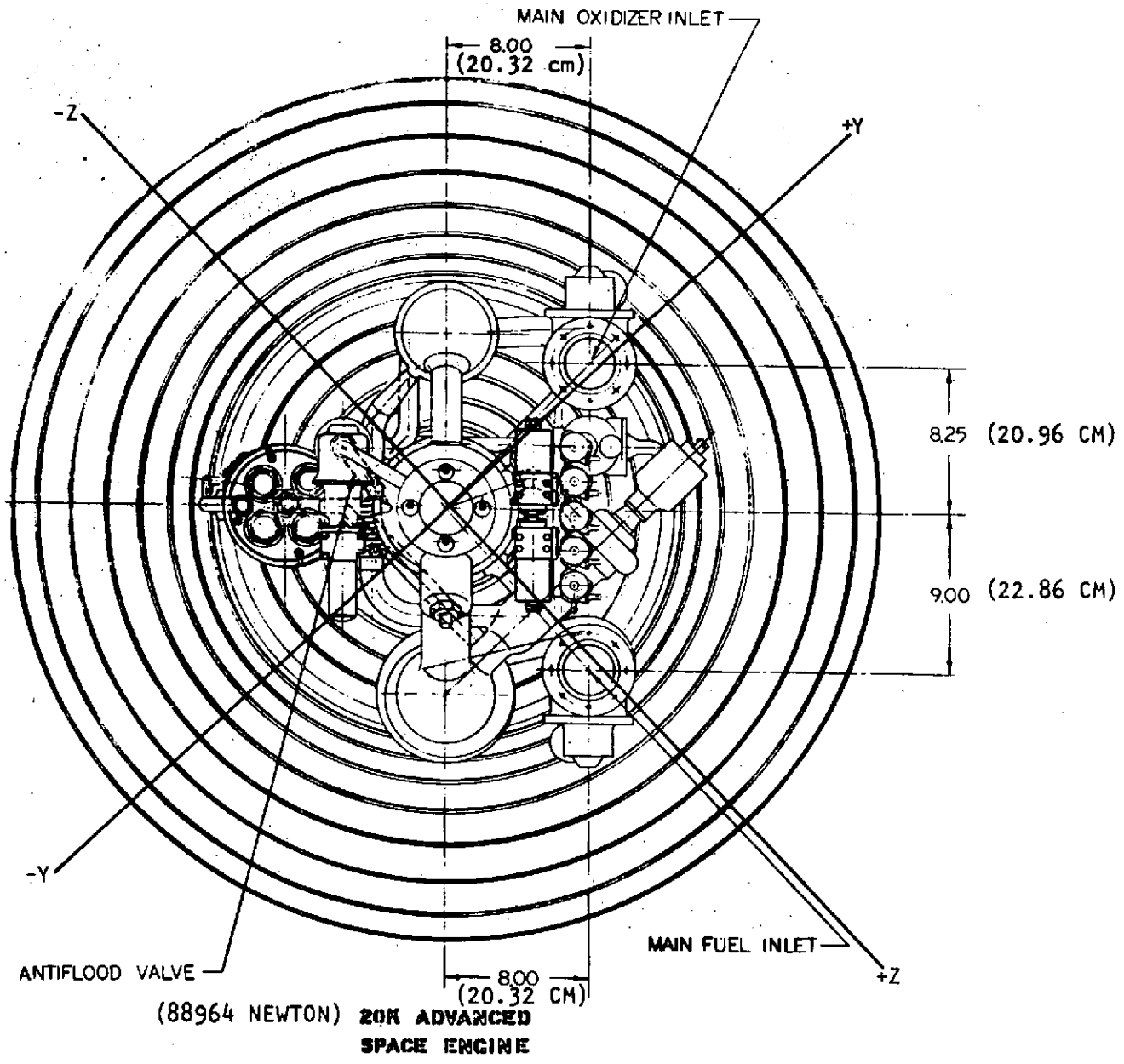

Figure 1-77. Advanced Space Engine, Aft View Showing Y- and Z-Axes

to the oxidizer turbine inlet. Oxidizer tank pressurization gas heat exchanger is located around the oxidizer turbine inlet duct.

All valves are line mounted, eliminating the need for additional supports and flexible bellows sections. Bellows used at this pressure become extremely rigid and may cause asymmetric loads if misaligned when installed. The entire system is in-place welded, eliminating heavy flanges, bolts, seal leakage problems, and thermal stress problems caused by flanged joints. Sufficient space is provided between components for the appropriate welding and removal equipment.

The pneumatic control system and electrical panel is located at the forward end of the engine for convenient interface accessibility. Provisions for thrust vector actuators are made by adding clevis attachments to the forward nozzle thrust chamber fuel manifold. Sufficient clearance is provided for gimbal actuators by appropriate location of engine system components.

STRUCTURAL ANALYSIS

The preliminary design structural analysis has been completed and a design evolved that will satisfy all service requirements and design criteria. Final details will be established through a final analysis during detail design. Materials to be used, operating temperatures, and mechanical properties are tabulated in Table B-1 of Appendix B. The criteria for yield safety factor, ultimate safety factor, fatigue, and stress rupture in Appendixes A and B have been followed.

The engine structural design criteria are stress level and life capability. Safety factors applied to stress and life are consistent with an engine that is to be man rated. The yield safety factor was computed by comparing the primary effective stress with the material minimum guaranteed yield strength at the maximum expected operating temperature. Yielding due to secondary stresses which are deflection-limited is controlled by the ultimate and/or fatigue safety factor.

The ultimate safety factor criteria is a factor of 1.4 on the stresses or strains that would cause failure whether the failure mode is tensile ultimate, creep rupture, buckling, or fatigue. The ultimate safety factor was computed by comparing: (1) the effective primary stress with the material ultimate failure strength, and/or (2) the effective peak strain with the material available elongation and low-cycle fatigue properties.

All pressure vessels in the engine were designed in accordance with the following structural verification criteria:

Proof Pressure = 1.2 x limit pressure at design temperature
Burst Pressure = 1.5 x limit pressure at design temperature
Limit Pressure = maximum expected operating pressure, including surges

Each subcomponent of the engine was analyzed to determine the required material thicknesses and the optimum shapes. The engine system was analyzed to determine required intercomponent connections and gimbal actuation requirements.

During the design of the engine system interconnects and major components, special attention was given to avoiding the consequences of hydrogen embrittlement. The alternative methods are:

1. Utilize materials shown to be not susceptible to embrittlement under conditions imposed.

2. Design to keep the stress levels low in those areas where the components will be in contact with hydrogen near room temperature.

3. In fabricated structures using welds, configure design so that welds are in low stress areas.

4. Pre-stress the component to above the yield point. This can be done with some parts, such as impellers, rotors, and pressures vessels, but is impractical for many structural parts.

5. Overlay the affected part with a coating of material that is not susceptible to hydrogen embrittlement, such as Incoloy 88 or copper.

The materials utilized in each major application, the environmental temperature, and corresponding material properties, as presented in Appendix B, are in conformance with the extensive materials investigations currently in process for the SSME.

ENGINE WEIGHT, CENTER OF GRAVITY, AND MOMENT OF INERTIA

Following major component design and final engine packaging, the physical characteristics of the engine were determined. The weight of the individual components was assessed and the total engine weight was determined as shown in Table 1-43 . Based on component mass distributions about the engine, the moments of inertia and centers of gravity (with respect to specific axis) were established and are presented in Table 1-44.

TABLE 1-44. ADVANCED SPACE ENGINE MASS PROPERTIES
(FIXED NOZZLE)

Weight = 337.0 lb (152.86 kg)

Center of Gravity $\overline{X}$ = +20.1 in. (51.1 cm)
$\overline{Y}$ = +1.1 in. (2.79 cm)
$\overline{Z}$ = -1.5 in. (-3.81 cm)

Moment of Inertia

Centroidal
I_{YY} = 35.6 slug-ft^2 (10280 kg-m^2)
I_{ZZ} = 36.0 slug-ft^2 (10396 kg-m^2)

About Gimbal Axes
I_{Y_G} = 65.2 slug-ft^2 (18827 kg-m^2)
I_{Z_G} = 65.5 slug-ft^2 (18914 kg-m^2)

TABLE 1-43. ADVANCED SPACE ENGINE DRY WEIGHT, 88,964 N (20K)

Description	Weight, pounds (kg)
Thrust Chamber	
Injector	18.0 (8.16)
Combustor	15.0 (6.80)
Nozzle	86.0 (39.1)
Gimbal Bearing	6.0 (2.72)
Fuel Pump	
Boost	7.5 (3.4)
Main	47.3 (21.45)
Oxidizer Pump	
Boost	16.8 (7.62)
Main	26.3 (11.9)
Valve	
Main Fuel	14.5 (6.58)
Main Oxidizer	14.5 (6.58)
Oxidizer Control (2)	25.0 (11.3)
Antiflood	1.2 (0.544)
Pneumatic	
Control Assembly	13.2 (5.99)
Plumbing	4.0 (1.81)
Electronic Control Assembly	7.0 (3.18)
Preburner	5.6 (2.54)
Igniter	
Dual Spark (2)	4.6 (2.09)
Body (2)	1.5 (0.68)
Ducting	
Fuel	4.8 (2.18)
Oxidizer	1.3 (0.59)
Hot Gas	4.6 (2.09)
Electrical Harness	3.0 (1.36)
Heat Exchanger	1.6 (0.726)
Interface Lines and Brackets	5.0 (2.27)
Seal Drains	1.0 (0.454)
Check Valves (5)	1.5 (0.68)
Flowmeters (2)	0.5 (0.227)
Total	337.0 (152.86)

TASK II: THRUST CHAMBER ASSEMBLY PRELIMINARY DESIGN

INJECTOR

The main injector on the advanced space engine is a coaxial type with a gas liquid element similar to that used on the Space Shuttle main engine. The selection of this configuration was based on high performance in addition to lightweight and relative ease of fabrication.

CONFIGURATION SELECTION

The injector assembly (Fig. 2-1) consists of 108 concentric elements with oxidizer flowing through the center orifice and fuel in the outer tube. The outer element length is sized for stability considerations and is shown in greater detail in Fig. 2-2 (flow directions indicated). The face plate consists of two parallel Rigimesh plates separated sufficiently to provide a hydrogen manifold for distributing hydrogen coolant through each plate for face coolant. Piston rings at the edges of the Rigimesh plates serve two purposes: (1) seal hydrogen coolant flow between the plates and outer body, (2) allow axial movement of the injector face plates caused by thermal growth of tube elements. This minimizes thermal stresses caused by the relative motion of injector Rigimesh plates to outer body.

The injector body is fabricated from a split INCO 718 steel forging. Splitting the body allows the installation of a one-piece cooled thermal liner prior to final assembly. The liner is used to provide a thermal barrier between the hot hydrogen gas and cold liquid oxygen. The outer shell is hydrogen cooled with the flow fed internally from the thrust chamber coolant discharge manifold. The flow continues to the manifold between the double Rigimesh face, into the fuel side of the injector and into the thrust chamber combustion zone.

The joint between the uncooled turbine discharge ducts and injector is designed to provide a temperature gradient from the uncooled to cooled section thereby minimizing thermal stresses. Designing the turbine discharge ducts as uncooled results in a much simpler more reliable design. A possible small weight penalty is realized by this design; however, the cost, simplicity, and improved reliability are considered more important.

The Rigimesh face is attached to the injector by the injector elements. Spacing of the plates is controlled by two types of sleeve lands that sandwich the inner plate nearer the injector, holding it mechanically into position. The outer plate is then supported on the inner surface by the sleeve lands and held into position by swaging the outer sleeve of the element into the countersunk holes in the Rigimesh face.

Fabrication of the injector assembly is state-of-the-art using techniques that are common practice at Rocketdyne. The sequence of assembly will be accomplished in the following manner. The elements are furnace brazed into the injector body following nickel plating of the body and elements. Cooling of the unit after brazing will be controlled to insure proper heat treatment of the INCO 718 material. Following the furnace braze cycle, the inner thermal shield

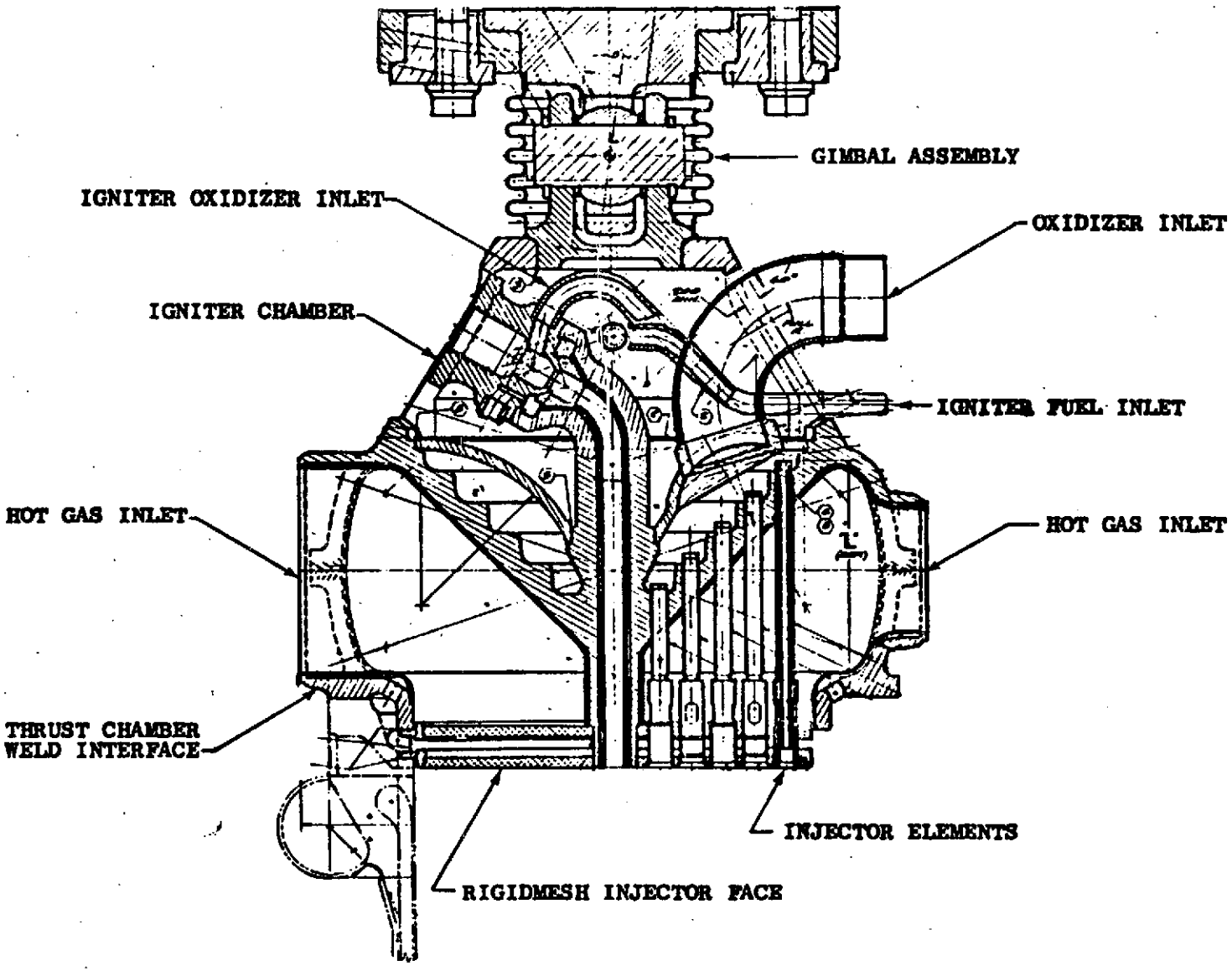

Figure 2-1. Thrust Chamber Injector and Gimbal Assembly

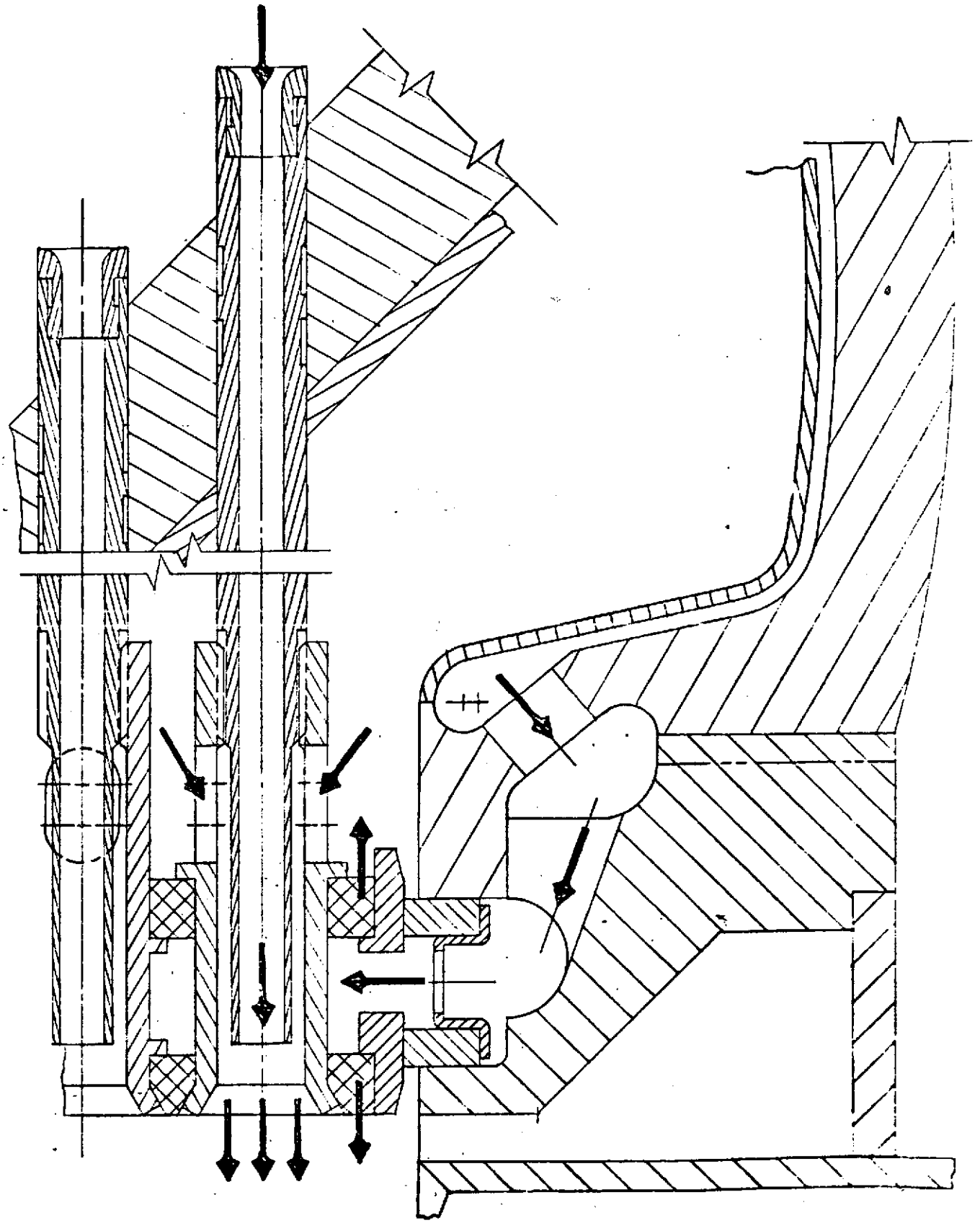

Figure 2-2. Injector Detail (4:1 Scale)

is assembled as a single piece unit. The lower body is then assembled to the upper body and EB welded as a final close out. The thermal liner is welded into the injector at the inlets of the turbine discharge to the injector, and at the aft end of the injector. The inner sleeves are then screwed on the elements followed by the inner Rigimesh plate. The outer element sleeves are installed and the outer Rigimesh plate installed and elements swaged in the tapered holes. The oxidizer dome is then electron-beam welded into place. The igniter body is now assembled to the center post and welded into position. The gimbal assembly and thrust mount is welded into position completing the injector assembly which is now ready for final weld to the thrust chamber assembly.

PERFORMANCE ANALYSIS

In oxygen/hydrogen systems (as well as other propellant combinations) the primary injector performance characteristics are largely dictated by two parameters. These limiting parameters are mixing/distribution efficiency, and evaporization/reaction efficiency. The methods of performance prediction and performance analysis outlined by the JANNAF committees are based on these two parameters for the description of injector efficiency.

The mixing/distribution characteristics of an injector are a function of the manifold flow distribution on a macroscopic scale, and the individual element mixing efficiency on a smaller scale. The manifold design of this injector provides the maximum manifold distribution volumes and flow areas, consistant with other design parameters (i.e., packaging, weight and "cutoff impulse"). LOX inlet velocities are moderate, and flow areas sufficient to maintain low cross velocity. The reduced inlet LOX metering orifices provide the most consistent method of flow control, with a minimum of sensitivity to external flow disturbances. The hot-gas manifolding is also designed to reduce inlet velocity and provide a minimum of local flow disturbances. The well-mixed, uniform mass distribution of the coaxial pattern selected for this injector also avoids any requirement for deliberate maldistribution such as film cooling or low mixture ratio barrier zone elements often required for thrust chamber compatibility.

The distribution of individual injection elements for this injector has been arranged to provide uniform mass injection distribution over the entire injector face. Maximum combustion chamber compatibility is provided in this manner by avoiding the adverse cross flowfields which result when the combusting mass attempts to flow from high mass to lower mass injection areas. This cross velocity is usually accompanied by mixture ratio striation as the fuel-rich light fractions are more easily transported than the oxidizer-rich heavy fractions. The result of this cross flow and mixture ratio striation is streaking of the combustion chamber wall.

The mixing efficiency of the individual elements is ensured by design features based on a wealth of Rocketdyne experience with high-performance gas-liquid coaxial injectors. A high velocity ratio between the gaseous fuel, and the liquid oxidizer, provides the high shear forces for droplet stripping and

momentum exchange between the fuel and oxidizer. This element is patterned after the highly developed, hot-fire demonstrated injector element in the SSME Main Engine injector. Table 2-1 shows the comparison of significant parameters between the two elements.

TABLE 2-1. COMPARISON OF INJECTOR PARAMETERS

Parameter	SSME	20K
LOX Injector Velocity, ft/sec (m/s)	97 (29.57)	91 (27.7)
LOX Metering Velocity, ft/sec (m/s)	441 (134.4)	359 (109)
Fuel Injector Velocity (gap), ft/sec (m/s)	1405 (428)	1712 (522)
Fuel Injector Velocity (expanded), ft/sec (m/s)	1154 (352)	1303 (397)
Face Area/Element, sq in. (cm^2)	0.412 (2.65)	0.168 (1.084)
Contraction Ratio	2.96	4.0
Distance to Throat, inch (cm)	14.0 (35.6)	8.5 (21.6)
L* (characteristic length), inch (cm)	30.6 (77.7)	27.3 (69.3)

Comparative history of various injectors and local mixing efficiencies versus a velocity related mixing parameters is shown in Fig. 2-3. This shows that the 88,964 newton (20,000-pound) thrust injector is operating in a region of high mixing efficiency similar to the SSME main injection element. The performance of the SSME main element has been well verified in extensive cold-flow mising tests, and also during demonstration firing.

Vaporization and reaction efficiency of coaxial elements has been extensively studied and modeled in various portions of the Rocketdyne organization. A very comprehensive combustion model has been developed by the Research Department at Rocketdyne, and the correlation between this model and actual engine experience is well documented.

This "NCSS" combustion model is used both as a performance prediction tool, and as a means of mapping the stability characteristics of the combusting streams in the combustion chamber. The final injector design configuration was input into this model, and the results indicate total vaporization, and reaction completed well upstream of the throat station. Figure 2-4 shows a plot of local c* efficiency predicted on the basis of vaporization and reaction completed at 15.24 cm (6 inches) from the injector face, with the throat distance at 21.6 cm (8.5 inches), leaving 6.35 cm (2.5 inches) of "safety factor."

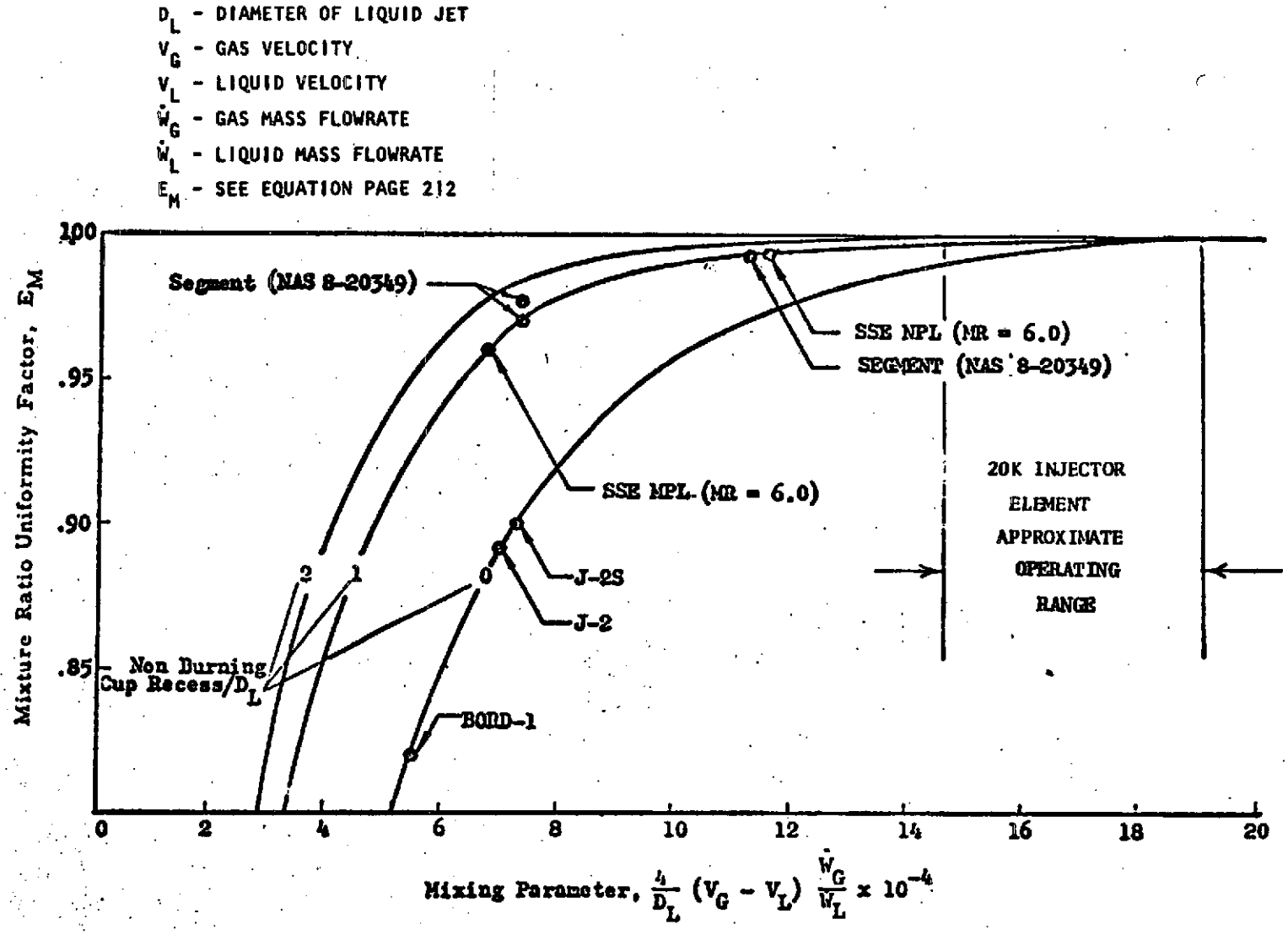

Figure 2-3. Coaxial Injection Element Mixing Characteristics

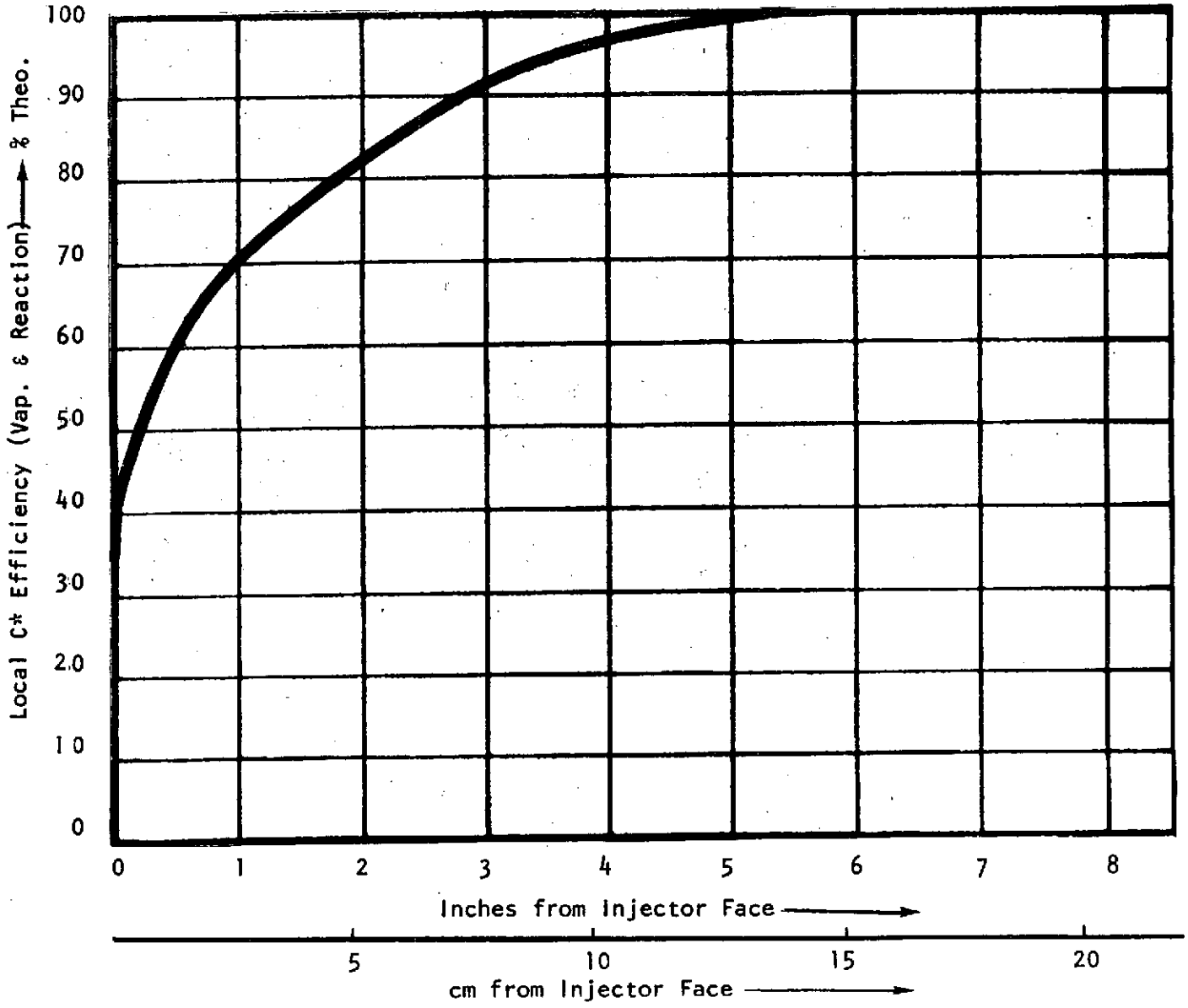

Figure 2-4. Predicted Local c* Efficiency Based on Vaporization and Reaction Limitations (From Combustion Model at Nominal Case)

Overall injection efficiency is normally expressed as the product of the mixing efficiency and c* efficiency, and the vaporization/reaction c* efficiency expressed in mathematical format:

$$c^*_{predicted} = c^*_{mixing} \times c^*_{vap}$$

This expresses injector c* efficiency. The actual measured c* efficiency is often moderated by "real combustion chamber," and "real nozzle" effects.

C^*_{mixing} is the c* efficiency based on the element mixture ratio distributions. This is a summation of mass weighted c* values for numerous stream tubes, compared with the theoretical value for perfect mixture ratio. This value is generally much higher than the "mixing efficiency" (E) which is an expression for mass-weighted distribution exclusive of propellant theoretical performance characteristics.

ηc^*_{vap} is the percentage of propellant vaporized and reacted in the combustion chamber (assumes perfect mixture ratio distribution, but includes dropsize vaporization characteristics, and reaction rates).

COMBUSTION STABILITY

Every effort has been taken to ensure combustion stability in the design of the ASE engine. Although the analysis, for the most part, was limited to a single-point evaluation, a conservative approach to stability was adopted and additional margin has been incorporated into the design in all critical areas. For simplicity due to the commonality of the subject matter, the analyses of both the main chamber combustor and the preburner are subsequently discussed in this section.

Both acoustic and feed-system-coupled stability were considered. Each of these types of instability involves coupling between the combustion process and the response of the combustion chamber. These differ primarily in that feed-system coupling is dependent on variations in propellant flowrate into the combustion chamber and, thus, as the name implies, is a function of the response characteristics of the propellant feed systems. Acoustic instability, on the other hand, is dependent only on coupling between the combustion process and the combustor wave dynamics, while feed system interaction is not required.

It is apparent, therefore, that the individual ("open loop") response of the feed system, combustor, and combustion process must be well known to carry out a meaningful stability evaluation.

Combustor Response Characteristics

Basic to all instability studies is the response of the combustor where the generation of chamber pressure occurs. Oscillations can occur only at frequencies at which the combustor has high response.

The response as a function of frequency of the main combustor is shown in Fig. 2-5. At very low frequencies, the gain is constant and its level is dependent on the normal choked-flow pressure/flowrate relationship. As the frequency is increased, the combustor wave response becomes more and more sluggish until it is finally unable to "keep up" with the oscillation frequency. The frequency at which this occurs is usually, but somewhat arbitrarily, taken as the point where the gain is reduced to 70 percent of its maximum steady-state (zero-frequency) level. This point is generally referred to as the "break frequency" and occurs at 210 Hz for the main combustor.

At frequencies below the break frequency, the combustor reacts as a bulk response and is capable of supporting flowrate-initiated (feed-system-coupled) chug or buzz oscillations.

In the band of frequencies between approximately 210 and 7000 Hz, the combustor is relatively unresponsive and generally will not support oscillations of any type.

At frequencies above the break frequency, the combustor is responsive only at or near frequencies corresponding to its normal wave motions. These wave motions are well defined through the use of acoustics and have acquired the name of the "acoustic modes" of the combustor. In chambers such as the ASE main combustor, only the transverse tangential and radial modes are of concern since the combustor exit (nozzle throat) allows much of the energy associated with longitudinal wave motion to escape.

As can be seen in Fig. 2-5, the ASE combustor is responsive only at specific frequency bands about the tangential modes at 7401, 12276, and 16883 Hz, and the first radial mode at 15,406 Hz. Oscillations at the higher order transverse modes are uncommon primarily because of the greater viscous dissipative forces associated with their high frequencies.

The acoustic response for the ASE preburner (Fig. 2-6) is similar to the main combustor except that the frequencies associated with the various modes are different and that the longitudinal modes are also shown. In the case of the preburner, the longitudinal modes are less well damped than in the main combustor because of the reflection point at the end of the combustor near the inlet to the fuel and oxidizer turbine hot-gas ducts.

Because of the low mixture ratio, the preburner break frequency is low at 78 Hz. The longitudinal modes occur at 3975, 7945, and 11,920 Hz, while the transverse modes are at 14,950 Hz and above.

Acoustic Stability

Acoustic instability is a coupled oscillation between the combustor wave motion (dynamic response) which has been shown to be well defined, and a sensitive combustion response which is far more tenuous. The potential for acoustic coupling can be evaluated through the use of the Priem analysis (Ref. 4). This analysis procedure predicts a dimensionless overpressure required to establish an

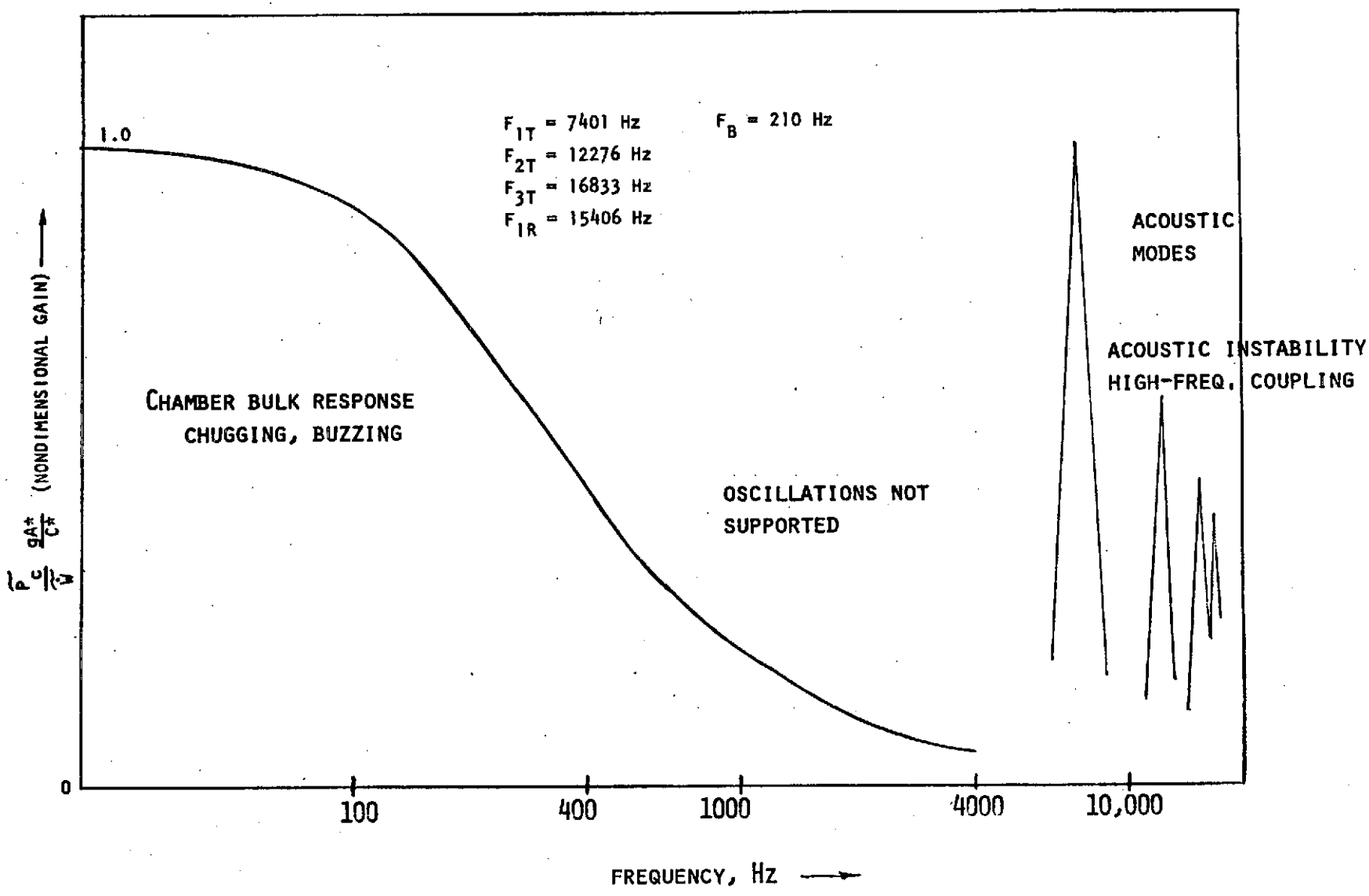

Figure 2-5. ASE Chamber Response, Main Combustor

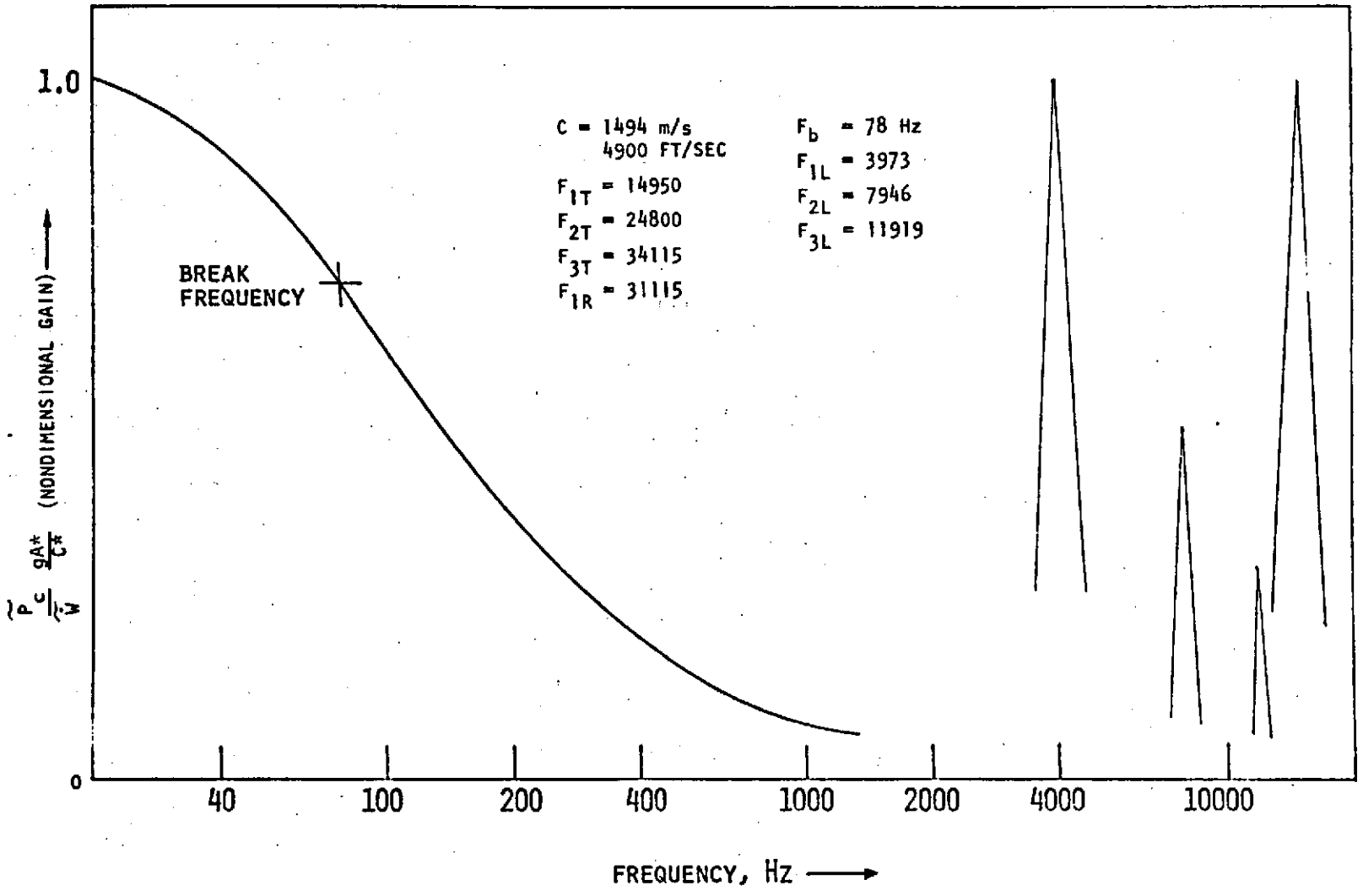

Figure 2-6. ASE Chamber Response, Preburner

instability. This overpressure index is a function of two intrinsic parameters, the accumulation of unburned propellant and the relative velocity between the liquid and gaseous species within the combustor.

The Priem analysis was performed for an unaided ASE main combustion chamber and is shown relative to other LOX/hydrogen coaxial engines in Fig. 2-7. The J-2 and J-2S exhibit dynamic stability to all but intermediate size bombs. They consistently damp both large and small disturbances. The cast segment engine has shown the ability to damp an established instability. The unaided ASE main combustion chamber (Fig. 2-7) has superior predicted stability (higher A_p) than any of these engines and should be dynamically stable.

It should be emphasized, however, that this conclusion is based on a single mainstage point analysis and that more critical conditions are usually encountered during transition. To preclude any possibility of sustaining an acoustic instability, an acoustic absorber has been included in the ASE main combustor design.

The Priem analysis was also performed for the main combustion chamber assuming that the absorber would negate the possibility of coupling with either the first or second transverse modes. The results of this analysis show (Fig. 2-8) that the A_p required to initiate a sustained instability was further increased by approximately an order of magnitude.

A similar analysis procedure was carried out for the ASE preburner combustor. Figure 2-9 shows the stability limits for the preburner relative to the reference engines. The preburner indicates greater stability than the main combustor, but an absorber has been included in the preburner design for additional stability margin. Curves are shown both with and without an acoustic absorber.

Absorber Design. The acoustic absorber for the main combustor was designed to suppress the transverse acoustic modes with primary emphasis assigned to the first tangential. Design calculations were carried out through optimization of the temporal damping coefficient (Ref. 5). This procedure entails solution of the wave equation for the combustor while replacing the rigid wall boundary conditions with those imposed by the absorber, where applicable.

The ASE absorber is composed of 16 individual acoustic absorber cavities distributed along the periphery of the injector end of the combustor. The total open area is equivalent to 10-percent of the chamber cross-sectional area.

A correlation was developed (Ref. 6) which shows that the required absorber open area is related inversely to the frequency of the oscillation to be damped with a further dependency on injector pattern. The upper half of Fig. 2-10 shows the industry-wide absorber experience. The lower half of the figure shows the same data and also shows that the ASE absorber lies in a favorable position (large open area) relative to the previous experience.

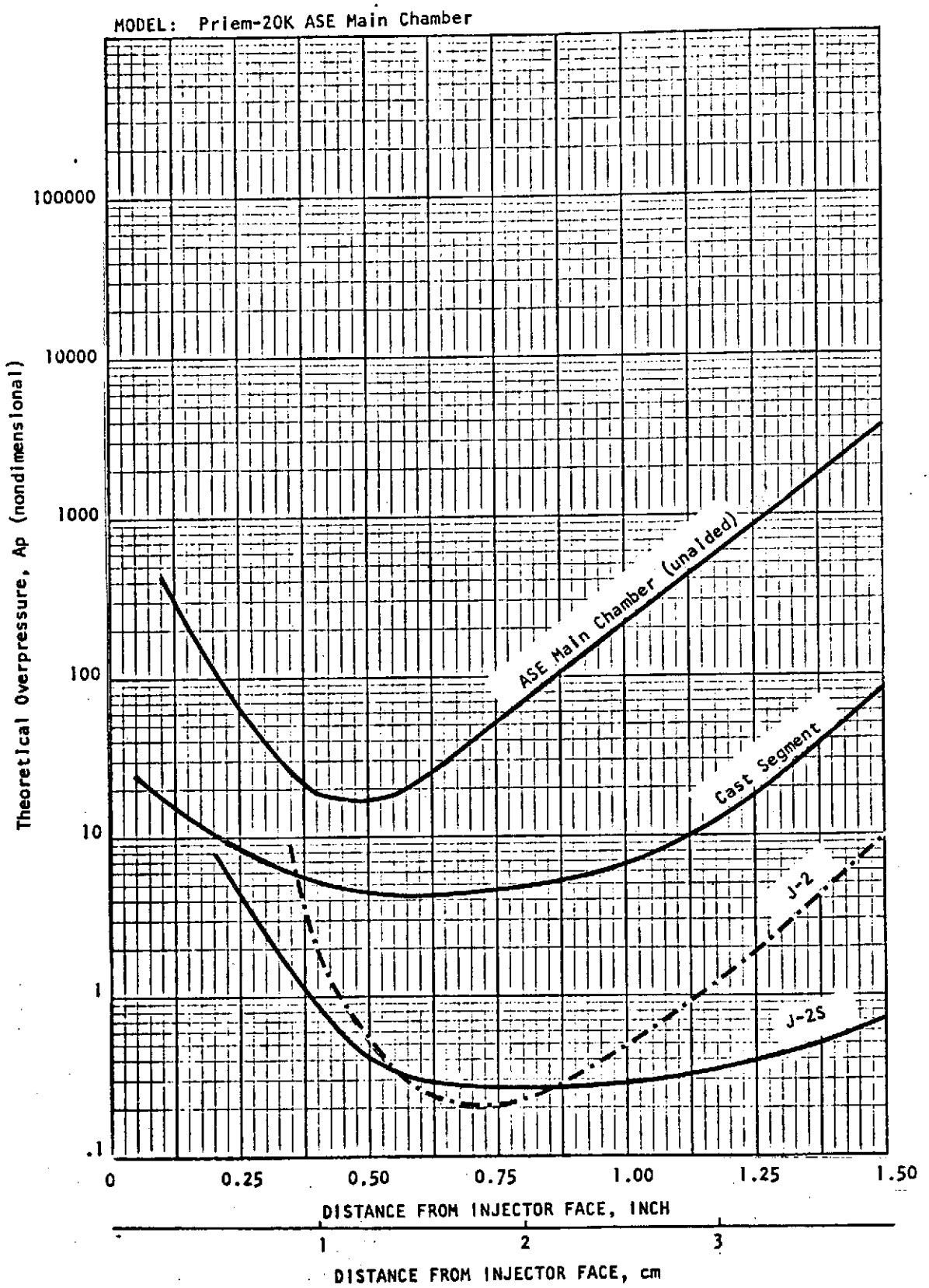

Figure 2-7. Priem Analysis with Unaided Main Combustion Chamber

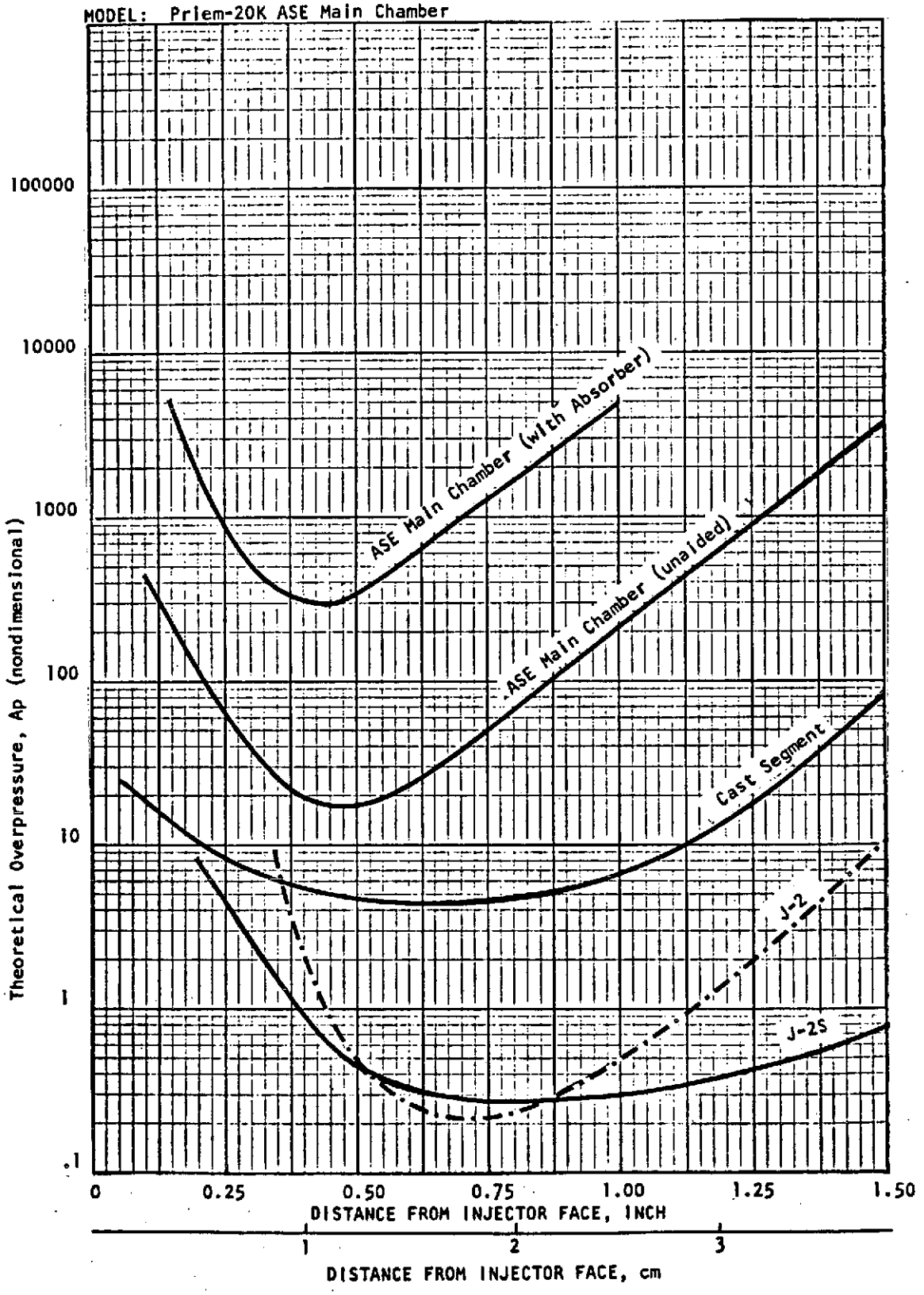

Figure 2-8. Priem Analysis of Main Combustion Chamber with Absorber

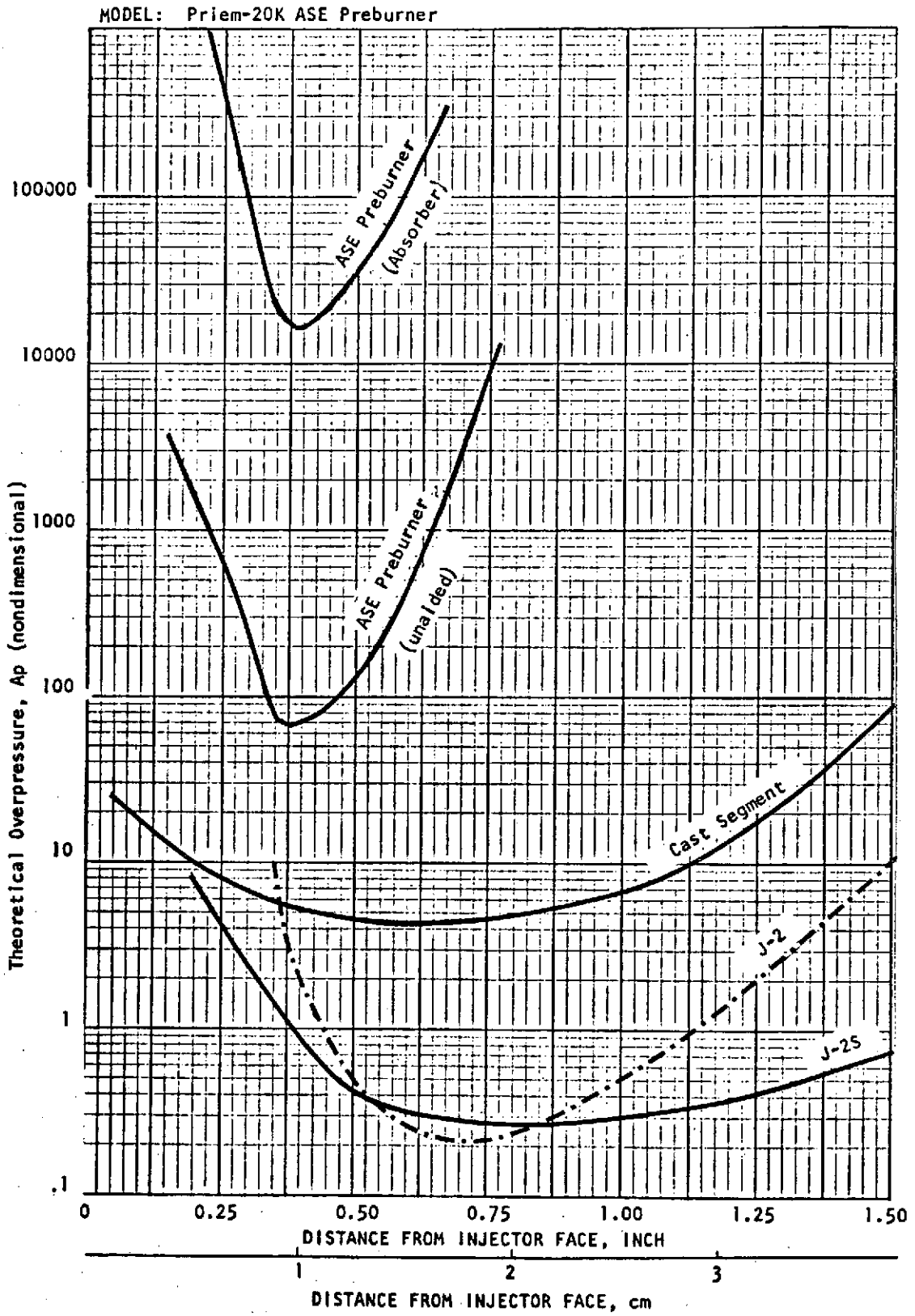

Figure 2-9. Priem Analysis with Preburner Combustor

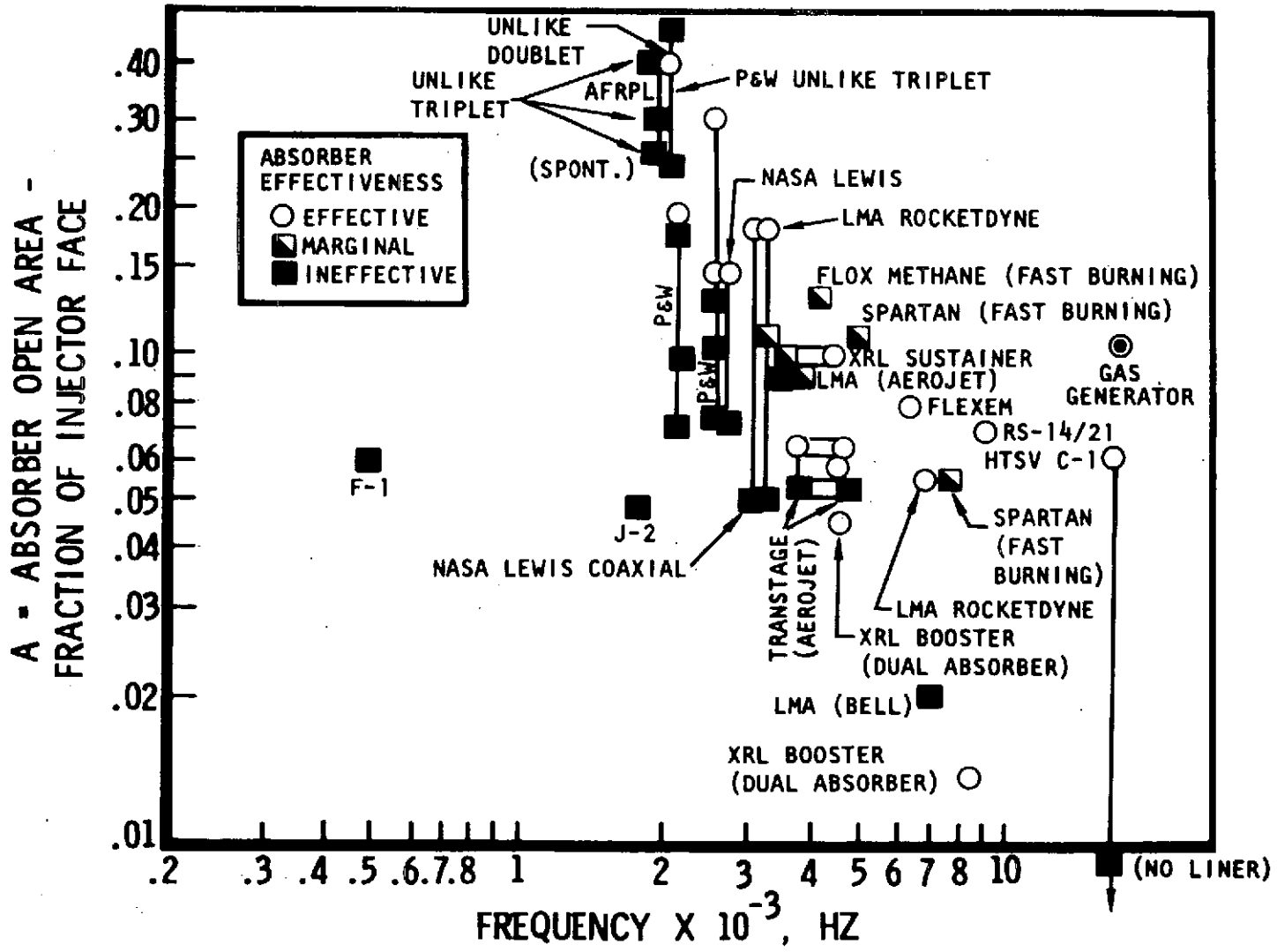

Figure 2-10. Absorber Experience

Figure 2-11 superimposes the damping curve with the transverse acoustic modes for the main combustor. It is apparent that the absorber has its maximum damping at the frequency corresponding to the first tangential mode, but that it also provides significant damping to the other transverse modes.

Additional stability margin has also been introduced into the preburner design through inclusion of an absorber. The preburner has a 14-percent open area relative to the combustor cross section and consists of six "L-shaped" 1/4-wave cavities spaced along the periphery of the injector-end and the combustion chamber. Figure 2-12 shows the damping provided by the preburner absorber as a function of absorber length. The optimized length of 1.55 cm (0.61 inch) was selected. This absorber is tuned for primary damping of the first tangential mode and provides damping to the other transverse modes. The same analysis procedure was used with this absorber as in the design of the main chamber acoustic cavity.

Feed-System-Coupled Stability

Feed-system-coupled stability may be separated into two major areas: low-frequency coupling which involves a bulk chamber response, and high-frequency or hybrid instability which involves coupling with the combustor acoustic modes.

There were two approaches to feed-system stability of the ASE engine. The first of these was to determine the "open loop" response characteristics of the major elements capable of coupling in an unstable feedback loop and then to design these components such that their responses were detuned relative to each other. The second was to construct a "double dead-time" analog simulation of the engine which allowed for much more detailed evaluation of the interaction of the engine components in the "closed loop" operational environment.

The basic mechanism of feed-system coupling is as shown in Fig. 2-13. For an oscillation to grow or sustain, the total loop gain must be greater than unity and the phase shift must be proper. One way to ensure against coupling of this type is to design the various components such that there are no common frequencies where each has significant gain. This approach has been carried out in the design of the ASE engine.

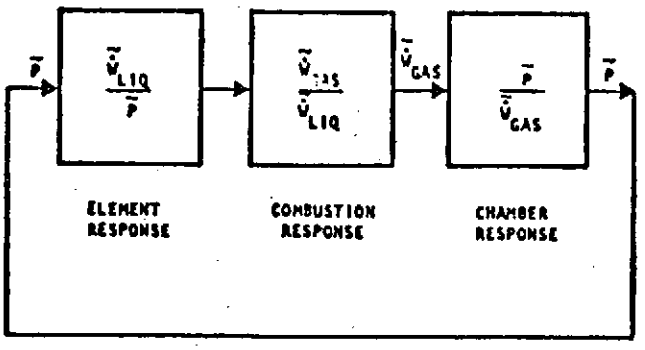

Figure 2-13. Feedback Loop/Feed-System Coupling

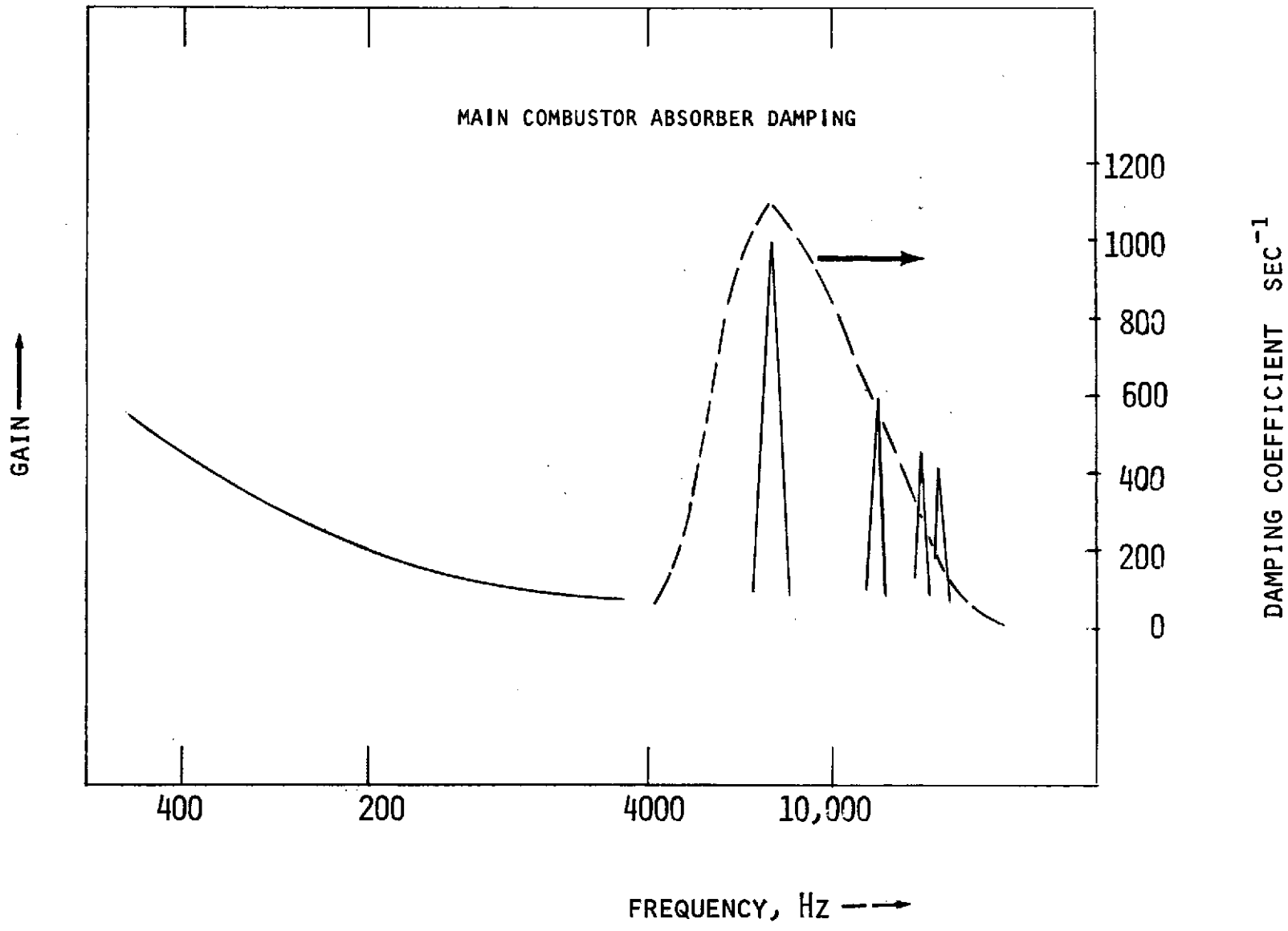

Figure 2-11. Main Combustor Absorber Damping

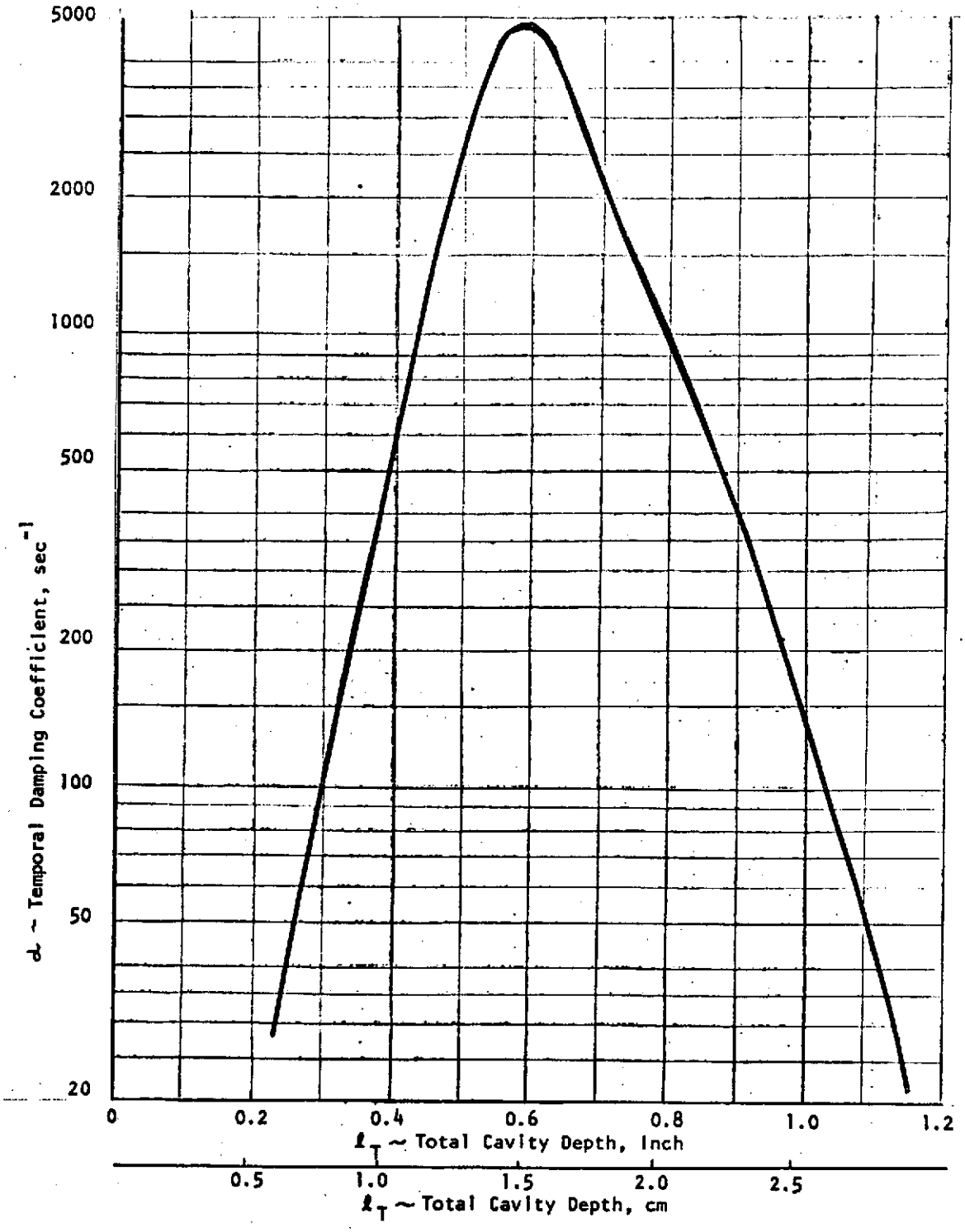

Figure 2-12. Preburner Acoustic Cavity Design, First Tangential Mode

The main combustion chamber response curve was shown in Fig. 2-1 and discussed in some detail. The main hydraulic response of interest in a coaxial injector is that of the oxidizer injection element. The element response is readily determined using finite-difference techniques and is shown in Fig. 2-14. The response of the hydraulic element is similar to the chamber acoustic response. It displays nearly constant gain at low frequencies, becomes somewhat sluggish and unresponsive, and finally responds only at the frequencies corresponding to its normal standing modes.

Determination of the combustion response is a somewhat greater problem and requires use of the Rocketdyne-developed LOX/hydrogen combustion mode. This model predicts the stripping, atomization, vaporization, and combustion of the oxidizer jet by the high-velocity hydrogen shroud as a function of the axial position in the cup recess and through the combustion chamber. Thus, an energy release profile such as shown (Fig. 2-15) may be generated for the combustor.

A rate of energy release may be determined by dividing the incremental mass consumed by the increment over which it was burned and relating this to a time delay by the time required for the propellants to arrive at that particular axial position. The time delay may be further related to frequency to determine the frequency-sensitive combustion response.

This response is shown for the main chamber (Fig. 2-16) and is divided into two areas. The higher-frequency area between 7000 and 33,000 Hz corresponds to the vaporization of propellant within the cup region, while the response below 7000 Hz corresponds to the combustion within the chamber region. The gain depicted in Fig. 2-16 is the amount of propellant vaporized per unit length. Due to the high-velocity hydrogen flow within the cup, the propellants vaporized in the cup do not burn until they enter the combustion chamber. The combustion gain for coupling an instability, therefore, is no greater in the cup than in the main chamber as might be interpreted from the plot.

In analyzing the response characteristics of the various elements, there are two comparisons which must be made. One of these is for the cup recess region while the other is for the combustion chamber.

The cup recess usually has a very high break frequency and, therefore, is capable of responding in a linear (bulk) fashion through the frequency range associated with the oxidizer element response. The important response comparison in the cup is between the element hydraulics and the combustion process. In making this response comparison for the ASE main combustor (Fig. 2-17) and preburner (Fig. 2-18), it is apparent that there are regions in which both the combustion and hydraulic components have gain. The combustion gain of interest, however, is the change in gas flowrate associated with a perturbation in injected liquid flowrate. The important fact for the ASE cup retion is that, although oxidizer is vaporized within the cup region, due to the high hydrogen velocity, these vaporized propellants do not ignite until they enter the combustion chamber. The actual cup combustion gain is, therefore, relatively low and coupling is not expected. If, on the other hand, the ASE had been designed with lower cup region velocities, ignition within the cup would occur and coupling would be anticipated.

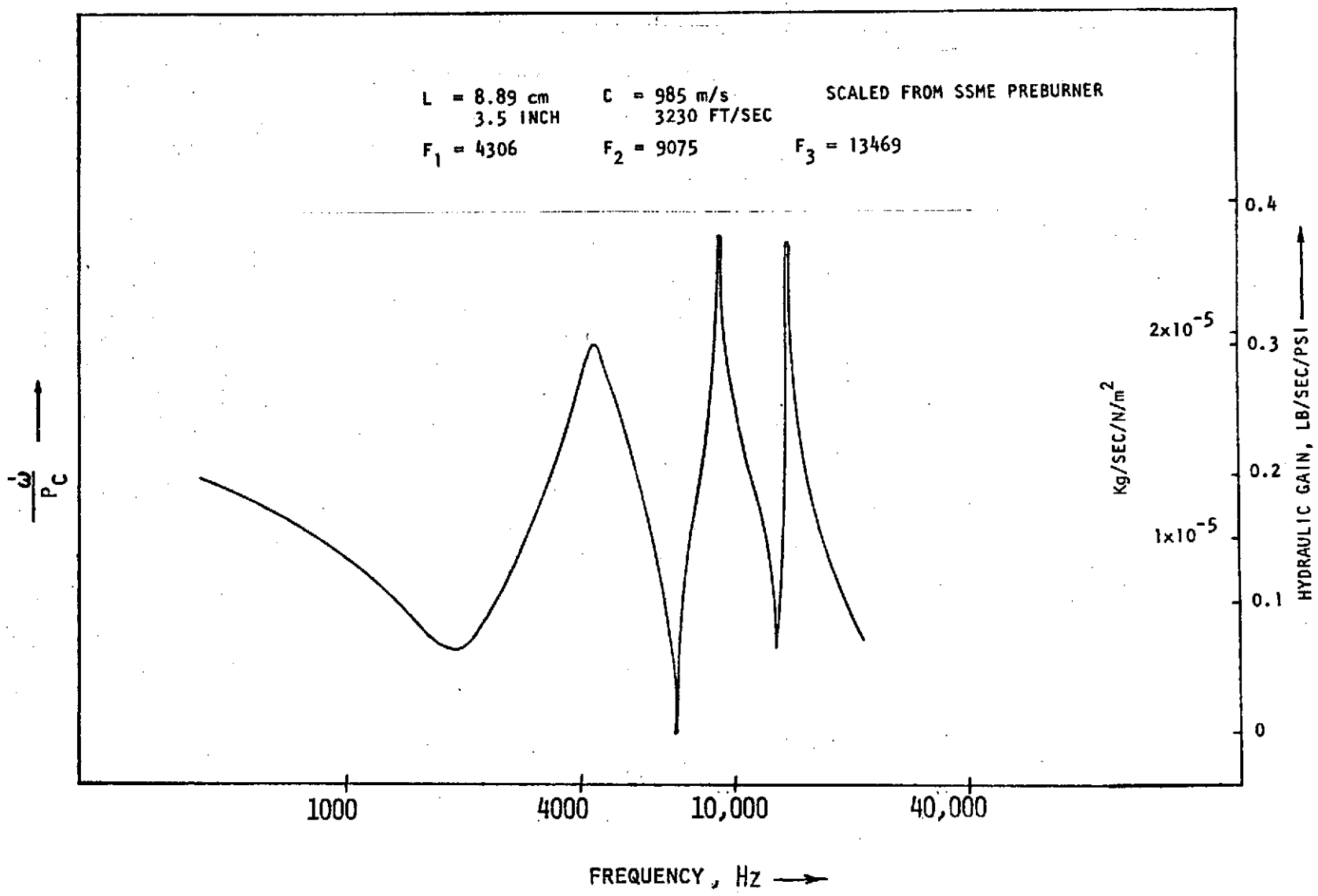

Figure 2-14. ASE Main Injector Oxidizer Element Response

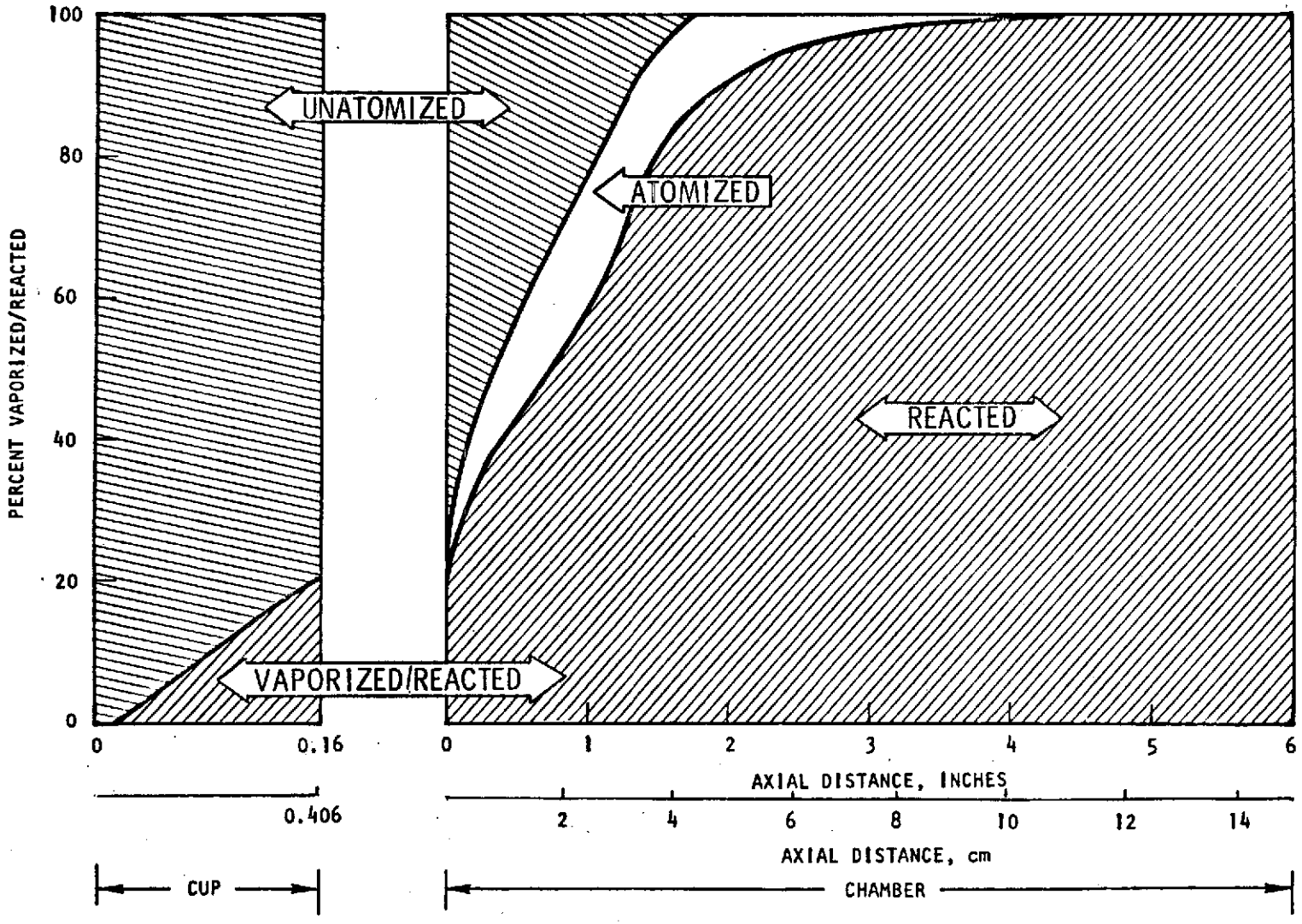

Figure 2-15. Reaction Profile

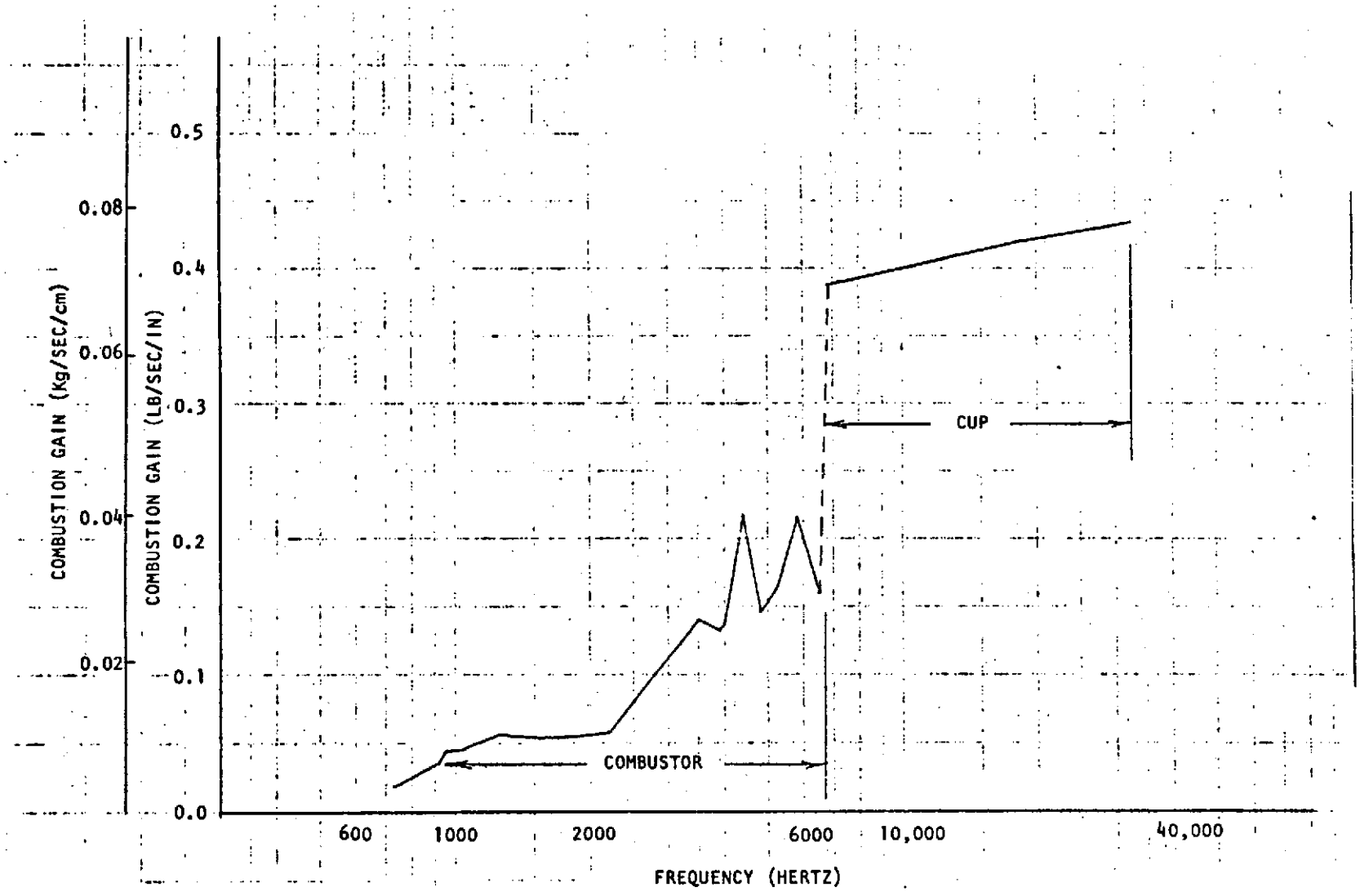

Figure 2-16. ASE Main Chamber Combustion Response

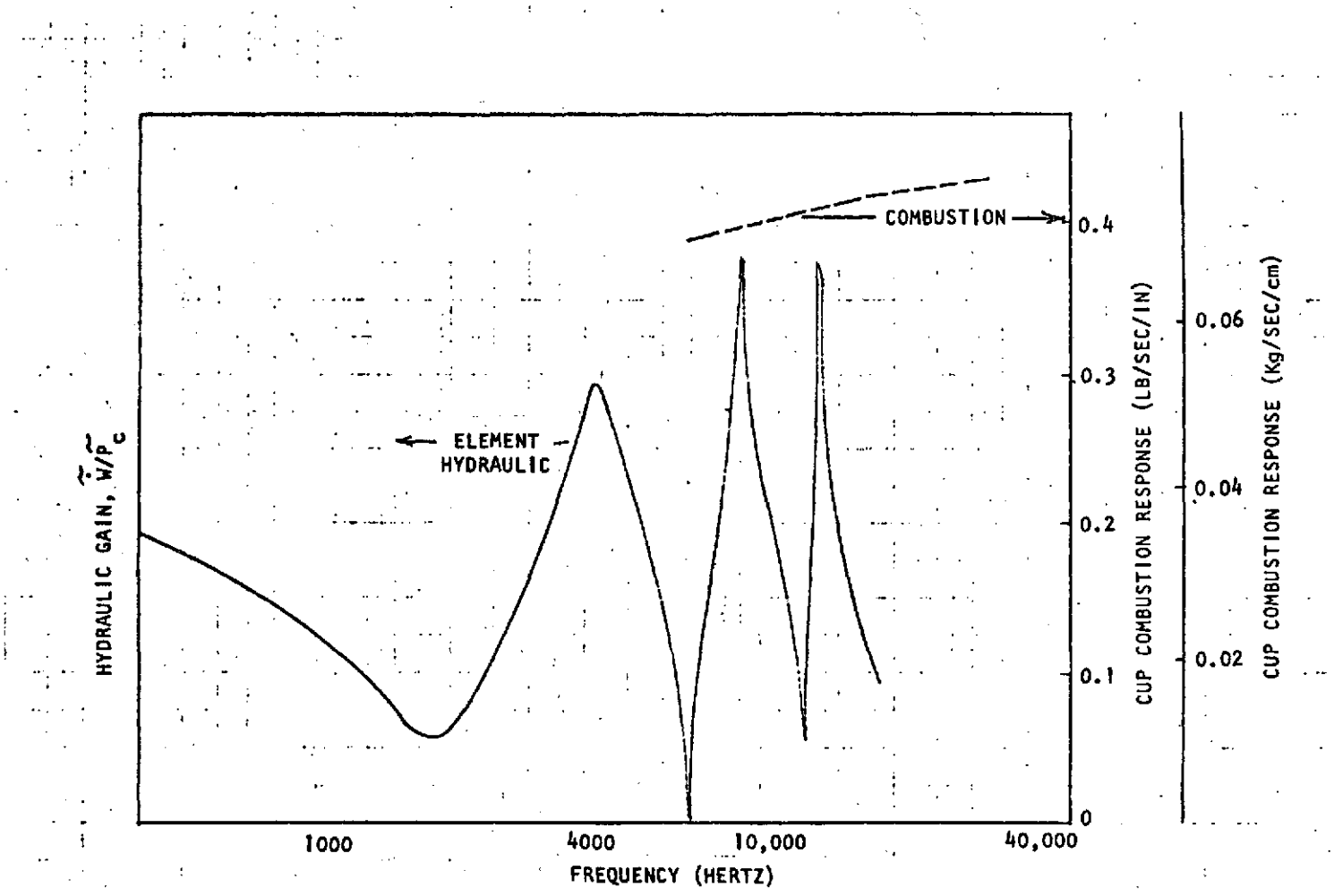

Figure 2-17. ASE Main Chamber

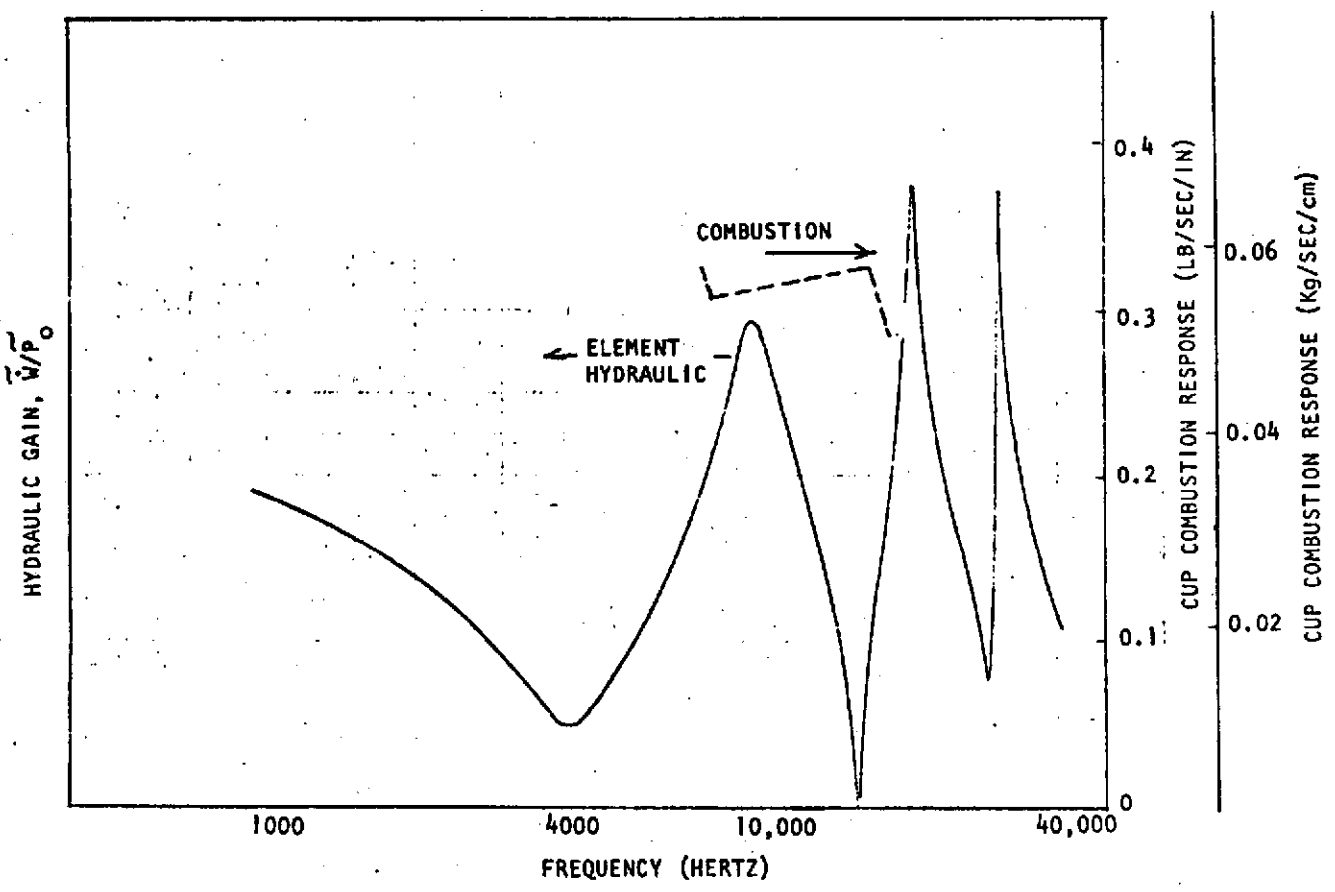

Figure 2-18. ASE Preburner

The response comparison must also be made for the combustion chamber region. In this case, the dynamic response of all three components (hydraulic, combustion, combustor wave motion) are important. Figure 2-19 shows the response comparison for the main chamber. The important observation here is that there is no frequency at which all three of the response plots have gain. Detuning has been accomplished in the design, and the main combustor should not couple in a high-frequency buzz or hydrid mode.

The same response comparison was made for the preburner (Fig. 2-20). The preburner combustor is also well detuned and no coupling is anticipated. Detuning of the hot-gas system was accomplished by providing ducts of significantly different length between the preburner and the two turbines.

Analog Simulation

In addition to the open-loop analysis of feed-system stability, a nonlinear mathematical model was constructed for the ASE system. This model represented the dynamics of the thrust chamber, preburner, and their liquid and gaseous feed systems. The model was mechanized for closed-loop solution on the analog computer and used to parametrically study the engine system stability in the frequency range of 0 to 3000 Hz.

A simplified schematic of the model is shown in Fig. 2-21. Somewhat further detail of the preburner system (Fig. 2-22) and main combustion chamber (Fig. 2-23) are also shown. The possibility of coupling between the preburner and the main chamber was allowed through the mechanization of the hot-gas system, as shown in Fig. 2-24.

The general formulation (Fig. 2-25) allowed for variation of both a time delay and klystron (clumping) lead term for each propellant. The model, therefore, may be described as a "double dead-time" model with klystron lead. The description was repeated for both the preburner and main chamber, and the two systems were coupled together through the hot-gas system.

Stability maps for the preburner and the main combustion chamber were generated to depict the system stability margin. These maps plot the boundary of incipient instability as a function of the oxidizer injector transport time delay and the oxidizer clumping time constant for fixed similar fuel parameters. In this manner, the system stability boundaries can be compared to the probable operating region of the engine to assess the degree of stability margin present. The maps obtained from this study are presented in Fig. 2-26 and 2-27.

Areas above the boundary of incipient instability are unstable while those below are stable. The separation of the incipient instability boundary from the probable operating region is the best indicator of the stability margin.

Results of the analog model studies showed no modes of instability due to coupling of either the preburner or the main chamber with the fuel or oxidizer feed systems. The lowest stability margin of the engine was associated with the preburner (Fig. 2-27). It should be noted that, even in this instance, the clumping lead time constant would have to be more than doubled from the probable operational region to cause instability.

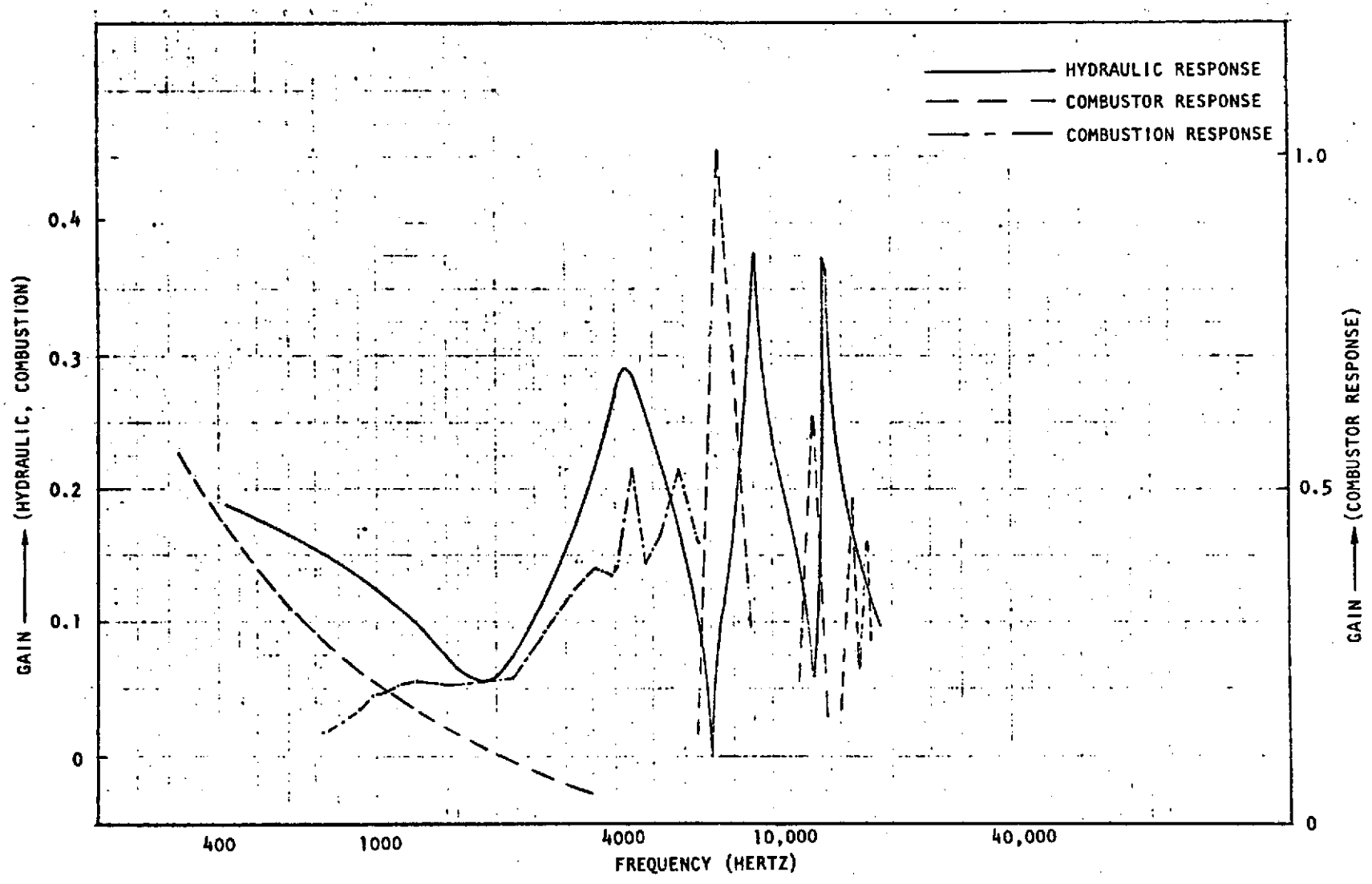

Figure 2-19. Response Comparison, ASE Main Chamber

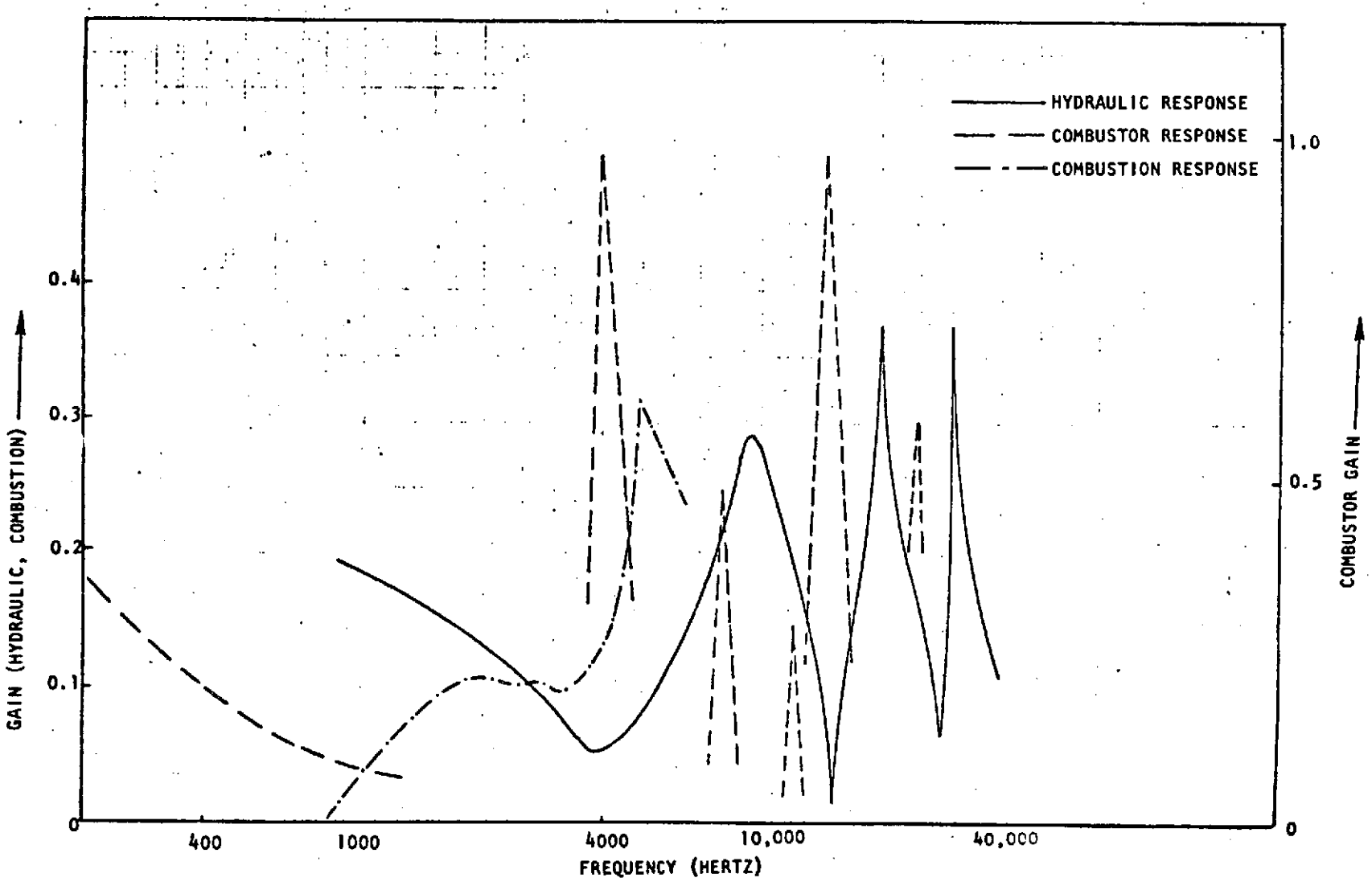

Figure 2-20. Response Comparison, ASE Preburner

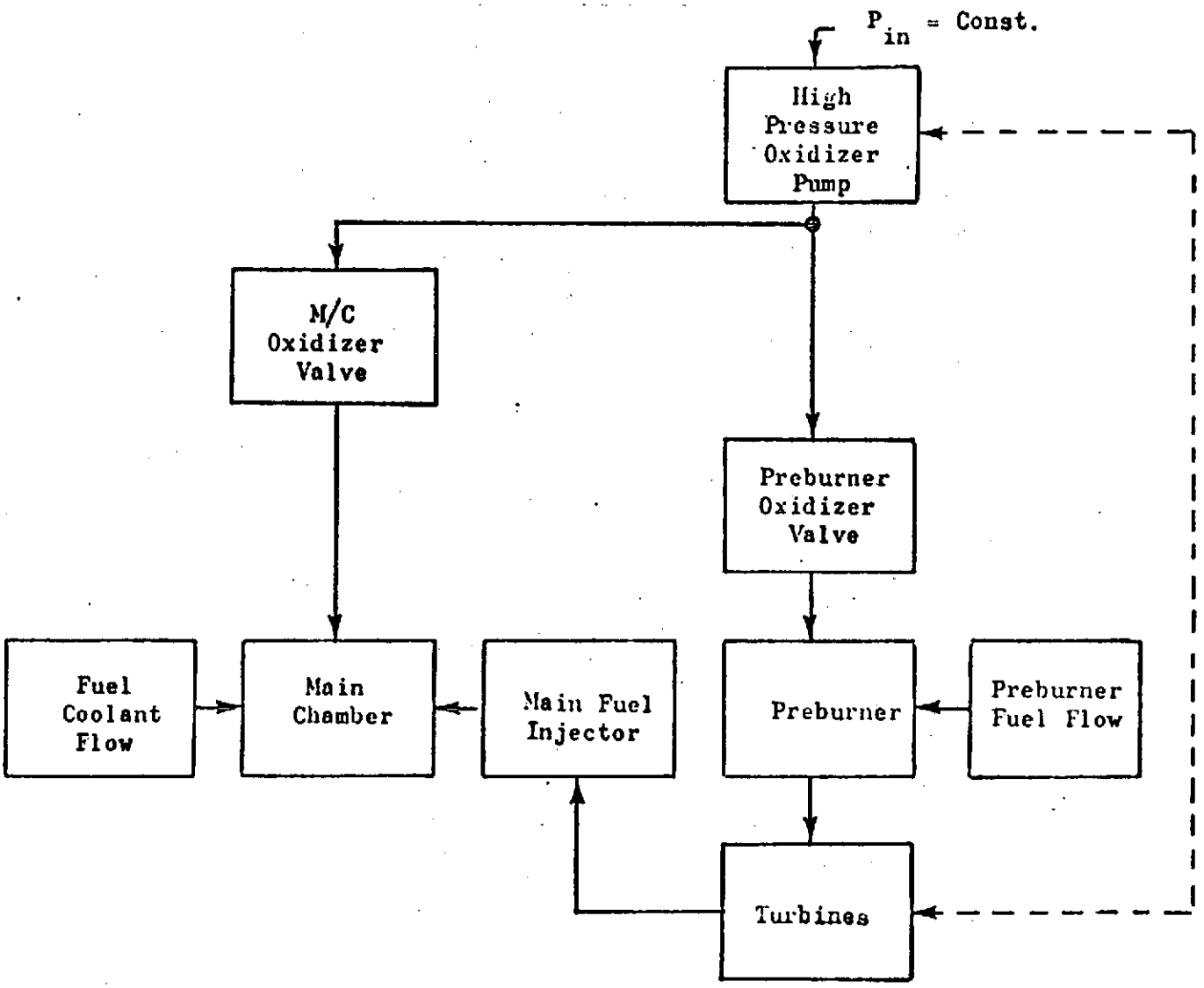

Figure 2-21. Analog Model Simiplified Schematic

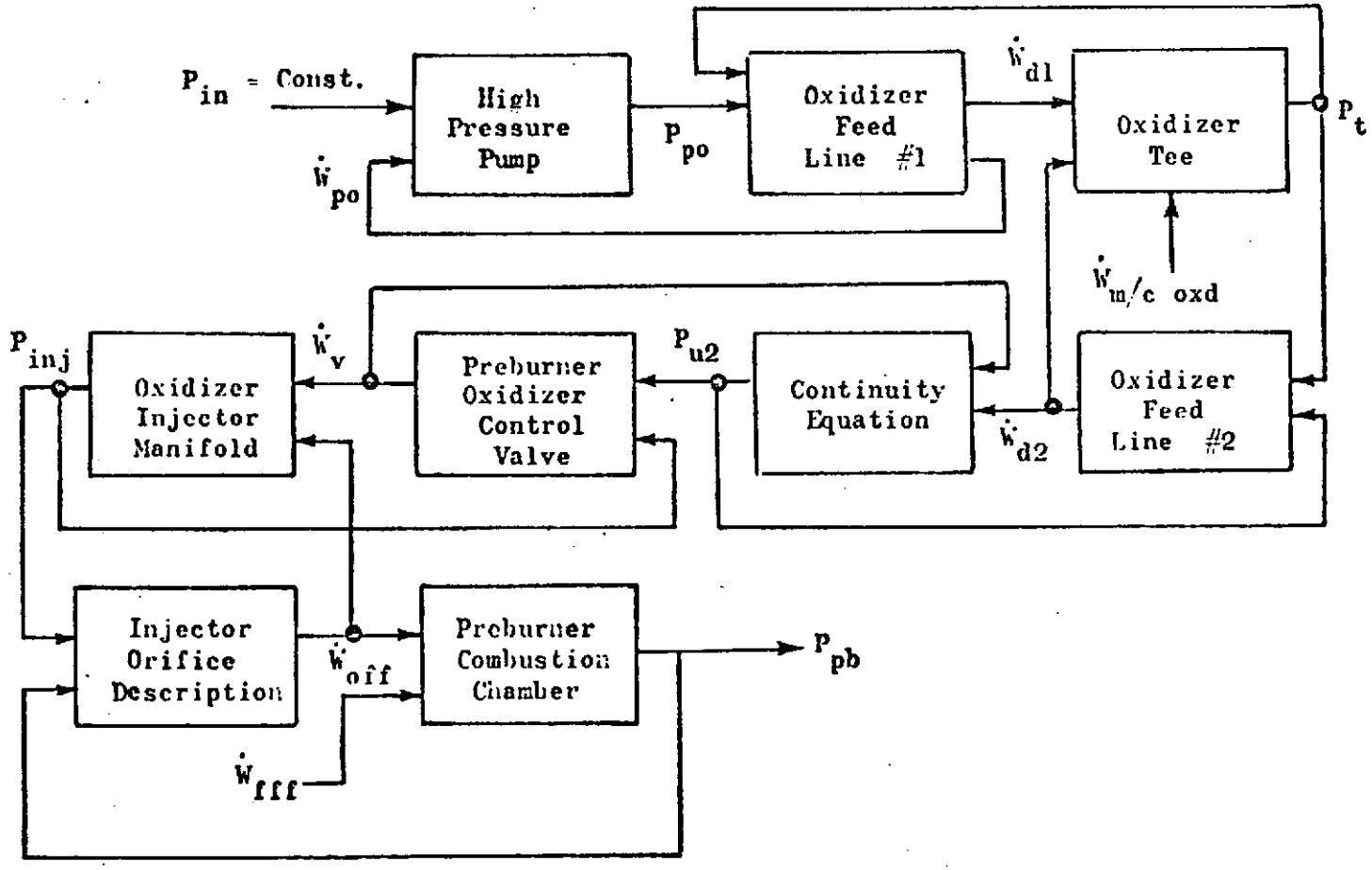

Figure 2-22. Preburner Model

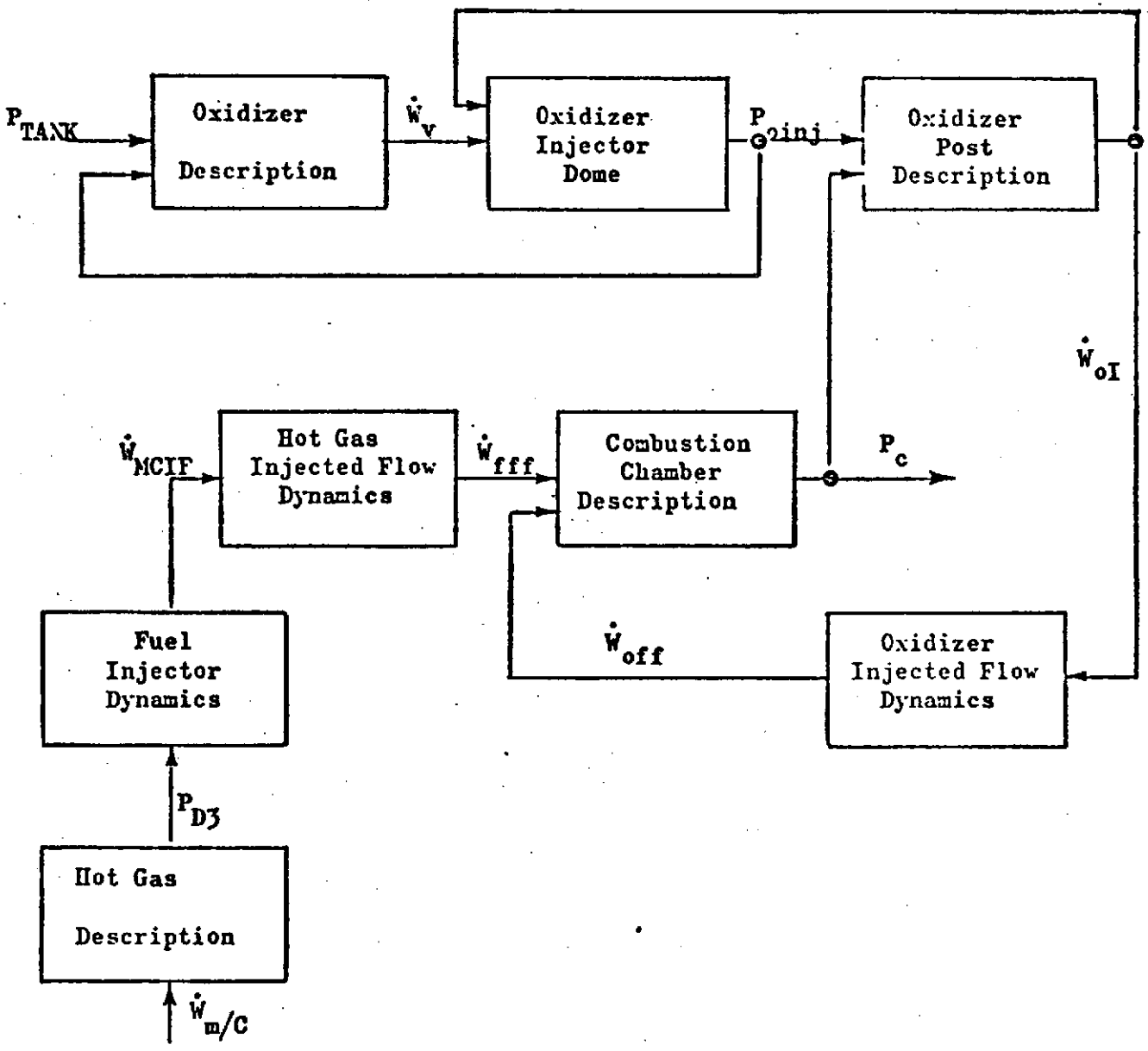

Figure 2-23. Main Chamber Model

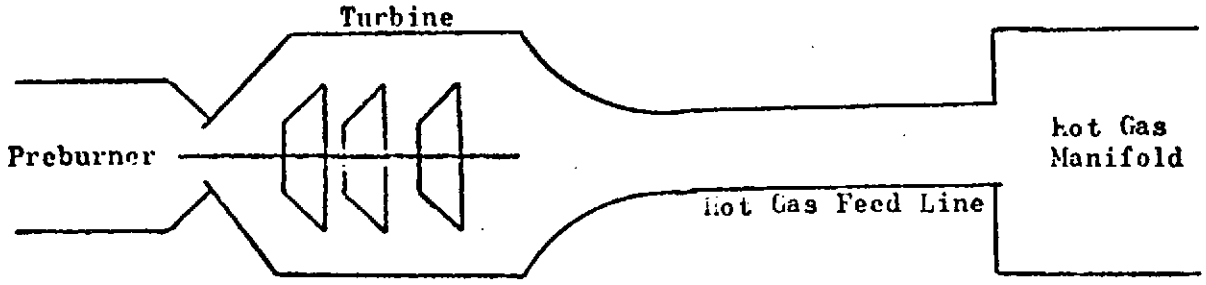

Figure 2-24. Hot-Gas System Model

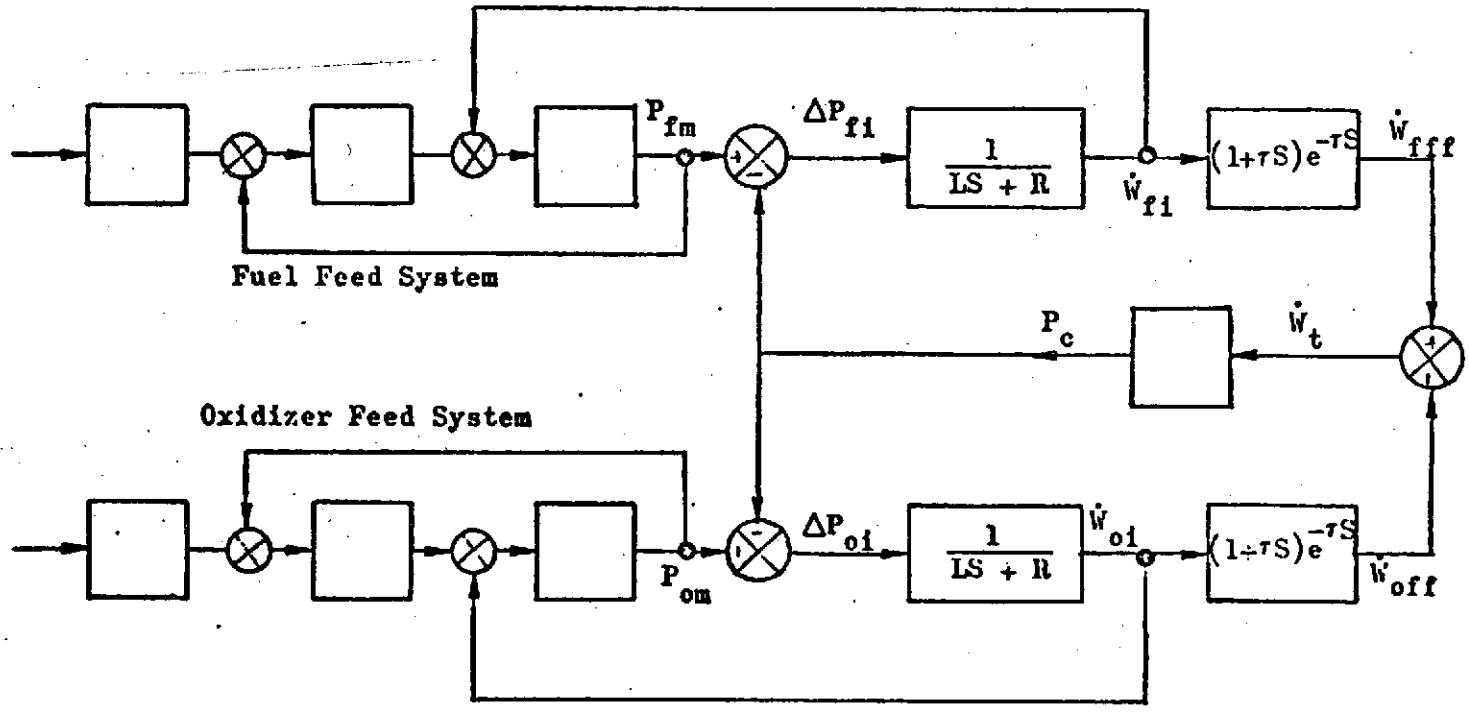

Where P_{fm}, P_{om} = Fuel & Oxidizer Manifold Pressure

$\dot{W}_{fi}$, $\dot{W}_{oi}$ = Fuel & Oxidizer Injector Flowrate

$\dot{W}_{fff}$, $\dot{W}_{off}$ = Fuel & Oxidizer Flowrate at Flame Front

P_c = Combustion Chamber Pressure

Figure 2-25. Typical Closed-Loop Feed System/Engine-Coupled Block Diagram

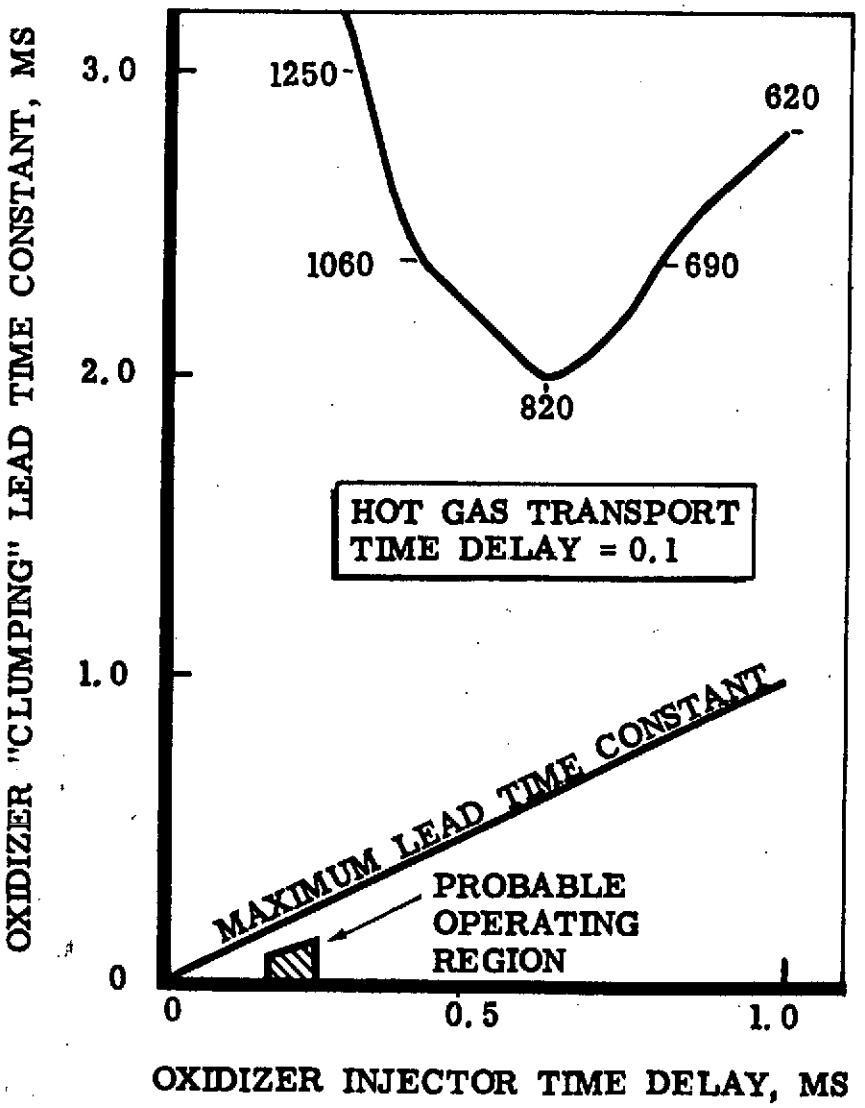

Figure 2-26. Stability Map for the Advanced Space Engine Main Combustion Chamber

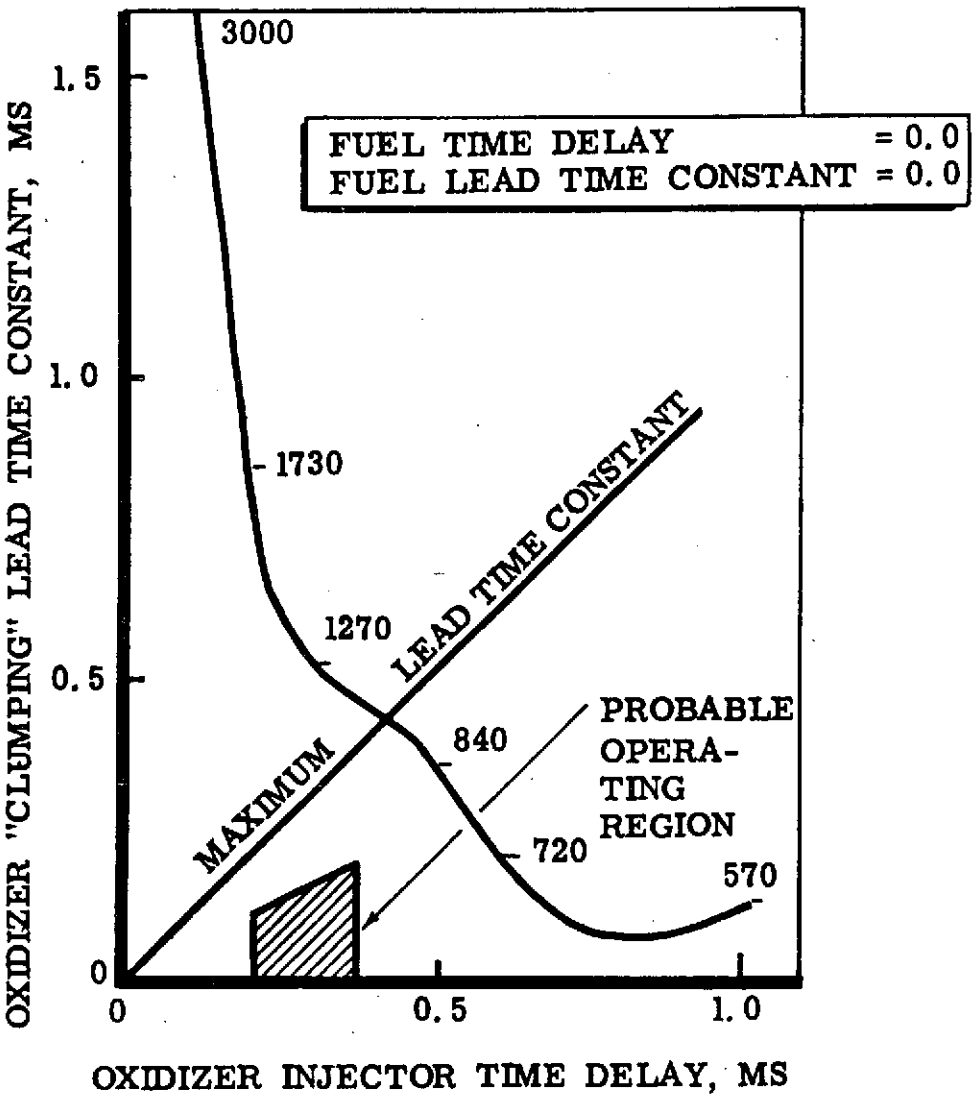

Figure 2-27. Stability Map for Advanced Space Engine Preburner

INJECTOR HEAT TRANSFER AND STRUCTURAL ANALYSIS

Flow requirements for the porous Rigimesh were analyzed on the basis of wall heat flux data taken in water-cooled experimental chambers at the injector end location. Due to the large percentage of face area displaced by the injector elements, the flow requirements are minimal (Fig. 2-28). The design range requirements of 0.091 to 0.136 kg/s (0.2 to 0.3 lb/sec) will result in face temperatures of 394 to 478 K (250 to 400 F) above the coolant injection temperature. Local injector element areas are to be cooled by the fuel-rich gases emanating from the annular injection region. Combustion and mixing delay lengths result in these areas attaining a temperature equal to the main fuel injection temperature.

The structural members of the injector are the gimbal attach plate, the inner cone, the outer shell, the injector face, and the oxygen injection elements (oxygen posts). There are three internal pressure cavities in the injector assembly: the oxygen manifold, the hot-gas cavity, and the coolant cavity formed by the injector faceplate and the backup structural faceplate. The external loads imposed on the injector assembly are the combustion chamber pressure acting on the faceplate, the reactions at the hot-gas manifold junction, and the gimbal bearing reaction. The forces at the hot-gas manifold interface are the result of gimbaling loads, vibration loads, acceleration loads, and forces that are transferred through the hot-gas manifold.

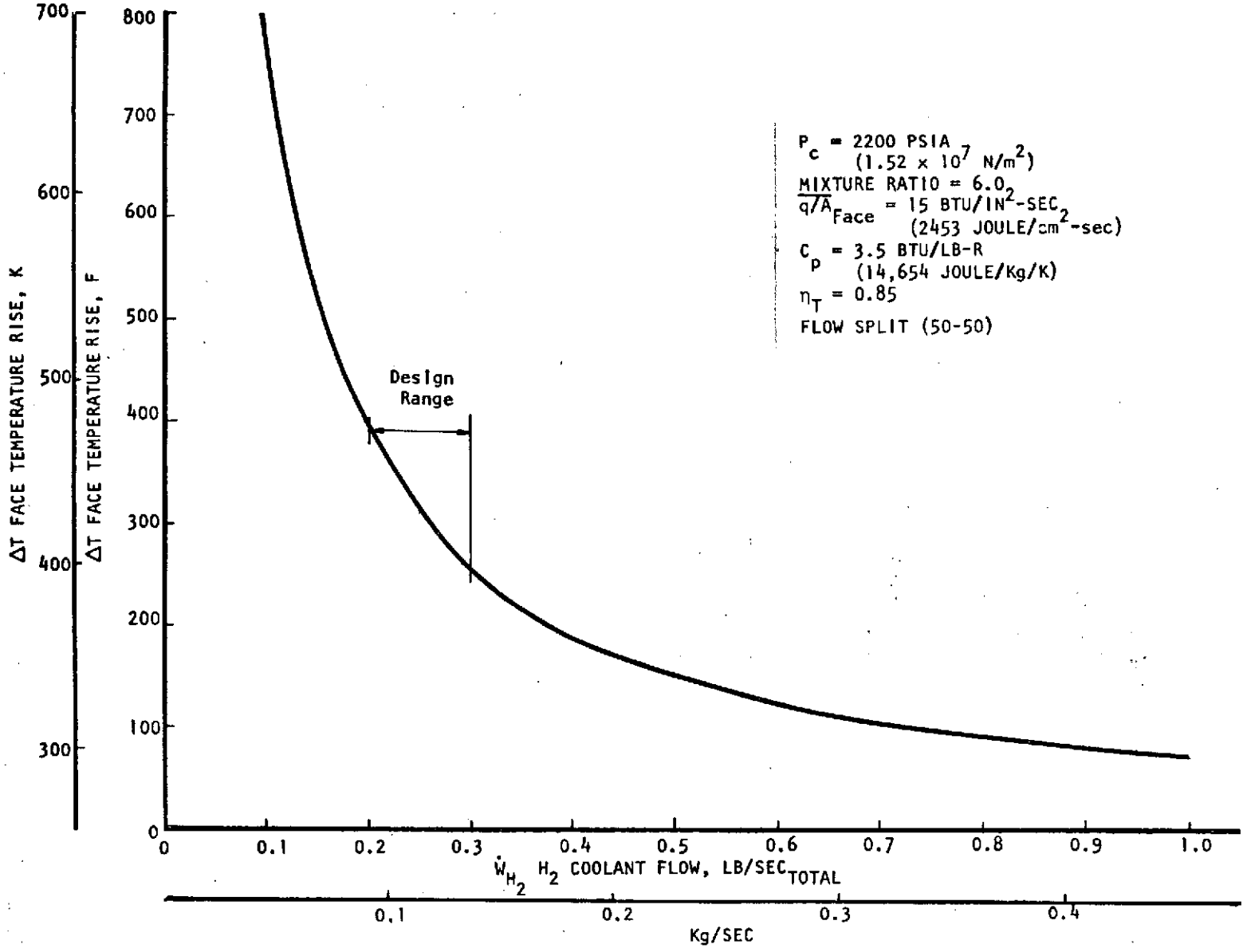

Figure 2-28. 20K (88,964 N) Injector Face Temperature Rise vs Transpirant H_2 Flow

THRUST CHAMBER

The thrust chamber design selected is based on recent design, fabrication, and test experience at Rocketdyne for high temperature and pressure applications. Included are thrust chamber configurations in the small 3558 to 111,206 N (8000 to 250,000 pound) thrust levels.

COMBUSTION CHAMBER CONFIGURATION SELECTION

The combustion chamber design selected (shown in Fig. 2-29) has a channel wall NARloy Z liner with electroformed nickel closeout coolant channels. An INCO 718 shell attached to the outer periphery of the combustion zone provides the required structural support.

The liner has 87 channels as hydrogen cooling passages from an expansion area ratio of 8 to the injector face. The coolant enters a manifold at the exit end through the channels and exits in the forward manifold and into the system.

Fabrication of the combustion zone starts with a spun NARloy Z liner machined to the final internal and external dimensions. The channels are then machined longitudinally into the liner. The INCO 718 manifold rings are furnace brazed onto either end of the NARloy Z liner. Detail machining of the rings for fuel passage and acoustic cavities are accomplished at this stage. Following the detail machining, the channel closeouts are electroformed to the proper thickness and machined. The INCO 718 stainless-steel jacket half shells are match machined to electroformed nickel, and EB welded into position. The hydrogen coolant manifolds are welded forming the closeout to the coolant passages.

NOZZLE CONFIGURATIONS

Two nozzle sections extend from an area ratio of 8 to 400, as shown in Fig. 2-29. The forward section from area ratio of 8 to 100 is a regeneratively cooled conventional tube-wall nozzle utilizing 450 A286 circular cross-section tubes. Coolant flow is supplied to the aft manifold, passes up the tubes and flows into the forward manifold. The nozzle is a conventional furnace brazed configuration with INCO 625 manifold rings and INCO 718 closeout manifolds. The nozzle is attached to the combustion zone at area ratio 8 by EB welding.

The second nozzle extends from area ratio 100 to 400 and is dump cooled with hydrogen supplied at the forward end manifold. The nozzle utilized 1250 A286 tubes to carry the hydrogen aft and exits at area ratio 400. The forward manifold ring material is INCO 625 with INCO 718 manifold closeout. Stainless-steel bands are used as stiffeners to react the low hoop stress.

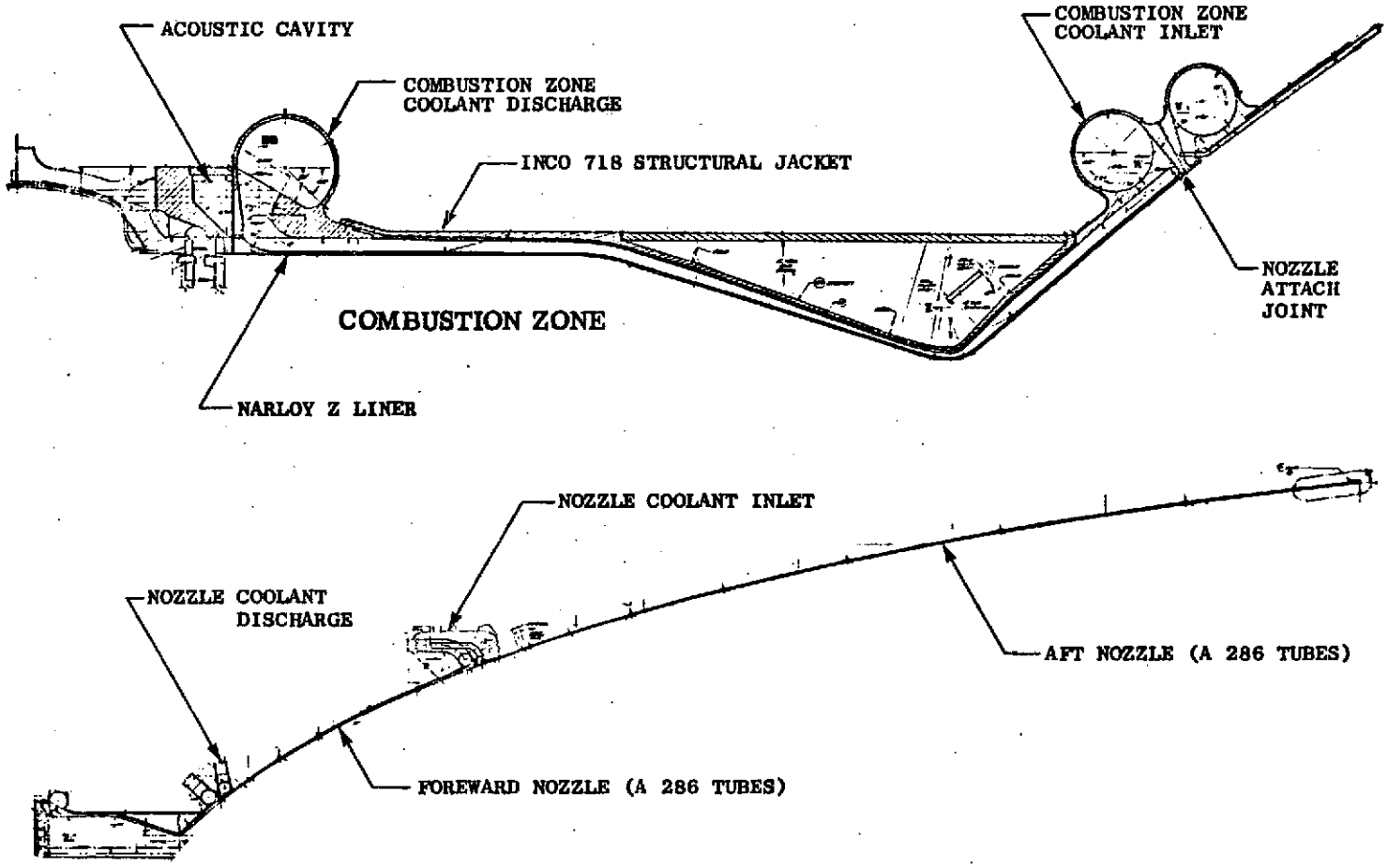

Figure 2-29. Combustion Chamber and Nozzle Designs

AERODYNAMIC AND HEAT TRANSFER ANALYSIS

During this study, significant effort was devoted to the definition of the thrust chamber coolant passage design geometry, operating wall temperatures, and thermal life aspects. Evaluation of the milled channel combustor liner, upper tubular wall nozzle and lower dump-cooled nozzle was completed.

Aerodynamic Aspects

Establishment of the throat upstream and downstream geometry together with the combustor internal geometry optimization allowed the definition of the wall geometry and accompanying nozzle performance and heat transfer. Specification of a 90-percent length optimum contour, 400:1 area ratio bell nozzle was made and accompanying viscous and potential flow efficiencies were defined. Figure 2-30 illustrates the throat Mach line values used as input to the nozzle characteristics solution program. Figure 2-31 illustrates the supersonic nozzle contour. Table 2-2 illustrates the combustion zone geometrical characteristics.

Study of the 90-percent length 400:1 area ratio bell indicated high potential flow performance and correction to the potential field performance was made to account for the viscous flow momentum loss by utilization of the Rocketdyne finite difference boundary layer solution. Selections of the comparatively sharp upstream and downstream throat radius ratios were made based on the recent analytical study (Fig. 2-32) which indicated substantial H_2 coolant pressure loss savings with no loss in potential field performance or nozzle shock introduction. Table 2-3 illustrates the boundary layer loss parameters for the selected design point.

Extensive 200 and 400:1 area ratio nozzle wind tunnel testing has been performed (Fig. 2-33), verifying the nozzle pressure distributions and wall heat transfer conditions. Figure 2-34 illustrates the nozzle pressure distributions for these tests showing good agreement with projected analytical results.

Combustor Design

Detailed computer analysis was performed to establish the coolant passage geometry required to maintain the wall surface temperatures at levels suitable for the high cyclic life requirements. Figure 2-35 illustrates the conservative combustor design heat flux profile at the 1.517×10^7 N/m^2 (2200 psia) design based on extrapolation of comprehensive lower pressure (0.517×10^7 N/m^2; 750 psia) water-cooled chamber data for a nearly identical geometrical configuration (Fig. 2-36 to 2-39). A peak heat flux of 13,410 (joules/cm^2-s (82 Btu/in.^{2}-sec) at a 1.27 cm (0.5 inch) distance upstream of the throat was specified for the 88,964 N (20K) design.

The selected coolant passage geometry for the 87-channel design is shown in Fig. 2-40. A coolant flow of 72.3 percent (MR = 6.0) is used in an uppass direction to cool the combustor. The combustor wall temperature distribution may be

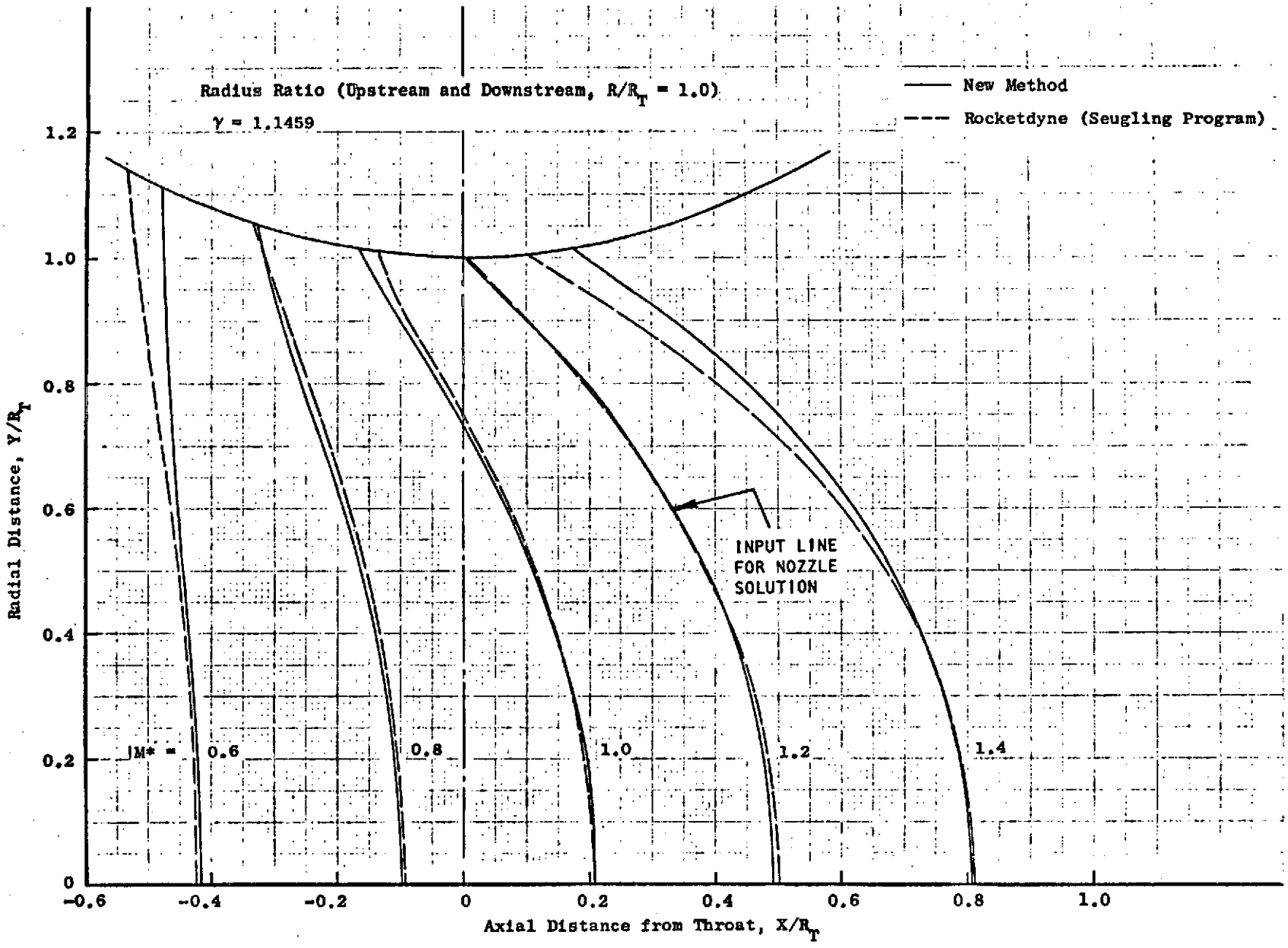

Figure 2-30. Transonic Flow Field

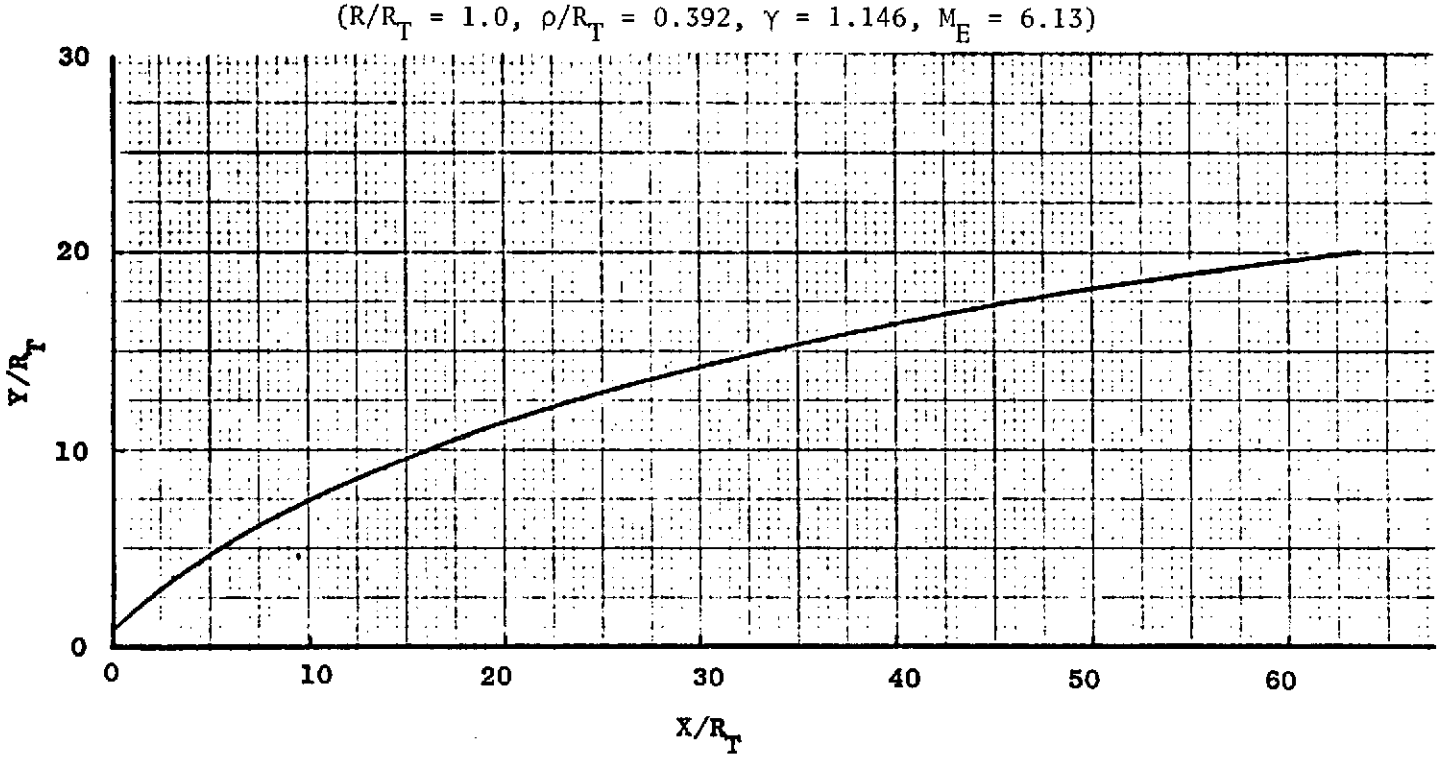

Figure 2-31. Nondimensional Nozzle Wall Contour
(ε = 400, 90-Percent L)

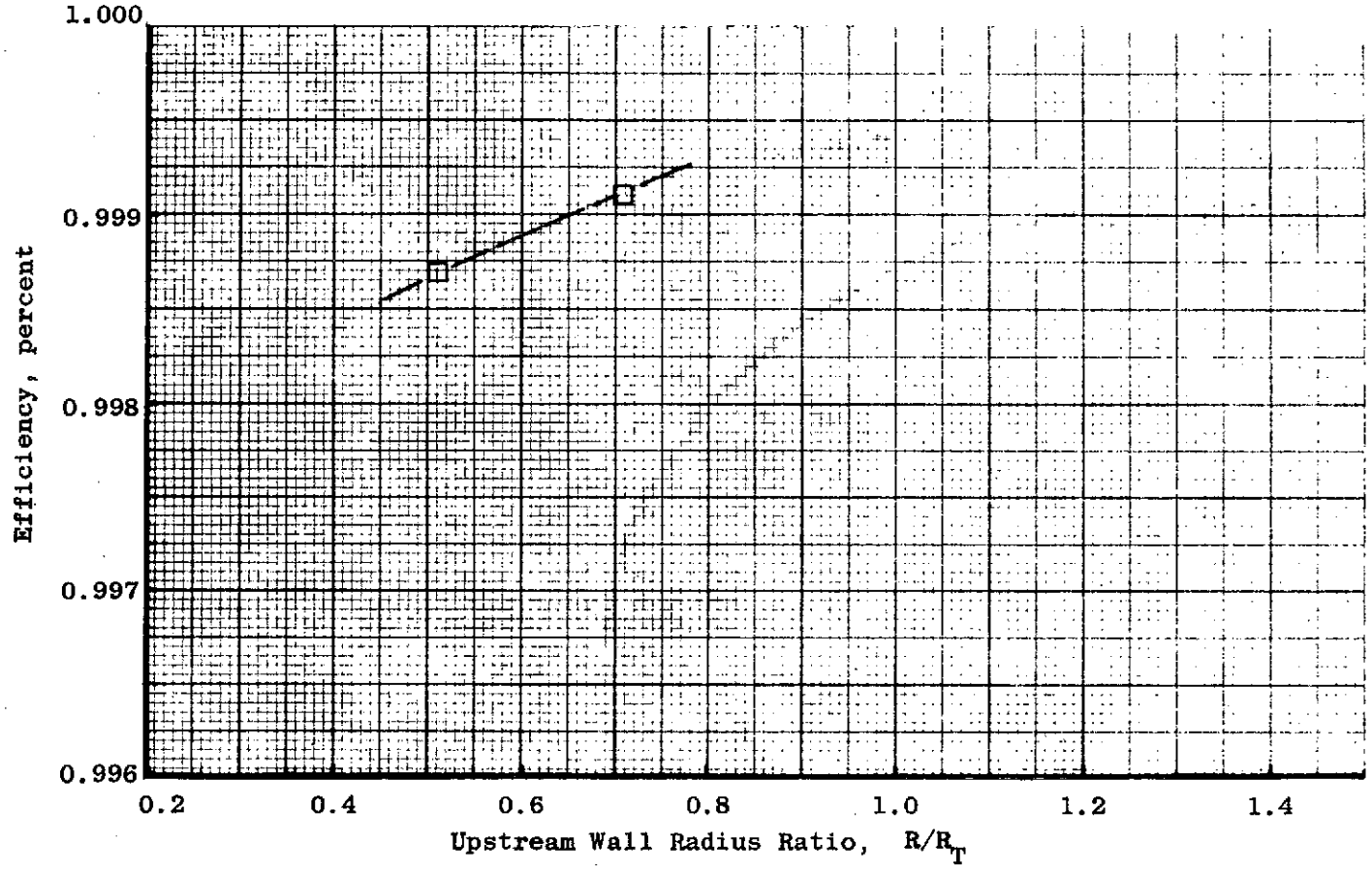

Figure 2-32. Effect of Upstream Wall Radius Ratio on Nozzle Performance (Typical, 100-Percent Length)

TABLE 2-2. ADVANCED OXYGEN-HYDROGEN ENGINE SYSTEM (88,964 N; 20K)
ε = 400:1 BELL
90% LENGTH

Vacuum Thrust, pounds (newtons)	20,000 (88,964)
Throat Stagnation Pressure, psia (N/m^2)	2200 (1.52×10^7)
Engine Mixture Ratio	6:1
c*, ft/sec (m/s)	7550 (2301)
Specific Impulse, seconds (N-s/kg)	473.4 (4642)
Propellant Flowrate, lb/sec (kg/sec)	42.247 (19.2)
Inviscid Aerodynamic Throat Area, $in.^2$ (cm^2)	4.5069 (0.699)
Geometric Throat Area, $in.^2$ (cm^2)	4.5473 (0.705)
Throat Discharge Coefficient at $R/R_T = 1.0$	0.9911
Throat Radius, in. (cm)	1.203 (3.06)
Throat Boundary Layer Displacement Thickness, in. (cm)	0.00044 (0.00112)
Upstream Throat Radius of Curvature, in. (cm)	1.203 (3.06)
Downstream Throat Radius of Curvature, in. (cm)	0.481 (1.22)
Combustion Zone Length, in. (cm)	8.5 (21.6)
Contraction Ratio	4.0:1
Convergence Half Angle, degrees (rad)	17 degree (0.297)
Nozzle Attach Area Ratio	8:1
Dump Cooled Nozzle Attach Area Ratio	100:1

TABLE 2-3. O_2/H_2 NOZZLE EXIT BOUNDARY LAYER PARAMETERS (88,964 N; 20K)

	P_c = 2200 psia ($1.517\ N/m^2 \times 10^7$)	P_c = 440 psia ($3.03 \times 10^6\ N/m^2$)	P_c = 28 psia ($193{,}053\ N/m^2$)
Momentum Thickness (θ_E), inch (cm)	0.221 (0.561)	0.306 (0.778)	0.530 (1.35)
Energy Thickness ($\emptyset_E$), inch (cm)	0.360 (0.914)	0.497 (1.26)	0.860 (2.18)
Velocity Thickness (δ_{VE}), inch (cm)	2.68 (6.81)	3.70 (9.4)	6.40 (16.3)
Displacement Thickness (δ^*_E), inch (cm)	0.402 (1.02)	0.554 (1.41)	0.958 (2.43)
Displacement Thickness at Throat ($10^3\ \delta^*_T$), inch (cm)	0.44 (1.12)	0.62 (1.57)	1.06 (2.69)
Momentum Reynolds Number (Re_θ)	1460	404	46
Thrust Coefficient Loss (ΔC_F)	0.061	0.084	0.146
Stanton Number ($10^3\ N_{ST}$)	1.33	1.84	3.18

$\overline{t}_w$ = 300 F (422 K); MR = 6.0

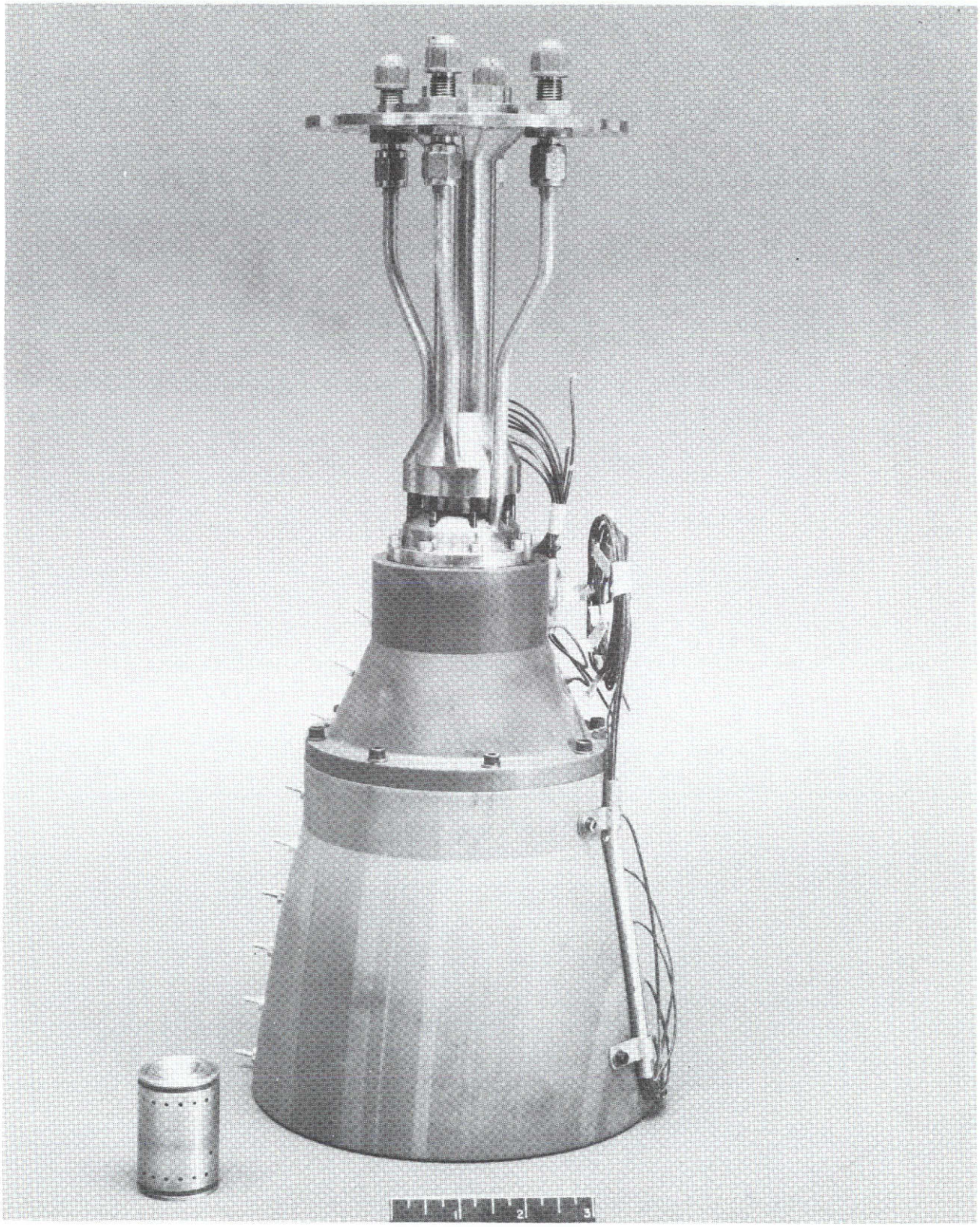

1XZ32-3/20/70-C1B

Figure 2-33. 400:1 Nozzle Wind Tunnel Test Model

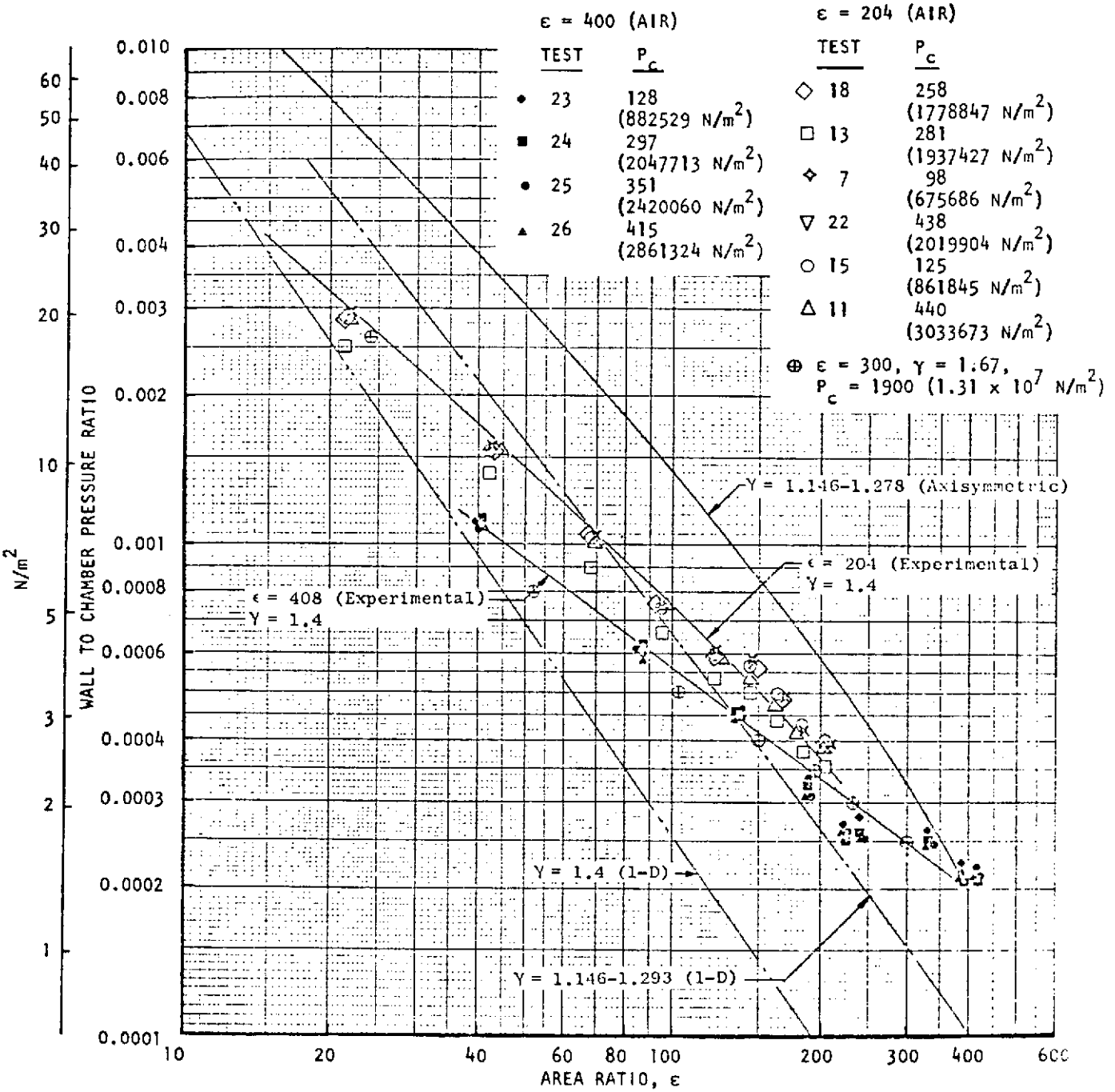

Figure 2-34. Nozzle Pressure Ratio Distribution High Area Ratio Models ($\gamma = 1.4$)

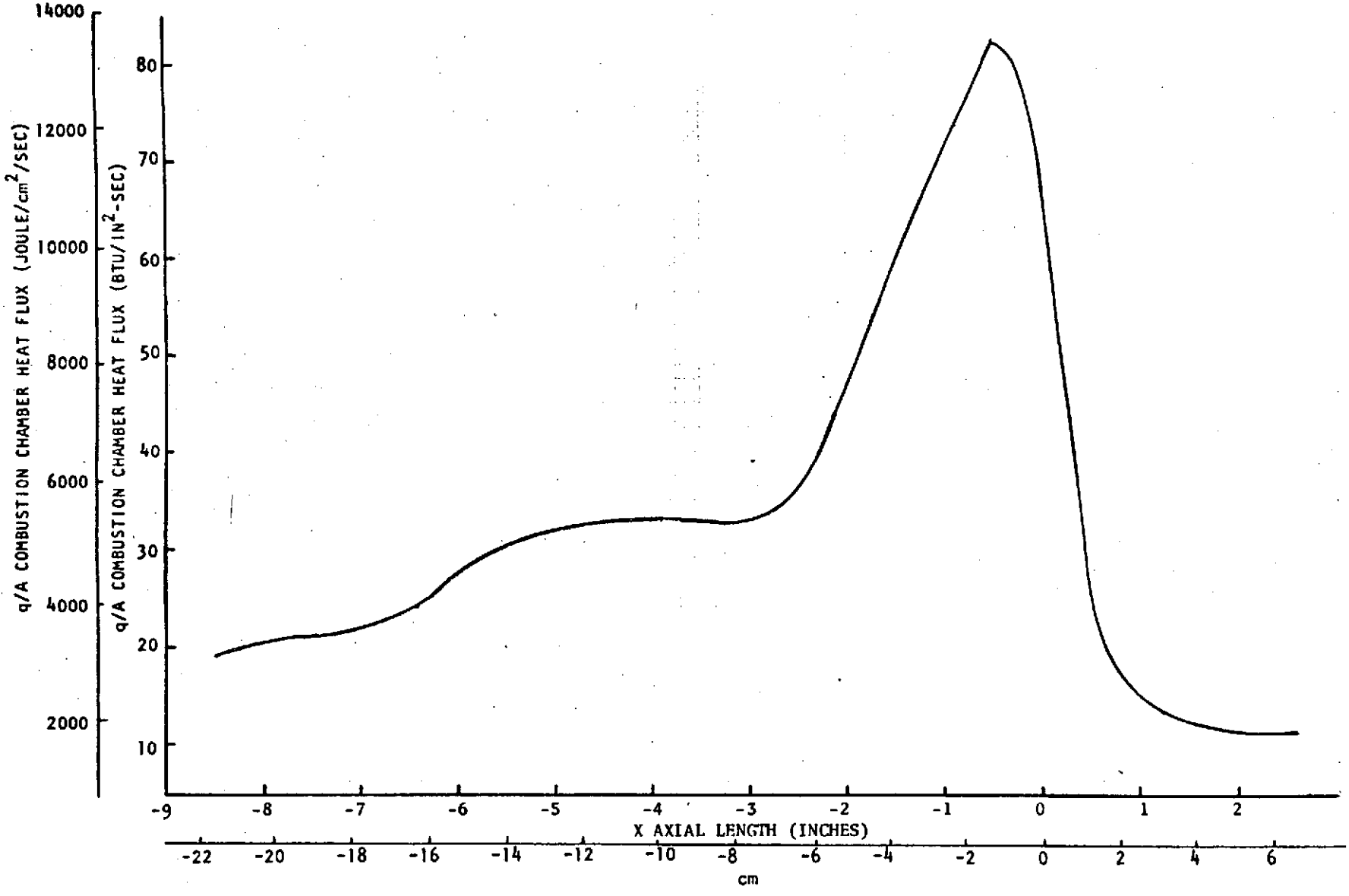

Figure 2-35. (88,964 N) 20K Combustion Chamber Wall Heat Flux vs Axial Length

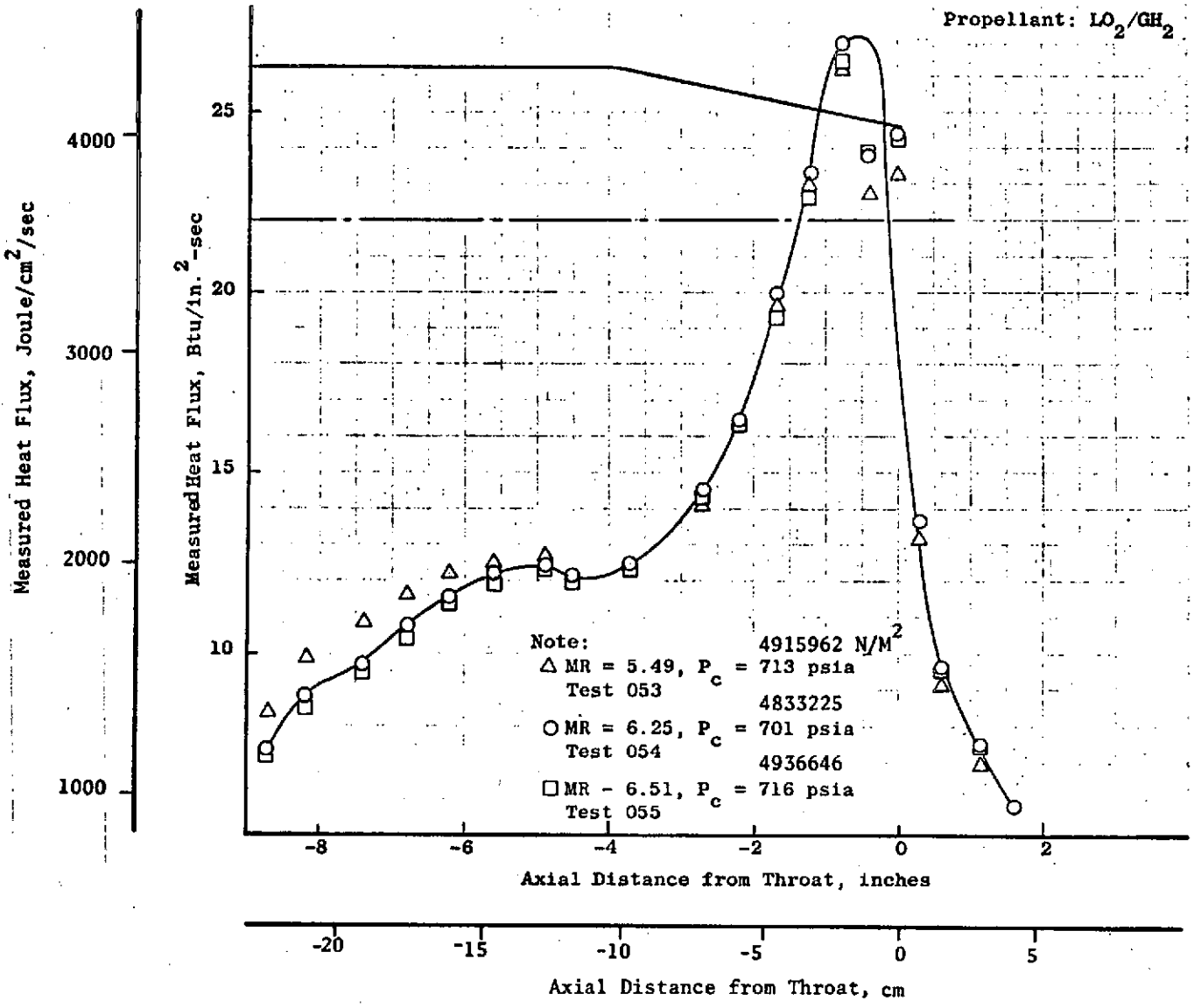

Figure 2-36. Cylindrical Chamber Wall Heat Flux Distribution, Mixture Ratio Influence, LO_2-GH_2

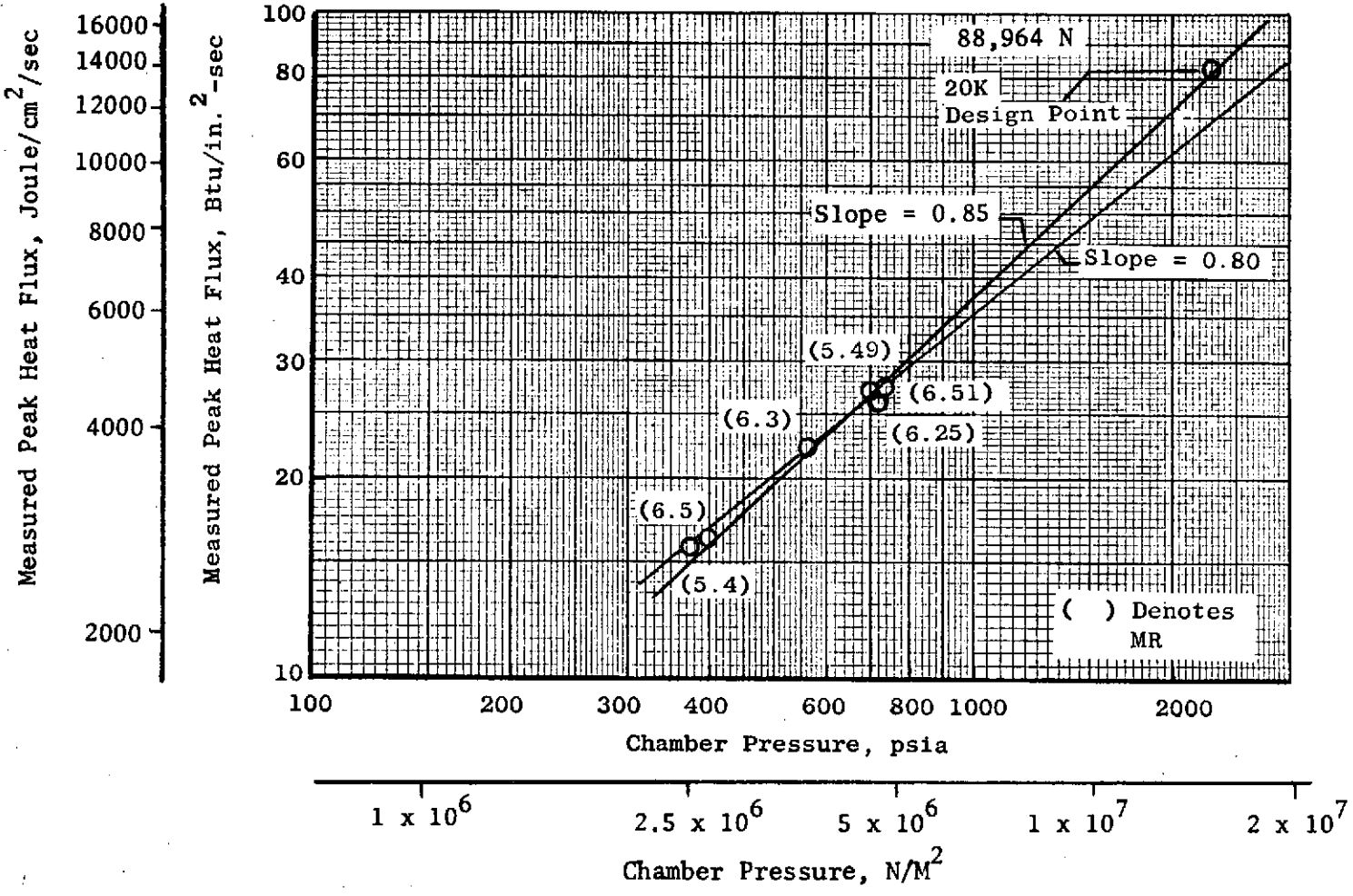

Figure 2-37. Peak Heat Flux Variation with Chamber Pressure

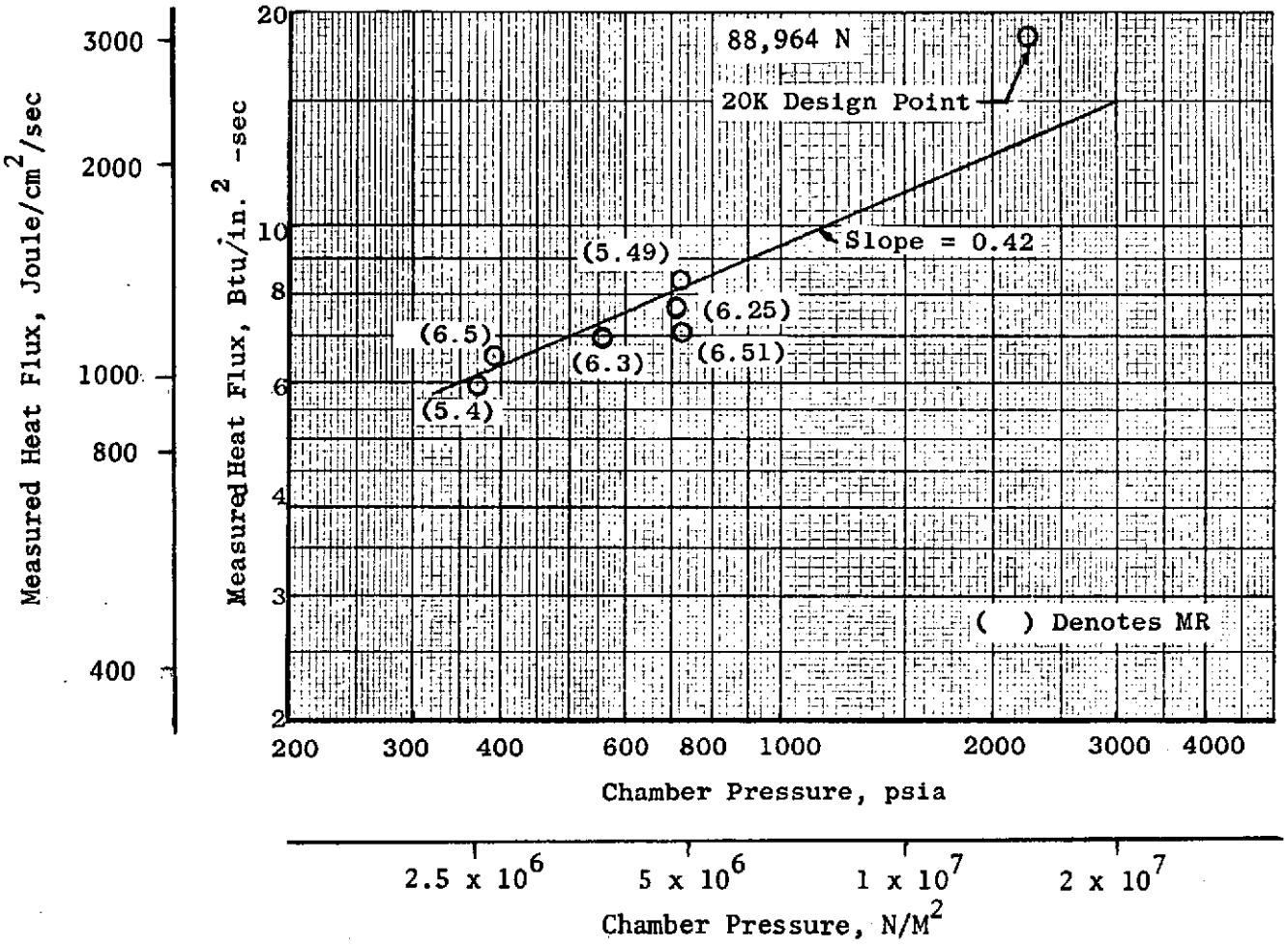

Figure 2-38. First Passage Heat Flux Variation with Chamber Pressure O_2/H_2 Experimental Data

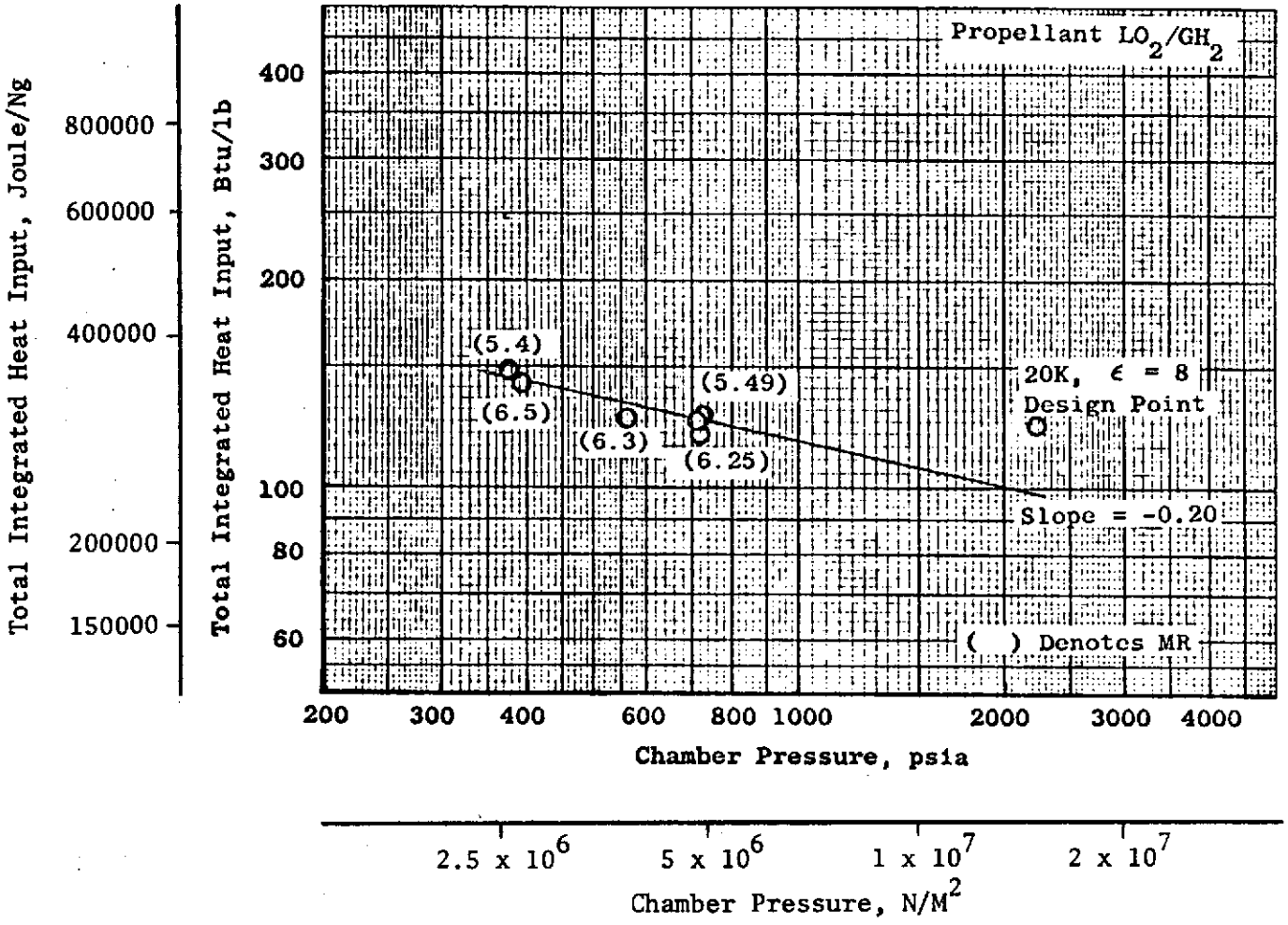

Figure 2-39. Cylindrical Chamber Experimental Integrated Heat Input Variation with Chamber Pressure ($\varepsilon = 4.0$)

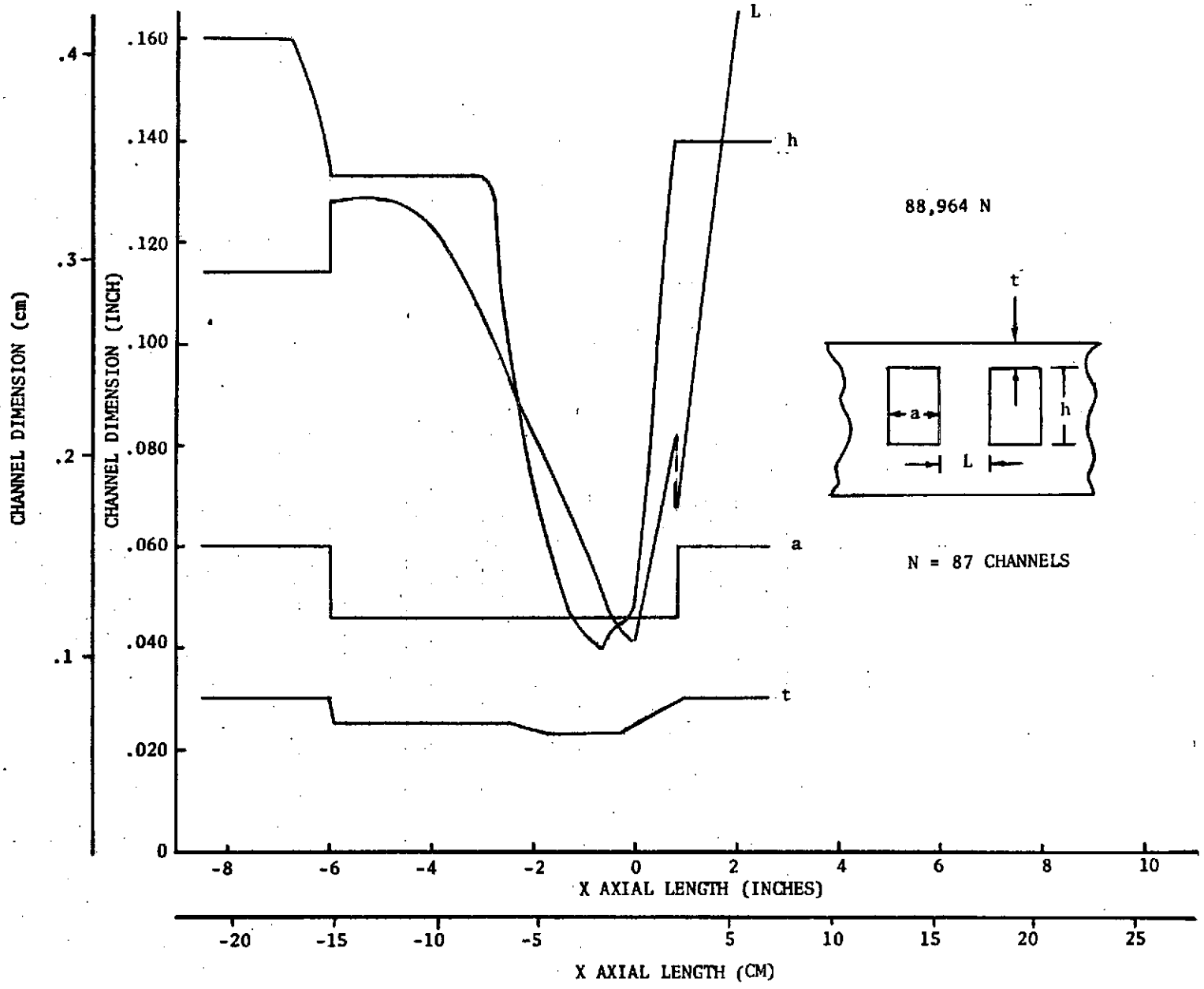

Figure 2-40. 20K O_2/H_2 Combustion Chamber Channel Design Geometry vs Axial Length

noted in Fig. 2-41. Cyclic life was found to be met with an 820 F throat wall temperature, as shown in Fig. 2-42. Cooling and pressure drop studies performed optimized the wall cooling and pressure drop relationships along the combustor wall for 40 stations.

Two-dimensional isotherm conditions for the $\varepsilon = 8$ nozzle uppass entrance are shown in Fig. 2-43. Throat region temperatures in the channel section are shown in Fig. 2-44. Injector region values are shown in Fig. 2-45. Coolant temperature rise versus axial length and coolant pressure drop distribution at nominal and off-mixture ratio design are shown in Fig. 2-46 and 2-47, respectively. As shown in another section of this report, the values determined result in satisfactory engine system balance conditions at the required mixture ratio levels.

Upper Nozzle Design

The 88,964 N (20K) upper tubular nozzle was developed as a configuration extending from an area ratio of 8 to 100 with circular tubes of 0.0178 cm (0.007 inch) thickness A286 material. Wall temperature distribution is shown in Fig. 2-48 for the preliminarily selected 450-tube configuration. Typical nozzle coolant temperature rises for both the upper and lower nozzle are illustrated in Fig. 2-49.

Figure 2-50 shows the nozzle heat flux profile versus axial distance. The comparatively low heat flux levels imposed allow for a low thermal conductivity A286 tube material. Analysis was conducted as a function of the number of upper nozzle coolant tubes, as shown in Fig. 2-51. Acceptable diameters 0.122 cm; (0.048 inch) are shown at the $\varepsilon = 8$ attach point for the selected 450-tube design with a tube diameter of 0.434 cm (0.171 inch) at the nozzle exit. The small tube diameters allow for a lightweight nozzle with minimum 0.018 cm (0.007) inch wall thickness values. As shown in Fig. 2-52, the wall thickness is within the strength requirement of the A286 wall material. Figure 2-53 shows the comparative characteristics of the A286 alloy selected. This material has been previously shown to provide good life characteristics, high strength, and ductility.

Dump-Cooled Nozzle Design

Figure 2-54 illustrates the dump-cooled nozzle wall temperature distribution versus length. A maximum design wall temperature of 1172 K (1650 F) is illustrated at the nozzle discharge point for a 1.172 kg/s (0.38 lb/sec) nominal flowrate. Only small wall-to-coolant temperature differences are present at the flow exit due to a high exit bulk temperature for performance.

Figure 2-55 shows the nozzle pressure drop for both the upper and lower (dump) nozzle sections. Both pressure drop levels are low as a result of the small imposed heat flux levels and excellent H_2 cooling ability.

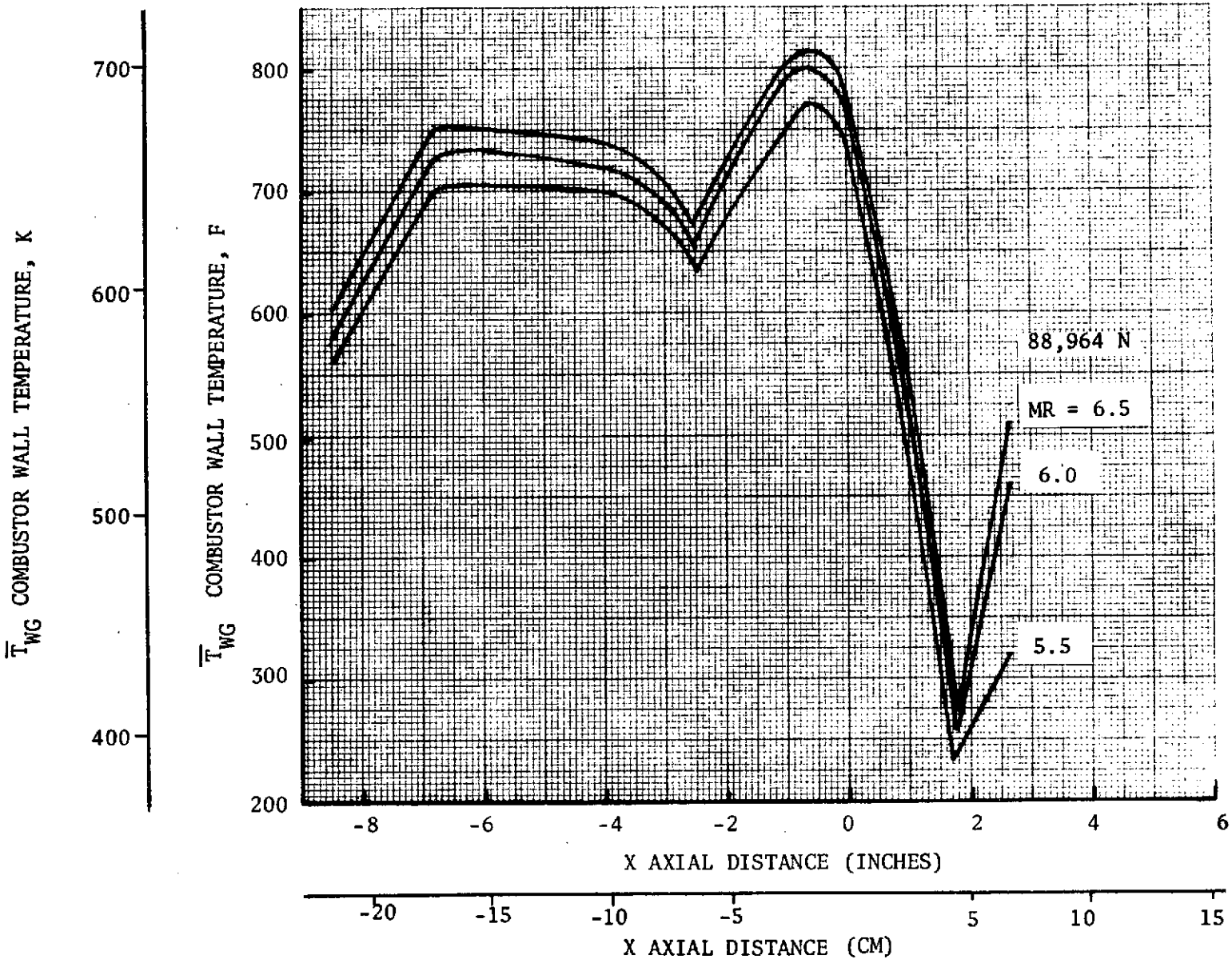

Figure 2-41. 20K O_2/H_2 Combustor Wall Temperature vs Axial Distance

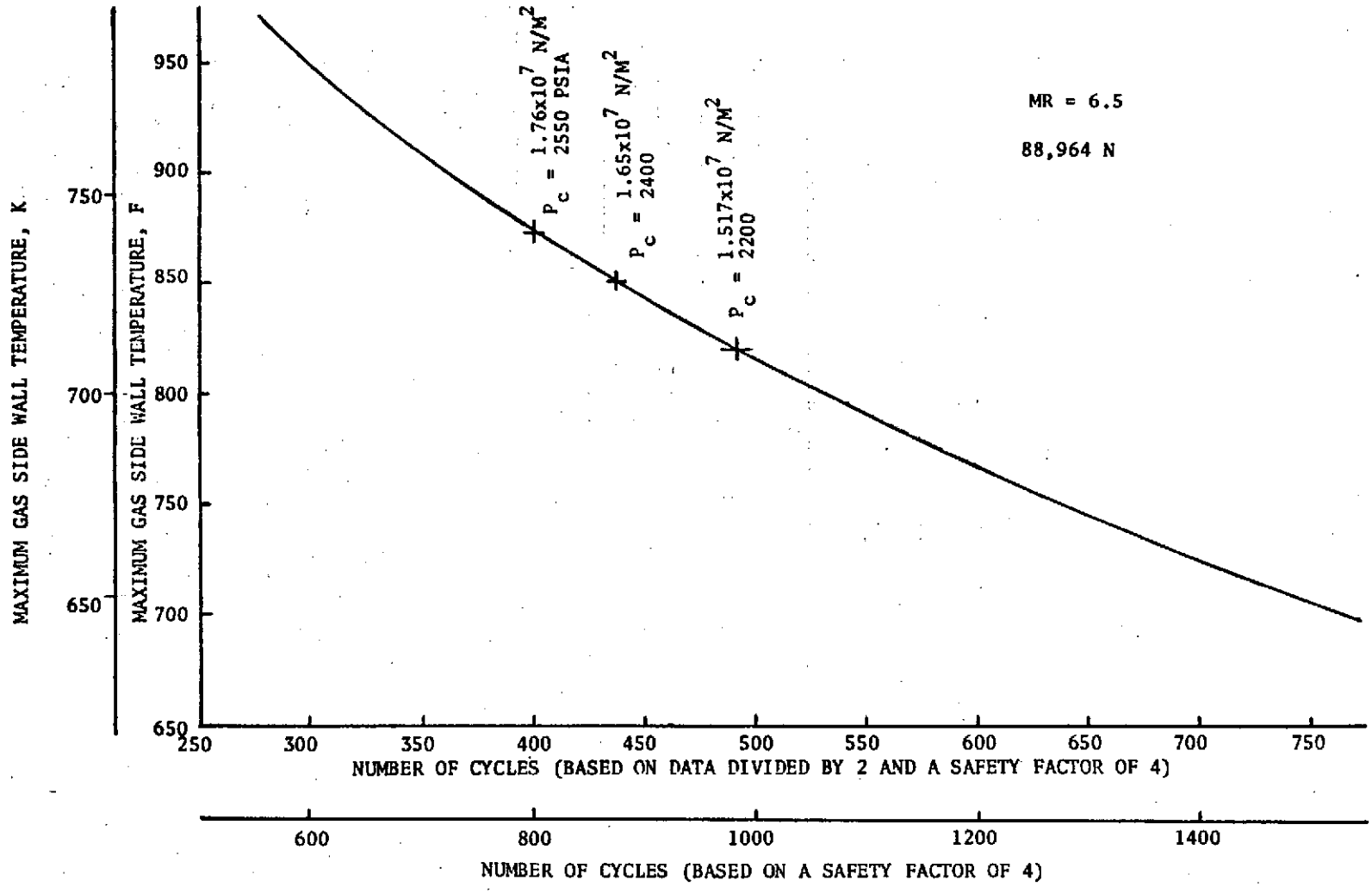

Figure 2-42. 20K Bell Life Cycle Parametric Data

20K MR=6.5

STATION NO. = 0 TWG(1-D) = 811.80 F
X (INCHES) = 2.6761 TWC(1-D) = 787.46 F
AREA RATIO = 14.9769 HC(1-D) = 0.9519E-02

CHANNEL DIMENSIONS (IN.)	THERMAL CONDUCTIVITY (BTU/IN-SEC-F)	COMBUSTION-GAS PARAMETERS	COOLANT PARAMETERS
WALL THICKNESS = 0.0300			TBULK = -371.00 F
CHANNEL HEIGHT = 0.1400	WALL = 0.4530E-02	TAW = 5735.06 F	TB/TWC EXPONENT = 0.550
CHANNEL WIDTH = 0.0600	CLOSEOUT = 0.9000E-03	HG = 0.2252E-02	MAX. CURVATURE = 1.400
LAND WIDTH = 0.1797		(BTU/IN2-S-F)	HC(REF.) = 0.2905E-01
CLOSEOUT THICK.= 0.1500			(BTU/IN2-S-F)

BETA = 1.896 AT ITERATION NUMBER 25

CONVERGENCE SATISFIED AT ITERATION = 92

HEAT BALANCE = 0.1259E-03 MAXIMUM DT/T = 0.4479E-04 AT NODE 61

TEMPERATURES (F)

524.81	521.36	512.44	504.52	505.52	506.77	507.30
495.32	495.76	486.44	477.63	479.40	481.16	481.65
474.62	470.51	460.37	448.37	453.29	456.65	457.75
450.77	446.59	434.49	414.66	428.77	434.32	435.88
351.78	345.23	325.01	288.84			
264.62	277.07	254.25	216.18			
254.15	245.98	220.47	174.10	130.99	106.62	98.74
219.67	215.62	204.15	187.73	182.63	179.09	177.63
207.66	205.99	201.64	196.51	195.33	194.55	194.28
204.66	203.85	201.32	198.56	197.96	197.57	197.45

FINAL COOLANT FILM COEFFICIENTS

0.010746	0.011471	0.011432	0.011421
0.010804			
0.011427			
0.010652	0.010255	0.010495	0.010576

FIN FACTOR = 1.3494

Figure 2-43. 20K Combustion Chamber ε = 8 Region Two-Dimensional Wall Temperature Distribution (P_c = 2200 psia, MR = 6.5)

20K MR=6.5

STATION NO. = 17 TNG(1-D) = 770.07 F
X (INCHES) = -0.8550 TWC(1-D) = 607.70 F
AREA RATIO = 2.6896 HC(1-D) = 0.8459E-01

CHANNEL DIMENSIONS (IN.)
WALL THICKNESS = 0.0230
CHANNEL HEIGHT = 0.0420
CHANNEL WIDTH = 0.0460
LAND WIDTH = 0.0560
CLOSEOUT THICK.= 0.1500

THERMAL CONDUCTIVITY (BTU/IN-SEC-F)
WALL = 0.4525E-02
CLOSEOUT = 0.9000E-03

COMBUSTION-GAS PARAMETERS
TAW = 5869.36 F
HG = 0.1442E-01 (BTU/IN2-S-F)

COOLANT PARAMETERS
TBULK = -260.65 F
Tb/TWC EXPONENT = 0.550
MAX. CURVATURE = 1.100
HC(REF.) = 0.1957E 00 (BTU/IN2-S-F)

BETA = 1.980 AT ITERATION NUMBER 25

CONVERGENCE SATISFIED AT ITERATION = 161
HEAT BALANCE = 0.1565E-03 MAXIMUM DT/T = 0.9725E-04 AT NODE 84

TEMPERATURES (F)

821.10	818.89	813.82	810.12	811.28	813.40	814.33
699.25	696.46	689.86	684.63	687.21	690.47	691.77
581.12	576.68	564.95	552.90	562.46	569.48	571.82
469.00	461.81	440.24	403.61	440.24	453.17	456.56
209.34	277.10	258.74	167.88			
164.77	151.20	110.46	43.45			
101.37	86.53	41.34	-37.76	-128.04	-171.73	-184.60
-19.48	-21.36	-26.67	-34.14	-40.24	-44.43	-45.90
-31.13	-31.31	-31.60	-32.45	-32.95	-33.29	-33.42
-32.03	-32.05	-32.14	-32.25	-32.32	-32.37	-32.41

FINAL COOLANT FILM COEFFICIENTS

0.092897	0.092910	0.092184	0.091995
0.108125			
0.122089			
0.131289	0.146210	0.158608	0.162031

FIN FACTOR = 0.9616

Figure 2-44. 20K Combustion Chamber Throat Region Two-Dimensional Wall Temperature Distribution (P_c = 2200 psia, MR = 6.5)

20K MR=6.5

STATION NO. = 39 TWG(1-D) = 851.02 F
X (INCHES) = -8.4645 TWC(1-D) = 809.12 F
AREA RATIO = 7.8961 HC(1-D) = 0.2251E-01

CHANNEL DIMENSIONS (IN.)
WALL THICKNESS = 0.0300
CHANNEL HEIGHT = 0.1600
CHANNEL WIDTH = 0.0500
LAND WIDTH = 0.1141
CLOSEOUT THICK.= 0.1500

THERMAL CONDUCTIVITY (BTU/IN-SEC-F)
WALL = 0.4535E-02
CLOSEOUT = 0.9000E-03

COMBUSTION-GAS PARAMETERS
TAW = 5724.12 F
HG = 0.3880E-02 (BTU/IN2-S-F)

COOLANT PARAMETERS
TBULK = -35.05 F
TL/TWC EXPONENT = 0.550
MAX. CURVATURE = 1.000
HC(REF.) = 0.4109E-01 (BTU/IN2-S-F)

BETA = 1.878 AT ITERATION NUMBER 25

CONVERGENCE SATISFIED AT ITERATION = 77

HEAT BALANCE = 0.1753E-03 MAXIMUM DT/T = 0.9952E-04 AT NODE 81

TEMPERATURES (F)

604.52	603.08	600.10	600.27	604.07	607.61	608.97
561.01	559.38	555.73	555.06	560.31	564.82	566.49
518.40	516.24	510.55	505.98	517.28	524.66	527.38
476.99	474.08	465.02	447.46	477.96	489.97	493.32
283.18	277.97	261.94	233.77			
171.24	166.96	154.24	133.52			
125.48	122.25	109.46	87.68	59.71	45.04	40.48
101.07	99.65	95.68	90.02	87.03	84.96	84.23
95.02	94.64	93.66	92.44	91.91	91.56	91.44
93.95	93.78	93.38	92.89	92.69	92.56	92.51

FINAL COOLANT FILM COEFFICIENTS

0.027070	0.026563	0.026397	0.026346
0.031379			
0.034191			
0.035736	0.036782	0.037365	0.037552

FIN FACTOR = 1.3664

Figure 2-45. 20K Combustion Chamber Injector Region Two-Dimensional Wall Temperature Distribution (P_c = 2200 psia, MR = 6.5)

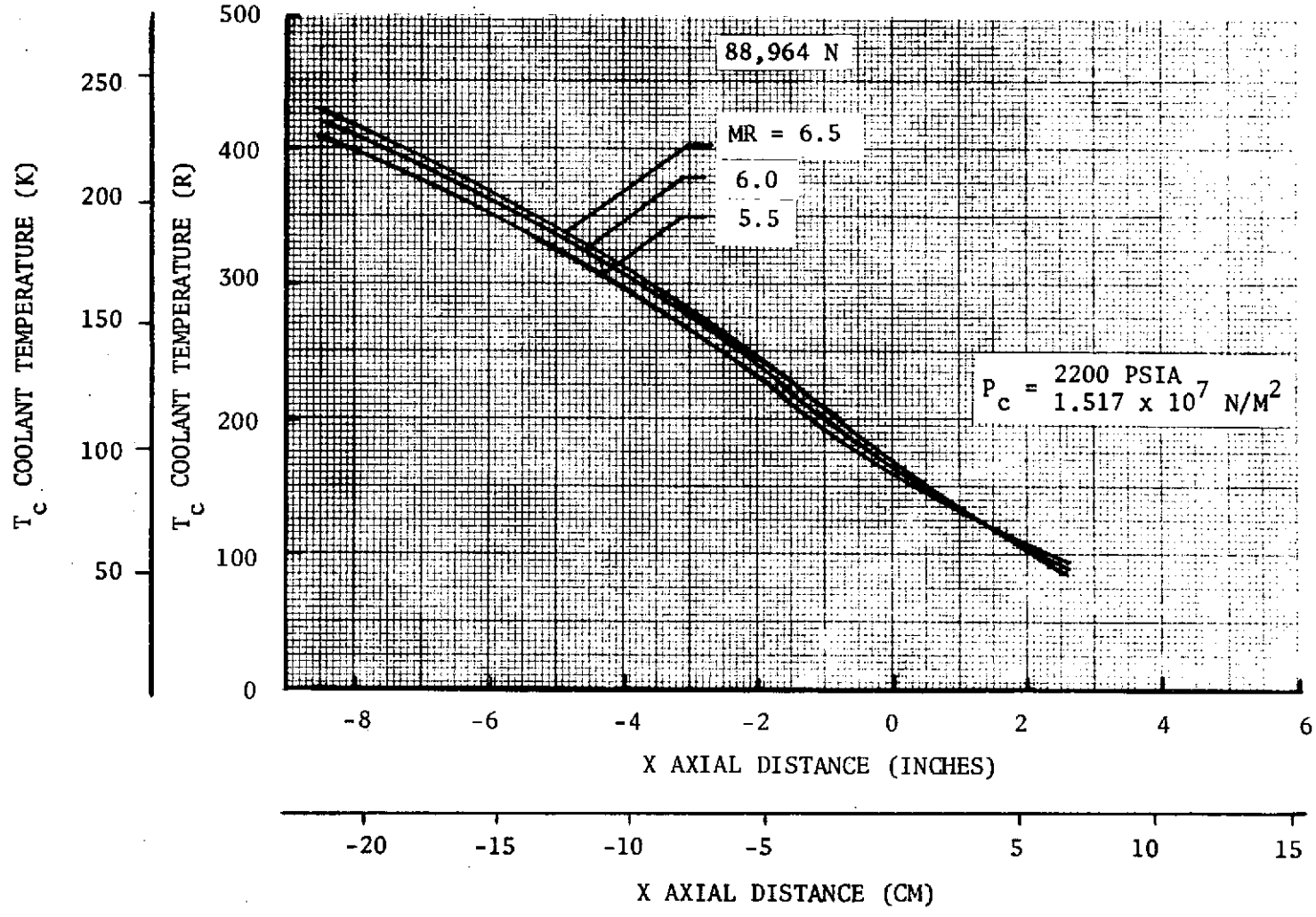

Figure 2-46. 20K Combustor Coolant Temperature Rise vs Length

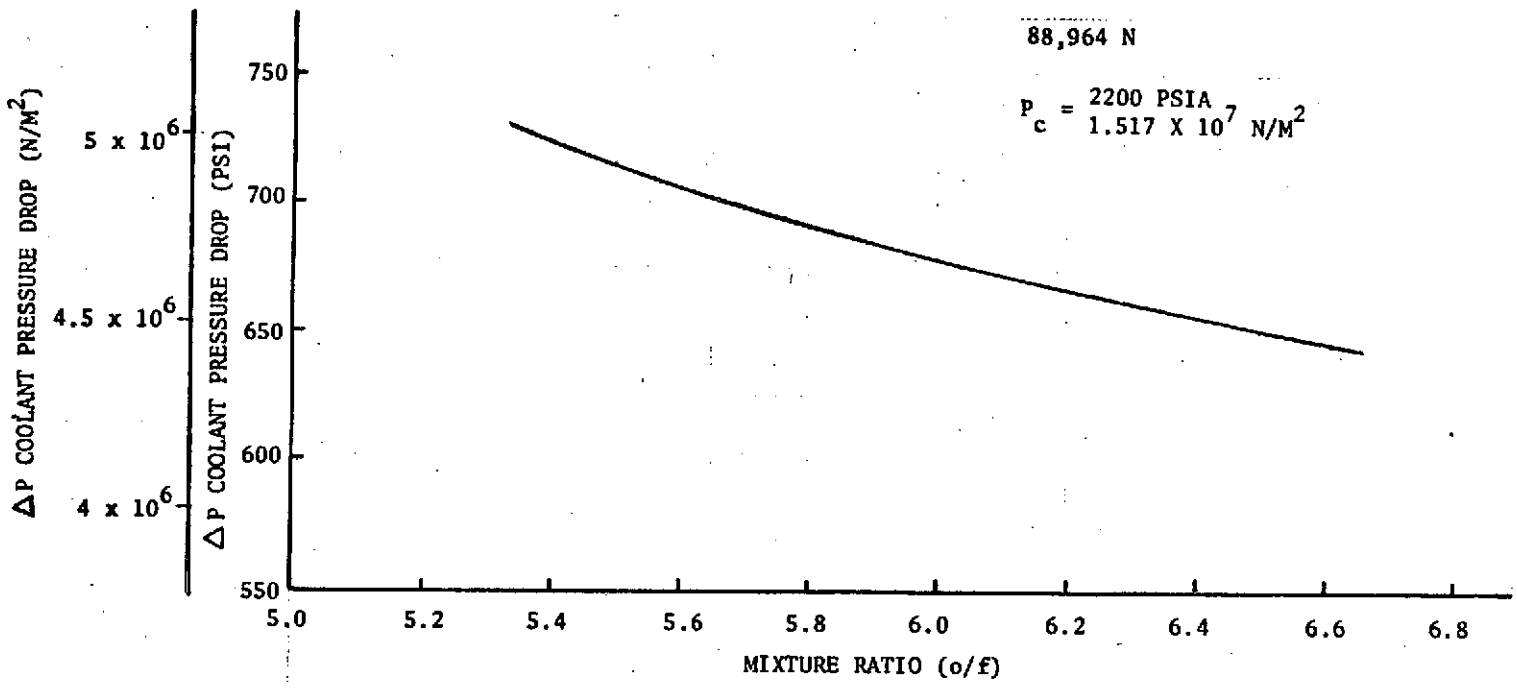

Figure 2-47. 20K Combustor Coolant Pressure Drop vs Mixture Ratio

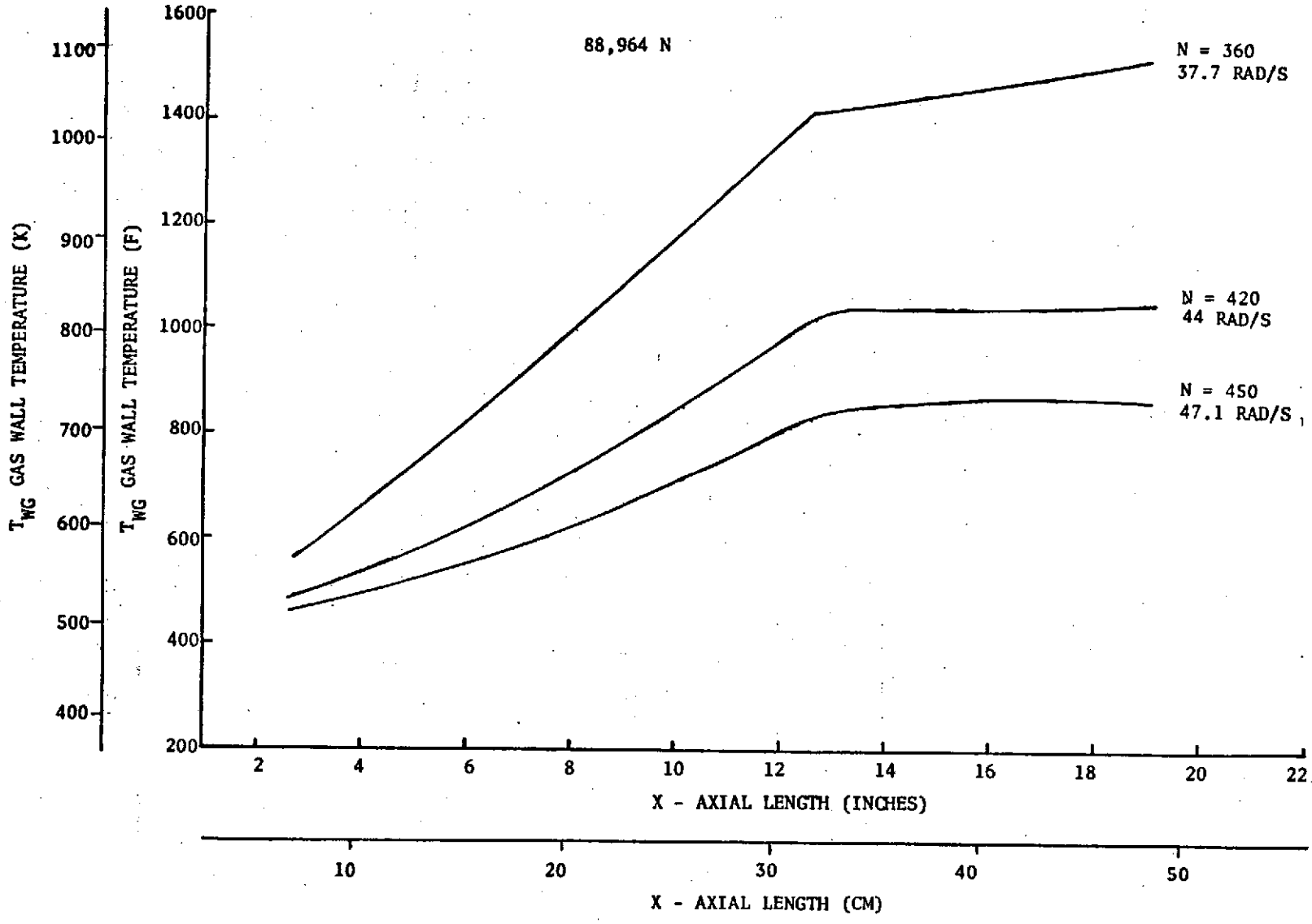

Figure 2-48. 20K Upper Nozzle (ε = 8-100, MR = 6.0) Wall Temperature versus Axial Length

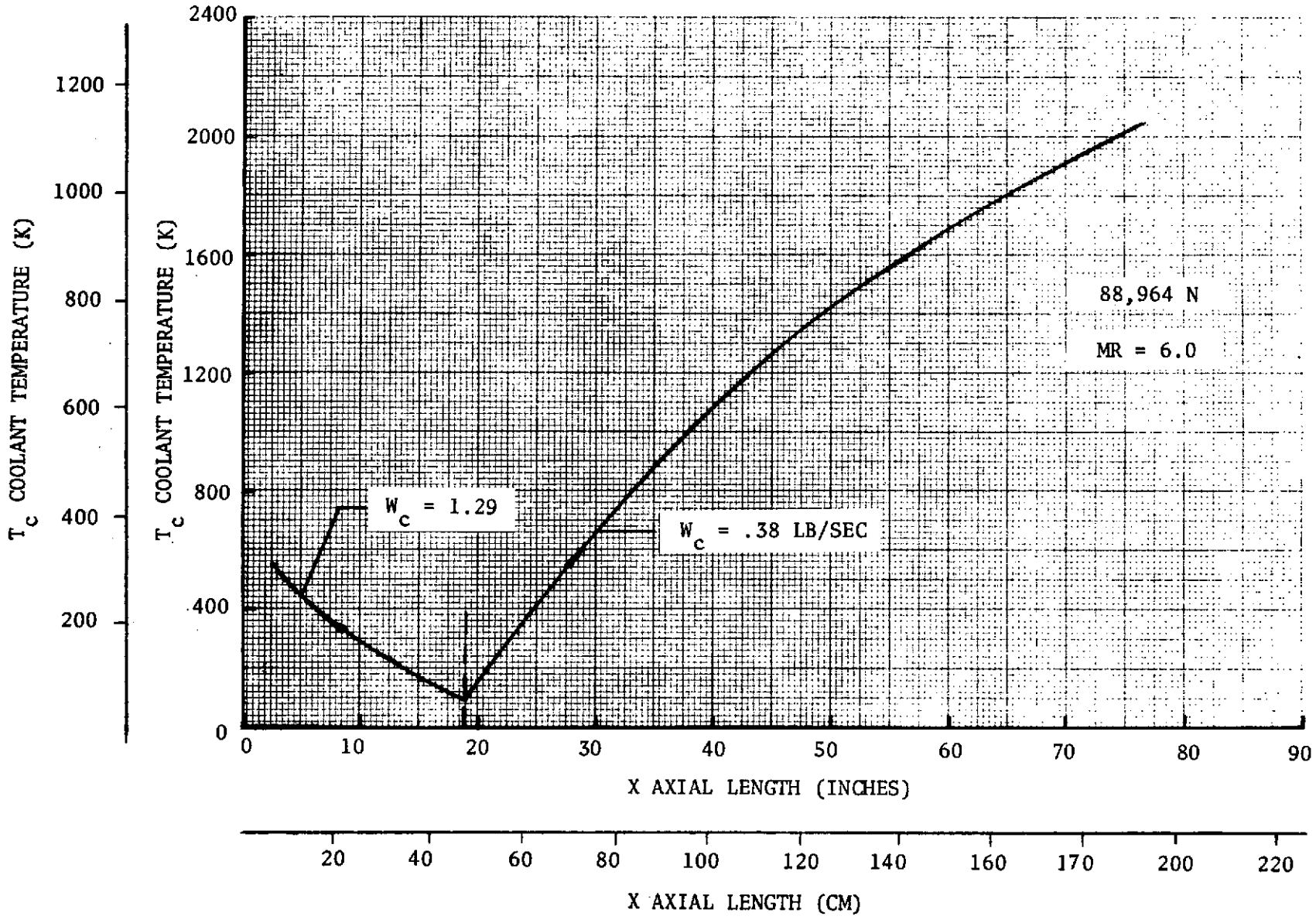

Figure 2-49. 20K ε = 400 Nozzle Coolant Temperature vs Axial Length

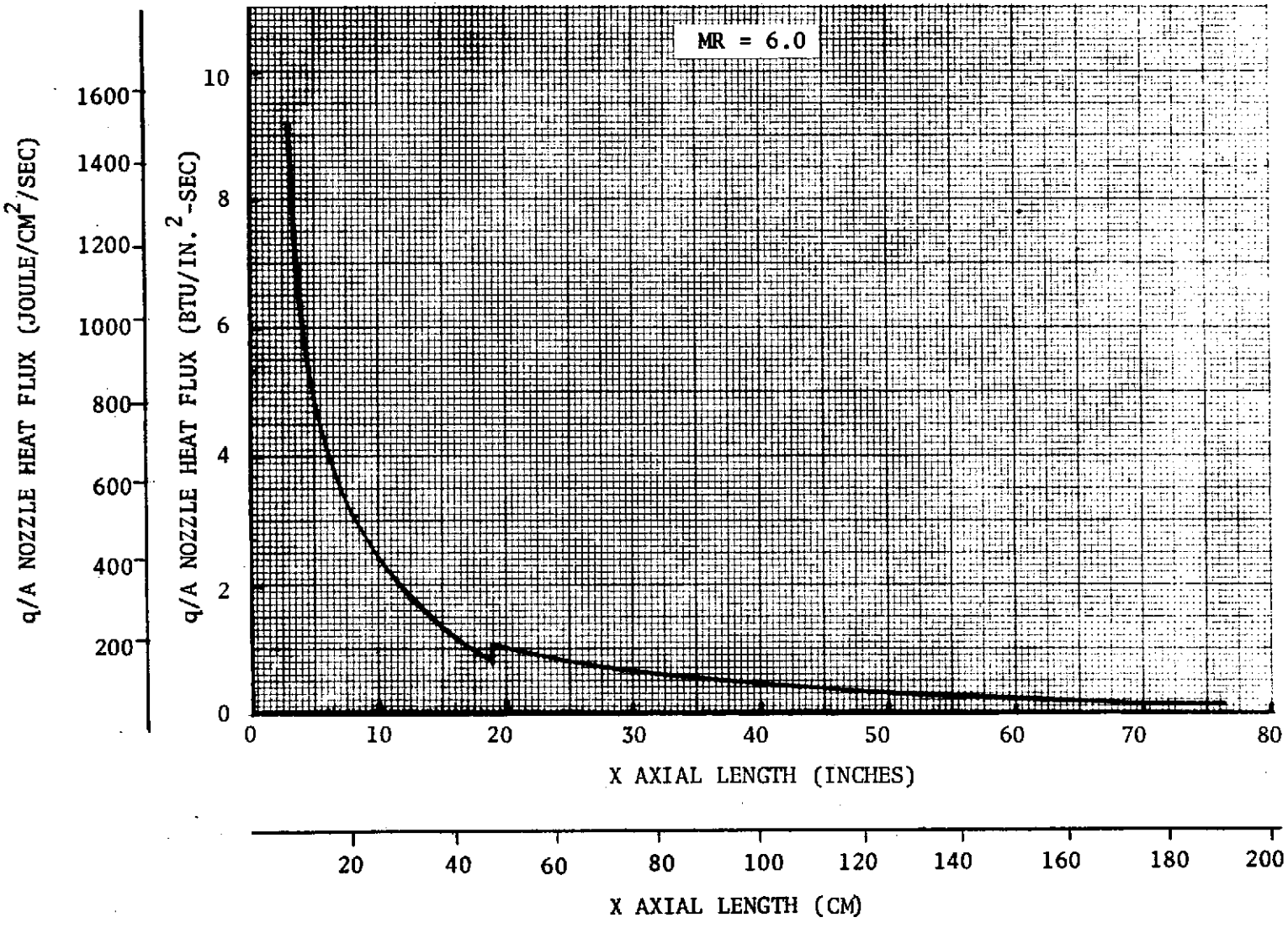

Figure 2-50. Nozzle Heat Flux vs Axial Length

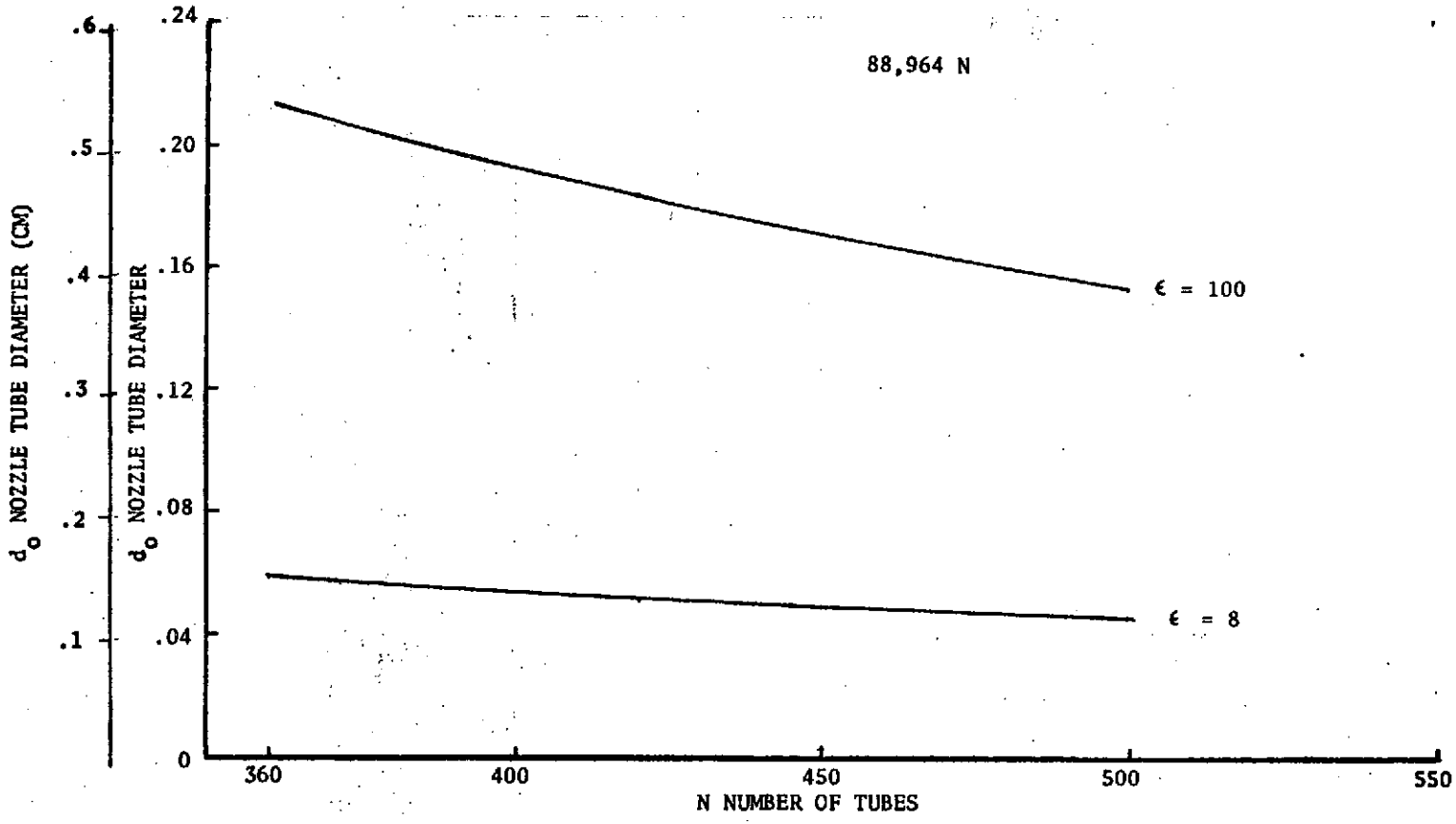

Figure 2-51. 20K Upper Nozzle Tube Diameter vs Number of Tubes

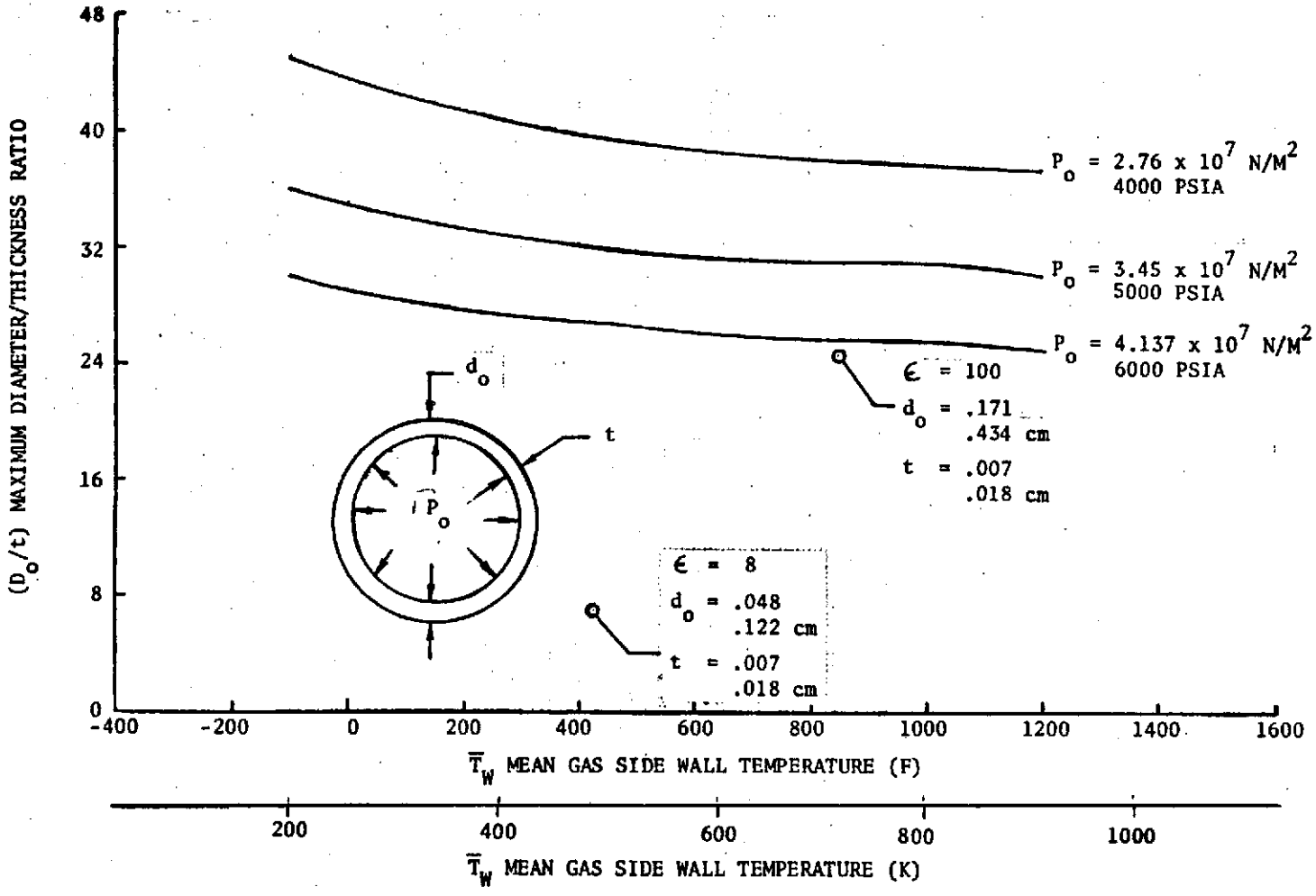

Figure 2-52. Maximum D_o/t vs Temperature, A-286 Nozzle

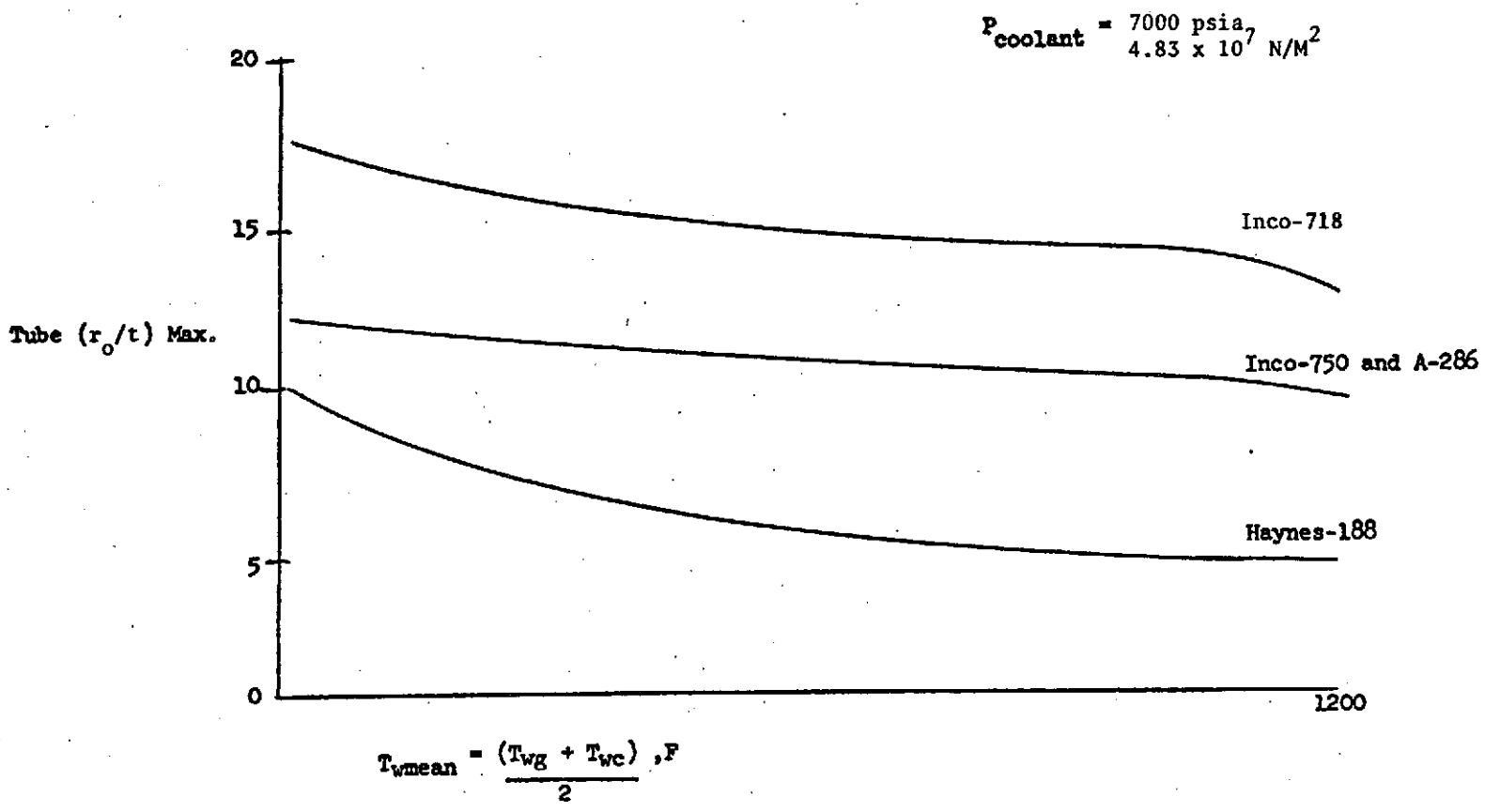

Figure 2-53. Pressure Stress Comparison of Allowable (Tube Radius/Wall Thickness) for Various Materials

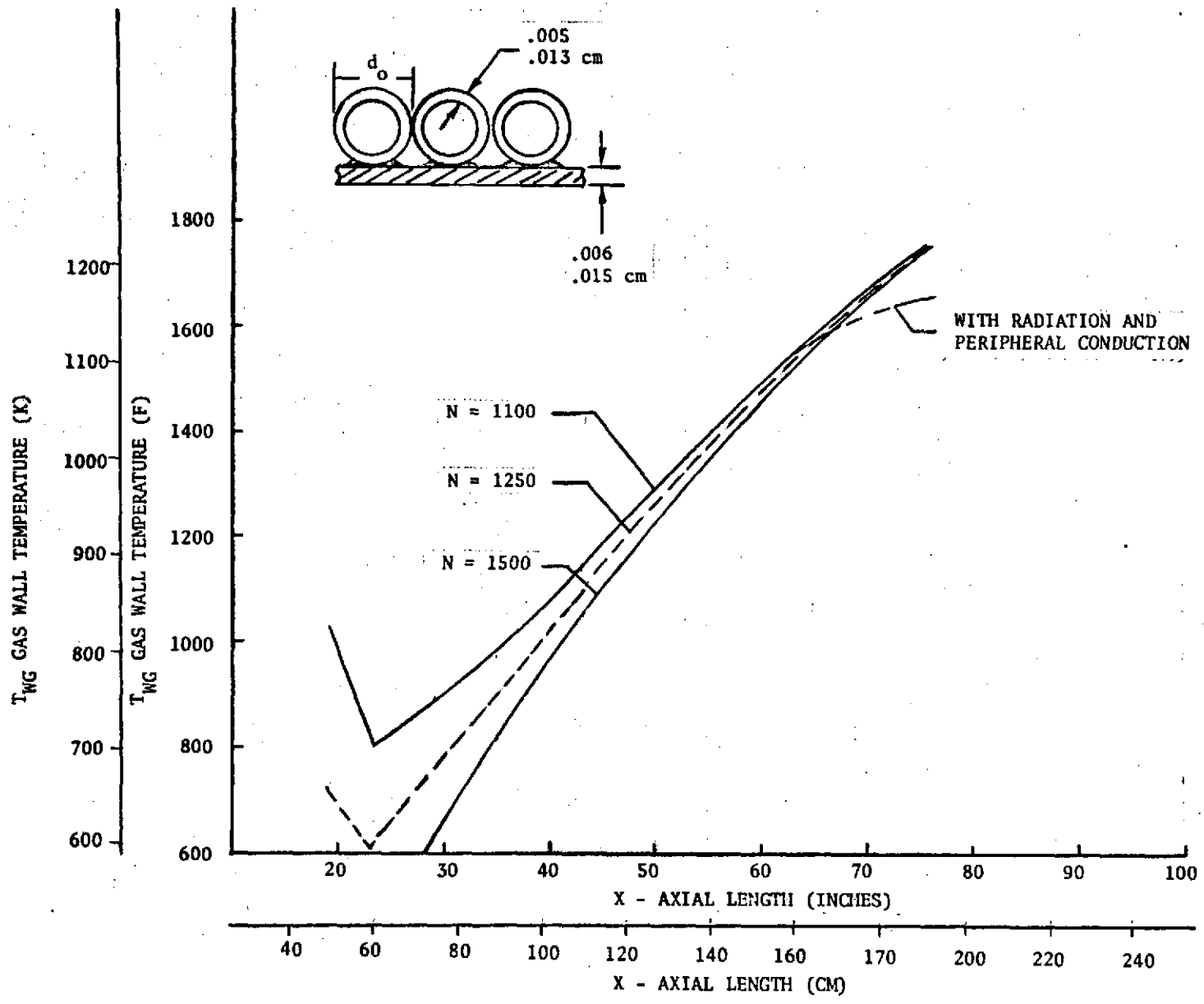

Figure 2-54. Dump Cooled Tubular Nozzle Extension (ε = 100 to 400) Gas Wall Temperature vs Axial Length ($\dot{W}_c$ = 0.38 lb/sec, 0.172 Kg/s)

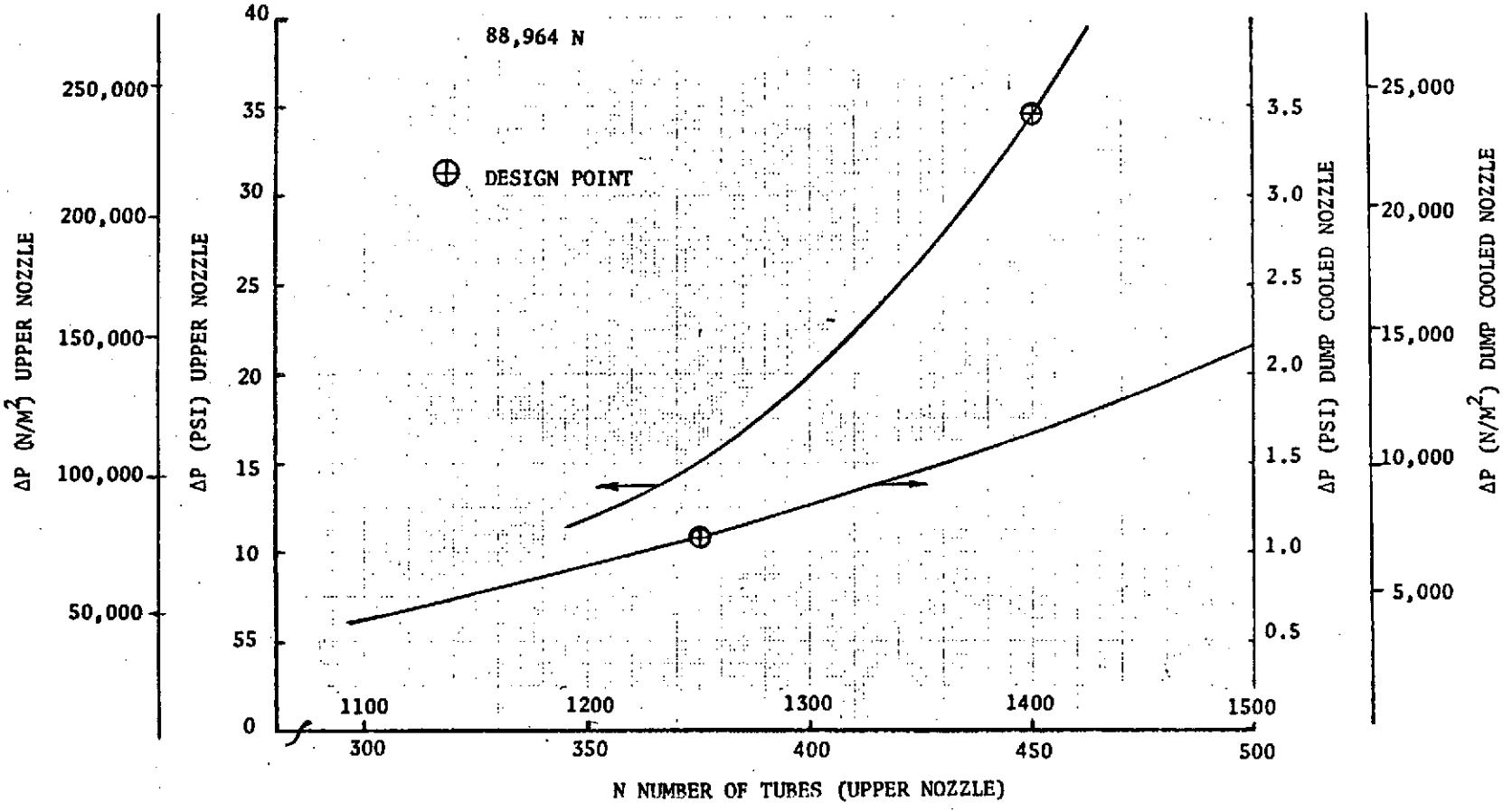

Figure 2-55. 20K (88,964 N) Nozzle Coolant Pressure Drop vs Number of Tubes

COMBUSTION CHAMBER STRUCTURAL ANALYSIS

The analysis of the thrust chamber was conducted utilizing the methods and criteria presented in Appendixes A and B.

Maximum use was made of design studies and analysis performed for the space shuttle engine, and the Advanced Hydrogen/Oxygen Thrust Chamber Design Analysis Program (NAS3-16774) conducted for the NASA-Lewis Research Center by Rocketdyne.

The main combustion chamber is structurally comprised of an inner thermal liner and an outer structural shell. The inner thermal liner acts as a barrier to protect the shell and is not used as a primary load-carrying member, except to contain its own coolant fluid pressure. The outer shell, commonly referred to as the jacket, acts as the vessel to contain the chamber pressure and transfer the nozzle thrust and external loads to the injector interface.

The main combustion chamber jacket was designed for the following operating loads: (1) chamber pressure, (2) thermal interaction with the liner, (3) nozzle thrust, (4) nozzle side loads during start and cutoff transients, (5) vibration loads, (6) aerodynamic loads, and (7) gimbaling and flight acceleration. Inconel 718 was selected for the jacket material to minimize weight.

Two factors were considered in sizing the coolant liner: thermal fatigue life and pressure-induced stresses. NARloy Z is a copper-base alloy developed at Rocketdyne specifically for the main combustion chamber liner of the SSME. The material was developed to have higher yield and rupture strength than commercially available copper-base alloys at elevated temperatures (810 K; 1000 F), thus containing the high coolant pressure more easily. The thermal conductivity and high ductility of copper were maintained to make it an ideal thrust chamber liner material. The low-cycle fatigue analysis of the liner was generalized to allow an optimization between heat transfer, performance, and stress. It was found in the Advanced Hydrogen/Oxygen Thrust Chamber Design Analysis Program (Ref. 7) that a maximum hot-gas wall surface temperature of 810 K (1000 F) resulted in a design life of 300 cycles with a safety factor of 4.

GIMBAL ASSEMBLY

Engine design requirements include provisions for thrust vector control by gimbaling the engine ±7 degrees in a square pattern. Acceleration rates are not to exceed 20 rad/s. This is accomplished by attaching two actuators to two clevises provided on the forward nozzle fuel manifold at 90 degrees from each other. A gimbal bearing located on the forward end of the engine has been designed to be capable of ±7 degree angulation, sustaining the full thrust load at all angles.

The gimbal configuration (Fig. 2-56) selected for this engine is designed specifically suited for this application because of the low thrust level. The gimbal consists of a clevis arrangement with a shaft and standard monoball assembly. A bellows is used to seal the gimbal assembly and react the torsional loads caused by gimbaling. The assembly is subassembled prior to welding to the engine thrust mount. The sequence of assembly consists of: (1) the monoball is pressed and staked into the forward part of the assembly, (2) the monoball assembly is then placed in the clevis with thrust washers on either side, and the pin pushed into position, (3) lock rings are placed on either side of the clevis to hold the pin in position, and (4) the bellows is slipped over the aft end of the clevis into position and welded at both ends to seal the bearing cavity. The monoball is self-lubricated by the fabroid seat on both the spherical seat and shaft. The entire assembly is welded to the engine thrust mount prior to welding the mount to the injector.

Thrust misalignment is adjusted by four eccentric bushings bolted through a slip ring attached to the forward end of the gimbal assembly. The entire assembly is trouble-free, requiring no service between overhauls.

Experience with this concept indicates its life should well exceed the engine overhaul requirements.

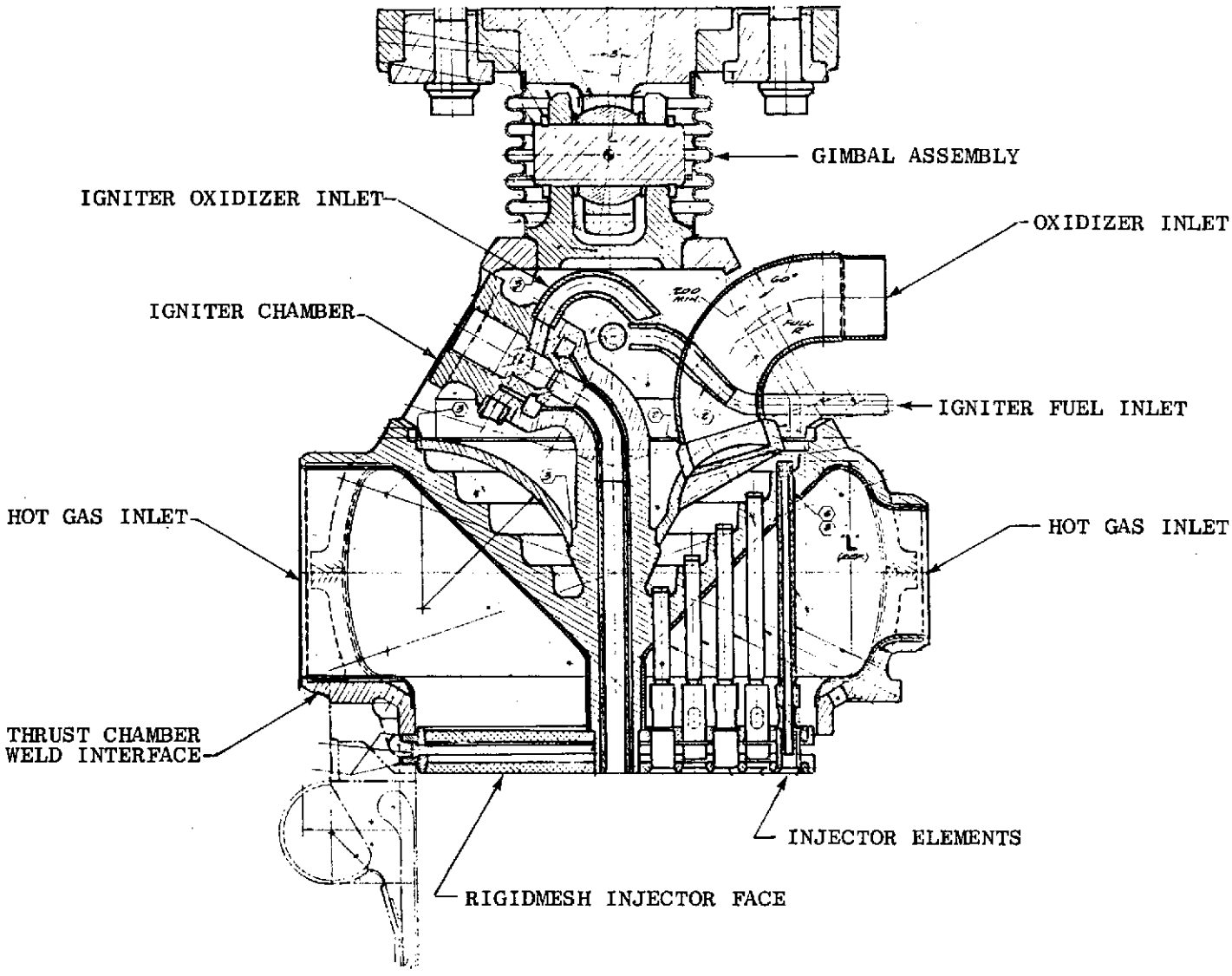

Figure 2-56. Thrust Chamber Injector and Gimbal Assembly

TASK III: PREBURNER PRELIMINARY DESIGN

PREBURNER ASSEMBLY

CONFIGURATION SELECTION

The advanced space engine system uses a single preburner to provide the hot gas to power the high-pressure fuel and oxidizer turbopumps. The preburner receives liquid oxygen from the high-pressure oxygen turbopump and high-pressure gaseous hydrogen from the discharge of the thrust chamber upper coolant jacket, oxidizer boost pump turbine, and fuel boost pump turbine. The preburner injector introduces the propellant into the combustor in a well-mixed fashion producing high performance, stable combustion. The preburner is directly attached to the inlet of the turbine on the high-pressure fuel turbopump. The hot-gas flow from the preburner is routed through a transition section where hot-gas flow for the high oxidizer turbopump is topped off through a branching elbow. The remaining hot gas then flows into the turbine manifold on the high-pressure fuel turbopump.

The preburner is designed to operate through a tank-head, idle-mode start into mainstage at any operating point defined within the limits of the engine mixture ratio excursion from 5.5 to 6.5. The design point preburner operating parameters are given in Table 3-1.

TABLE 3-1. PREBURNER NOMINAL OPERATING PARAMETERS

Chamber Pressure, psia	3377 (2.328 x 10^7 N/m^2)
Combustion Temperature, R	1896 (1309 K)
Mixture Ratio	0.82
Total Flowrate, lb/sec	9.18 (4.164 kg/s)
Fuel Inlet Temperature, R	490 (528 K)
Oxidizer Inlet Temperature, R	162 (346 K)

The structural features of the preburner have been designed to meet the requirements of a service free life of 60 thermal cycles or 2 hours accumulated run time, and service life between overhauls of 300 thermal cycles or 10 hours accumulated run time.

The preburner igniter is an assembly consisting of a one-piece body, 18 self-contained coaxial injection elements, faceplates, fuel manifold torus with two inlet, and oxidizer manifold and inlet (Fig. 3-1). The self-contained coaxial injection elements discharge liquid oxygen from a center post whose exit is recessed behind the plane of the injector face. Gaseous hydrogen is injected from an annulus around each oxidizer post. Each element is a unit in which oxidizer and fuel metering is provided. The oxidizer flow is controlled primarily by the rounded entrance orifice at the upstream end of the oxidizer post. The rounded entrance minimizes entrance effects so that the pressure drop accurately controls the relationship between the orifice and post diameters. The fuel flow is metered by the 16 entrance slots and the annulus area between

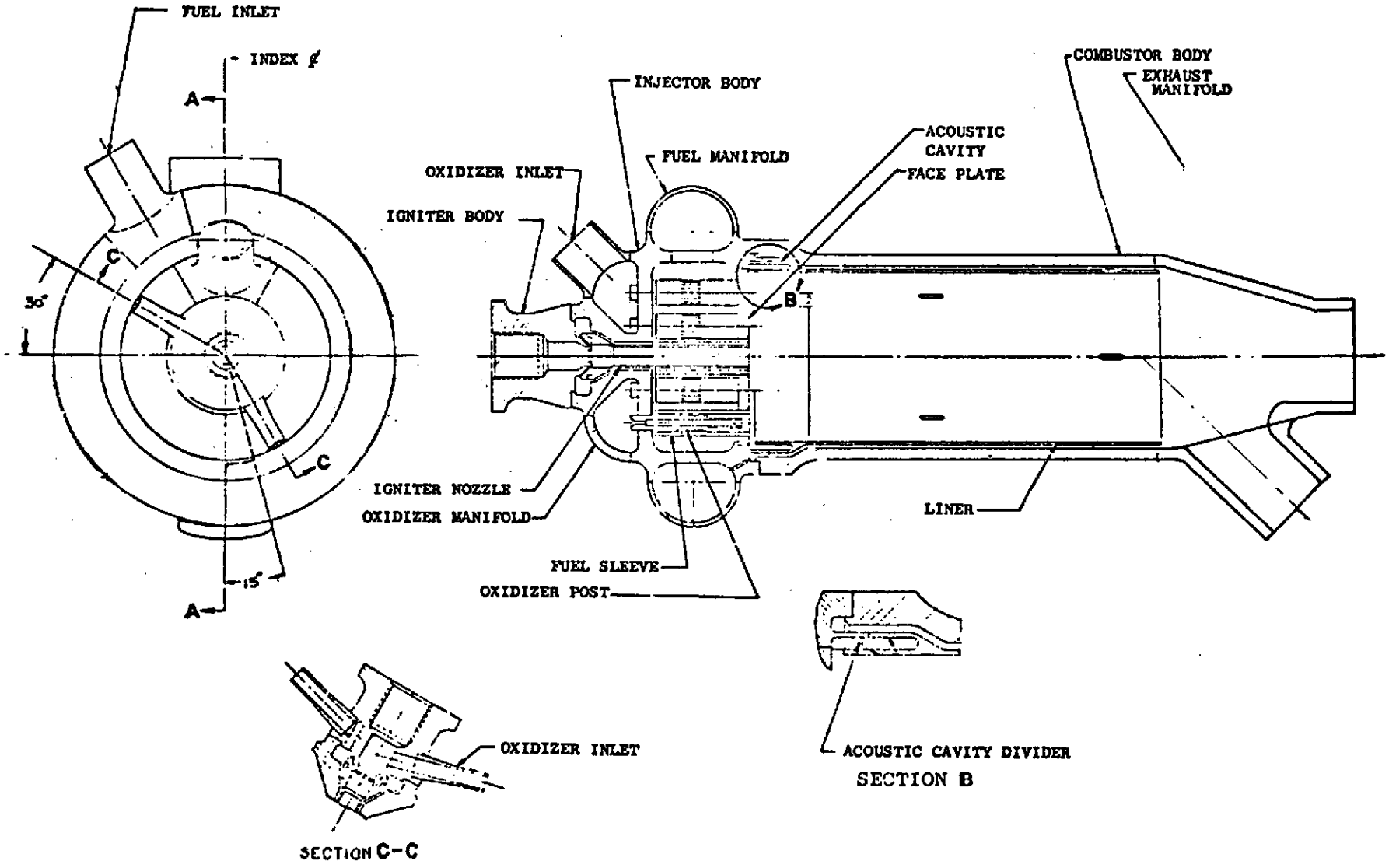

Figure 3-1. Advanced Space Engine Preburner Assembly

the oxidizer post and fuel sleeve. The slots are designed so that the width is less than the minimum width of the fuel annulus to provide a filtering capability to prevent contamination from plugging the fuel annulus. Cold-flow tests on the SSME preburner elements, designed using the same basic criteria, have shown that a 26-percent restriction of the slot entrance area results in only a 2-percent reduction in flowrate. Special consideration to prevent a reduction in element fuel flowrate is warranted because a reduction in element fuel flowrate raises the element mixture ratio and produces the potential for a high-temperature streak in the combustor.

The preburner injector is a lightweight design. The self-contained elements, brazed to the injector body and faceplate, provide a path through which the pressure loads across the faceplate are carried to the injector body. This reduces faceplate distortion and allows a thinner faceplate to be used. Low weight also results from the use of a braze/welded injector assembly since bolts, flanges, and seals are not required.

The preburner combustor is a cylindrical combustion chamber with an exhaust manifold which provides the transition section to interface with the turbine manifold on the fuel turbopump and the branch elbow to split off flow to the oxidizer turbopump. A fuel-cooled liner is used within the cylindrical combustor body for life, durability, and light weight. Six acoustic absorber cavities are provided in the liner below the injector face. Coolant flow for the liner is supplied from the injector fuel inlet manifold through 12 orifices. The liner produces an effective thermal barrier for the structural outer wall and requires only 2 percent of the preburner fuel flow. Dimples on the liner center the liner within the combustor body to maintain a constant area annulus for the coolant flow. Low preburner weight is enhanced by welding the lines and combustor body to the injector.

The ignition source for the preburner is an air gap igniter mounted in the center of the injector. This igniter location was selected over an igniter location in the combustor wall because it will not: (1) impinge high-temperature hot gas against the combustor wall, (2) interfere with the flow streams of the injector elements, (3) require an envelope in a high strain region of the preburner structure, and (4) compromise the use of a liner and acoustic absorbers. The principal disadvantage of using a center-mounted igniter is the potential for directing the high-temperature ignition flame into the turbine. Measures to prevent this have been taken by designing the igniter to operate at an overall mixture ratio equal to the preburner mixture ratio and using a coaxial igniter exhaust nozzle to enhance mixing.

PERFORMANCE ANALYSIS

The preburner has been designed to produce high combustion efficiency and thoroughly mixed, uniform temperature exhaust gas. The key feature of the preburner design which controls performance is the coaxial element deisng. Although the main emphasis is placed on designing the injection characteristics of the coaxial elements to produce performance and mixing, consideration is also given to factors that control the element pattern, number of elements, and element spacing.

The preburner injection pattern has 18 elements approximately equally spaced 0.5 inch on center in a pattern of concentric rows. The selection of the injection pattern and number of elements was based on the minimum practical spacing between elements that fabricational limits would allow, the minimum element flowrate that can be metered with reasonably sized orifices and annuli, and a number of elements that would complete a concentric row pattern with almost equal spacing.

Low element flowrate and close element spacing are design objectives for the preburner due to performance and weight considerations. The element flowrate must be selected so that the diameter of the oxidizer jet is small enough to allow the oxidizer to be completely atomized before the surrounding annular jet of gaseous hydrogen has full expanded into the combustion chamber. The mechanisms through which the coaxial element produces atomization, vaporization, and mixing are a function of the relative velocity between the low-velocity liquid oxidizer and the high-velocity gaseous fuel. Atomization of the oxidizer in a region of high relative velocity is desirable since the atomization rate increases with relative velocity while the mean oxidizer drop size decreases. Small drops increase the rate of vaporization by providing more available surface area per unit mass for heat transfer. A high-velocity fuel stream also enhances vaporization because the film coefficient on the surface of the drops increases with the relative velocity between the drop and the fuel stream.

Two techniques were used in the design of the preburner element to ensure high performance. First, a recess oxidizer post was used to increase the atomization rate and minimize the oxidizer drop size by forcing the hydrogen to remain at a high velocity around the oxidizer jet for the length of the recess. Secondly, the element was designed for complete atomization of the oxidizer in the high fuel velocity region of the element flowfield.

The performance of the preburner coaxial element was evaluated using the Rocketdyne steady-state combustion computer model, "NCSS". The preburner coaxial element has an oxidizer post recess of 0.254 cm (0.100 inch), a total flowrate of 0.231 kg/s (0.51 lb/sec) at the design point (corresponding to 18 elements), an oxidizer jet velocity of 24.4 m/s (80 ft/sec), and an expanded fuel velocity in the recess of 213 m/s (700 ft/sec). The selection of the recess depth and propellant velocities was based in the successful SSME full-scale preburner coaxial element design. The results of this analysis are summarized in Fig. 3-2 through 3-4. It can be seen from Fig. 3-2 that total vaporization and reaction of the oxidizer is predicted within 7.62 cm (3.0 inches) from the injector face. Figure 3-3 shows that the fuel velocity remains high in the recess and decreases rapidly within the first 1.27 cm (0.5 inch) from the injector face. The recess produces 11 percent atomization and complete atomization occurs within the first 1.27 cm (0.5 inch), Fig. 3-2. The drops produced are small, ranging from 60 to 104 microns in diameter, Fig. 3-4. The remaining 6.35 cm (2.5 inches) are required for complete vaporization and reaction.

The mixing capability of the element design was evaluated using design criteria recently acquired during cold-flow testing of the SSME preburner coaxial elements, conducted according to Ref. 18. From the results of this testing, a

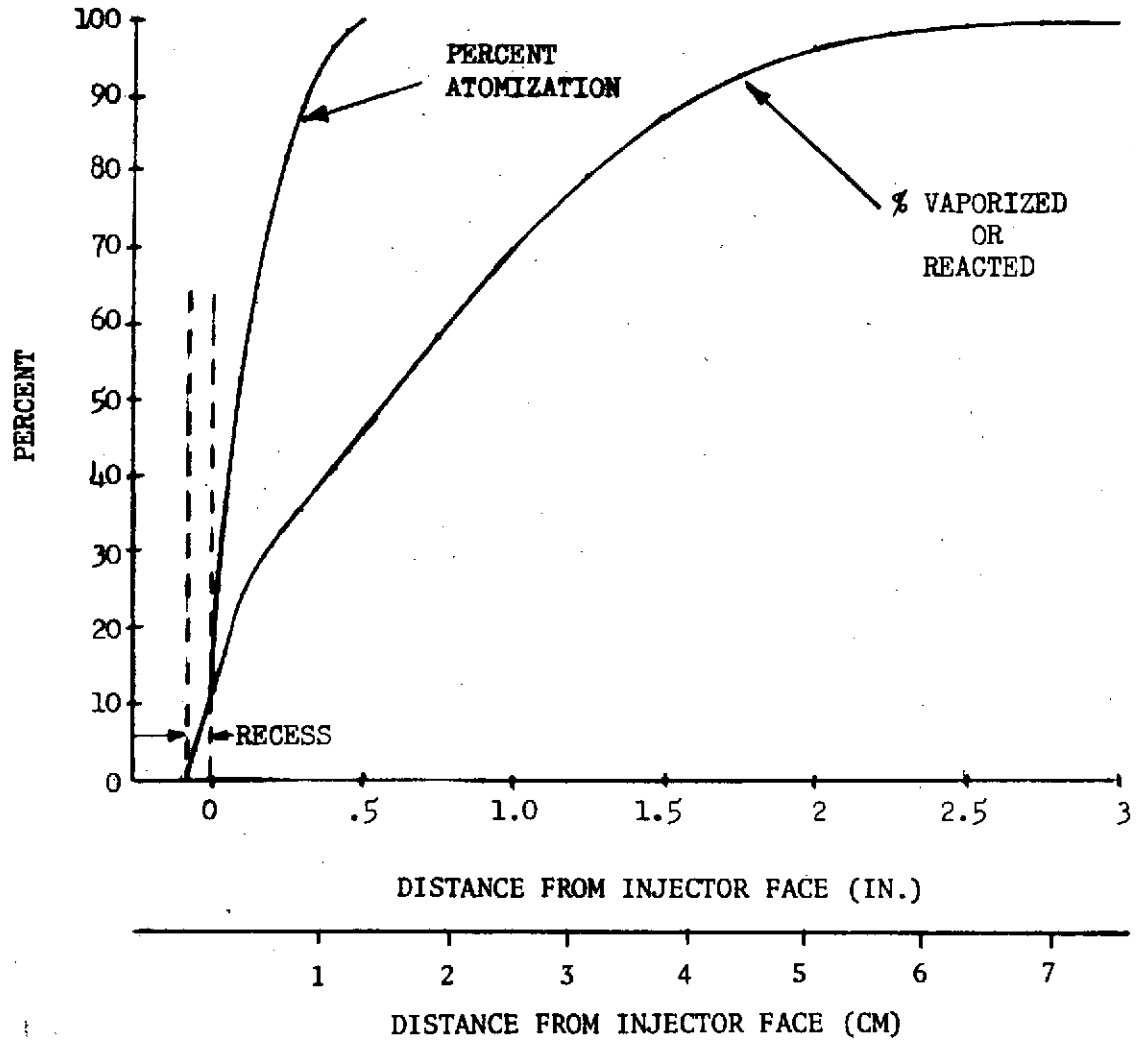

Figure 3-2. Preburner Coaxial Element

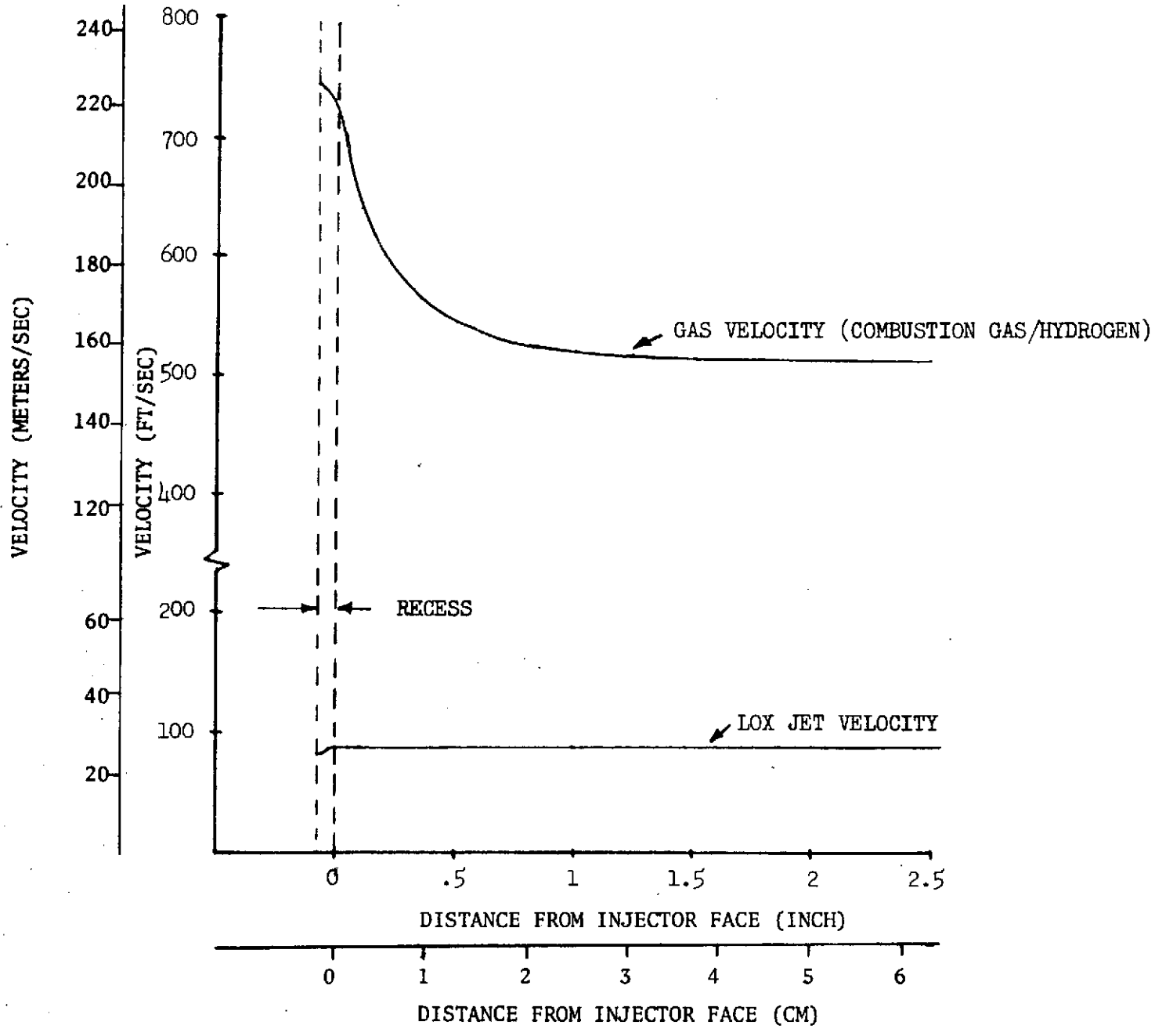

Figure 3-3. Preburner Coaxial Element

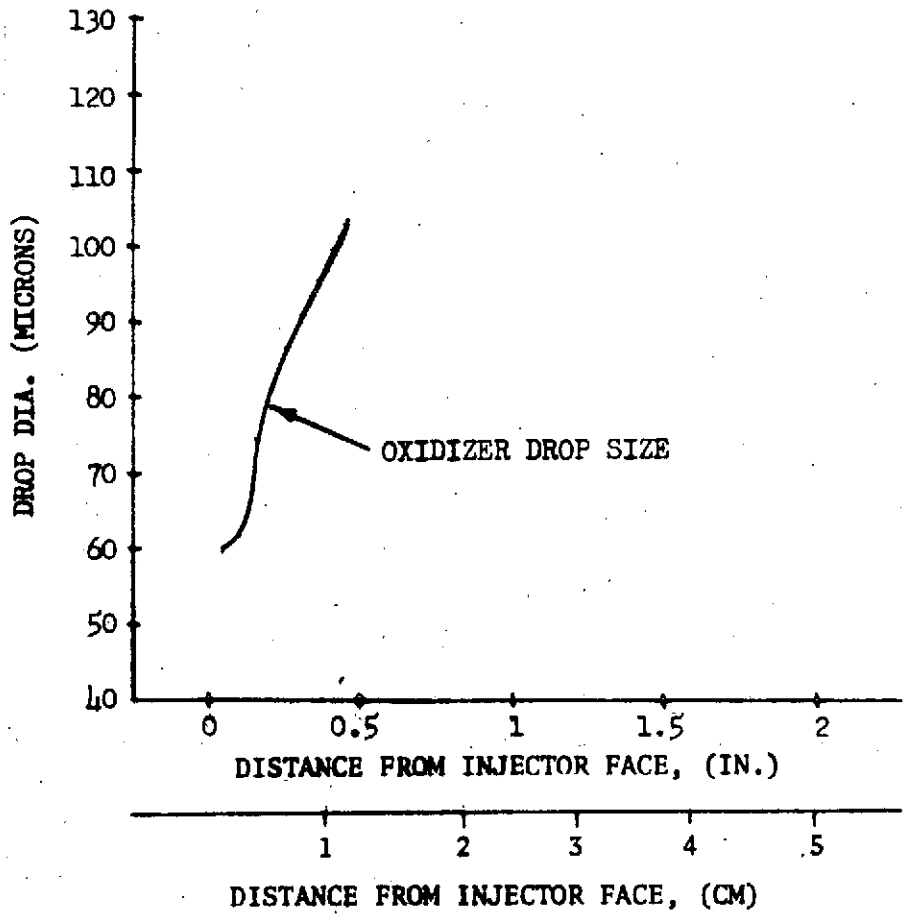

Figure 3-4. Preburner Coaxial Element

relationship has been established between the injected propellant densities and velocities, and the mixing uniformity parameter E_m (Fig. 3-5). The mixing uniformity parameter represents a mass-weighted measure of the deviation of the mixture ratio distribution across the element flowfield from the overall element mixture ratio. The mixing uniformity parameter, E_m, is defined below:

$$E_m = 100 \left[1 - \sum_i^n \frac{\dot{w}_i}{\dot{w}_t} \frac{(R-r_i)}{R} - \sum_i^n \frac{\dot{w}_i}{\dot{w}_t} \frac{(R-\bar{r}_i)}{(R-1)}\right]$$

where

$\dot{w}_i/\dot{w}_t$ = mass

R = ratio of total oxidizer to total oxidizer plus fuel (total flow)

r_i = ratio of local oxidizer flow in a streamtube to the total flow in streamtubes for which $r_i < R$

$\bar{r}_i$ = ratio of local oxidizer flow in a streamtube to the total flow in streamtubes for which $r_i > R$

From Fig. 3-5, it can be seen that the mixing uniformity factor varies universely with the nondimensionless product of the ratio of the injected gas density to liquid density to the two-thirds power, and the ratio of the injected gas velocity to liquid velocity. The cold-flow distribution data from which this plot was prepared were measured at a location 12.7 cm (5 inches) from the injector face. It can be seen from Fig. 3-5 that, for the preburner nondimensionless density/velocity parameter of 0.58 at the design point, the predicted mixing uniformity parameter is approximately 0.95 percent. This indicates that the element would produce thorough mixing and uniform temperature exhaust gas.

COMBUSTION STABILITY

All features of the preburner design that have a potential effect on combustion stability were controlled to provide maximum preburner stability. The recessed coaxial element injector design is inherently stable, because the stripping action of the high-velocity hydrogen produces small oxidizer droplets that are vaporized so rapidly that they are relatively insensitive to transverse acoustic disturbances. This was verified by performing a Priem analysis on the preburner. Although the results of this analysis indicated that the preburner should be dynamically stable, an acoustic absorber was included in the design for additional stability margin. The absorber had a 14-percent open area relative to the combustor cross section and consists of six L-shaped, quarter-wave cavities spaced along the periphery of the injector end of the combustion chamber.

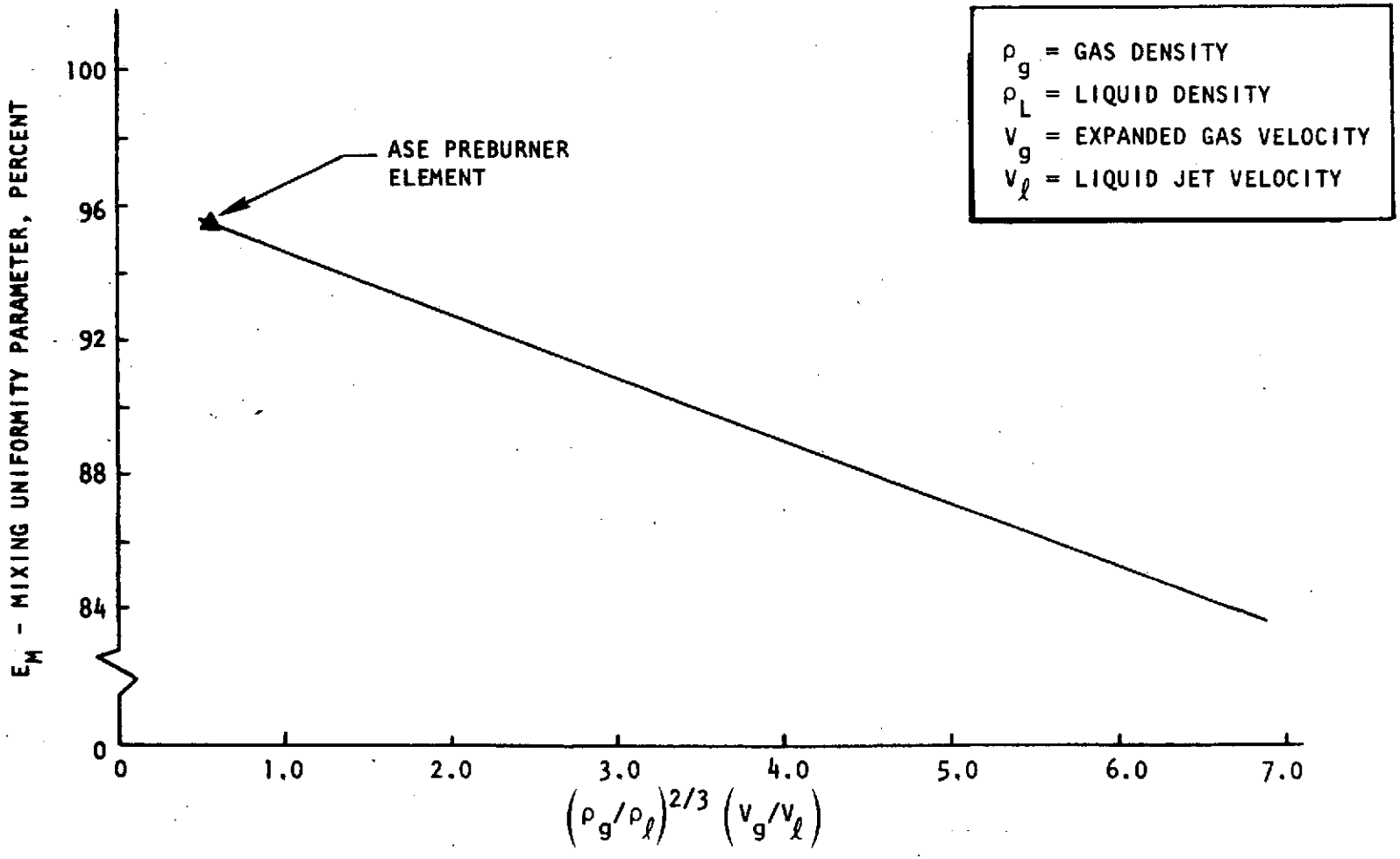

Figure 3-5. SSME Preburner Coaxial Element Cold-Flow Mixing Tests

The feed-system-coupled stability of the preburner was evaluated using two approaches: (1) an analysis of the response characteristics of the major elements capable of coupling in an unstable feedback loop, and (2) an analysis using a "double dead-time" analog simulation of the engine that allows for a detailed evaluation of the interaction of the engine components in a closed-loop operational environment.

As a result of the open-loop analysis, the preburner was designed so that the hydraulic response, the combustion response (determined using the Rocketdyne Steady-State Combustion Model), and the combustor response have no common frequencies where each has a significant gain.

To accomplish the closed-loop analysis, a nonlinear mathematical model of the engine system was mechanized on the analog computer. A stability map was generated to depict the stability margin for the preburner. The map consists of a plot of boundary of incipient instability relative to the probable operating region, as a function of the oxidizer injector transport time delay and the oxidizer clumping time constant for fixed similar fuel parameters. The results showed no modes of instability due to coupling of the preburner.

A more complete discussion of the combustion stability analysis is presented in conjunction with the main thrust chamber stability analysis under Task II. The discussions were combined because of the commonality of the subject matter.

HEAT TRANSFER AND STRESS ANALYSIS

A steady-state heat transfer analysis of the preburner combustor wall temperature profile was conducted to support structural analyses. The combustor wall temperature profile was determined for the worst-case preburner operating conditions corresponding to a preburner combustion temperature of 383 K (2030 R) at the maximum engine operating point. The resulting temperature profile is given in Fig. 3-6.

A structural and life analysis was conducted on the preburner for the most critical combinations of pressure and thermal loading. The temperatures and pressures used are shown in Fig. 3-6 and 3-7. Minimum safety factors of 1.1 on yield strength, 1.4 on ultimate strength, and 4 on life were used while limiting total creep of 1.0 percent.

The fundamental theory used in life prediction analysis is that failure depends on the accumulation of creep damage and fatigue damage. Data obtained from material fatigue specimens and test data of actual hardware or, if test data are unavailable, the method of universal slopes is used in the life analysis.

The life analysis is based on a definition of the stress-strain-time-temperature history during each operating cycle. Creep damage is evaluated from the stress-time-temperature cycle and fatigue damage from the strain-time-temperature cycle.

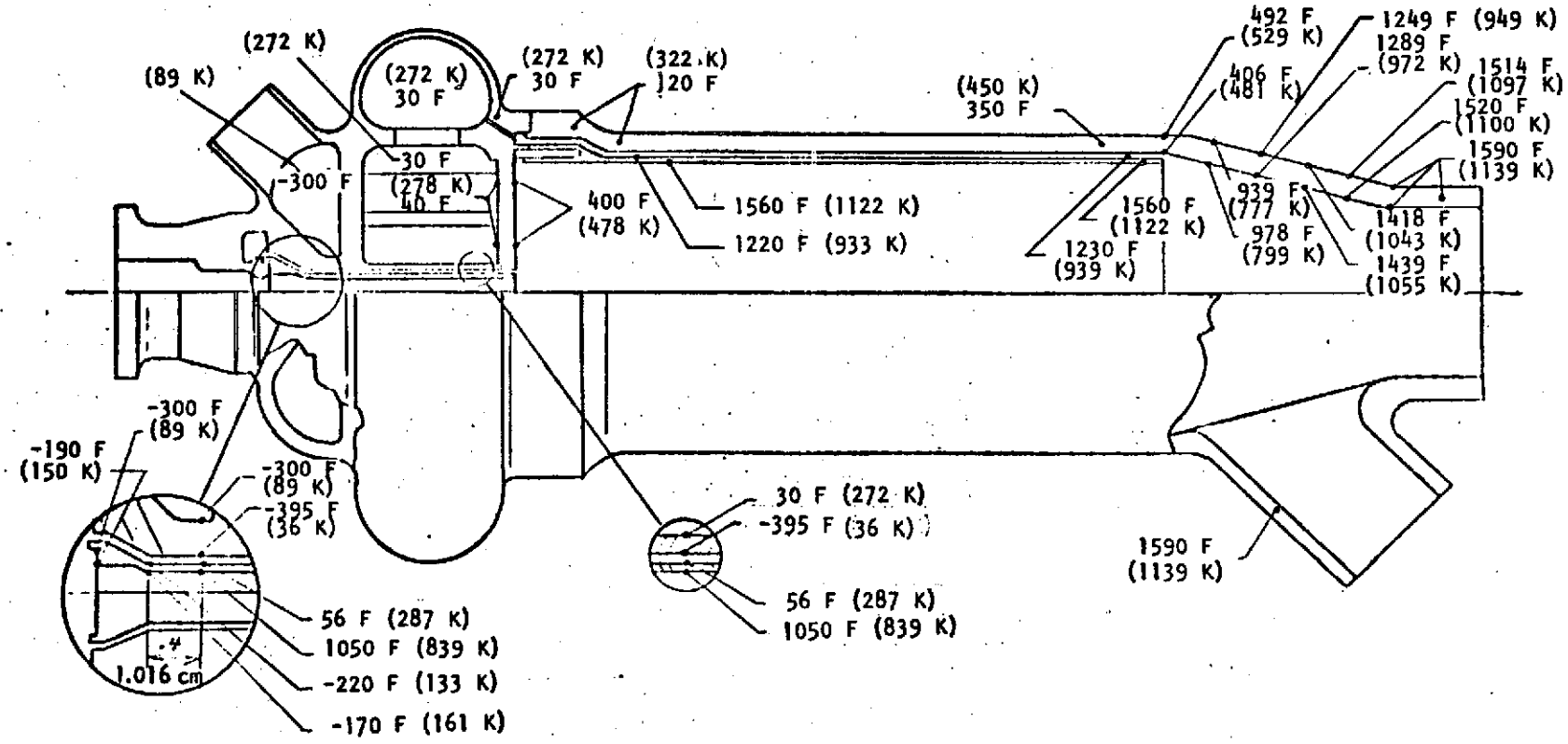

Figure 3-6. Preburner Temperature Distribution

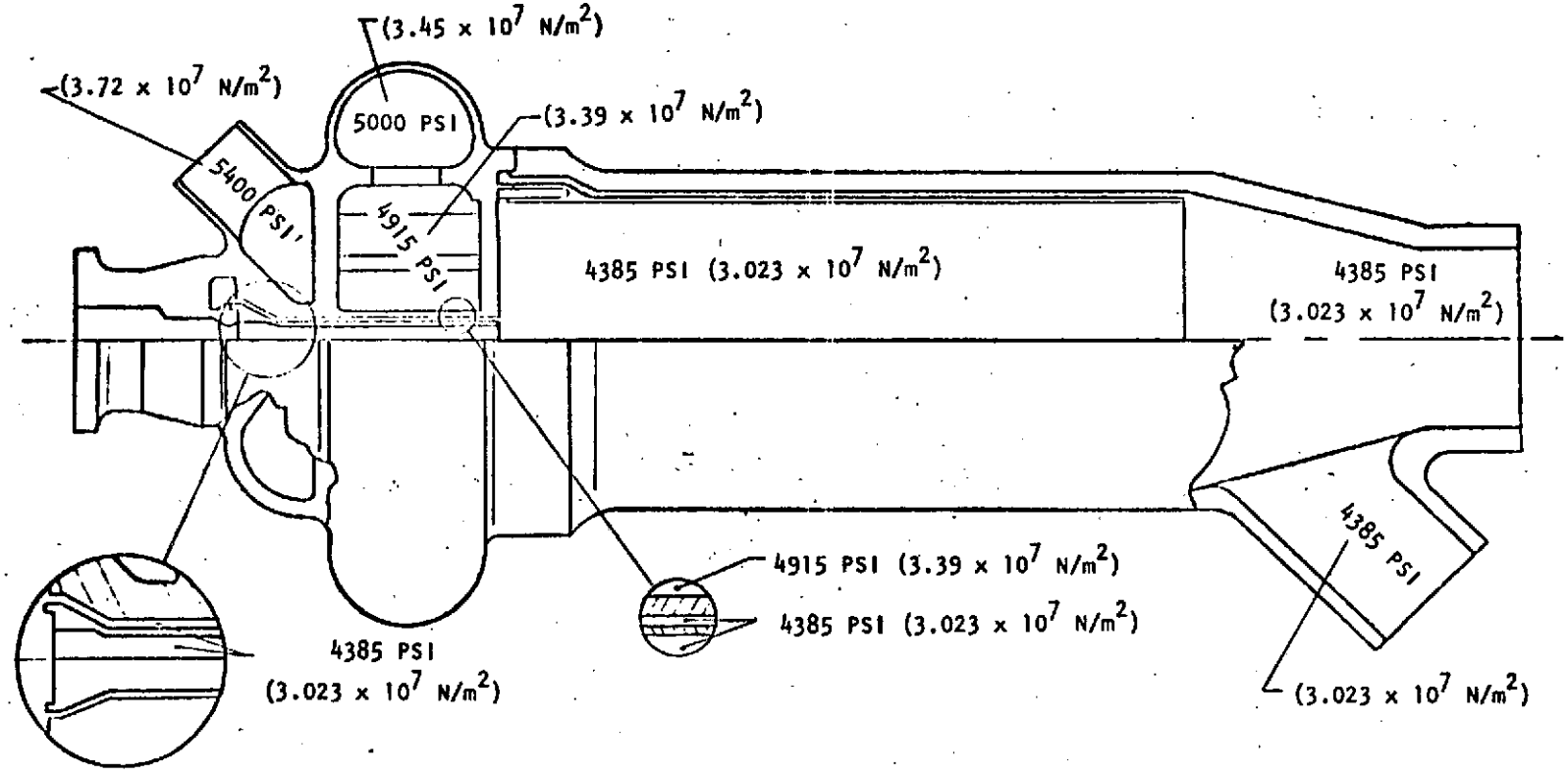

Figure 3-7. Pressure Distribution Preburner, 20K (88,964 N), Advanced Space Engine

The increment of creep damage, $\Delta\phi_c$, is determined by the ratio of the time spent at a particular stress level, t, to the time-to-rupture at that stress level, t_r. This is presented mathematically as:

$$\Delta\phi_c = \left(\frac{t}{t_{r\phi}}\right)$$

$\Delta\phi_c$ = creep damage

t = time at stress σ

t_r = time to rupture at the stress σ

The total creep damage, ϕ_c, is given by:

$$\phi_c = \sum \Delta\phi_c$$

Fatigue damage, ϕ_f, is determined by the ratio of the actual number of cycles (starts and stops), applied at a particular strain range, to the number of cycles which would cause failure at that strain range.

A generalized life equation is used to consider the total damage caused by the interaction of low cycle fatigue and creep rupture. The equation takes the following form:

$$4\,\phi_f + 4\,\phi_c = 1.0$$

The safety factor of 4 is applied to the typical fatigue and creep rupture life.

For purposes of modeling, the preburner was divided into three physical parts: the combustor body, the igniter, and the injector body. The combustor body was modeled as an axisymmetric thin shell of revolution and analyzed for stresses, strains, and deflections by the computer. The igniter was also modeled as an axisymmetric thin shell of revolution. The injector body, however, was modeled as an axisymmetric finite element model.

Those areas of the preburner considered most critical or of the most interest are shown in Fig. 3-8, and the basic strength and life values are shown in Tables 3-2 and 3-3, respectively. Figure 3-9 shows the deflection of the injector faceplate. Its maximum relative displacement is 1.016 mm (0.004 inch).

The materials used in the preburner design are shown in Fig. 3-8. The igniter body, faceplate, propellant manifolds, liner, and combustor body are fabricated from Inconel 625. This material was selected primarily because of its high strength in the range of temperatures that will occur on the preburner and its low susceptibility to hydrogen embrittlement. In addition, Rocketdyne has established machining, brazing, and welding techniques for this material. CRES

304L is used for the self-contained injector elements because it has adequate strength for this application and is easily machined and brazed. The uncooled combustor exhaust manifold is Haynes 188. Although this material is somewhat more difficult to machine than Inconel 625, it was selected for this part due to its higher strength at temperatures near the preburner combustion temperatures. Haynes 188 also has low susceptibility to hydrogen embrittlement.

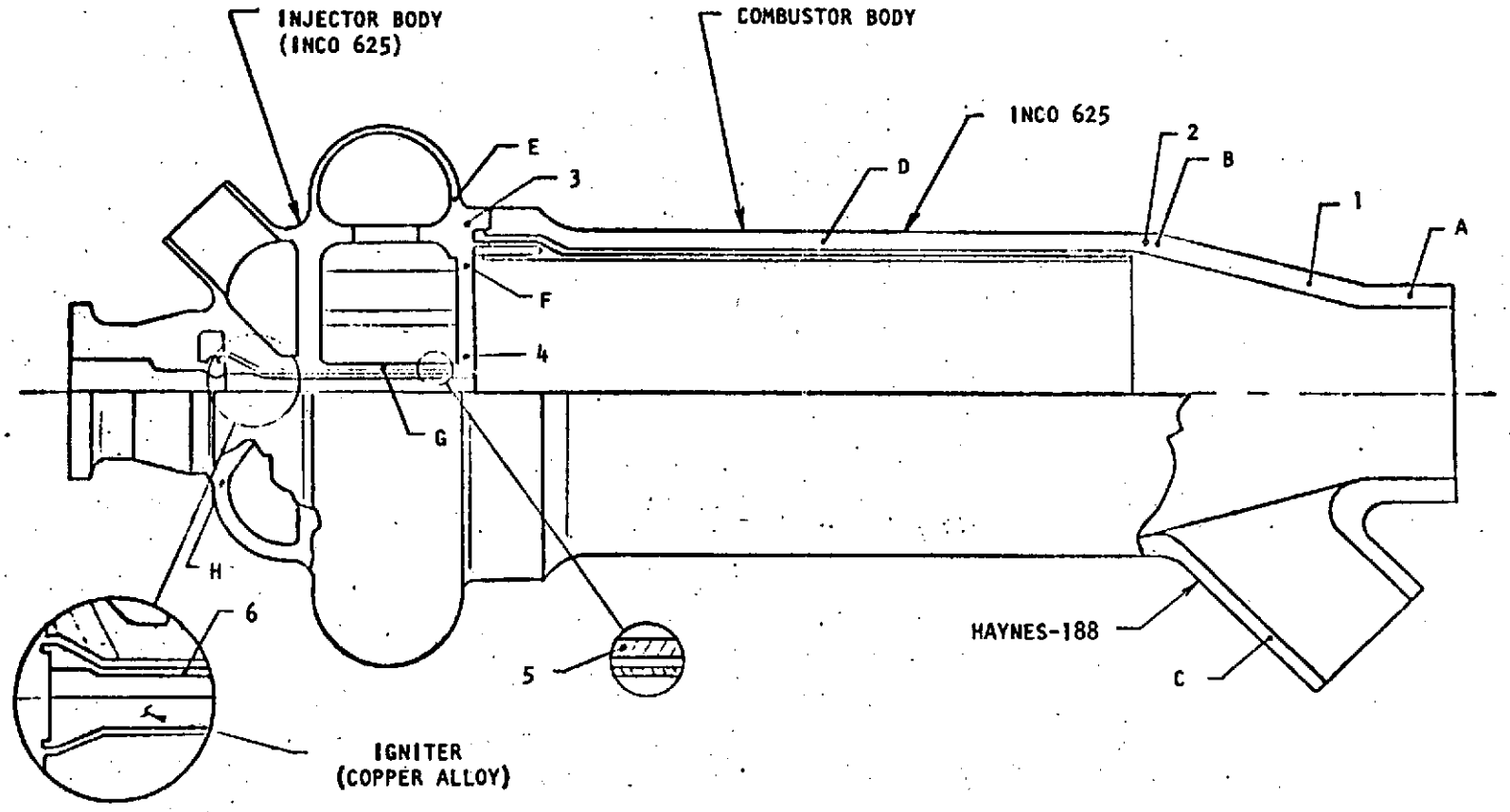

Figure 3-8. Preburner, 20K (88,964 N), Advanced Space Engine

TABLE 3-2. PREBURNER, 88,964 N (20K) ADVANCED SPACE ENGINE BASIC STRENGTHS

Point (1)	Temperature, F (K)	σ_{eff}, psi (2) (N/m^2)	F_{ty}, psi (3) (N/m^2)	F_{tu}, psi (4) (N/m^2)	F.S.$_{yield}$	F.S.$_{ult.}$
A	1590 (1139)	12,600 (8.68×10^7 N/m^2)	24,000 (1.65×10^8)	43,000 (2.965×10^8)	1.90	3.41
B	750 (672)	29,090 (2.005×10^8)	32,000 (2.206×10^8)	92,000 (6.343×10^8)	1.10	3.16
C	1590 (1139)	12,600 (8.68×10^7)	24,000 (1.65×10^8)	43,000 (2.965×10^8)	1.90	3.41
D	492 (529)	38,427 (2.649×10^8)	45,500 (2.93×10^8)	102,000 (7.033×10^8)	1.11	2.66
E	30 (272)	39,744 (2.74×10^8)	56,000 (3.86×10^8	116,000 (7.998×10^8)	1.41	2.92
F	265 (403)	22,700 (1.565×10^8)	48,000 (3.31×10^8)	106,000 (7.308×10^8)	2.11	4.67
G	-129 (184)	19,600 ($1,351 \times 10^8$)	60,000 (4.137×10^8)	124,000 (8.55×10^8)	3.06	6.32
H	-300 (89)	23,400 (1.613×10^8)	73,000 (5.033×10^8)	145,000 (9.997×10^8)	3.11	6.19

(1) Points shown in Fig. 3-8

(2) Effective Stress

(3) Tensile yield strength at operating temperature

(4) Tensile ultimate strength at operating temperature

NOTE: Material of fabrication is shown in Fig. 3-8

TABLE 3-3. PREBURNER, 88,964 N (20K) ADVANCED SPACE ENGINE LIFE DATA

Point ①	Temperature, F (K)	Fatigue			Creep			4 ($\phi_f + \phi_c$)
		ε_{eff}, in./in. (cm/cm) ②	N_f ③	$\phi_f = (\frac{300}{N_f})$	σ_{eff}, psi (N/m^2) ④	t_r, hours ⑤	$\phi_c = (\frac{10}{t_r})$	
1	1480 (1078	0.0034 (0.0086)	4400	0.068	16644 (1.147×10^8)	700	0.014	0.32
2	700 (644)	0.0037 (0.0094)	40,000	0.0075	29090 (2.005×10^8)	Negligible	Negligible	Negligible
3	40 (278)	0.0010 (0.0025)	10^6	Negligible (0.653×10^8)	9476 (0.653×10^8)	↓	↓	↓
4	355 (453)	0.0030 (0.0076)	10^5	0.003	5744 (0.396×10^8)			
5	-200 (144)	0.0013 (0.0033)	10^6	Negligible	Negligible			
6	550 AVE. (561)	0.0101 (0.0257)	15,000	0.020	Negligible			

① Points shown in Fig. 3-8

② Effective strain range

③ Cycles to failure at operating temperature and effective strain

④ Effective stress

⑤ Time to rupture at operating temperature and effective stress

NOTE: Operating cycles = 300, and exposure time = 10 hours

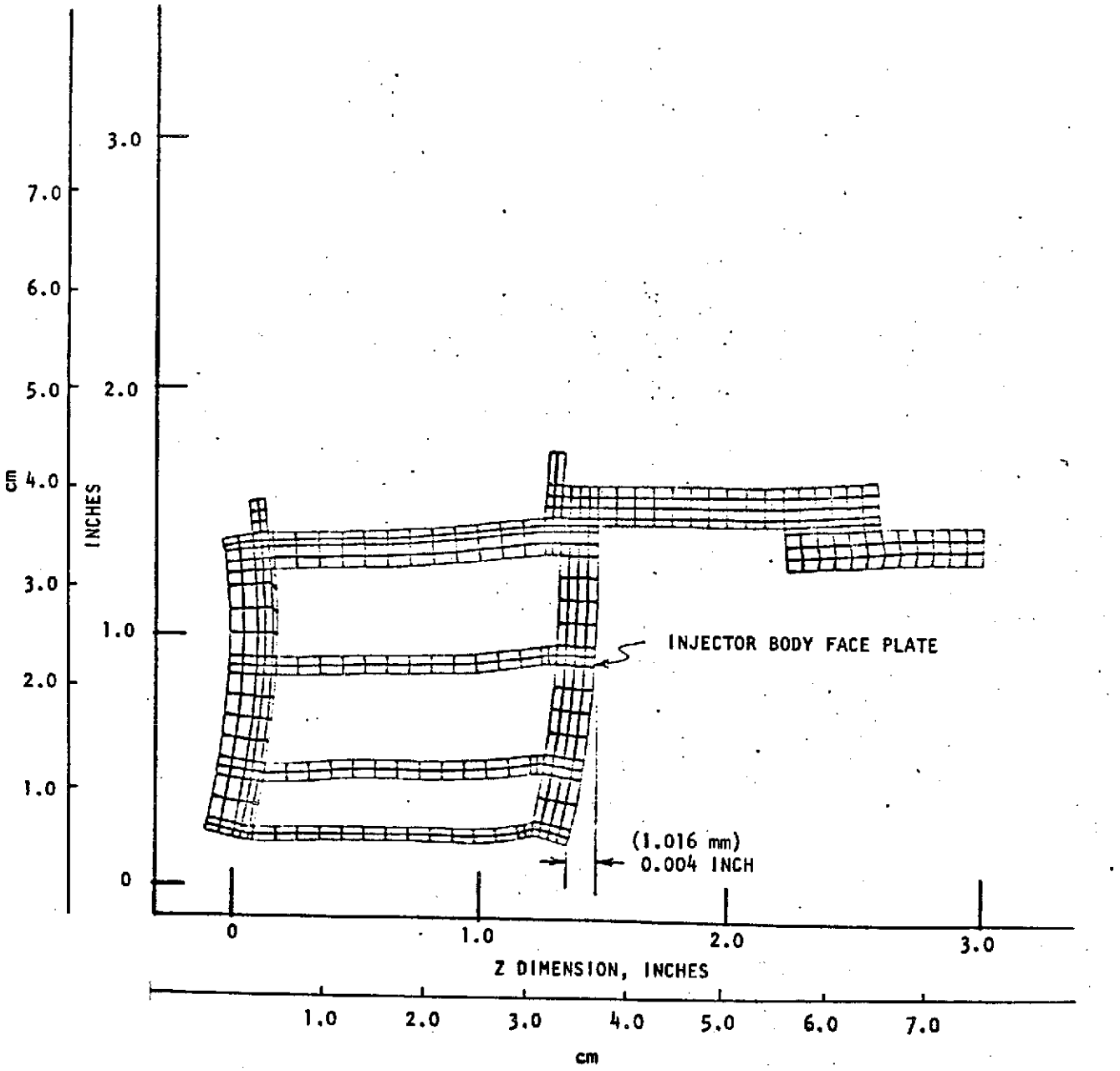

Figure 3-9. Preburner-Injector Body Worst Condition at Mainstage

TASK IV: TURBOPUMP PRELIMINARY DESIGN

LOW-PRESSURE OXIDIZER TURBOPUMP

CONFIGURATION SELECTION AND PERFORMANCE

The purpose of the LOX boost pump is to increase the available NPSH (net positive suction head) at the inlet of the main LOX pump to a level which will facilitate a high performance and weight effective overall design. The specific requirements, presented in Table 4-1, are to raise the pressure of liquid oxygen from 108,592 N/m^2 (15.75 psia) at the inlet to 598,120 N/m^2 (86.75 psia). The design flowrate is 16.68 kg/s (36.78 lb/sec) or 235 gpm. The available NPSH is specified at 5.97 joule/kg (2 feet) minimum. It is further specified that the design be based on a suction performance corresponding to 2.3 inlet velocity heads, i.e., NPSH = $2.3\ c_m^2/2g$.

The design parameters obtained to satisfy the above requirements are noted in Table 4-1. A single inducer stage pump was selected with a rotor speed of 678 rad/s (6475 rpm). The inducer includes four full and four partial vanes, with a constant 9.6-cm (3.78-in.) diameter, resulting in a moderate tip speed of 32.6 m/s (107 fps). The inlet flow coefficient was established at 0.07 and the head coefficient at 0.42. The overall pump efficiency is 70 percent. The value of the flow coefficient was dictated by low inlet velocity. The selection of the head coefficient value was based on experimental data obtained with Rocketdyne's MK-25 inducer, which demonstrated a head coefficient of 0.53, with a rotor efficiency of 91 percent in water.

The performance characteristics of the low pressure oxidizer pump are presented in Fig. 4-1. The curves represent a design speed of 678 rad/s (6475 rpm), at an engine mixture ratio of 6.5. Developed head requirement and operating speed increase at lower mixture ratios at constant engine thrust, as indicated in Fig. 4-1 by the 5.5 MR H-Q point. The head flow characteristic displays a good negative slope over the operating range, a desirable feature for system stability.

The analysis of the low pressure oxidizer turbopump included an accounting of all internal flows and pressures. The results of that analysis are presented in Fig. 4-2. Flow through the bearing lube circuit is maintained as a result of two factors: (1) the friction pumping effect of the inducer hub, and (2) the static pressure rise across the volute diffuser vanes.

The propellant provided to drive the low pressure, oxidizer turbine is GH_2, at essentially ambient temperature 305 K; 550 R) and inlet and exhaust pressures of 3.003×10^7 N/m^2 and 2.61×10^7 N/m^2 (4355 and 3787 psia), respectively (see Table 4-2).

The turbine selected is a single row axial impulse type rotating at 678 rad/s (6475 rpm) and using a 710 percent admission nozzle. The wheel pitch diameter is 11.43 cm (4.5 inches), resulting in a pitch line velocity of 38.7 m/s (127 fps) and a pitch line velocity to gas isentropic spouting velocity ratio (u/c_o) of 0.0624. The turbine delivers 10,887 watts (14.6 shaft horsepower), with the flowrate at 0.249 kg/s (0.55 lb/sec). The combination of low blade

TABLE 4-1. ASE LOW-PRESSURE LOX TURBOPUMP DESIGN PARAMETERS (MR = 6.5)

- Pump
  - System Requirements

P_S, psia (N/m^2)	15.75 (108,592)
P_D, psia (N/m^2)	86.75 (598,120)
$\dot{W}$, lb/sec (kg/s)	36.78 (16.68)
NPSH, ft, min (joule/kg)	2.0 (5.97)

  - Design Parameters

Type	Inducer
N, rpm (rad/s)	6475 (678)
ϕ_{Inl}	0.07
ψ_{Stg}	0.42
η, percent	70
Specific Speed	2325 (0.8510 nondimensional)
Suction Specific Speed	59,400 (21.74 nondimensional)
Inducer Tip Diameter, inches (cm)	3.78 (9.6)
U_{Tip}, fps (m/s)	107 (32.6)
Hub Diameter at Inlet, inches (cm)	1.135 (2.88)
Hub Diameter at Discharge, inches (cm)	3.500 (8.89)
Number of Inducer Blades at Inlet	4
Number of Inducer Blades at Discharge	8
Blade Tip Angle at Inlet, degrees	7
Blade Tip Angle at Discharge, degrees	65

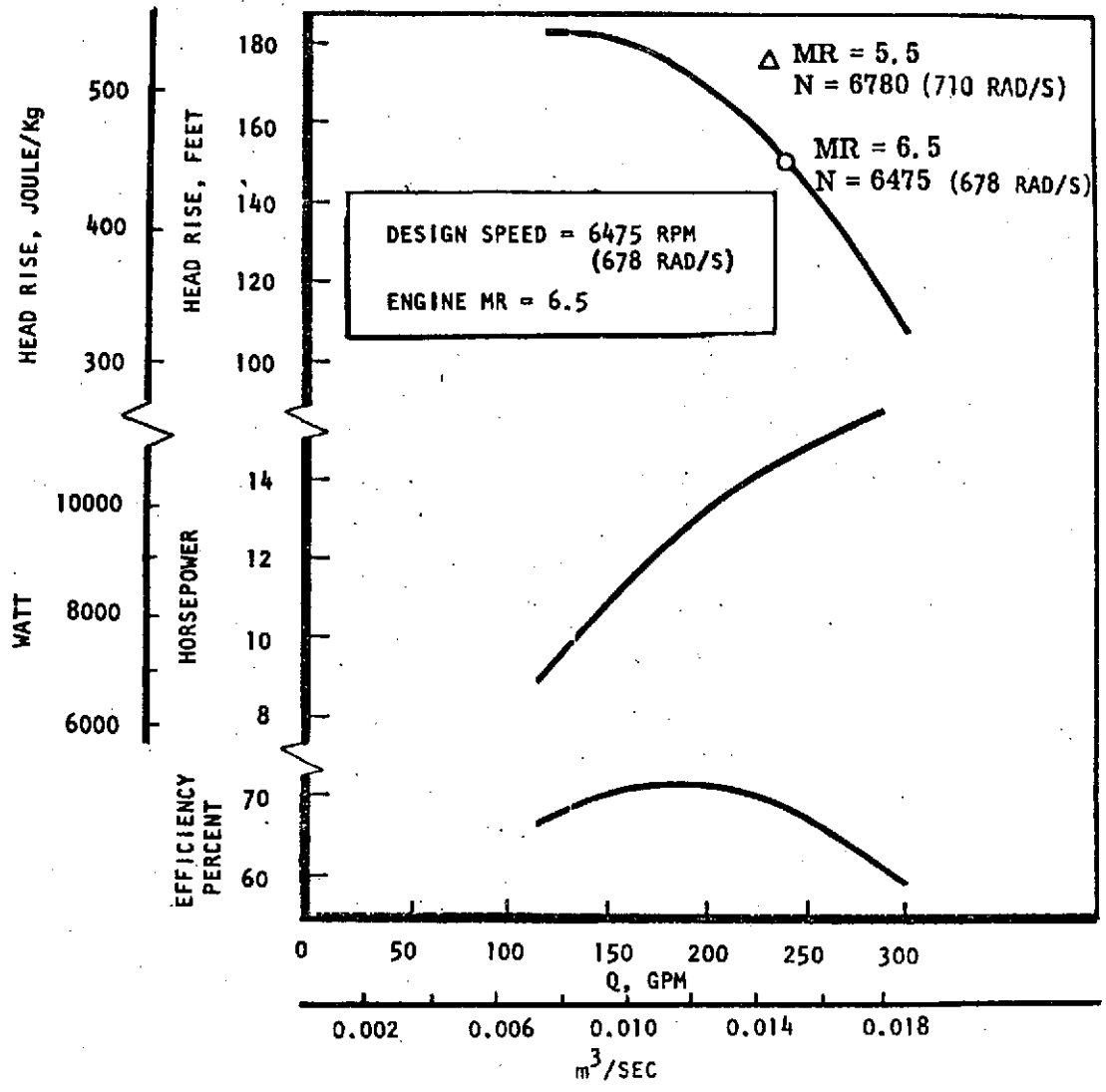

Figure 4-1. ASE Low-Pressure Oxidizer Pump Predicted Performance Map

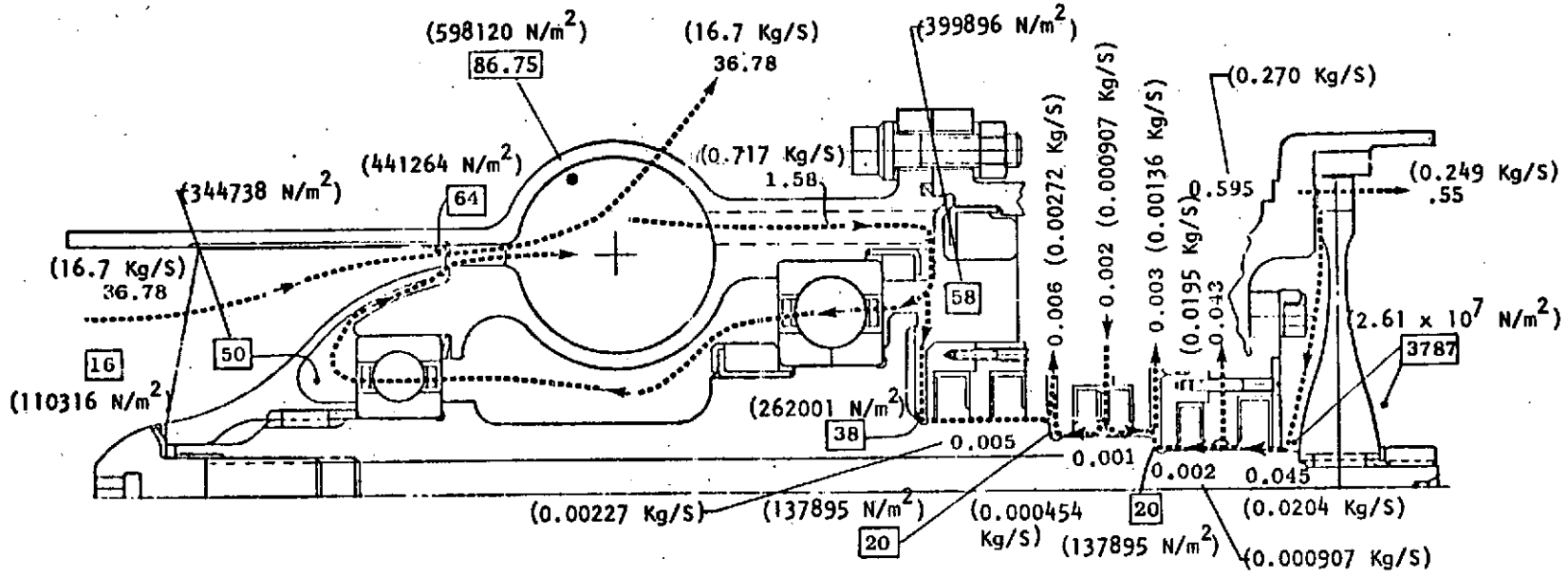

NUMBERS WITH ARROWS = FLOW, LB/SEC
BOXED NUMBERS = STATIC PRESSURE, PSIA
MIXTURE RATIO = 6.5
N = 6475 (678 RAD/S)

Figure 4-2. ASE Low-Pressure Oxidizer Turbopump Flow and Pressure Schedule

TABLE 4-2. ASE LOW-PRESSURE LOX TURBOPUMP DESIGN PARAMETERS (MR = 6.5)

- Turbine
  - System Constraints

Fluid	GH_2
T_{t_1}, R (K)	550 (561)
P_{t_1}, psia (N/m^2)	4355 (3.003×10^7)
P_{t_2}, psia (N/m^2)	3787 (2.611×10^7)

  - Design Parameters

Type	Partial Admission, Single-Stage Impulse
ϵ, percent	7.0
N, rpm (rad/s)	6475 (678)
bhp (watts)	14.6 (10,887)
D_m, inches (cm)	4.5 (11.4)
U_m, fps (m/s)	127 (38.7)
Number of Nozzle Passages	2
Number of Rotor Blades	78
Nozzle Inlet Angle, degrees	90
Nozzle Exit Angle, degrees	16
Nozzle Passage Height, inch (cm)	0.25 (0.635)
Rotor Blade Inlet Angle, degrees	17
Rotor Blade Exit Angle, degrees	25
Rotor Blade Height, inch (cm)	0.25 (0.635)
U/C_o(t-t)	0.0624
η, percent	22.5
$\dot{W}$, lb/sec (kg/s)	0.55 (0.249)

speed and low arc of admission results in a modest 22.5 percent turbine efficiency. In assessing the turbine efficiency, it should be remembered that the 10,887 watts (14.6 horsepower) required of this turbine represents less than 1 percent of the total turbomachinery power of the engine, therefore, the impact on system performance is very small.

The turbine efficienty characteristic as a function of pitch line velocity to gas isentropic spouting velocity ratio is shown in Fig. 4-3.

DESIGN DESCRIPTION

The low pressure oxidizer turbopump (Fig. 4-4) includes two external housings: the pump volute, which also serves as an inlet, inducer tunnel and bearing support; and the turbine housing which also supports the shaft seals and incorporates the drain and purge lines. The two housings are attached through a low pressure flange joint.

The rotating members consist of the inducer, shaft, turbine disk and retaining nuts, bolts, and locking features. The rotor is supported by a 30-mm angular contact bearing on the pump end and a 50-mm angular contact bearing on the turbine side.

The pumping element consists of an axial flow inducer of constant OD and contoured hub, containing four full and four partial vanes which discharges through ten guide vanes into a scroll shaped volute which delivers the fluid through a single pipe. The fluid is diffused slightly through the guide vanes and further diffused through the volute.

In the turbine, ambient gaseous hydrogen is admitted through a nozzle that extends over 7 percent of the circumference and incorporates two nozzle passages. After the nozzle, the gas passes through 78 blades in the turbine disk and returns to the engine through an exhaust collector.

To prevent mixing of the pump and turbine fluids, a seal package consisting of three controlled gap shaft seals is used. Details of the seal design are given elsewhere in this report.

THRUST BALANCE

Because of the high pressure level, the turbine contributes a large component to the rotor axial thrust. Conversely, because of the low pressure levels in the pump, conventional methods of counterbalancing the thrust, such as properly locating and sizing wear rings, are impractical in this case. Since the turbine is a partial admission impulse type, there is no appreciable pressure drop across the wheel and the turbine thrust component consists of pressure applied over the area inside the turbine seal diameter. This thrust component was minimized by reducing the seal diameter to the minimum consistent with structural and rotor dynamic considerations. Then the thrust (turbine end) bearing size was selected such that it could carry the residual axial load. Because of the

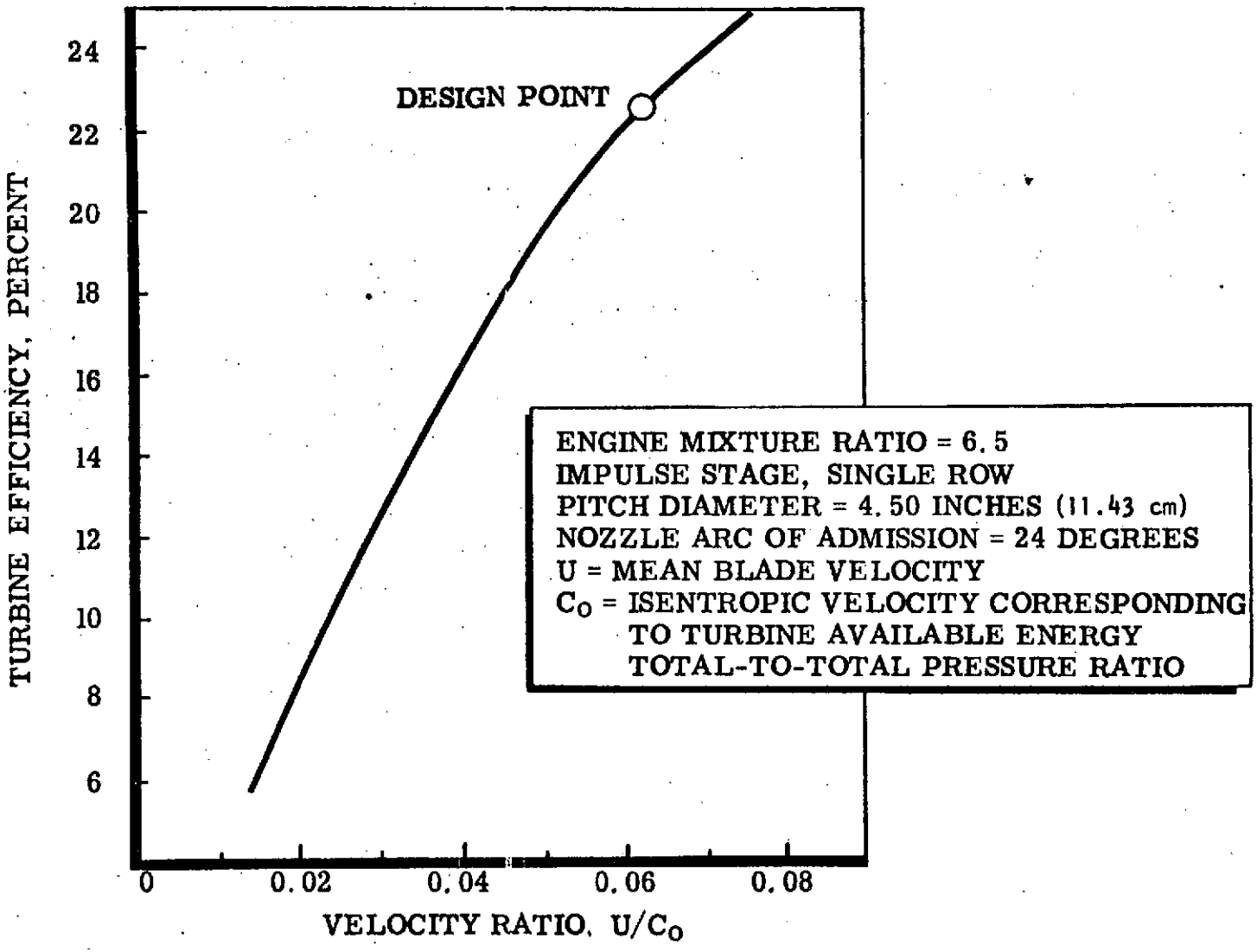

Figure 4-3. ASE Low-Pressure Oxidizer Turbine

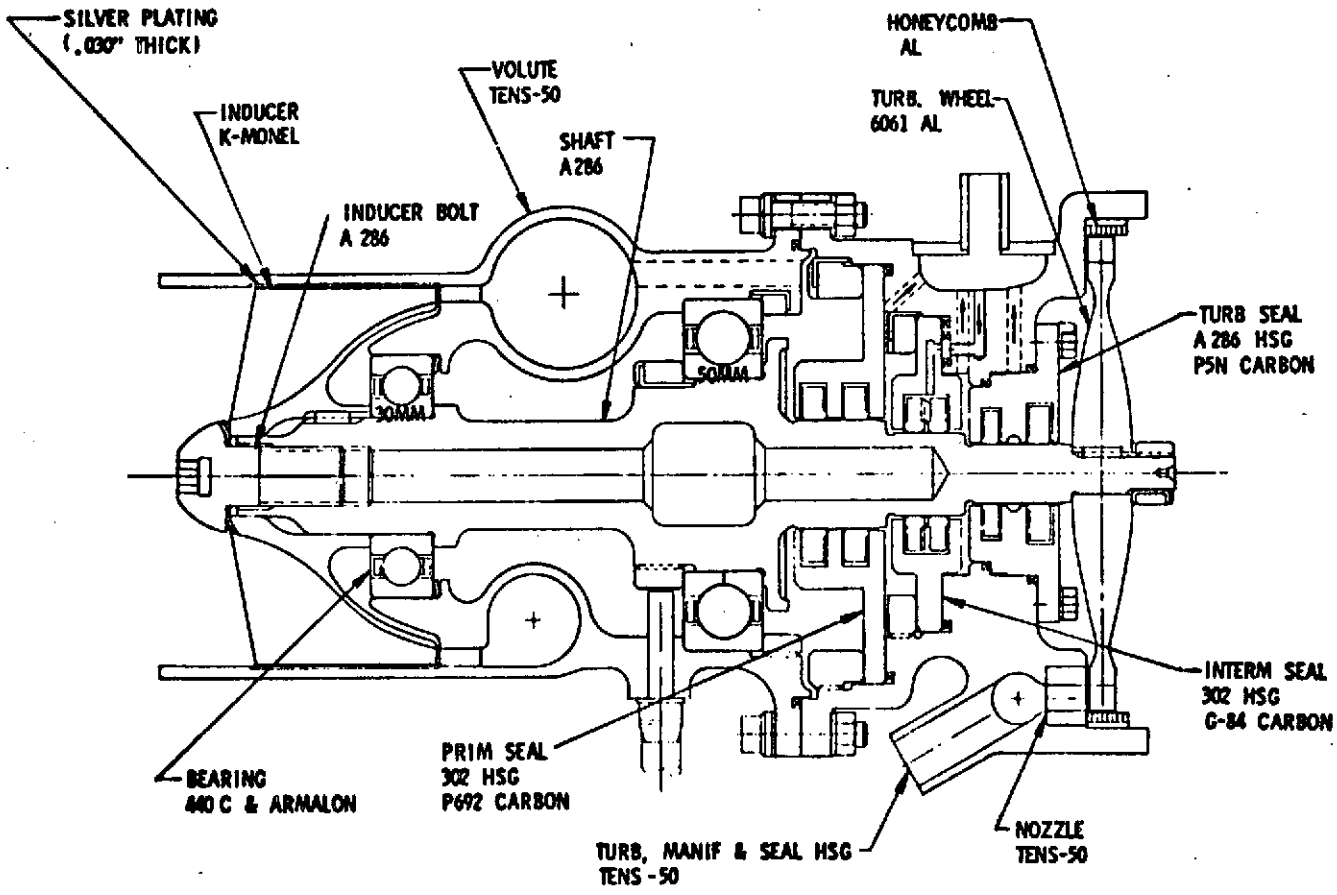

Figure 4-4. ASE Low-Pressure LOX Turbopump

low speeds involved this is a very practical solution; the 50-mm thrust bearing selected can carry the residual thrust of 6672 N (1500 lb) and meet the life requirements by a wide margin.

BEARINGS

Bearing lubrication in the low pressure oxidizer turbopump is accomplished by tapping 0.00063 m^3/sec (10 gpm) of liquid oxygen from the volute and introducing it through a cored passage to a region behind the turbine end bearing (see Fig. 4-5). The fluid is then passed through the turbine end bearing and pump end bearing, and is returned to the main pump flow loop behind the inducer discharge.

The detail design parameters for both bearings are presented in Fig. 4-5. Races and balls of both bearings are made of consumable electrode vacuum melt 440-C stainless steel. The case is one piece Armalon (glass fabric-filled Teflon) with no external reinforcement. The quality of Armalon will be controlled by Rocketdyne specification RB0130-013 to ensure adequate peel strength and uniform properties.

The front bearing is angular contact type, of 30-mm bore, resulting in a modest 0.2 million DN (bore diameter, mm times shaft speed, rpm). The static axial load capacity is 28,913 N (6500 lb). In contrast, the bearing is subjected only to a spring preload of 222 N (50 lb) which is applied to prevent ball skidding. The predicted B-10 life of the pump end bearing is over 1000 hours. The turbine end bearing was designed as a split inner race type, to permit the inclusion of the maximum number of balls for high axial load capability. Its bore side is 50 mm, resulting in a conservative DN value of under 0.4 million. The static axial load capacity of the turbine end bearing is 44,482 N (10,000 lb). In contrast, it carries a net thrust of 6672 N (1500 lb), which yields a B-10 life of over 200 hours.

SHAFT SEALS

To preclude mixing liquid oxygen from the pump with GH_2 from turbine, the two regions are separated by three seal assemblies as shown in Fig. 4-6.

All three seals are of the controlled gap type, with two seal rings in each. The controlled gap concept was selected for this application primarily because it has low drag torque, a "must" for idle mode starts. This concept also minimizes power absorption during steady-state operation and permits very long service life.

Pump fluid will be contained by the primary LOX seal. The small amount of oxygen that flows past the seal will be drained overboard from the cavity formed by the primary and intermediate seals. Pumping ribs are included upstream of the primary LOX seal to reduce the pressure to a level that will vaporize the fluid. By this technique, the mass flowrate through the seal is greatly reduced. The concept was used on the APS liquid oxygen turbopump with excellent results.

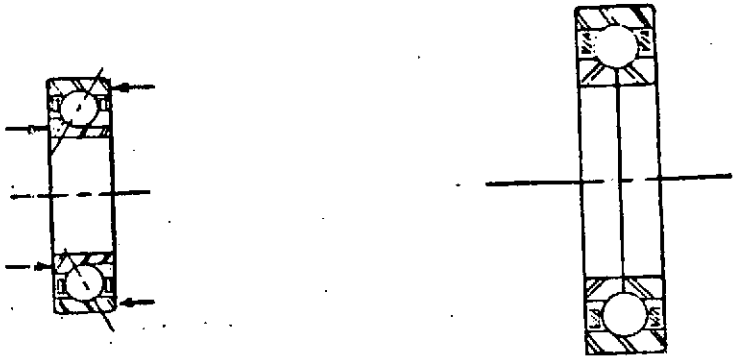

	PUMP END	TURBINE END
TYPE	ANGULAR CONTACT	SPLIT INNER RING
BORE, MM	30	50
DN	0.2×10^6	0.4×10^6
PITCH DIAMETER, INCHES	1.8 (4.57 cm)	2.75 (6.99 cm)
BALL DIAMETER	0.375 (0.953 cm)	0.4375 (1.111 cm)
NUMBER OF BALLS	12	14
RACE AND BALL MATERIAL	440-C	440-C
CAGE MATERIAL	ARMALON	ARMALON
AXIAL STATIC CAPACITY, LB	6500 (28913 N)	10,600 (47151 N)
AXIAL LOAD, POUNDS	50 (222 N)	1530 (6806 N)
B_{10} FATIGUE LIFE, HOURS	>1000	215

Figure 4-5. Low-Pressure LOX Turbopump Bearing Design Parameters

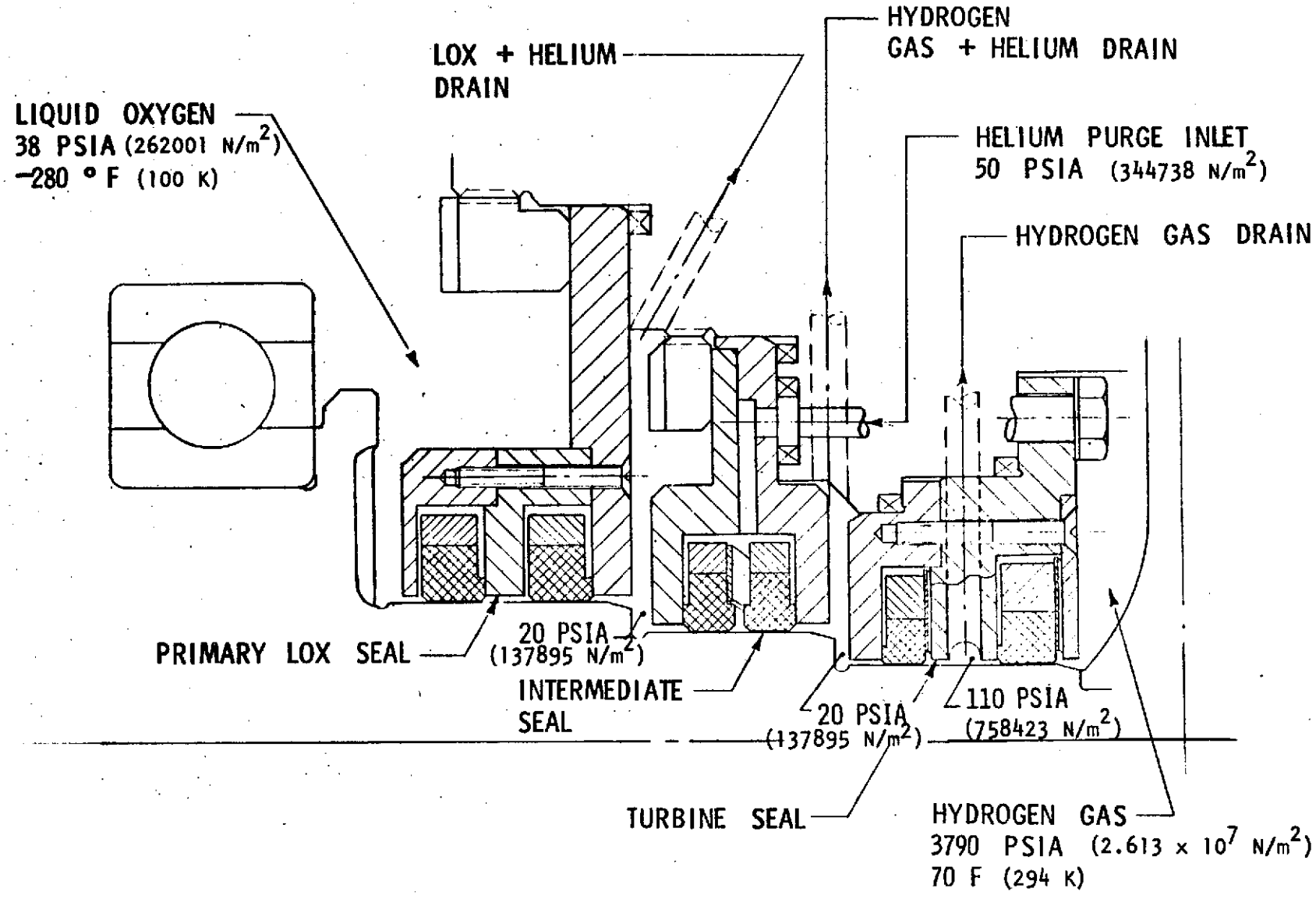

Figure 4-6. ASE Low-Pressure Oxidizer Turbopump Seals

Because of the high pressures involved on the turbine side, sealing and drainage is accomplished in two steps: an overboard drain is included downstream of the first segment to reduce the pressure between the two segments to 758,423 N/m^2 (110 psia), and the small amount of GH_2 that leaks past the second ring is drained overboard.

To provide absolute separation of the pump and turbine fluids, an intermediate seal is incorporated between the two drain areas with a GHe purge that maintains the cavity between the two rings at 344,738 N/m^2 (50 psia). Thus, before LOX or GH_2 can leak across the intermediate gear, it has to overcome this 344,738 N/m^2 (50 psia) barrier.

The materials selected for the seal components are noted in Table 4-3. A diametral clearance of 0.005 cm (0.002 inch) is specified between the sealing rings and the shaft.

TABLE 4-3. ASE LOW-PRESSURE LOX TURBOPUMP SHAFT SEAL DATA

Seal	Housing Material	Seal Ring Material	Retaining Ring Material	Shaft Material	Shaft Surface Treatment	Diameter Clearance, inches
Primary LOX	302	P 692 Carbon	A 286	A 286	CR Plate	0.002 (0.005 cm)
Intermediate	302	G 84 Carbon	A 286	A 286	CR Plate	0.002 (0.005 cm)
Turbine	A 286	P 5N Carbon	A 286	A 286	CR Plate	0.002 (0.005 cm)

The LPOTP baseline design is oriented to a system in which the main shutoff valve is located upstream of the pump. Thus, there are no long wet coast periods with stringent static sealing requirements. Should a requirement be established to mount the main valve downstream of the LOPTP, a liftoff seal can be incorporated into the design with a small amount of modification into the cavity between the thrust bearing and the primary seal.

The liftoff seal contains two concentric bellows between its nose and the supporting housing. The cavity between these two bellows is pressurized during coast conditions which presses the nose of the seal against the mating part, limiting static leakage values to approximately 6.299×10^{-6} kg/s (0.05 lb/hr). Immediately prior to start, the bellows pressure is vented, which allows the nose to "lift off" the mating part, thus preventing any degradation of the mating surface due to rubbing.

This type of liftoff seal can be incorporated into the LPOTP on a retrofit basis, as shown in Fig. 4-7, by incorporating actuation pressure parts into the housing and modifying the primary seal retaining nut.

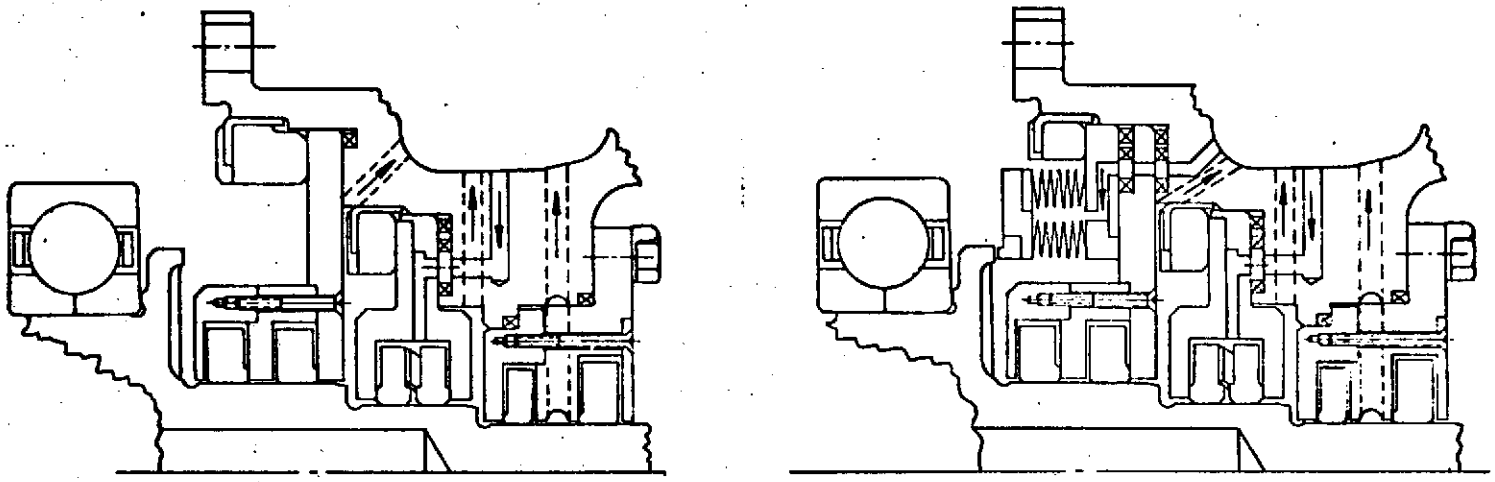

Figure 4-7. Low-Pressure Oxidizer Turbopump with Concentric Bellows Liftoff Seal

CRITICAL SPEED ANALYSIS

The critical speeds were calculated with a finite element method. The shaft was approximated as a series of concentrated masses and inertias connected by elastic beam elements. Forward synchronous precession was assumed and the bearings were modeled as linear springs to ground. The tyroscopic effect of each rotating mass was included.

The rotor critical speed for the low pressure turbopump is indicated in Fig. 4-8 as a function of the turbine end bearing spring rates. Trends due to the front bearing spring rates are shown in a parametric form; at the predicted combination of spring rates, the lowest critical speed is located above 3142 rad/s (30,000 rpm). Since the operating speed of the turbopump is below 1047 rad/s (10,000 rpm), no rotordynamic problems are anticipated.

MATERIAL SELECTION AND STRESS ANALYSIS

The materials selected for the low pressure oxidizer turbopump components are indicated in Fig. 4-4.

The pump housing will be cast from Tens-50 aluminum as an integral piece. To reduce tip seal leakage, the inducer-to-housing radial clearance has to be maintained close. Protections against hard metal-to-metal rubbing is provided by incorporating 0.168-cm (0.030-inch)-thick silver lining, applied by plating, on the inner diameter of the housing adjacent to the inducer.

Because of the low temperatures involved, the turbine housing can also be cast from Tens-50 aluminum. The three nozzle passages are electrical discharge machined in a Tens-50 aluminum block which is then EB welded into a milled cavity in the turbine housing.

The inducer itself will be machined from K-Monel forging, which has demonstrated exceptional ability to withstand hazardous conditions in LOX such as rubbing and foreign object impact without exploding. The shaft will be machined from A-286 forging.

Low tip speeds and ambient temperature permit the use of 6061 aluminum for the turbine wheel. Blades will be machined integral with the disk by electrical discharge method. Retaining nuts and bolts will be made of A-286, and lock tabs of 302 stainless steel.

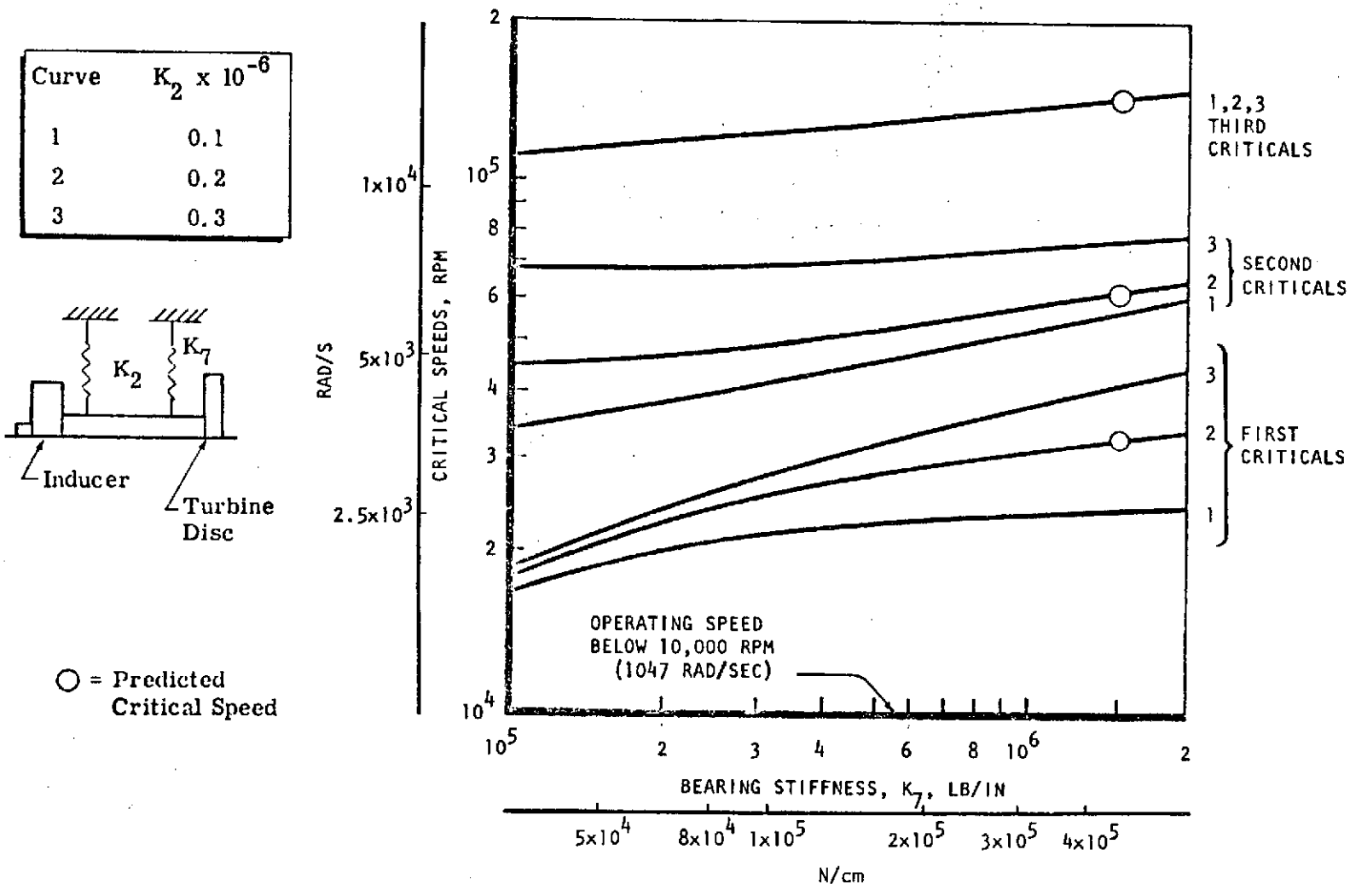

Figure 4-8. ASE Low-Pressure LOX Turbopump

LOW-PRESSURE FUEL TURBOPUMP

CONFIGURATION SELECTION AND PERFORMANCE

The function of the low-pressure fuel pump is to raise the pressure of liquid hydrogen from tank pressure to a level which will remove NPSH as a speed limiting criterion for the main pump and thus permit a high performance weight effective design. Since, by virtue of its function, the design of this pump is suction performance oriented, the design point was selected at an engine mixture ratio of 5.5, where both speed and delivered flow are highest and, therefore, the demands on suction performance are most severe. The specific measurements for this operating point are presented in Table 4-4.

The high suction performance requirement and low developed head automatically channelled the selection of the pump to a single-stage inducer type. The principal design parameters are noted in Table 4-4. The operating speed of the turbopump was established at 3068 rad/s (29,300 rpm), the maximum consistent with the suction performance requirements. A flow coefficient of 0.065 was selected for good suction capability. The diameter of the inducer was established at 8.382 cm (3.300 inches), which resulted in a moderate tip speed of 128.6 m/s (422 ft/sec) and a required head coefficient of 0.31.

The pump performance was calculated using Rocketdyne's Inducer Analysis Program. The characteristics obtained are presented in Fig. 4-9 . The head-flow curve has a steep negative slope in the anticipated operating range, which is important from a system stability standpoint. Pump overall efficiency at the design point is 70 percent, and the required shaft power is 21,998 watts (29.5 hp). The effect of operating at higher engine mixture ratio is illustrated in the figure by the 6.5 mixture ratio H-Q point: both speed and flowrate are slightly lower. The internal flow and pressure distribution is shown in Fig.4-10 .

Here, as in the case of the low-pressure LOX turbopump, the bearing coolant flow is maintained by the friction pumping effect of the inducer hub and by the static pressure rise across the volute guide vanes.

The drive system to be used for the pump has been defined by system studies as a gas turbine propelled by hydrogen gas heated to essentially ambient temperature by passing through the thrust chamber coolant tubes. The inlet pressure and temperature of the gas and the exhaust pressure are as noted in Table 4-5. The low power level and attendant low flowrate dictated a partial admission turbine.

The rotational speed of the turbine was fixed at 3068 rad/s (29,300 rpm) by pump considerations and the decision to have the pump and turbine rotor elements on the same shaft.

To obtain the best turbine performance at the established speed, several turbine diameters were evaluated. As the pitch diameter is increased, the tip speed to gas spouting velocity is increased which tends to improve efficiency. However, with increasing diameter the degree of admission has to be reduced to maintain the required flow area, since blade height cannot be reduced below approximately

TABLE 4-4. ASE LOW-PRESSURE FUEL TURBOPUMP DESIGN PARAMETERS (MR = 5.5)

- Pump
  - System Requirements

P_S, psia (N/m^2)	16.65 (114,798)
P_D, psia (N/m^2)	72.13 (497,319)
$\dot{W}$, lb/sec (kg/s)	6.33 (2.871)
NPSH, ft, min (joule/kg)	5 (14.945)

  - Design Parameters

Type	Inducer
N, rpm (rad/s)	29,300 (3068)
$D_{Inducer}$, inches (cm)	3.300 (8.382)
U_{Tip}, fps (m/s)	422 (128.6)
ϕ_{Inl}	0.065
ψ_{Stg}	0.31
η, percent	70
Specific Speed	2835 (1.0376, nondimensional)
Suction Specific Speed	99,130 (36.28, nondimensional)
Hub Diameter at Inlet, inch (cm)	1.000 (2.54)
Hub Diameter at Discharge, inches(cm)	2.930 (7.44)
Number of Inducer Blades at Inlet	4
Number of Inducer Blades at Discharge	4
Blade Tip Angle at Inlet, degrees	6.5
Blade Tip Angle at Discharge, degrees	43.1

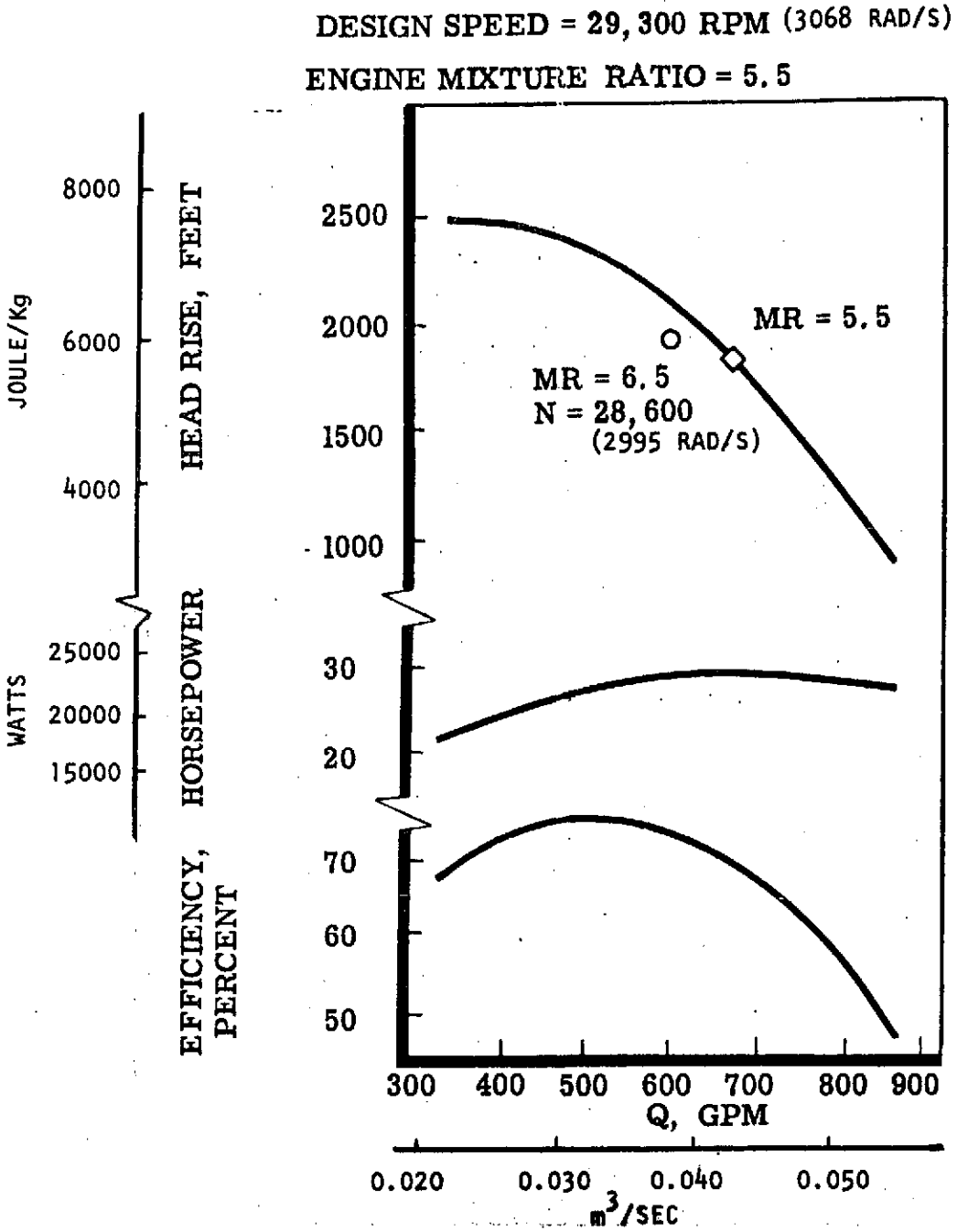

Figure 4-9 . ASE Low-Pressure Fuel Pump Predicted Performance Map

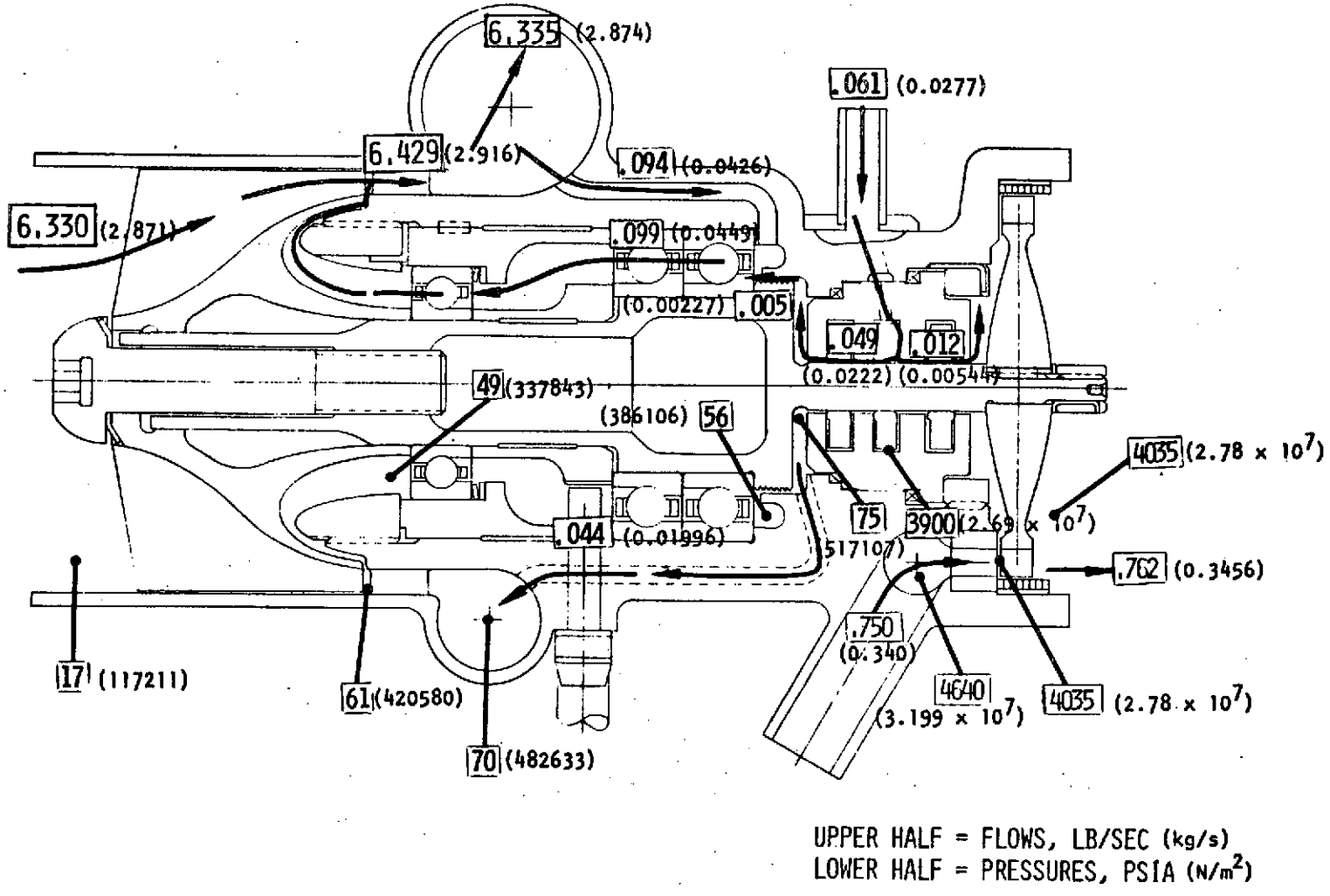

Figure 4-10. ASE Low-Pressure Fuel Turbopump Internal Flow and Pressure Schedule (MR = 5.5)

TABLE 4-5. ASE LOW-PRESSURE FUEL TURBOPUMP DESIGN PARAMETERS (MR = 5.5)

- Turbine
  - System Constraints

Fluid	GH_2
T_{t_1}, R (K)	492 (529)
P_{t_1}, psia (N/m^2)	4640 (3.199×10^7)
P_{t_2}, psia (N/m^2)	4035 (2.782×10^7)
P/R (t-t)	1.15

  - Design Parameters

Type	Partial Admission, Single-Stage, Impulse
ϵ, percent	8.5 (32 degrees)
N, rpm (rad/s)	29,300 (3068)
bhp (watts)	29.5 (21,998)
D_m, inches (cm)	2.75 (6.985)
U_m, fps (m/s)	351 (106.98)
Number of Nozzle Passages	2
Number of Rotor Blades	63
Nozzle Inlet Angle, degrees	90
Nozzle Exit Angle, degrees	16
Rotor Blade Inlet Angle, degrees	20
Rotor Blade Exit Angle, degrees	25
Nozzle Passage Height, inch (cm)	0.22 (0.559)
Rotor Blade Height, inch (cm)	0.22 (0.559)
U/C_o	0.185
η_o(t-t), percent	39.8
$\dot{W}$, lb/sec (kg/s)	0.75 (0.34)

0.635 cm (0.25 inch) without performance penalty. From this analysis, it was found that the performance peaks out at 8.5 percent admission and a pitch diameter of 6.99 cm (2.75 inches), Table 4-5. The corresponding tip speed is 106.98 m/s (351 ft/sec) and the wheel speed-to-gas mounting velocity ratio is 0.185.

Turbine efficiency as a function of pitch line velocity to gas isentropic spouting velocity ratio is present in Fig. 4-11. The combination of low tip speed and small arc of admission limit the efficiency at the design point to 39.8 percent. The low turbine efficiency has very little engine effect on engine overall performance since the 21,998 watts (29.5 horsepower) required by the low-pressure fuel pump represents only 1 percent of the total turbomachinery horsepower on the engine. A gas flowrate of 0.229 m/s (0.75 lb/sec) is required to develop the 21,998 watts (29.5 shaft horsepower).

DESIGN DESCRIPTION

The entire low-pressure fuel turbopump is contained in a single cast aluminum housing which fulfills the function of inducer tunnel, pump volute, bearing and seal support, and turbine housing (Fig. 4-12). Components are assembled into the housing from both ends; the only external joints involved are those required for fluid entry or discharge. This approach yields the lowest weight by eliminating bulky flanges and offers the highest reliability by providing a self-contained sealed package.

Pump working elements consist of a four-bladed inducer of constant 8.382 cm (3.300 inches) diameter and contour hub. The fluid is discharged from the inducer through 10 stationary diffuser vanes, collected in the volute and delivered through a single discharge duct to the inlet of the high-pressure fuel turbopump. The velocity of the fluid is reduced through the diffuser vanes and, thereby, friction losses in the volute are minimized.

Turbine propellant is introduced through a 1.219-cm (0.48-inch) diameter inlet into a manifold extending over a small segment of the circumference. The gas is expanded to exhaust pressure level through two nozzle passages. The turbine wheel includes 63 unshrouded impulse type blades, machined integral with the disk. A honeycomb seal of small cell size is situated opposite the wheel tip, to facilitate a close clearance. The clearance will be set only large enough to permit assembly, and the wheel will be allowed to wear in its own clearance during the initial test.

The rotor is comprised of the shaft, on which the bearing inner races and spacer are retained, the inducer, turbine disk, and fasteners. To transmit the developed torque, the turbine disk is keyed to the shaft. Relative rotation between the inducer and shaft is precluded by an integral key at the pump end of the shaft. A solid shaft is not required from stress or rotordynamic considerations; therefore, material is removed from the center to reduce weight and moment of inertia.

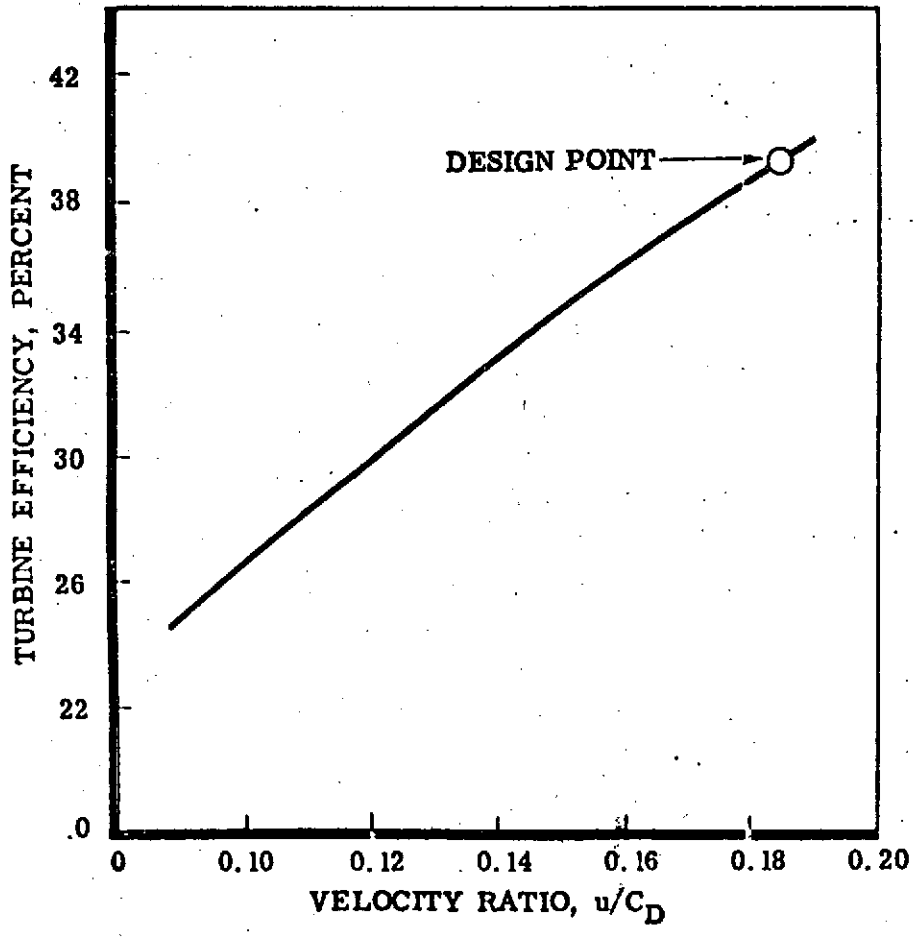

ENGINE MIXTURE RATIO = 5.5

IMPULSE STAGE, SINGLE ROW

PITCH DIAMETER, D_m = 2.75 in. (6.985 cm)

NOZZLE ARC OF ADMISSION = 32 DEGREES

C_D = ISENTROPIC VELOCITY CORRESPONDING TO TURBINE AVAILABLE ENERGY (Btu/lb) TOTAL-TO-TOTAL PRESSURE RATIO

Figure 4-11. ASE Low-Pressure Fuel Turbine

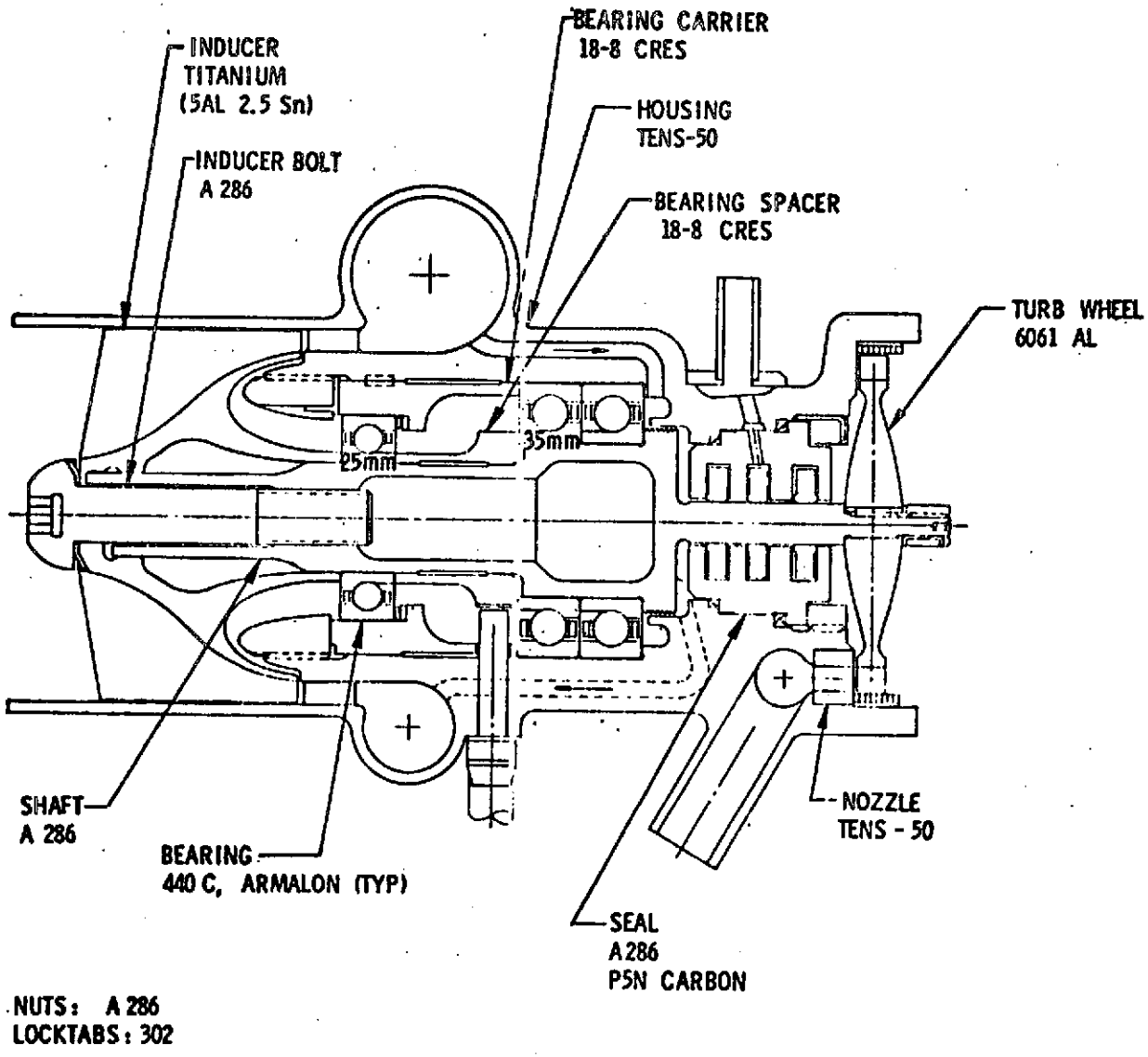

Figure 4-12. ASE Low-Pressure Fuel Turbopump Layout

THRUST BALANCE

As a result of the high-pressure levels in the turbine region, the turbine component of the rotor axial thrust is substantial. Since the turbine is a partial admission impulse type, the pressure on either side of the disk is equal; the thrust component originates from the pressure acting over the area enclosed by the shaft seal. The capability to counteract this thrust in the pump is limited because of low available pressure. To achieve a simple and effective thrust control, the turbine component is minimized by reducing the shaft seal diameter to the smallest allowable from a stress and rotordynamic standpoint. Then, a pair of thrust bearings of sufficient size is selected to carry the residual loads. The shaft diameter at the seal was finalized at 0.953 cm (0.375 inch) which resulted in a wet rotor load of 3292 N (740 pounds). The pair of 35-mm bearings used in the design can carry that axial load with ample life margin.

BEARINGS

The rotor is supported by a 20-mm ball bearing on the pump end and a pair of 35-mm ball bearings on the turbine end. DN values at the design speed are moderate, 0.6 and 1 million, respectively.

The internal design details of the bearings are noted in Table 4-6. Each bearing is of angular contact type, with one piece Armalon cage and 440C races and balls. The pump end bearing carries radial rotor loads only. To preclude ball skidding and scoring, it is axially loaded to a constant 200 N (45 pounds) with a Belleville spring.

With small loads and low DN values, the predicted B_{10} life of the pump end bearing is very high, in excess of 1000 hours.

The pair of turbine end bearings share a total rotor axial thrust of 3292 N (740 pounds). Assuming that the load is not shared equally, and that one of the bearings carries 60 percent of this load, the predicted B_{10} life is 204 hours, twice the 100-hour minimum stipulated.

Bearing lubrication is accomplished by bleeding off 0.029 m/s (0.094 lb/sec) liquid hydrogen from the volute discharge through a cored passage to the turbine side of the thrust bearings.

The coolant passes through the turbine end bearings and the pump end bearing and returns to the main pump flow at the discharge of the inducer. The circulation flow is maintained by pressure differentials created by the disk friction pumping action of the inducer hub and by the rise in static pressure realized through the diffuser vanes.

SHAFT SEAL

The shaft seal design of the low-pressure fuel turbopump is based on a vehicle installation in which the main shutoff valve is located upstream of the pump; thus, there is no static scaling requirement during coast periods.

TABLE 4-6. ASE LOW-PRESSURE FUEL TURBOPUMP
BEARING DESIGN PARAMETERS

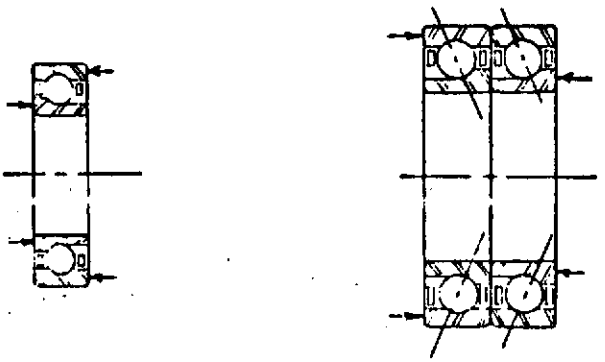

	Pump End	Turbine End
Type	Angular Contact	Angular Contact (Pair)
Bore, mm	20	35
DN	0.6×10^6	1.02×10^6
Pitch Diameter, inches (cm)	1.2 (3.048)	1.9 (4.826)
Ball Diameter, inches (cm)	0.21875 (0.5556)	0.3125 (0.7938)
Number of Balls	11	12
Race and Ball Material	440C	440C
Cage Material	Armalon	Armalon
Axial Static Capacity, pounds (Newton)	1600 (7117)	4400 (19,572)
Axial Load, pounds (newton)	45 (200)	740/pair (3292)
B_{10} Fatigue Life, hours	>1000	204

Since pump and turbine fluids are pure hydrogen, separations of these regions is not required from the standpoint of chemical or mechanical compatibility. To minimize GH_2 flow from the turbine to the pump, a controlled gap floating ring seal is included to seal the shaft.

In analyzing the heat balance of the pump fluid, it was found that if all assumptions with regard to fluid properties, amount of friction heating, bearing heat input, and turbine gas seal leakage stacked the wrong way, the fluid passing through the pump would absorb sufficient heat to make the NPSH available at the inlet of the main pump marginal. To be on the safe side, provisions are made in the design to stop turbine gas leakage into the pump by pressurizing the shaft seal with liquid hydrogen to be tapped from the high-pressure pump. The necessity of such a hydrogen injection system will be assessed based on actual fluid temperature measurement in the early phase of the development program. If not required, the injection port will be discontinued or used for instrumentation purposes.

Details of the shaft seal and the materials selected are noted in Fig. 4-13. By incorporating a sealing lip on both faces of the turbine side ring, the seal can be used in its present configuration with or without hydrogen injection.

CRITICAL SPEED ANALYSIS

The rotordynamic characteristics of the low-pressure fuel turbopump are presented in Fig. 4-14 . Critical speeds are indicated as a function of rear bearing spring rates, with trends due to front bearing spring rate shown in parametric curves. The lowest critical speed is predicted at 4189 rad/s (40,000 rpm). This is above the maximum operating speed of the turbopump by more than the stipulated 20 percent margin.

MATERIAL SELECTION AND STRESS ANALYSIS

Because of low-pressure levels in the pump, ambient temperature in the turbine, and moderate tip speeds, the components in the low-pressure fuel turbopump are generally lightly stressed. Materials and wall thicknesses, with the exception of the turbine manifold, are governed by nonstructural considerations such as manufacturing capability.

The housing will be cast from Tens-50 aluminum. Due to casting technique limitations, the minimum wall thicknesses would be the same from steel or aluminum (the latter is a particularly weight-effective choice for the pump region). It is well suited for turbine manifold material because it is unaffected by hydrogen embrittlement, whereas most steels would deteriorate at the high-pressure ambient temperature GH_2 environment. The same reasoning led to choosing 6061 aluminum for the turbine wheel material. The blades are machined integral with the disk.

From a strength standpoint, aluminum would be acceptable for the inducer; however, a harder material is preferable to resist nicks and dents in the leading edge from foreign particles. Titanium, used in many hydrogen inducer applications, was selected.

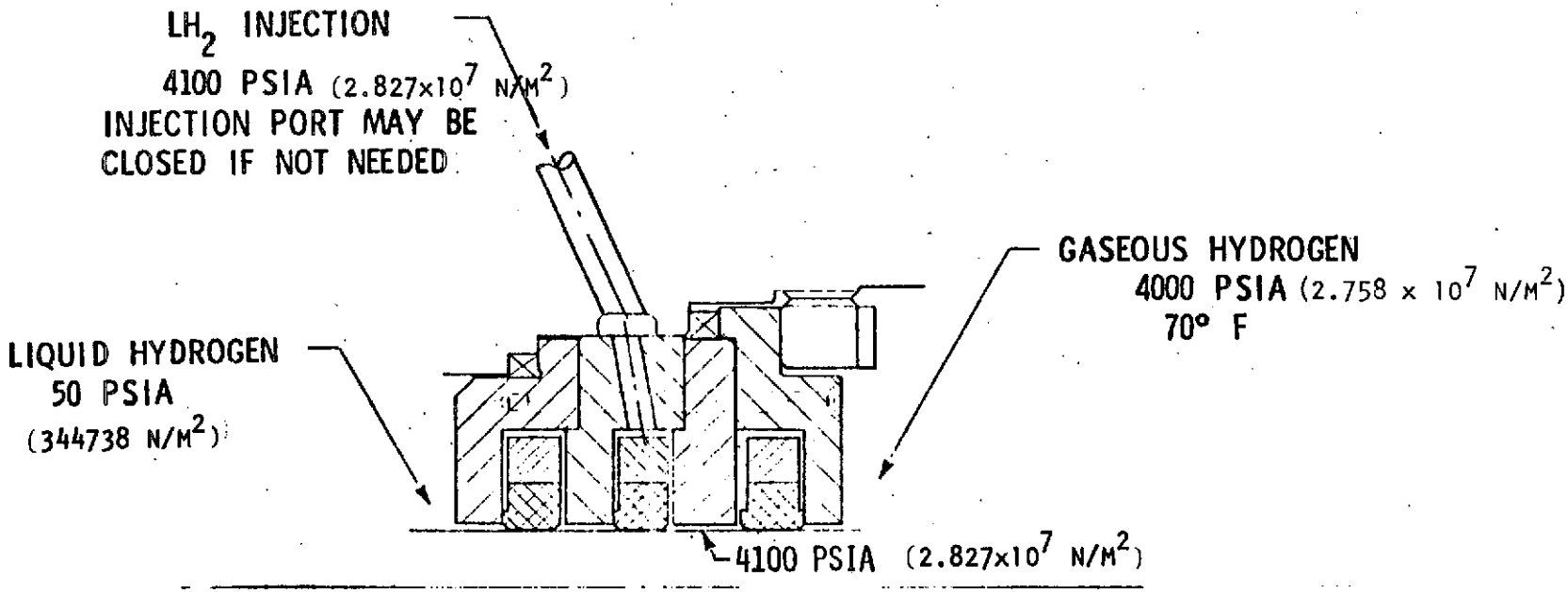

HOUSING MATERIAL	A 286
SEAL RING MATERIAL	P 5N CARBON
RETAINING RING MATERIAL	A 286
SHAFT MATERIAL	A 286
SHAFT SURFACE TREATMENT	CHROME PLATE
DIAMETRAL CLEARANCE, IN.	0.002 (0.0051 cm)

Figure 4-13. ASE Low-Pressure Fuel Turbopump Seal

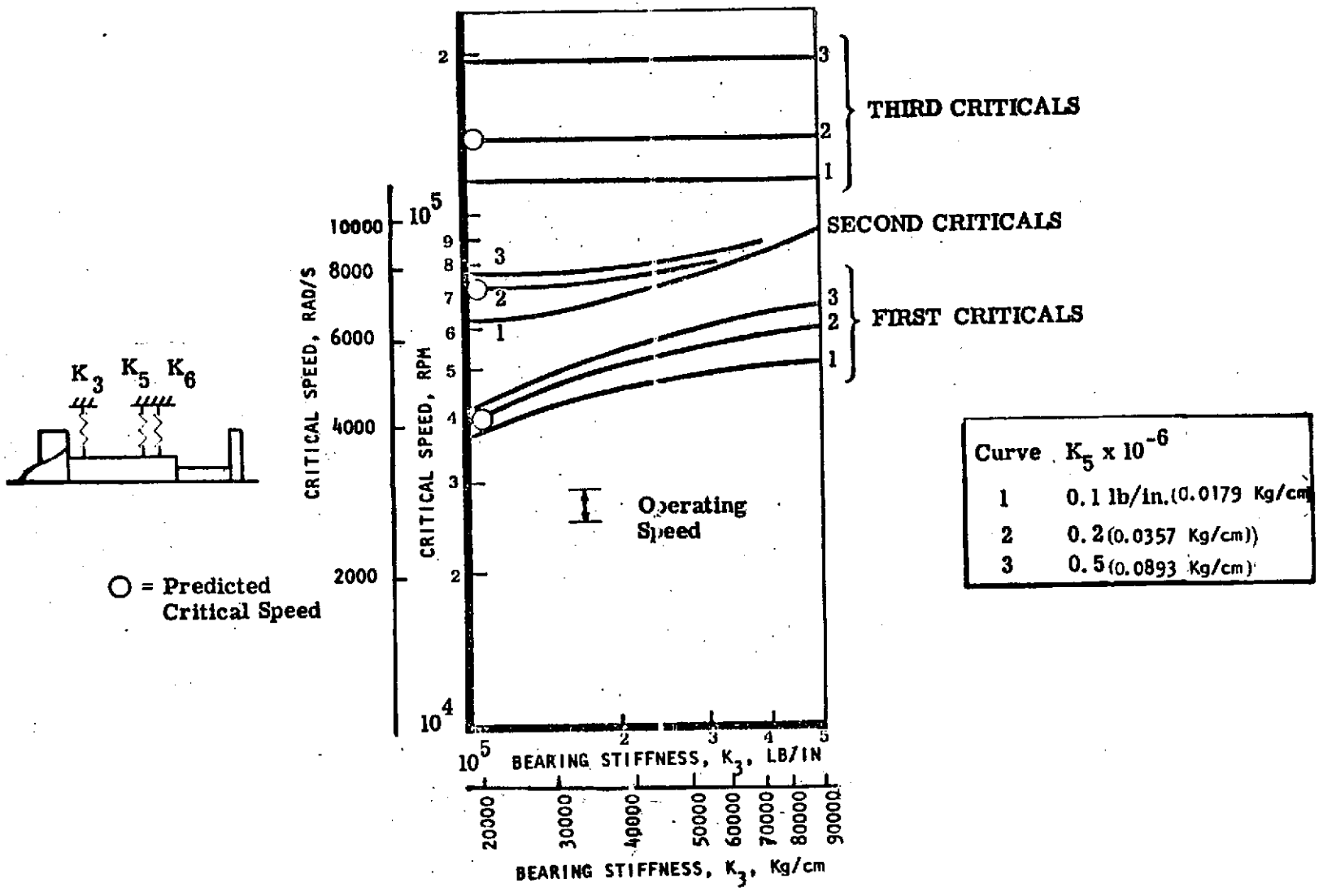

Figure 4-14. ASE Low-Pressure Fuel Turbopump Rotor Critical Speeds

The properties required of the shaft material are: (1) a hard mounting surface for the bearings, (2) a hard-chrome-plateable surface for the shaft seals, (3) and high strength and modulus of elasticity to permit a minimum shaft diameter at the turbine seal. The A-286 alloy was selected because it meets all the above requirements, and it has a successful history in many cryogenic applications.

HIGH-PRESSURE OXIDIZER TURBOPUMP

CONFIGURATION SELECTION AND PERFORMANCE

The function of the high-pressure oxidizer pump is to raise the pressure of liquid oxygen from 529,173 to 2.687 x 10^7 N/m^2 (76.75 to 3897 psia), at a delivered flowrate of 16.68 kg/s (36.78 lb/sec).

This function is accomplished with an inducer plus a single-stage centrifugal impeller configuration. An inducer is included in the design to minimize the required NPSH. Lower NPSH capability maintains the boost pump discharge pressure at a low level, and permits the main pump to run at a higher speed with correspondingly higher efficiency and smaller size. The detail hydrodynamic design parameters are listed in Table 4-7. The design speed is 8168 rad/s (78,000 rpm), which in conjunction with the 5.969 cm (2.35 inch) impeller tip diameter results in a moderate 244 m/s (800 fps) tip speed. At the selected rotor speed, the specific speed of the pump is 0.5124 nondimensional (1400), which places it in a good performance range for a centrifugal pump, facilitating an overall efficiency of 70 percent.

The pump performance map for the high-pressure oxidizer turbopump is presented in Fig. 4-15. The curves represent constant speed performance at 8168 rad/s (78,000 rpm), with the 6.5 engine mixture ratio point indicated at 0.01483 m^3/s (235 gpm) 16.68 kg/s (36.78 lb/sec). Operating points for 6.0 and 5.5 engine mixture ratio are shown to illustrate pump parameter trends over the range of engine operation. The highest speed point is at 9006 rad/s (86,000 rpm) for a nominal engine operating at 5.5 mixture ratios.

To establish pump performance, an internal flow and pressure schedule was prepared. The results of that analysis are given in Fig. 4-16.

The turbine of the high-pressure oxidizer pump receives its propellant form the preburner at an inlet temperature of 1053 K (1896 R) and an inlet pressure of 2.321 x 10^7 N/m^2 (3367 psia). The turbine discharges to a system pressure of 1.710 x 10^7 N/m^2 (2475 psia), Table 4-8.

The turbine selected is a single-stage impulse type, of 25-percent admission, developing 549,581 watts (737 shaft horsepower) at 8168 rad/s (78,000 rpm). Partial admission is necessary to avoid a blade height lower than 0.635 cm (0.25 inch) which would result in a higher performance penalty. The wheel pitch diameter is 10.8 cm (4.25 inches), resulting in 440 m/s (1445 fps) pitch line velocity. The ratio of pitch line velocity to gas isentropic spouting velocity is 0.364, yielding an overall turbine efficiency of 66 percent (Fig. 4-17). The required gas flowrate is 1.143 kg/s (2.52 lb/sec).

DESIGN DESCRIPTION

The mechanical arrangement of the high-pressure oxidizer turbopump is shown in Fig. 4-18. The turbopump has two major housings. The pump housing, which includes the discharge volute, serves as a mount for pump wear rings and balance piston orifices, both bearings, and the primary seal. The other major housing

TABLE 4-7. ASE HIGH-PRESSURE LOX TURBOPUMP DESIGN PARAMETERS (MR = 6.5)

- Pump
  - System Requirements

Fluid	LOX
P_S, psia (N/m^2)	76.75 (529,173)
P_D, psia (N/m^2)	3897 (2.687×10^7)
$\dot{W}$, lb/sec (kg/s)	36.78 (16.683)

  - Design Parameters

Type	Inducer Plus First-Stage Centrifugal
N, rpm (rad/s)	78,000 (8168)
Inducer to Diameter, inches (cm)	1.57 (3.988)
Inducer Hub Diameter at Inlet, inch (cm)	0.610 (1.55)
Inducer Hub Diameter at Discharge, inch (cm)	0.800 (2.032)
Inducer Blade Tip Angle at Inlet, degrees	10.0
Inducer Blade Tip Angle at Inlet (rms), degrees	13.2
Inducer Blade Tip Angle at Discharge (rms), degrees	18.0
Impeller Inlet Tip Diameter, inches (cm)	1.57 (3.988)
Impeller Tip Diameter, inches (cm)	2.35 (5.97)
Impeller Blade Tip Angle at Inlet, degrees	10.0
Impeller Blade Discharge Angle, degrees	27
Number of Inducer Blades at Inlet	3
Number of Inducer Blades at Discharge	3
Number of Impeller Blades at Inlet	5
Number of Impeller Blades at Discharge	5
U_{Imp}, fps (m/s)	800 (243.84)
ϕ_{Disch}	0.12
ψ_{Stg}	0.40
η, percent	70
Specific Speed	1435
Suction Specific Speed	31,000

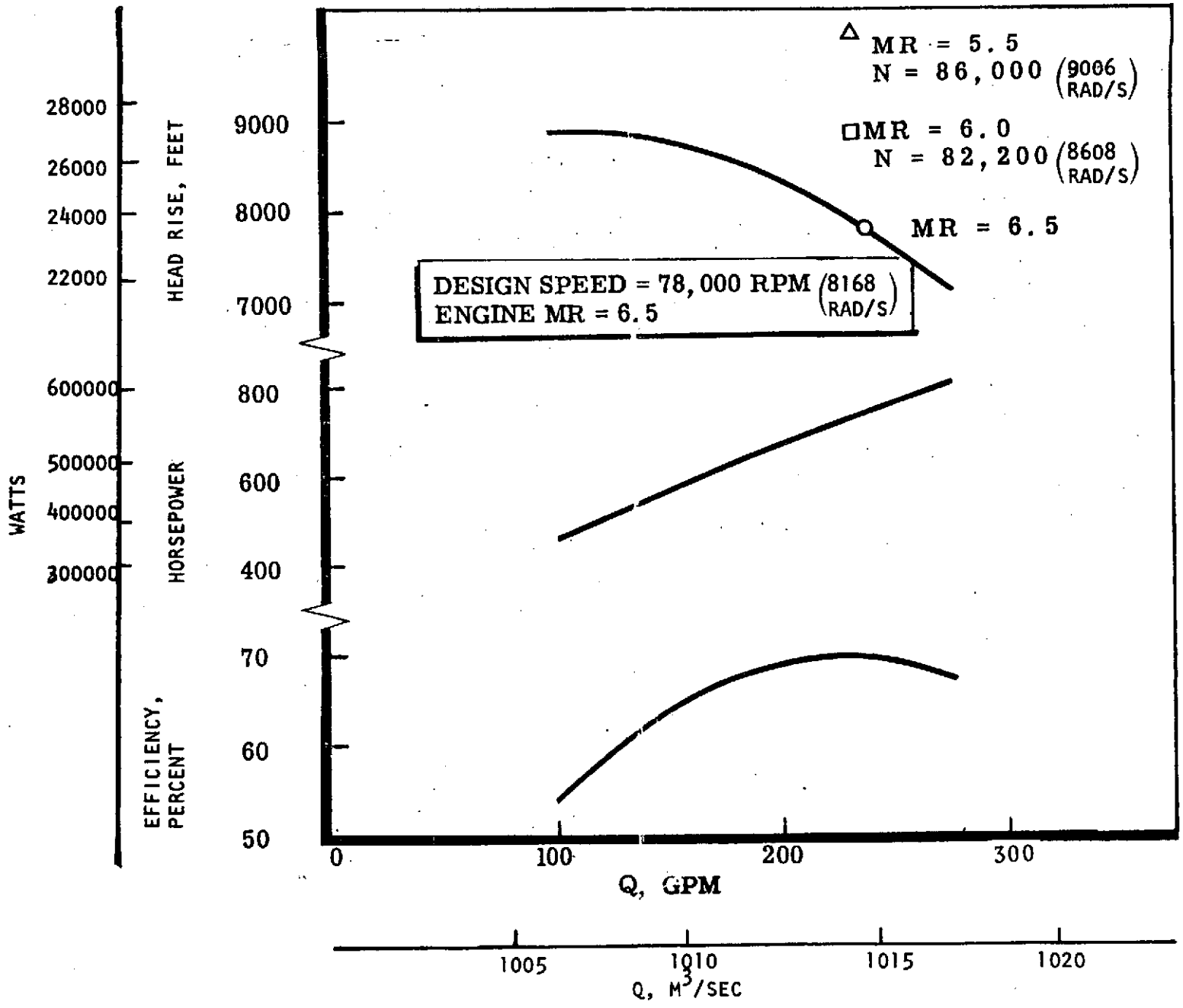

Figure 4-15. ASE High-Pressure LOX Pump Predicted Performance Map

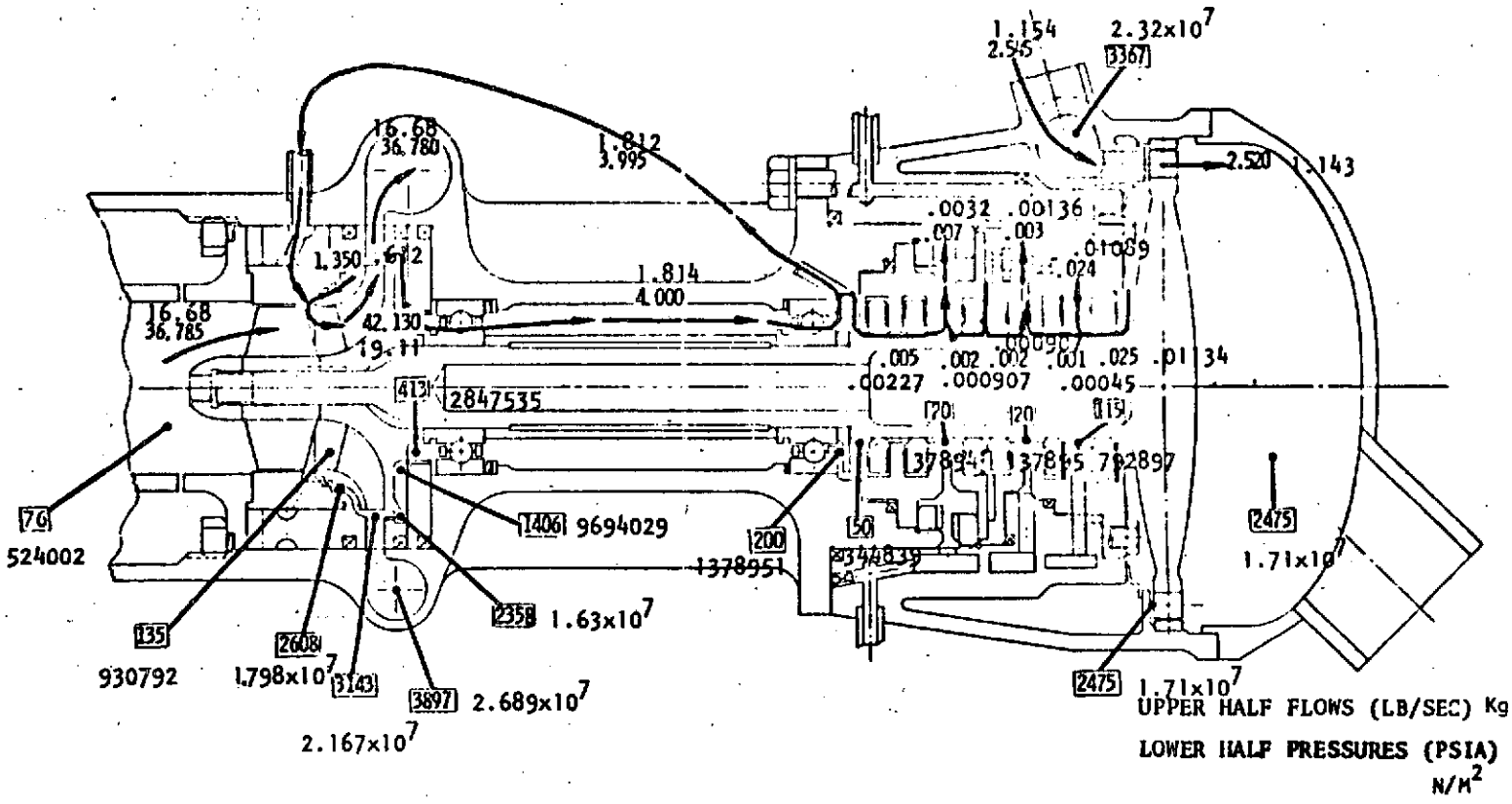

Figure 4-16. ASE High-Pressure LOX Turbopump Internal Flows and Pressures

TABLE 4-8. ASE HIGH-PRESSURE LOX TURBOPUMP DESIGN PARAMETERS

- Turbine
  - System Constraints

Fluid	Preburner Hot Gas (H_2O + H_2)
T_{t_1}, R (K)	1896 (1309)
P_{t_1}, psia (N/m^2)	3367 (2.321×10^7)
P_{t_2}, psia (N/m^2)	2475 (1.706×10^7)

  - Design Parameters

Type	Partial Admission, Single-Stage, Impulse
N, rpm (rad/s)	78,000 (8168)
bhp (watts)	737 (549,581)
ϵ, percent	25
U/C_o	0.37
η, percent	67
$\dot{W}$, lb/sec (kg/s)	2.52 (1.143)
D_m, inches (cm)	4.25 (10.8)
U_m, fps (m/s)	1445 (440)
Number of Nozzle Passages	12
Number of Rotor Blades	74
Nozzle Inlet Angle, degrees	90
Nozzle Exit Angle, degrees	16
Rotor Blade Inlet Angle, degrees	26
Rotor Blade Exit Angle, degrees	25
Nozzle Passage Height, inch (cm)	0.25 (0.635)
Rotor Blade Height, inch (cm)	0.25 (0.635)

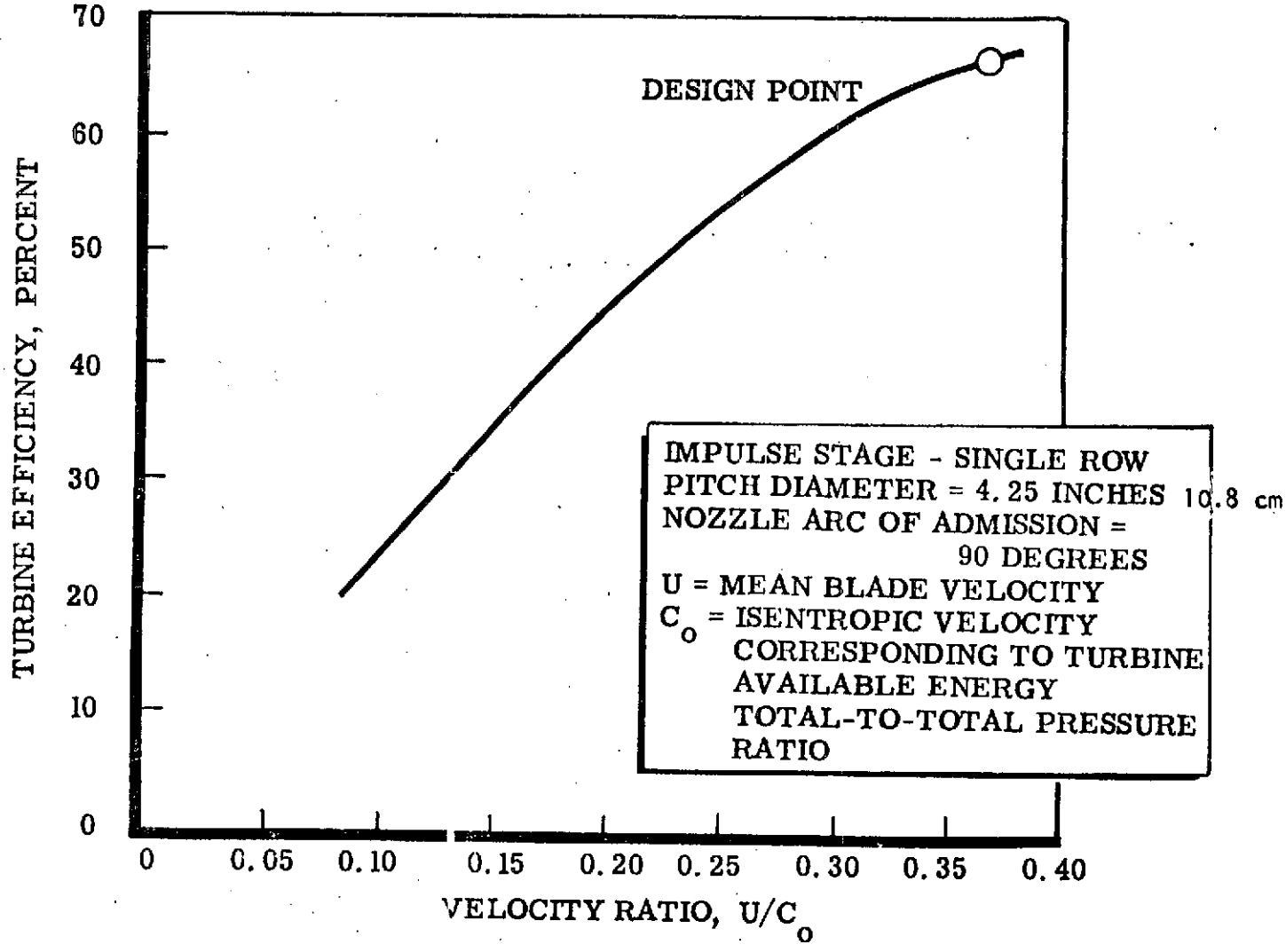

Figure 4-17. ASE High-Pressure Oxidizer Turbine

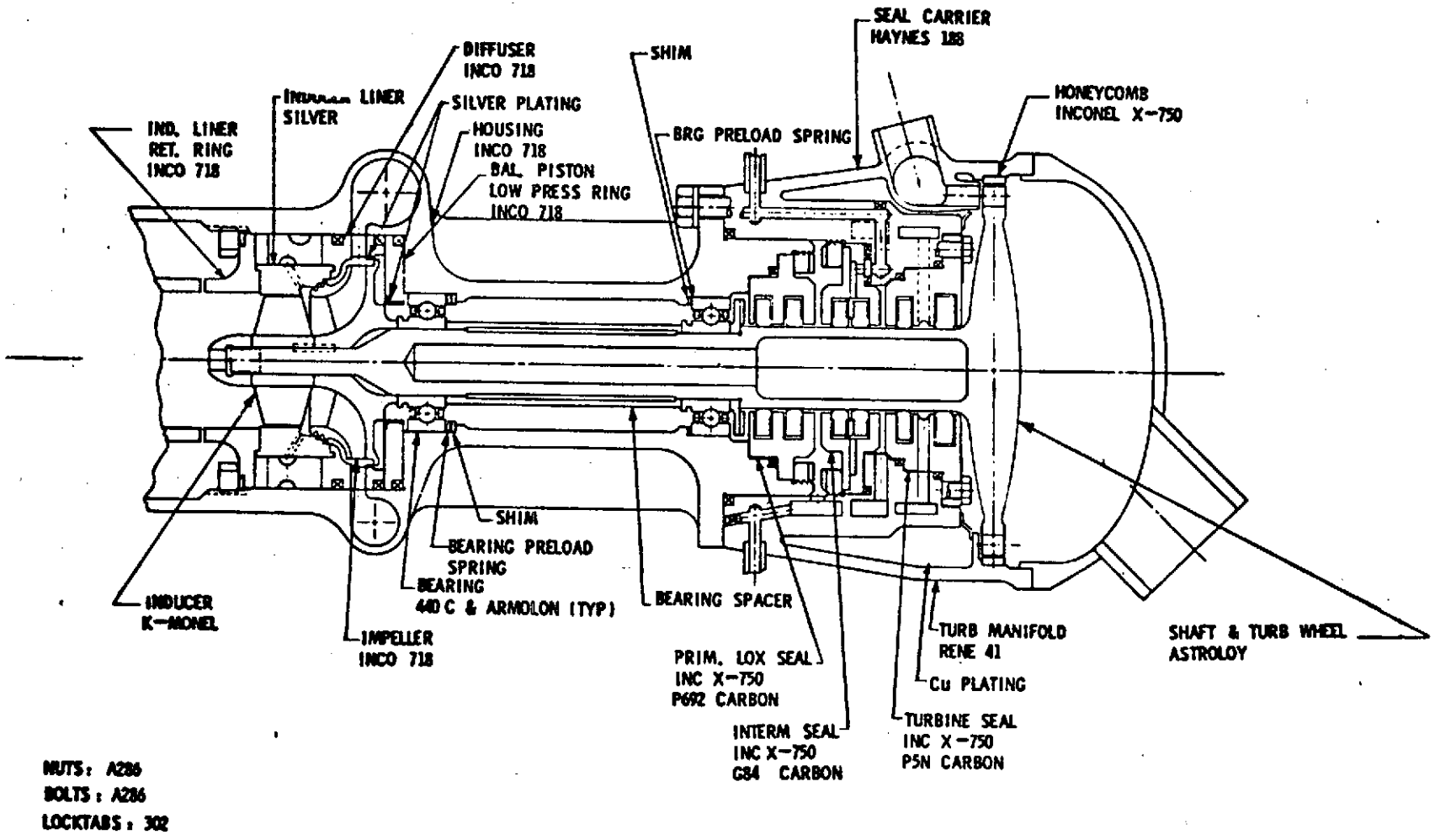

Figure 4-18. ASE High-Pressure Oxidizer Turbopump

is the turbine manifold which supports the nozzle, the intermediate and turbine seals, and provides drainage and purge access to all shaft seals. The only external joint in the turbopump, other than those required to admit and discharge flow, is where these two housings are attached. This joint is exposed to the pressure level of the pump primary seal drain, which is less than 241,317 N/m^2 (35 psia).

The pumping elements consist of a three-bladed inducer of constant diameter and tapered hub, and a shrouded impeller containing five full vanes with a discharge angle of 27 degrees. Liquid oxygen discharged from the impeller passes through 13 diffuser passages into the volute where it is collected and delivered through a single discharge duct. To improve suction performance and minimize internal fluid recirculation, a silver inducer liner is used, which will permit close vane tip clearance. The same silver liner is also utilized for a stepped labyrinth seal on the impeller front shroud.

Propellant gas is admitted to the turbine through a single inlet. The flow splits in the manifold and passes to two nozzle segments located 180 degrees from each other. Splitting of the nozzles is necessary to avoid a large bearing reaction load which would result from an unsymmetrical turbine wheel blade loading. Each nozzle segment contains six convergent subsonic passages, through which the gas is expanded fully to the exhaust pressure. The turbine wheel includes 74 impulse type blades, machined integral with the disk.

The rotor is supported by two 20-mm ball bearings, and consists principally of an integral shaft and turbine disk, inducer, impeller, and a primary seal slinger.

THRUST BALANCE

To guarantee reliable bearing operation for the stipulated 10-hour cycle life at the high speeds involved, the bearings must be subjected to limited, closely installed loads. Radial loads are minimized by the use of diffuser vanes in the pump and by symmetrical nozzle arrangement. To exercise a tight control over the residual rotor axial loads, a self-compensating, nonrubbing balance piston is used (Fig. 4-19). The rotating member of the balance piston is integral with the back shroud of the impeller. To operate the piston, LOX is bled from the impeller discharge and passed into the balance piston cavity through the high-pressure orifice formed by an extension of the impeller rear shroud and a silver plated section of the diffuser ring. From the balance piston cavity, LOX passes into the bearing cavity, through the low-pressure orifice formed by the impeller hubs, and silver-plated inner diameter of the low-pressure ring. From the bearing cavity, the LOX is returned to the eye of the impeller through a cast passage in the pump housing.

The performance characteristics of the balance piston are shown in Fig. 4-20. The total travel from the position where the high-pressure orifice is axially aligned to the position where the low-pressure orifice is aligned, is established at 0.0254 cm (0.010 inch). The net pressure force on the balance piston as function of axial position between the two orifices, is indicated by the ordinate. The difference between the heads at the extreme positions reflects

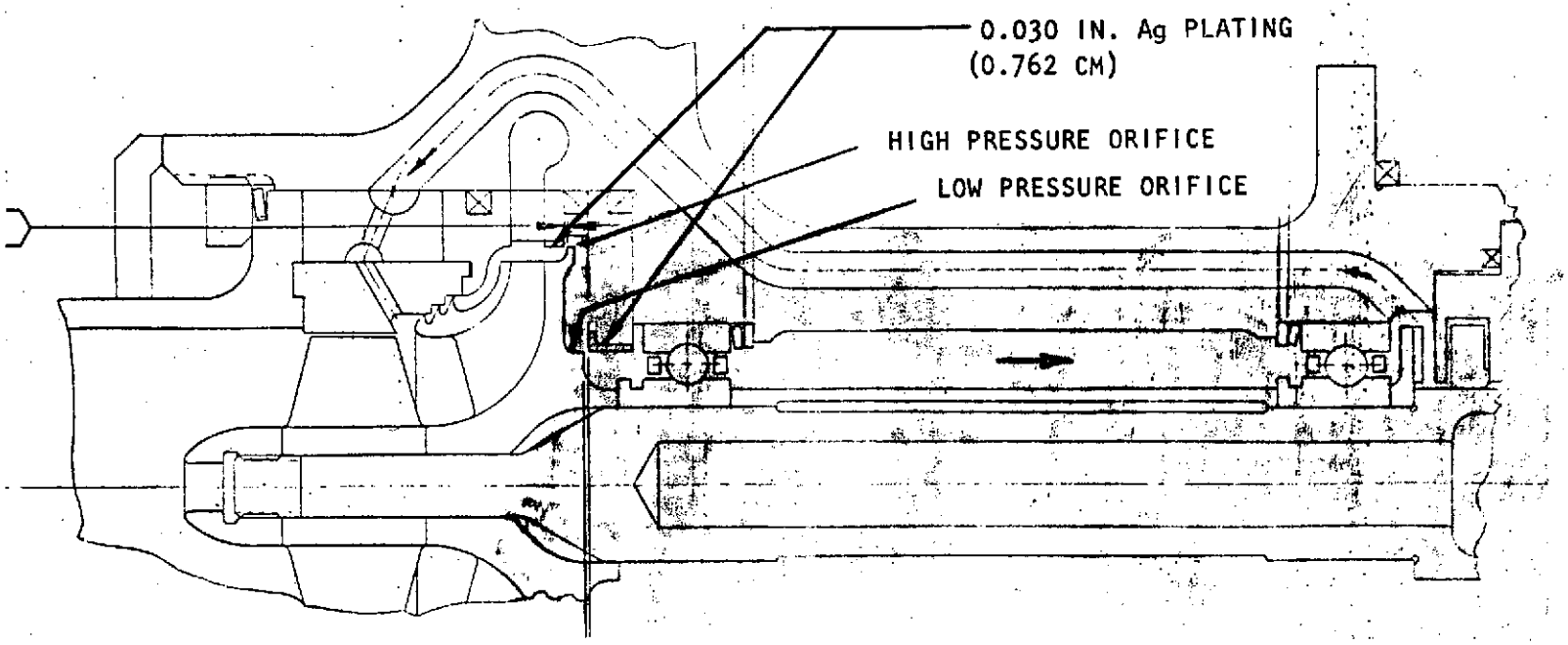

Figure 4-19. Axial Force Balance Piston

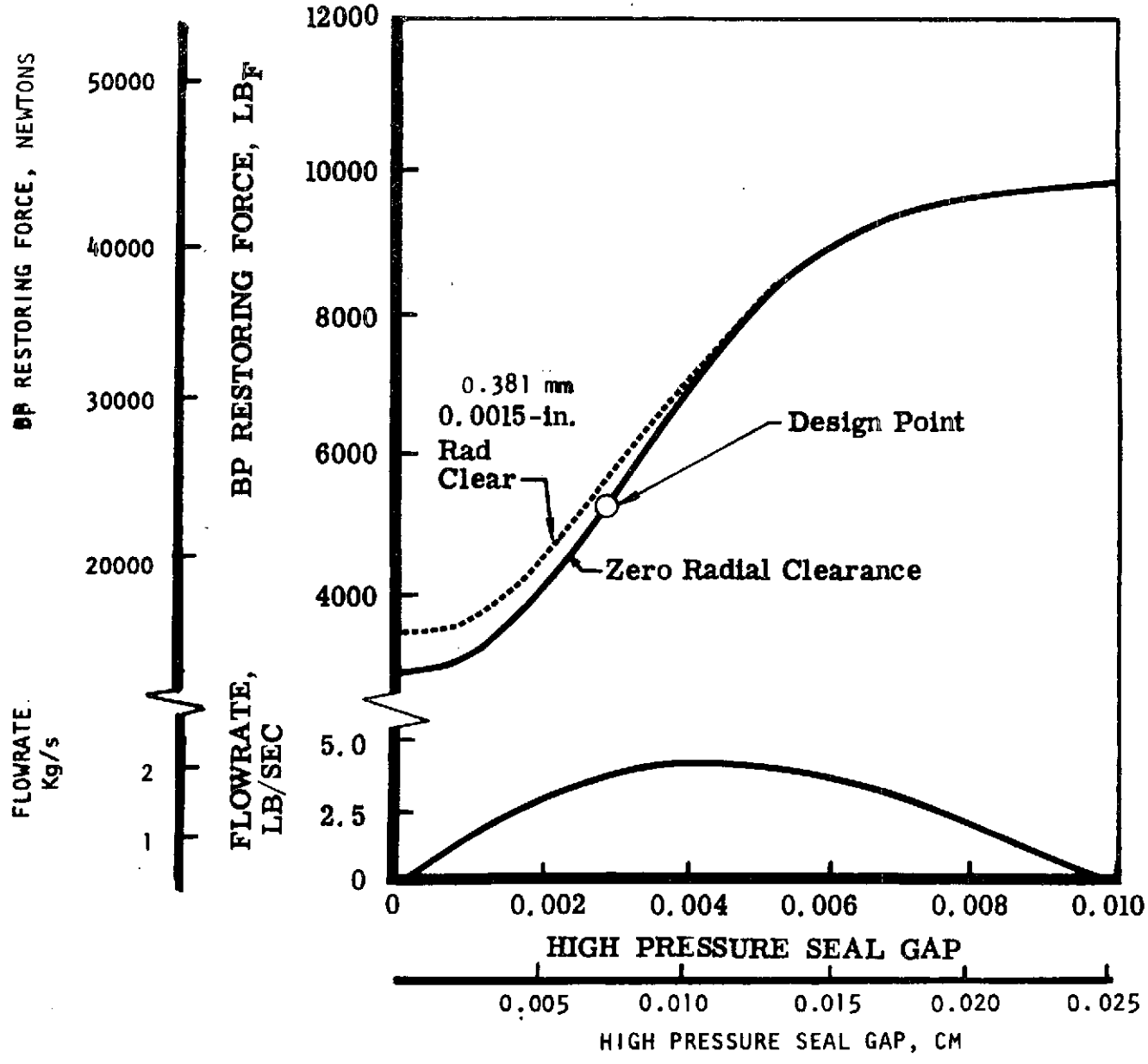

Figure 4-20. ASE High-Pressure LOX Turbopump Balance Piston Performance

the load margin of the piston, i.e., the change in residual rotor thrust which the piston can balance. The range shown is equal to approximately 70 percent of the sum of the pressure forces on the rotor in one direction, and thus represents a very large margin.

Because metal-to-metal rubbing presents an explosion hazard in liquid oxygen, a balance piston design in which the surfaces forming the orifices can bottom and rub heavily on each other is unacceptable. In the proposed design, the flow is restricted by maintaining a small radial clearance between the rotating and stationary members when the two members are axially aligned. Hazardous radial rubbing is avoided by adding 0.0762 cm (0.030 inch) silver plating to the inner diameter of the stationary part.

BEARINGS

Two angular contact type 20-mm ball bearings are used to support the rotor. The bearings are preloaded with Belleville springs axially to prevent ball skidding and to take up the internal radial clearance. The Belleville springs are shimmed so that the bearings will carry the rotor axial thrust during transient start and shutdown phase, when speeds and pressures are below the level required for effective balance piston functioning. During steady-state operation, the axial load on the bearings is only that provided by the preload springs.

The design of the bearings and principal parameters are shown in Fig. 4-21. At the design speed of 8168 rad/s (78,000 rpm), the DN value is 1.6 million which is realistic in light of recent bearing test history on the APS pump and other programs.

The races and balls will be made from consumable electrode vacuum melt 440-C stainless steel. The cage is one-piece Armalon, with no external reinforcement. The quality of Armalon will be controlled by Rocketdyne specification RB0130-013 to ensure satisfactory properties.

The static axial load capacity of the bearings is 7117 N (1600 pounds). A preload of 1165 N (262 pounds) will be applied by the Belleville springs. The calculated B-10 life at that load is 250 hours.

Bearing lubrication is accomplished with the balance piston fluid, i.e., liquid oxygen from the impeller discharge is bled off and passed through the high- and low-pressure orifices into the bearing cavity. After passing through both bearings, the fluid is returned through a cast passage in the housing to the impeller inlet.

SHAFT SEALS

To preclude mixing liquid oxygen from the pump with GH_2 from the turbine, the two regions are separated by three seal assemblies as shown in Fig. 4-22.

All three seals are of the controlled gap type, with two seal rings in each. The controlled gap concept was selected for this application primarily because

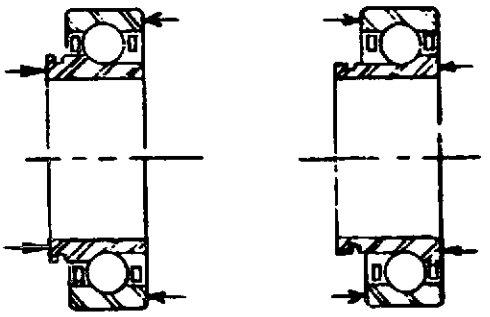

TYPE	ANGULAR CONTACT
BORE, MM	20
DN	1.6×10^6
PITCH DIAMETER, INCHES	1.22 (3.10 cm)
BALL DIAMETER, INCHES	0.21875 (0.5556 cm)
NUMBER OF BALLS	11
RACE AND BALL MATERIAL	440-C
CAGE MATERIAL	ARMALON
AXIAL STATIC CAPACITY	1600 (7117 N)
AXIAL LOAD, POUNDS	262 (1165 N)
B_{10} FATIGUE LIFE, HOURS	250

Figure 4-21. ASE High-Pressure LOX Turbopump Bearing Design Parameters

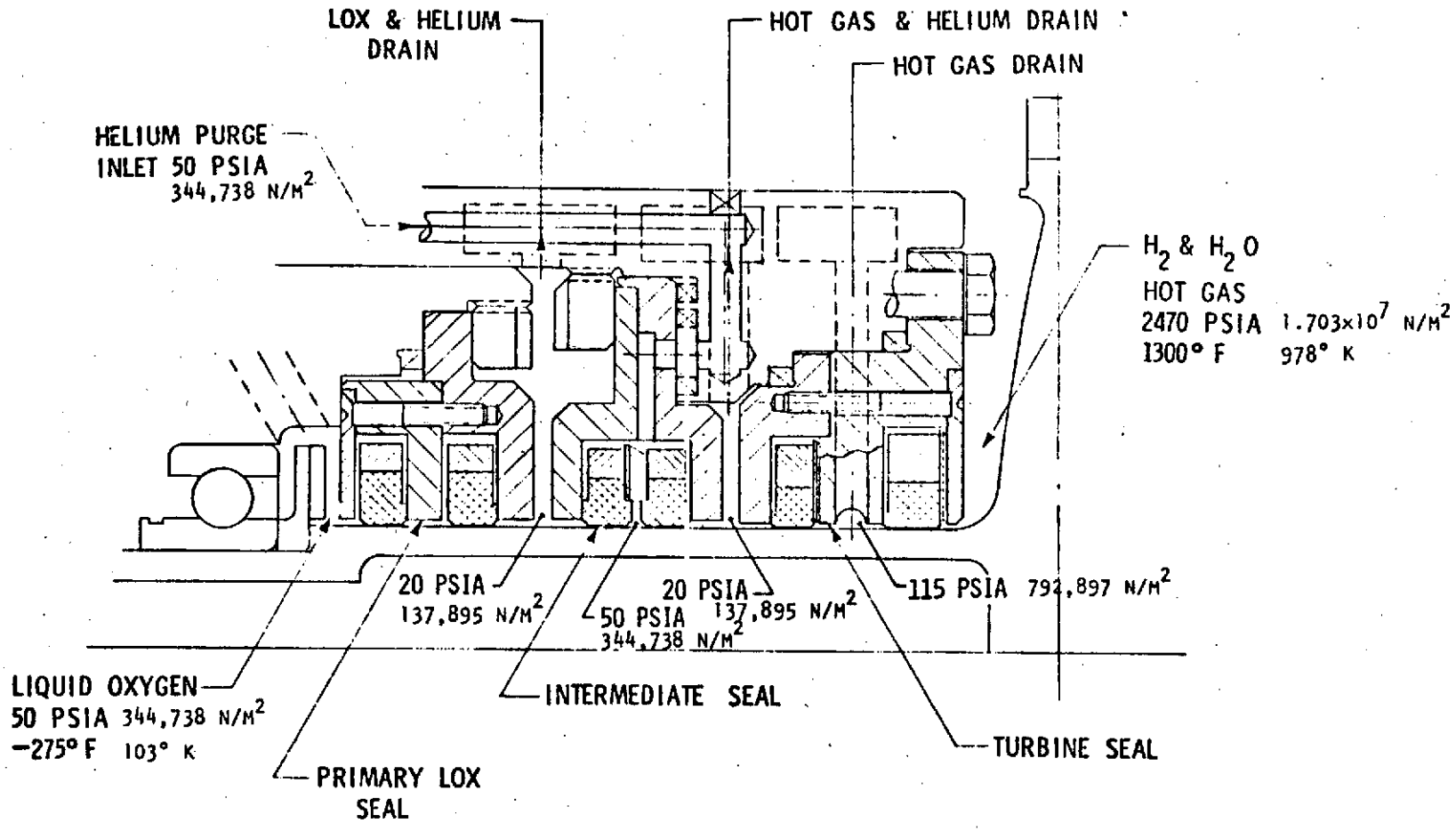

Figure 4-22. ASE High-Pressure Oxidizer Turbopump Seals

it has low drag torque, a "must" for idle mode starts. This concept also minimizes power absorption during steady-state operation and permits very long service life.

Pump fluid will be contained by the primary LOX seal. The small amount of oxygen which flows past this seal will be drained overboard from the cavity formed by the primary and intermediate seals. A slinger containing pumping ribs is included upstream of the primary LOX seal to reduce the pressure to a level which will vaporize the fluid. With this technique, the mass flowrate through the seal is greatly reduced. The concept was used on the APS liquid oxygen turbopump with excellent results.

On the turbine side, because of the high pressures involved, sealing and drainage is accomplished in two steps: an overboard drain is included downstream of the first segment which reduces the pressure between the two segments to 792,897 N/m^2 (115 psia); the small amount of GH_2 which leaks past the second ring is also drained overboard.

To provide absolute separation of the pump and turbine fluids, an intermediate seal is incorporated between the two drain areas with a GHe purge which maintains the cavity between the two rings at 344,738 N/m^2 (50 psia). Thus, before LOX or GHe can leak across the intermediate gear, it has to overcome this 344,738 N/m^2 (50 psia) barrier.

The materials selected for the seal components are noted in Table 4-9. A diametral clearance of 5.08 mm (0.002 inch) is specified between the sealing rings and the shaft.

TABLE 4-9. ASE HIGH-PRESSURE LOX TURBOPUMP SHAFT SEAL DATA

Seal	Housing Material	Seal Ring Material	Retaining Ring Material	Shaft Material	Shaft Surface Treatment	Diameter Clearance, inches
Primary LOX	INCO X-750	P 692 Carbon	Astroloy	Astroloy	CR Plate	0.002 (0.00508 cm)
Intermediate	INCO X-750	G 84 Carbon	Astroloy	Astroloy	CR Plate	0.002 (0.00508 cm)
Turbine	INCO X-750	701-65 Amcermet	Astroloy	Astroloy	Tungsten Carbide	0.002 (0.00508 cm)

CRITICAL SPEED ANALYSIS

The rotordynamic characteristics of the high-pressure oxidizer turbopump are shown in Fig.4-23 . Calculated critical speeds are plotted versus the front bearing radial stiffness, and the effect of rear bearing radial stiffness is indicated by parametric curves. With the projected spring rates, the first

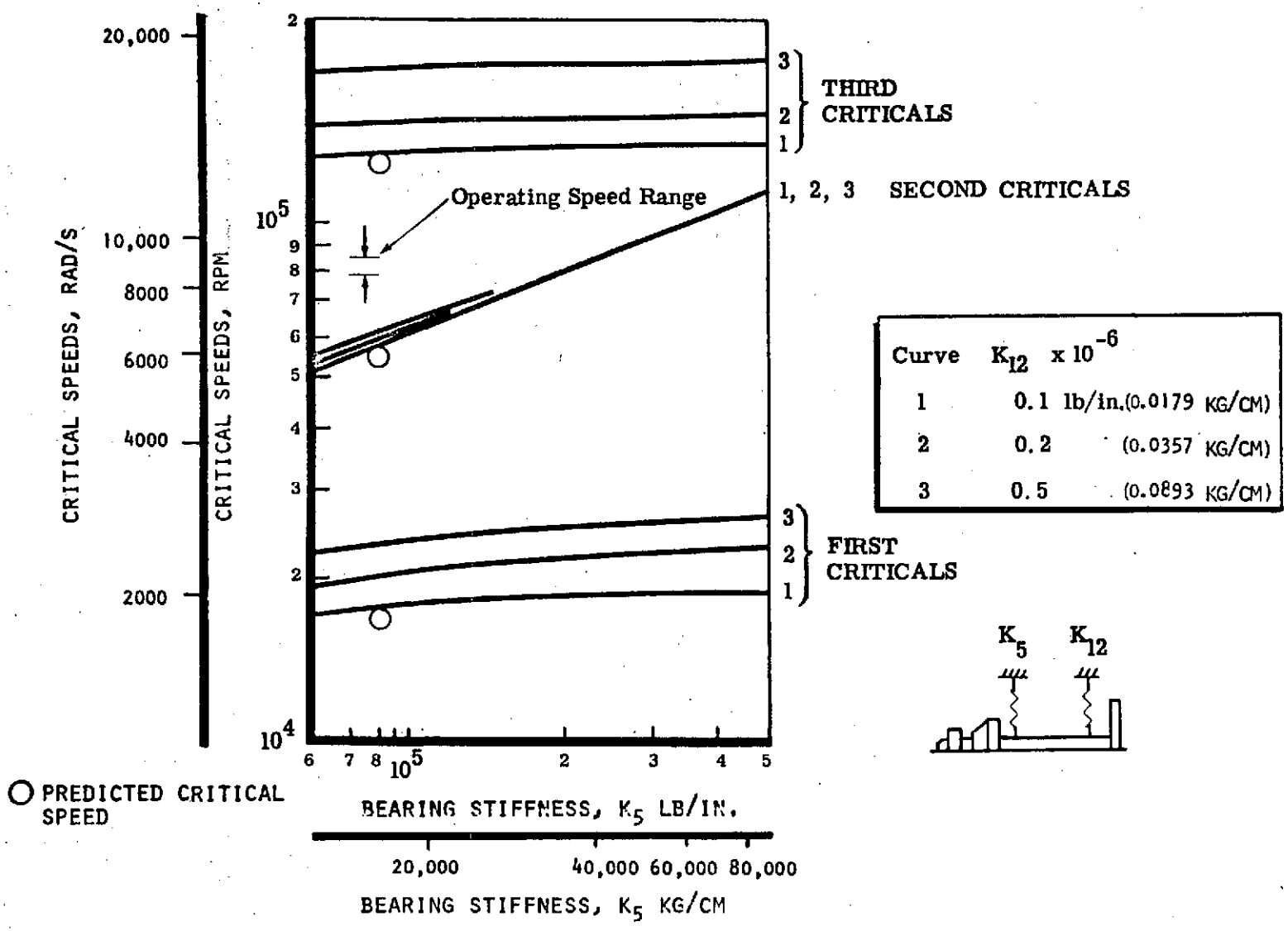

Figure 4-23. ASE High-Pressure LOX Turbopump Rotor Critical Speeds

critical speed is at approximately 1780 rad/s (17,000 rpm), the second critical at 5760 rad/s (55,000 rpm), and the third, or bending mode, critical is at 14,137 rad/s (135,000 rpm).

The operating range of the turbopump is free of critical speeds, by substantially more margin than the 25 percent stipulated in the Statement of Work.

MATERIAL SELECTION AND STRESS ANALYSIS

The materials selected for the low-pressure oxidizer turbopump have extensive background in similar turbopump applications. The pump housing will be cast from INCO 718, which has excellent cryogenic properties and good casting quality. For the same reason, INCO 718 was also selected for the impeller casting material. The inducer will be machined from K-Monel forging, because of its strength properties and because K-Monel has demonstrated excellent qualities of resisting explosion in LOX due to rubbing or foreign object damage. The seal carrier-manifold assembly will be a welded composite with the seal carrier being fabricated from Haynes 188 and the manifold from Rene' 41. Rene' 41 was selected for the manifold because of its superior strength qualities at the high turbine inlet temperature.

The nozzle flow passages will be formed by electrical discharge machining, and the nozzle ring will be welded to the manifold.

Rocketdyne has extensive experience in welding Rene' 41 on larger and more complex parts, which will be applicable to the fabrication of the oxidizer manifold. To preclude degradation of Rene' 41 material properties from high-pressure hydrogen environment, copper plating will be applied to areas which are subject to plastic strain.

The turbine disk and shaft will be forged from Astroloy and friction welded. Before welding of the actual parts is attempted, Astroloy samples will be friction welded to work out proper sequence and technique. If the weld samples indicate that a consistently sound weld is difficult to obtain, the center hole in the shaft will be deleted and the shaft and disk will be machined from an integral forging.

The turbine disk hub thickness has been established at 16.51 mm (0.650 inch). The calculated short-time burst speed is 13,509 rad/s (129,000 rpm), and the long-time burst speed is 10,786 rad/s (103,000 rpm). Based on 1089 K (1500 F) wheel average temperature, a 20 percent margin on burst speed is maintained. A 20 percent burst speed margin has also been included in the impeller design.

HIGH-PRESSURE FUEL TURBOPUMP

CONFIGURATION SELECTION AND PERFORMANCE

To increase the calibration margin of the engine, the fluid-dynamic design point of the high-pressure fuel turbopump was established at 6.5 engine mixture ratio. At that engine balance point, the turbopump is required to deliver 2.567 kg/s (5.66 lb/sec) of liquid hydrogen, raising the pressure from 462,845 N/m^2 (67.13 psia) to 3.085 x 10^7 N/m^2 (4475 psia). Maximum power condition occurs at 5.5 engine mixture ratio, which imposes a pump discharge pressure requirement of 3.296 x 10^7 N/m^2 (4780 psia) with a nominal engine. To include margin to handle engine-to-engine variation at 5.5 mixture ratio, this discharge pressure requirement is further increased to a maximum of 3.836 x 10^7 N/m^2 (5560 psia). Thus, the design of the high-pressure fuel turbopump was performed to achieve a best efficient point at 6.5 mixture ratio, but with structural capability to operate at 5.5 mixture ratio with a 2σ engine.

In establishing the configuration of the high-pressure fuel turbopump, the most important decision to be made was relative to the number of stages to be employed in the pump. Potentially applicable configurations were: two-stage pump, either with series or back-to-back impellers, and three-stage pump with series impeller arrangement.

To compare the configurations on an equal basis, it was assumed that engine P_c and shaft speed were constant. Pump discharge pressure was also maintained fixed and it was assumed that with the less efficient pump the turbine inlet temperature was increased to make up the additional power requirement.

In Table 4-10, the pertinent criteria are compared. The factors which carried the most weight in the decision were: atainable pump efficiency, impeller tip speed, required turbine temperature.

The attainable pump efficiency is a function of the stage specific speed. Because of low pump flowrate and high head requirement, the specific speed with all three configurations evaluated is substantially below the optimum level for centrifugal pumps 0.732, nondimensional ($\approx$2000). With the three-stage pump, a higher stage specific speed is realized because the head produced per stage is smaller. As a result, the stage efficiency of the three-stage configuration is higher (65 versus 56 percent).

To make up for the lower efficiency of the two-stage pump in the engine balance, the turbine inlet temperature would have to be increased from 1044 K to 1167 K (1880 to 2100 R), and calibration margin would have to be sacrificed or, if the turbine temperature were maintained constant, the thrust chamber pressure would have to be lowered approximately 275,903 N/m^2 (400 psia).

Although not evaluated in Table 4-10, the back-to-back configuration is subject to a further performance degradation relative to the other two when overall pump efficiency is computed, because it requires a separate balance piston to control axial thrust, which adds to internal recirculation losses.

TABLE 4-10. ASE HIGH-PRESSURE FUEL PUMP CONFIGURATION SELECTION CRITERIA

P_c = 2200 psi (1.517×10^7 N/m^2); N = 88,270 rpm (9244 rad/s)

Number of Stages	2	2	3
Configuration	Series	Back to back	Series
Impeller Type	Shrouded	Shrouded	Shrouded
Head Rise$_{Nom}$ (6.5 MR), feet (m)	133,000 (40,540)	133,000 (40,540)	133,000 (40,540)
U_{Nom} (6.5 MR), fps (m/s)	2020 (615.7)	2020 (615.7)	1640 (499.89)
U_{Max} (5.5 MR and 2σ + margin), fps (m/s)	2280 (694.94)	2280 (694.94)	1865 (568.41)
Stage Specific Speed (6.5 MR)	501	501	660
Stage, percent	56	56	65
Balance Piston	Integral	Separate	Integral
Impeller (OD), inches (cm)	5.23 (13.28)	5.23 (13.28)	4.25 (10.80)
Impeller Tip Width, inch (cm)	0.073 (0.185)	0.073 (0.185)	0.093 (0.236)
Impeller Fabrication (diameter over tip width ratio)	71.7	71.7	45.7
Crossover Type	Internal	External	Internal
Diffuser Velocity Ratio	5.65	5.65	4.43
Turbine Temperature (5.5 MR), R (K)	2100 (1167)	2100 (1167)	1880 (1044)

The tip speed of the impeller is set by the head coefficient and the head to be produced per stage. Since head coefficient values are the same for the three configurations, and the head developed per stage in the three-stage pump is smaller (two-thirds), the required tip speed is correspondingly lower. The comparative values shown in Table 4-10 for maximum discharge pressure, are 79.3 m/s (2280 fps) for two stage and 64.9 m/s (1865 fps) for the three stage.

As explained later, low pump flowrates and attendant small impeller blade height necessitate using shrouded impellers. Although tip speeds up to 96.7 m/s (2780 fps) have been achieved with shrouded impellers, this was accomplished with diffusion-bonded titanium impellers fabricated under laboratory conditions at very high expense. To keep cost and procurement lead time within line, the impeller would have to be cast. The maximum two-stage tip speed of 79.3 m/s (2280 fps) is approaching the practical limit for a cast, shrouded-titanium impeller. In this region, even a small increase in tip speed necessitates a substantial increase in hub length, to carry the centrifugal loads. It was projected that as a result, the overall length of the two- and three-stage series configurations would be approximately the same, and the back-to-back two-stage pump would be longer because of the separate balance piston feature. Since the diameter of the three-stage pump would be smaller, it was concluded that the three-stage pump would have the smallest envelope and also the lowest weight.

The number of component parts in the three-stage pump is higher by one crossover and one impeller and, therefore, it is slightly more complex and more expensive. Because the impeller diamter-to-tip-width ratio is smaller, the three-stage impeller is easier to cast.

In summary, although slightly more complex and more costly, the three-stage pump offers better efficiency and, therefore, lower turbine temperature or higher P_c. It is more conservative on tip speed, easier to fabricate, and its envelope and weight are smaller. It was concluded that the three-stage pump configuration had more advantages for this engine application and, therefore, was selected for preliminary design.

With the general type of the pump established, alternatives for detail configuration were evaluated.

Pump Inlet Orientation

The location of the pump inlet at the opposite end from the turbine, as opposed to locating it between the pump and turbine, was based primarily on the liquid hydrogen pressure level which has to be maintained on the pump side of the shaft dynamic seal to prevent ingress of turbine gases into the pump. Since the pressure on the turbine side of the seal is 1.696×10^7 N/m^2 (2460 psia) it is desirable to maintain the pressure on the pump side at approximately 2.068×10^7 N/m^2 (3000 psia). Therefore, it is advantageous to have the pump features with the highest pressure level, i.e., the last-stage impeller adjacent to the turbine.

The radial entry volute-type inlet configuration of the pump was selected to optimize engine packaging and to provide prewhirl at the first-stage impeller inlet. It is anticipated that the low-pressure pump will have a scroll-shaped volute with a radial discharge and that the high-pressure fuel turbopump will be mounted to the engine with pump inlet side down. Under those conditions, the fluid is transferred from the low-pressure pump to the high-pressure pump most efficiently, both from the standpoint of fluid friction and engine weight with a radial inlet on the high-pressure pump.

A volute-type inlet is used to provide prewhirl at the first-stage impeller inlet. The impeller inlet prewhirl permits a larger impeller discharge blade angle for reduced stress as well as a reduced inlet relative velocity for increased impeller efficiency. The volute-type inlet provides low losses, permits the bearings to be located outboard of the impeller inlet and results in engine installation flexibility.

Impeller Type

The use of shrouded versus open-face impellers was evaluated. Open-face impellers are easier to fabricate and are capable of higher tip speeds. However, the combination of high speeds and low flowrates results in very low impeller blade heights in this turbopump. As a result, the clearance between the impelelr vanes and housing would have to be held impractically close to maintain high performance. Furthermore, small changes in the axial position of the rotor would bring about large shifts in pump performance. In contrast, with a shrouded impeller, there is no need to hold the axial clearance close, and performance is independent of rotor position. Despite the fact that the impeller hub length has to be increased to carry the shroud centrifugal loads and fabrication is more difficult, performance considerations dictate that shrouds be used. An important side benefit of adding shrouds is that the stiffness of the impeller is increased which, in turn, reduces the relative deflection in the balance piston. This is of particular significance because of the high-pressure loads involved.

Diffuser Type

The use of radial vaned diffusers, as opposed to an open volute with one or two tongues, was evaluated. The radial vane configuration was selected for three reasons. By reducing the velocity of the fluid in the volute to approximately half of the impeller discharge velocity, fluid friction losses, which are proportional to velocity squared, are reduced. The pressure gradient around the periphery of the impeller will be less with a vaned diffuser; therefore, the radial loads will be smaller. Finally, the diffuser vanes provide an efficient tie for the pressure vessel formed by the volute walls and, thereby, reduce the housing wall thickness requirement.

Turbine Orientation

The direction of turbine propellant flowrate is somewhat arbitrary. Rotor axial thrust can be balanced and engine packaging can be accommodated whether the flow is toward or away from the pump. However, with a three-stage pump, the liquid hydrogen pressure level at the shaft seal is between the turbine

inlet and exhaust pressures and, thus, if the turbine exhaust is on the pump side, the seal leakage flow is in the proper direction, i.e., toward the turbine. In contrast, if the turbine inlet is on the pump side, the seal pressure has to be raised artifically. For this reason, the turbine was oriented with the exhaust on the pump side.

Pump Performance

The predicted performance of the pump, shown in Fig. 4-24, is based on Rocketdyne's computer program for prediction of stage performance when pumping an incompressible fluid and a second computer program which includes the influence of hydrogen properties to evaluate the effect of leakage flowrates upon fluid density and upon impeller enthalpy changes. Pump fluid flow passages will be designed to ensure pressure gradients that will produce efficient diffusion and freedom from flow separation. Flow analyses will be conducted by procedures developed at Rocketdyne which have resulted in efficient rocket engine pump designs. The principal pump parameters are presented in Table 4-11. In Fig. 4-25, the calculated internal pressures and temperatures are shown.

Turbine Performance

In designing the turbine, certain factors exert great influence on the type of turbine adopted. These factors are:

1. Desired efficiency level
2. Reliability
3. Maximum load capability
4. Variable load characteristics
5. Ease of manufacturing

These considerations affect the final design configuration with respect to physical dimensions, type of turbine, and blade stress and vibrations. The projected application for the 88,964 N (20K) engine turbine places a premium on turbine performance; therefore, an efficiency increase at moderate weight penalty becomes economical. This, combined with the very high energy level of the working fluid, justifies the use of a multistage turbine with relatively high blade speed.

The internal efficiency of a turbine is the ratio of the actual power produced to the theoretical power available in an isentropic expansion from the total pressure and temperature at the inlet of the turbine to the static pressure at its exhaust. For the turbine under consideration, the shaft horsepower is the only useful output; the residual kinetic energy is unavoidable. The major factors that affect the performance are:

1. Isentropic velocity ratio
2. Stage reaction

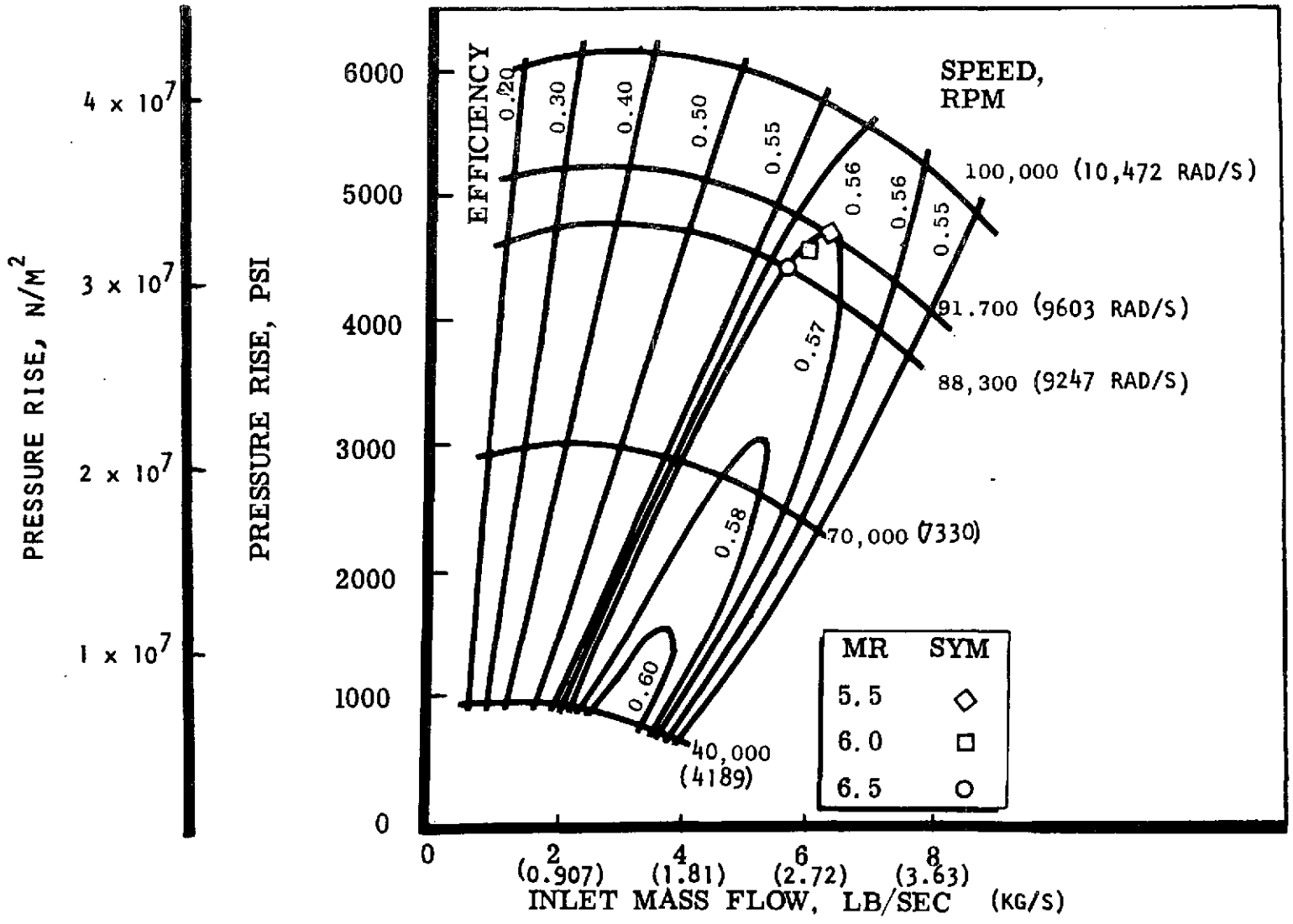

Figure 4-24. ASE High-Pressure Fuel Pump Predicted Performance

TABLE 4-11. ASE HIGH-PRESSURE FUEL TURBOPUMP DESIGN PARAMETERS (MR = 6.5)

- Pump
  - System Requirements

P_S, psia (N/m^2)	62.13 (428,371)
P_D, psia (N/m^2)	4475 (3.085×10^7)
$\dot{W}$, lb/sec (kg/s)	5.66 (2.567)

  - Design Parameters

Type	Three-Stage Centrifugal
N, rpm (rad/s)	88,270 (9244)
U_{Tip}, fps (m/s)	1640 (57.07)
$\phi_{Discharge}$	0.10
$\psi_{Stagnation}$	0.60
η, percent	57
Impeller Inlet Hub Diameter, inch (cm)	0.950 (2.41)
Impeller Inlet Tip Diameter, inches (cm)	1.810 (4.60)
Impeller Tip Diameter, inches (cm)	4.250 (10.800)
Impeller Blade Angle at Inlet (rms), degrees	14.9
Impeller Blade Angle at Discharge, degrees	45
Stage Specific Speed	620
Number of Blades at Impeller Inlet	5
Number of Blades at Impeller Discharge	10
Number of Diffuser vanes	13

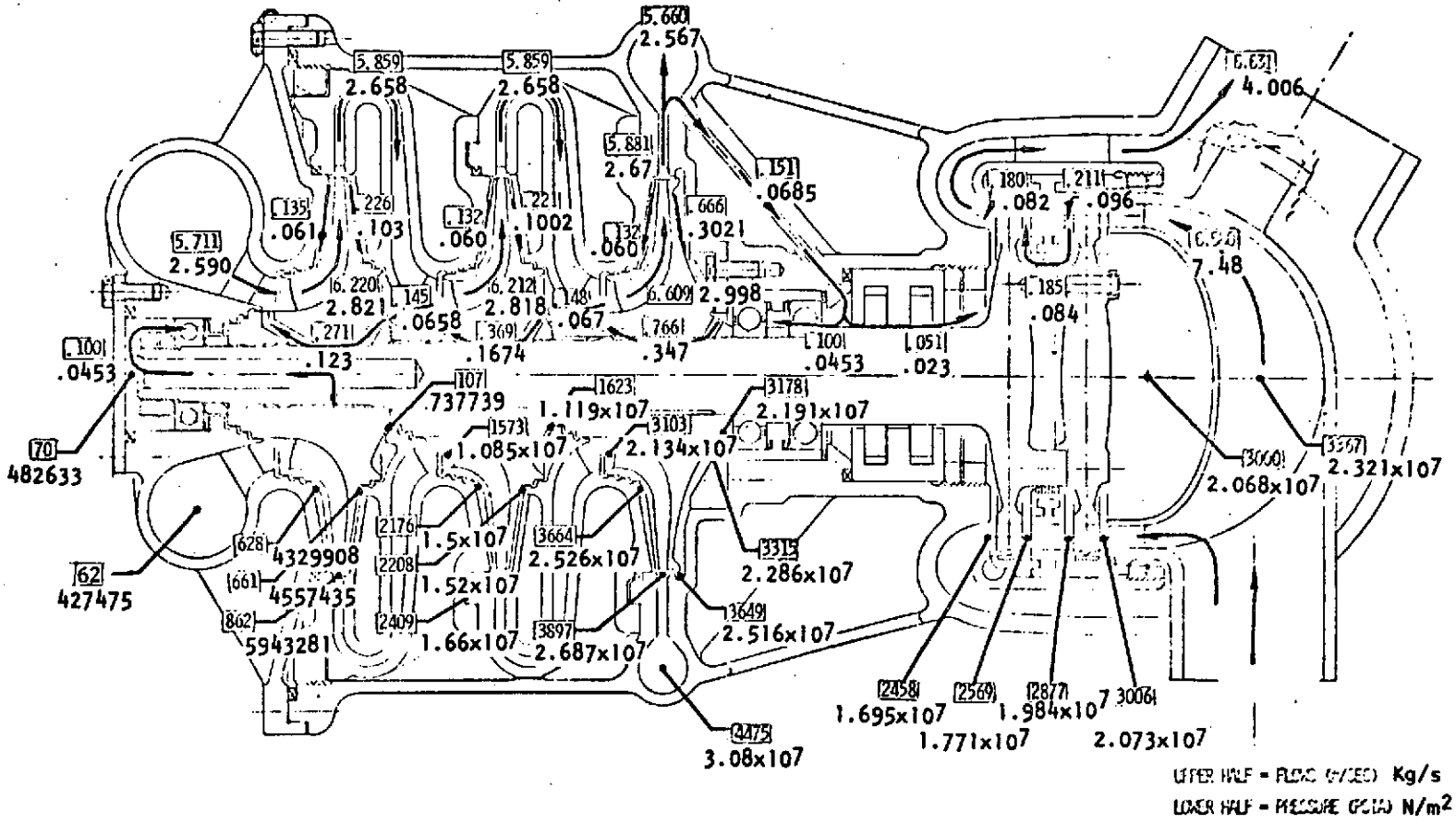

Figure 4-25. ASE High-Pressure Fuel Turbopump Internal Flows and Pressures

3. Leakage losses
4. Pressure ratio
5. Parasitic losses

The first factor may be considered as the single most important affecting the performance level of a stage and, in general, dictates the number of stages.

The aerothermodynamic design procedure employs the equation of continuity together with reasonable and consistent values of expansion and kinetic energy coefficients for nozzle blades, two-dimensional friction, and incidence losses. Results of the element-by-element calculations can be expressed in terms of diagram efficiency as a function of the isentropic velocity ratio. Diagram efficiencies are basically two dimensional in that they include only profile, incidence, surface friction, and wake losses. An actual turbine stage has certain additional losses which are:

1. End losses (annulus wall boundary layer and leakage)
2. Interstage seal leakage and leakage interference
3. Parasitic friction losses

End losses are primarily a function of nozzle and rotor blade height, configuration (shrouded or open-ended blades) operating tip clearances, and amount of reaction. Short nozzles contribute strongly to increased end losses.

A commonly used tool for presenting turbine performance is a diagram which shows the turbine stage efficiency as a function of the ratio of wheel tip speed to gas spouting velocity (U/C_o). The diagram is shown in Fig. 4-26. The design velocity ratio of $U/C_o = 0.485$ results in a turbine efficiency of 80 percent. For optimum performance, 28 percent of reaction was employed. The turbine efficiency is also influenced by two additional criteria--Reynolds number (Re) and Mach number (M). Usually, it can be said that the Reynolds number becomes an important criterion for the turbine efficiency only if the Reynolds number is lower than 2×10^5. It will be found that for the subject turbine, $Re > 2 \times 10^5$ so that, in this proposal, the Reynolds number is not significant.

The Mach number is mainly a criterion for the rotor blade design since it is a fact that the nozzle design point efficiency is independent of the Mach number. Generally, subsonic rotor blades can be equipped with blunt leading edges without ill effect on performance. The turbine operates in the subsonic region and leading edges are employed for long life and optimum off-design performance. The data used for the turbine performance analysis are based on average loss coefficients (selected after an exhaustive study of the available experimental and analytical data) which usually are obtained in good aerodynamic design practice. It is of equal importance to note that the efficiencies quoted are based on a certain amount of clearance between rotor tip and shroud. It is assumed that the radial clearances of the turbine tip are 2 percent of the blade height. Likewise, the ratio of trailing edge thickness to blade spacing is an important criterion for the turbine

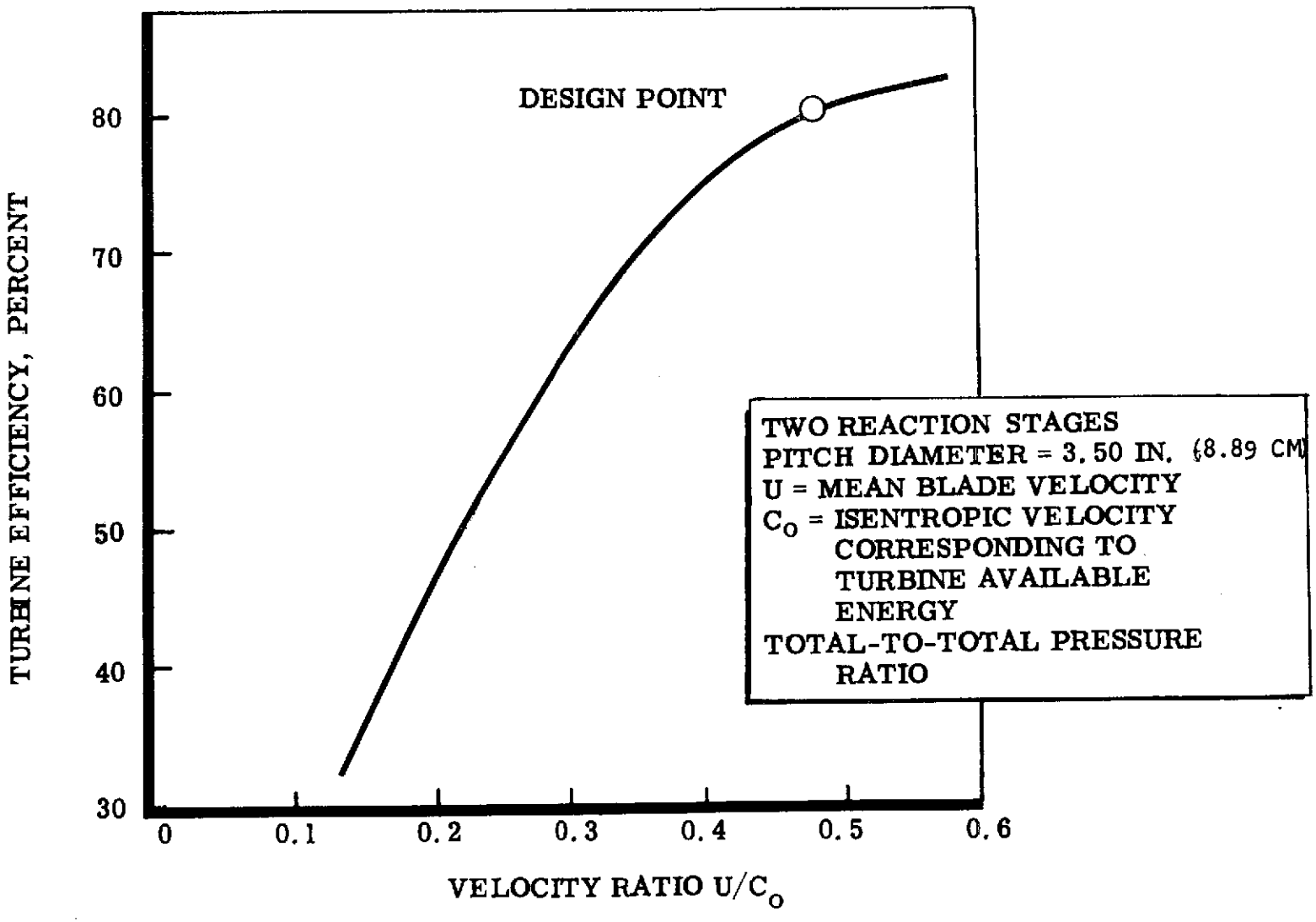

Figure 4-26. ASE High-Pressure Fuel Turbine

efficiency. The efficiencies quoted are the total-to-total efficiencies and the reference pressures for the turbine stage are the total inlet pressure and total exit pressure. Blading performance is affected to a large extent by the aerodynamic loading on the profiles. The resultant force acting on a profile corresponds to the integrated pressure differences between the convex and concave surfaces. In closely pitched blades, these differences and their accompanying turbulence losses are reduced. However, losses due to surface friction are thereby increased. Wide pitching decreases surface friction loss, but aerodynamic loading is increased. This may induce stalling with a rapid drop in performance.

Aerodynamic loading is a function of the cascade solidity or chord/pitch ratio. The permissible ranges of blading solidity for standard profiles have been fairly accurately established by test.

The determination of the correct flow access is the most important step in the design of an efficient turbine. If these flow curves are wrong, the pressure downstream of the blade rows will differ from those used in the velocity diagram. This will cause the approach velocities of the following blade row to have fluid angles that deviate from the blade angle design and this will reduce the performance of the turbine.

The turbine parameters selected as a result of the analysis are presented in Table 4-12.

DESIGN DESCRIPTION

The selected turbopump design, shown in Fig. 4-27, consists of a three-stage centrifugal pump of series impeller arrangement, powered by a two-stage full-admission axial-flow reaction turbine. The pump design features of series impellers and integral balance piston lend themselves to a well-integrated design with a minimum number of parts and fewest external joints. The turbopump is a self-sufficient unit, which requires no externally supplied lubricants, heaters, purges, or drains.

The external housings consist of three major parts: the inlet, which supports the front bearing and provides axial retention for the crossover; the housing, which serves as the major pressure vessel and incorporates the pump volute, bearing and seal supports, and the turbine nozzle and stator supports; and, finally, the turbine manifold through which turbine hot gas is introduced and discharged, and which is in-place welded to the housing at assembly.

Liquid hydrogen is introduced to the pump through a scroll-shaped radial inlet which imparts prewhirl to the fluid. From the inlet, the liquid hydrogen enters the first-stage impeller which is fully shrouded with backwardly curved blades with a discharge angle of 45 degrees. Fully shrouded impellers are used to minimize the sensitivity of impeller axial position upon efficiency and axial rotor force. Backwardly curved impeller blades and inlet prewhirl are used to obtain a stable operating characteristic with wide flow range capability and maximum efficiency. The number of impeller blades (five partial and five full) is selected to provide minimum slip and, therefore,

TABLE 4-12. ASE HIGH-PRESSURE FUEL TURBOPUMP DESIGN PARAMETERS (MR = 6.5)

- Pump
  - System Constraints

Fluid	Preburner Hot Gas ($H_2 + H_2O$)
T_{t_1}, R (K)	1896 (1309)
P_{t_1}, psia (N/m^2)	3367 (2.321×10^7)
P_{t_2}, psia (N/m^2)	2462 (1.697×10^7)

  - Design Parameters

Type	Two-stage, pressure componded
N, rpm (rad/s)	88,270 (9243)
bhp (watts)	2340 (1,744,938)
ϵ, percent	100
D_m, inches (cm)	3.5 (8.89)
U_m, fps (m/s)	1350 (46.98)
U/C_o	0.485
η_o t-t, percent	80.0
$\dot{W}$, lb/sec (kg/s)	6.58 (2.985)
Number of First-Stage Nozzle Vanes	41
Number of First-Stage Rotor Blades	69
Number of Second-Stage Nozzle Vanes	39
Number of Second-Stage Rotor Blades	65
First-Stage Nozzle Valve Height, inch (cm)	0.25 (0.635)
First-Stage Rotor Blade Height, inch (cm)	0.25 (0.635)
Second-Stage Nozzle Vane Height, inch (cm)	0.27 (0.686)
Second-Stage Rotor Blade Height, inch (cm)	0.27 (0.686)
Nozzle Inlet Angle, degrees	90
Nozzle Exit Angle, degrees	16
First Rotor Inlet Angle, degrees	38
First Rotor Exit Angle, degrees	25
Second Nozzle Inlet Angle, degrees	85
Second Nozzle Exit Angle, degrees	16
Second Rotor Inlet Angle, degrees	37
Second Rotor Exit Angle, degrees	25

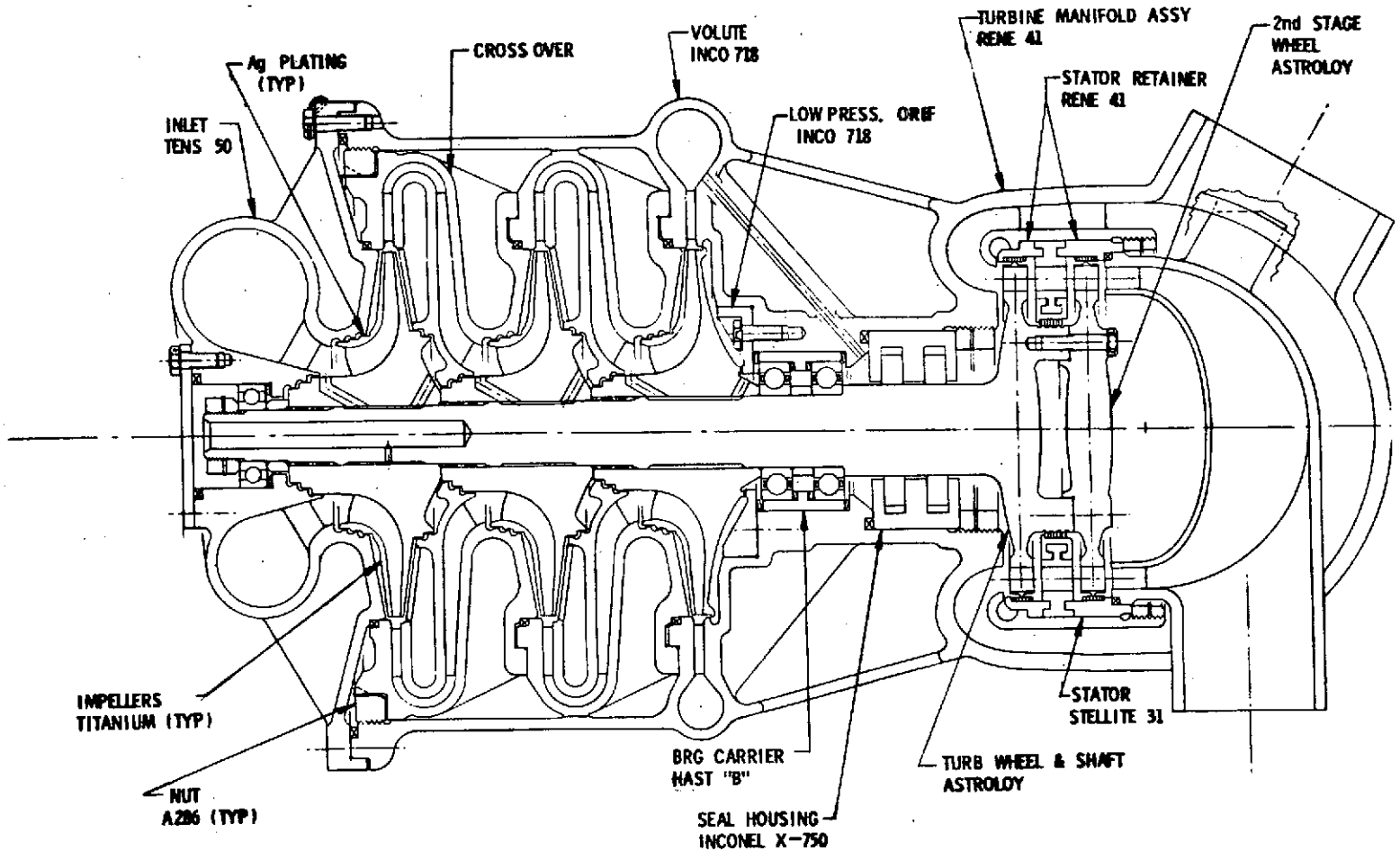

Figure 4-27. ASE High-Pressure Fuel Turbopump

maximum H-Q slope consistent with the selected head coefficient as well as to provide adequate structural support for the shroud.

From the first-stage impeller, the fluid is discharged into a radial diffuser which provides flow matching the crossover vane system and reduces the impeller discharge velocity. It maintains minimum impeller radial forces over a wide flow range. The radial diffuser is followed by a vaneless turning passage which directs the flow radially inward into the vaned crossover passage. This section of the flow path provides the remainder of diffusion required to match the second-stage impeller inlet. It provides prewhirl at the second-stage inlet to minimize the impeller inlet relative velocity for higher impeller efficiency while reducing the amount of diffusion required by the crossover for minimum crossover pressure drop. After the second-stage impeller, the fluid passes through the second crossover and third-stage impeller, which are hydrodynamically identical to the first crossover and other two impellers, respectively.

From the second-stage impeller, the liquid hydrogen enters the second-stage vaned diffuser in which the flow passages will be similar to those of the first-stage diffuser. The vaned diffuser reduces the volute velocity for reduced friction losses and matches the volute over a wide flow range to produce a minimum impeller radial load. The diffuser vane number will be selected for minimum envelope, wide flow range, and to avoid reinforcement of pressure waves at the volute exit generated by the impeller blades passing diffuser vanes. In addition to the advantage they represent from a hydrodynamic standpoint, the second-stage diffuser vanes fulfill an important mechanical function--they provide a structural tie across what would otherwise be a C-shaped pressure vessel at the volute. As a result, tongue stresses and required wall thickness are reduced, realizing a sizable weight saving.

The liquid hydrogen emitting from the second-stage diffuser is collected in a volute and delivered through a single-discharge pipe. As noted above, with the vaned diffuser, pressure gradients around the periphery of the impeller will be maintained at a low level and, as a result, a double discharge with attendant complexity and weight penalty is not required.

Internal recirculation in the pump is controlled by step laybrinth seals located at the impeller front shrouds and at the hubs. To maintain pump performance at a high level, tight laybrinth clearances have to be maintained. To facilitate this, the stationary platforms of the labyrinth seals will be plated with 2.54 mm (0.010-inch) thick silver. With this provision, the clearances will be set to a minimum value needed to assemble the parts and the labyrinth teeth will be allowed to machine their own clearance into the silver. It is estimated that approximately 0.762 mm (0.003-inch) clearance can be maintained on the diameter by this technique.

The torque from the turbine is transmitted through spline joints between the shaft and impellers. All splines are located outside the main impeller hub stress envelopes to preclude spline separation due to radial growth and to avoid introducing stress concentration into the highly stressed section of the impeller. To ensure that positive piloting is maintained under all operating

conditions, and to avoid excessive press fits, the impeller pilots are also located in sections which are not subject to high radial growth.

THRUST BALANCE

The axial thrust of the rotor is absorbed by a self-compensating, double-acting balance piston, which is integral with the third-stage impeller backplate (Fig. 4-28). The balance piston operates between the high-pressure and low-pressure orifices and absorbs the axial loads so the bearings operate with only their controlled preloads.

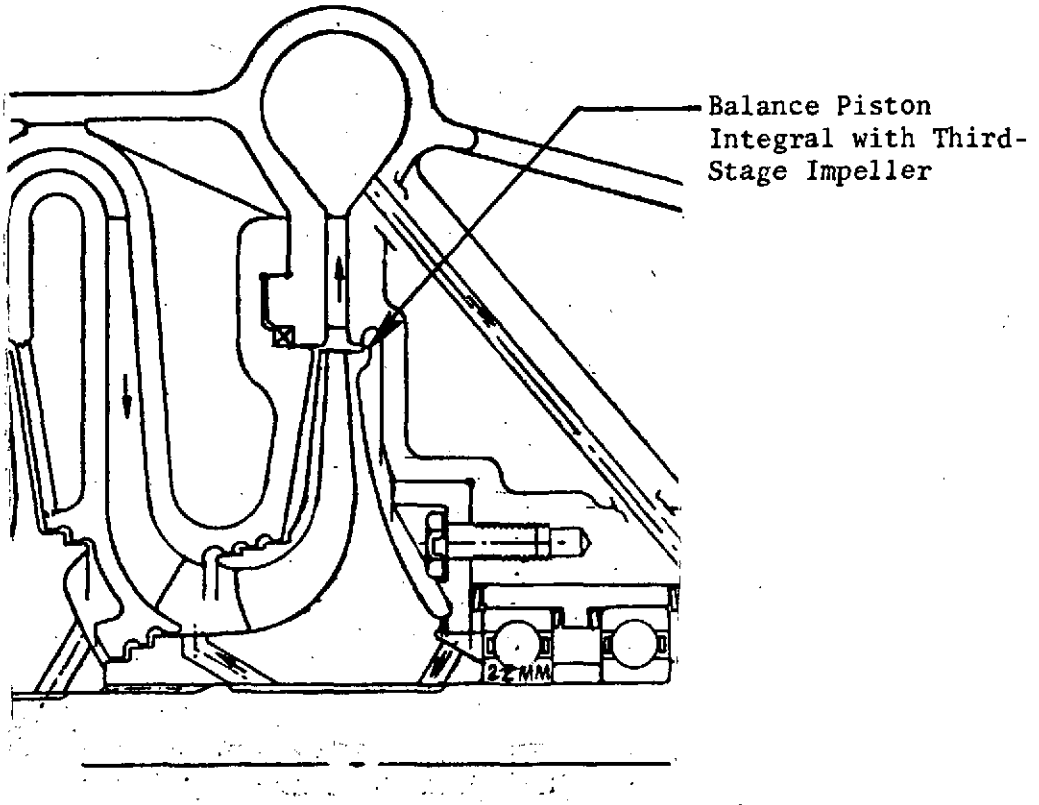

Figure 4-28. Balance Piston

To bring the rotor residual loads within the balancing capability of the piston, wear rings are added to the first- and second-stage impellers and fluid is bled back into the impeller inlets.

To operate the piston, liquid hydrogen is bled from the discharge of the third-stage impeller, passed through a high-pressure orifice located at the impeller tip, then through a low-pressure orifice into the bearing cavity. From there, the balance piston fluid is returned through the hub into the inlet of the second-stage impeller.

The high-pressure orifice element in the impeller overlaps radially the stationary element in the volute housing at all operating conditions. An overlap (Fig. 4-29) is preferred for maximum capability and for sensitivity to axial

movement of the balance piston. The degree of overlap is the result of assembly tolerances, thermal contraction rates, centrifugal effects on the impeller and pressure growth of the volute housing. Preliminary calculations indicate the overlap will be 1.016 mm (0.004 inch) during operation.

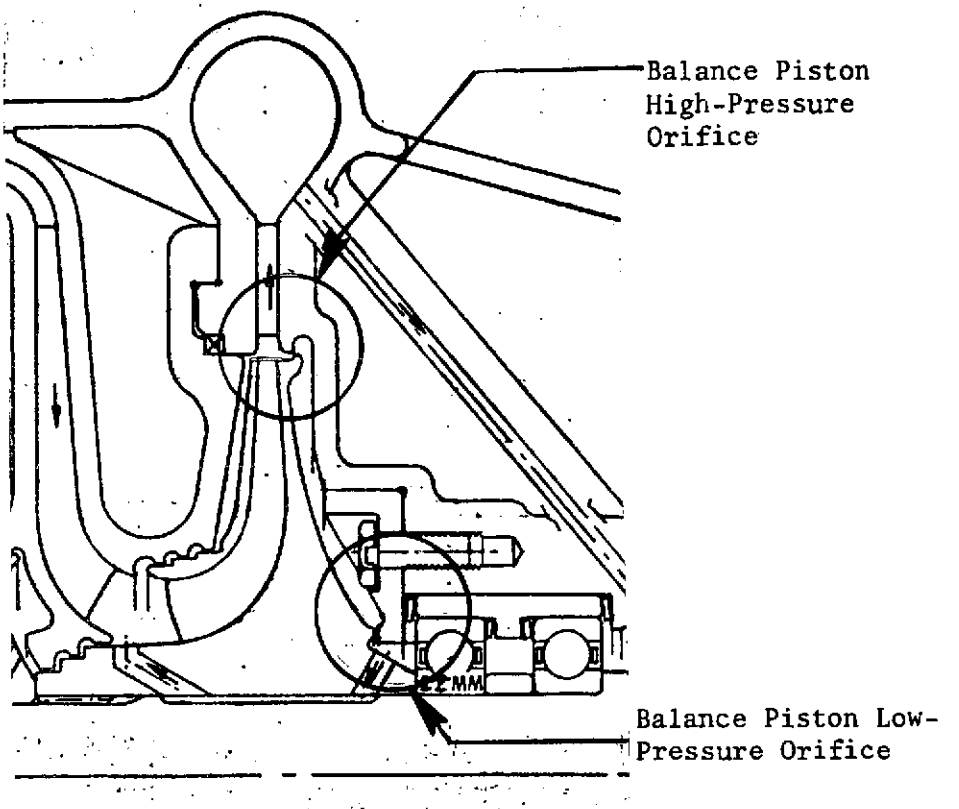

Figure 4-29. High-Pressure Orifice Element/Volute Housing Stationary Element Overlap

The restoring force developed by the balance piston as a function of axial position relative to the orifices is shown in Fig. 4-30.

The major parts of rotor assembly are comprised of the three impellers, an integral shaft, and turbine first-stage and second-stage wheels. The rotor is supported with a pair of 22-mm ball bearings at the turbine end and a 17-mm ball bearing mounted on the pump end. The outer races of the rear bearing pair and axial preload springs are contained in a cartridge which is free to move axially. Stops are provided for the turbine end cartridge which will permit start and shutdown transient loads to be absorbed by the bearings. By this method, rubbing at the balance piston orifices is eliminated during start and cutoff, and at steady-state conditions the bearings are subjected only to the preloads dictated by bearing dynamics.

To provide the transient load-carrying capability in both directions with angular contact bearings, two bearings were required at the turbine end. The pump end bearing carries radial loads only and it is axially preloaded to reduce bearing internal clearances and keep the balls from skidding.

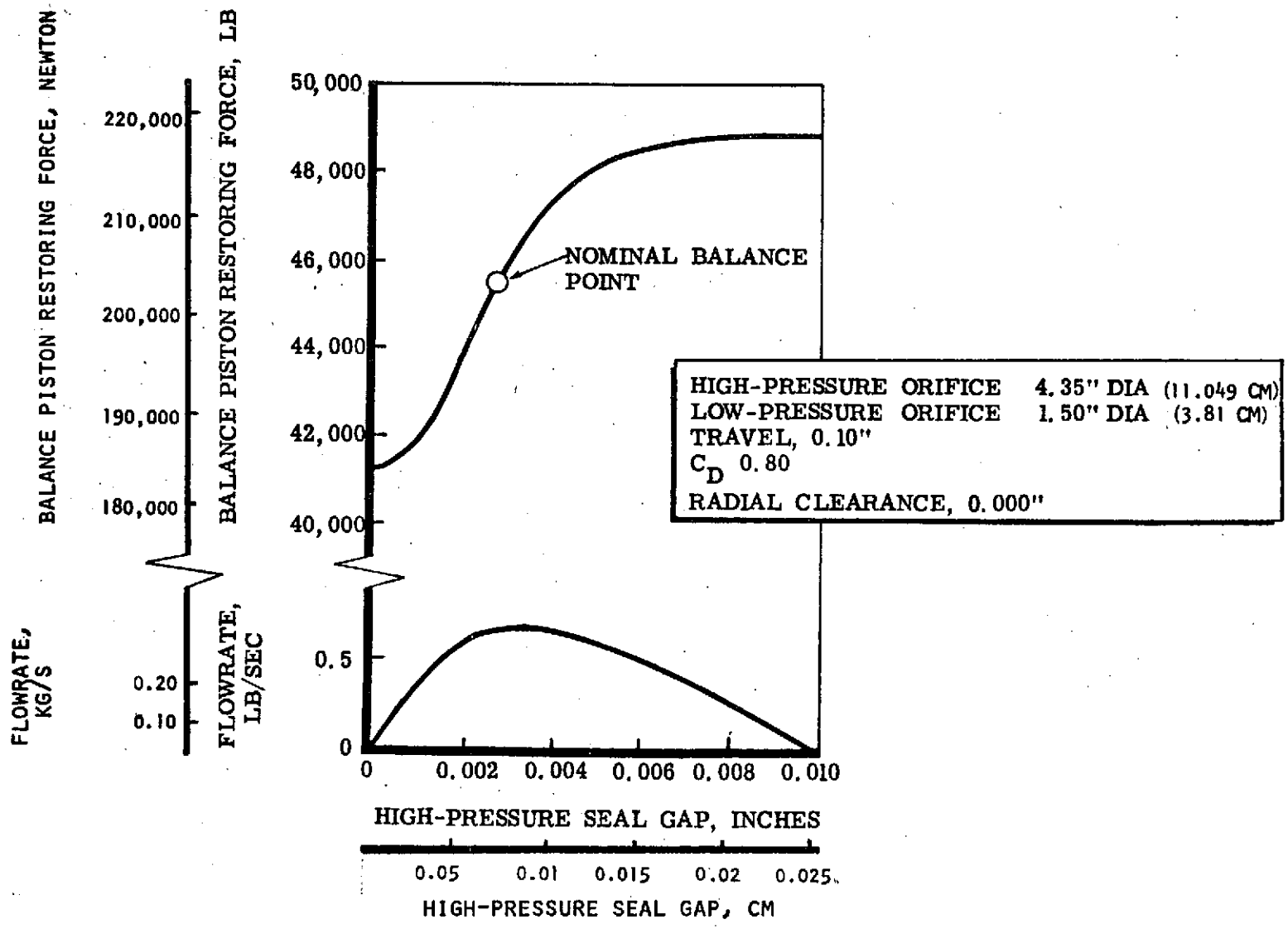

Figure 4-30. ASE High-Pressure Fuel Turbopump Balance Piston Performance

Bearing lubrication is provided for ball bearing as well as hybrid operation by internal recirculation of liquid hydrogen. To lubricate the pump end bearing, LH_2 is tapped through radial holes in the rear hub of the first-stage impeller and passed through a center hole in the shaft to the front of the bearings. From there, the coolant passes through the bearing and returns through a step-labyrinth restriction to the main pump flow at the first-stage impeller inlet. Although the flow quantity can be controlled elsewhere, the labyrinth is included to maintain the local pressure at the bearings above vapor pressure. To lubricate the rear bearings, fluid is bled from the volute discharge to the turbine side of the bearings. From there the coolant passes through both bearings, mixes with the balance piston fluid, and returns to the inlet of the second-stage impeller.

Hot-gas propellant enters the turbine through a dome-shaped inlet manifold, passes through the two nozzle rows and rotor stages in the direction of the pump, turns 180 degrees, and leaves the turbine flowing away from the pump.

Since interstage losses can be relatively high in a high-pressure turbine of this size, rotor blade tips on both stages are shrouded. Shroud tip leakage is minimized by maintaining a close clearance between the shroud tip and a small cell size honeycomb insert brazed to the stator. The clearance will be set at minimum consistent with assembly requirements and the shroud will be allowed to wear itself in. The same approach will be used to reduce gas leakage between the second-stage nozzle and rotor.

On both wheels, the blades and blade shrouds will be integral with the disk, and flow passages will be produced by electrical-discharge machining. The second-stage nozzle will be cast as individual blades, which will be assembled in the continuous inner shroud through a feed slot and will be clamped at the outer diameter by retaining rings on either side.

SHAFT SEAL

The liquid hydrogen seal is designed to minimize operating leakage, consistent with the 10-hour life and 300-start requirement. Static sealing is not required since the propellant valve located upstream of the pump is closed during the coast period. The liquid hydrogen pump fluid and the hydrogen-rich steam (H_2 + H_2O) turbine hot gas are compatible; therefore, fluid seperation is not required which allows the seal leakage to be drained into the turbine area to eliminate overboard propellant loss. The selected seal configuration and predicted leakage is shown in Fig. 4-31.

A double floating-ring, controlled-gap seal has been selected as the best compromise between leakage, life, and reliability. The labyrinth-type seals were rejected due to the higher leakage losses. The design technology of the floating-ring concept is considered to be sufficiently developed to allow design of a seal to meet the requirements with a high probability of success. Floating-ring seals have demonstrated satisfactory operation in the H-1, RS-17, MK-19, IR&D LH_2 programs, and several commercial applications.

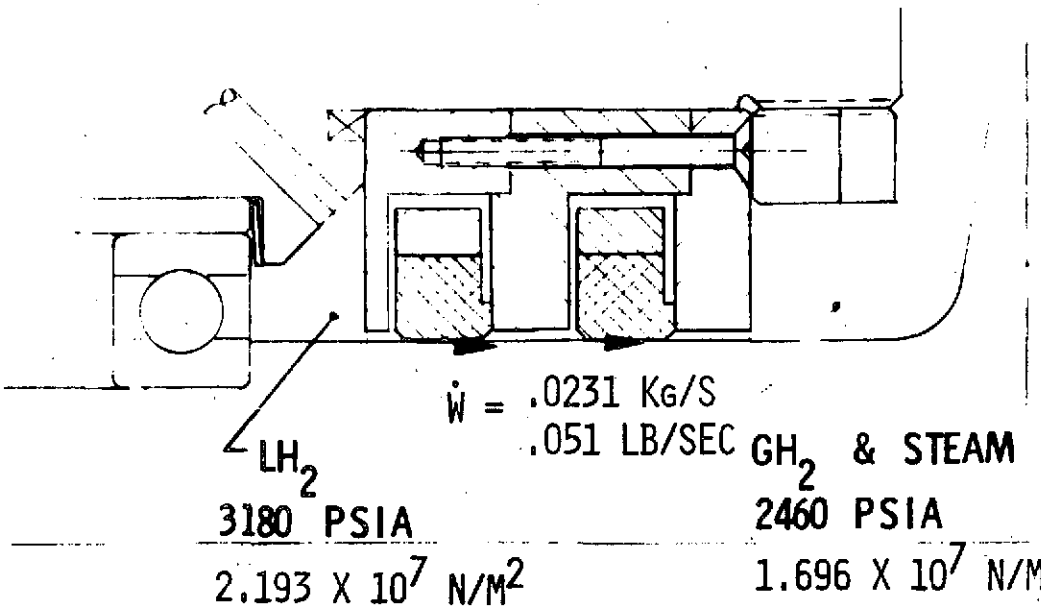

SEAL HOUSING MATERIAL:	A286
SEAL RING MATERIAL:	P5N CARBON
RETAINING RING MATERIAL:	ASTROLOY
SHAFT MATERIAL:	ASTROLOY
SHAFT SURFACE TREATMENT:	TUNGSTEN CARBIDE
DIAMETRAL CLEAR (IN):	.002 .508 MM

Figure 4-31. ASE High-Pressure Fuel Turbopump Shaft Seal Data

The floating ring consists of an inner carbon ring and an Astroloy ring for strength. The inner ring is maintained in compressive hoop stress and retained with an interference fit. The radial pressure load is supported by the composite ring in compressive hoop stress. The axial pressure force is partially balanced by relieving the axial contact surface. The seal-ring-to-shaft operating clearance 0.762 mm (0.003-inch dimetral) has been selected to provide minimum leakage and sufficient margin to allow for the thermal and pressure deflections. Additional sealing effectiveness and fail-safe allowance is obtained by stacking two rings in series. The rings are free to be centered by the shaft location and are restrained from rotation with tangs on the outer ring. The shaft surface is coated with tungsten carbide for additional wear resistance. The self-lubricating qualities of fused fluoride materials have been demonstrated by NASA (Reference: NASA-TN D-2348). The material was successfully tested at Rocketdyne on an Air Force technology contract (FO-4611-67-C-0116) and an IR&D LH_2 program.

BEARINGS

Rolling-element bearings have been used widely in high-speed rocket engine turbopumps because of their advantages in: (1) large-capacity-to-volume ratio, (2) ability to operate independently of external pressurizing systems, (3) ability to survive particulate contamination, (4) ability to start with minimum preconditioning, (5) high radial spring rate, and (6) low heat generation and coolant consumption. Among the rolling-element bearing designs, the angular contact ball bearings are most easily adapted to turbopump operating requirements. These bearings have the capability of absorbing axial and radial loads. The preload may be varied to obtain a range of radial stiffness to control shaft dynamics and critical speeds. The bearings also can compensate for temperature gradients without inducing thermal instability, and can be paired for axial shaft position control in both directions. The angular-contact ball bearings are particularly suitable for high-speed (high DN) applications because the balls have minimum tendency for nonrolling motion (as opposed to rollers which can skew), and the cage can be one-piece element.

In the design of angular-contact rolling-element bearings, the bearing bore size is kept to a minimum, consistent with shaft strength and bearing load capacity, to reduce the effects of centrifugal force on the rolling elements at high DN's. In selecting ball size, a design optimization is made between minimizing centrifugal force and heat generation (minimum ball size) and adequate load capacity (maximum ball size).

In a high-speed bearing design, a minimum allowable diametral clearance must be maintained to avoid thermally induced radial interference. To accomplish this, a proper combination of contact angle and total curvature must be selected. A design tradeoff is made between maximum radial stiffness, which requires a minimum contact angle, and maximum thrust capacity, which requires a maximum contact angle.

Bearing life is limited by either rolling-contact fatigue or wear of the raceways, balls, and cage. Fatigue life which can be calculated is used as a design criterion; wear life is difficult to determine because of lack of data.

For evaluating actual bearing life, fatigue life if a relatively valid criterion to use, since the bearing operating conditions of speed, external loads, and internal loads, and internal inertial forces on rolling elements are all considered. These operating factors also affect wear life in relatively the same manner.

The significant parameters of the bearing design are listed in Table 4-13.

CRITICAL SPEED ANALYSIS

A finite element method was used to determine the rotor's critical speeds and mode shapes. The rotor was modeled as a series of concentrated masses and inertias connected by massless elastic beam elements. The analysis includes gyroscopic effects and shear deformation.

In analyzing the ball bearing design, the bearings were treated as linear springs to ground.

The critical speeds as a function of bearing spring rate are presented in Fig. 4-32. At the predicted spring rates, the first critical speed is at 5341 rad/s (51,000 rpm), and the third or bending mode critical is at 14,137 rad/s (135,000 rpm). There is a satisfactory margin between the operating speed range and critical speed locations.

MATERIAL SELECTION AND STRESS ANALYSIS

The materials and processes selected for the high-pressure fuel turbopump have been selected on the basis of extensive Rocketdyne usage in similar applications and/or recent developments at Rocketdyne and throughout the industry. Extensive use of materials having high strength-to-weight ratios is being made to minimize turbopump weight. Surfaces of components which are subject to plastic strain and which are exposed to an environment of high-pressure hydrogen-rich steam in the temperature range of 144 to 1144 K (-200 to 1600 F) will be copper plated to prevent strength degradation due to that environment. Rocketdyne has demonstrated that copper plating protects the base metal from hydrogen environment embrittlement at hydrogen pressures up to 6.895×10^7 N/m^2 (10,000 psi).

Electrodeposited copper from pyrophosphate baths will be employed so that controlled thicknesses can be deposited with a minimum of special tooling. In certain locations, internal anodes will be required due to the throwing power limitations of a copper-plating system.

The principal pressure vessel of the turbopump is the volute housing. It also reacts the crossover separating load transmitted through the turbopump inlet housing. Of paramount importance is minimizing backplate (balance piston) axial deflection. This is accomplished by providing a ribbed-ring backplate structure. Additional support is provided by the turbine housing which functions in parallel with the volute backplate.

The volute scroll is a closed load loop by virtue of the integral discharge diffuser vanes. This provides a more efficient structure than a C clamp-type

TABLE 4-13. ASE HIGH-PRESSURE FUEL TURBOPUMP BEARING DESIGN PARAMETERS

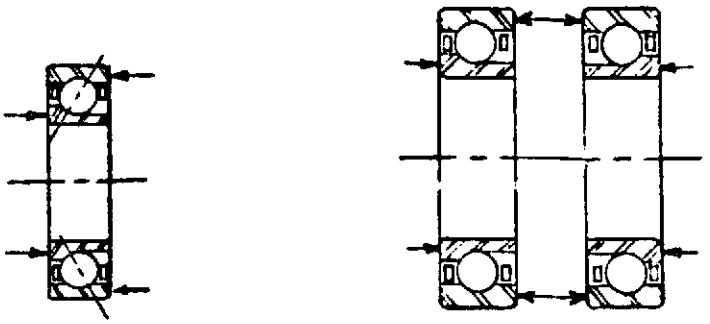

	Pump End	Turbine End
Type	Angular Contact	Angular Contact
Bore, mm	17	22
DN	1.5×10^6	1.9×10^6
Pitch Diameter, inches (cm)	1.02 (2.591)	1.27 (3.226)
Ball Diameter, inch (cm)	0.21875 (9556)	0.21875 (0.556)
Number of Balls	10	12
Race and Ball Material	440C	440C
Cage Material	Armalon	Armalon
Axial Static Capacity (newton)	1450 (6450)	1740 (7740)
Axial Load, pounds (newton)	250 (1112)	250 (1112)
B_{10} Fatigue Life, hours	100	120

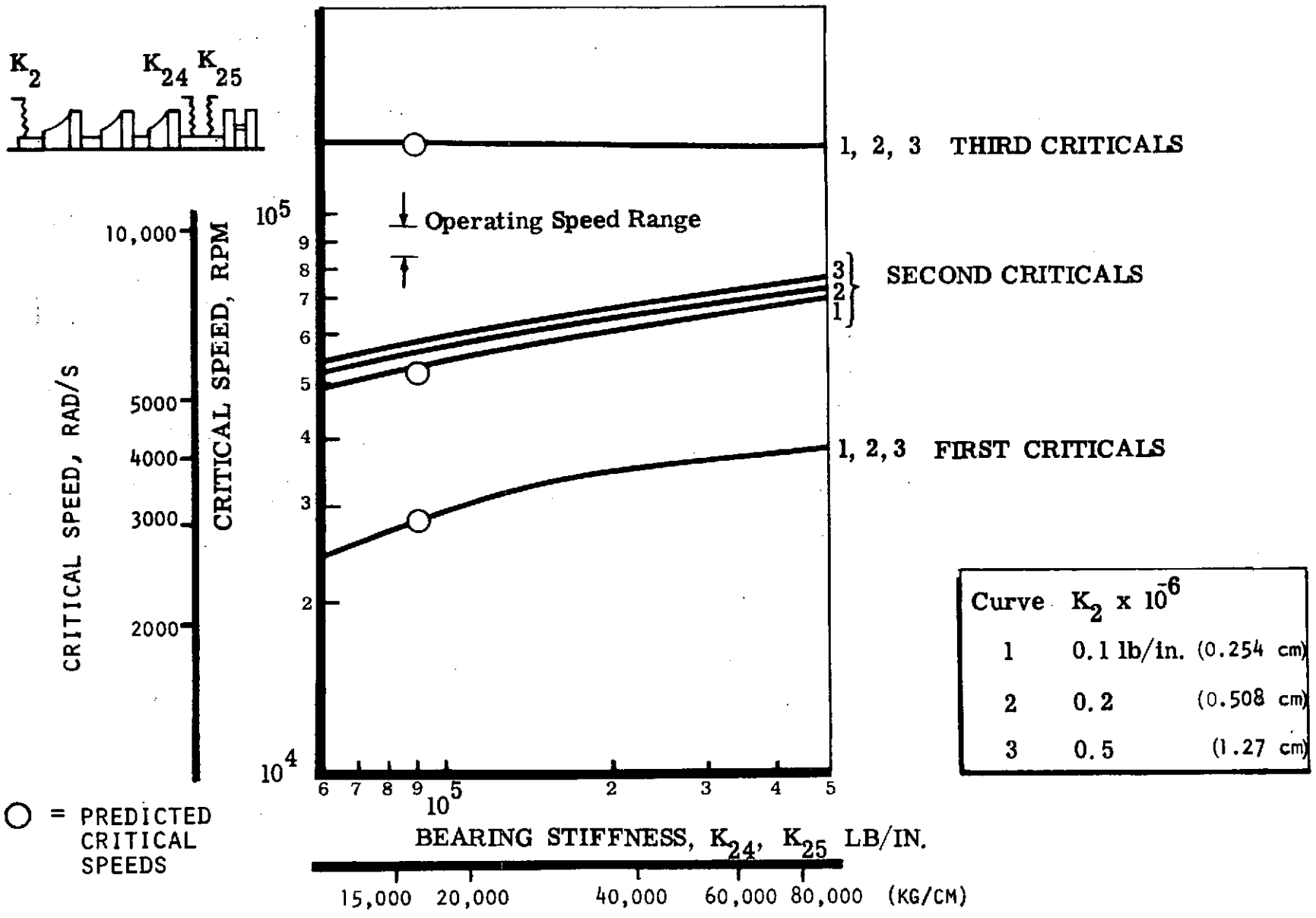

Figure 4-32. ASE High-Pressure Fuel Turbopump Rotor Critical Speeds

volute with separate diffuser vanes. Because of high strength and good casting quality, INCO 718 has been selected for the housing material.

For similar reasons, the crossover is also made of INCO 718. The crossovers are subjected to a combination of axial and radial pressure loading as well as internal passage pressure loading; they function structurally as a ring. The axisymmetric portions are held plane by the action of the crossover vanes and ribs.

Since the bearing DN plays such an important part in establishing rotational speed and, therefore, the general configuration of the turbopump, detail calculations were made to determine the minimum diameter required to carry the predicted loads. The shaft was structurally sized to carry three types of loading:

1. Torque
   a. Steady-state torque $\sim T_o$
   b. Alternating torque $\sim T_a$*
2. Axial load $\sim P_A$
3. Side load $\sim P_S$ which results in bending moments

The following equation is used to calculate fatigue factors of safety:

$$F.S. = 1\Bigg/\sqrt{\left(\frac{\sigma_o}{L_b F_{ty}} + \frac{K_t \sigma_a}{F_e}\right)^2 + 3\left(\frac{\tau_o}{L_s F_{ty}} + \frac{K_{ts} \tau_a}{F_e}\right)^2}$$

where

σ_o = steady direct stress
= axial load/area

σ_a = alternating direct stress**
= bending stress due to side load

τ_o = steady shear stress
= torque/polar section modulus

τ_a = alternating shear stress
= 5 percent of steady shear stress

K_t = theoretical stress concentration in bending

*The alternating torque is assumed to be a percentage of the steady torque and is dependent upon the application.

**The side load is assumed to be fixed in space relative to the rotor and, consequently, gives rise to an alternating stress.

K_{ts} = theoretical stress concentration factor in torsion

F_{tu} = ultimate tensile strength

F_e = endurance limit stress for complete stress reversal

$$L_b = \frac{16}{3\pi}\left[\frac{1-(d_i/d_o)^3}{1-(d_i/d_o)^4}\right]$$

$$L_s = \frac{4}{3}\left[\frac{1-(d_i/d_o)^3}{1-(d_i/d_o)^4}\right]$$

d_i = shaft inner diameter

d_o = shaft outer diameter

Based on these calculations, the predicted torque will be transmitted with an adequate safety factor, using the 22-mm turbine end bearing and spline arrangement shown in the baseline design. The development of this equation can be found in "Stress Concentration Design Factors," by R. E. Peterson, 1953.

The impellers are cast titanium (5Al-2.55Sn titanium) with an integral shroud. The impeller blades are subjected to both hydrodynamic and centrifugal loading. The centrifugal loading is the major consideration in the impeller structural design. The hydrodynamic blade loading is small due to the low fluid density (LH_2).

The impeller backplate is structurally sized to support the vane and shroud loading in addition to its own centrifugal loading. The hoop resistance of the shroud is conservatively neglected. The backplate has a burst speed at least 20 percent greater than the maximum operating speed.

A "burst efficiency factor" is utilized to predict the backplate burst speed. This factor is dependent on the ratio of the average tangential stress to maximum tangential stress and upon the ability of the backplate material to redistribute the centrifugal loading (i.e., material elongation).

Burst tests conducted at Rocketdyne utilizing shrouded titanium impellers have shown that a burst efficiency factor of 1.0 is attainable.

The turbine housing is fabricated from Rene' 41 material. This material is selected because of its superior high-temperature strength. The housing is copper plated internally to protect against the deleterious effects of hydrogen environment on the rupture strength and low cycle fatigue life.

The housing is structurally sized to provide safety factors of 1.4 on ultimate strength, 1.1 on yield strength, and 1.0 on 1-percent creep in 10 hours.

An additional requirement is to design for a low cycle fatigue life of 300 cycles times a factor of safety of 4.

The integrally bladed turbine wheels are made from Astroloy forgings. The disks are structurally sized to react the blade centrifugal rim load as well as the centrifugal force acting on the disk mass. Like the impeller backplate, a burst efficiency factor is used to the wheel burst speed. The second-stage wheel burst speed is 13,823 rad/s (132,000 rpm) based on a burst efficiency factor of 0.83. The second-stage wheel burst speed will be slightly higher than the first due to the restraint offered by the shaft.

The blade is structurally sized to maintain a factor of safety of 1.4 on a modified Goodman diagram. The blade alternating stress is assumed equal to the gas bending stress. Additionally, the blade steady-state stress is limited to the 10-hour, 1-percent creep limit.

Additional discussion of turbopump materials selected and methods of fabrication planned is presented under "Component Fabrication."

FABRICATION

The high head, relatively low-flow requirements of the LH_2 turbopump establishes a design with very small hydrodynamic passages. Because of this, fabrication of some of the components requires advanced techniques to maintain dimensional tolerances and obtain the surface finish required to meet performance characteristics. A discussion of the fabrication method to be used in the most important components of the turbopump follows.

Crossovers

The crossovers take the flow from one stage, diffuse it and direct it to the next stage. Crossovers will be cast from INCO-718 in two main pieces. The investment process will be used with ceramic cores for the hydrodynamic passages. Cores are placed in a die representing the external housing surface and wax is then injected around the cores. The die is then removed and the was pattern is dipped in a (ceramic) slurry to form the pour surface. The wax is then melted out and the pattern is ready for casting. This process gives excellent surface finish and maintains the internal hydrodynamic passages to specified dimensional tolerances. Following casting, the two pieces will be welded together to form the complete crossover. After machining the seal lands on the assembly, they will be silver plated to allow rubbing contact with the labyrinth seals in the impeller to occur without damage.

Pump Impellers

The pump impellers will be cast of titanium alloy (5Al-2.55Sn-Ti) using the same process as for the crossovers. Because of titanium's reactivity, however, the cores will be made of solid graphite instead of ceramic. To make the graphite cores, a die will be made to apply pressure to form the cores. Following wax injection and removal of the outside die, the pattern will be dipped and coated with a graphite instead of a ceramic slurry. A similar impeller has recently been successfully cast in INCO 718.

In the above processes, the key to obtaining satisfactory hydrodynamic passage shapes and surface finishes is the use of the cores. Without the cores, the shape and surface finish of the passages cannot be maintained as flow of the slurry into the small passage areas cannot be adequately controlled.

Pump Inlet

The pump inlet will be cast of Tens-50 aluminum using the conventional investment casting process. Special cores will not be required as the hydrodynamic passages are of sufficient cross section to be adequately filled with slurry using the dipping process. Following the final machining of the seal lands, they will be silver plated to allow rubbing contact with the labyrinth seals in the impeller to occur without damaging either the housing or the impeller.

Pump Housing

The volute subassembly of the housing will consist of two INCO 718 castings. One casting will include the major portion of the volute torus and the flange for bolting to the inlet casting. The second casting will include the turbine bearing support as well as the diffuser vanes. These two castings and the turbine turnaround passage will be welded together to form the subassembly.

The turbine nozzle fluid dynamic passages will be formed using the EDM process. The nozzle ring then will be welded into the inlet domes, which in turn will be secured to the exhaust dome through baffle plates. The manifold will be in-place welded to the housing at the turbopump assembly.

Turbine Second-Stage Nozzle

The turbine second-stage nozzle vanes will be individually cast from Haynes Stellite 31 and assembled and held in place in the pump volute and turbine nozzle assembly by the two-piece slotted turbine tip seal support rings. Cast Stellite nozzle vanes have been used successfully in all of the Mark 3 (Thor and Atlas) turbines.

Turbine Wheels

The first-stage turbine disk and shaft and the second-stage disk will be made from Astroloy forgings with the blade passages formed using the EDM process to allow the use of shrouded blades. Astroloy was chosen to obtain the desired high strength at high temperature. Turbine wheels of similar size and design were fabricated from Astroloy for the small hydrogen and oxygen turbopumps recently completed (Contract NAS8-27794).

Turbine Inlet and Discharge Manifold

The turbine inlet and discharge manifold is a simple fabricated assembly made up of formed parts of Rene' 41 material. Here, again, Rocketdyne's experience with Rene' 41 in the Mark 10 turbopump will ensure a reliable assembly.

Hydrogen Embrittlement

Since the liquid hydrogen turbopump will be operating in a hydrogen environment, the problem of hydrogen embrittlement of the materials used in its fabrication must be considered. The materials used in the major components of the turbopump are shown in Fig. 4-27. Since some of these materials are susceptible to hydrogen embrittlement under certain conditions, its effects are significant only at near-room temperatures and at stress levels above the yield; specific steps will be taken to avoid the problem.

The methods used to overcome the problem of hydrogen embrittlement are:

1. Design to keep the stress levels low in those areas where the components will be in contact with hydrogen near room temperature.
2. In fabricated structures using welds, configure the design so that the welds are in low-stress areas.
3. Prestress the components above the yield point. This can be done with some parts such as impellers, wheels, and pressure vessels, but is impractical in many structural parts.
4. Overlay the affected part with a coating of material that is not susceptible to hydrogen embrittlement such as Incoloy-88 or copper.

TASK V: VALVES, IGNITION SYSTEM, AND CONTROLS PRELIMINARY DESIGN

VALVES AND PNEUMATIC CONTROLS

An analysis was conducted to determine the optimum valve locations to provide adequate engine control yet minimize impact on the engine cycle.

The long-term coast requirements of the engine, the difficulty of minimizing turbopump dynamic seal leakage, and the necessity of preventing turbine heat soakback into the tanked propellants during coast resulted in locating the propellant shutoff valves at the boost pump inlets. In this manner the engine is isolated during coast. The residual propellants in the engine are dispelled during controlled shutdown of the engine after firing. The primary engine control valves that provide thrust and mixture control were located on the oxidizer side because of start and cutoff considerations (precise shutoff of oxidizer), availability of pressure drop, and the significant impact on the engine of fuel system controls. The latter consideration is based on the fact that the engine is pressure drop limited on the fuel side, requiring either an increase in pump discharge pressure or a decrease in chamber pressure to accommodate the additional pressure drop required for a modulating control valve.

The actuation mechanisms selected were pneumatics for the inlet valves and electrical for the modulating control valves. The valves and pneumatic controls are shown schematically in Fig. 5-1.

MAIN OXIDIZER AND FUEL INLET VALVES

Butterfly, poppet, and ball valve configurations were considered for the inlet valve applications. The butterfly and poppet configurations were rejected because of their inherent high pressure drop. This is particularly critical on this engine because of the very low start NPSP requirements.

Selected Configuration

The configuration selected was a modified ball or eyelid valve with a liftoff seal and actuated by a four-way solenoid valve (Fig. 5-2). The same valve is used in both applications to reduce fabrication and maintenance costs without sacrificing weight and performance. The eyelid design significantly reduces weight, thus overcoming the major drawback of ball-type valves. Some of the components of this valve are also used in the oxidizer control valves. The eyelid design was chosen because of its low pressure drop characteristics when full open. A liftoff seal patterned after the NASA-LeRC contract effort to minimize leakage through a captive plastic seat concept was included to increase the valve life. The cam-actuated liftup arrangement prevents scrubbing during valve actuation. The pneumatic actuator was selected because of its relating compactness and fast response. Welded flanges were utilized to accomplish zero leakage and weight reduction.

Design Operating Characteristics

The shaft is rotated by a crank attached to the pneumatic actuator that is controlled by a four-way solenoid valve. A cam keyed to the shaft lifts the

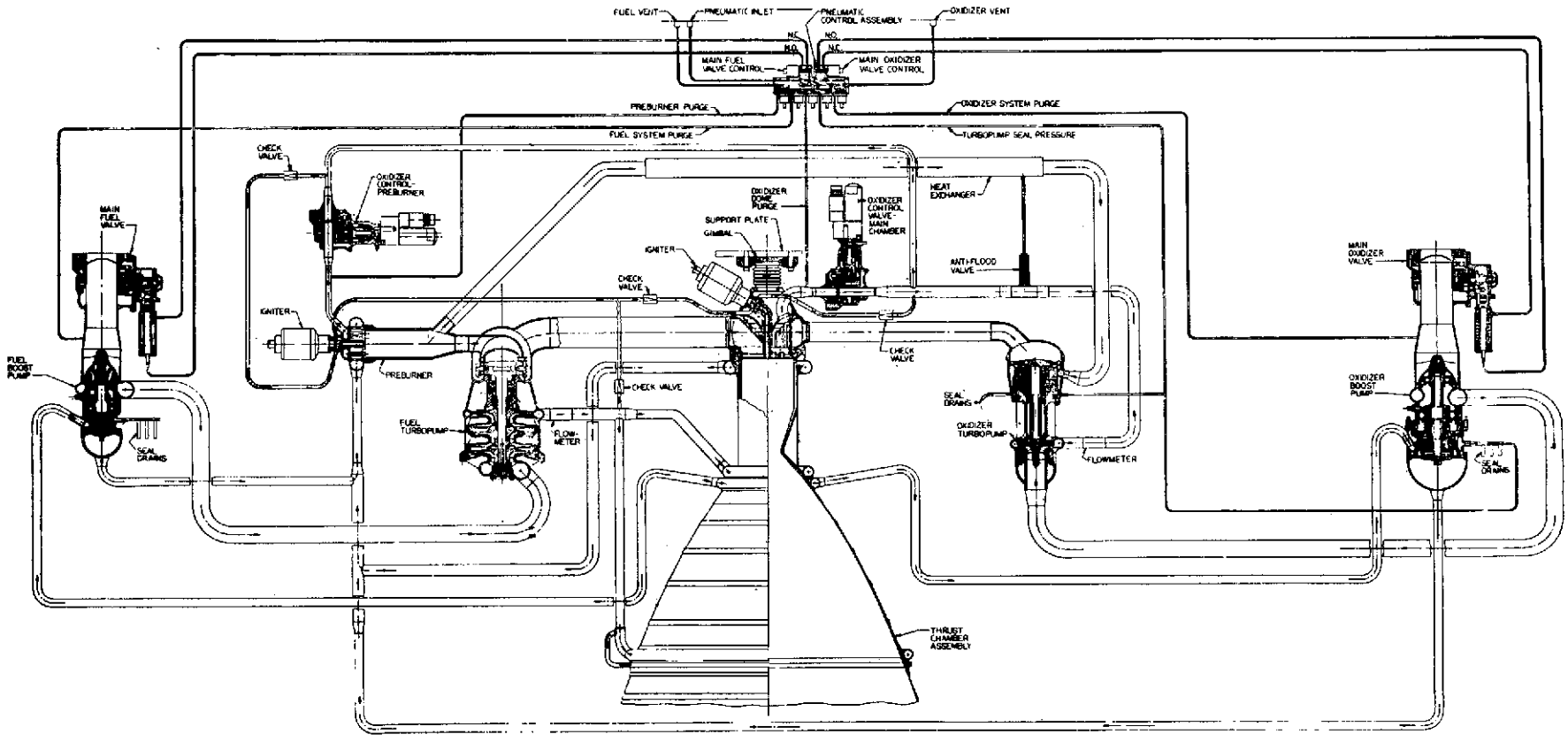

Figure 5-1. Advanced Space Engine Schematic (88,964 N; 20K)

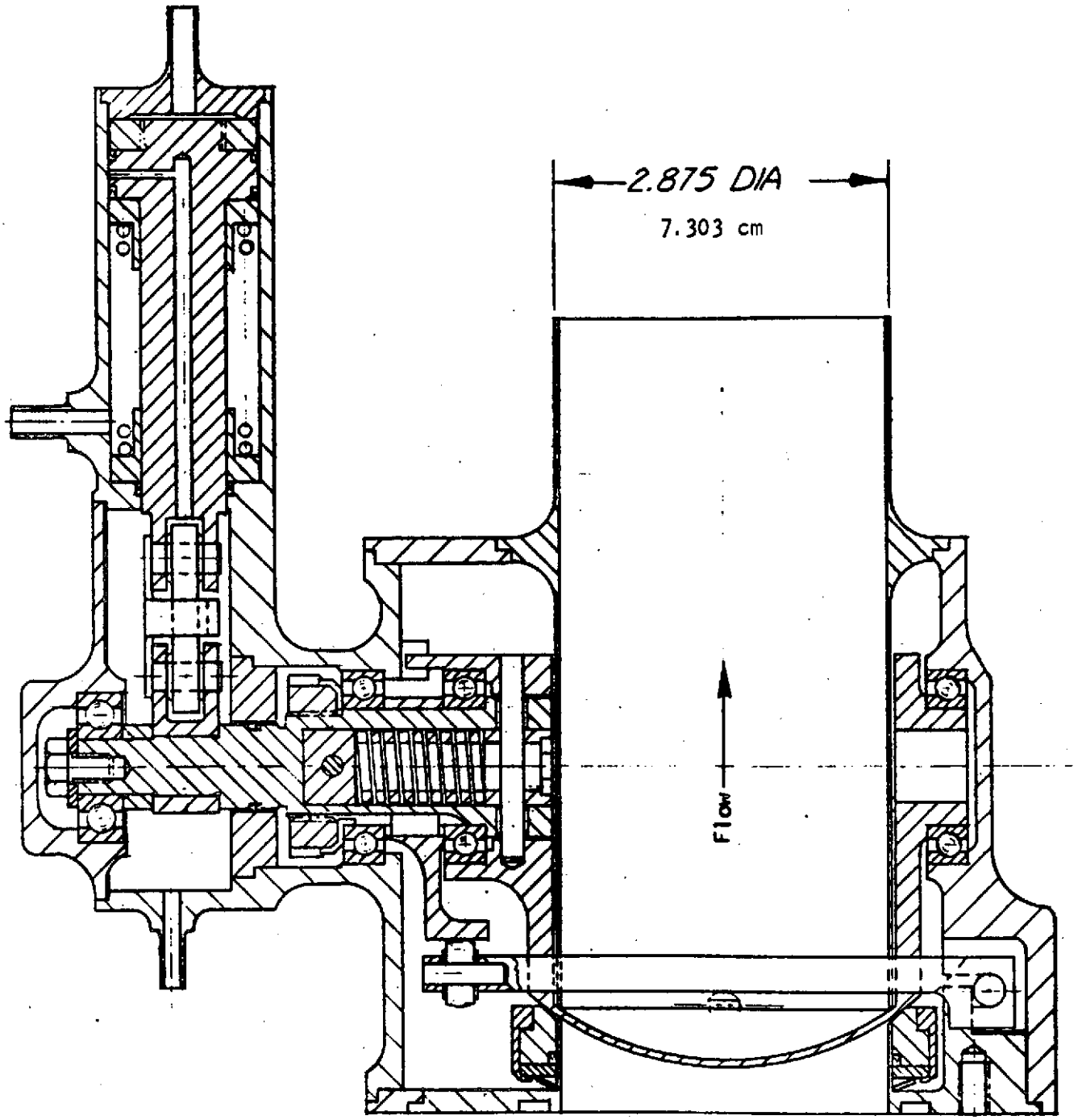

Figure 5-2. Main Propellant Valve

main seal from the valve's spherical seat when rotated 20 degrees. The cam follower is mounted on a yoke which applies an even load to lift the seal assembly. The valve rotates 70 degrees between full-closed and full-open positions; however, there will be some propellant flow as soon as the seal is lifted. A torsion spring pinned to the shaft at one end and the valve at the other keeps the valve against a stop in the housing until the shaft rotates the 20 degrees. It then maintains a load between the shaft and valve during valve actuation.

MAIN AND PREBURNER OXIDIZER CONTROL VALVES

The main oxidizer and preburner control valves are utilized as part of the closed-loop control system to provide mixture ratio control and thrust control, respectively. Though butterfly, poppet and ball-type valves were considered, the ball-type valve was considered best suited because of its uniformity of control over the range of operation. The lack of on-board hydraulics (and potential problems during coast) and lack of adequate pneumatic servovalves resulted in the selection of electric motor actuators. Though electric motor drives can be large and heavy, by maintaining the valve torque requirement as low as practical, the size and weight of the motors was kept relatively small.

Selected Configuration

The configuration selected for these tasks is a modified ball or eyelid valve with a liftoff seal actuated by a 28-vdc rotary actuator (Fig. 5-3). The same size valve is used in both applications to reduce fabrication and maintenance costs without sacrificing weight and performance. The liftoff seal was included to increase the valve life and prevent oxidizer leakage during start and cutoff. This feature may not be required for the main oxidizer control valve and therefore may be eliminated based on further study.

Design Operating Characteristics

The rotary actuator is bolted to the valve body and keyed to the shaft. The shaft is rotated 20 degrees to fully lift the main seal from the valve's spherical seat through a cam keyed to the shaft. The cam follower is mounted on a yoke which applies an even load to the seal assembly. The valve rotates 53 degrees between full closed and full open positions; however, there will be some flow as soon as the seal is lifted. A torsion spring pinned to the shaft at one end and the valve at the other keeps the valve against a stop in the housing until the shaft has rotated the 20 degrees. It then maintains a load between the shaft and valve during valve actuation.

The actuator is operated by 28 vdc. The operating life is 10,000 cycles under an operating load of 16.95 ±3.39 joules (150 ±30 in./lb). The stop-to-stop time is from a maximum of 6 seconds at 18 volts to 0.5 second minimum at 32 volts. Position is indicated by a potentiometer built into the rotary actuator.

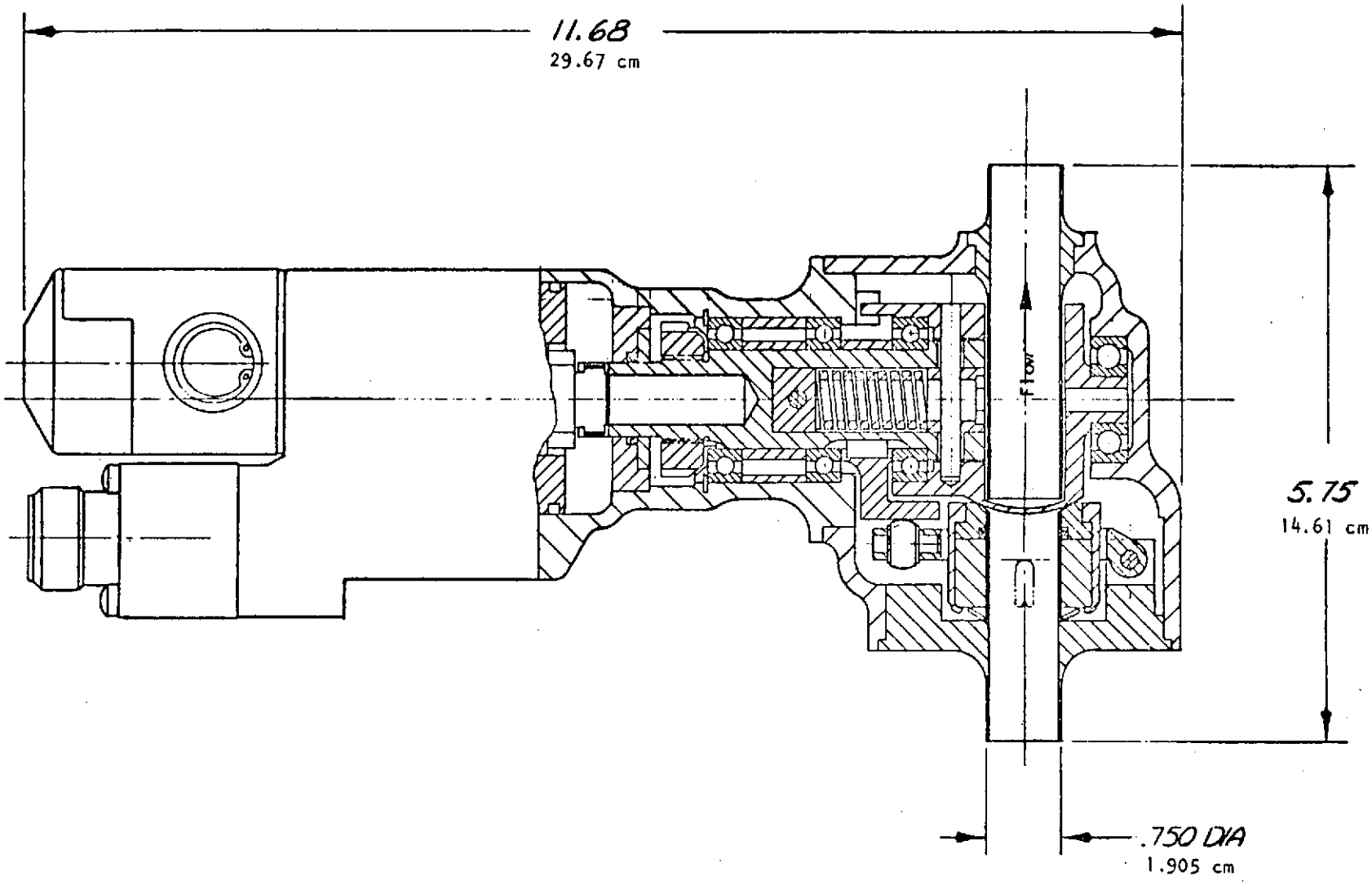

Figure 5-3. Control Valve

PNEUMATIC CONTROL PACKAGE

The pneumatic control package provides helium through solenoid valves to actuate the main valves, pressurize the turbopump seals, and to purge the oxidizer and fuel systems, oxidizer dome, and preburner.

Selected Configuration

The three-way and four-way solenoid valves selected were designed and used on other Rocketdyne engines. A common housing or manifold is used to reduce the volume and weight of the system (Fig. 5-4). All mating lines are welded in place during engine assembly.

Design Operating Characteristics

Each valve is individually actuated when its solenoid receives a command signal. The common housing for the three-way valves also includes filters in the outlet ports. The four-way valve housings are mounted on the manifold and have filters in their outlet ports. All valve inlets are protected by a single large filter located in the inlet passage of the manifold.

SYSTEM PNEUMATIC REQUIREMENTS

Based on system pneumatic control valve and purge requirements, an estimate of typical mission engine pneumatic requirements has been completed and is presented in Table 5-1. A typical mission was utilized to provide preliminary information pending identification of maximum system requirements. The engine purges may be eliminated based on further study, but are included to provide a conservative estimate.

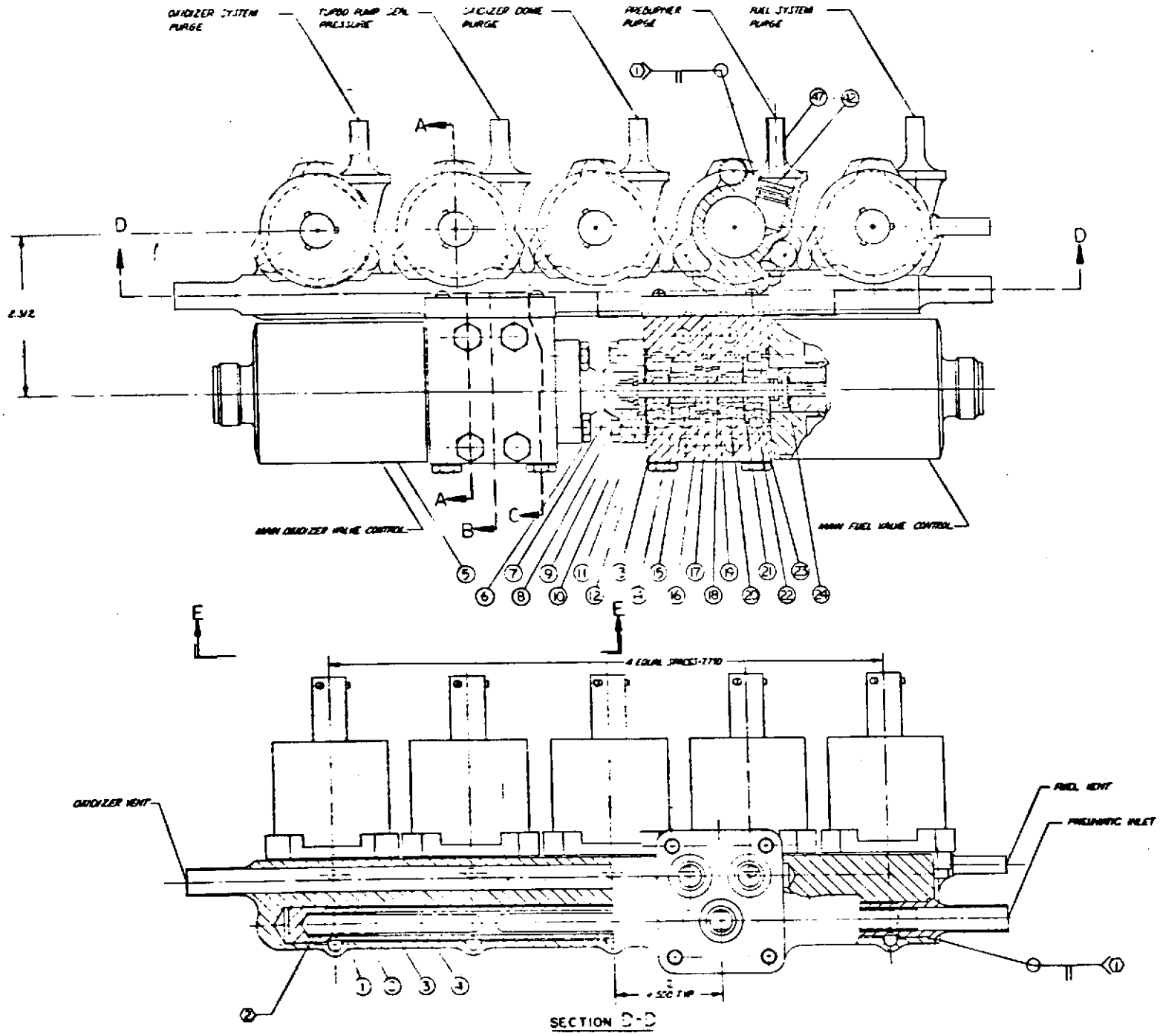

Figure 5-4. Pneumatic Control Package

TABLE 5-1. PNEUMATIC SYSTEM REQUIREMENTS

(Representative Mission: 14 days in orbit, 6 starts, 0.4 hour hot-fire duration)

Function	Number of Components	Total Usage Requirements	Total Mission He Requirements, scim ③
Pneumatic Component Leakage			
He Supply Isolation Valve	1	2 scim ① (5.46×10^{-7} m^3/sec)	40,300 (0.6604)
Regulator and Relief Valve	1	50 scim ② (1.366×10^{-5} m^3/sec)	1,200 (0.0197)
Purge Solenoid Valves	4	240 scim ② (6.55×10^{-5} m^3/sec)	5,760 (0.0944)
Turbopump Seal Pressure Solenoid	1	60 scim ③ (1.639×10^{-5} m^3/sec)	120 (0.00197)
Main Valve Control Solenoids	2	150 scim ② (4.097×10^{-5} m^3/sec)	3,600 (0.0589)
Main Valve Actuators	2	300 scim ② (8.194×10^{-5} m^3/sec)	7,200 (0.1180)
Main Valve Actuation	2	2,600 sci/start (0.0426 m^3)	15,600 (0.2556)
Pump Seal Purge	2	32,000 scim (8.74×10^{-3} m^3/sec)	768,000 (12.585)
Oxidizer System Purge	-	3,800 sci/firing (0.0623 m^3)	22,800 (0.3736)
Fuel System Purge	-	7,500 sci/firing (0.1229 m^3)	45,000 (0.7374)
		Total Required	909,580 sci (14.905 m) ③
			5.3 pounds (23.58 N)

① Continuous during orbital coast

② Continuous during engine firing

③ 20 seconds per engine firing

IGNITION SYSTEM

CONFIGURATION SELECTION AND DESIGN

An air-gap igniter is used in both the preburner and thrust chamber to provide the source of ignition energy at start. This type of ignition system was selected after a comprehensive review of the state-of-the-art ignition systems. The primary requirements of the ignition system are: (1) the igniters be capable of operating at start with cold propellants supplied at tank head/idle mode pressures producing repeatable, reliable ignition of the preburner and thrust chamber, and (2) the igniters be of configuration which can be designed to meet the life requirements of the engine. The ignition systems considered to be the most applicable were the combustion wave igniter, the ASI (augmented spark igniter), and the air-gap igniter. Each of these systems appeared to have potential for meeting the ignition system requirements; however, the air-gap igniter appears superior due to the potential for high spark electrode durability, predictable and repeatable ignition conditions at the spark electrode, and a higher temperature downstream of the igniter exit to enhance main propellant ignition.

The air-gap igniters used in the preburner and thrust chamber are basically the same configuration. The main difference is that the thrust chamber igniter has been rotated 60 degrees from the engine centerline to accommodate packaging under the gimbal. This requires a 30-degree elbow to be placed in the igniter nozzle.

The air-gap igniter uses an integral spark plug and exciter assembly for ignition, an oxygen/hydrogen injector, and a combustor/nozzle for ducting the hot gas to the injector (Fig. 5-5). Oxidizer is injected from an annular manifold around the spark electrode. A small amount of fuel is injected into the igniter combustor/nozzle where it mixes with the oxidizer downstream of the electrode producing an oxidizer-rich combustion (MR $\approx$ 40:1). The bulk of the igniter fuel flows through the nozzle coolant liner and is discharged at the injector face.

The air-gap igniter has the capability for rapid re-ignition with minimum delay in the event of a flameout during the start transition. It also provides a high mixture ratio near the electrode for reliable ignition and produces a hot core for main propellant ignition. The extremely high mixture ratio of the hot core is also advantageous for main propellant ignition because the hydrogen discharged from the coolant liner drives the hot-core temperature higher through the stoichiometric point before it is totally mixed with the igniter flow. Other advantages of the air-gap igniter are: (1) the oxidizer flow around the electrode provides cooling for the electrode and minimizes the potential for erosion from combustion, and (2) the injection technique using impinging fuel orifices below the electrode produces predictable conditions for ignition.

The igniter geometry in the region of the spark electrode, oxidizer annulus, and fuel orifice is similar to that tested under Contract NAS3-14348 and company-sponsored programs. The igniter propellant manifolds and combustor/nozzle geometry have been modified slightly to accommodate optimum packaging

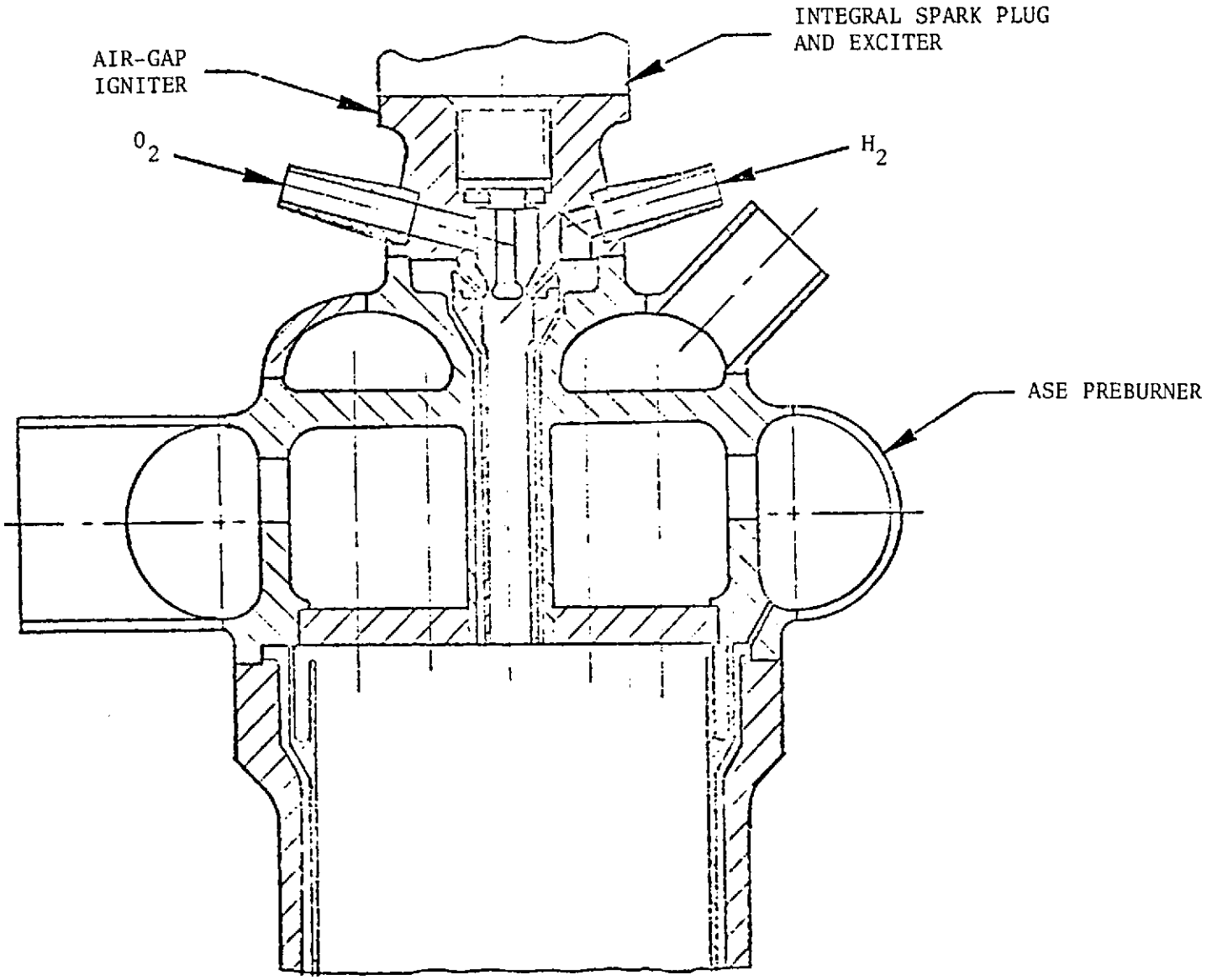

Figure 5-5. ASE Preburner Air-Gap Igniter

in the injector. A coaxial-type nozzle exit was selected for the igniter to allow mixture to take place downstream of the injector face to enhance main propellant ignition and allow the igniter to operate similar to an injector element during mainstage. The integral spark plug and exciter is attached to the igniter with a threaded joint. The seal at this point is integral with the spark plug.

OPERATING CHARACTERISTICS

The propellants for the preburner and thrust chamber igniters are supplied from the discharge of the high-pressure fuel and oxidizer turbopumps (Fig. 5-1). At start, the propellants at the supply points will be at cryogenic temperatures but appreciable heating in the supply lines is anticipated. Successful ignition of the air-gap igniter was demonstrated under company-sponsored hot-fire testing with a hardware temperature of 56 K (100 R) and propellant temperatures of 78 K (140 R) hydrogen and 114 K (206 R) oxygen (Ref. 9).

The igniter flow circuits are a fixed hydraulic resistance system. As a result, the igniter flowrates at mainstage increase above the ignition level due to the greater available pressure drops. The trend from ignition to mainstage is illustrated in Table 5-2 for a preburner and thrust chamber igniter sized for a total flowrate of 0.0454 kg/s (0.100 lb/sec) at start. This is the best design from the standpoint of engine simplicity, however, measures may be required to economize igniter fuel at mainstage. Minimum acceptable igniter flowrates at start will be defined during development testing. If the resulting mainstage igniter fuel flowrate is too high with a fixed hydraulic resistance system, valves can be incorporated into the igniter system which will either reduce the igniter flowrates at mainstage or totally shut off the igniter propellants and circulate a low-level gaseous purge through the igniters to prevent accumulation of water vapor.

TABLE 5-2. IGNITER NOMINAL OPERATING PARAMETERS

	Start		Mainstage	
	P/B	M/C	P/B	M/C
Chamber Pressure, psia (N/m^2)	100 (689476)	100 (689476)	3377 (2.328×10^7)	2200 (1.517×10^7)
Core Temperature, R (K)	3860 (2144)	3860 (2144)	5060 (2811)	4560 (2533)
Overall Temperature, R (K)	1360 (756)	1360 (756)	810 (450)	1060 (589)
Core Mixture Ratio	40	40	25	31
Overall Mixture Ratio	0.8	0.8	0.8	0.62
Total Flowrate, lb/sec (kg/s)	0.1 (0.0454)	0.1 (0.0454)	0.1 (0.0454)	0.479 (0.2173)
Oxidizer Inlet Temperature, R (K)	162 (90)	162 (90)	162 (90)	162 (90)
Fuel Inlet Temperature, R (K)	37 (20.6)	37 (20.6)	37 (20.6)	90 (50)

The integral spark plug and exciter has complete redundancy to provide high reliability. Each assembly contains two complete capacitance discharge exciters packaged in a single can to minimize weight and packaging envelope. The spark plug is divided into isolated spearate halves to which the exciters are connected, providing two redundant spark plug and exciter assemblies in a single package.

The envelope of the integral spark igniter and a schematic typical of each of the capacitive exciters are shown in Fig. 5-6. The operating parameters of the spark igniter are given in Table 5-3.

TABLE 5-3. INTEGRAL SPARK IGNITER OPERATING PARAMETERS

Input Voltage, volts	24 to 32
Input Current, ampere	1*
Stored Energy, millijoules	30 to 50*
Delivered Energy, millijoules	10*
Spark Rate, sparks/second	200

*For each exciter

MATERIAL SELECTION AND STRESS ANALYSIS

A heat transfer analysis of the steady-state temperature profile in the preburner and thrust chamber igniters was performed for conditions at start and mainstage. The results showed that although the igniter core temperatures greatly increased at mainstage, the nozzle coolant flowrate increased to a greater extent providing adequate cooling.

A structural and life analysis of the igniters showed both igniters to be structurally adequate and capable of meeting the life requirements of the engine. A more complete discussion of the preburner igniter stress analysis is given in the preburner discussion. The conditions within the thrust chamber igniter were less severe due to the lower mainstage pressure level and lower thermal gradient across the liner wall.

The igniter bodies are fabricated from Inconel 625 and the liner material is NARloy. Both the preburner and thrust chamber igniters are brazed/welded assemblies which are then welded to the injectors.

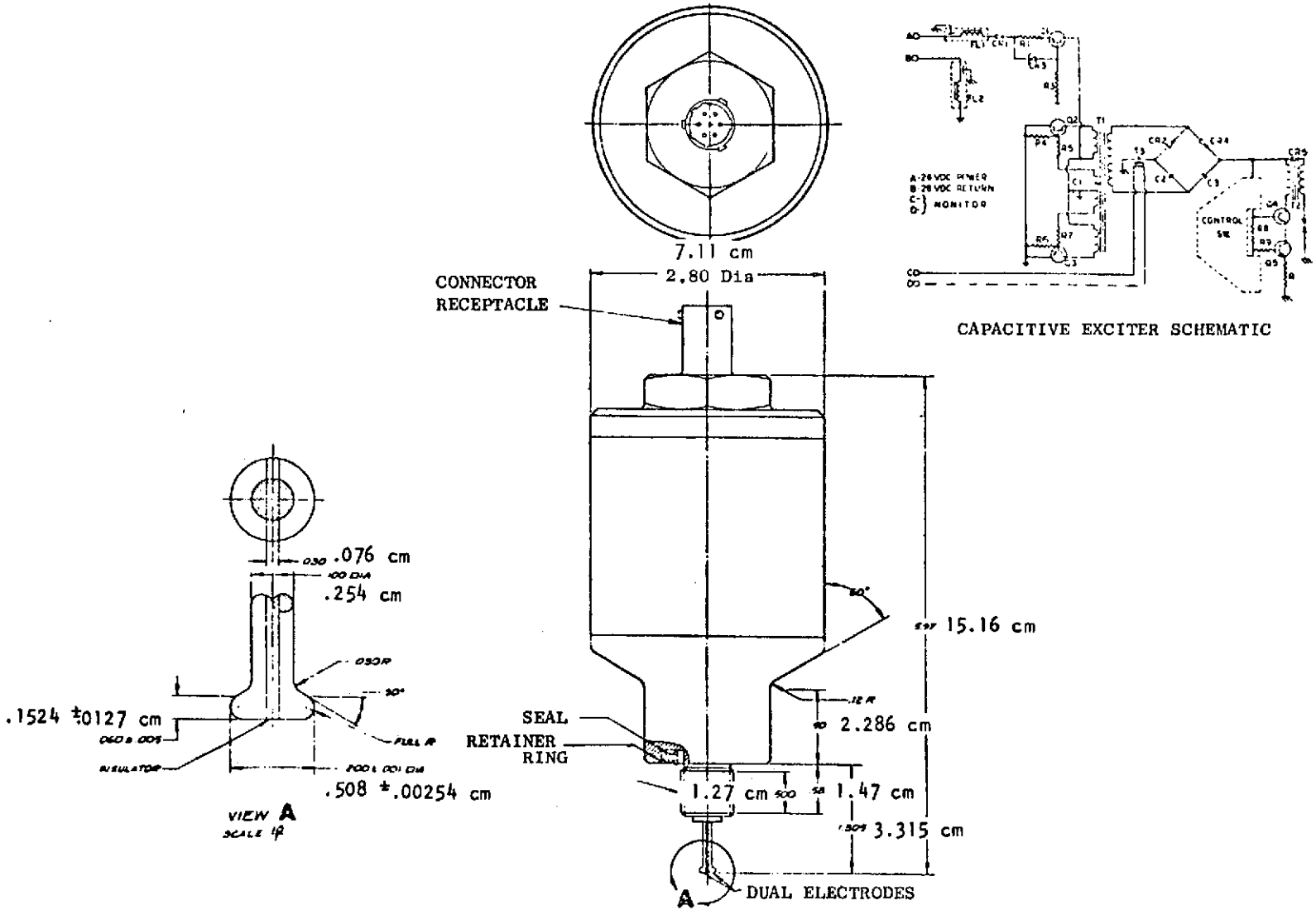

Figure 5-6. Integral Spark Igniter

CONTROL SYSTEM

An analysis of the engine control requireemtns, instrumentation, and state of the art of applicable approaches were conducted for synthesis of a control system to meet the engine requirements. A discussion of these analyses are subsequently presented. The ground rules for conducting the requirements were:

1. Providing constant thrust ±2 percent at full thrust
2. Providing mixture ratio control within ±2 percent of any desired value within the range of 5.5 to 6.5 at full thrust
3. Providing safe, stable, and reliable operation during start, idle, and mainstage modes of operation
4. Providing multiple restart capability

The control system design also includes:

1. Instrumentation requirements for engine checkout and control
2. Control system schematics, valve operation sequence, and control unit block diagram
3. Control unit preliminary designs define:
   a. Overall dimensions
   b. Internal components
   c. Interface and power requirements

Though it was intended to provide a breadboard controller, the readily available technology from concurrent programs provide an excellent basis for early assessment of the characteristics for a flight-type design.

Based on a fail-safe design approach baselined at the initiation of the study, an engine electrical control system was defined. The overall engine electrical control system is depicted in block form in Fig. 5-7, where it can be seen that the electrical control system elements can be grouped as follows:

1. Controls
   a. Throttling valve actuators (electrical)
   b. Solenoid or pilot valves (purges + control)
   c. Spark exciters
2. Transducers
   a. Pressure
   b. Temperature
   c. Flow
   d. Speed
   e. Position

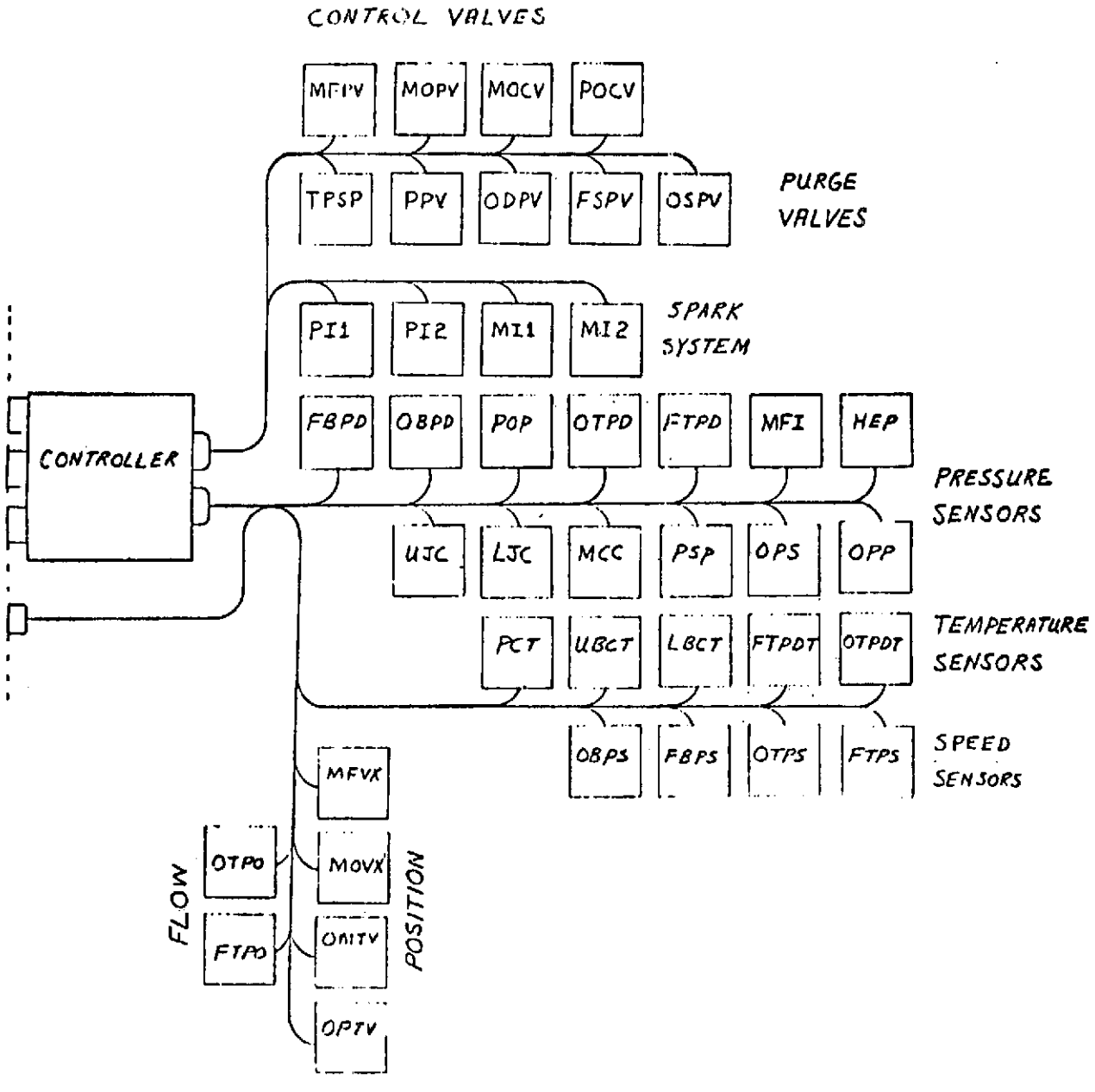

Figure 5-7. Engine Electrical System Block Diagram

3. Associated Harnesses
4. Engine Control Assembly

The engine controller block diagram is presented in Fig. 5-8. The instrumentation requirements and engine sequencing (previously discussed in this report) are presented in Table 5-4 and Fig. 5-9 (abbreviations defined in Tables 5-4 and 5-5).

ENGINE CONTROLLER MECHANICAL FEATURES

The controller electronics are housed in a sealed and pressurized canister, as shown in Fig. 5-10. The cover is held to the faceplate by a V-band clamp. A clamp of this type provides uniform pressure to the O-ring seal, easy access, and overall lighter assembly weight than a bolt ring. A maximum leak rate of 5×10^{-6} cc/sec/atm can be met with this assembly technique. The unit will be initially pressurized to approximately 103421 N/m^2 (15 psia) with dry GN_2. This establishes an inert atmosphere inside the assembly and prevents moisture entering due to thermal and/or pressure cycling.

All circuit boards are mounted to the faceplate and are separated one from the other by a series of "Becon" printed circuit connectors mounted to the periphery of the circuit board (Fig. 5-11). In this way, a given circuit can be carried from the connector interface board through a series of in-line contacts to the top board or any intermediate board.

The integrated circuit leads are welded to swaged thermals. This eliminates the potential heat soakback into the chip that soldering can cause, while providing the greater reliability of a weld joint.

The transistors of the power circuits are heat-sunk to a ring mounted to the faceplate.

COMPONENT TECHNOLOGY AND CONTROLLER CIRCUITRY DESIGN

To minimize controller size, weight, and power dissipation, a hybrid controller configuration was chosen. The use of CMOS LSI circuitry and components is emphasized for several reasons:

1. Five to 10 times higher functional density than comparable TTL SSI/MSI
2. Inherent circuit reliability achieved through simplified manufacturing process
3. Reduced number of interconnects required per functional subsystem
4. Lower power dissipation than comparable TTL circuitry by a factor of 10 to 1000.

NASA preferred parts were reviewed for this application and can utilized for discrete semiconductors and components where applicable. However, the TTL integrated circuits were bypassed in favor of CMOS MSI/LSI for the reasons noted above. It is noted that NASA is considering approval of certain MOS/CMOS devices for Space Shuttle program use in the near future. Several

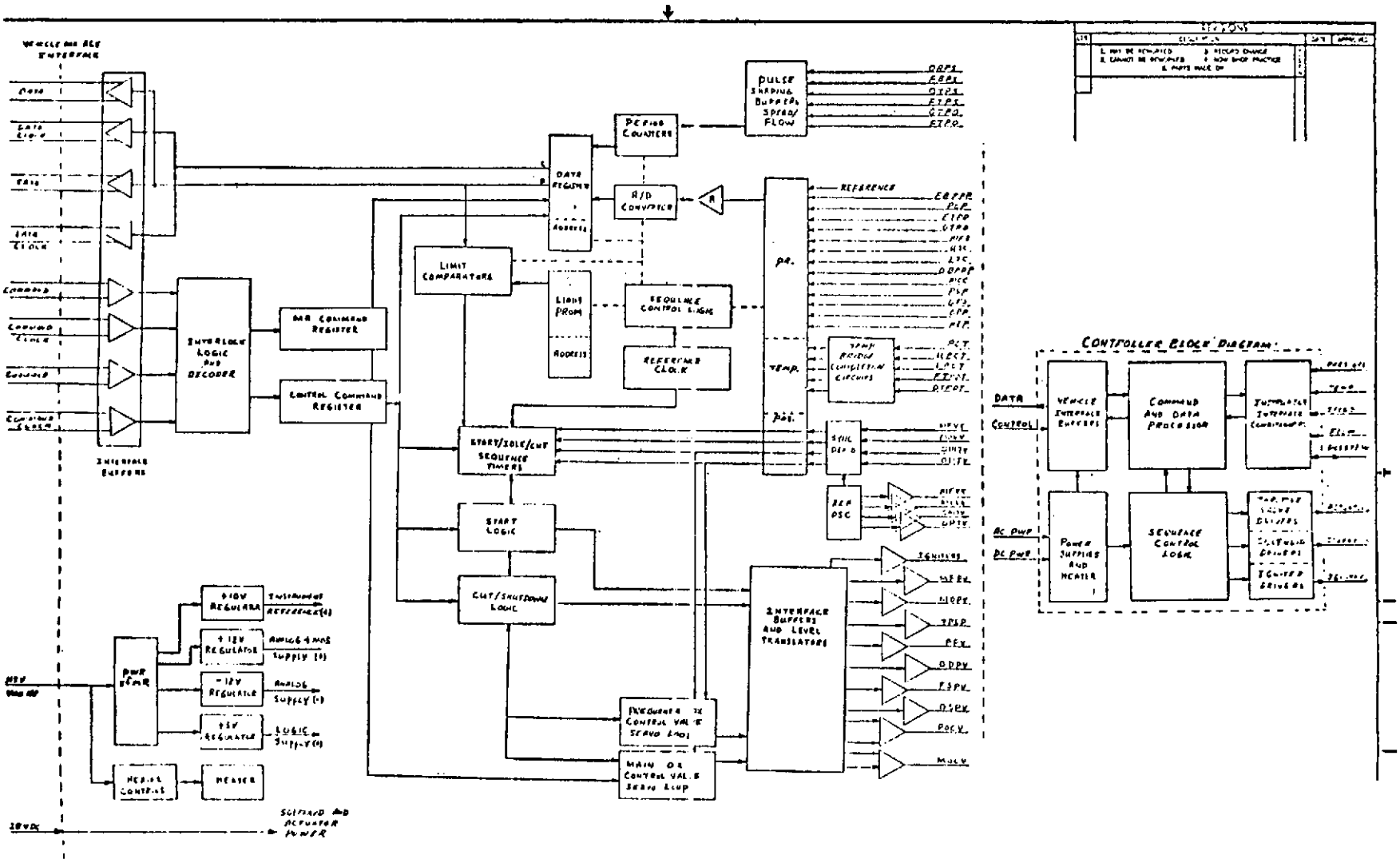

Figure 5-8. Controller Block Diagram

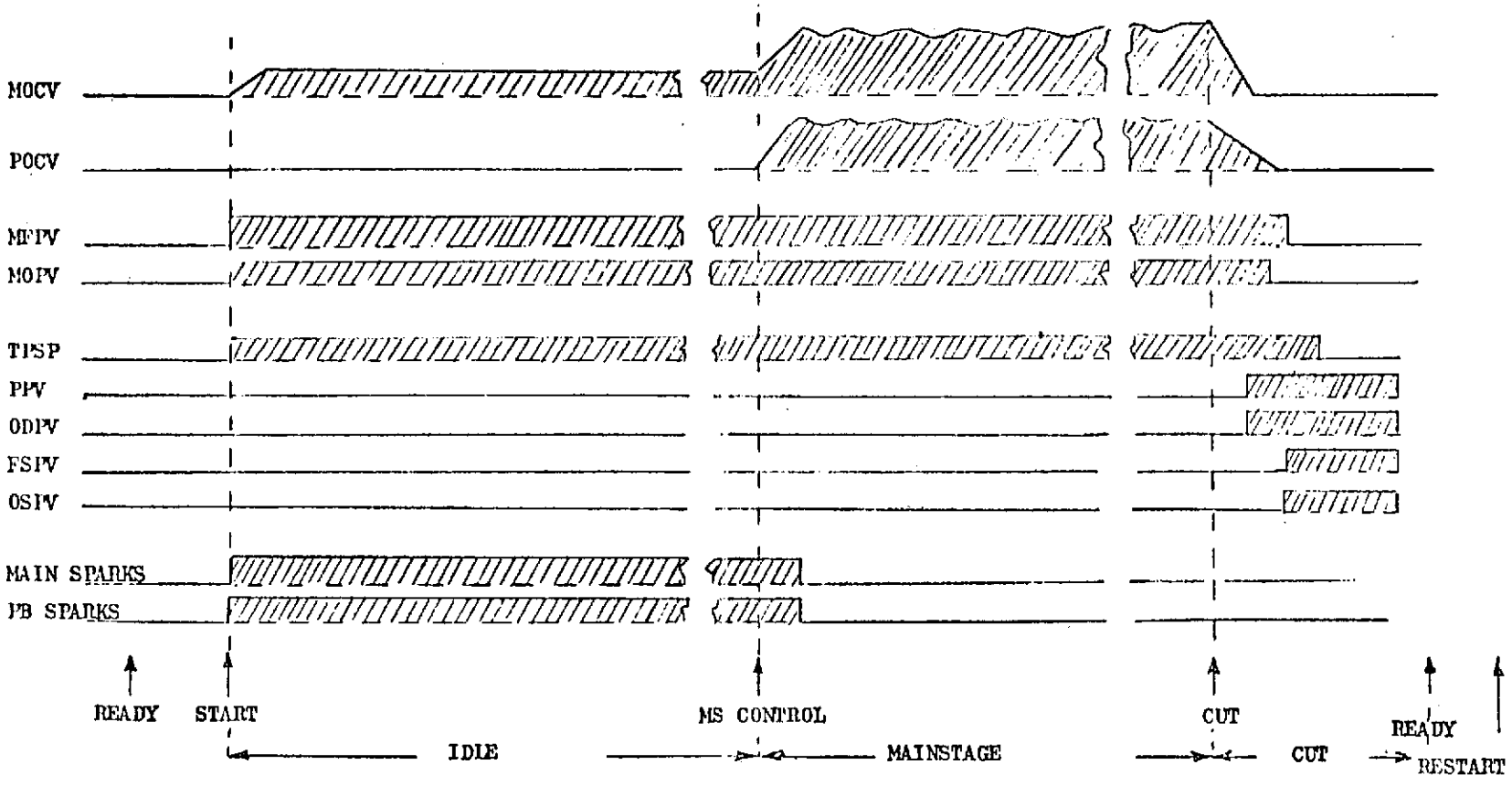

Figure 5-9. ASE Engine Control Valve Sequencing

TABLE 5-4. ENGINE INSTRUMENTATION REQUIREMENTS

Pressures	Instrument Type	Function 1	2	3	4	5	6	Abbreviation
Fuel Boost Pump Discharge	RC7003*	X			X			FBPDP
Oxidizer Boost Pump Discharge	RC7001	X			X			OBPDP
Preburner Outlet	RC7001				X		X	POP
Fuel Turbopump Discharge	RC7001	X		X	X		X	FTPD
Oxidizer Turbopump Discharge	RC7003*	X		X	X		X	OTPD
Main Fuel/Gas Injection	RC7001				X			MFI
Upper/Lower Jacket Coolant Discharge Pressure	RC7003*				X			UJC/LJC
Main Combustion Chamber	RC7001		X		X		X	MCC
Pneumatic System	RC7001				X	X	X	PSP
Oxidizer Pumps-Seals (purge)	RC7001				X	X	X	OPS
Oxidizer Purge System	RC7001				X	X	X	OPP
Heat Exchanger	RC7001						X	HEP
Temperatures								
Preburner Chamber	RC7004	X	X		X		X	PCT
Upper/Lower Bulk Coolant Temperature	RC7003*				X		X	UBCT/LBCT
Fuel Turbopump Discharge	RC7003*				X			FTPDT
Oxidizer Turbopump Discharge	RC7003*			X	X			OTPDT
Flowrates								
Oxidizer Turbopump Outlet	RC7005	X	X	X			X	OTPO
Fuel Turbopump Outlet	RC7005	X	X	X			X	FTPO
Speeds								
Oxidizer and Fuel Boost Pumps	RC7005				X		X	OBP/FBP
Oxidizer and Fuel Turbopumps	RC7005				X		X	OTP/FTP
Valve Positions								
Main Fuel Valve	POT	X			X	X	X	MFVX
Main Oxidizer Valve	POT	X			X	X	X	MOVX
Oxidizer Throttle Valve (main)	LVDT	X	X	X	X	X	X	OMTM
Oxidizer Throttle Valve (preburner)	LVDT	X	X	X	X	X	X	OPTV

Functions:

1. Engine Start and Cutoff Control
2. Engine Thrust Control
3. Mixture Ratio Control
4. Engine Monitor/Checkout
5. Engine Ready
6. Engine Limit Control

* Integral Pressure/Temperature Elements

TABLE 5-5. ABBREVIATIONS

MFPV = Main Fuel Pilot Valve
MOPV = Main Oxidizer Pilot Valve
MOCV = Main Oxidizer Control Valve
POCV = Preburner Oxidizer Control Valve
PPV = Preburner Purge Valve
ODPV = Oxidizer Dome Purge Valve
FSPV = Fuel System Purge Valve
OSPV = Oxidizer System Purge Valve
PI 1 = Preburner Igniter No. 1
PI 2 = Preburner Igniter No. 2
MI 1 = Main Igniter No. 1
MI 2 = Main Igniter No. 2
TPSP = Turbopump Seal Purge

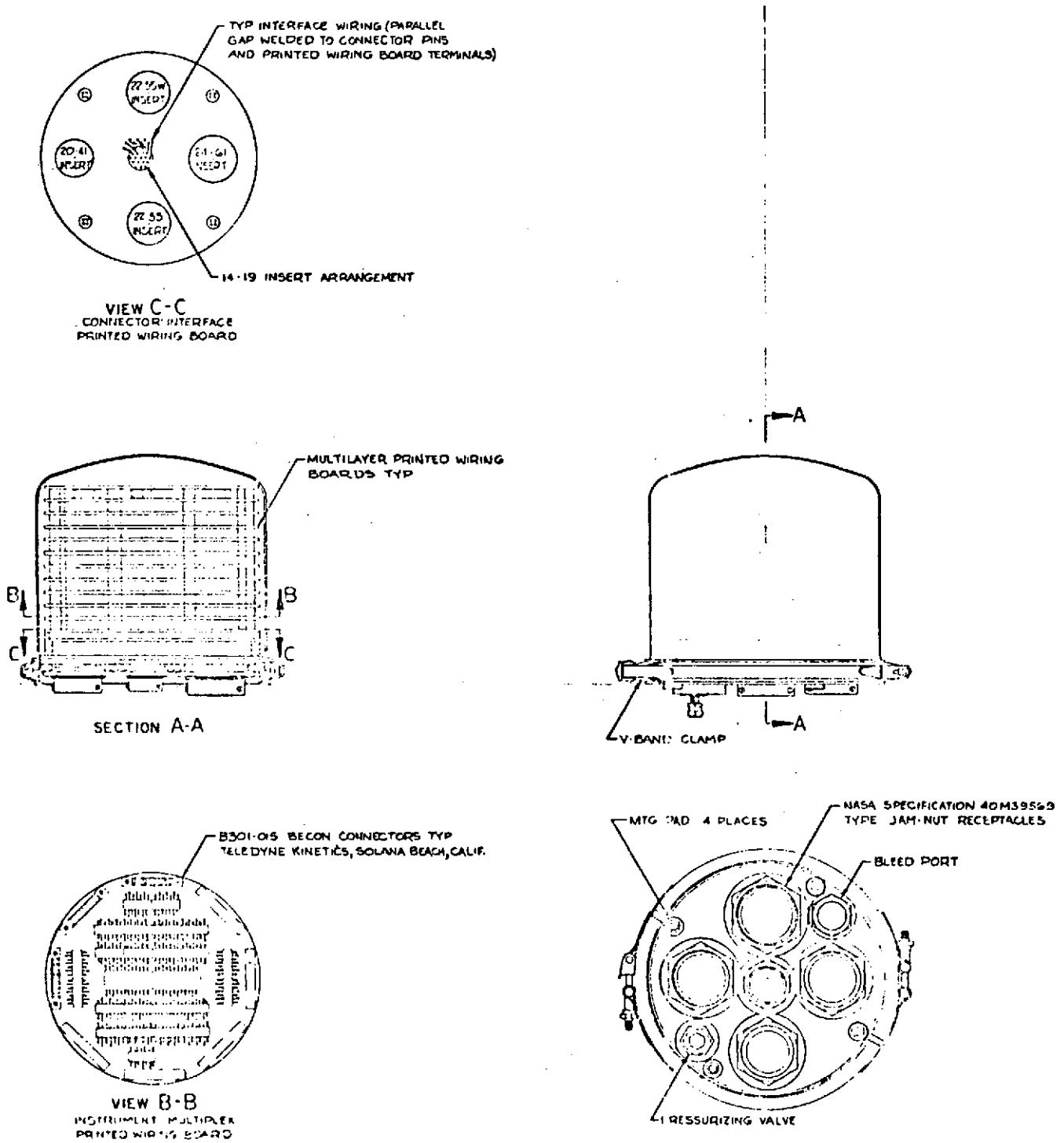

Figure 5-10. Engine Controller

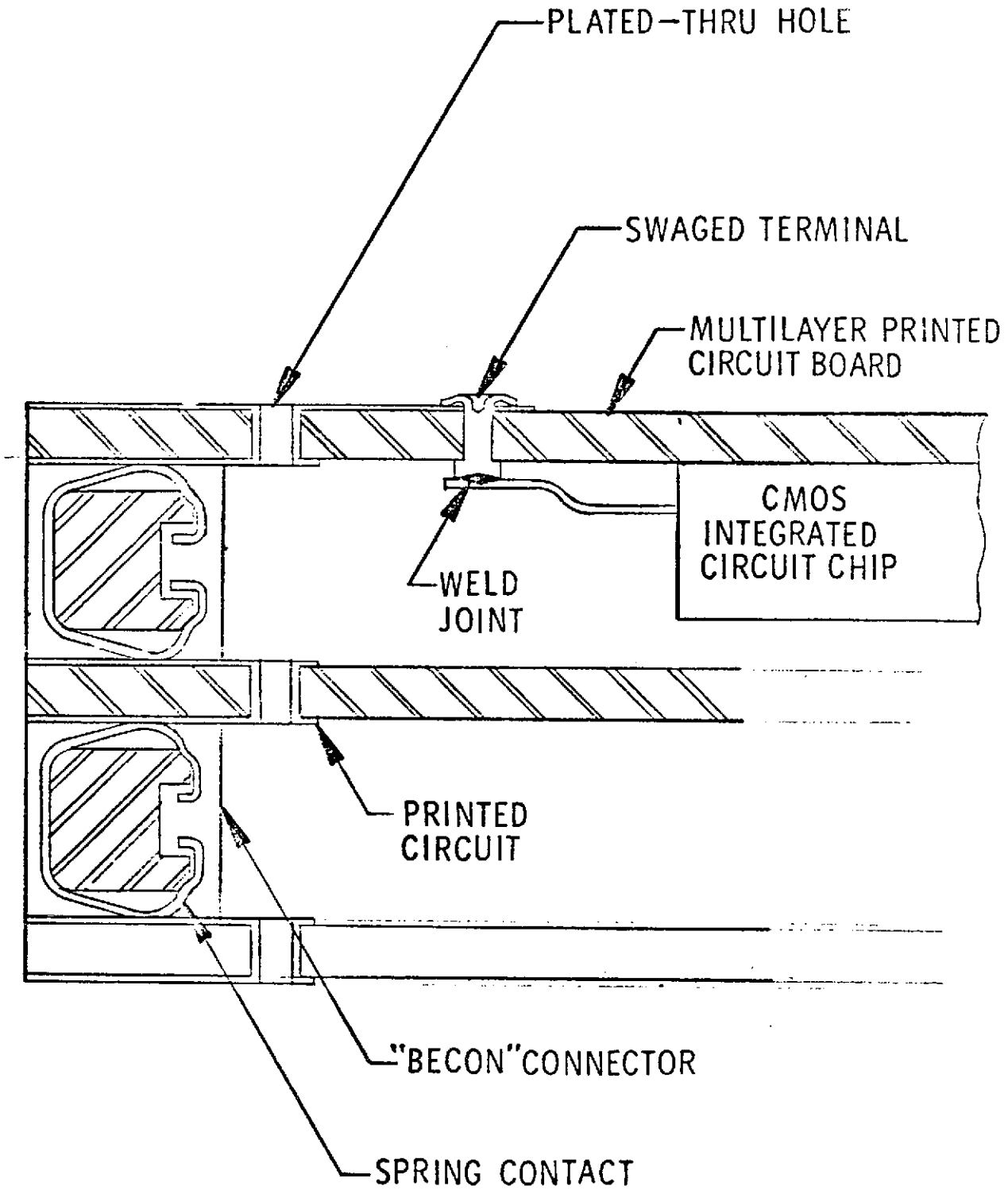

Figure 5-11. Typical PCB Assembly

manufacturers are presently introducing MOS product lines. Although no manufacturers are presently approved by NASA as sources for MOS devices, two manufacturers have NASA-approved TTL lines.

From approximations of circuits required, it is indicated that a complexity level of approximately 200 circuits and associated discrete components will be required. The controller package is sized based on this approximation. Alternate circuitry and optimum subsystem function assignment may lead to some slight simplification, but major reductions in component count and interconnects can be made through custom large-scale integration of functional subsystems. Several manufacturers offer computer-aided design programs for custom integration of circuits. Utilization of custom LSI could reduce component count by as much as two to three times with attendant deductions in interconnects and resultant increased reliability.

POWER REQUIREMENTS

The major power requirements can be approximated and tabulated as follows:

Item	No. of Units	Watts Each	Total Watts	
			Peak	Steady-State
Transducers				
Pressure/Temperature	18	0.1	1.8	
Speed/Flow	6	---	0	
Position	4	0.2	0.8	
Total			2.6	2.6
Actuators	2	210/90	420	90*
Solenoids	7	30	150*	90*
Spark System	4	10	40	40
Controller	1	35/25	35	25

*Corrected for % Duty Cycle and Sequence

From the approximatations, the power demand profile shown in Fig. 5-11 can be constructed. Figure 5-11 indicates that the peak system power requirement, approximately 600 watts, occurs at the initiation of mainstage. "Average" power dissipation for the system is anticipated to be on the order of 175 to 200 watts with peak demands of 400 to 600 watts (500 watts typical) occurring during operational phase transitions and during MR/P_c-commanded excursion transients.

INTERFACE REQUIREMENTS

Power

Total power requirements are defined in Fig. 5-12 and the above table. For general purpose usage, including igniter, throttle valve actuators, solenoid

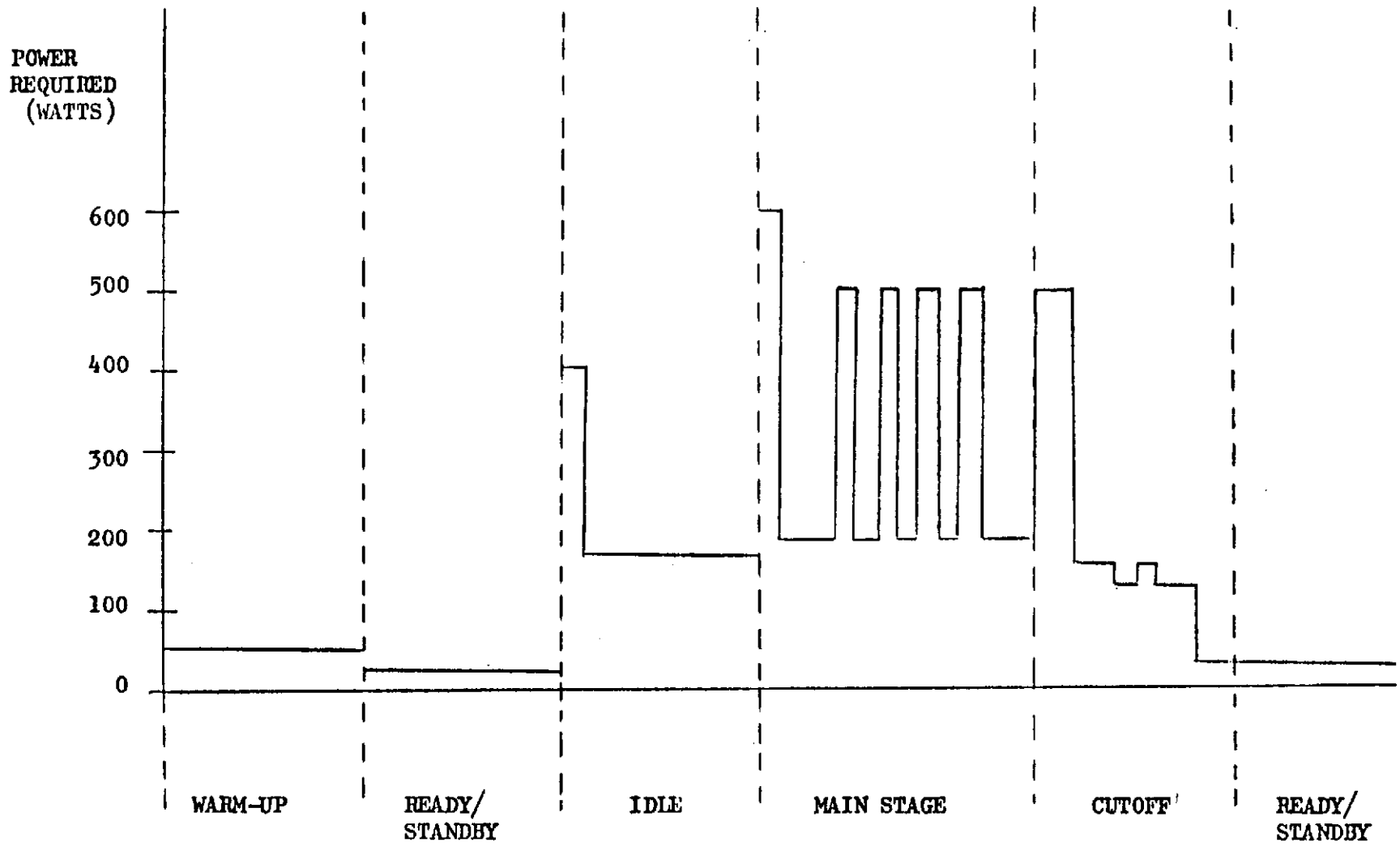

Figure 5-12. Power Requirements

valves, and interface driver excitation, 28 vdc is required. Power required to supply the controller internal regulators that provide logic, analog, and instrument reference supplier is 115 vac, 400 Hz, and 1 ϕ. Power demand is essentially constant at approximately 25 watts. The 28 vdc and 115 vac may be supplied from either vehicle or AGE sources.

Commands

Commands are received as an 18-bit word serial command clocked by the command source clock at a TBD (nominal 1-m Hz) rate. Two-bit positions are reserved for register control, 8-bit positions for MR command, and 8-bit positions for engine checkout and sequencing control commands. Inputs are TTL compatible and present an equivalent 9415 line receiver typical load. Commands may be transmitted from either the vehicle or AGE sources. Interlock logic is provided to lock out the nonoperational channel of the parallel input.

Data

Multiplexed engine data, including command check, controller status, controller reference, and transducer data are transmitted on the data bus as a 16-bit serial word, 1-m Hz nominal bit rate. Eight bits are reserved for the data address and 8 bits for the variable value. Serial transmission occurs in 16-bit bursts, nominal 1-m Hz rate, at a frequency of approximately 2K words/second. Output line drivers are TTL compatible and are equivalent to 9414 line drivers. Vehicle/AGE busses are parallel with individual drivers.

TASK VI: ENGINE DEVELOPMENT PROGRAM PLANS

To provide the full scope of information necessary for vehicle system assessment, the contract was extended to include determination of alternative engine program development plans and related costs. Also included were studies of packaging the engine to conform to a common interface and design of a retractable nozzle for minimizing engine stowed length. The plans are defined below.

Program Plan I - Minimum cost development of Flight Certified Engine (FCE). A minimum cost development program is defined as one that is not constrained to a tight (short) schedule and which makes optimum use of available facilities, hardware, and manpower to achieve the development of the engine at least cost. Overtime pay is likely to be minimized.

Program Plan II - Minimum time development of FCE. A minimum time development is defined as one that is constrained to a short schedule. Duplication of facilities and hardware is likely and considerable use is made of overtime to speed up operations and accomplish the goals quickly.

The results of the analysis are presented in Table 6-1. As shown, the shortening of the DDT&E effort by one year (from 59 months to 47 months) increases the cost by approximately 7 million dollars. The difference is primarily due to additional facility, tooling, STE and hardware requirements to facilitate the shorter schedule. The DDT&E cost in both cases includes five deliverable engines for vehicle integration support and related GSE. Also as shown, a total production cost for 50 engines plus spares is approximately 48 million dollars. The resulting first unit production cost of 1.46 million dollars reflects all associated costs of tooling, engineering support, etc. The 50-engine production costs at a rate of two per month were derived utilizing a 90-percent learning curve for manpower and 95 percent for material. The 10-year operational support effort includes continued engine testing concurrent with field operations to achieve the full 10-hour life demonstration as well as field support operations.

The study to determine the impact of packaging the engine to the RL10A-3-3 interface configuration was conducted and it was determined there was no significant impact on the engine in either cost or weight.

The retractable nozzle design study resulted in a design capable of reducing the engine length for transportation in the Space Shuttle to 128.27 cm (50.5 inches). The pneumatically operated system also results in an engine weight increase of 21.32 kg (47 pounds) with additional weight reduction possible through material substitution and removal of excess material. The impact on development cost was determined to be $1,338,000 and the increase in the per unit engine cost was $63,000.

The results of these analyses in conjunction with the engine configuration design studies provide well-defined bases for utilization in the Space Tug vehicle studies.

TABLE 6-1. ALTERNATIVE DEVELOPMENT PLAN SUMMARY

	PLAN I (Minimum Cost)	PLAN II (Minimum Time)
Development Program Duration (months)	59	47
DDT&E Cost	90,301,000	97,093,000
Production Cost (50 engines)	47,820,000	47,820,000
Unit Production Cost (1st unit/last unit)	($1.46\overline{M}$/$.907\overline{M}$)	($1.46\overline{M}$/$.907\overline{M}$)
Operations Cost (Continued life demonstration and 10-year field support)	11,550,000	11,550,000
Total	149,671,000	156,463,000

PLAN I: MINIMUM COST PROGRAM

The minimum cost ASE development program (Plan I) will be accomplished in 59 months. The engine, ground support equipment (GSE) and mockups will be designed, tested and verified in accordance with the overall program schedule shown in Fig. 6-1. Formal demonstrations will be performed to provide the basis for Preliminary Flight Certification (PFC) and Final Flight Certification (FFC). The objective of minimum cost will be achieved by:

1. Optimum Use of existing facilities for fabrication, assembly and testing.

2. Employing knowledge gained from similar rocket engine development programs such as the Space Shuttle Main Engine (SSME).

3. Scheduling major program milestones realistically to minimize need for premium time labor.

4. Emphasizing analyses and component testing early in the program to minimize engine testing.

Activities leading toward accomplishment of each phase of the development program are presented herein.

The production program will be a 46-month effort initiated by long-lead hardware release following Critical Design Review (CDR). The first engine will be delivered in month 68, and the desired two-per-month rate will be achieved by month 70. The fiftieth engine will be delivered in month 93.

The Operations and Flight Support (O&FS) effort will be initiated with engine integration efforts at the outset of the program and will continue through 10 years of operational support. The operational support is assumed to begin at point of initial operational capability (IOC) which, in turn, is assumed to occur following FFC. The 10-year effort will be completed 15 years and 11 months (191 months) after program go-ahead.

DEVELOPMENT PLAN

The minimum cost development program for an advanced space engine capable of a vacuum thrust of (88,964 newtons) 20,000 pounds will consist of a design demonstration phase and a certification phase. The design demonstration phase will require approximately 40 months to complete. This phase will emphasize analysis and component testing to verify basic concepts and features prior to initial engine testing. Intensive laboratory testing will be conducted to verify functional characteristics and structural margins of critical components. Additionally, hot-fire tests will be accomplished on component subassemblies such as the thrust chamber assembly and turbopumps to verify performance and service life predictions.

Page intentionally left blank

Page intentionally left blank

Initial design releases for procurement of long-lead hardware to support component, subsystem, and engine testing will be completed 9 months from program start. All detail parts drawings for the first R&D engine will be released 12 months from program start. A preliminary design review is scheduled 30 months after program start to allow for feedback of design information resulting from the extensive component test program and early engine system testing. Following completion of the PDR, the engine design will be essentially frozen. Only mandatory design changes resulting from customer request and engine testing will be allowed thereafter. The Critical Design Review is scheduled 50 months from program start. After completion of the CDR, the design will be frozen except for changes required by changes to the Contract End Item (CEI) specification.

Thrust chamber assembly hot-fire tests will be initiated approximately 18 months after program start. Preburner hot-fire testing will commence approximately 12 months after program start. Low- and high-pressure turbopump hot-fire testing will be initiated approximately 14 and 19 months, respectively, after program start. Simulation of the engine operating environment will be stressed during subsystem hot-fire testing. These tests will be accomplished on existing test facilities at the Santa Susana Field Laboratory which have been modified for the specific engine hardware.

The first site engine test will be conducted approximately 25 months after program start, with the first altitude simulation test conducted approximately 26 months after program start. These engine test stands also will be located at the Santa Susana Field Laboratory. The two site test stands will be existing facilities which have been modified for testing the advanced space engine. Engines tested in these facilities will have a nozzle expansion ratio (ϵ) of 8:1 to preclude nozzle separation side loads. The primary test objectives to be achieved with these engines include:

1. Evaluation of engine ignition characteristics (preburner and main chamber)

2. Evaluation of engine sequencing

3. Evaluation of engine input requirements such as NPSH, propellant inlet temperatures, etc.

4. Evaluation of engine service life

The altitude simulation engine test facility also will be modification of an existing facility; however, major changes will be required. Engines tested in this facility will have a nozzle expansion ratio (ϵ) of 400:1. The primary objectives of testing in this facility include, in addition to those listed for the site test facilities, performance evaluation under altitude simulation conditions and start and shutdown transient characteristics.

The certification phase of the development program will occur during the last 19 months of the program. Major emphasis during this period will be directed toward the demonstration of flight readiness. All major performance parameters will be

demonstrated to be within CEI specification limits by PFC, except for service-free life and life between overhauls. Program control to assure completion of all required demonstrations to achieve certification will be by means of Design Verification Specifications (DVS). Completion of the certification demonstration described in each of the DVS's will provide the basis for PFC. The test requirements for the PFC demonstration are given in the engine development section of this plan.

Component and subsystem testing will be continued during the certification phase but at a reduced rate necessary to support engine testing and field operations. The most significant milestone of the certification phase will be completion of the Final Flight Certification test program. The requirements for this program are also given in the engine development section of this plan. The test effort is summarized in Fig. 6-2.

Component Testing

The minimum-cost development program (Plan I) provides for a concentrated component development program prior to initial engine testing. This effort will consist of early verification of all functional components through laboratory and subsystem hot-fire testing. Thermal and mechanical fatigue life, structural integrity, performance and operational characteristics will be evaluated and verified. Approximately 1500 component level tests will be conducted in the laboratory which will simulate the engine environment in all practicable limits.

Subsystem hot-fire testing will be concentrated on the verification of life, stability and performance. Testing of the thrust chamber assembly, low- and high-pressure oxidizer and fuel pumps with preburners will be accomplished at test facilities located at the Santa Susana Field Laboratory. Approximately 750 subsystem hot-fire tests will be conducted to verify requirements and assumptions, thereby minimizing the extent of engine testing required. The specific requirements for component testing of each component and subsystem are delineated in the following paragraphs.

Turbomachinery. The 88,964 N (20,000 pound) thrust advanced space engine turbomachinery consists of four turbopumps: one low-pressure and one high-pressure pump for each propellant, liquid oxygen and liquid hydrogen. The high-pressure turbines are driven by hot gas (H_2 plus H_2O), while the low-pressure turbines are driven by ambient-temperature GH_2. Because the engine uses a topping cycle, the operating characteristics of the pumps and turbines are critical and interdependent with each other and with the rest of the system. Therefore, engine balance requirements and design analysis of the turbomachinery will be critical to successful engine operation.

The minimum-cost program is success oriented and, as such, assumes that no major turbopump development problems will be encountered. The primary objectives of the turbopump test program are to verify the performance and mechanical integrity of the four turbopumps at the engine operating conditions. It is assumed that the technology for the turbopump bearings and seals will be available from current technology program(s). Therefore, no separate testing of these components will be required. A complete engine balance will be firmly established early in

Page intentionally left blank

the program, providing a basis for turbopump operating requirements. The technology available from the SSME and other engine programs will be utilized to a maximum to reduce the development risks and eliminate the need for extensive development testing.

The four turbopumps, a high-pressure oxidizer, high-pressure fuel, low-pressure oxidizer, and low-pressure fuel, will be tested separately. In this manner, the operating characteristics of each of the four turbopumps can be determined independently. This approach also allows testing of each of the turbopumps without being dependent on the availability of one or more of the other turbopumps.

A total of three each high- and low-pressure oxygen and hydrogen turbopump assemblies will be utilized during the component hot-fire test program. Each high-pressure turbopump will be recycled at least once to allow disassembly inspection for life assessment. Two of the low-pressure turbopumps are planned for disassembly inspection. The individual test duration and accumulated life prior to recycle will be based on test data and concurrent analyses. The schedule for fabrication and testing of the turbomachinery is shown in Fig. 6-3, with a breakdown of the individual tests shown in Fig. 6-4 and 6-5.

Turbine Development Testing. Initially, a turbine from each turbopump will be subjected to a series of 20 spin tests on a dynamometer in the Rocketdyne Canoga Park Development Laboratory. The test series will be conducted using gas nitrogen and will result in complete turbine mapping when the difference in gas properties between the gaseous nitrogen and the actual gases utilized by the turbines in the engine are accounted for analytically. Five different power levels at four different inlet pressures will be investigated to establish the turbine maps.

Low-Pressure Turbopump Testing. The low-pressure turbopumps, by virtue of their relative simplicity, low rotational speed which is below the rotor first critical speed, and low turbine gas temperature, require less development than the high-pressure turbopumps. Initial testing will be conducted to verify the hydrodynamic performance of the pump (Test d, Fig. 6-4).

Suction performance testing will be investigated in a series of three 200-second-duration tests (e, f, and g, Fig. 6-4). Efficiency of the pumps will be determined utilizing the pump H-Q performance and known performance of the turbines obtained during dynamometer testing.

As testing proceeds, the mechanical integrity of the pumps will be verified (test h through o, Fig. 6-4) to the point that it is considered safe to install the turbopump on an engine. All full-life integrity verification testing will be conducted on the engine. This eliminates the need for full-life demonstrations at both the component level and on the engine which conforms to the minimum-cost philosophy.

High-Pressure Turbopump Testing. The initial testing conducted with the high-pressure turbopumps (tests a through g, Fig. 6-5) will utilize ambient hydrogen gas to drive the turbines. The tests will be utilized to gain mechanical integrity confidence and initial hydrodynamic performance data. Full-power,

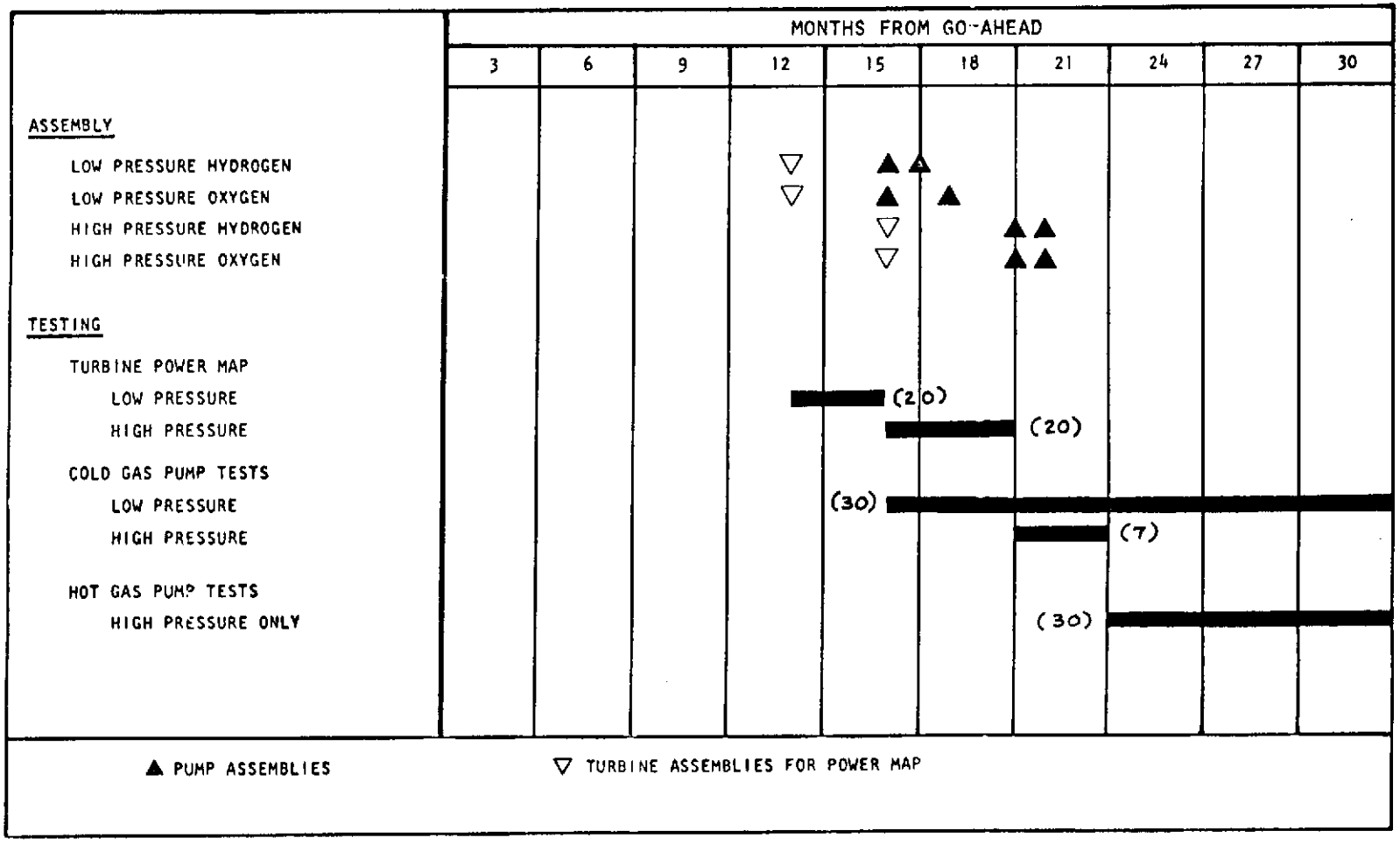

Figure 6-3. Component Turbomachinery Assembly and Test Schedule

Test Type	T/P Unit	Propellants		No. of Tests	Duration seconds	Remarks
		Pump Oxid/Fuel	Turbine			
Map Turbine in Dynamometer Facility	--	--	GN_2	20	200 EA	
Ambient Gas T/P Spins in T/P Test Facility	1st	LO_2/LH_2	GH_2			
(a) Ramp to 50% Design Speed at Nom. Q/N		↓	↓	1	30	Bring to speed slowly
(b) Ramp to 75% Design Speed at Nom. Q/N				1	30	Bring to speed slowly
(c) Ramp to 100% Design Speed at Nom. Q/N				1	30	Bring to speed slowly
(d) Vary Q at Design Speed				1	200	G-Q, Eff. Type Test
(e) NPSH vs HD at Nom. Q/N and Speed				1	200	Suction Performance Check
(f) NPSH vs HD at 5.5 M/R Q and N				1	200	Suction Performance Check
(g) NPSH vs HD at 6.5 M/R Q and N				1	200	Suction Performance Check
(h) Ramp to 110% Speed				1	30	Overstress Check
(i) Full Duration at Nom. Q and N				1	2000	
(j) Full Duration at 5.5 M/R Q and N				1	2000	
(k) Full Duration at 6.5 M/R Q and N				1	2000	
(l) Repeat (e)				1	200	
(m) Repeat (f)				1	200	
(n) Repeat (g)				1	200	
(o) Full Duration at Highest Turbine HP Condition				1	2000	
Repeat (a) through (o)	2nd	LO_2/LH_2	GH_2	15	9520	

Figure 6-4. Low-Pressure Oxidizer and Fuel Turbopump Development Test (Program 1)

Test Type	Unit	Propellants		No. of Tests	Duration seconds	Remarks
		Pump Oxid/Fuel	Turbine			
Map Turbine in Dynamometer Facility	--	--	GN_2	20	200 EA	
Ambient Gas T/P Spins in T/P Test Facility	1st	LO_2/LH_2	GH_2			
(a) Ramp to 50% Design Speed at Nom. Q/N				1	30	Bring to Speed Slowly
(b)) Ramp to 75% Design Speed at Nom. Q/N				1	30	Bring to Speed Slowly
(c) Ramp to 100% Design Speed at Nom. Q/N				1	5	High Acceleration Ramp Analyze for Critical Speed
(d) Vary Q at Design Speed				1		H-Q, EFF, Type Test
(e) NPSH vs HD at Nom. Q/N and Speed				1		Suction Performance Check
(f) NPSH vs HD at Low Q/N and Nom. Speed				1		Suction Performance Check
(g) NPSH vs HD at High Q/N and Nom. Speed				1		Suction Performance Check
Hot Gas T/P Tests in T/P Test Facility	1st	LO_2/LH_2	H_2+H_2O			
(h) Ramp to 100% Design Speed at Nom. Q/N				1	5	High Acceleration Ramp. Facility, T/P Checkout
(i) Vary Q at Design Speed				1	200	H-Q Type Test
(j) Full Duration at Nom. Q and N				1	2000	
(k) Full Duration at Nom. Q and N for 5.5 M/R				1	2000	
(l) Full Duration at Nom. Q and N for 6.5 M/R				1	2000	
(m) Ramp to 110% Speed at Nom. Q/N					30	Overstress Check
(n) NPSH vs HD at Nom. Q/N and Speed				2	200 EA	Suction Performance Check
(o) NPSH vs HD at 5.5 M/R Q and N				2	200 EA	Suction Performance Check
(p) NPSH vs HD at 6.5 M/R Q and N				2	200 EA	Suction Performance Check
(q) Vary Q at 80% Speed (LH_2 T/P Only)				1	200	Determine Effects of Compressibility on Efficiency
(r) Vary Q at 90% Speed (LH_2 T/P Only)				1	200	Determine Effects of Compressibility on Efficiency
(s) Full Duration at Highest Turbine HP Condition				1	2000	
Repeat (h) through (s) Above	2nd	LO_2/LH_2	H_2+H_2O	15	9835	

Figure 6-5. High-Pressure Oxidizer and Fuel Turbopump Development Tests (Program I)

full-duration testing will then commence, utilizing perburner hot-gas products to drive the turbines (tests h through s, Fig. 6-5). Periodic inspections of the turbine components will be conducted to verify structural integrity after exposure to full power, pressure, thermal, and rotational stresses.

Testing will emphasize determination of hydrodynamic performance characteristics over the full range of operating conditions required to operate the engine at mixture ratios of 5.5 to 6.5. Suction performance tests will be conducted to verify that the input conditions to the high-pressure pumps as provided by the low-pressure pumps will be satisfactory.

As in the case of the low-pressure turbopumps, full-life integrity verifications will be conducted at the engine level.

Also during these tests, sufficient instrumentation will be provided to ensure that the rotor dynamics of the turbopump assemblies remain within acceptable limits. Disassembly and inspection of the hardware after testing will determine if any unusual conditions such as excessive wear has occurred.

The data from the high-pressure as well as the low-pressure turbopump tests will be utilized in the engine start model and mainstage computer programs to ensure engine compatibility.

Controls and Valves. The 88,964 N (20,000 pound) thrust advanced space engine requires four primary control valves (main oxidizer valve, main fuel valve, preburner oxidizer control valve, and main chamber oxidizer control valve), an antiflood valve to prevent oxidizer flow to the heat exchanger until hot gas is flowing through it, and numerous check valves to prevent reverse flow of the propellants.

The basic technology for these valves has been established under numerous related programs at Rocketdyne, and only verification testing in the Development Laboratory will be necessary under the minimum-cost program.

The controls and valves component test plan shown in Table 6-1 provides for completing the specified types of tests on individual valve assemblies in accordance with the schedule presented in Fig. 6-6. The two main propellant valves (O_2 and H_2) are identical in design to minimize cost, as are the preburner oxidizer valve and the main chamber oxidizer valve. The required quantities of each valve are shown in Table 6-2, which provides sufficient hardware for functional and destructive testing.

Water Flow Test. The purpose of this test is to verify that the component can meet the fluid flowrate and pressure drop requirements specified. This verification can be accomplished most economically with water, and will be conducted in the flow area of the Engineering Development Laboratory at Rocketdyne.

Tests will be performed to establish the flow versus ΔP characteristics of the component, and the envelope of flowrate versus ΔP at various valve positions will be explored. Posttest inspection of the component will be made to ensure that no

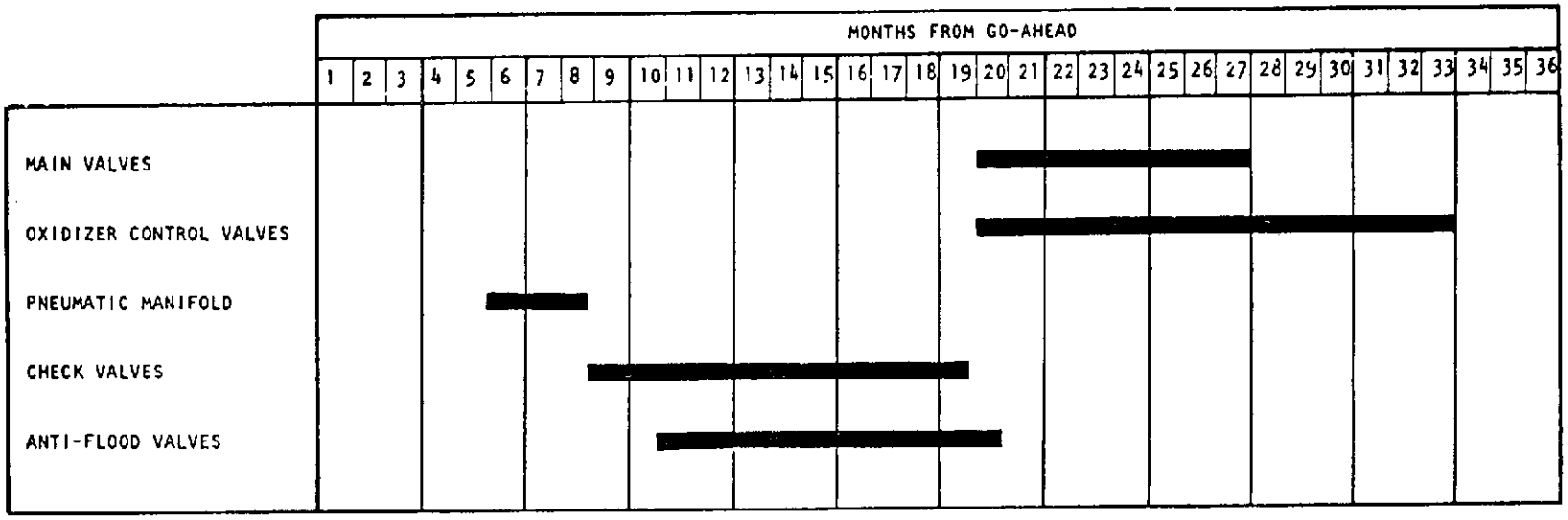

Figure 6-6. Controls and Valves Test Schedule

TABLE 6-2. CONTROLS AND VALVES TEST PLAN

Component	Tests Required								
	Proof Test	Leak and Functional	Water Flow (ΔP)	Dynamic Torque	Environmental	Endurance	Ignition Proof	Vibration	Burst
Main Propellant Valves (MOV/MFV)	3	3	1	1	0	2	0	2	1
Oxidizer Control Valve (Preburner and Main Chamber)	3	3	1	1	0	2	1	2	1
Pneumatic Manifold	2	2	-	-	0	1	1	0	1
Antiflood Valve	3	3	1	-	0	2	0	2	1
Purge and ASI Check Valves	6	6	2	-	0	4	0	4	2

Number of assemblies required:

Main Propellant Valves: 3

Oxidizer Control Valves: 3

Pneumatic Manifold: 2

Antiflood Valve: 3

Purge and ASI Check Valves: 6

abnormal degradation of the mechanical elements occurred. These data will be compared to the requirements at the specified differential pressures, and the data will be correlated with the flow coefficients used in the design to establish the valve size. Testing one unit is sufficient to generate flow versus P data for the component.

Verification will be considered complete when the envelope of flow versus ΔP has been completed as described above and when analytical correlation indicates that the flowrate and pressure drop requirements are met.

Dynamic Flow Torque Test. The purpose of this test is to verify that the actuator loads encompass the maximum dynamic torque loads of the component. This verification can be accomplished in conjunction with the water flow test.

The fluid dynamic torque will be measured while flowing water through the valve at several valve positions over its full angular travel. The dynamic flow torque test data will be used to establish the fluid dynamic flow torque during the excursion of the component and will be compared with the flow torque coefficients used in the design to establish the power requirements of the actuator.

Verification will be considered complete when the test data have been recorded and correlated to verify the requirements.

Endurance Test. The purpose of this test is to verify that the component can meet the specified cycle/environment requirements in Table 6-3. Ambient, cryogenic, and high-temperature cyclic and functional testing will be conducted in the mechanical area of the Rocketdyne Engineering Development Laboratory to demonstrate this capability.

The values will be functionally tested, cycled under the required environment, and functionally tested at selected points in the cycle series, and again at the conclusion of each test series.

Verification will be considered complete when the units have successfully completed the required cycles and have subsequently met the functional test requirements.

Vibration Test. The purpose of this test is to verify that the component can meet specified vibration requirements. To demonstrate this, each component will be subjected to tests conducted in the vibration area of the Rocketdyne Engineering Development Laboratory.

Components will be mounted to a vibration table with a three-phase stabilizing fixture simulating the engine mounting configuration. The component will be thermally conditioned to 88.9 ±27.8 K (160 ±50 R) during vibration, and will be vibrated in its normal engine operating mode (open) as experienced during engine operation. With the valve open, pressures will be applied to the propellant inlet port, and acceleration levels will be monitored at various points on the component

TABLE 6-3. ENDURANCE CYCLE TEST REQUIREMENTS

	MOV AND MFV	OCV	AFV	CV	Pneumatic Manifold
Ambient Temperature					
T = 530 R (294 K)					
Pressurized Cycles	3,300	3,300	3,300	3,300	3,300
Cryogenic Temperature					
T = 160 ±50 R (88.9 ±27.8 K)					
Pressurized Cycles	682	682	682	682	451
Zero Pressure Cycles	440	440	440	--	--
High-Temperature					
$T = 590\ ^{+10}_{-0}$ R ($327.8\ ^{+\ 5.6}_{-\ 0}$ K)					
Ambient Pressure Cycles	1,540	1,540	1,540	1.540	1,540
Modulation Tests					
T = 160 ±50 R (88.9 ±27.8 K)					
2.5% Range					
26% Nominal Position	--	40,000	--	--	--
36% Nominal Position	--	4,000	--	--	--
Total Cycles	5,962	49,962	5,962	5,522	5,291

to determine acceleration amplification. A functional test will be performed after completing vibration in each axis. The component will be disassembled and inspected following the final functional test.

The acceleration amplification factor between the input to the vibration table and the greatest output on the component will be used to predict peak acceleration loads on all component appendages. These loads will be correlated with the vibration levels measured during engine hot-fire tests. In the event the engine test levels are more severe, additional vibration tests will be conducted to verify the revised requirements. In the event the engine test vibration levels are less severe, the requirements will be revised accordingly prior to testing additional units.

Verification will be considered complete when the units specified have successfully met the functional test requirements and no structural damage or detrimental wear are noted during posttest disassembly.

Burst Test. The purpose of this test is to verify that the component can meet specified ultimate pressure and safety factor criteria requirements. The test will be conducted in the mechanical area of the Rocketdyne Engineering Development Laboratory.

Strain gage data will be used to determine the working stress and to verify that the component meets the minimum yield factor of safety at the limit pressure. Burst test data will also be evaluated to verify that the component meets the requirements for minimum ultimate factor of safety and the minimum ultimate pressure as defined.

Verification will be considered complete when one unit completes the burst test and the resulting data shows that the component meets the minimum yield factor of safety without yielding which is detrimental to proper operation and also meets the minimum ultimate factor of safety and ultimate pressure as defined.

Functional Test. The purpose of this test is to establish the functional condition of the component. This will be accomplished by performing leakage and actuation tests in the clean room area of the Rocketdyne Engineering Development Laboratory.

The functional test will be conducted prior to and subsequent to individual verification tests, noted in Table 6-4, subsequent to each axis of vibration test, and after specified number of cycles during the endurance test.

The leakage test will be conducted at both ambient and cryogenic temperatures with the component thermally conditioned to the temperature specified. The leakage will be measured using helium over the pressure range specified.

TABLE 6-4. FUNCTIONAL TESTS

Verification Test	Number of Units Allocated	Minimum Number of Units	Minimum Number of Tests per Unit
Vibrate all Valves	2*	2*	1*
Endurance			
MOV/MFV	2	2	1
OCV	2	2	1
AFV	2	2	1
CV (2 designs)	2 (each design)	2 (each design)	

*One pneumatic manifold

The actuation test will be conducted at both ambient and cryogenic temperatures with the componet thermally conditioned to the temperature specified. Travel time from full closed to full open and return to full closed will be measured.

The functional test data will be correlated with data from prior tests to determine whether the specific verification test adversely affected the functional performance of the component. The functional test does not verify any specific requirement but merely establishes the functional condition of the component during a specific verification test and is a criteria for establishing the successful completion of the specific verification test.

Development testing of the combustion devices will be accomplished through a series of laboratory tests and component hot-fire tests at the Santa Susana Field Laboratory. The schedule for accomplishing the required tests is presented in Fig. 6-7. The following is a description of the tests planned for each device.

Ignition System. The ignition system for the 88,964 N (20K) ASE consists of two spark-initiated ASI assembly units, one each for the preburner and main chamber. Basically, each unit consists of a common integral air-gap spark igniter, a fuel-oxidizer injection scheme, and a combustion chamber. The overall development schedule for both the spark igniter units and the ASI assemblies is shown in Fig. 6-8.

The integral spark igniter development will consist of preliminary design, breadboard igniter lab testing, final design, and lab testing of the finalized concept.

Key lab tests include functional, electrical/electronic, vibration, environmental, pressure and leak verification testing. Twelve equivalent spark units are required for the lab test series: five units in a 6-month prototype optimization effort to evaluate the funcational and electrical characteristics, and seven units in a 9-month final verification effort to demonstrate vibration, environmental, pressure, and leakage characteristics.

Development of the ASI assemblies for both the preburner and the main chamber will consist of materials and processes testing, cold-flow lab testing, and igniter-only hot-fire testing at both low and high pressure. The low-pressure hot-fire testing will demonstrate the engine ignition sequence, while the high-pressure (mainstage) testing will investigate steady-state operating mixture ratio and demonstrate cooling and durability.

Two assemblies (one of each type for the preburner and the main chamber) will be required for the lab testing, and four assemblies (two of each type) will be required for the hot-fire testing. Initial testing will be conducted with prototype igniter units, and additional testing will use the final design. Seventy low-pressure tests (ignition-only) of 5-second average duration will evaluate start characteristics and spark energy requirements for the preburner ASI. An additional 35 high-pressure (mainstage) tests of 50 seconds average duration will be conducted to evaluate power level and mixture ratio, cooling, and life characteristics Along with the preburner ASI tests will be 30 low-pressure and 35 high-pressure tests on the main thrust chamber ASI.

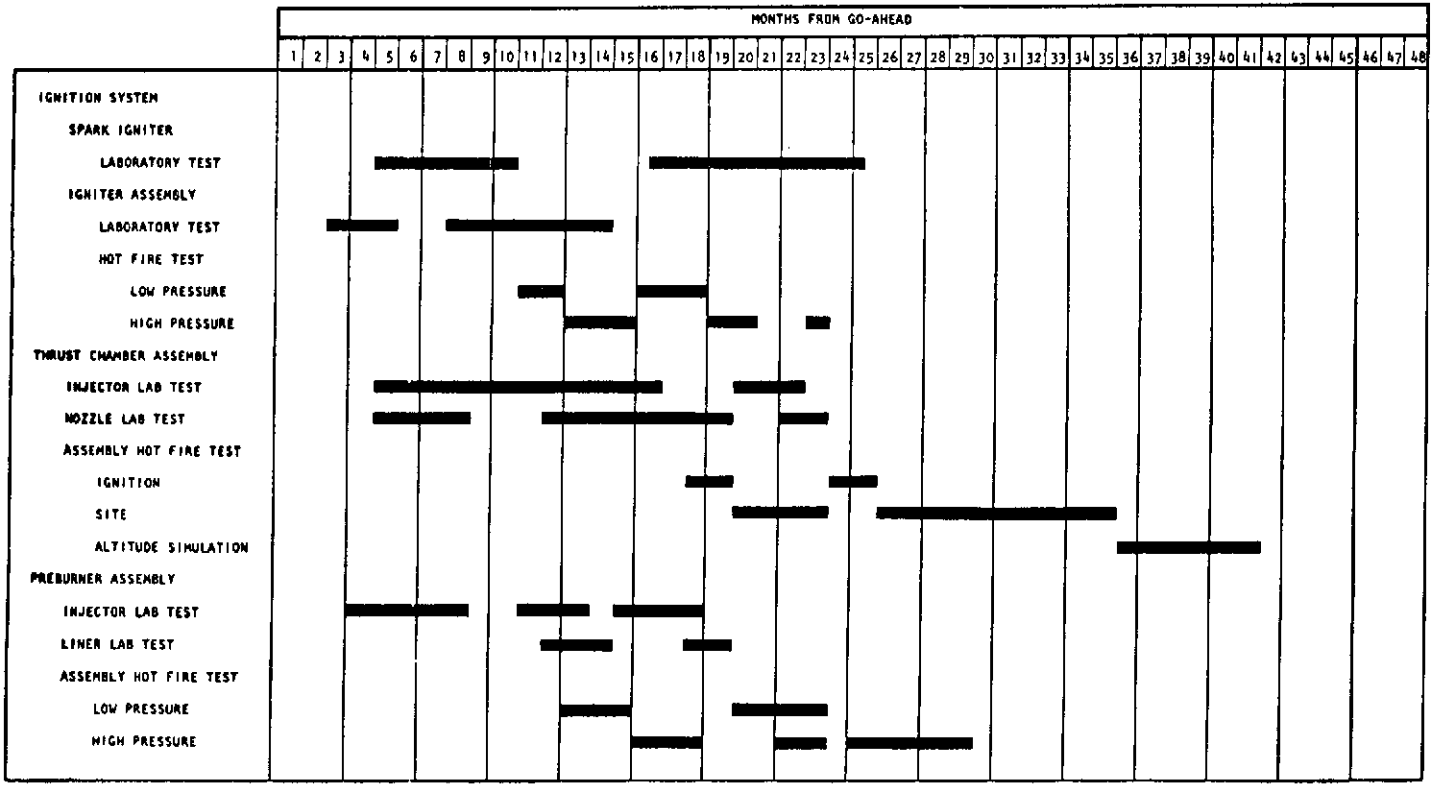

Figure 6-7. Combustion Devices Test Schedule

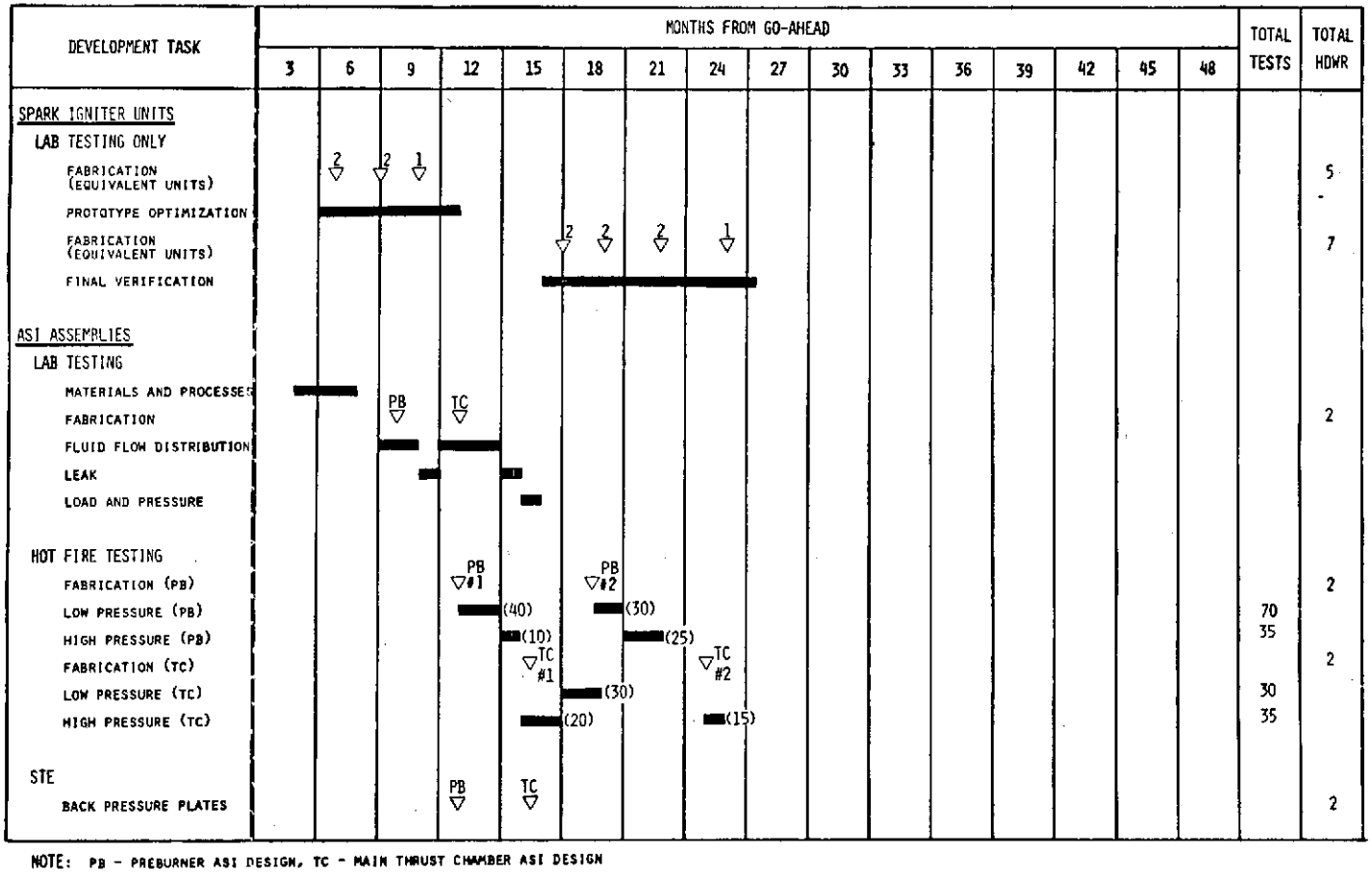

NOTE: PB - PREBURNER ASI DESIGN, TC - MAIN THRUST CHAMBER ASI DESIGN

Figure 6-8. Ignition System Development

To simulate engine conditions, two special backpressure plates (one for the preburner and one for the main chamber) must be fabricated to accomplish the hot-fire test program.

Thrust Chamber Assembly. The thrust chamber assembly consists of major components such as the injector, combustion chamber with a short nozzle ($\epsilon = 8$), a regeneratively cooled nozzle extension to $\epsilon = 100$, and a dump-cooled nozzle extension from $\epsilon = 100$ to $\epsilon = 400$. These chamber component designs will be finalized and detailed for thrust chamber-only testing and for engine testing. Chamber-only test hardware will vary only in hot-gas manifolding and interface attachment techniques. The overall development schedule for the thrust chamber is shown in Fig. 6-9, and consists of both cold-flow lab testing and hot-fire chamber-only testing.

Primary lab tests will include injector element flow, injector assembly flow, nozzle wind tunnel, nozzle coolant flow distribution, acoustic cavity tuning, leak, load, and pressure testing.

Twelve individual injector elements will be fabricated to study the element flow characteristics, and a full-scale injector flow model will be fabricated to study the injector flow distribution and element vortex shedding. An acoustic cavity model will also be built to perform the acoustic cavity tuning studies for the injector.

One nozzle wind tunnel model will be fabricated to study the nozzle flow and separation characteristics associated with the 400:1 extension, and a full-scale nozzle will be fabricated to perform flow distribution studies. A thrust chamber assembly from the hot-fire program will be used to perform the leak, load, pressure, and gimbaling tests. A special leak test fixture must also be fabricated to perform the leak test.

Six chamber assemblies will be fabricated to conduct the hot-fire test program, the first four with a short 8:1 nozzle, and the last two with a full 400:1 nozzle. Two preburners and two turbine and hot-gas manifold simulators will be part of the STE required for these tests.

A total of 40 low-pressure ignition tests (5 seconds average duration) will be conducted to establish the ignition requirements and start and cutoff sequences. One hundred sixty additional high-pressure-sea level tests (100 seconds average mainstage duration) will be conducted with the short nozzle chambers to establish injector performance, power level, mixture ratio, and structural and cooling characteristics. Seventy-five stability bombs will be used during this test series to evalute combustion stability. The fifth and sixth units, having a full 400:1 nozzle, will be used to establish the altitude performance characteristics, and to demonstrate the complete assembly cooling and structural integrity. Six high-pressure altitude tests will be conducted on these two units.

Preburner. The preburner will supply high-pressure hot gas to drive the oxidizer and fuel turbopump turbines for engine application. Also, preburners

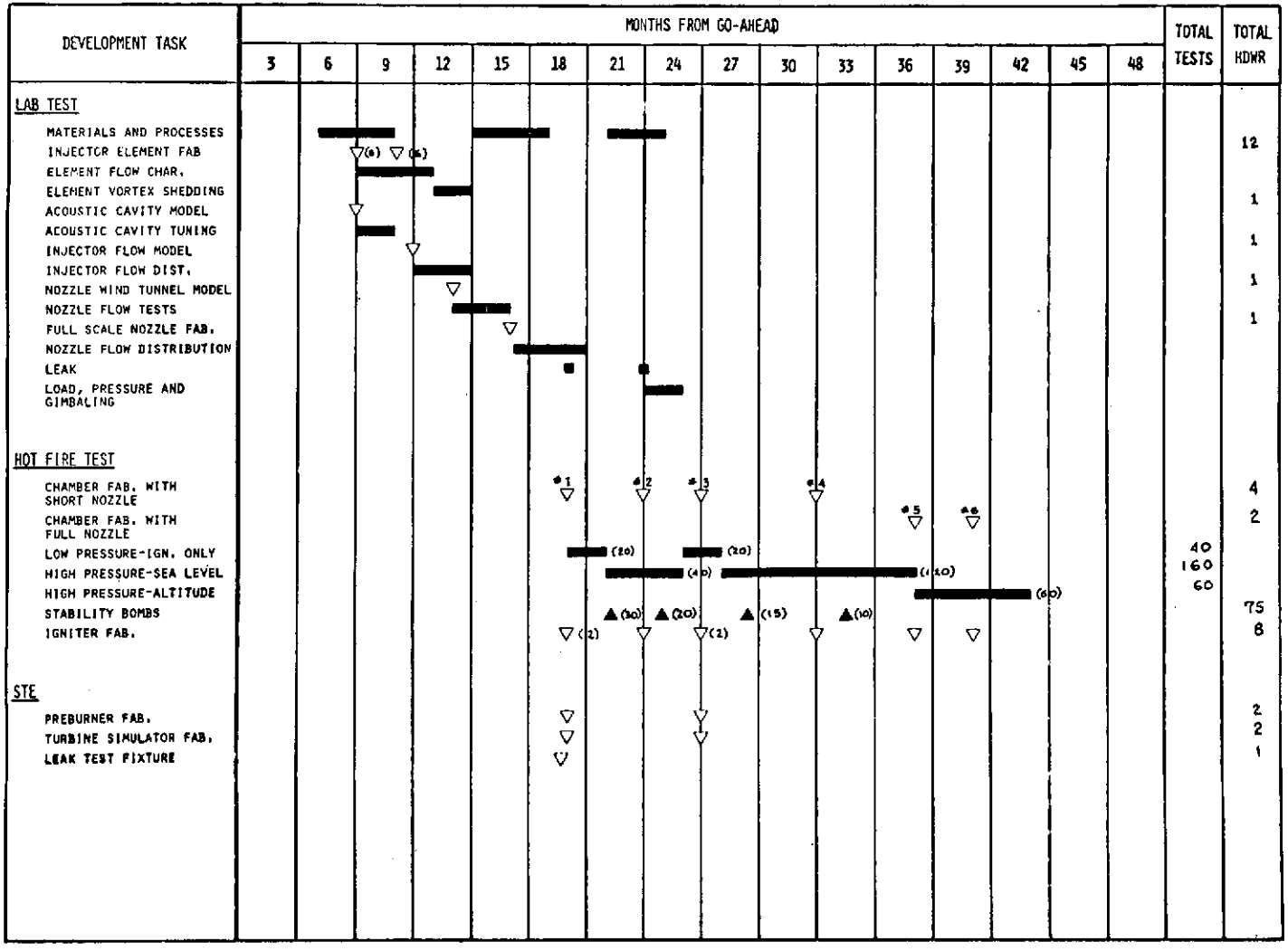

Figure 6-9. Thrust Chamber Assembly Development

will be used to supply hot gas for thrust chamber and for turbopump component testing. Detailed designs will be made for the engine preburner and for component use, including preburner-only testing. All preburner designs will be nearly the same except for possible attachment deviations. The overall development schedule for the preburner assembly is shown in Fig. 6-10, and consists of both cold-flow lab testing and hot-fire preburner-only testing.

The preburner will be subjected to lab verification testing such as injector element and injector flow distribution, liner coolant flow, leak, load, pressure, and acoustic cavity tuning.

Six different injector elements will be fabricated to study the element flow characteristics, and a full injector assembly will be made to study total face-flow distribution. An acoustic cavity model will also be built to perform the cavity tuning studies.

A full preburner liner will be fabricated to evaluate the coolant flow characteristics in terms of uniformity, pressure drop, and leakage. (This unit subsequently will be used in the first hot-fire hardware assembly.) Another preburner assembly from the hot-fire program will be used to perform the load and pressure tests.

Six flanged preburner assemblies will be fabricated to support the hot-fire program. Preburner-only hot-fire testing will include 60 low-pressure ignition tests (5 seconds average duration) to verify start capability under different propellant conditions, and 110 high-pressure mainstage tests of 100 seconds average duration will be conducted to verify performance, duration capability, life, cooling, stability, and hot-gas temperature profile uniformity. Forty stability bombs will be used in the high-pressure stability demonstrations, and two temperature rakes will be part of the STE required to evaluate the temperature profile. Two turbine backpressure simulators must also be fabricated to permit the preburner-only testing.

Ground Support Equipment. Ground Support Equipment (GSE) will be designed, fabricated, and demonstrated on a schedule that provides support of engine system testing, as shown in Fig. 6-11. The equipment operation will be verified during the early portions of the engine system test program and during the PFC and FFC portions of the development effort. Total equipment required is delineated in Table 6-5.

The GSE allocations shown in Table 6-5 assume delivery of complete sets of equipment as required to support three engine integration sites: the vehicle contractor plant, a NASA test site (e.g., MSFC or MTF) and a launch site. This equipment will be delivered concurrent with prototype engine delivery during the DDT&E phase of the grogram. The additional engine handlers, covers, and closures would be delivered during the 50-engine production phase of the program.

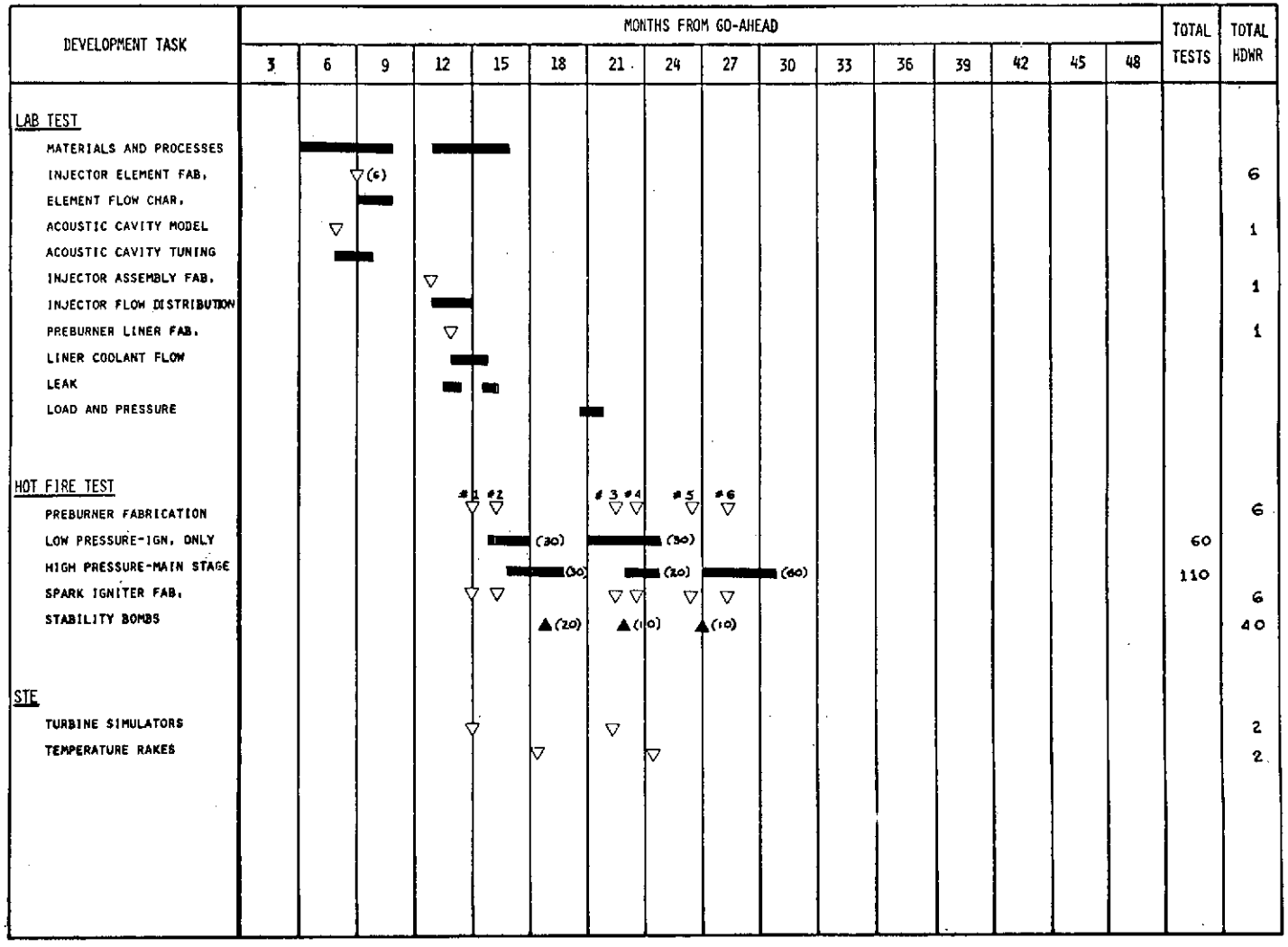

Figure 6-10. Preburner Assembly Development

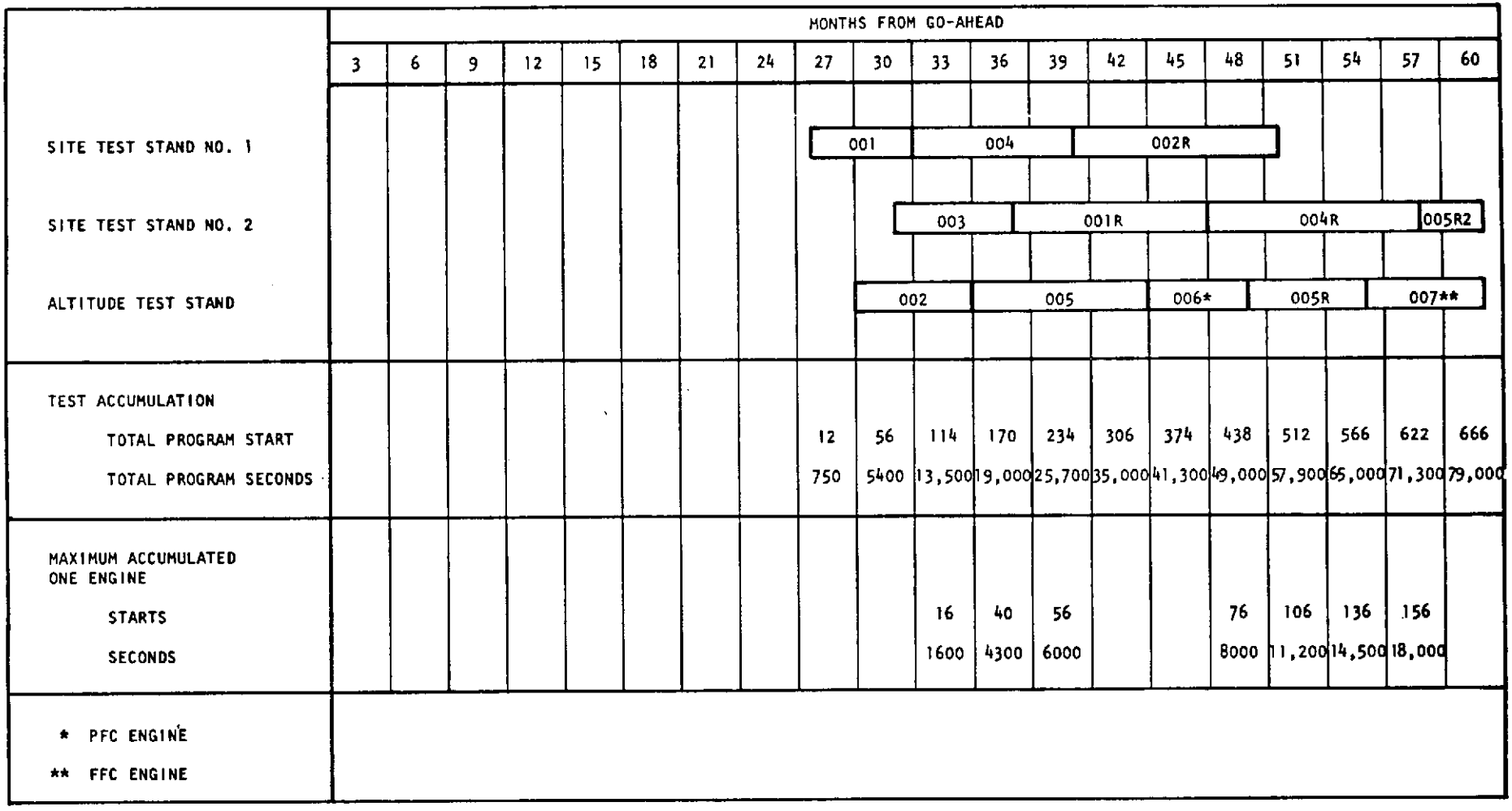

Figure 6-11. Engine Systems Test Schedule

TABLE 6-5. GSE ALLOCATIONS

Item	Development	Prototype	Production
Handling and Transport			
1.1 Handler, Engine (and Cover)	5	3	20
1.2 Sling, Handler (and Cover)	2	3	--
1.3 Sling, Engine, Rotating	2	3	--
1.4 Installer, Engine	1	3	--
1.5 Hoist Adapter	1	3	--
1.6 Covers and Closures, Set	5	3	20
1.7 Pad, Thrust Chamber Interior Protection	2	3	--
Test, Maintenance, and Servicing			
2.1 Console, Engine Electro/Pneumatic Checkout	1	3	--
2.2 Test Set, Engine	1	3	--
2.3 Test Set, Installed Engine	1	3	--
2.4 Flow Tester, Pneumatic (Atmospheric)	2	6	--
2.5 Flow Tester, Pneumatic (High Pressure)	2	6	--
2.6 Leak Detector, Mass Spectrometer	1	3	--
2.7 Tool Set, Special	1	3	--
2.8 Welding Set (and Cutters)	2	4	--
Control			
3.1 Control Test Panels (2)	1	3	--
Internal Inspection			
4.1 Borescope and Foreign Object Retrieval Set	1	2	--

Engine System Testing

Engine development testing will demonstrate that the flight configuration engine meet all the requirements of the engine Model Specification. A 12-engine development program consisting of 666 tests will be conducted. Overall engine development and verification test objectives are listed in Table 6-6. The engine system test schedule is shown in Fig. 6-11.

Development Tests. A 10-engine development test program, including two exploratory engines and five recycled engines, will be completed. The exploratory test series, consisting of 15 tests on each of two engines, will be conducted on the first two new engines assembled. The first engine will have a nozzle area ratio of 8:1, and will be tested on one of the site test stands at the Santa Susana Field Laboratory (SSFL). The second engine will have a nozzle area ratio of 400:1 and will be tested on the altitude simulation test facility at SSFL. The primary objective of this testing is to define engine ignition, start and shutdown transient characteristics. Additionally, engine interactions will be evaluated at both site and altitude conditions. Data obtained from these early tests will be used to improve the engine computer model.

A total of 516 site and altitude simulation tests are planned during the development phase. The primary objectives of this phase of the engine test program are:

1. Evaluate engine operational and performance characteristics at site and altitude conditions

2. Demonstrate, through a series of limits and overstress tests, the margin of safety inherent in the engine system

3. Demonstrate the combustion stability characteristics of the engine during a typical mission duty cycle, including idle mode, mainstage and restart conditions.

4. Certify through demonstration tests that the engine system will meet all requirements specified in the engine model specification. (Note: Service life between overhauls and maintainability will be demonstrated during the Flight Support Program.)

5. Demonstrate the adequacy of special servicing procedures and test equipment

6. Validate Field Operating Instructions manuals.

This phase of the engine testing will certify the capability of the engine to meet program requirements. Engine service-free life will be domonstrated by the completion of the Final Flight Certification Test Program. Each engine in this phase of testing will accumulate additional operating duration to demonstrate a continued service-life growth. Five engines will be recycled at least one time

TABLE 6-6. ENGINE DEVELOPMENT AND VERIFICATION TEST

Objectives	New Engines							Recylced Engines				
	001	002	003	004	005	006	007	101	102	104	105	205
Ignition-only Tests												
Site	X											
Altitude		X										
Site Operational and Performance Evaluation	X		X	X				X	X			X
Altitude Operational and Performance Evaluation		X			X						X	
Stability Mapping of Main Injector			X		X						X	X
Limits and Over Stress Testing												
Engine Mixture Ratio		X	X		X			X			X	X
NPSH			X	X	X				X		X	X
Engine Ambient Environment					X						X	X
Duration		X	X		X						X	X
Maximum Time Between Firings					X						X	
Minimum Time Between Firings					X						X	
Preliminary Flight Certification (Alt)						X						
Final Flight Certification (Alt)							X					

with one engine recycled twice to allow evaluation of service-life growth on engine components. During each recycle, engine disassembly will be accomplished to the extent necessary to allow inspection. At least one of the recycled engines will accumulate in excess of 150 starts (see Fig. 6-11) or one-half of the starts required to demonstrate service life between overhauls by the completion of the FFC.

Special Test Equipment. Conduct of the engine system development test effort will require special test equipment (STE). Significant STE items required are:

1. Simulated altitude test positions. The position(s) will be used initially for thrust chamber component testing and then modified to accomdate engine system testing.

2. A heat exchanger during site testing of the 8:1 ϵ engine. This heat exchanger will simulate the 100:1 portion of the engine nozzle by conditioning hydrogen to the temperature normally provided to the turbines for the low-pressure pumps.

3. A system capable of gimbaling the engine. The system will consist of two actuators, a programmer, and a hydraulic fluid supply system. The system is needed as STE because it is not provided as part of the engine equipment.

Preliminary Flight Certification Program. A one-engine Preliminary Flight Certification test program will be conducted commencing 42 months from program start. This program will demonstrate the capability of the engine to meet all CEI specification requirements except service-free life and service life between overhauls. The engine used for this program will be an R&D engine assembled per production criteria, including inspection and quality assurance standards. An engine test program consisting of 40 tests and approximately 5700 seconds, including one test of 1200 seconds duration, will be completed. Major external input and operating variables will be demonstrated to their limit values during the PFC test program, as follows:

1. Vacuum thrust at idle mode and mainstage

2. Step and ramp mixture ratio variation

3. Maximum and minimum combinations of oxidizer and fuel prestart and mainstage inlet pressures and temperatures

4. Limit values of turbopump speed, turbopump discharge pressure, preburner temperature, and main combustor chamber coolant flow

All tests will be conducted in the altitude simulation test facility. Upon completion of the program, the engine will be completely disassembled for inspection.

Final Flight Certification Program. A one-engine Final Flight Certification test program will be conducted commencing 53 months from program start (Fig. 6-1). This program will demonstrate the capability of the engine to meet all CEI specification requirements except service life between overhauls. The engine used for this program will be of the flight configuration in all respects. An engine test program consisting of 60 tests and approximately 9000 seconds, including one test of 2000 seconds duration, will be completed. Major external input and operating variables, including all those listed for PFC, will be demonstrated to their limit values during the FFC program. All tests will be conducted in the altitude simulation test facility. Upon completion of the program, the engine will be completely disassembled for inspection. The engine will then be recycled for use in the O&FS service life demonstration program.

Reliability and Maintainability

The reliability program will be based on the concept that reliability is an inherent product design characteristic that must be incorporated and improved by a concentrated effort early in the design phase and maintained by tight controls throughout the development and production phases.

Reliability-oriented design requirements will be included in design requirement specifications. Reliability will be considered as a qualitative and quantitative parameter in trade studies. Reliability predictions will be prepared using appropriate data sources to determine the feasibility of meeting the quantitative reliability requirements.

Reliability analyses will evaluate application of components relative to system-imposed functional and environmental stresses, such as containment level and surge pressures. A Faliure Mode and Effect Analysis (FMEA) will identify reliability-critical areas for application of appropriate engineering attention. A criticality analysis will provide a quantitative ranking of critical failure modes.

Design reviews are chaired by an independent team within the Reliability organization to provide a critical review of the design status versus the design requirements at key milestones in the design phase.

The established problem/failure reporting, analysis, corrective action, and follow-up system will be implemented for this program and in accordance with specified requirements.

Reliability assessments will be prepared at major program milestones and other key points in the program. The assessments will utilize testing accomplished to date and reliability analyses to ensure that all potential degrading sources affecting reliability have been identified and evaluated, and corrective action initiated.

To provide a means of control and evaluation of the Reliability Program at any point in time, a computerized monitoring system will be used to maintain current records of the following:

1. The FMEA
2. Design Review
3. Design Verification
4. History of Serialized Parts
5. Engine Test Reports
6. UCR/FAR

Maintainability Program. The maintainability program for the ASE will be concerned with the following key factors:

1. Engine replacement capability on the vehicle
2. Checkout capability
3. Component replacement capability
4. Accessibility for external and internal visual inspection of critical areas
5. Fault isolation

Early in the design certification phase of the program, maintainability studies and analyses will be conducted, based on other similar rocket engine programs such as the SSME, to define parameters for use by the system designers to ensure that the preceding key factors are considered and implemented into the engine design. Program control to assure incorporation of maintainability features into the engine design will be by means of the Design Verification Specification (DVS) and by informal and formal design reviews. Component and engine system tests are planned to demonstrate that maintainability concepts have been incorporated into the engine design.

System Safety Program. Early in the program, a Preliminary Hazard Analysis (PHA) will be conducted to ensure complete definition of hazard-producing energy sources (external as well as internal) and establishment of design criteria for their control. The entire engine life cycle will be considered, with emphasis on normal and emergency situation operational activities.

As the detailed designs evolve, a Subsystem Hazard Analysis (SHA) will be prepared. The SHA provides a detailed evaluation of possible equipment, component, procedural, and externally induced faults that could result in hazardous events.

MANUFACTURING PLAN

The fundamental approach to ASE manufacturing will be to fabricate all engine hardware in the production shop to production drawings. This includes development and prototype deliverable hardware as well as the 50 production engines and their spares. The Master Schedule for the ASE is shown in Fig. 6-12.

All deliverable engines will be produced in accordance with the Master Schedule. The engines designated for the formal demonstration portions of the PFC and FFC programs also will be fabricated in accordance with the Master Schedule. The remainder of the development hardware must be produced at an irregular pace as required to support development testing, however, and will be expedited as necessary. The expedited hardware will undergo exactly the same fabrication sequences as the production hardware, but flow times between operations will be minimized. The manufacturing schedule for the minimum-cost program is shown in Fig. 6-13.

Hardware fabricated during the DDT&E phase of the program, including the five prototype deliverables, will be manufactured on soft tooling. Production hardware will be fabricated on hard tooling which will provide a capability of increased delivery rate, if desired. Increased delivery rates would reduce the total cost of the production phase.

OPERATION AND FLIGHT SUPPORT PLAN

An Operational and Flight Support (O&FS) plan has been developed as a part of the Advanced Space Engine (ASE) program study. O&FS planning considers the effort associated with integrating the ASE into the Space Shuttle program tug and the support required for a 10-year operational flight program.

Engine integration support planning includes such activities as (1) resolving ASE/tug interface problems and providing technical assistance during prototype ASE installation in the tug, (2) providing technical and spares support during tug propulsion ground testing, and (3) providing technical and spares support during flight testing leading to Final Flight Certification of the integrated ASE and tug. Integration planning also provides for personnel training and technical manuals support necessary for achieving an Initial Operating Capability (IOC) at FFC.

Operational support planning provides for field technical support, engine contractor's in-plant sustaining engineering, and spare hardware. An in-plant hardware overhaul/refurbishment effort is planned, as is field maintenance support.

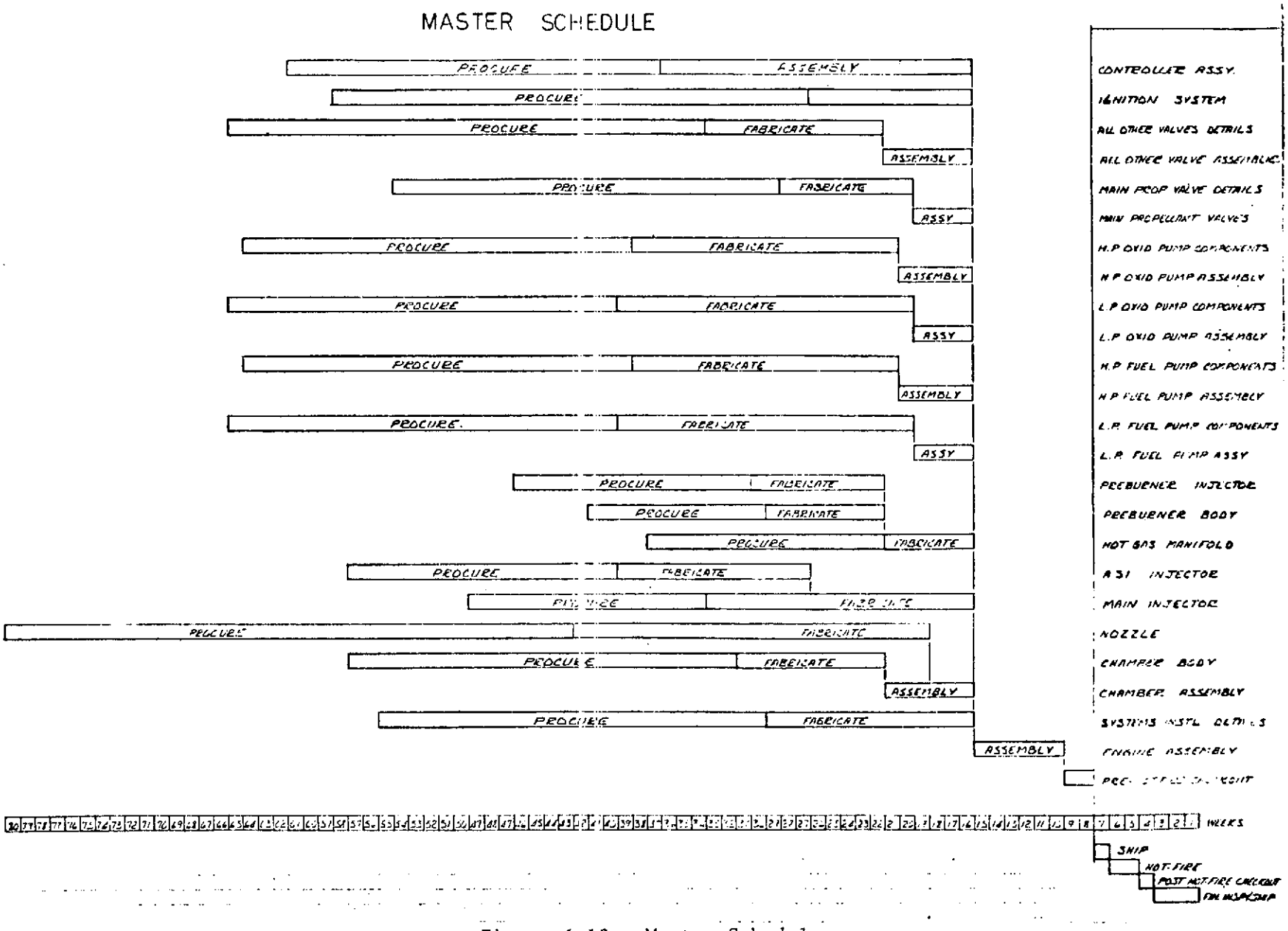

Figure 6-12. Master Schedule

Page intentionally left blank

Objectives for O&FS planning are:

- To make a preliminary determination of support resource requirements
- To establish the basic support concepts
- To estimate the support program effort

In developing the plan, certain ground rules and assumptions were established to place dimensions on the support program and for determining suitable support approaches. These ground rules and assumptions are shown in Table 6-7.

The next step in the support study and planning sequence was to develop a maintenance concept since this is the basis of most support resource requirement. The concept is presented in the ASE Maintenance section of this plan.

Support approaches were then selected and support efforts scheduled to meet overall program phasing. The results of this study effort are summarized in the Support Approach section.

Finally, a support cost analysis was made. Although results of the O&FS cost analysis are presented elsewhere with other ASE program cost data, the methods used in developing the cost and related considerations are described in this O&DS plan's final section.

ASE Maintenance

The ASE maintenance program is planned toward the following objectives:

Interface with tug operations

Provide routine and corrective maintenance within allotted turnaround time

Ensure a flight-ready system at time of launch

Be cost effective

A workable maintenance program that would meet these objectives was established by: (1) reviewing the design concept and service life requirements for routine maintenance requirements, (2)identifying comparable components (from other engines) engines) and reviewing their problem rates to determine corrective maintenance requirements, and (3) reviewing the projected mission model* for the volume and rate of maintenance activity. In addition, tug ground operations planning* was analyzed for maintenance opportunities. Using the information derived, and with due consideration for the support implications of various alternatives, a concept was developed (see Fig. 6-14). It is presented in the following paragraphs.

*Preliminary Data Package, Space Tug System Studies, dated April 1973.

TABLE 6-7. PROGRAM GROUND RULES AND ASSUMPTIONS

- A space tug requires one 88,964 N (20K) Advanced Space Engine (ASE).
- The integrated space tug propulsion system is subjected to a ground test program prior to Final Flight Certification (FFC).
- The ground test program is conducted at a government installation, such as Mississippi Test Facility (MTF).
- The first prototype ASE is delivered to the ground test facility for installation and test in the propulsion test article.
- Twenty propulsion test article hot-fire tests are conducted.
- Two flight configuration space tugs are assembled prior to FFC using prototype ASE's.
- One prototype engine is available as a spare for ground test operations and one is available as a spare for pre-FFC flight test operations.
- ASE 's are installed during space tug assembly operations at the vehicle contractor's facility.
- The completed space tug can be delivered to the launch site for first flight within 2 months of the ASE delivery date.
- Kennedy Space Center (KSC) is the launch operations location.
- Five flight tests are conducted between Preliminary Flight Certification and FFC.
- Space tugs are retrieved and returned by the shuttle orbiter to the launch site during all pre-FFC flights.
- The operational period is 10 years and starts at FFC.
- Flight rate is an average of 20 per year during the operational period.
- Fourteen days are available for space tug turnaround activities between flights.
- Prototype ASE's used in the first two space tugs are phased out of flight operations within 1 year of FFC.
- During the first 5 years of the operational period, 43 space tugs are assembled and the two pre-FFC space tugs are re-configured with production ASE's.
- Five production engines are available as spares for post-FFC flight operations.

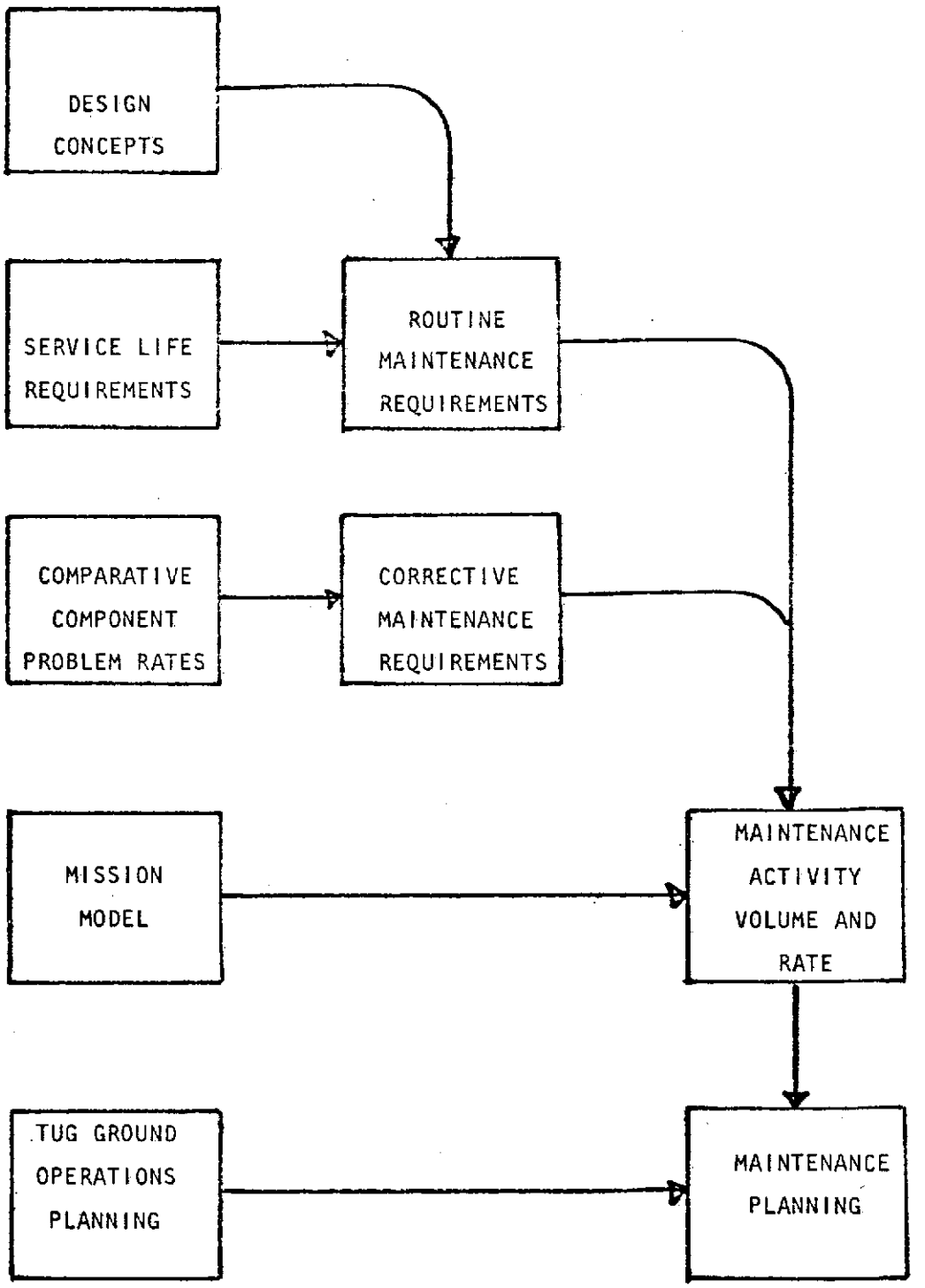

Figure 6-14. Maintenance Program Study

Rountine Maintenance

ASE routine maintenance consists of subsystem purging, hardware inspection, internal leak testing, valve actuation, control system sequencing, and sensor checks. These activities are integrated into tug processing as shown in Table 6-8. (KSC preliminary planning* shows a 62-hour period between payload removal and payload installation. Table 6-8 assumes reinstallation of the same tug, although it is understood that the next orbiter mission may not require a tug or that an alternate tug may be used.)

Postflight purging of ASE subsystems supplements in-flight purges to remove combustion products (H_2O) from engine subsystems and expels moist air which may have been drawn into the engine during the shuttle vehicle's re-entry. The purging is accomplished at the safe and purge area.

The inspection and internal leak testing aid in identifying the need for corrective action. However, the primary source for revealing corrective action needs is flight data which are reviewed after flight for anomalies and problem trends. The inspection is done in the tug maintenance and checkout facility and includes an external visual inspection of the complete engine and internal inspection of the engine's hot sections and rotating machinery. Internal inspection is made through the chamber throat and preburner and turbopump ports using special internal inspection equipment.

Internal leak testing of the main propellant valves ensures positive propellant shutoff, which is essential for safe starts and multiple restart capability. This testing is done following refurbishment during other checkout and test operations. If the tug is to be stored, the testing is done before and after the storage period.

Although oxidizer control valve actuation, control system sequencing, and flight instrumentation sensor functioning are evaluated through flight data analysis, these items are rechecked during preflight operations, ensuring that problems have not developed since the last ASE flight operation. These tests are assumed to be automatic and controlled either by a tug controller system or tug GSE. Control system sequencing is reverified as part of the launch readiness testing on the pad.

In addition to the above ASE routine maintenance requirements for tugs in process flow, periodic checking of humidity indicators is necessary for ASE's stored individually or in stored tugs.

Corrective Maintenance

ASE corrective maintenance is performed on the tug, in the site shop, and at the depot. Factors which determine the level of maintenance dictate that the depot is the more feasible location for most ASE corrective maintenance. These factors include:

*KSC Space Shuttle Processing Study, dated 6 March 1973.

TABLE 6-8. TUG/ASE PROCESSING

	LOCATION		TUG PROCESSING ACTIVITY		ASE MAINTENANCE
I.	LANDING FACILITY		SHUTTLE RECOVERY		---
II.	SAFE AND PURGE AREA	a.	SAFE AND PURGE	a.	SUBSYSTEMS PURGE
		b.	REMOVE FROM SHUTTLE ORBITER	b.	---
III.	TUG MAINTENANCE AND CHECKOUT	a.	DEMATE FROM SPACECRAFT (if spacecraft retrieved)	a.	---
		b.	POST-FLIGHT INSPECTION	b.1.	EXTERNAL VISUAL INSPECTION
				2.	INTERNAL INSPECTION
		c.	REFURBISH	c.	CORRECTIVE MAINTENANCE
		d.	CHECKOUT AND TEST	d.	MAIN VALVE INTERNAL LEAK TEST
		e.	MATE TO SPACECRAFT	e.	---
		f.	INTERFACE VERIFICATION	f.	---
		g.	INTEGRATED SYSTEM TEST	g.1.	OXIDIZER CONTROL VALVES SLEW CHECK
				2.	CONTROL SYSTEM SEQUENCE TEST
				3.	FLIGHT INSTRUMENTATION SENSOR CHECKS
IV.	ORBITER MAINTENANCE AND CHECKOUT FACILITY	a.	INSTALL IN ORBITER	a.	---
		b.	INTERFACE VERIFICATION	b.	---
		c.	INTEGRATED SYSTEM TEST	c.	---
V.	SHUTTLE INTEGRATION FACILITY	a.	SHUTTLE BUILD UP	a.	---
		b.	INTEGRATED SYSTEM TEST	b.	---
VI.	LAUNCH PAD	a.	MATE SHUTTLE TO PAD SYSTEM	a.	---
		b.	INTERFACE VERIFICATION	b.	---
		c.	LAUNCH READINESS TEST	c.	CONTROL SYSTEM SEQUENCE TEST
		d.	LOAD PROPELLANTS AND PRESSURANTS	d.	---
		e.	COUNTDOWN AND LAUNCH	e.	---

C-5

- Welded component assemblies and engine joints
- Low frequency of corrective maintenance requirements
- High-pressure reverification requirements
- Adequate spare engine availability
- Apparent ease of engine replacement

The basic maintenance concepts are:

- Thread fastened components are replaced at the site
- Welded joint components in low-pressure systems (tank head, control system, or drain pressures) are replaced at the site
- Welded joint components in high-pressure systems are replaced at the depot
- All defective components that must be removed for refurbishment are refurbished at the depot

Table 6-9 provides an estimated number of problems by component for a 200-flight profile and contains the potential disposition of these problems based on the concept.

Support Approach

The basic support problem is to provide the skills, material, and equipment needed to sustain ASE engines used in approximately 200 flights during a 10-year period of operations. However, the scope of the problem is expanded by the need for integrating an advanced design engine into a new vehicle and the need for support during attendant engine integration activities. The support problem presents two phases of requirements and is, therefore, resolved by two phases of activity.

The first phase, the engine integration period, is supported primarily by the engine contractor. During this period, the engine contractor performs the following:

- Identifies support resource requirements
- Plans the support activity in detail
- Provides field site technical support to the tug assembly operations during installation of prototype engines in the initial two tugs

TABLE 6-9. PROBLEM DISPOSITION

					REPAIR DISPOSITION						
		Components Per Engine	Comparable Component Problem Rate/ 1000 MDC	Estimated ASE Problems/ 200 MDC	Repair In Tug	Replace Component In Tug	Remove Engine, Replace Component at Site, Reinstall Engine	Replace Engine, Return To Depot	Replace Component at Depot	Refurbish Component at Depot	Discard Component
1.	Igniter	2	2.3	0.9		0.9					0.9
2.	Fuel Pump	1	12.0	2.4				2.4	2.4	2.4	
3.	Fuel Boost Pump	1	12.0	2.4				2.4	2.4	2.4	
4.	Main Fuel Valve	1	1.5	0.3			0.3			0.3	
5.	Oxidizer Control Valve	2	1.0	0.4				0.4	0.4	0.4	
6.	Main Oxidizer Valve	1	1.0	0.2			0.2			0.2	
7.	Anit-Flood Valve	1	1.0	0.1				0.1	0.1	0.1	
8.	Oxidizer Boost Pump	1	12.0	2.4				2.4	2.4	2.4	
9.	Oxidizer Pump	1	12.0	2.4				2.4	2.4	2.4	
10.	Heat Exchanger	1	<0.1	<0.1							
11.	Control Valves	7	3.1	4.3		4.3				4.3	
12.	Thrust Chamber and Preburner Assembly										
	a. Gimbal Assembly	1	<0.1	<0.1							
	b. Preburner	1	<0.1	<0.1							
	c. Dome-Injector/ Combustor	1	7.5	1.5				1.5	1.5		1.5
	d. Nozzle	1	7.5	1.5	0.7			0.8	0.8	0.8	
13.	Electrical Control Assembly	1	6.0	1.2		1.2				1.2	
14.	Electrical Harness	2	1.2	0.5		0.5				0.5	
15.	Tubing and Ducting	19	0.8	3.0		1.6		1.4	1.4	2.3	0.7
16.	Check Valves	8	3.1	5.0		1.2		3.8	3.8		5.0
17.	Flowmeters	2	<0.1	<0.1							
18.	Seal Drains	2	0.5	0.2		0.2					0.2
19.	Sensors										
	a. Pressure	14	1.0	2.8		2.8					2.8
	b. Temperature	5	4.5	4.5		4.5					4.5
	c. Position	2	1.0	0.4		0.4					0.4
	d. Flow	4	1.5	1.2		1.2					1.2
	e. Pump Speed	4	2.0	1.6		1.6					1.6

- Provides field site technical support to the tug propulsion test operations during ground hot-fire testing with a prototype engine

- Provides field site technical support to launch operations during the preliminary test flights of the tug

- Prepares and issues technical manuals covering prototype engine and GSE operating requirements and maintenance procedures for engine integration activities

- Prepares and issued technical manuals covering production engine and GSE operating requirements and maintenance procedures for operational activities

- Trains the engine contractor personnel who provide field support; trains tug assembly contractor personnel who perform engine related activities; trains the NASA personnel who manage or perform in activities related to engine installation, test, or flight; and trains those personnel who will provide ASE field site maintenance.

- Performs a detailed analysis of prototype and production engine spare hardware needs for engine integration activities and submits a recommended spares list to NASA.

- Upon NASA approval, releases prototype spares for manufacture and purchase in time for delivery with the first engine. Also provides in-plant warehousing for depot level spares.

- Upon NASA approval, releases initial production spares for manufacture and purchase in time for delivery of the first production engine.

- Provides a field maintenance support for engines and GSE used in tug propulsion test and flight operations.

- Provides depot level engine/component overhaul-refurbishment support in-plant for returned hardware.

Tug assembly contractor personnel perform all engine installation, inspection, and test activities during tug assembly operations. Also, the tug assembly contractor or NASA provide warehousing for spares delivered to the various sites.

During the second phase, a transition is made from the earlier phase of producing initial resources and supporting activity that is primarily developmental. The support is redirected as a sustaining effort; however, the transition is not abrupt. The engine contractor's transitioning efforts are:

- Continued field site technical support of tug assembly operations through to completion of this operation
- Updating technical manuals based on the 10C experience
- Training of personnel for the production engine configuration
- Delivery of initial production engine spare hardware
- Updating prototype engine spare hardware configuration for use with the production engine
- Turning over field maintenance of the engine and GSE to NASA, the tug vehicle contractor, or an operations contractor

To sustain the operational and flight support program, the engine contractor provides:

- Field site technical support for launch operations
- In-plant engineering assistance
- Spares management and warehousing
- Usage spare hardware
- Depot-level engine/component overhaul and refurbishment

Figure 6-15 provides a time-phased chart of O&FS milestones keyed to program milestones and periods.

Support Cost Analysis

To estimate the effort required for the ASE O&FS program, the various support activities and products were assigned to the following cost packages:

Engine Integration

1. Logistics Engineering
2. Field Support
3. Manuals
4. Training
5. Spares Management
6. Spares

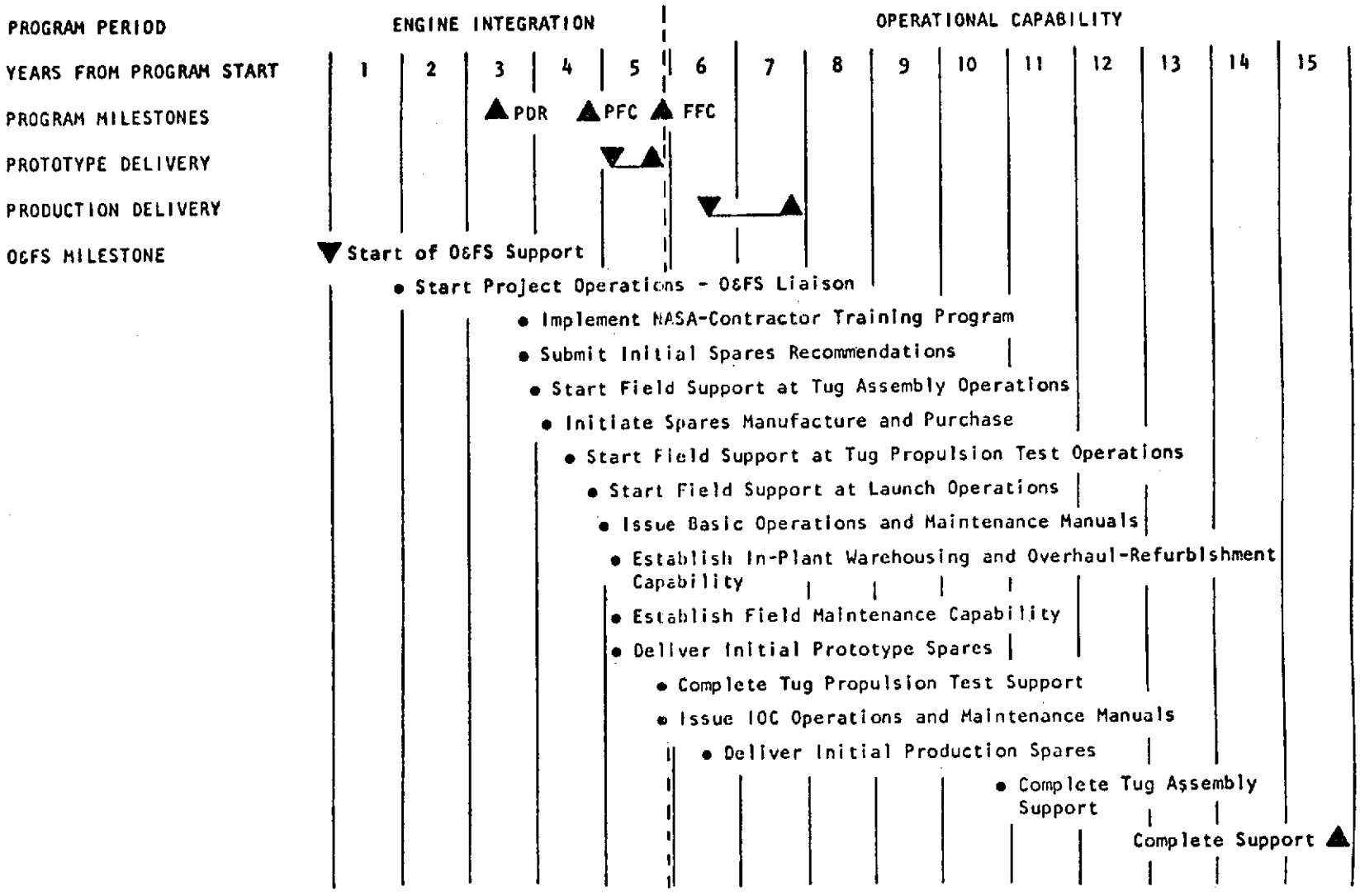

Figure 6-15. Support Program Milestones (Program 1)

Operations Support

1. Field Maintenance and Refurbishment
2. Field Engineering
3. Sustaining Engineering
4. Spares
5. Engine/Component Overhaul

The scope of effort and method used to estimate costs for each package are described in the following paragraphs.

Engine Integration

Logistics Engineering. Logistics Engineering is the in-plant effort for determining support requirements, planning support, and coordinating with Field Support at the sites. Manpower for this effort is based on complexity of the program and on the number, types, and duration of Field Support activities coordinated with.

Field Support. Field Support is the technical assistance activity provided at the various program operations locations. It includes a site O&FS liaison effort at the customer's project operations site. Manpower for these efforts are based on the number, scope, and duration of operations supported.

Manuals. Manuals effort includes: (1) the writing and production of basic issue operating requirements and maintenance procedures manuals for the prototype engine and GSE, (2) issuing changes to the basic manuals, and (3) preparing operating and maintenance manuals for the production engine in the 10C environment. Manpower is based on scope of engine tasks to be covered, complexity of the engine, type and scope of GSE, and an estimate of the number of pages, illustrations, and change pages needed.

Training. Training includes the preparation of training materials, including visual aids, and the conduct of training courses in the operation and maintenance of the engine and GSE. Manpower is based on the probable scope of classes and diversity of subjects to be covered. No training equipment (other than visual slides) is anticipated.

Spares Management. Spares Management consists of: (1) analyzing the hardware design and reviewing failure data to estimate spare hardware needs, (2) submitting spares recommendations to the customer, (3) releasing spares for manufacture/pruchase and monitoring progress and delivery, (4) processing engines/components returned to repair, and (5) providing warehousing services. Manpower is based on volume of projected spares needs, traffic in returned engine/components, and the spares production and warehousing durations.

Spares. Spares for the engine integration effort consists of a set of replacements for prototype engines used in tug propulsion test and the pre-FFC launch operations. This set of replacement hardware is estimated at 80 percent of one engine worth of parts. The estimate is based on projected problems for the anticipated number of mission duty cycles (MDC), the probable repair disposition, the reorder/refurbish pipeline time, and the warehousing location. The problem disposition table in the ASE Maintenance section of this plan was used in making the spares selection. The table is based on the 200-flight mission profile; since the tug propulsion test operations and pre-FCC flight operations will consist of 25 MDC's, the table's data was adjusted accordingly for prototype spares requirements. Since projected problems for most prototype engine components will be less than 0.5, most of the items selected as spares are insurance items. Table 6-10 identifies prototype spares selected during the study. Each part was rated according to relative material and labor value and selected parts ratings summed to obtain the 80 percent of one engine estimate.

Operations Support

Field Maintenance and Refurbishment. The field maintenance and refurbishment effort consists of the technician and inspection support for tug propulsion test operations (although pre-FFC) and launch operations. It includes all engine and GSE routine and corrective maintenance at the site, including engine removal and installation. It does not include site laboratory maintenance assistance for such things as parts cleaning, gage calibration, etc. (Such maintenance is usually provided by a site contractor who supports all systems, and requirements are difficult to predict at this time.) Since the projected routine maintenance loading is the processing of one tug at a time, per site, and corrective maintenance is infrequent, a minimum crew level of effort is projected for the duration of activity at each site.

The support approach is to transfer field maintenance and refurbishment to NASA or an operations contractor at FFC. However, the cost will continue and are, therefore, included in this study (pre-FFC maintenance costs are identified as nonrecurring; post-FFC are identified as recurring).

Field Engineering. The Field Engineering activity is the field site technical assistance provided to the tug assembly operations and to launch operations. It is a continuation of field support provided at these locations during engine integration and manpower is based on the scope and duration of operations supported.

Sustaining Engineering. Sustaining Engineering includes: (1) the in-plant engineering activity for engine service life demonstration and problem resolution, (2) technical manual updating, (3) training, and (4) spares management and warehousing. Manpower is generally based on the same factors as described under Engine Integration for those efforts, as applied to a long-term operational program.

TABLE 6-10. ASE SPARES

	Component	Quantity Per Engine	Prototype Spares Quantity (PreFCC Activity)	Initial Production Spares Quantity	* Updated Configuration Spares Quantity	Usage Repair Material Sets and Replacement Units
1.	Igniter	2	1	2	---	1 unit
2.	Fuel Pump	1	1	---	1	2 sets
3.	Fuel Boost Pump	1	1	---	1	2 sets
4.	Main Fuel Valve	1	1	---	1	---
5.	Oxidizer Control Valve	2	1	---	1	---
6.	Main Oxidizer Valve	1	1	---	1	---
7.	Anti-Flood Valve	1	1	---	1	---
8.	Oxidizer Boost Pump	1	1	---	1	2 sets
9.	Oxidizer Pump	1	1	---	1	2 sets
10.	Heat Exchanger	1	---	1	---	---
11.	Control Valves	7	2	---	2	4 sets
12.	Thrust Chamber and Preburner Assembly					
	a. Gimbal Assembly	1	---	1	---	---
	b. Preburner	1	---	1	---	---
	c. Dome/Injector/ Combustor	1	1	---	1	2 units
	d. Nozzle	1	1	---	1	2 sets
13.	Electrical Control Unit	1	1	---	1	1 set
14.	Electrical Harness	2	2	---	---	2 sets
15.	Tubing and Ducting	19	**1	---	---	**2 sets
16.	Check Valves	8	2	3	---	5 units
17.	Flowmeters	2	---	2	---	---
18.	Seal Drains	2	**1	---	---	**1 set
19.	Sensors					
	a. Pressure	14	2	2	---	3 units
	b. Temperature	5	2	2	---	5 units
	c. Position	2	2	2	---	---
	d. Flow	4	1	1	---	1 unit
	e. Pump Speed	4	4	2	2	2 units

* Prototype spares updated, as required, to production configuration.

** Set of materials - retained as one of post-FFC usage repair material sets.

Spares. Spares for the Operations Support period consists of an initial production spares level, prototype spares updated to the production engine configuration, and usage material and units. The identity of items selected and their numbers are in Table 6-10.

The set of initial production spares is estimated at 20 percent of one engine worth of parts. The items were selected on the same basis as described for Engine Integration spares but with the concept that prototype spares would be updated where possible. The resulting stock level would approximate 100 percent of an engine worth of parts.

The 15 prototype items identified for updating as production spares were selected as the best candidates for such updating. It is recognized, however, that such updating may not be possible for some parts and that others may be used as is. Material costs for updating these parts was based on 23 percent of component's original material costs, the same figure as is used for estimating refurbishment costs. (Labor costs for updating are included in the Engine/Component overhaul package.)

The usage material and replacement units were selected on the basis of the repair disposition (see ASE Maintenance section). Quantities are based on projected problems and a ground rule that the initial spares level be preserved. Usage items were not included for insurance spares, items with a problem projection less than 0.5 for the 200 MDC. Usage spare units were rated, as in the case of initial spares, and estimated at 40 percent of one engine worth. Usage material for each of the 18 sets was estimated at 23 percent of the component's original material costs.

Engine/Component Overhaul

Review of the mission profile, number of engines, and service life requirements shows that no scheduled engine overhauls are required. Therefore, the scope of work in this effort consists of: (1) replacing discrepant components on returned engines, (2) refurbishing discrepant components, and (3) providing the labor to update prototype spares.

The number of components replaced on engines returned to the depot was determined by summing that data in the problem disposition study for the 200 flight operations program. That sum was increased by 12.5 percent for pre-FFC activity (25 MDC's). The result was approximately 20.

To determine the labor for the replacement of 20 components in terms of engine assembly labor, two factors were judged: (1) component remove and replace time was two and one-half times that required in initial engine assembly, (2) 15 major components largely account for engine assembly time, or each of the 15 represent 6.6 percent of the engine's assembly time. The number of components, 20, was multiplied by 2.5 and 6.6 percent to obtain a labor estimate of 330 percent of one engine assembly labor.

Discrepant components requiring refurbishment at the depot were tabulated from the problem distribution study and multiplied by 35 percent of the average component's original fabrication cost.

Prototype spares updating labor was estimated by multiplying their number by 35 percent of the average component's original fabrication labor.

DATA AND DOCUMENTATION

Data and documentation for the ASE was estimated based on the data lists shown in Tables 6-11, 6-12, and 6-13 for the DDT&E, Production, and O&FS phases of the program, respectively. The lists shown in the tables were generated through evaluation of the SSME data requirements. Cost estimates for the data do not include engineering effort necessary to originate the reports; the originator's efforts are changed to the appropriate product subaccount.

FACILITIES

The fundamental assumption in generating ASE facilities estimates is that SSME facilities will be available at the time required to support the Advanced Space Engine. Table 6-14 defines the facilities allocated to major system and subsystem testing.

TABLE 6-11. DDT&E DATA LIST

Item	Frequency	No. Issues
Plan, Configuration Management	Semi-AN	10
Engineering Change Proposals	AR	70
Plan, First Article Configuration Inspection	O-Time	--
Package, First Article Configuration Inspection	O-Time	--
Minutes, First Article Configuration Inspection	O-Time	--
Specification Maintenance	AR	--
Preliminary Interface Revision Notice	AR	--
Record Engineering Change Proposal	AR	--
Lists, Configuration Identification	AR	--
Report, Configuration Identification and Status	Mo*	10
Agenda, Critical Design Review	O-Time	1
Package, Critical Design Review (CDR) Engine and GSE	O-Time	1
Minutes, Critical Design Review	O-Time	1
Facilities Utilization Plan	Semi-AN	10
Real and Installed Property Status Report	Semi-AN	10
Operational and Flight Support (O&FS) Plan	Semi-AN	10
Operating Requirements and Procedures Manual	O-Time	1
Maintenance, Repair, and Parts List Manual	O-Time	1
Ground Support Equipment Use, Maintenance, and Repair Manual	O-Time	1
Major Spares Status Report	Mo**	12
Recommended Support Parts List (RSPL)	Qtly***	3
Support Parts Priced Exhibit	Bl-Mo**	6
Program Management Plan	Semi-AN	10
Program Management Summary	Mo	59
Cost, Schedule, and Performance Measurement Report	Mo	59
NASA 533 Financial Management Report, Monthly	Mo	59
NASA 533 Financial Management Report, Quarterly	Qtly	15
Indirect Cost/Manpower Data,Monthly and Quarterly	Mo/Qtly	15
Propellant and Pressurants Use Report	Mo	59
Propellant and Pressurant Forecasts	Qtly	15
Unit Cost Report	Qtly***	3

*Monthly after 1st engine delivery
**First Report 2 months prior to engine delivery
***Quarterly after first engine delivery

TABLE 6-11. (Continued)

Item	Frequency	No. Issues
New Technology Report	Mo	59
New Technology Annual Report	Ann.	5
Program Review Data (Agenda and Handouts)	Qtly	15
Program Review Minutest	Qtly	15
Motion Picture Film Progress Report	Ann	5
Data Requirement Change Proposal	Semi-AN	10
Logic Networks and Key Milestone Charts	Mo	59
Reliability Program Plan	Semi-AN	10
Reliability Operating Procedures	Semi-AN	10
Failure Mode, Effect, and Criticality Analysis	Semi-AN	10
Maintenance Significant Items List	Semi-AN	10
Parts List and Approval Status, E.E.E. (to CDR)	Semi-AN	8
Design Review Minutes (to CDR)	Mo	48
Maturity Assessment and Test Summary Report	Mo	59
Nonconformance Status and Trend Summary Report	Mo	59
Quality Program Plan	Ann	5
Quality Assurance Manual Procedures	O-Time	1
Final Inspection and Acceptance Checkout Plan	O-Time	1
Final Inspection and Acceptance Checkout Procedure	Ann	5
Engine Log Book	Each Engine	5
System Safety Plan	Semi-AN	10
Hazard Analyses Reports	AR	4
Safety Analysis Report	Qtly	15
Accident/Incident Report	AR	10
List and Describe, Ground Support Equipment (GSE)	Semi-AN	10
Plan, Program Development	Semi-AN	10
Design Verification Specification (DVS)	Qtly	15
Drawing, Lists, Form 1, Specifications, and Microfilm	Mo	59
Plan, Structural Assessment	Qtly	15
Component Stress Analysis Structural Loads and Design Criteria	Qtly	15

TABLE 6-11. (Concluded)

Item	Frequency	No. Issues
Model, Engine Controller	Qtly	15
Data, Engine System Test, Microfilm/Tape	Per test	682
Model, Engine Data Reduction and Prediction	AR	9
Report Preliminary Flight Certification (PFC)	O-Time	1
Report, Final Flight Certification (FFC)	O-Time	1
Ptan, Flight Certification	O-Time	1
Specification CEI (Engine and GSE)	Semi-AN	10
Engine Control Design Document	Qtly	15
Engine Controller Operating Information	O-Time	1
Materials Control Reports		
1. Main Combustion Chamber	Qtly	12
2. Nozzle	Qtly	12
3. Main Injector	Qtly	12
4. Oxidizer Preburner	Qtly	12
5. High-Pressure Oxidizer Turbopump	Qtly	12
6. Low-Pressure Oxidizer Turbopump	Qtly	12
7. High-Pressure Fuel Turbopump	Qtly	12
8. Low-Pressure Fuel Turbopump	Qtly	12
9. Main Valve	Qtly	12
10. Gimbal Bearing	Qtly	12
11. Systems	Qtly	12
12. Controller	Qtly	12
13. Plan, Manufacturing	Semi-AN	10

TABLE 6-12. PRODUCTION PHASE DATA LIST

Item	Frequency	No. Issues
Program Management Plan	Semi-AN	8
Program Management Summary	Mo	46
Cost, Schedule and Performance Measurement Report	Mo	46
NASA 533 Financial Management Report, Monthly	Mo	46
NASA 533 Financial Management Report, Quarterly	Qtly	11
Indirect Cost/Manpower Data, Monthly and Quarterly	Mo	46
Propellant and Pressurants Use Report	Mo	46
Propellant and Pressurant Forecasts	Qtly	11
Unit Cost Report*	Qtly	11
Logic Networks and Key Milestone Charts	Mo	46
Plan, Manufacturing	Semi-AN	8

TABLE 6-13. O&FS PHASE DATA LIST

Item	Frequency	No. Issues
Operating Requirements and Procedures Manual	AR	--
Maintenance, Repair, and Parts List Manual	AR	--
Ground Support Equipment Use, Maintenance, and Repair Manual	AR	--
Major Spares Status Report	AR	--
Request for Disposition Report (RFD)	AR	--
Program Management Plan	Semi-AN	20
Program Management Summary	Mo	120
Cost, Schedule, and Performance Measurement Report	Mo	120
NASA 533 Financial Management Report, Monthly	Mo	120
NASA 533 Financial Management Report, Quarterly	Qtly	40
Indirect Cost/Manpower Data, Monthly and Quarterly	Mo	120

TABLE 6-14. MINIMUM COST PROGRAM FACILITIES

System/Subsystem	Location	Modification
Oxidizer Turbomachinery		
High-Pressure Turbopump	Coca-1A	Minor
Low-Pressure Turbopump	Coca-1A	Minor
Fuel Turbomachinery		
High-Pressure Turbopump	Coca-1B	Minor
Low-Pressure Turbopump	Coca-1B	Minor
Ignition Systems	Coca-4A	Minor
Precombustor	Coca-4C	Minor
Thrust Chamber Assembly		
Ambient	Coca-1C	Minor
Altitude*	Coca	Major
Engine System		
Ambient	Coca-1C	Minor
Altitude Position No. 1	Coca	Major
Altitude Position No. 2	Coca	Major

*Thrust chamber altitude position converts to engine System position.

COSTS

Cost estimates for the minimum-cost ASE program were generated separately for three distinct phases: DDT&E, Production, and Operations and Flight Support (O&FS). All estimates are in 1973 dollars and do not include fee, propellants or capital expenditures. Consumables are assumed to be GFE and the quantities required are included. The DDT&E estimate includes five deliverable prototype engine systems, GSE to support three sites, and a mock-up engine. These items are detailed separately in the estimate, allowing for convenient reallocation of the costs to other phases of the program, if desired. The production phase estimate is for 50 units at a peak rate of 2 per month, which is reached in the third month of deliveries. A 90-percent learning curve was used for fabrication hours and a 95-percent curve was used for material (primarily mortality reduction).

The O&FS estimate includes a 240-start, 8-hour test program to complete the service life demonstration for the engine. This cost also is separately identified and may be reallocated as desired.

All costs were generated to a product-oriented work breakdown structure. The item-by-item breakdown is included in the subsequent pages.

COST SUMMARY

The minimum-cost program cost estimate is $149,671,000.

DDT&E	$ 90,301,000
Production	47,820,000
O&FS	11,550,000
Total	$149,671,000

DDT&E Summary

00XXX	Combustion Devices	$ 10,121,000
01XXX	Turbomachinery	11,586,000
02XXX	Controls and Valves	3,712,000
03XXX	Ground Support Equipment (GSE)	1,223,000
04XXX	Engine Systems	26,566,000
05XXX	Program Management	6,689,000
06XXX	Deliverables	8,304,000
07XXX	Tooling and STE	2,506,000
08XXX	Integration and Engine Support	3,032,000
09XXX	Data and Documentation	5,653,000
10XXX	Facilities	2,700,000
	Subtotal	$ 82,092,000
	Development Contingency	8,209,000
	Total	$ 90,301,000

Production Summary

00XXX	Hardware	$ 34,667,000
01XXX	Acceptance Test	1,994,000
02XXX	Initial Spares	143,000
03XXX	Engineering	826,000
04XXX	Tooling	3,653,000
05XXX	Program Management	3,479,000
07XXX	Manufacturing Services	2,758,000
08XXX	GSE	300,000
	Total	$ 47,820,000

First Unit Cost.. The first unit cost of $1,460,000 includes ammortization over 50 units of engineering, tooling, program management and manufacturing services costs. It is developed as follows:

Fabrication Labor	$ 599,000
Material	421,000
Quality Control	114,000
Test Labor	38,000
Engineering	17,000
Tooling	102,000
Program Management	70,000
Manufacturing Services	99,000
Total	$1,460,000

O&FS Summary

00XXX	Field Support	$ 3,000,000
01XXX	Engine and Component Overhaul	929,000
02XXX	Engineering	2,938,000
03XXX	Spares	683,000
04XXX	Program Management	3,198,000
05XXX	Facilities Maintenance	133,000
06XXX	Service Life Demonstration	669,000
	Total	$11,550,000

Consumables

The following consumables are required for the ASE program:

Item	DDT&E	Production	O&FS
Liquid Oxygen, tons	51,107	3,690	18,450
Liquid Hydrogen, K-lbs.	16,631	933	4,665
Liquid Nitrogen, tons	7,105	513	2,565
GN_2, K-scf	725,200	36,000	180,000
He, K-scf	21,270	1,200	6,000
Alcohol, pounds	2,345,000	420,000	2,100,000

Detailed Costs

The detailed costs for each phase of the program are included in the following pages.

DDT&E

PLAN I

011XX	LPOP		$ 2,527,000	
0111X	Engineering	$ 510,000		
0112X	Fabrication	870,000		
0113X	Material	671,000		
0114X	Component Test	308,000		
0115X	Quality Control	168,000		
012XX	HPFP		$ 3,363,00	
0121X	Engineering	$ 710,000		
0122X	Fabrication	1,208,000		
0123X	Material	829,000		
0124X	Component Test	388,000		
0125X	Quality Control	228,000		
013XX	HPOP		$ 3,303,000	
0131X	Engineering	$ 710,000		
0132X	Fabrication	1,192,000		
0133X	Material	789,000		
0134X	Component Test	388,000		
0135X	Quality Control	224,000		
02XXX	Components			$ 3,712,000
021XX	Electronics		$ 1,386,000	
0211X	Engineering	$ 548,000		
0212X	Fabrication	50,000		
0213X	Material	606,000		
0214X	Component Test	100,000		
0215X	Quality Control	82,000		
022XX	Main Valves		$ 898,000	
0221X	Engineering	$ 88,000		
0222X	Fabrication	488,000		
0223X	Material	184,000		
0224X	Component Test	53,000		
0225X	Quality Control	85,000		

DDT&E

PLAN I

00XXX	Combustion Devices			$ 10,121,000
000XX	Thrust Chamber Assembly		$ 6,843,000	
0001X	Engineering	$1,342,000		
0002X	Fabrication	2,537,000		
0003X	Material	1,443,000		
0004X	Component Test	1,057,000		
0005X	Quality Control	464,000		
001XX	Ignition System		$ 1,657,000	
0011X	Engineering	$ 660,000		
0012X	Fabrication	136,000		
0013X	Material	392,000		
0014X	Component Test	428,000		
0015X	Quality Control	41,000		
002XX	Precombuster Assembly		$ 1,621,000	
0021X	Engineering	$ 425,000		
0022X	Fabrication	411,000		
0023X	Material	62,000		
0024X	Component Test	657,000		
0025X	Quality Control	66,000		
01XXX	Turbomachinery			$ 11,586,000
010XX	LPFP		$ 2,393,000	
010XX	Engineering	$ 401,000		
0102X	Fabrication	884,000		
0103X	Material	632,000		
0104X	Component Test	308,000		
0105X	Quality Control	168,000		

DDT&E

PLAN I

023XX	Control Valves		$ 1,428,000	
0231X	Engineering	$ 348,000		
0232X	Fabrication	392,000		
0233X	Material	454,000		
0234X	Component Test	150,000		
0235X	Quality Control	84,000		
03XXX	Ground Support Equipment			$ 1,223,000
031XX	Development of GSE		$ 1,223,000	
0311X	Engineering	$ 643,000		
0312X	Fabrication	150,000		
0313X	Material	311,000		
0314X	Component Test	80,000		
0315X	Quality Control	39,000		
04XXX	Engine Systems			$26,566,000
041XX	Engine Development		$14,307,000	
0411X	Engineering	$9,734,000		
0412X	Fabrication	808,000		
0413X	Material	102,000		
0414X	Component Test	3,533,000		
0415X	Quality Control	130,000		
042XX	PFC		$ 1,872,000	
0421X	Engineering	$ 822,000		
0422X	Fabrication	130,000		
0423X	Material	16,000		
0424X	Test	883,000		
0425X	Quality Control	21,000		
043XX	FPC		$ 7,932,000	
0431X	Engineering	$6,146,000		
0432X	Fabrication	130,000		
0433X	Material	16,000		
0434X	Test	1,619,000		
0435X	Quality Control	21,000		

DDT&E

PLAN I

044XX	Reliability and Service Free Demo.		$ 2,455,000	
0441X	Engineering	$1,269,000		
0442X	Fabrication	235,000		
0443X	Material	30,000		
0444X	Test	883,000		
0445X	Quality Control	38,000		
05XXX	Program Management			$ 6,689,000
051XX	Program Management		$ 565,000	
052XX	Program Control		989,000	
053XX	Configuration Control		622,000	
054XX	Reliability		2,021,000	
55XX	Quality Assurance		865,000	
056XX	Manufacturing Services		252,000	
057XX	Travel and Subsistence		250,000	
058XX	Computer Services		1,125,000	
06XXX	Deliverables			$ 8,304,000
061XX	Ground Test Engines		$ 2,449,000	
0611X	Fabrication	$1,317,000		
0612X	Material	848,000		
0613X	Acceptance Test	37,000		
0614X	Quality Control	247,000		
062XX	PFC Engines		$ 2,449,000	
0621X	Fabrication	$1,317,000		
0622X	Material	848,000		
0623X	Acceptance Test	37,000		
0624X	Quality Control	247,000		
063XX	FCE Engines		$ 1,226,000	
0631X	Fabrication	$ 659,000		
0632X	Material	424,000		
0633X	Acceptance Test	19,000		
0634X	Quality Control	124,000		

DDT&E

PLAN I

064XX	GSE		$ 1,137,000	
0641X	Fabrication	$ 340,000		
0642X	Material	708,000		
0643X	Quality Control	89,000		
065XX	Mockup		$ 79,000	
0651X	Engineering	$ 28,000		
0652X	Fabrication	44,000		
0653X	Material	7,000		
066XX	Spares		$ 964,000	
0661X	Fabrication	$ 527,000		
0662X	Material	339,000		
0663X	Quality Control	98,000		
07XXX	Tooling and STE			$ 2,506,000
071XX	Tooling		$ 293,000	
0711X	Factory Tooling (NR)	$ 151,000		
0712X	Factory Tooling (REC)	142,000		
072XX	STE		$ 2,213,000	
0721X	Factory STE (NR)	$ 80,000		
0722X	Factory STE (REC)	133,000		
0723X	Test STE (NR)	2,000,000		
08XXX	Integration and Engine Support			$ 3,032,000
081XX	Engineering		$ 1,592,000	
082XX	Field Support		457,000	
083XX	Manuals		284,000	
084XX	Training		226,000	
085XX	Spares Management		196,000	
086XX	Logistics		277,000	
09XXX	Data			$ 5,653,000
091XX	Engineering		$ 2,899,000	
092XX	Management		473,000	
093XX	Program Support		2,281,000	
10XXX	Facilities			$ 2,700,000
101XX	Administration		-	
102XX	Test		$ 2,700,000	
103XX	Shop		-	
	Total DDT&E Cost			$82,092,000
	Development Contingency			8,209,000
			Total	$90,301,000

PRODUCTION

			PLAN ALL
00XXX	Hardware		$34,667,000
001XX	Fabrication	$16,520,000	
002XX	Material	14,597,000	
003XX	Quality Control	3,560,000	
01XXX	Acceptance Test		$ 1,994,000
011XX	Quality Control	$ 81,000	
012XX	Test Labor	1,913,000	
02XXX	Initial Spares		$ 143,000
021XX	Fabrication	$ 66,000	
022XX	Material	63,000	
023XX	Quality Control	14,000	
XXX	Engineering		$ 826,000
031XX	Sustaining Engineering	$ 826,000	
04XXX	Tooling		$ 3,653,000
041XX	Production (NR)	$ 1,363,000	
042XX	Recurring	2,290,000	
05XXX	Program Management		$ 3,479,000
051XX	Program Management	$ 275,000	
052XX	Program Control	165,000	
053XX	Data and Documentation	1,385,000	
054XX	Quality Assurance	1,169,000	
055XX	Configuration Management	485,000	
07XXX	Manufacturing Services		$ 2,758,000
071XX	Manufacturing Services	$ 2,758,000	
08XXX	GSE		$ 300,000
081XX	Fabrication	$ 90,000	
082XX	Material	186,000	
083XX	Quality Control	24,000	
	Total Production Cost		$47,820,000

OPERATIONS

				PLAN ALL
00XXX	Field Support			$ 3,000,000
001XX	Maintenance and Refurbishment		$ 1,501,000	
002XX	Field Engineering		1,499,000	$ 929,000
01XXX	Engine and Component Overhaul			
011XX	Fabrication Labor		$ 703,000	
012XX	Material		112,000	
013XX	Quality Control		114,000	
02XXX	Engineering			$ 2,938,000
021XX	Sustaining Engineering		$ 1,406,000	
022XX	Logistics Support		1,542,000	
03XXX	Spares			$ 683,000
031XX	Engine Spares		$ 539,000	
0311X	Fabrication Labor	$ 239,000		
0312X	Material	249,000		
0313X	Quality Control	51,000		
032XX	GSE		$ 144,000	
0321X	Fabrication Labor	$ 430,000		
0322X	Material	90,000		
0323X	Quality Control	11,000		
04XXX	Program Management			$ 3,198,000
041XX	Program Management		$ 424,000	
042XX	Program Control		283,000	
043XX	Data and Documentation		1,715,000	
044XX	Quality Assurance		65,000	
045XX	Configuration Control		211,000	
046XX	Travel & Relocation		500,000	
05XXX	Facilities Maintenance			$ 133,000
051XX	Tooling Maintenance		$ 133,000	
06XXX	Service Life Demo.			$ 669,000
061XX	Test		$ 644,000	
062XX	Quality Control		25,000	
	Total Operations Cost			$11,550,000

PLAN II: MINIMUM TIME PROGRAM

The minimum time development program (Plan II) will be accomplished in 49 months. The engine, ground support equipment (GSE), and mockups will be designed, tested, and verified in accordance with the overall program schedule shown in Fig. 6-16. Formal demonstrations will be performed to provide the basis for Preliminary Flight Certification (PFC) and Final Flight Certification (FFC). The objective of minimum time will be achieved by:

1. Maximum use of facilities for fabrication, assembly and testing, including double shifting and premium time labor.

2. Employing knowledge gained from similar rocket engine development programs such as the SSME to reduce laboratory testing prior to start of engine testing.

3. Initiating engine system testing as hardware is available and prior to completion of component design verification testing.

4. Completing some component verification testing on the engine.

Activities leading toward accomplishment of each phase of the development program are presented herein.

The production program will be a 46-month effort initiated by long-lead hardware release following Critical Design Review (CDR). The first engine will be delivered in month 58, and the desired two-per-month rate will be achieved by month 60. The fiftieth engine will be delivered in month 82.

The Operations and Flight Support effort will be initiated with engine integration efforts at the outset of the program and will continue through 10 years of operational support. The operational support is assumed to begin at IOC which, in turn, is assumed to occur following FFC. The 10-year effort will be completed 13 years and 11 months after program go-ahead.

DEVELOPMENT PLAN

The minimum time development program for an advanced space engine capable of a vacuum thrust of 88964 Newtons (20,000 pounds) will consist of a design demonstration phase and a certification phase. The design demonstration phase will require approximately 33 months. This phase will emphasize design and analysis to allow an early start for engine system testing. Component and subsystem laboratory and hot-fire verification testing will be conducted concurrent with engine testing. The first engine system will be assembled and started in test as soon as hardware is available. Initial engine testing will be concerned with component development as well as engine system operating characteristics. Component testing could be diverted to support resolution of engine operating problems rather than verification of design.

Page intentionally left blank

Initial design releases for procurement of long-lead hardware to support component, subsystem, and engine testing will be completed 7 months from program start. All detail parts drawings for the first R&D engine will be released 10 months from program start. A preliminary design review is scheduled 22 months after program start to allow for feedback of design information resulting from the extensive component test program and early engine system testing. Following completion of the PDR, the engine design will be essentially frozen. Only mandatory design changes resulting from customer request and engine testing will be allowed thereafter. The Critical Design Review is scheduled 38 months from program start. After completion of the CDR, the design will be frozen except for changes required by changes to the CEI specification.

Thrust chamber assembly hot-fire tests will be initiated approximately 12 months after program start. Low- and high-pressure turbopump hot-fire testing will be initiated approximately 12 and 15 months, respectively, after program start. These tests will be accomplished on existing test facilities at the Santa Susana Field Laboratory which have been modified for the specified engine hardware.

The first site engine test will be conducted approximately 19 months after program start, with the first altitude simulation test conducted approximately 21 months after program start. These engine stands will also be located at the Santa Susana Field Laboratory. The two site test stands will be existing facilities which have been modified for testing the ASE. Engines tested in these facilities will have a nozzle expansion ratio (ϵ) of 8:1 to preclude nozzle separation side loads. The primary test objectives to be achieved with these engines include:

1. Evaluation of engine ignition characteristics (preburner and main chamber).
2. Evaluation of engine sequencing.
3. Evaluation of engine input requirements such as NPSH, propellant inlet temperatures, etc.
4. Evaluation of engine service life.

The altitude simulation engine test facility also will be a modification of an existing facility; however, major changes will be required. This facility will be designed for testing of the thrust chamber assembly at altitude-simulating conditions, as well as the engine systems. Engines tested in this facility will have a nozzle expansion ratio (ϵ) of 400:1. The primary objectives of testing in this facility include all those listed for the site test facilities but under altitude-simulating conditions. Additionally, the major objectives of engine performance and start and shutdown transient characteristics will be evaluated on this test facility.

The certification phase of the development program will occur during the last 14 months of the program. Major emphasis during this period will be directed toward the demonstration of flight readiness. All major performance parameters will be demonstrated to be within CEI specification limits by PFC except for service-free life and life between overhaul. Program control to assure completion

of all required demonstrations to achieve certification will be by means of Design Verification Specifications (DVS). Completion of the certification demonstration described in each DVS will provide the basis of PFC. The test requirements for the PFC demonstration are given in the engine development section of this plan. Component and subsystem testing will be continued during the certification phase at a rate necessary to complete DVS verification requirements prior to PFC. The most significant milestone of the certification phase will be completion of the Final Flight Certification test program. The requirements for this program are also given in the engine development section of this plan. The test effort is summarized in Fig. 6-17.

Component Testing

The minimum time development program (Plan II) provides for a concentrated component development program concurrent with engine testing. This effort will consist of verification of all functional components through component laboratory and subsystem hot-fire testing as well as engine system testing. Thermal and mechanical fatigue life, structural integrity, performance and operational characteristics will be evaluated and verified. Approximately 1500 component level tests will be conducted in the laboratory which will simulate the engine environment in all practicable limits.

Subsystem hot-fire testing will be concentrated on the verification of component, function, stability and performance. Component life demonstration will be accomplished with the engine testing. Testing of the thrust chamber assembly, low-pressure and high-pressure oxidizer and fuel pumps with preburners will be accomplished at test facilities located at the Santa Susana Field Laboratory. Approximately 750 subsystem hot-fire tests will be conducted to verify requirements and assumptions. The specific requirements for component testing of each component and subsystem are delineated in the following paragraphs.

Turbomachinery. The 88,964 Newtons (20,000 pounds) thrust advanced space engine turbomachinery consists of four turbopumps: one low-pressure and one high-pressure pump for each propellant, liquid oxygen and liquid hydrogen. The high-pressure turbines are driven by hot gas (H_2 + H_2O), while the low-pressure turbines are driven by ambient temperature GH_2. Because the engine uses a topping cycle, the operating characteristics of the pumps and turbines are critical and interdependent with each other and with the rest of the system. Therefore, engine balance requirements and design analysis of the turbomachinery will be critical to successful engine operation.

The minimum time program is success oriented and, as such, assumes that no major turbopump development problems will be encountered. The primary objectives of the turbopump test program are to verify the performance and mechanical integrity of the four turbopumps at the engine operating conditions. It is assumed that the technology for the turbopump bearings and seals is available. Therefore, no separate testing of these components will be required. A complete engine balance will be firmly established early in the program providing a basis for turbopump operating requirements. The technology available from the SSME and other engine programs will be utilized to a maximum to reduce the development risks and eliminate the need for extensive development testing.

Page intentionally left blank

The four turbopumps (a high-pressure oxidizer, high-pressure fuel, low-pressure oxidizer, and a low-pressure fuel) will be tested separately. In this manner, the operating characteristics of each of the four turbopumps can be determined independent of each other. This also allows testing of each of the turbopumps without being dependent on the availability of one of more of the other turbopumps, and allows a compression of the test schedule by simultaneous test series.

A total of two each high-pressure and low-pressure oxygen and hydrogen turbopump assemblies will be utilized during the component hot-fire test program. The schedule for fabrication and testing of the turbomachinery is shown in Fig. 6-18 with a breakdown of the individual tests shown in Fig. 6-19 and 6-20.

Turbine Development Testing. Initially, a turbine from each turbopump will be subjected to a series of 20 spin tests on a dynamometer in the Rocketdyne Canoga Park Development Laboratory. These tests will be conducted at lower-than-normal speed using gaseous nitrogen to develop a complete turbine map knowing the difference in gas properties between the gaseous nitrogen and the actual gases utilized by the turbines in the engine. Five different power levels at four different inlet pressures will be investigated to establish the turbine maps.

Low-Pressure Turbopump Testing. The low-pressure turbopumps, by virtue of their relative simplicity, low rotational speed, which is below the rotor first critical speed, and low turbine gas temperature, require less development than the high-pressure turbopumps. Initial testing will be conducted to verify the hydrodynamic performance of the pump (Test d, Fig. 6-19).

Suction performance testing will be investigated in a series of three 200-second-durations tests (e, f, and g, Fig. 6-19). Efficiency of the pumps will be determined utilizing the pump H-Q performance and known performance of the turbines obtained during dynamometer testing.

As testing proceeds, the mechanical integrity of the pumps will be verified (test h through o, Fig. 6-19) to the point that it is considered safe to install the turbopump on an engine. All full-life integrity verification testing will be conducted on the engine. This eliminates the need for full-life demonstrations at both the component level and on the engine which conforms to the minimum-cost philosophy.

High-Pressure Turbopump Testing. The initial testing conducted with the high-pressure turbopumps (tests a through g, Fig. 6-20) will utilize ambient hydrogen gas to drive the turbines. The tests will be utilized to gain mechanical integrity confidence and initial hydrodynamic performance data. Full-power, full-duration testing will then commence, utilizing preburner hot-gas products to drive the turbines (tests h through s, Fig. 6-20 . Periodic inspections of the turbine components will be conducted to verify structural integrity after exposure to full power, pressure, thermal, and rotational stresses.

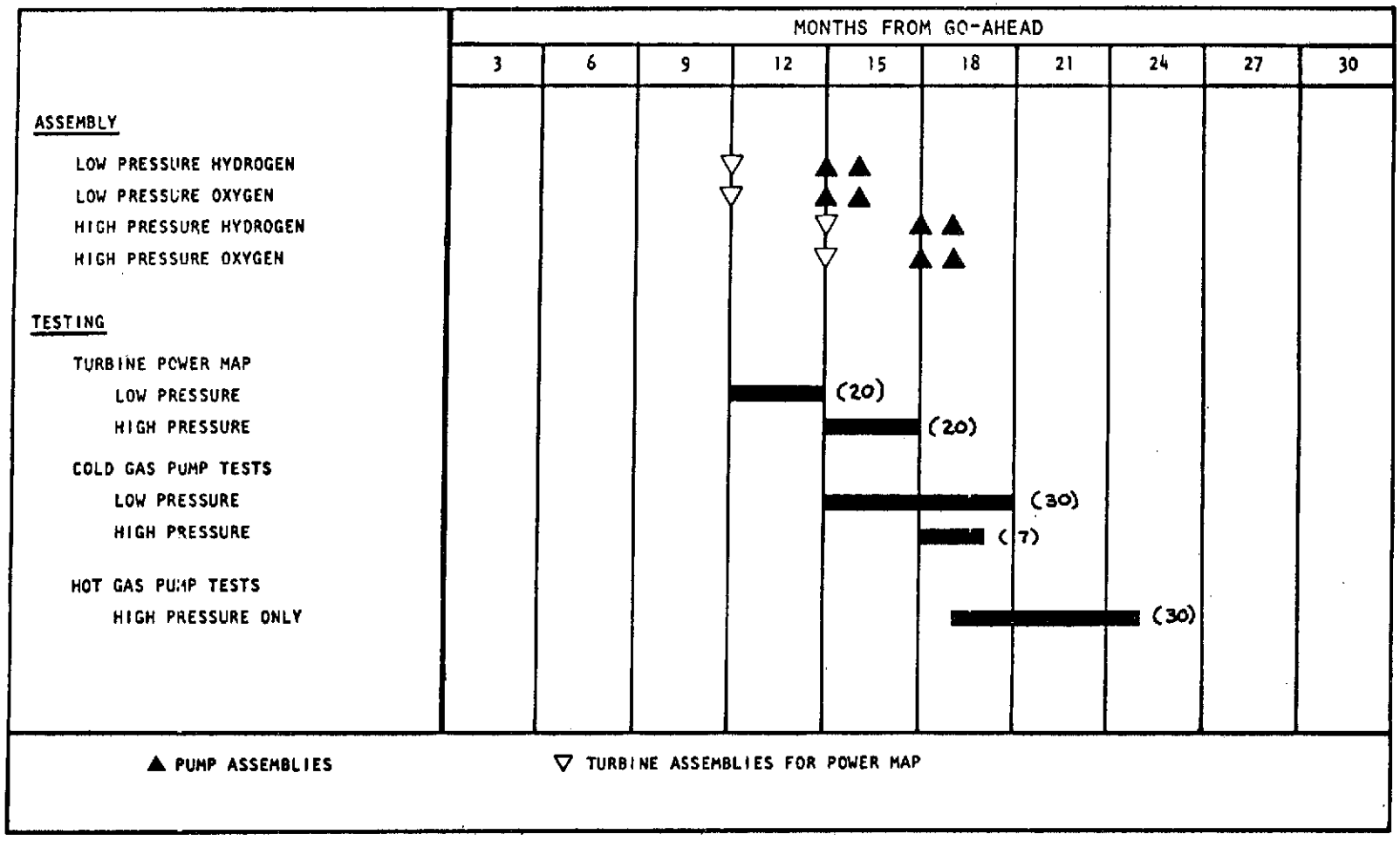

Figure 6-18. Component Turbomachinery Assembly and Test Schedule

Test Type	T/P Unit	Propellants: Pump Oxid/Fuel	Propellants: Turbine	No. of Tests	Duration seconds	Remarks
Map Turbine in Dynamometer Facility	--	--	GN_2	20	200 EA	
Ambient Gas T/P Spins in T/P Test Facility	1st	LO_2/LH_2	GH_2			
(a) Ramp to 50% Design Speed at Nom. Q/N		↓	↓	1	30	Bring to speed slowly
(b) Ramp to 75% Design Speed at Nom. Q/N				1	30	Bring to speed slowly
(c) Ramp to 100% Design Speed at Nom. Q/N				1	30	Bring to speed slowly
(d) Vary Q at Design Speed				1	200	G-Q, Eff. Type Test
(e) NPSH vs HD at Nom. Q/N and Speed				1	200	Suction Performance Check
(f) NPSH vs HD at 5.5 M/R Q and N				1	200	Suction Performance Check
(g) NPSH vs HD at 6.5 M/R Q and N				1	200	Suction Performance Check
(h) Ramp to 110% Speed				1	30	Overstress Check
(i) Full Duration at Nom. Q and N				1	2000	
(j) Full Duration at 5.5 M/R Q and N				1	2000	
(k) Full Duration at 6.5 M/R Q and N				1	2000	
(l) Repeat (e)				1	200	
(m) Repeat (f)				1	200	
(n) Repeat (g)				1	200	
(o) Full Duration at Highest Turbine HP Condition				1	2000	
Repeat (a) through (o)	2nd	LO_2/LH_2	GH_2	15	9520	

Figure 6-19. Low-Pressure Oxidizer and Fuel Turbopump Development Test (Program 2)

Test Type	Unit	Propellants		No. of Tests	Duration seconds	Remarks
		Pump Oxid/Fuel	Turbine			
Map Turbine in Dynamometer Facility	--	--	GN_2	20	200 EA	
Ambient Gas T/P Spins in T/P Test Facility	1st	LO_2/LH_2	GH_2			
(a) Ramp to 50% Design Speed at Nom. Q/N				1	30	Bring to Speed Slowly
(b)) Ramp to 75% Design Speed at Nom. Q/N				1	30	Bring to Speed Slowly
(c) Ramp to 100% Design Speed at Nom. Q/N				1	5	High Acceleration Ramp Analyze for Critical Speed
(d) Vary Q at Design Speed				1		H-Q, EFF, Type Test
(e) NPSH vs HD at Nom. Q/N and Speed				1		Suction Performance Check
(f) NPSH vs HD at Low Q/N and Nom. Speed				1		Suction Performance Check
(g) NPSH vs HD at High Q/N and Nom. Speed				1		Suction Performance Check
Hot Gas T/P Tests in T/P Test Facility	1st	LO_2/LH_2	H_2+H_2O			
(h) Ramp to 100% Design Speed at Nom. Q/N				1	5	High Acceleration Ramp. Facility, T/P Checkout
(i) Vary Q at Design Speed				1	200	H-Q Type Test
(j) Full Duration at Nom. Q and N				1	2000	
(k) Full Duration at Nom. Q and N for 5.5 M/R				1	2000	
(l) Full Duration at Nom. Q and N for 6.5 M/R				1	2000	
(m) Ramp to 110% Speed at Nom. Q/N					30	Overstress Check
(n) NPSH vs HD at Nom. Q/N and Speed				2	200 EA	Suction Performance Check
(o) NPSH vs HD at 5.5 M/R Q and N				2	200 EA	Suction Performance Check
(p) NPSH vs HD at 6.5 M/R Q and N				2	200 EA	Suction Performance Check
(q) Vary Q at 80% Speed (LH_2 T/P Only)				1	200	Determine Effects of Compressibility on Efficiency
(r) Vary Q at 90% Speed (LH_2 T/P Only)				1	200	Determine Effects of Compressibility on Efficiency
(s) Full Duration at Highest Turbine HP Condition				1	2000	
Repeat (h) through (s) Above	2nd	LO_2/LH_2	H_2+H_2O	15	9835	

Figure 6-20. High-Pressure Oxidizer and Fuel Turbopump Development Tests (Program 2)

Testing will emphasize determination of hydrodynamic performance characteristics over the full range of operating conditions required to operate the engine at mixture ratios of 5.5 to 6.5. Suction performance tests will be conducted to verify that the input conditions to the high-pressure pumps as provided by the low-pressure pumps will be satisfactory.

As in the case of the low-pressure turbopumps, full-life integrity verifications will be conducted at the engine level.

Also during these tests, sufficient instrumentation will be provided to ensure that the rotor dynamics of the turbopump assemblies remain within acceptable limits. Disassembly and inspection of the hardware after testing will determine if any unusual conditions such as excessive wear has occurred.

The data from the high-pressure as well as the low-pressure turbopump tests will be utilized in the engine start model and mainstage computer programs to ensure engine compatibility.

Controls and Valves. The 88,964 Newtons (20,000 pounds) thrust advanced space engine requires four primary control valves (main oxidizer valve, main fuel valve, preburner oxidizer control valve, and main chamber oxidizer control valve), an antiflood valve to prevent oxidizer flow to the heat exchanger until hot gas is flowing through it, and numerous check valves to prevent reverse flow of the propellants.

The basic technology for these valves has been established under numerous related programs at Rocketdyne, and only verification testing in the Development Laboratory will be necessary under the minimum-time program.

The controls and valves component test plan shown in Table 6-15 provides for completing the specified types of tests on individual valve assemblies in accordance with the schedule presented in Fig. 6-21 The two main propellant valves (O_2 and H_2) are identical in design to minimize cost, as are the preburner oxidizer valve and the main chamber oxidizer valve. The required quantities of each valve are shown in Table 6-15, which provides sufficient hardware for functional and destructive testing.

Water Flow Test. The purpose of this test is to verify that the component can meet the fluid flowrate and pressure drop requirements specified. This verification can be accomplished most economically with water, and will be conducted in the flow area of the Engineering Development Laboratory at Rocketdyne.

Tests will be performed to establish the flow versus ΔP characteristics of the component, and the envelope of flowrate versus ΔP at various valve positions will be explored. Posttest inspection of the component will be made to ensure that no abnormal degradation of the mechanical elements occurred. These data will be compared to the requirements at the specified differential pressures, and the data will be correlated with the flow coefficients used in the design to establish the valve size. Testing one unit is sufficient to generate flow versus ΔP data for the component.

TABLE 6-15. CONTROLS AND VALVES TEST PLAN

Component	Tests Required								
	Proof Test	Leak and Functional	Water Flow (ΔP)	Dynamic Torque	Environmental	Endurance	Ignition Proof	Vibration	Burst
Main Propellant Valves (MOV/MFV)	3	3	1	1	0	2	0	2	1
Oxidizer Control Valve (Preburner and Main Chamber)	3	3	1	1	0	2	1	2	1
Pneumatic Manifold	2	2	-	-	0	1	1	0	1
Antiflood Valve	3	3	1	-	0	2	0	2	1
Purge and ASI Check Valves	6	6	2	-	0	4	0	4	2

Number of assemblies required:

Main Propellant Valves: 3

Oxidizer Control Valves: 3

Pneumatic Manifold: 2

Antiflood Valve: 3

Purge and ASI Check Valves: 6

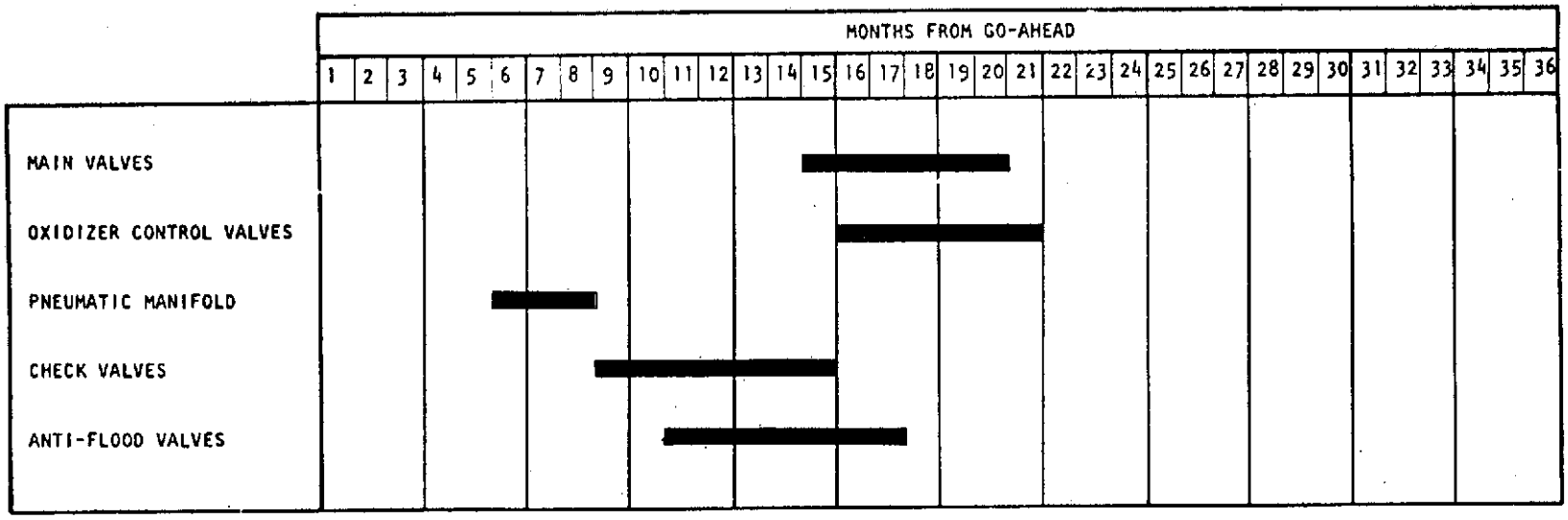

Figure 6-21. Controls and Valves Test Schedule

Verification will be considered complete when the envelope of flow versus ΔP has been completed as described above and when analytical correlation indicates that the flowrate and pressure drop requirements are met.

Dynamic Flow Torque Test. The purpose of this test is to verify that the actuator loads encompass the maximum dynamic torque loads of the component. This verification can be accomplished in conjunction with the water flow test.

The fluid dynamic torque will be measured while flowing water through the valve at several valve positions over its full angular travel. The dynamic flow torque test data will be used to establish the fluid dynamic flow torque during the excursion of the component and will be compared with the flow torque coefficients used in the design to establish the power requirements of the actuator.

Verification will be considered complete when the test data have been recorded and correlated to verify the requirements.

Endurance Test. The purpose of this test is to verify that the component can meet the specified cycle/environment requirements in Table 6-16. Ambient, cryogenic, and high-temperature cyclic and functional testing will be conducted in the mechanical area of the Rocketdyne Engineering Development Laboratory to demonstrate this capability.

The values will be functionally tested, cycled under the required environment, and functionally tested at selected points in the cycle series, and again at the conclusion of each test series.

Verification will be considered complete when the units have successfully completed the required cycles and have subsequently met the functional test requirements.

Vibration Test. The purpose of this test is to verify that the component can meet specified vibration requirements. To demonstrate this, each component will be subjected to tests conducted in the vibration area of the Rocketdyne Engineering Development Laboratory.

Components will be mounted to a vibration table with a three-plane stabilizing fixture simulating the engine mounting configuration. The component will be thermally conditioned to (88.9 K ± 27.8 K) 160 ±50 R during vibration, and will be vibrated in its normal engine operating mode (open) as experienced during engine operation. With the valve open, pressures will be applied to the propellant inlet port, and acceleration levels will be monitored at various points on the component to determine acceleration amplification. A functional test will be performed after completing vibration in each axis. The component will be disassembled and inspected following the final functional test.

The acceleration amplification factor between the input to the vibration table and the greatest output on the component will be used to predict peak acceleration loads on all component appendages. These loads will be correlated with the vibration levels measured during engine hot-fire tests. In the event the engine test levels are more severe, additional vibration tests will be conducted to

TABLE 6-16. ENDURANCE CYCLE TEST REQUIREMENTS

	MOV AND MFV	OCV	AFV	CV	Pneumatic Manifold
Ambient Temperature					
T = 530 R (294 K)					
Pressurized Cycles	3,300	3,300	3,300	3,300	3,300
Cryogenic Temperature					
T = 160 ±50 R (88.9 ±27.8 K)					
Pressurized Cycles	682	682	682	682	451
Zero Pressure Cycles	440	440	440	--	--
High-Temperature					
T = 590 $^{+10}_{-0}$ R (327.8 + 5.6 K)					
Ambient Pressure Cycles	1,540	1,540	1,540	1,540	1,540
Modulation Tests					
T = 160 ±50 R (88.9 ±27.8 K)					
2.5% Range					
26% Nominal Position	--	40,000	--	--	--
36% Nominal Position	--	4,000	--	--	--
Total Cycles	5,962	49,962	5,962	5,522	5,291

verify the revised requirements. In the event the engine test vibration levels are less severe, the requirements. In the event the engine test vibration levels are less severe, the requirements will be revised accordingly prior to testing additional units.

Verification will be considered complete when the units specified have successfully met the functional test requirements and no structural damage or detrimental wear are noted during posttest disassembly.

Burst Test. The purpose of this test is to verify that the component can meet specified ultimate pressure and safety factor criteria requirements. The test will be conducted in the mechanical area of the Rocketdyne Engineering Development Laboratory.

Strain gage data will be used to determine the working stress and to verify that the component meets the minimum yield factor of safety at the limit pressure. Burst test data will also be evaluated to verify that the component meets the requirements for minimum ultimate factor of safety and the minimum ultimate pressure as defined.

Verification will be considered complete when one unit completes the burst test and the resulting data shows that the component meets the minimum yield factor of safety without yielding which is detrimental to proper operation and also meets the minimum ultimate factor of safety and ultimate pressure as defined.

Functional Test. The purpose of this test is to establish the functional condition of the component. This will be accomplished by performing leakage and actuation tests in the clean room area of the Rocketdyne Engineering Development Laboratory.

The functional test will be conducted prior to and subsequent to individual verification tests, noted in Table 6-17, subsequent to each axis of vibration test, and after specified number of cycles during the endurance test.

The leakage test will be conducted at both ambient and cryogenic temperatures with the component thermally conditioned to the temperature specified. The leakage will be measured using helium over the pressure range specified.

The actuation test will be conducted at both ambient and cryogenic temperatures with the component thermally conditioned to the temperature specified. Travel time from full closed to full open and return to full closed will be measured.

The functional test data will be correlated with data from prior tests to determine whether the specific verification test adversely affected the functional

TABLE 6-17. FUNCTIONAL TESTS

Verification Test	Number of Units Allocated	Minimum Number of Units	Minimum Number of Tests per Unit
Vibrate all Valves	2*	2*	1*
Endurance			
MOV/MFV	2	2	1
OCV	2	2	1
AFV	2	2	1
CV (2 designs)	2 (each design)	2 (each design)	

*One pneumatic manifold

performance of the component. The functional test does not verify any specific requirement but merely establishes the functional condition of the component during a specific verification test and is a criteria for establishing the successful completion of the specific verification test.

Combustion Devices. The combustion devices required for the 88,964 N (20,000 pounds) thrust advanced space engine are: (1) an ignition system for the preburner and main chamber, (2) a preburner, and (3) a thrust chamber assembly.

Development testing of the combustion devices will be accomplished through a series of laboratory tests and component hot-fire tests at the Santa Susana Field Laboratory. The schedule for accomplishing the required tests is presented in Fig. 6-22. The following is a description of the tests planned for each device.

Ignition System. The ignition system for the 88,964 Newtons (20K ASE consists of two spark-initiated ASI assembly units, one each for the preburner and main chamber. Basically, each unit consists of a common integral air-gap spark igniter, a fuel-oxidizer injection scheme and a combustion chamber. The overall development schedule for both the spark igniter units and the ASI assemblies is shown in Fig. 6-23.

The integral spark igniter development will consist of preliminary design, breadboard igniter lab testing, final design, and lab testing of the finalized concept.

Key lab tests will include functional, electrical/electronic, vibration, environmental, pressure and leak verification testing. Twelve equivalent spark units are required for the lab test series: five units in a 4-month prototype optimization effort to evaluate the functional and electrical characteristics, and seven units in a 6-month final verification effort to demonstrate vibration, environmental, pressure, and leakage characteristics.

Development of the ASI assemblies for both the preburner and the main chamber will consist of materials and processes testing, cold-flow lab testing, and igniteronly hot-fire testing at both low and high pressure. The low-pressure hot-fire testing will demonstrate the engine ignition sequence, while the high-pressure (mainstage) testing will investigate steady-state operating mixture ratio and demonstrate cooling and durability.

Two assemblies (one of each type for the preburner and the main chamber) will be required for the lab testing, and six assemblies (three of each type) will be required for the hot fire testing. Initial testing will be conducted with prototype igniter units, and additional testing will use the final design. Forty-five low-pressure tests (ignition only) of 5 seconds average duration will evaluate start characteristics and spark energy requirements for the preburner ASI. An additional 30 high-pressure (mainstage) tests of 50 seconds average duration will be conducted to evaluate power level and mixture ratio, cooling, and life characteristics. Coincident with the preburner ASI tests will be 50 low-pressure and 35 high-pressure tests on the main thrust chamber ASI.

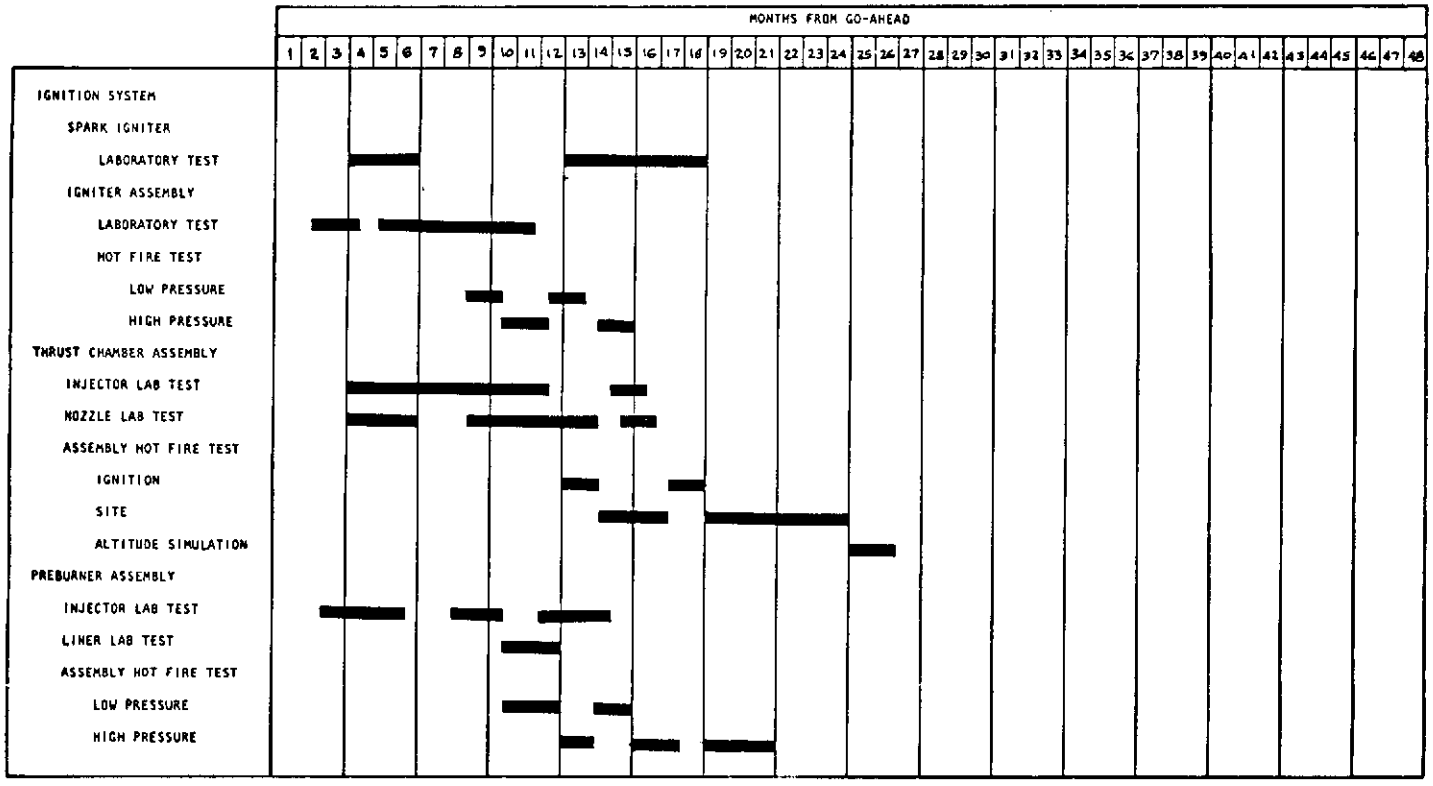

Figure 6-22. Combustion Devices Test Schedule

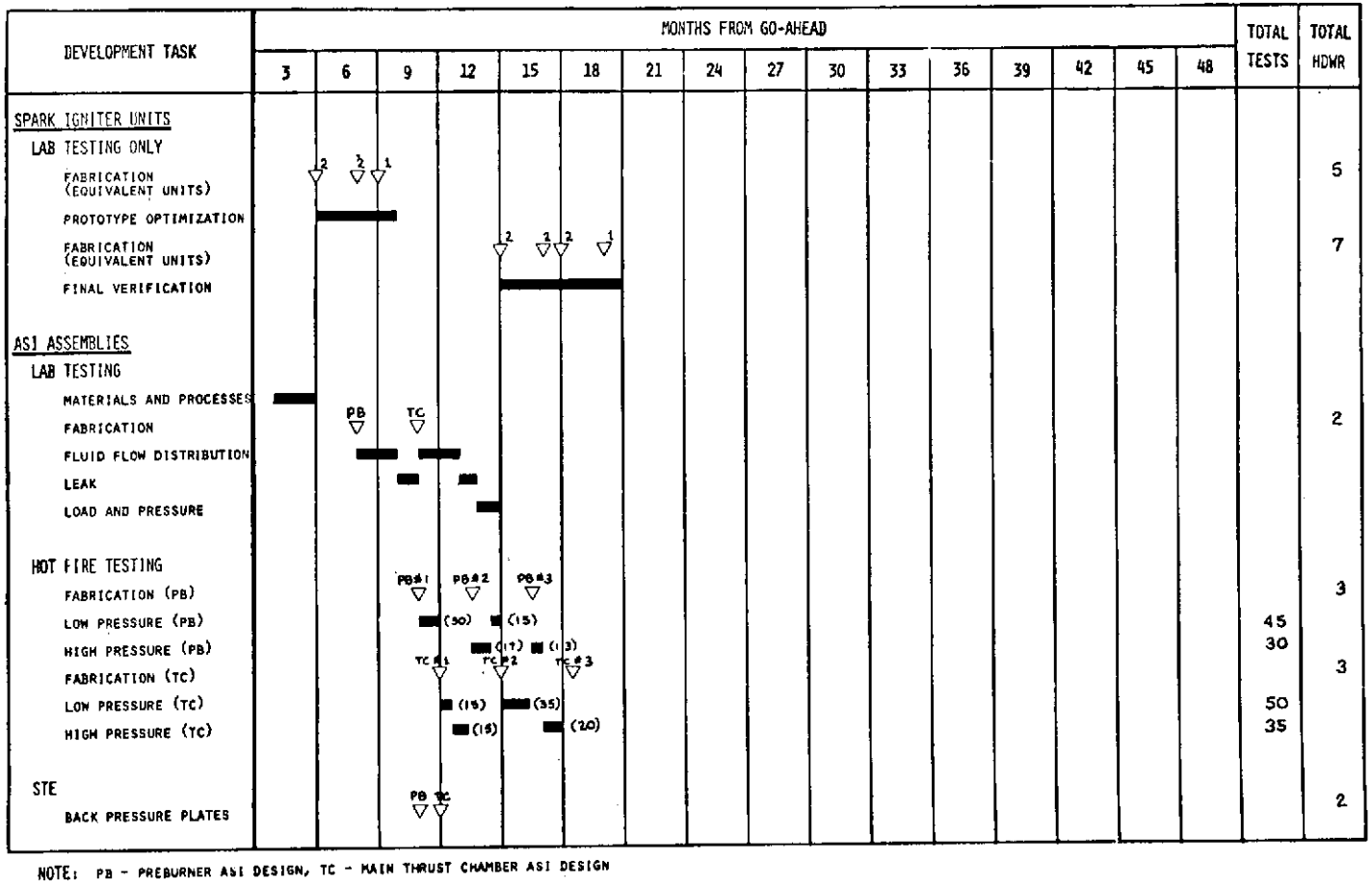

NOTE: PB - PREBURNER ASI DESIGN, TC - MAIN THRUST CHAMBER ASI DESIGN

Figure 6-23. Ignition System Development

To simulate engine conditions, two special back-pressure plates (one for the preburner and one for the main chamber) must be fabricated to accomplish the hot fire test program.

Thrust Chamber Assembly. The thrust chamber assembly consists of major components such as the injector, combustion chamber with a short nozzle ($\epsilon = 8$), a regeneratively cooled nozzle extension to $\epsilon = 100$, and a dump-cooled nozzle extension from $\epsilon = 100$ to $\epsilon = 400$. These chamber component designs will be finalized and detailed for thrust chamber-only testing and for engine testing. Chamber-only test hardware will vary only in hot-gas manifolding and interface attachment techniques. The overall development schedule for the thrust chamber is shown in Fig. 6-24, and consists of both cold-flow lab testing and hot-fire chamber-only testing.

Primary lab tests will include injector element flow, injector assembly flow, nozzle wind tunnel, nozzle coolant distribution, acoustic cavity tuning, leak, load, and pressure testing.

Twelve individual injector elements will be fabricated to study the element flow characteristics, and a full-scale injector flow model will be fabricated to study the injector flow distribution and element vortex shedding. An acoustic cavity model will also be built to perform the acoustic cavity tuning studies for the injector.

One nozzle wind tunnel model will be fabricated to study the nozzle flow and separation characteristics associated with the 400:1 extension, and a full-scale nozzle will be fabricated to perform flow distribution studies. A thrust chamber assembly from the hot-fire program will be used to perform the leak, load, pressure, and gimbaling tests. A special leak test fixture must also be fabricated to perform the leak test.

Nine chamber assemblies will be fabricated to conduct the hot-fire test program, the first six with a short 8:1 nozzle, and the last three with a full 400:1 nozzle. Three preburners and two turbine and hot-gas manifold simulators will be part of the STE required for these tests.

A total of 50 low-pressure ignition tests (5 seconds average duration) will be conducted to establish the ignition requirements and start and cutoff sequences. One hundred forty additional high-pressure-sea level tests (100 seconds average mainstage duration) will be conducted with the short nozzle chambers to establish injector performance, power level, mixture ratio, and structural and cooling characteristics. Seventy-five stability bombs will be used during this test series to evaluate combustion stability. The seventh, eighth, and ninth units, having a full 400:1 nozzle, will be used to establish the altitude performance characteristics, and to demonstrate the complete assembly cooling and structural integrity. Fifty-five high pressure altitude tests will be conducted on these three units.

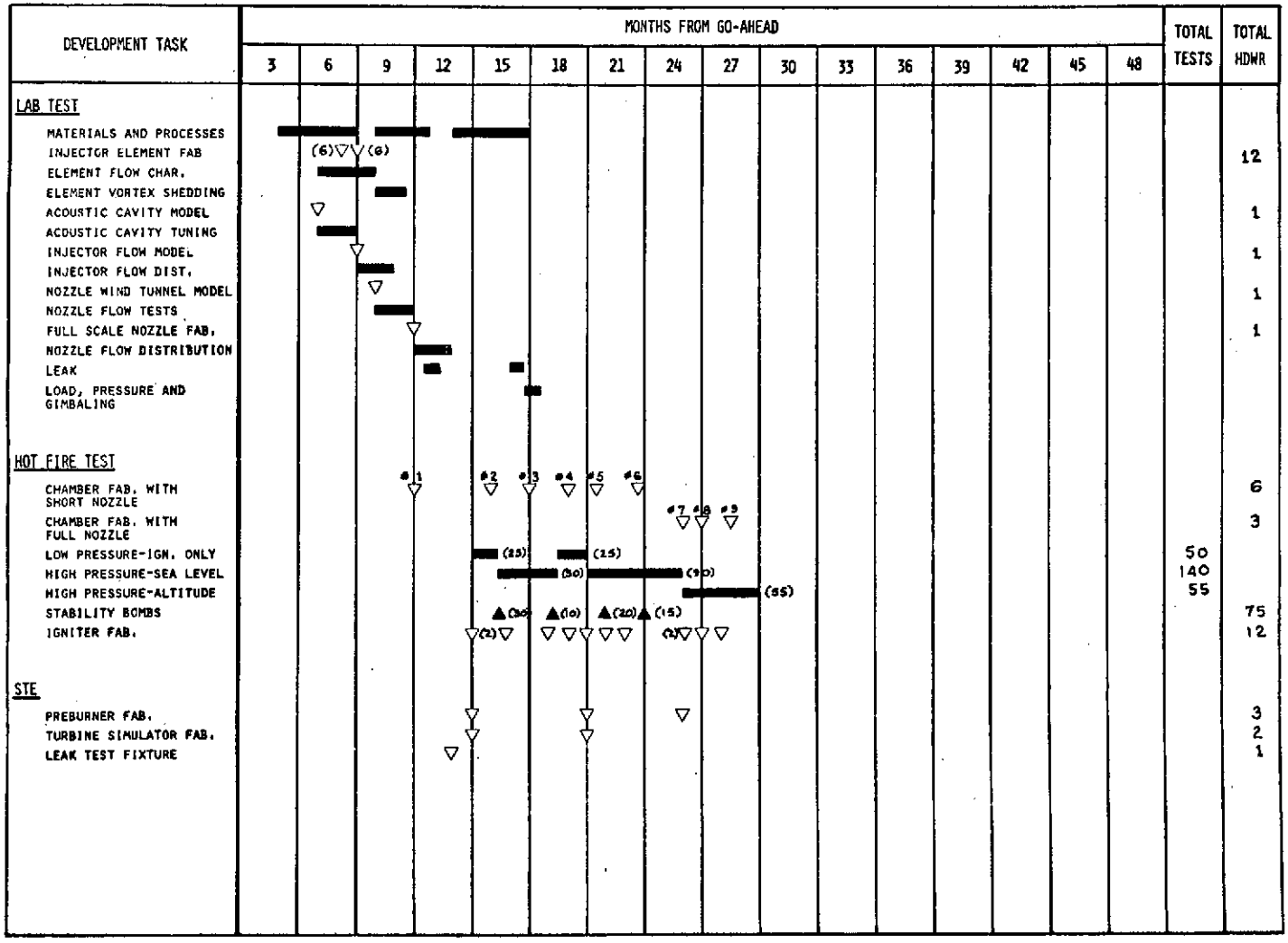

Figure 6-24. Thrust Chamber Assembly Development

Preburner. The preburner will supply high-pressure hot gas to drive the oxidizer and fuel turbopump turbines for engine application. Also, preburners will be used to supply hot gas for thrust chamber and for turbopump component testing. Detailed designs will be made for the engine preburner and for component use, including preburner-only testing. All preburner designs will be nearly the same except for possible attachment deviations. The overall development schedule for the preburner assembly is shown in Fig. 6-25, and consists of both cold-flow lab testing and hot-fire preburner-only testing.

The preburner will be subjected to lab verification testing such as injector element and injector flow distribution, liner coolant flow, leak, load, pressure, and acoustic cavity tuning.

Six different injector elements will be fabricated to study the element flow characteristics, and a full injector assembly will be made to study total face-flow distribution. An acoustic cavity model will also be built to perform the cavity tuning studies.

A full preburner liner will be fabricated to evaluate the coolant flow characteristics in terms of uniformity, pressure drop, and leakage. (This unit subsequently will be used in the first hot-fire hardware assembly.) Another preburner assembly from the hot-fire program will be used to perform the load and pressure tests.

Seven flanged preburner assemblies will be fabricated to support the hot-fire program. Preburner-only hot-fire testing will include 60 low-pressure ignition tests (5 seconds average duration) to verify start capability under different propellant conditions, and 107 high-pressure mainstage tests of 100 seconds average duration will be conducted to verify performance, duration capability, life, cooling, and stability, and hot-gas temperature profile uniformity. Forty stability bombs will be used in the high-pressure stability demonstrations, and two temperature rakes will be part of the STE required to evaluate the temperature profile. Three turbine backpressure simulators must also be fabricated to permit the preburner-only testing.

Ground Support Equipment. Ground Support Equipment (GSE) will be designed, fabricated, and demonstrated on a schedule that provides support of engine system testing, as shown in Fig. 6-16. The equipment operation will be verified during the early portions of the engine system test program and during the PFC and FFC portions of the development effort. Total equipment required is delineated in Table 6-18

The GSE allocations shown in Table 6-18 assume delivery of complete sets of equipment as required to support three engine integration sites: the vehicle contractor plant, a NASA test site (e.g., MSFC or MTF) and a launch site. These equipment will be delivered concurrent with prototype engine delivery during the DDT&E phase of the program. The additional engine handlers, covers, and closures would be delivered during the 50-engine production phase of the program.

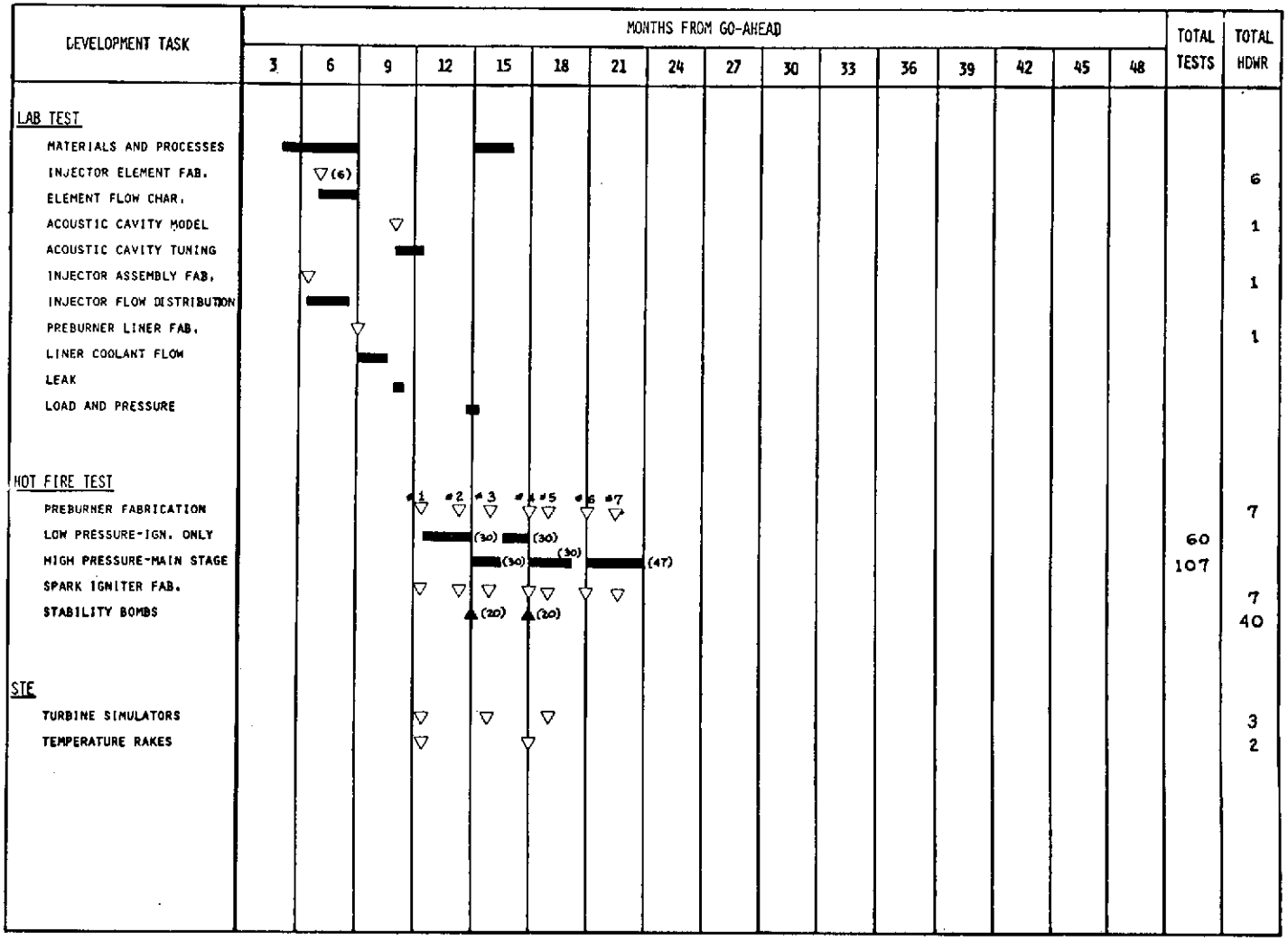

Figure 6-25. Preburner Assembly Development

TABLE 6-18. GSE ALLOCATIONS

Item	Development	Prototype	Production
Handling and Transport			
1.1 Handler, Engine (and Cover)	5	3	20
1.2 Sling, Handler (and Cover)	2	3	--
1.3 Sling, Engine, Rotating	2	3	--
1.4 Installer, Engine	1	3	--
1.5 Hoist Adapter	1	3	--
1.6 Covers and Closures, Set	5	3	20
1.7 Pad, Thrust Chamber Interior Protection	2	3	--
Test, Maintenance, and Servicing			
2.1 Console, Engine Electro/Pneumatic Checkout	1	3	--
2.2 Test Set, Engine	1	3	--
2.3 Test Set, Installed Engine	1	3	--
2.4 Flow Tester, Pneumatic (Atmospheric)	2	6	--
2.5 Flow Tester, Pneumatic (High Pressure)	2	6	--
2.6 Leak Detector, Mass Spectrometer	1	3	--
2.7 Tool Set, Special	1	3	--
2.8 Welding Set (and Cutters)	2	4	--
Control			
3.1 Control Test Panels (2)	1	3	--
Internal Inspection			
4.1 Borescope and Foreign Object Retrieval Set	1	2	--

Engine System Testing

Engine development testing will demonstrate that the flight configuration engine meets all the requirements of the engine Model Specification. A 13-engine development program consisting of 790 tests will be conducted. Overall engine development and verification test objectives are listed in Table 6-19 The engine system test schedule is shown in Fig. 6-26.

Development Tests. An 11-engine development test program, including two exploratory engines and six recycled engines, will be completed. The exploratory test series, consisting of 15 tests on each of two engines, will be conducted on the first two new engines assembled. The first engine will have a nozzle area ratio of 8:1, and will be tested on one of the site test stands at the Santa Susana Field Laboratory (SSFL). The second engine will have a nozzle area ratio of 400:1 and will be tested on the altitude simulation test facility at SSFL. The primary objective of this testing is to define engine ignition, start and shutdown transient characteristics. Additionally, engine interactions will be evaluated at both site and altitude conditions. Data obtained from these early tests will be used to improve the engine computer model.

A total of 671 site and altitude simulation tests are planned during the development phase. The primary objectives of this phase of the engine test program are:

1. Evaluate engine operational and performance characteristics at site and altitude conditions

2. Demonstrate, through a series of limits and overstress tests, the margin of safety inherent in the engine system

3. Demonstrate the combusion stability characteristics of the engine during a typical mission duty cycle, including idle mode, mainstage and restart conditions.

4. Certify through demonstration tests that the engine system will meet all requirements specified in the engine model specification. (Note: Service life between overhauls and maintainability will be demonstrated during the Flight Support Program.)

5. Demonstrate the adequacy of special servicing procedures and test equipment.

6. Validate Field Operating Instructions manuals.

This phase of the engine testing will certify the capability of the engine to meet program requirements. Engine service-free life will be demonstrated by the completion of the Final Flight Certification Test Program. Each engine in this phase of testing will accumulate additional operating duration to demonstrate a continued service-life growth. Five engines will be recycled at least one time with two engines recycled twice to allow evaluation of service-life growth on

TABLE 6-19. ENGINE DEVELOPMENT AND VERIFICATION TEST

Objectives	New Engines							Recycled Engines					
	001	002	003	004	005	006	007	101	102	104	105	201	205
Ignition-only Tests													
Site	X												
Altitude		X											
Site Operational and Performance Evaluation	X		X	X				X	X			X	X
Altitude Operational and Performance Evaluation		X			X						X		X
Stability Mapping of Main Injector			X		X						X		
Limits and Over Stress Testing													
Engine Mixture Ratio		X	X		X			X			X	X	X
NPSH			X	X	X				X		X		X
Engine Ambient Environment					X						X		X
Duration		X	X		X						X	X	X
Maximum Time Between Firings					X						X		
Minimum Time Between Firings					X						X		
Preliminary Flight Certification (Alt)						X							
Final Flight Certification (Alt)							X						

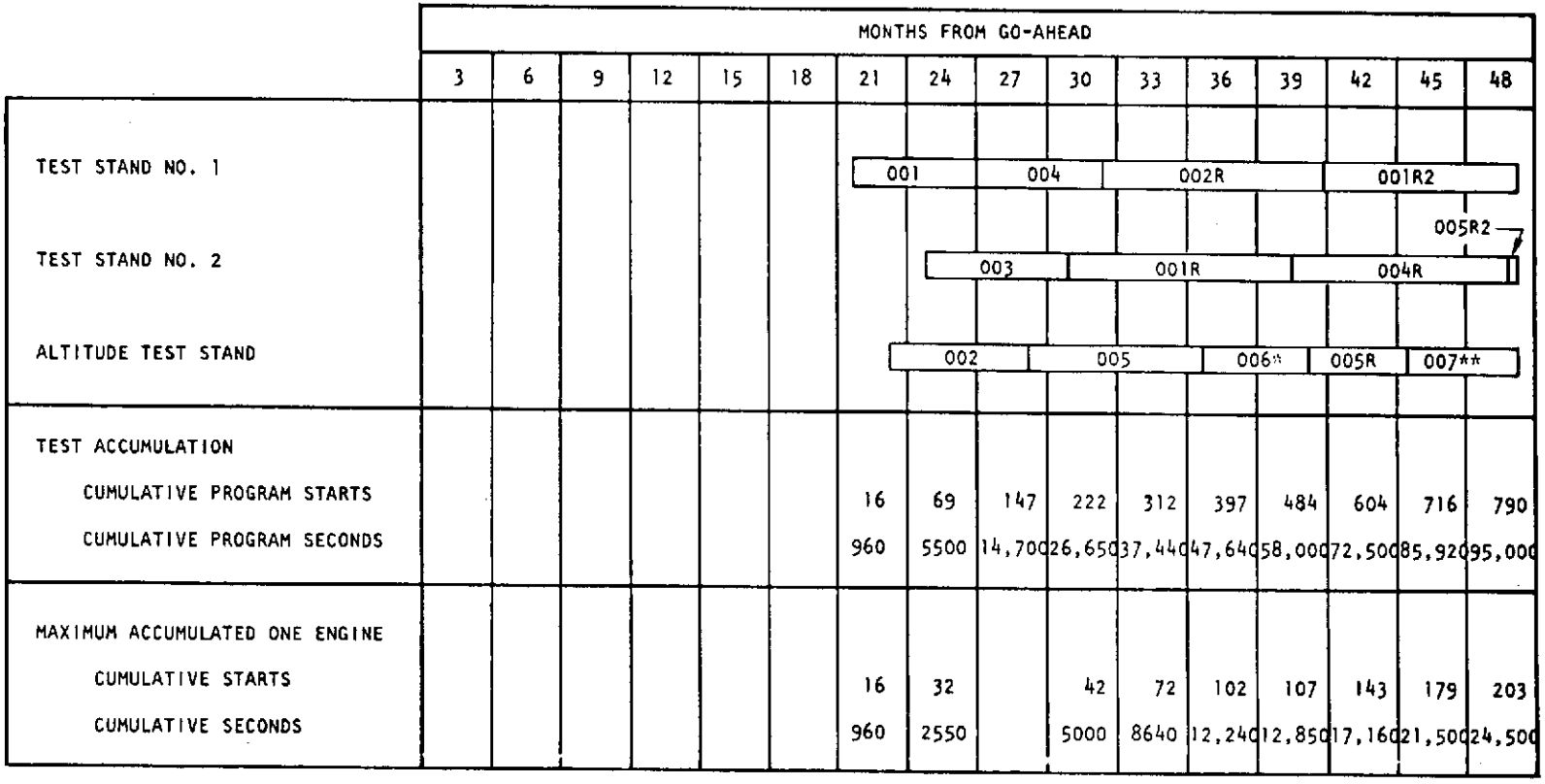

* PFC ENGINE

** FFC ENGINE

Figure 6-26. Engine Systems Test Schedule

engine components. During each recycle, engine disassembly will be accomplished to the extent necessary to allow inspection. At least one of the recycled engines will accumulate in excess of 150 starts (see Fig. 6-43) or one-half of the starts required to demonstrate service life between overhauls by the completion of the FFC.

Special Test Equipment. Conduct of the engine system development test effort will require special test equipment (STE). Significant STE items required are:

1. Simulated altitude test positions. The position(s) will be used initially for thrust chamber component testing and then modified to accommodate engine system testing.

2. A heat exchanger during site testing of the 8:1 ϵ engine. This heat exchanger will simulate the 100:1 portion of the engine nozzle by conditioning hydrogen to the temperature normally provided to the turbines for the low-pressure pumps.

3. A system capable of gimbaling the engine. The system will consist of two actuators, a programmer, and a hydraulic fluid supply system. The system is needed as STE because it is not provided as part of the engine equipment.

Preliminary Flight Certification Program. A one-engine Preliminary Flight Certification test program will be conducted commencing 34 months from program start. This program will demonstrate the capability of the engine to meet all CEI specification requirements except service-free life and service life between overhauls. The engine used for this program will be an R&D engine assembled per production criteria, including inspection and quality assurance standards. An engine test program consisting of 40 tests and approximately 5700 seconds, including one test of 1200 seconds duration, will be completed. Maior external input and operating variables will be demonstrated to their limit values during the PFC test program, as follows:

1. Vacuum thrust at idle mode and mainstage

2. Step and ramp mixture ratio variation

3. Maximum and minimum combinations of oxidizer and fuel prestart and mainstage inlet pressures and temperatures

4. Limit values of turbopump speed, turbopump discharge pressure, preburner temperature, and main combustor chamber coolant flow

All tests will be conducted in the altitude simulation test facility. Upon completion of the program, the engine will be completely disassembled for inspection.

Final Flight Certification Program. A one-engine Final Flight Certification test program will be conducted commencing 53 months from program start (Fig. 6-16).

This program will demonstrate the capability of the engine to meet all CEI specification requirements except service life between overhauls. The engine used for this program will be of the flight configuration in all respects. An engine test program consisting of 64 tests and approximately 10,000 seconds, including one test of 2000 seconds duration, will be completed. Major external input and operating variables, including all those listed for PFC, will be demonstrated to their limit values during the FFC program. All tests will be conducted in the altitude simulation test facility. Upon completion of the program, the engine will be completely disassembled for inspection. The engine will then be recycled for use in the O&FS service life demonstration program.

Reliability and Maintainability

The reliability program will be based on the concept that reliability is an inherent product design characteristic that must be incorporated and improved by a concentrated effort early in the design phase and maintained by tight controls throughout the development and production phases.

Reliability-oriented design requirements will be included in design requirement specifications. Reliability will be considered as a qualitative and quantitative parameter in trade studies. Reliability predictions will be prepared using appropriate data sources to determine the feasibility of meeting the quantitative reliability requirements.

Reliability analyses will evaluate application of components relative to system-imposed functional and environmental stresses, such as containment level and surge pressures. A Failure Mode and Effect Analysis (FMEA) will identify reliability-critical areas for application of appropriate engineering attention. A criticality analysis will provide a quantitative ranking of critical failure modes.

Design reviews are chaired by an independent team within the Reliability organization to provide a critical review of the design status versus the design requirements at key milestones in the design phase.

The established problem/failure reporting, analysis, corrective action, and follow-up system will be implemented for this program and in accordance with specified requirements.

Reliability assessments will be prepared at major program milestones and other key points in the program. The assessments will utilize testing accomplished to date and reliability analyses to ensure that all potential degrading sources affecting reliability have been identified and evaluated, and corrective action initiated.

To provide a means of control and evaluation of the Reliability Program at any point in time, a computerized monitoring system will be used to maintain current records of the following:

1. The FMEA
2. Design Review
3. Design Verification
4. History of Serialized Parts
5. Engine Test Reports
6. UCR/FAR

Maintainability Program. The maintainability program for the ASE will be concerned with the following key factors:

1. Engine replacement capability on the vehicle
2. Checkout capability
3. Component replacement capability
4. Accessibility for external and internal visual inspection of critical areas
5. Fault isolation

Early in the design certification phase of the program, maintainability studies and analyses will be conducted, based on other similar rocket engine programs such as the SSME, to define parameters for use by the system designers to ensure that the preceding key factors are considered and implemented into the engine design. Program control to assure incorporation of maintainability features into the engine design will be by means of the Design Verification Specification (DVS) and by informal and formal design reviews. Component and engine system tests are planned to demonstrate that maintainability concepts have been incorporated into the engine design.

System Safety Program. Early in the program, a Preliminary Hazard Analysis (PHA) will be conducted to ensure complete definition of hazard-producing energy sources (external as well as internal) and establishment of design criteria for their control. The entire engine life cycle will be considered, with emphasis on normal and emergency situation operational activities.

As the detailed designs evolve, a Subsystem Hazard Analysis (SHA) will be prepared. The SHA provides a detailed evaluation of possible equipment, component, procedural, and externally induced faults that could result in hazardous events.

MANUFACTURING PLAN

The fundamental approach to ASE manufacturing will be to fabricate all engine hardware in the production shop to production drawings. This includes development and prototype deliverable hardware as well as the 50 production engines and their spares. The Master Schedule for the ASE is shown in Fig. 6-27.

All deliverable engines will be produced in accordance with the Master Schedule. The engines designated for the formal demonstration portions of the PFC and FFC programs also will be fabricated in accordance with the Master Schedule. The remainder of the development hardware must be produced at an irregular pace as required to support development testing, however, and will be expedited as necessary. The expedited hardware will undergo exactly the same fabrication sequences as the production hardware, but flow times between operations will be minimized. The manufacturing schedule for the minimum-cost program is shown in Fig. 6-28.

Hardware fabricated during the DDT&E phase of the program, including the five prototype deliverables, will be manufactured on soft tooling. Production hardware will be fabricated on hard tooling which will provide a capability of increased delivery rate, if desired. Increased delivery rates would reduce the total cost of the production phase.

OPERATION AND FLIGHT SUPPORT PLAN

An Operational and Flight Support (O&FS) plan has been developed as a part of the Advanced Space Engine (ASE) program study. O&FS planning considers the effort associated with integrating the ASE into the Space Shuttle program tug and the support required for a 10-year operational flight program. The support program milestones are presented in Fig. 6-29. The overall support effort will be conducted as described under Plan I.

DATA AND DOCUMENTATION

Data and documentation for the ASE were estimated based on the data lists shown in Tables 6-20, 6-21, and 6-22 for the DDT&E, Production, and O&FS phases of the program, respectively. The lists shown in the tables were generated through evaluation of the SSME data requirements. Cost estimates for the data do not include engineering effort necessary to originate the reports; the originators' efforts are changed to the appropriate product subaccount.

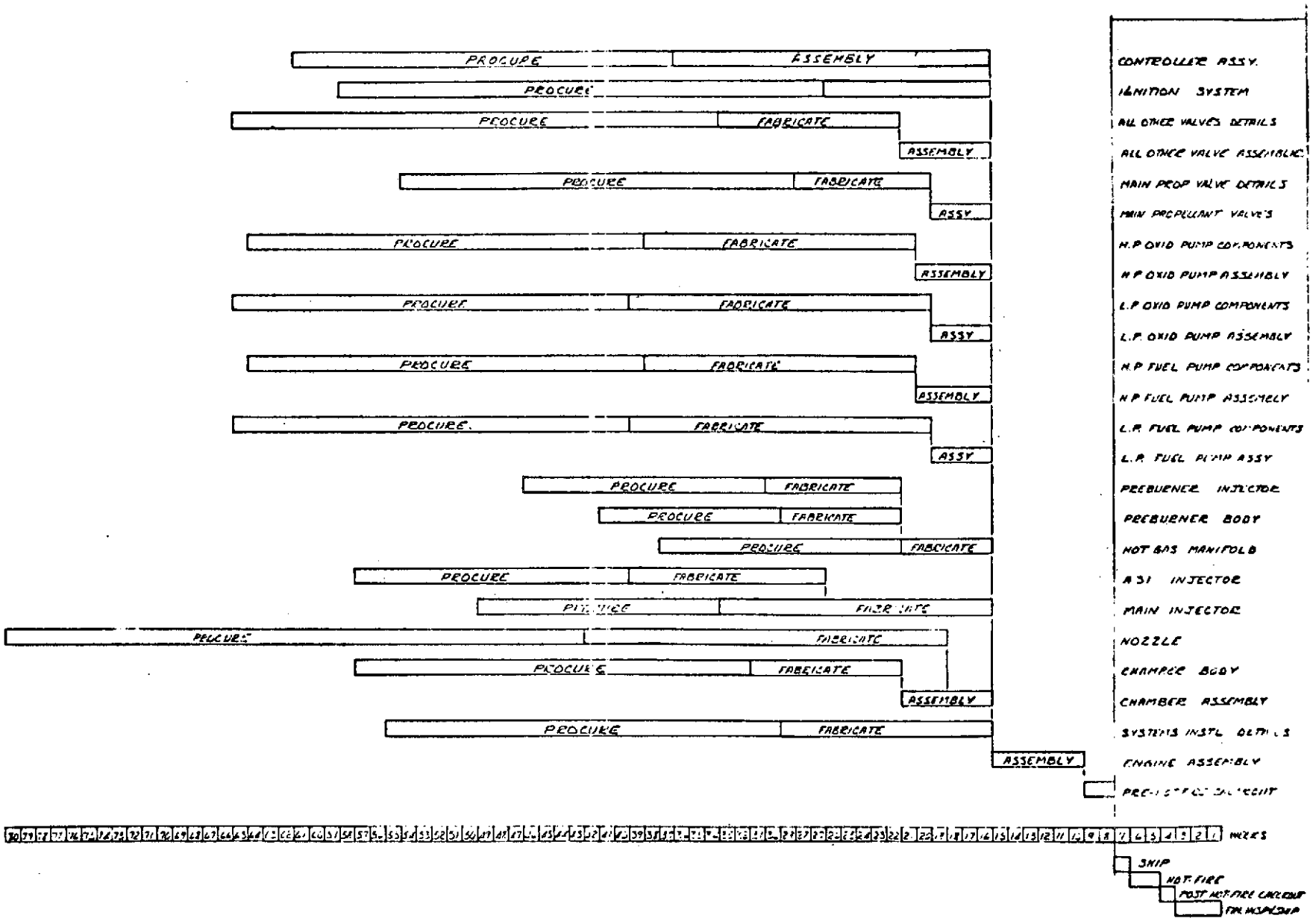

Figure 6-27. Master Schedule

Page intentionally left blank

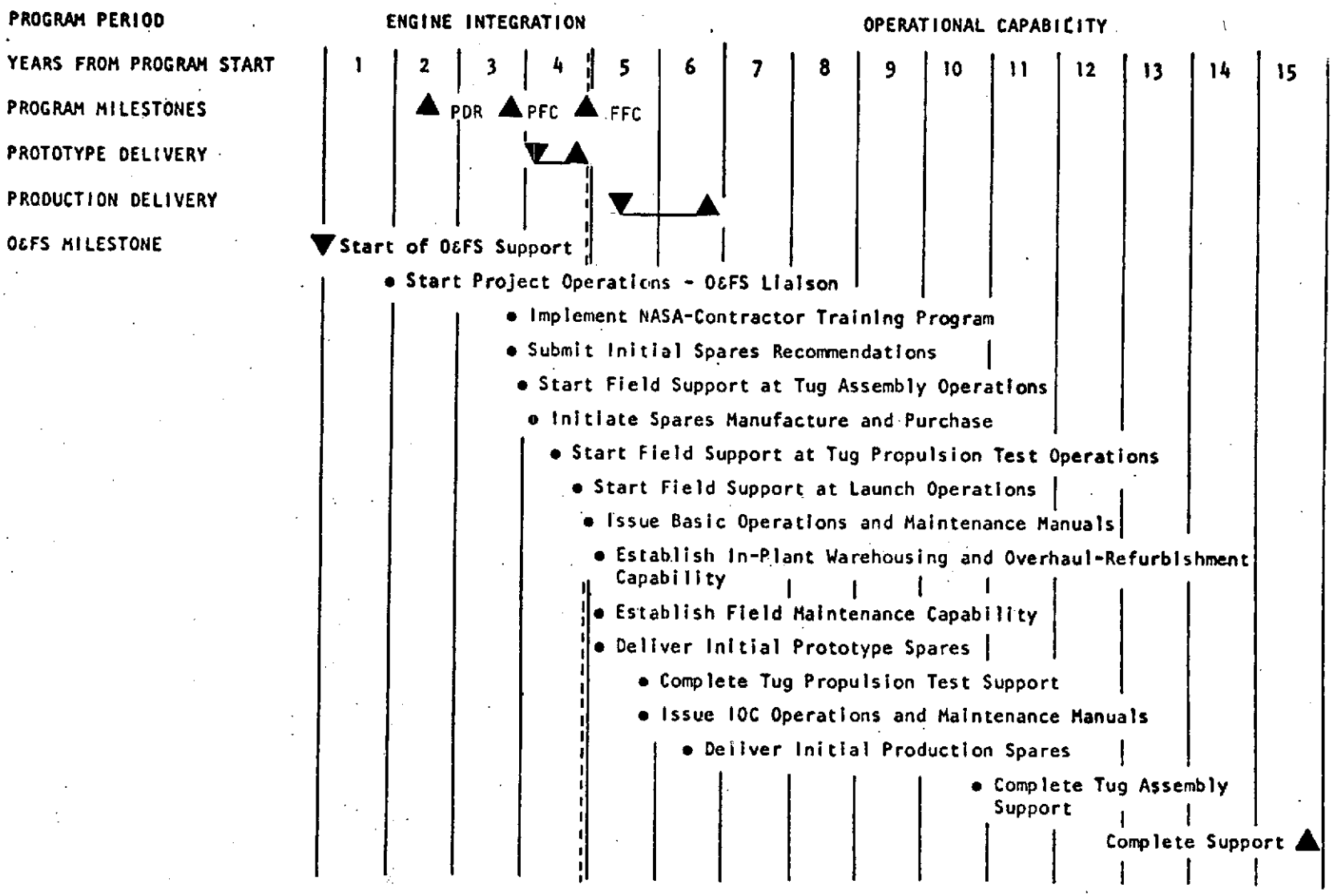

Figure 6-29. Support Program Milestones (Program 2)

PRECEDING PAGE BLANK NOT FILMED

TABLE 6-20. DDT&E DATA LIST

Item	Frequency	No. Issues
Plan, Configuration Management	Semi-AN	10
Engineering Change Proposals	AR	70
Plan, First Article Configuration Inspection	O-Time	--
Package, First Article Configuration Inspection	O-Time	--
Minutes, First Article Configuration Inspection	O-Time	--
Specification Maintenance	AR	--
Preliminary Interface Revision Notice	AR	--
Record Engineering Change Proposal	AR	--
Lists, Configuration Identification	AR	--
Report, Configuration Identification and Status	Mo*	10
Agenda, Critical Design Review	O-Time	1
Package, Critical Design Review (CDR) Engine and GSE	O-Time	1
Minutes, Critical Design Review	O-Time	1
Facilities Utilization Plan	Semi-AN	10
Real and Installed Property Status Report	Semi-AN	10
Operational and Flight Support (O&FS) Plan	Semi-AN	10
Operating Requirements and Procedures Manual	O-Time	1
Maintenance, Repair, and Parts List Manual	O-Time	1
Ground Support Equipment Use, Maintenance, and Repair Manual	O-Time	1
Major Spares Status Report	Mo**	12
Recommended Support Parts List (RSPL)	Qtly***	3
Support Parts Priced Exhibit	Bl-Mo**	6
Program Management Plan	Semi-AN	10
Program Management Summary	Mo	59
Cost, Schedule, and Performance Measurement Report	Mo	59
NASA 533 Financial Management Report, Monthly	Mo	59
NASA 533 Financial Management Report, Quarterly	Qtly	15
Indirect Cost/Manpower Data, Monthly and Quarterly	Mo/Qtly	15
Propellant and Pressurants Use Report	Mo	59
Propellant and Pressurant Forecasts	Qtly	15
Unit Cost Report	Qtly***	3

*Monthly after 1st engine delivery
**First Report 2 months prior to engine delivery
***Quarterly after first engine delivery

TABLE 6-20. (Continued)

Item	Frequency	No. Issues
New Technology Report	Mo	59
New Technology Annual Report	Ann.	5
Program Review Data (Agenda and Handouts)	Qtly	15
Program Review Minutest	Qtly	15
Motion Picture Film Progress Report	Ann	5
Data Requirement Change Proposal	Semi-AN	10
Logic Networks and Key Milestone Charts	Mo	59
Reliability Program Plan	Semi-AN	10
Reliability Operating Procedures	Semi-AN	10
Failure Mode, Effect, and Criticality Analysis	Semi-AN	10
Maintenance Significant Items List	Semi-AN	10
Parts List and Approval Status, E.E.E. (to CDR)	Semi-AN	8
Design Review Minutes (to CDR)	Mo	48
Maturity Assessment and Test Summary Report	Mo	59
Nonconformance Status and Trend Summary Report	Mo	59
Quality Program Plan	Ann	5
Quality Assurance Manual Procedures	O-Time	1
Final Inspection and Acceptance Checkout Plan	O-Time	1
Final Inspection and Acceptance Checkout Procedure	Ann	5
Engine Log Book	Each Engine	5
System Safety Plan	Semi-AN	10
Hazard Analyses Reports	AR	4
Safety Analysis Report	Qtly	15
Accident/Incident Report	AR	10
List and Describe, Ground Support Equipment (GSE)	Semi-AN	10
Plan, Program Development	Semi-AN	10
Design Verification Specification (DVS)	Qtly	15
Drawing, Lists, Form 1, Specifications, and Microfilm	Mo	59
Plan, Structural Assessment	Qtly	15
Component Stress Analysis Structural Loads and Design Criteria	Qtly	15

TABLE 6-20. (Concluded)

Item	Frequency	No. Issues
Model, Engine Controller	Qtly	15
Data, Engine System Test, Microfilm/Tape	Per test	682
Model, Engine Data Reduction and Prediction	AR	9
Report Preliminary Flight Certification (PFC)	O-Time	1
Report, Final Flight Certification (FFC)	O-Time	1
Ptan, Flight Certification	O-Time	1
Specification CEI (Engine and GSE)	Semi-AN	10
Engine Control Design Document	Qtly	15
Engine Controller Operating Information	O-Time	1
Materials Control Reports		
1. Main Combustion Chamber	Qtly	12
2. Nozzle	Qtly	12
3. Main Injector	Qtly	12
4. Oxidizer Preburner	Qtly	12
5. High-Pressure Oxidizer Turbopump	Qtly	12
6. Low-Pressure Oxidizer Turbopump	Qtly	12
7. High-Pressure Fuel Turbopump	Qtly	12
8. Low-Pressure Fuel Turbopump	Qtly	12
9. Main Valve	Qtly	12
10. Gimbal Bearing	Qtly	12
11. Systems	Qtly	12
12. Controller	Qtly	12
13. Plan, Manufacturing	Semi-AN	10

TABLE 6-21. PRODUCTION PHASE DATA LIST

Item	Frequency	No. Issues
Program Management Plan	Semi-AN	8
Program Management Summary	Mo	46
Cost, Schedule and Performance Measurement Report	Mo	46
NASA 533 Financial Management Report, Monthly	Mo	46
NASA 533 Financial Management Report, Quarterly	Qtly	11
Indirect Cost/Manpower Data, Monthly and Quarterly	Mo	46
Propellant and Pressurants Use Report	Mo	46
Propellant and Pressurant Forecasts	Qtly	11
Unit Cost Report*	Qtly	11
Logic Networks and Key Milestone Charts	Mo	46
Plan, Manufacturing	Semi-AN	8

TABLE 6-22. O&FS PHASE DATA LIST

Item	Frequency	No. Issues
Operating Requirements and Procedures Manual	AR	--
Maintenance, Repair, and Parts List Manual	AR	--
Ground Support Equipment Use, Maintenance, and Repair Manual	AR	--
Major Spares Status Report	AR	--
Request for Disposition Report (RFD)	AR	--
Program Management Plan	Semi-AN	20
Program Management Summary	Mo	120
Cost, Schedule, and Performance Measurement Report	Mo	120
NASA 533 Financial Management Report, Monthly	Mo	120
NASA 533 Financial Management Report, Quarterly	Qtly	40
Indirect Cost/Manpower Data, Monthly and Quarterly	Mo	120

FACILITIES

The fundamental assumption in generating ASE facilities is that SSME facilities will be available at the time required to support the Advanced Space Engine. Table 6-23 defines the facilities allocated to major system and subsystem testing.

COSTS

Cost estimates for the minimum-time ASE program were generated separately for three distinct phases: DDT&E, Production, and Operations and Flight Support (O&FS). All estimates are in 1973 dollars and do not include fee, propellants, or capital expenditures. Consumables are assumed to be GFE and the quantities required are included. The DDT&E estimate includes five deliverable prototype engine systems, GSE to support three sites, and a mock-up engine. These items are detailed separately in the estimate, allowing for convenient reallocation of the costs to other phases of the program, if desired. The production phase estimate is for 50 units at a peak rate of 2 per month, which is reached in the third month of deliveries. A 90-percent learning curve was used for fabrication hours and a 95-percent curve was used for material (primarily mortality reduction).

The O&FS estimate includes a 240-start, 8-hour test program to complete the service life demonstration for the engine. This cost also is separately identified and may be reallocated as desired.

All costs were generated to a product-oriented work breakdown structure. The item-by-item breakdown is included in the subsequent pages.

COST SUMMARY

The minimum-time program cost estimate is $149,671,000.

DDT&E	$ 97,093,000
Production	47,820,000
O&FS	11,550,000
Total	$149,671,000

TABLE 6-23. MINIMUM TIME PROGRAM FACILITIES

System/Subsystem	Location	Modification
Oxidizer Turbomachinery		
High-Pressure Turbopump	CTL-IV, Cell-26A	Major
Low-Pressure Turbopump	CTL-IV, Cell-26A	Major
Fuel Turbomachinery		
High-Pressure Turbopump	CTL-IV, Cell-26B	Major
Low-Pressure Turbopump	CTL-IV, Cell-26B	Major
Ignition Systems	CTL-III, Module I	Major
Precombustor	CTL-III, Module I	Major
Thrust Chamber Assembly		
Ambient	CTL-IV, Cell-29	Major
Altitude*	CTL-IV, Cell-29	Major
Engine System		
Ambient	CTL-IV, Cell-27	Major
Altitude Position #1	CTL-IV, Cell-29	Major
Altitude Position #2*	CTL-IV, Cell-29	Major

*Thrust chamber altitude position converts to engine System position.

DDT&E Summary

00XXX	Combustion Devices	$11,718,000
01XXX	Turbomachinery	16,630,000
02XXX	Controls and Valves	4,194,000
03XXX	Ground Support Equipment (GSE)	1,248,000
04XXX	Engine Systems	21,215,000
05XXX	Program Management	5,766,000
06XXX	Deliverables	8,320,000
07XXX	Tooling and STE	7,140,000
08XXX	Integration and Engine Support	2,751,000
09XXX	Data and Documentation	4,284,000
10XXX	Facilities	5,000,000
Subtotal		$88,266,000
	Development Contingency	8,727,000
Total		$97,093,000

Production Summary

00XXX	Hardware	$34,667,000
01XXX	Acceptance Test	1,994,000
02XXX	Initial Spares	143,000
03XXX	Engineering	826,000
04XXX	Tooling	3,653,000
05XXX	Program Management	3,479,000
07XXX	Manufacturing Services	2,758,000
08XXX	GSE	300,000
Total		$47,820,000

First Unit Cost. The first unit cost of $1,460,000 includes ammortization over 50 units of engineering, tooling, program management, and manufacturing services costs. It is developed as follows:

Fabrication Labor	$ 599,000
Material	421,000
Quality Control	114,000
Test Labor	38,000
Engineering	17,000
Tooling	102,000
Program Management	70,000
Manufacturing Services	99,000
Total	$1,460,000

O&FS Summary

00XXX	Field Support	$3,000,000
01XXX	Engine and Component Overhaul	929,000
02XXX	Engineering	2,938,000
03XXX	Spares	683,000
04XXX	Program Management	3,198,000
05XXX	Facilities Maintenance	133,000
06XXX	Service Life Demonstration	669,000
	Total	$11,550,000

Consumables

The following consumables are required for the ASE program:

Item	DDT&E	Production	O&FS
Liquid Oxygen, tons	51,107	3,690	18,450
Liquid Hydrogen, K-lbs	16,631	933	4,665

Item	DDT&E	Production	O&FS
Liquid Nitrogen, tons	7,105	513	2,565
GN_2, K-scf	725,200	36,000	180,000
He, K-scf	21,270	1,200	6,000
Alcohol, pounds	2,345,000	420,000	2,100,000

Detailed Costs

The detailed costs for each phase of the program are included in the following pages.

DDT&E

PLAN II

00XXX	Combustion Devices			$11,718,000
000XX	Thrust Chamber Assembly		$8,232,000	
0001X	Engineering	$1,489,000		
0002X	Fabrication	3,190,000		
0003X	Material	1,802,000		
0004X	Component Test	1,181,000		
0005X	Quality Control	570,000		
001XX	Ignition System		$1,719,000	
0011X	Engineering	$ 696,000		
0012X	Fabrication	152,000		
0013X	Material	433,000		
0014X	Component Test	413,000		
0015X	Quality Control	25,000		
002XX	Precombuster Assembly		$1,767,000	
0021X	Engineering	$ 585,000		
0022X	Fabrication	418,000		
0023X	Material	63,000		
0024X	Component Test	636,000		
0025X	Quality Control	65,000		
01XXX	Turbomachinery			$16,630,000
010XX	LPFP		$2,678,000	
0101X	Engineering	$ 475,000		
0102X	Fabrication	987,000		
0103X	Material	700,000		
0104X	Component Test	332,000		
0105X	Quality Control	184,000		

DDT&E

PLAN II

011XX	LPOP		$ 2,840,000	
0111X	Engineering	$ 610,000		
01112X	Fabrication	971,000		
01113X	Material	743,000		
01114X	Component Test	332,000		
01115X	Quality Control	184,000		
012XX	HPFP		$ 3,637,000	
0121X	Engineering	$ 682,000		
0122X	Fabrication	1,392,000		
0123X	Material	948,000		
0124X	Component Test	358,000		
0125X	Quality Control	257,000		
013XX	HPOP		$ 7,475,000	
0131X	Engineering	$ 682,000		
0132X	Fabrication	1,374,000		
0133X	Material	903,000		
0134X	Component Test	4,264,000		
0135X	Quality Control	252,000		
02XXX	Components			$ 4,194,000
021XX	Electronics		$ 1,567,000	
0211X	Engineering	$ 718,000		
0212X	Fabrication	54,000		
0213X	Material	652,000		
0214X	Component Test	100,000		
0215X	Quality Control	43,000		
022XX	Main Valves		$ 1,015,000	
0221X	Engineering	$ 112,000		
0222X	Fabrication	551,000		
0223X	Material	206,000		
0224X	Component Test	53,000		
0225X	Quality Control	93,000		

DDT&E

PLAN II

023XX	Control Valves		$ 1,612,000	
0231X	Engineering	$ 428,000		
0232X	Fabrication	438,000		
0233X	Material	504,000		
0234X	Component Test	150,000		
0235X	Quality Control	92,000		
03XXX	Ground Support Equipment			$ 1,248,000
031XX	Development of GSE		$ 1,248,000	
0311X	Engineering	$ 653,000		
0312X	Fabrication	155,000		
0313X	Material	320,000		
0314X	Component Test	80,000		
0315X	Quality Control	40,000		
04XXX	Engine Systems			$21,215,000
041XX	Engine Development		$13,780,000	
0411X	Engineering	$9,296,000		
0412X	Fabrication	838,000		
0413X	Material	105,000		
0414X	Component Test	3,411,000		
0415X	Quality Control	130,000		
042XX	FPC		$ 1,265,000	
0421X	Engineering	$ 785,000		
0422X	Fabrication	130,000		
0423X	Material	17,000		
0424X	Test	312,000		
0425X	Quality Control	21,000		
043XX	FFC		$ 3,970,000	
0431X	Engineering	$2,513,000		
0432X	Fabrication	130,000		
0433X	Material	17,000		
0434X	Test	1,289,000		
0435X	Quality Control	21,000		

DDT&E

PLAN II

044XX	Reliability and Service Free Demo.		$ 2,200,000	
0441X	Engineering	$1,210,000		
0442X	Fabrication	313,000		
0443X	Material	41,000		
0444X	Test	586,000		
0445X	Quality Control	50,000		
05XXX	Program Management			$ 5,766,000
051XX	Program Management		$ 367,000	
052XX	Program Control		745,000	
053XX	Configuration Control		232,000	
054XX	Reliability		2,038,000	
055XX	Quality Assurance		911,000	
056XX	Manufacturing Services		98,000	
057XX	Travel and Subsistence		225,000	
058XX	Computer Services		1,150,000	
06XXX	Deliverables			$ 8,320,000
061XX	Ground Test Engines		$ 2,474,000	
0611X	Fabrication	$1,317,000		
0612X	Material	873,000		
0613X	Acceptance Test	37,000		
0614X	Quality Control	247,000		
062XX	PFC Engines		$ 2,474,000	
0621X	Fabrication	$1,317,000		
0622X	Material	873,000		
0623X	Acceptance Test	37,000		
0624X	Quality Control	247,000		
063XX	FCE Engine		$ 1,238,000	
0631X	Fabrication	$ 659,000		
0632X	Material	437,000		
0633X	Acceptance Test	18,000		
0634X	Quality Control	124,000		

DDT&E

PLAN II

064XX	GSE		$ 1,080,000	
0641X	Fabrication	$ 340,000		
0642X	Material	651,000		
0643X	Quality Control	89,000		
065XX	Mockup		$ 79,000	
0651X	Engineering	$ 28,000		
0652X	Fabrication	44,000		
0653X	Material	7,000		
066XX	Spares		$ 975,000	
0661X	Fabrication	$ 527,000		
0662X	Material	348,000		
0663X	Quality Control	100,000		
07XXX	Tooling and STE			$ 7,140,000
071XX	Tooling		$ 310,000	
0711X	Factory Tooling (NR)	$ 155,000		
0712X	Factory Tooling (REC)	155,000		
072XX	STE		$ 6,830,000	
0721X	Factory STE (NR)	$ 83,000		
0722X	Factory STE (REC)	147,000		
0723X	Test STE (NR)	6,600,000		
08XXX	Integration and Engine Support			$ 2,751,000
081XX	Engineering		$ 1,349,000	
082XX	Field Support		419,000	
083XX	Manuals		284,000	
084XX	Training		226,000	
085XX	Spares Management		196,000	
086XX	Logistics		277,000	
09XXX	Data			$ 4,284,000
091XX	Engineering		$ 2,272,000	
092XX	Management		350,000	
093XX	Program Support		1,662,000	
10XXX	Facilities			$ 5,000,000
102XX	Test		$ 5,000,000	
	Total DDT&E Cost			$88,266,000
	Development Contingency			8,727,000
			Total	97,093,000

PRODUCTION

			PLAN ALL
00XXX	Hardware		$34,667,000
001XX	Fabrication	$16,520,000	
002XX	Material	14,597,000	
003XX	Quality Control	3,560,000	
01XXX	Acceptance Test		$ 1,994,000
011XX	Quality Control	$ 81,000	
012XX	Test Labor	1,913,000	
02XXX	Initial Spares		$ 143,000
021XX	Fabrication	$ 66,000	
022XX	Material	63,000	
023XX	Quality Control	14,000	
03XXX	Engineering		$ 826,000
031XX	Sustaining Engineering	$ 826,000	
04XXX	Tooling		$ 3,653,000
041XX	Production (NR)	$ 1,363,000	
042XX	Recurring	2,290,000	
05XXX	Program Management		$ 3,479,000
051XX	Program Management	$ 275,000	
052XX	Program Control	165,000	
053XX	Data and Documentation	1,385,000	
054XX	Quality Assurance	1,169,000	
055XX	Configuration Management	485,000	
07XXX	Manufacturing Services		$ 2,758,000
071XX	Manufacturing Services	$ 2,758,000	
08XXX	GSE		$ 300,000
081XX	Fabrication	$ 90,000	
082XX	Material	186,000	
083XX	Quality Control	24,000	
	Total Production Cost		$47,820,000

OPERATIONS

				PLAN ALL
00XXX	Field Support			$ 3,000,000
001XX	Maintenance and Refurbishment		$ 1,501,000	
002XX	Field Engineering		1,499,000	$ 929,000
01XXX	Engine and Component Overhaul			
011XX	Fabrication Labor		$ 703,000	
012XX	Material		112,000	
013XX	Quality Control		114,000	
02XXX	Engineering			$ 2,938,000
021XX	Sustaining Engineering		$ 1,406,000	
022XX	Logistics Support		1,542,000	
03XXX	Spares			$ 683,000
031XX	Engine Spares		$ 539,000	
0311X	Fabrication Labor	$ 239,000		
0312X	Material	249,000		
0313X	Quality Control	51,000		
032XX	GSE		$ 144,000	
0321X	Fabrication Labor	$ 430,000		
0322X	Material	90,000		
0323X	Quality Control	11,000		
04XXX	Program Management			$ 3,198,000
041XX	Program Management		$ 424,000	
042XX	Program Control		283,000	
043XX	Data and Documentation		1,715,000	
044XX	Quality Assurance		65,000	
045XX	Configuration Control		211,000	
046XX	Travel & Relocation		500,000	
05XXX	Facilities Maintenance			$ 133,000
051XX	Tooling Maintenance		$ 133,000	
06XXX	Service Life Demo.			$ 669,000
061XX	Test		$ 644,000	
062XX	Quality Control		25,000	
	Total Operations Cost			$11,550,000

COMMON ENGINE INTERFACE AND RETRACTABLE NOZZLE STUDY

An analysis of the repackaging of the Advanced Space Engine to the RL10A-3-3 engine installation and the impact of a retractable nozzle design was conducted. The engine interface was modified to conform to the dimensions shown in Fig. 6-30. A lightweight retractable nozzle mechanism was designed to minimize the stowed length of the engine while the vehicle is being transported in the Space Shuttle to and from orbit. The impact of the changes on the engine design and the resulting changes in weight, development cost and production unit costs were assessed and are subsequently discussed. To aid in understanding the discussion, the engine layout including both the modified interface and retractable nozzle is presented in Fig. 6-31.

COMMON ENGINE INTERFACE

The design of the engine system was investigated to determine the impact of compatibility with the RL10A-3-3 engine installation. Changes required for interface compatibility included interchanging the main oxidizer turbopump location with the fuel due to the close mounting of the boost pumps to the main turbopumps. This necessitated changing the relative position of the boost turbopump both circumferencially and axially to match RL10A-3-3 inlet flanges.

The preburner was relocated opposite the original position resulting in a slightly longer line between the preburner and main fuel turbopump. The preburner discharge duct to the main oxidizer turbopump was also slightly increased in length.

The gimbal actuator thrust chamber pickup points were shifted further outboard because the RL10A-3-3 engine locations were located inside the advanced space engine thrust chamber due to the larger area ratio nozzle. This relocation would not affect the actuator length since it would mean only slight rotation.

Changing engine packaging to meet the RL10A-3-3 engine interface points does not affect the overall packaging concept and results in a suitable packing arrangement. There would be no discernable impact on engine weight or cost if this configuration were adopted at the initiation of the development program.

RETRACTABLE NOZZLE DESIGN

To meet the requirement of minimizing the stowed length of the engine while being transported in the Space Shuttle and also provide a large area ratio nozzle for high performance, a design study of alternative retractable nozzle concepts was conducted. The ground rules for an acceptable approach were lightweight, positive acting and nozzle retention, and reliability with suitable redundancy of key operating points.

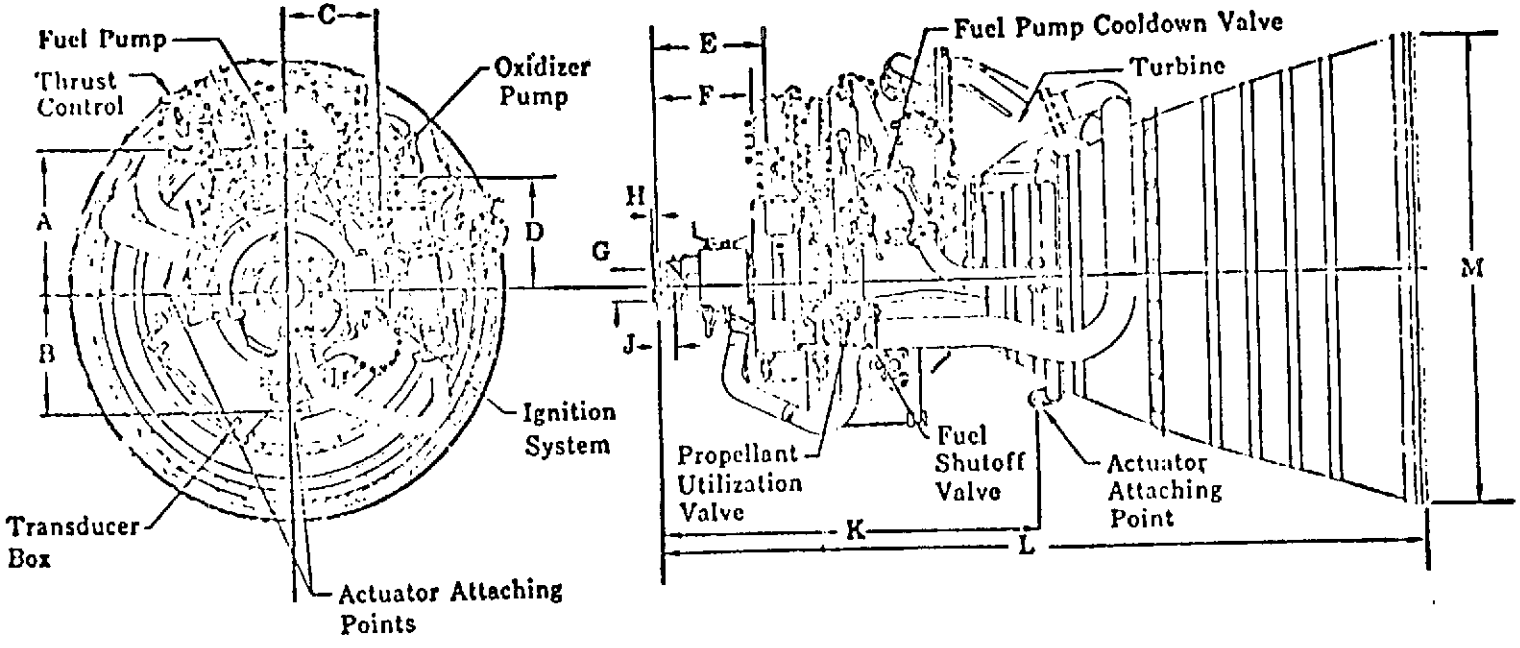

A - 29.85	D - 23.92	G - 7.305	K - 83.50	(cm)
11.750	9.419	2.876	32.874	(in.)
B - 25.84	E - 24.39	H - 0.610	L - 178.05	(cm)
10.172	9.603	0.240	70.10	(in.)
C - 20.65	F - 22.19	J - 3.81	M - 100.43	(cm)
8.128	8.738	1.500	39.54	(in.)

DIMENSIONS ARE NOMINAL IN CM (IN.) AT ROOM TEMPERATURE

Figure 6-30. RL10A-3-3 Engine Installation

Page intentionally left blank

Concept Selection

The concepts considered were:

- Cable-pulley system
- Ball screw and column
- Differential ball screws
- Rack and pinion
- Journal drive
- Telescoping actuators
- Flexible nozzle
- Three single ball screws
- Chain drive
- Pneumatically actuated with guide tubes

The ball screw, rack and pinion, and journal concepts were rejected because of the difficulty in screw synchronization and complexity in providing a suitable drive. Also, the weight was considered excessive, particularly if any redundancy of the system were included. The cable-pulley and chain drive approaches were not sufficiently positive acting and tended to be complex. Also, the electric motor drive required resulted in high weight. The telescoping nozzle and flexible nozzle concepts were rejected based on questionable reliability. The concept selected was the pneumatically actuated design with guide tubes to provide nozzle stability.

Concept Design

The skirt's light weight enabled the selection of the pneumatic-actuated system consisting of three equally spaced actuators, as previously shown in Fig. 6-29. Adjacent to these are three guide tubes. The guide tubes and actuators are supported at the forward end by adjustable bipods attached to the thrust chamber injector. The journal's mating with the guide tubes and supporting the skirt is made of a virtually friction-free material called Rulon J (Dixon Corporation). A latching mechanism is located at both ends of the guide tubes. The mechanism features a spring-loaded latching device which is unlatched pneumatically. The aft end of the actuators are attached to the skirt near the exit ring.

When fully retracted, the height of the engine from the gimbal mounting surface to the exit is 128.27 cm (50.50 inches). The forward end of the actuators and associated structure protrudes the mounting plane approximately 15.24 cm (6 inches). The diameter of these protrusions is approximately 12.7 cm (5 inches).

A flexible hose will be used to supply the dump coolant to the retractable nozzle. Short flexible hoses are required on the forward end of the actuators because of the slight angulation during actuation. The internal portage feature to extend and retract the actuators eliminated the requirements for long external flex hoses.

The alignment of the guide tubes is accomplished by adjustable rod ends on the bipods. The aft end of the guide tube is attached to the chamber structure through a mono-ball bearing. This permits the alignment without bending the tubes.

A spring-loaded, TFE-covered seal is used between the fixed and extended nozzle. Both surfaces in contact with the seal are cooled, making this type of seal practical to use in this application.

The aft end of the fixed nozzle is uncooled to reduce the discontinuity between nozzles. This uncooled ring is made of nickel -- a good heat conductor.

A weight analysis of the retraction system was conducted and is presented in Table 6-24. The liberal use of titanium and thin-wall tubing has resulted in a change in engine weight of 21.32 kg (47 pounds). Further reductions may be possible with further analysis. The low magnitude of the forces involved resulting from low temperature and pressure make a low-weight system practical.

Operating Characteristics

A single four-way solenoid valve is required to control this system. As soon as helium pressure is allowed to the engine, the helium flows through the normally open port of the four-way valve to the forward unlatching devices which in turn feeds the helium to the extending side of the actuators. This pressure remains on until an electric signal to the four-way valve vents the normally open side and allows helium pressure through the normally closed side to the aft unlatching devices which, in turn, feeds helium to the retracting side of the actuators. When the nozzle is fully retracted, the forward latches are engaged and a limit switch deactivates the four-way solenoid valve, thus venting the system. The schematic of the system is shown in Fig. 6-32.

Cost Analysis

An analysis of the development and unit production cost impact of incorporating the retractable nozzle was conducted and the increase in development cost was determined to be $1,338,000 for the DDT&E phase of the program. The increase in unit production cost is projected to be $63,000, based on delivery of 50 engines at a rate of two engines per month.

TABLE 6-24

WEIGHT CHANGE - ADVANCED SPACE ENGINE WITH RETRACTABLE NOZZLE

ITEM	DESCRIPTION	WEIGHT, pounds (kg)	
1.	Redesign fuel manifolds and move from ϵ = 100 to ϵ = 186. Incorporate extendable nozzle attach ring and add 3 actuator points	+ 6.0	(2.72)
2.	Add nickel guide and closeout rings	+ 9.9	(4.49)
3.	Add 3 mechanical locks aft	+ 1.4	(0.635)
4.	Add nozzle positioning ring	+11.8	(5.35)
5.	Add 3 guide struts and attachments	+ 1.1	(0.499)
6.	Add 3 nozzle actuator aft points	+ 0.8	(0.363)
7.	Add 3 nozzle actuators including forward locks	+10.2	(4.63)
8.	Add 3 forward supports, a frame and fittings. Includes rod end and mono-ball attachment.	+ 3.7	(1.68)
9.	Add 1 four-way solenoid valve and modify pneumatic control	+ 0.7	(0.318)
10.	Add 3 limit switches on retractor	+ 1.0	(0.454)
11.	Modify electrical harness for control loops of nozzle extension	+ 0.4	(0.181)
		47.0	(21.3)

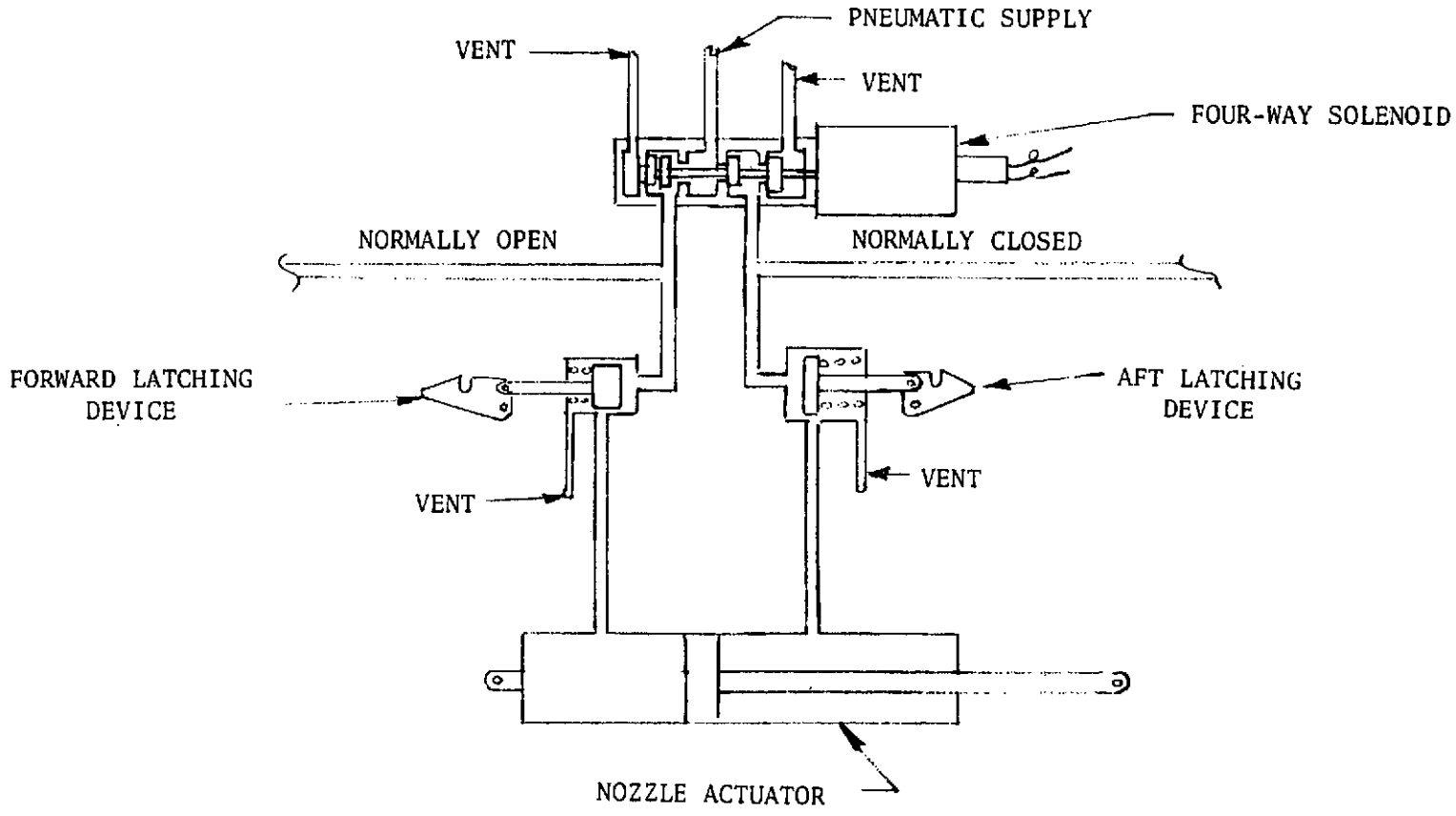

Figure 6-32. Nozzle Retraction Schematic

DISCUSSION OF RESULTS

The Advanced Space Engine preliminary design was conducted to resolve the best approach among several technical choices to subsequently allow focusing of component research, study of component interaction, and study of system dynamics. This effort would thus provide a basis for the required technology prior to full development of an engine for Space Tug application (Fig. 7-1).

To meet the requirements of the Space Tug, a high-performance, lightweight engine is required. Also, features directed toward vehicle optimization, such as low NPSH, autogenous pressurization, idle mode, etc., were investigated.

The basis of the engine design was the configuration selection study conducted during the initial part of the program from a number of design alternatives (Table 7-1); the baseline engine configuration (Fig. 7-2) was selected.

As established as a ground rule, the baseline configuration was nonthrottling; however, the impact of throttling was studied and determined to be capable of incorporation by modification of the baseline design. The primary features of the baseline engine are: single preburner, GH_2 turbine-driven boost pumps, and split-flow thrust chamber. The single preburner was selected because of nonthrottling requirement, limited engine inlet temperature and pressure variation (resulting from space application), and relative simplicity. The dual preburner was found to be preferable for deep throttling but not of sufficient overall advantage. The physical and operational flexibility of the GH_2 turbine boost pump drive resulted in its selection. The ability to optimize the flow through parallel paths of the split-flow thrust chamber and, thus, improve chamber pressure by approximately 1,378,951 N/m^2 (200 psi) resulted in its selection.

Following selection of the concept, engine and major component analysis and design was conducted. The engine is designed to provide a specific impulse of 473.4 seconds at a nominal mixture ratio of 6.0:1 and a thrust of 88,964 Newtons (20,000 pounds). The projected engine dry weight is 152.86 kg (337 pounds) and the engine inlet NPSH requirements are 0/0 (feet of LO_2/LH_2) and 5.97/44.8 joules/kg (2/15 feet) in idle mode and mainstage, respectively. The results of dynamic analyses conducted during the study indicated satisfactory start and idle mode operation for both cold (restart) and warm (long-term coast in space) conditions (Fig. 7-3). The capability of providing autogenous pressurization during mainstage was verified; however, better definition of pressurization flowrates and desired temperature during start are required.

Appropriate packaging (Fig. 7-4) of the engine was conducted to ensure minimum interconnect pressure drops while providing access for system maintainability. The interconnecting lines are joined by in-place welding, a process considered sufficiently developed and directly applicable based on engine operational requirements.

A concentric element injector configuration (Fig. 7-5) was selected for the main thrust chamber assembly because of its demonstrated high performance. The thrust chamber, composed of a combustion chamber (up to ϵ = 8:1), a fixed nozzle (ϵ = 8:1

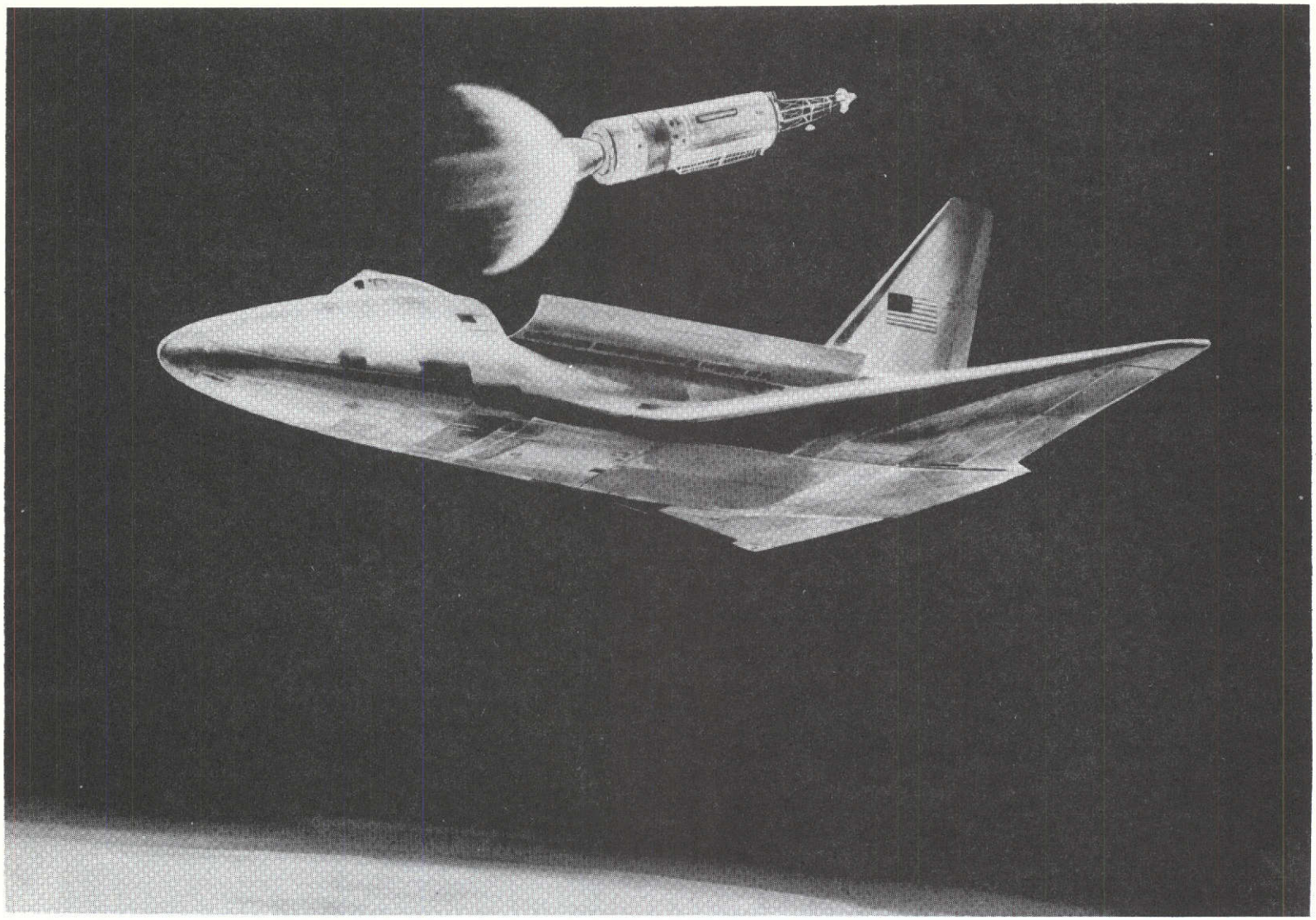

Figure 7-1. Space Tug

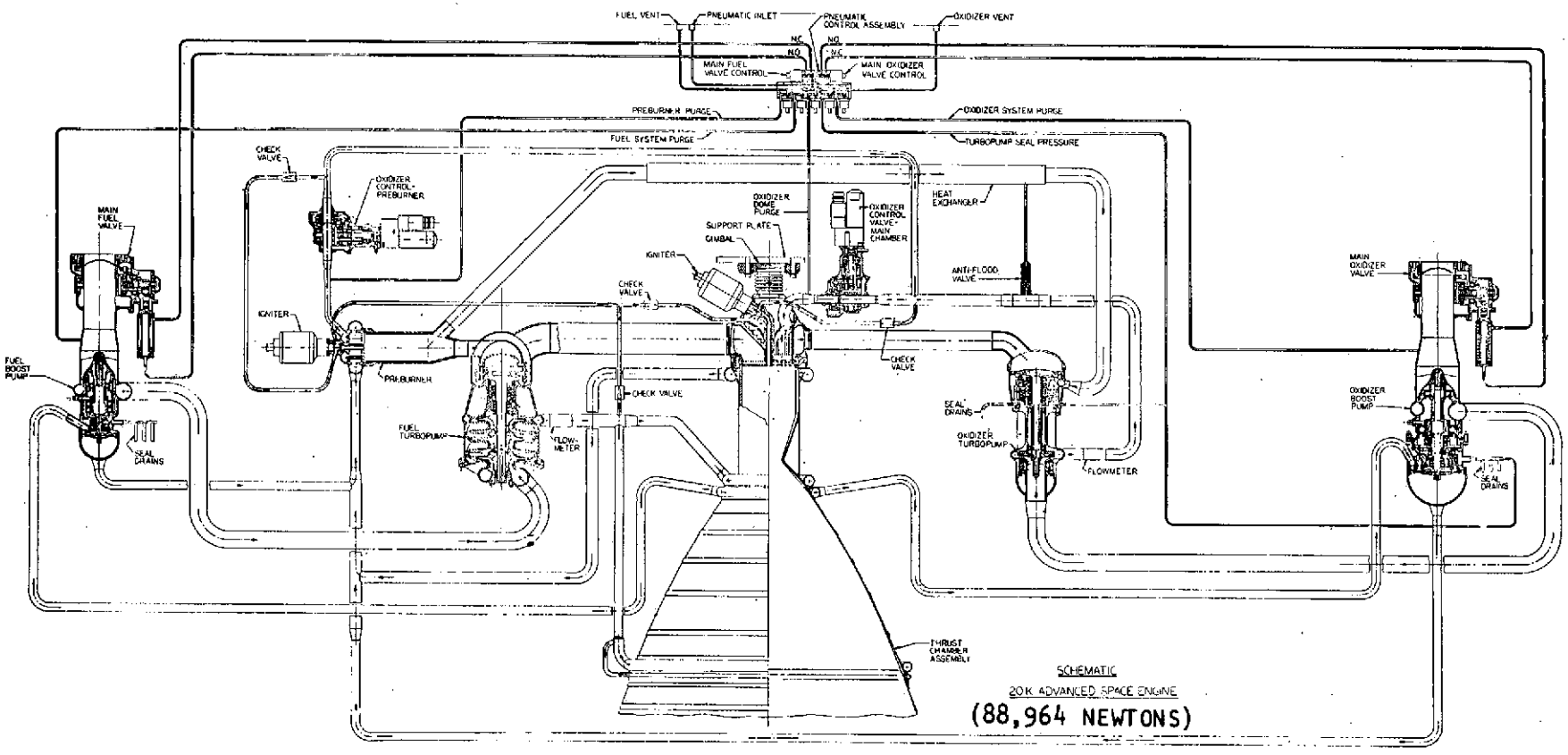

Figure 7-2. Engine Schematic

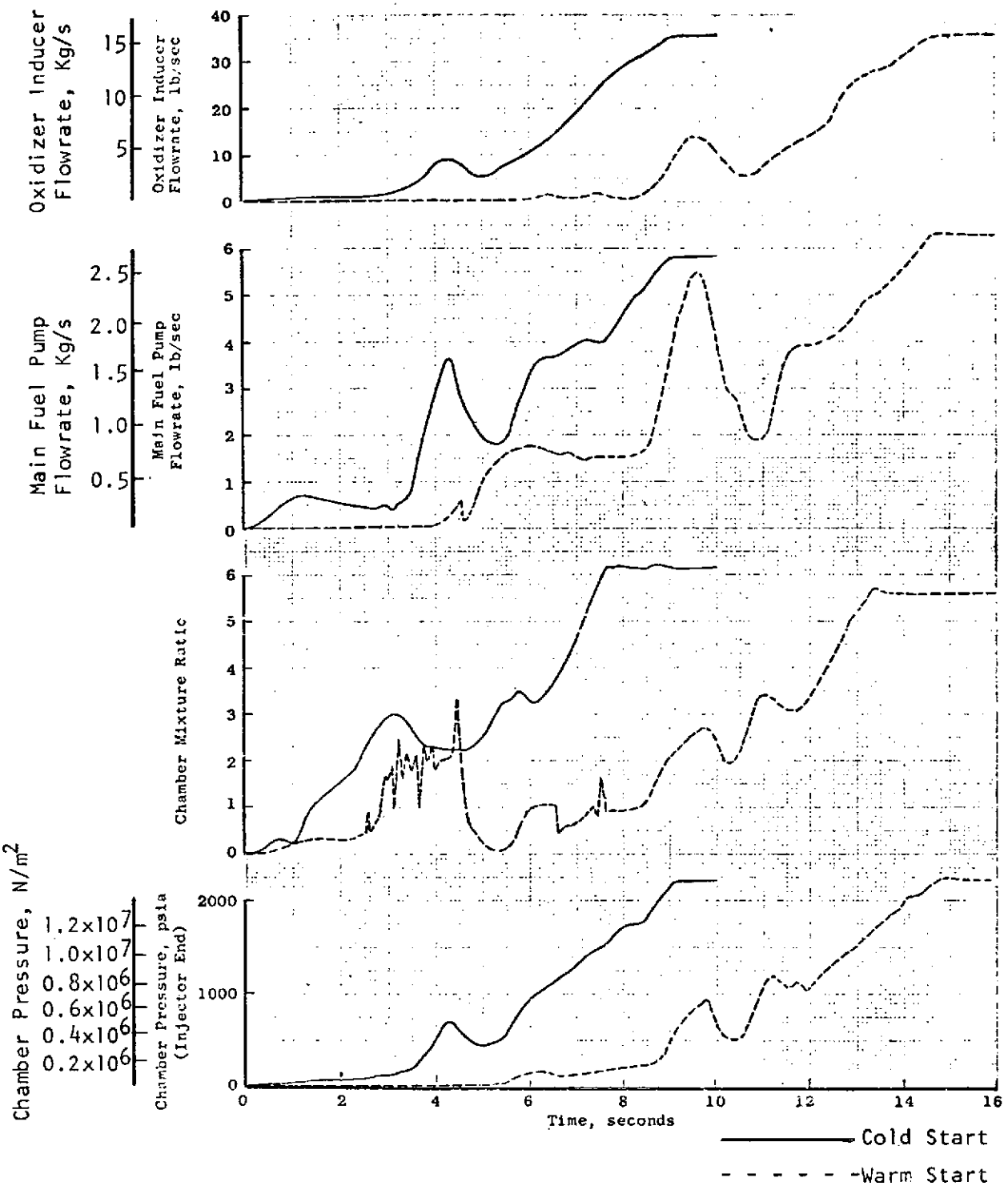

Figure 7-3. Idle Mode Operation

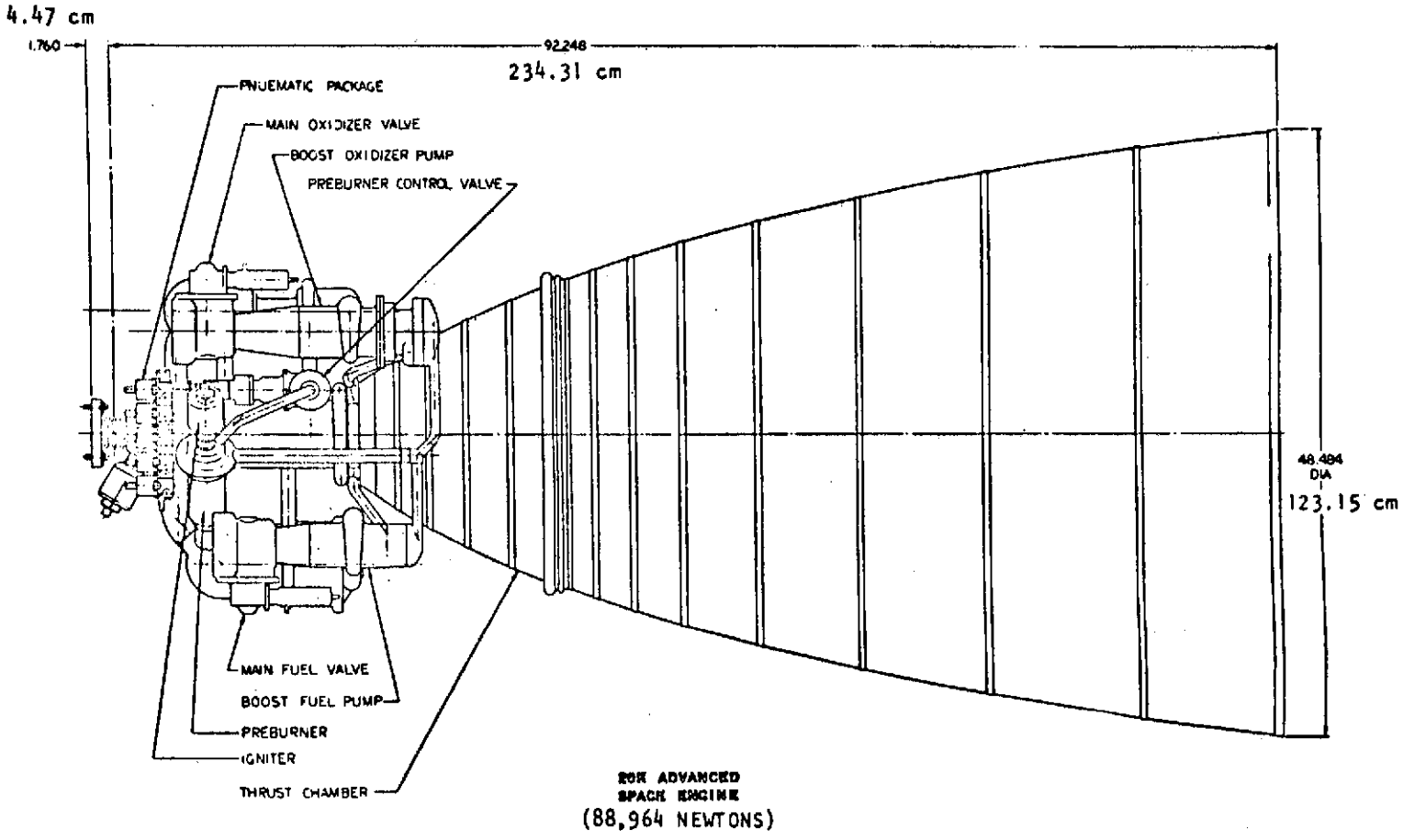

Figure 7-4. Baseline Engine Package

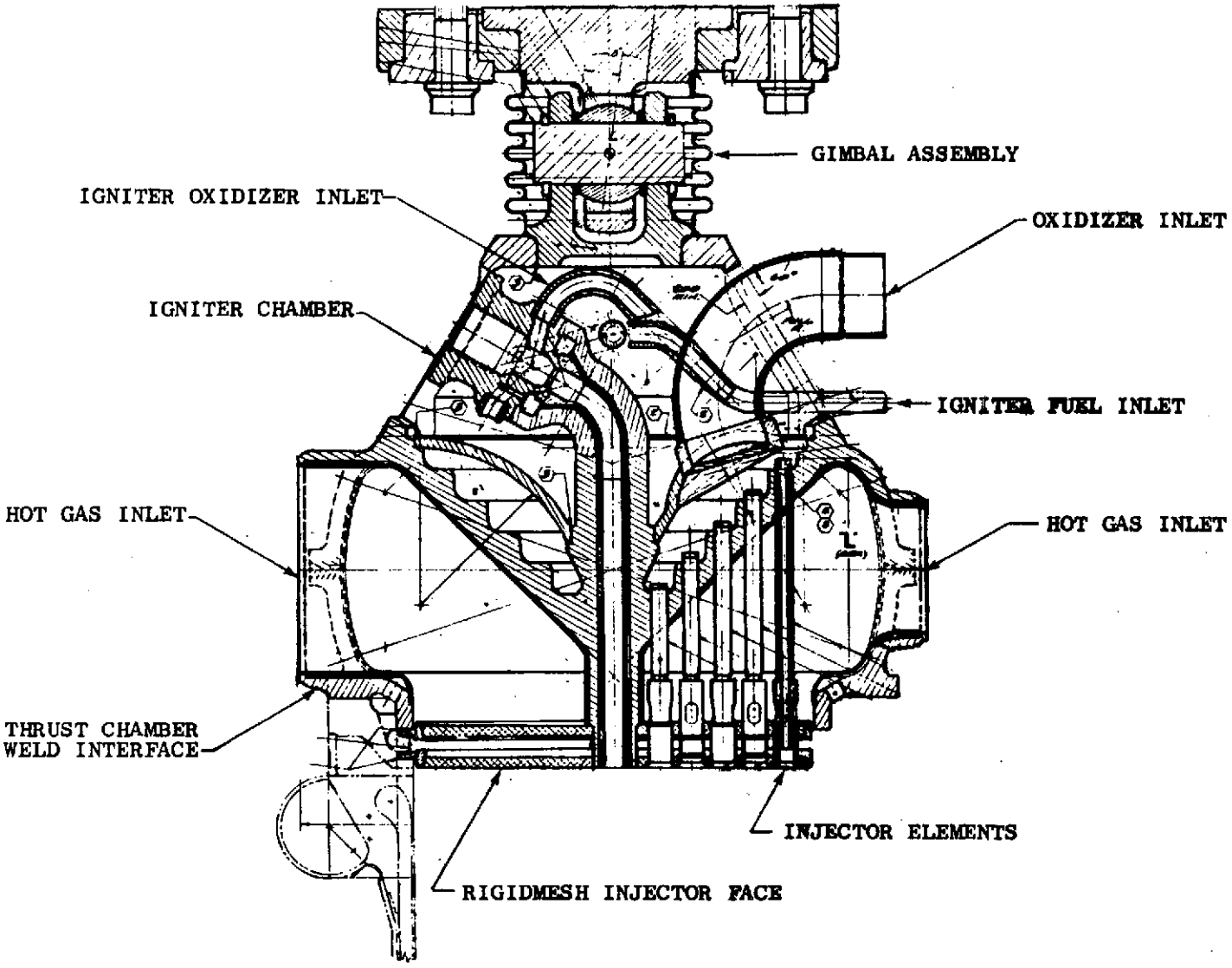

Figure 7-5. Thrust Chamber Injector and Gimbal Assembly

TABLE 7-1. DESIGN ALTERNATIVES

Design Configuration	Operational Mode
Boost Pump Drive Methods	Throttling Requirements
Gears	No Throttling
Hydraulic Turbine	6:1 Throttling*
Hydrogen Gas Turbines	Design Point Net Positive Suction Head, feet (joules/kg)
Regenerative Cooling Scheme	LO_2: 0** 2 (5.97) 16 (47.8)
Pass and a Half	LH_2: 0** 15 (44.8) 60 (179.3)
Split	Start Mode
Preburner Configuration	Normal
Single Preburner	Pressurized Idle
Dual Preburner Separately Supplying Combustion Products to Each Turbine	Tank-Head Idle

*Perturbation of Baseline Design Only
**Tank-Head Idle Mode Start Only

to 100:1), and a dump-cooled nozzle (ϵ = 100:1 to 400:1). The combustion chamber (Fig. 7-6) utilized a spun and slotted NARloy-Z liner with electroform closeout and an Inco-718 structural jacket. The high heat capacity and strength at elevated temperature of the NARloy-Z makes it desirable in this application. The fixed nozzle (Fig. 7-6) composed of A-286 tubes is cooled by the hydrogen ultimately used to drive the boost pump turbines. The dump-cooled nozzle, specifically designed for light weight because of the moderate loads applied, is also composed of A-286 tubes.

The single preburner configuration (Fig. 7-7) is essentially solid wall with some film cooling. This configuration was selected to avoid the complexities of regenerative cooling a small combustor.

The low-speed boost pumps (Fig. 7-8 and 7-9) were sized to meet the start and mainstage inlet requirements (low speed) and yet provide sufficient developed head to assure the main pumps adequate NPSH. The main turbopumps (Fig. 7-10 and 7-11) were thus optimized for maximum performance and therefore operate at very high speed during mainstage.

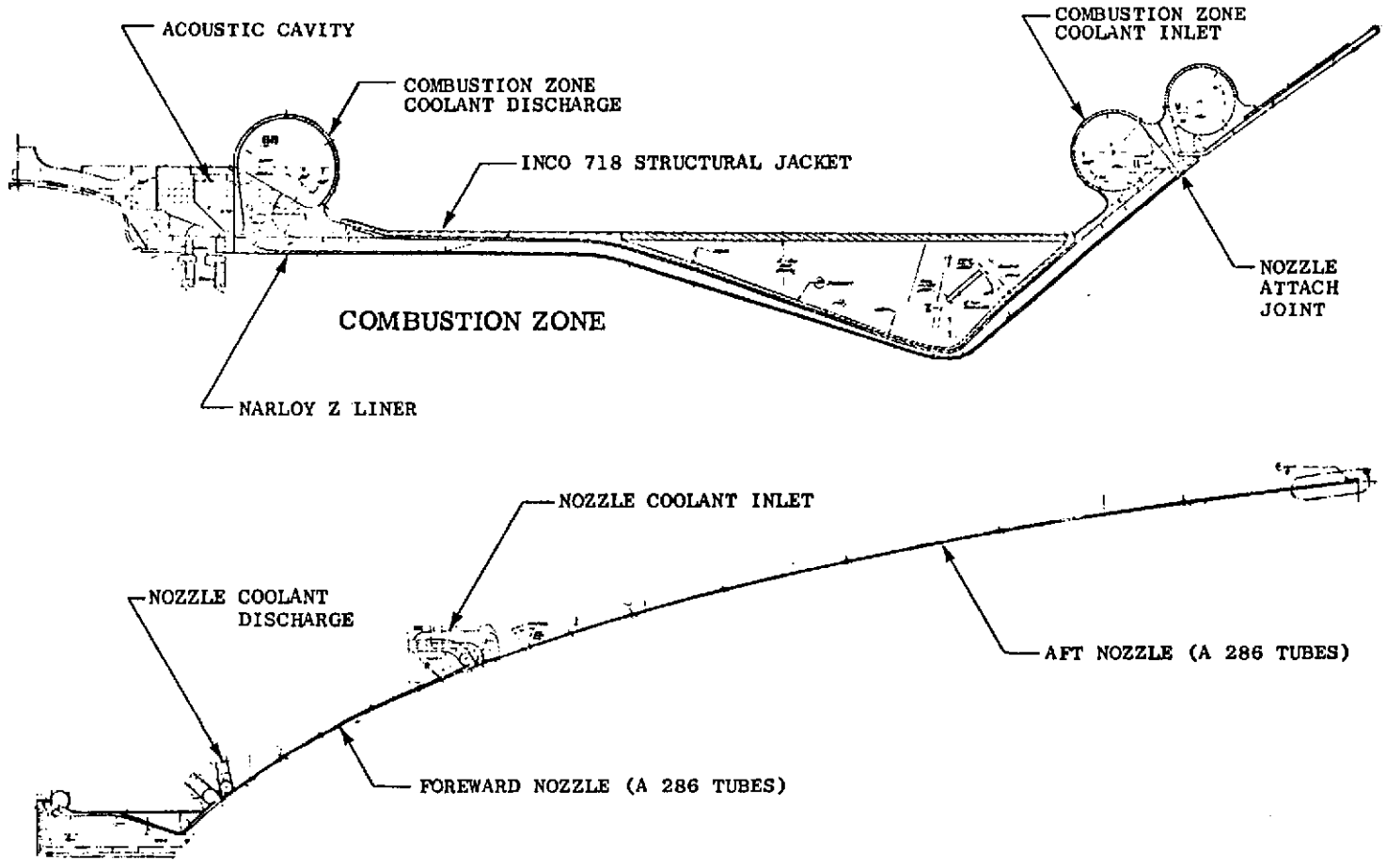

Figure 7-6. Combustion Chamber and Nozzle Designs

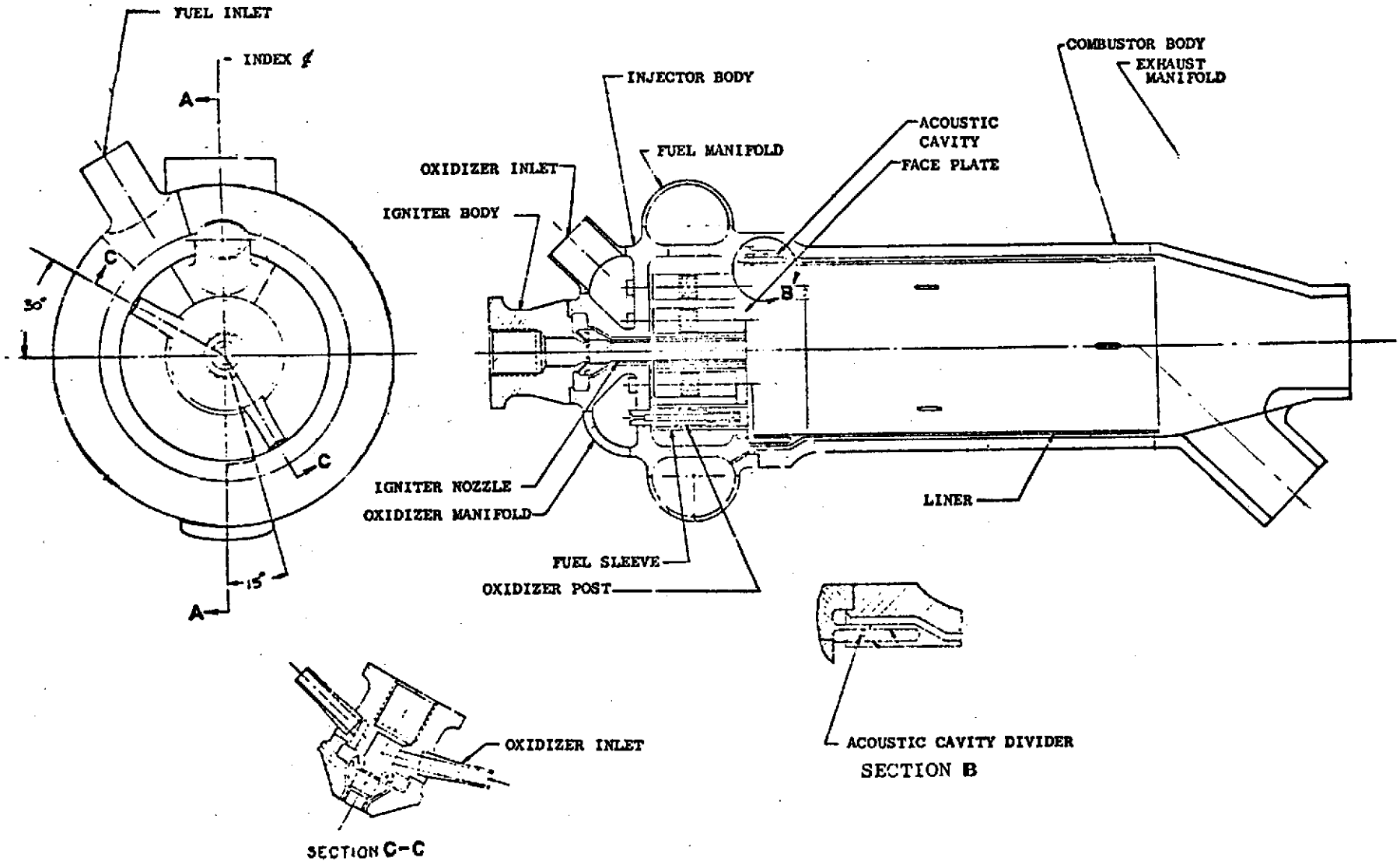

Figure 7-7. Advanced Space Engine Preburner Assembly

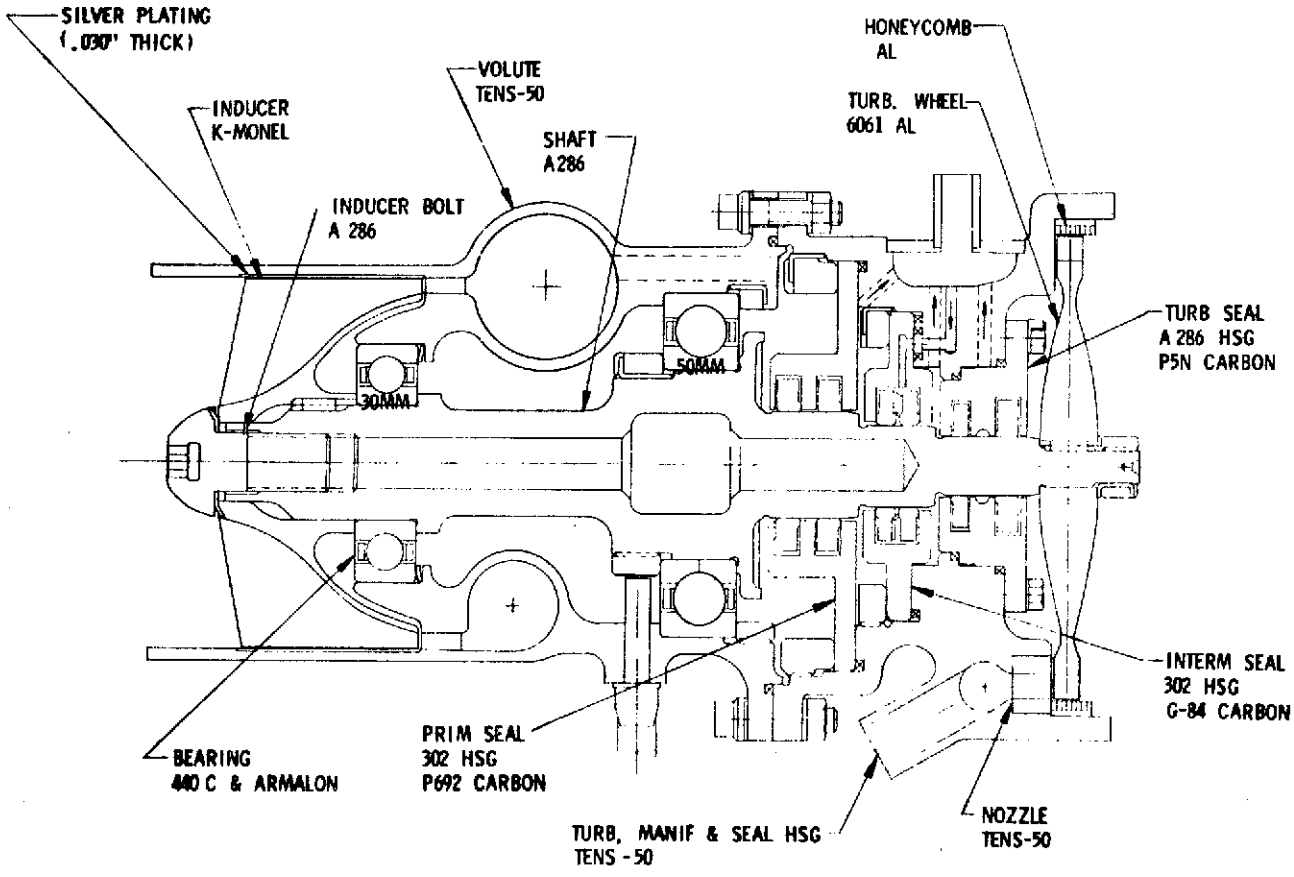

Figure 7-8. ASE Low-Pressure LOX Turbopump

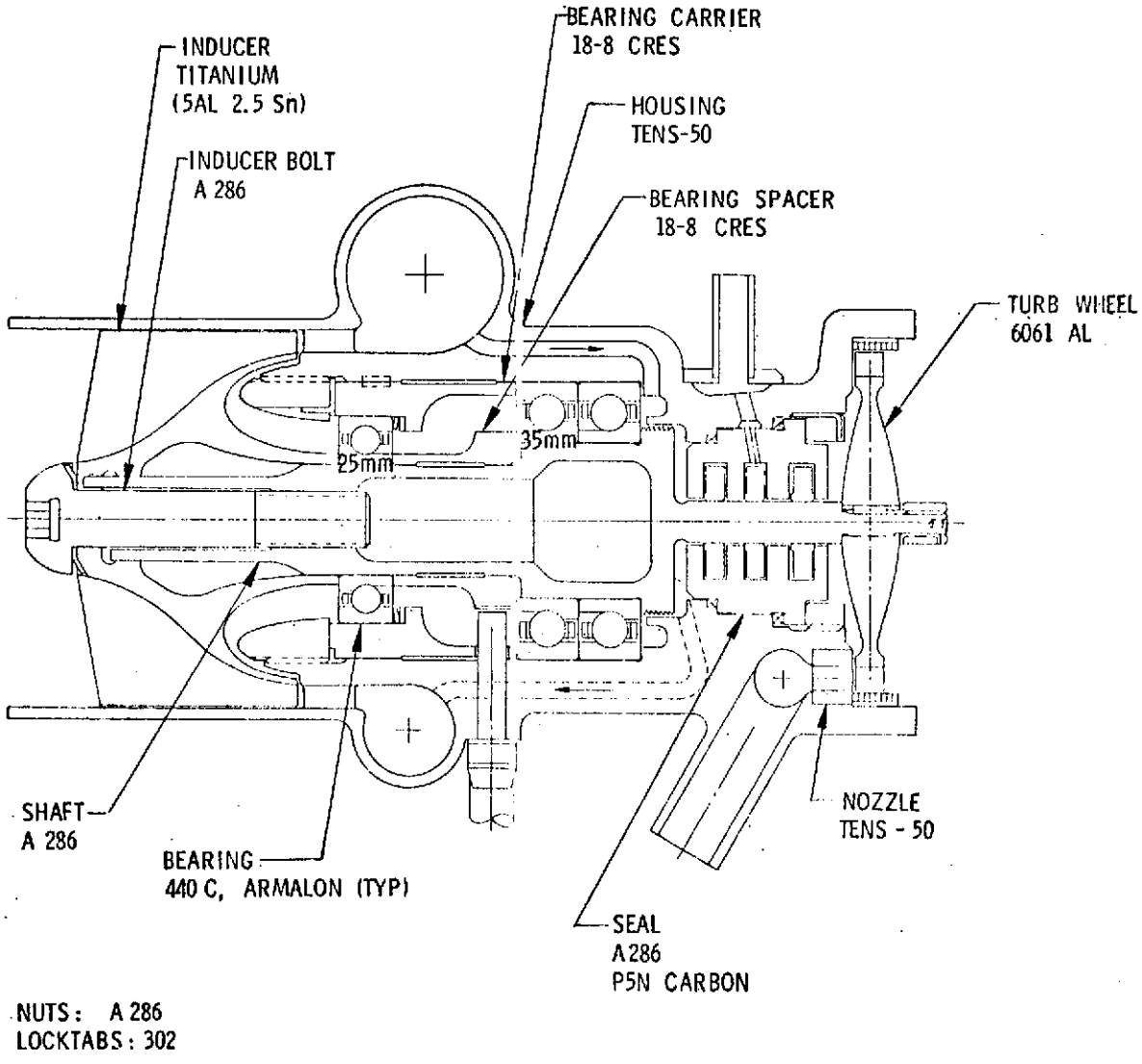

Figure 7-9. ASE Low-Pressure Hydrogen Turbopump

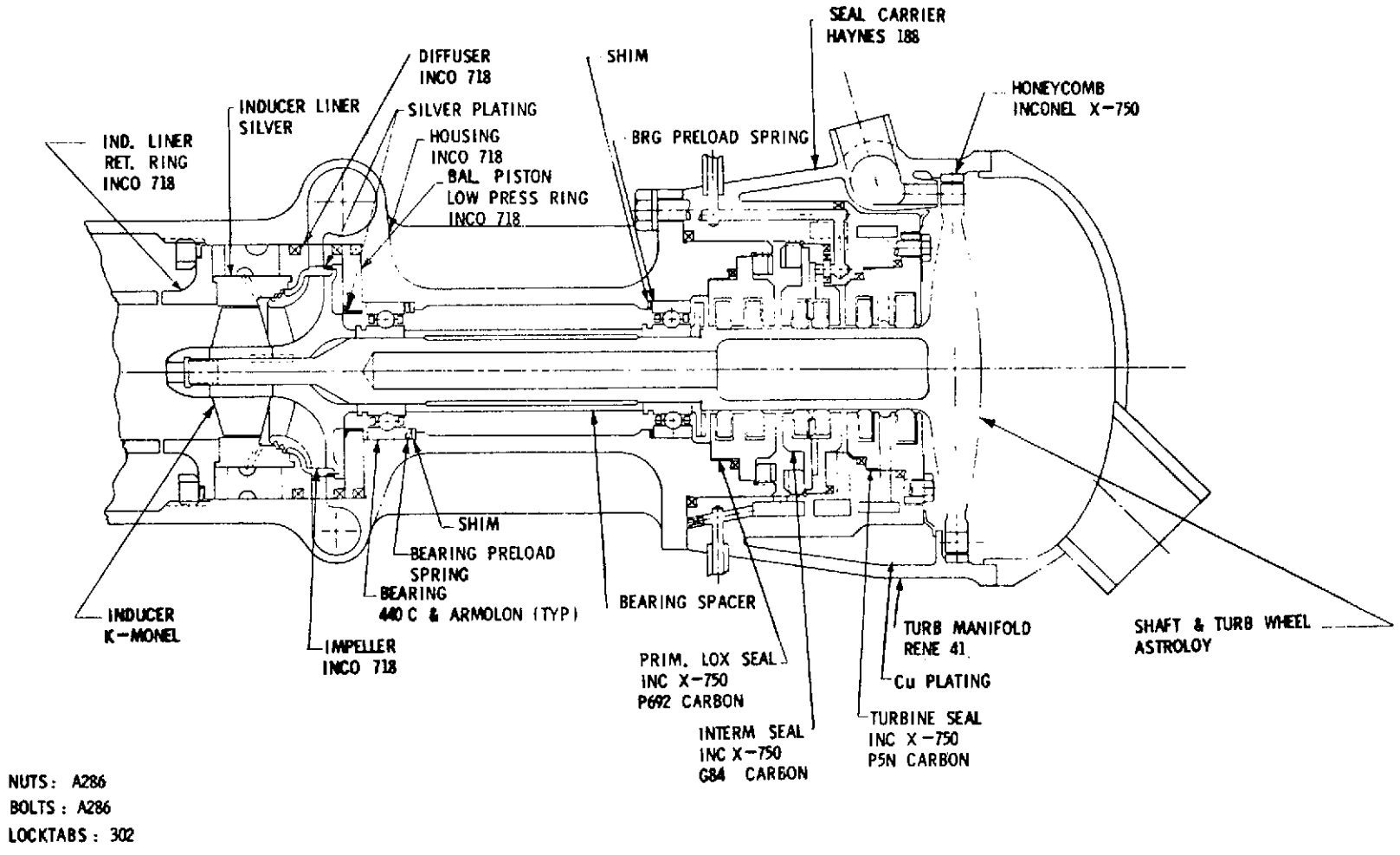

Figure 7-10. ASE High-Pressure Oxidizer Turbopump

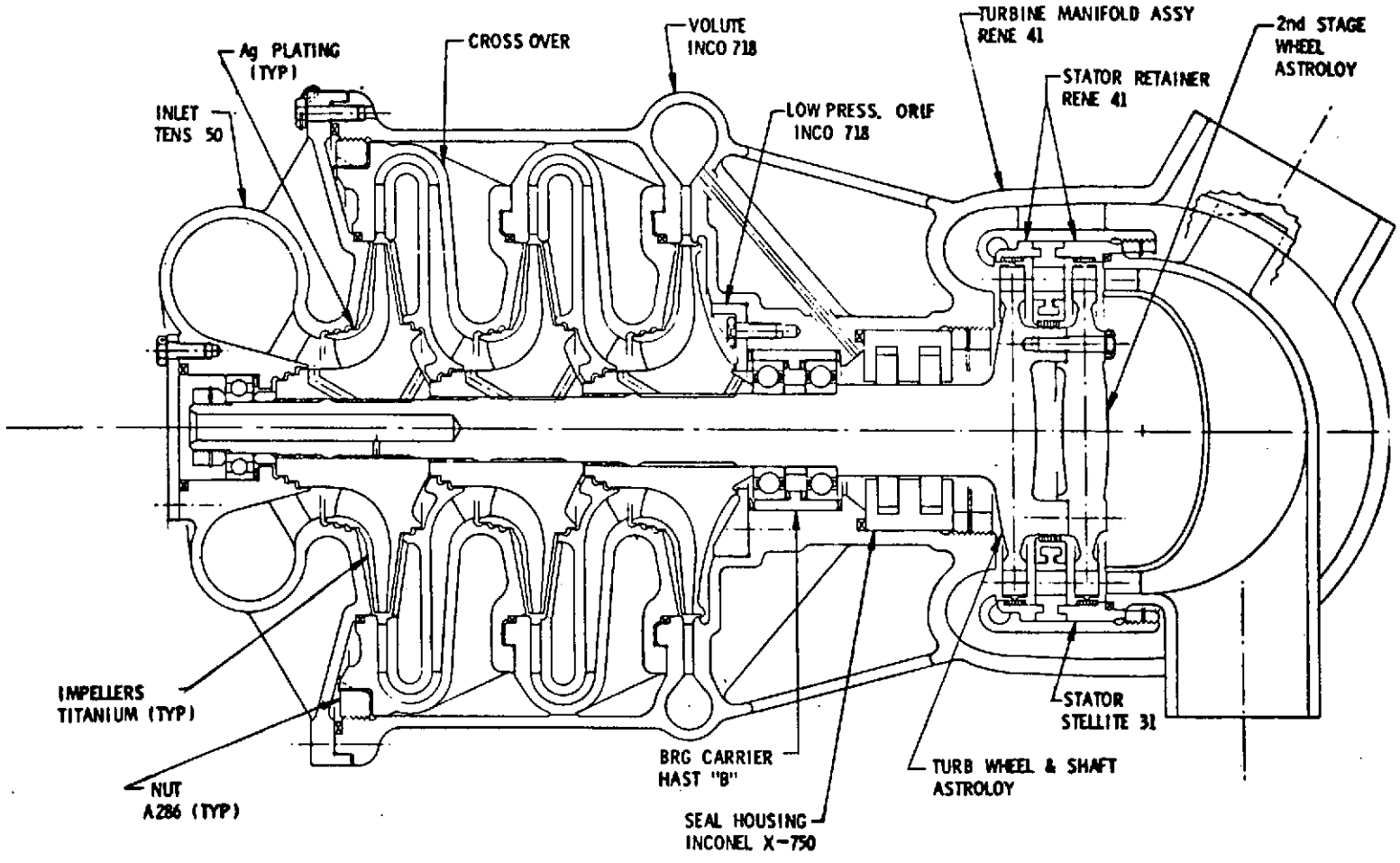

Figure 7-11. ASE High-Pressure Fuel Turbopump

The main LO_2 turbopump was designed with a single stage (and inducer) to avoid complexities of adding an additional stage for supplying the preburner. The additional developed head provided to the main injector results in a high-pressure drop design (very desirable for throttling applications). After significant effort in assessing the relative merits of two-stage and three-stage main LH_2 pump configurations, the three-stage configuration was selected because of its superior performance (four points of efficiency), smaller size 2.54-cm (1-inch) length and 2.54-cm (1-inch) diameter, and lighter weight 2.722 kg (6 pounds).

Because of the nonthrottling baseline, a two-modulating-valve control system, in conjunction with the main inlet valves, was implemented. The valves (Fig. 7-12 and 7-13) were located to control preburner and main injector oxidizer flowrates. This approach not only provides good engine control but also avoids increased fuel-side pressure drop that would directly impact chamber pressure.

The preburner and main chamber igniter concept (Fig. 7-14) was selected from the prior NASA-LeRC studies (Contracts NAS3-14350 and NAS3-14351) and company-funded technology effort. The air-gap design was selected because of its wider temperature range of operation than others investigated.

The fail-safe control system was designed based on current technology. With adequate provisions for control, instrumentation on redundancy of key functions, an engine controller (Fig. 7-15) weighing only approximately 3.175 kg (7 pounds) was determined to be practical. To provide a lightweight package, emphasis was placed on utilizing the results of controlled circuitry studies currently in progress for the SSME. The basic instrumentation requirements (Table 7-2) were analyzed and selected with respect to specific requirements of engine checkout, start, and operational phases. Abbreviations are defined in Table 7-3.

Analysis of alternative "minimum cost" and "minimum-time" development plans was conducted. This effort included DDT&E, production of 50 engines, and 10-year operational support costs. The results indicate that the shortening of the development schedule by 1 year (from 59 to 47 months) increases the cost of the minimum-time program by approximately 7 million dollars. The difference is primarily due to the additional facility, tooling, STE, and hardware requirements to facilitate the shorter schedule.

The concluding effort directed under the contract was an analysis of packaging the engine to meet a common interface (RL10A-3-3 interface configuration) and design of a suitable retractable nozzle configuration. It was determined that meeting the common interface had negligible effect on the engine concept. A retractable nozzle system was designed (Fig. 7-16) which allows shortening the engine stowed length to only 128.27 cm (50.5 inches) and increases the weight by 21.319 kg (47 pounds).

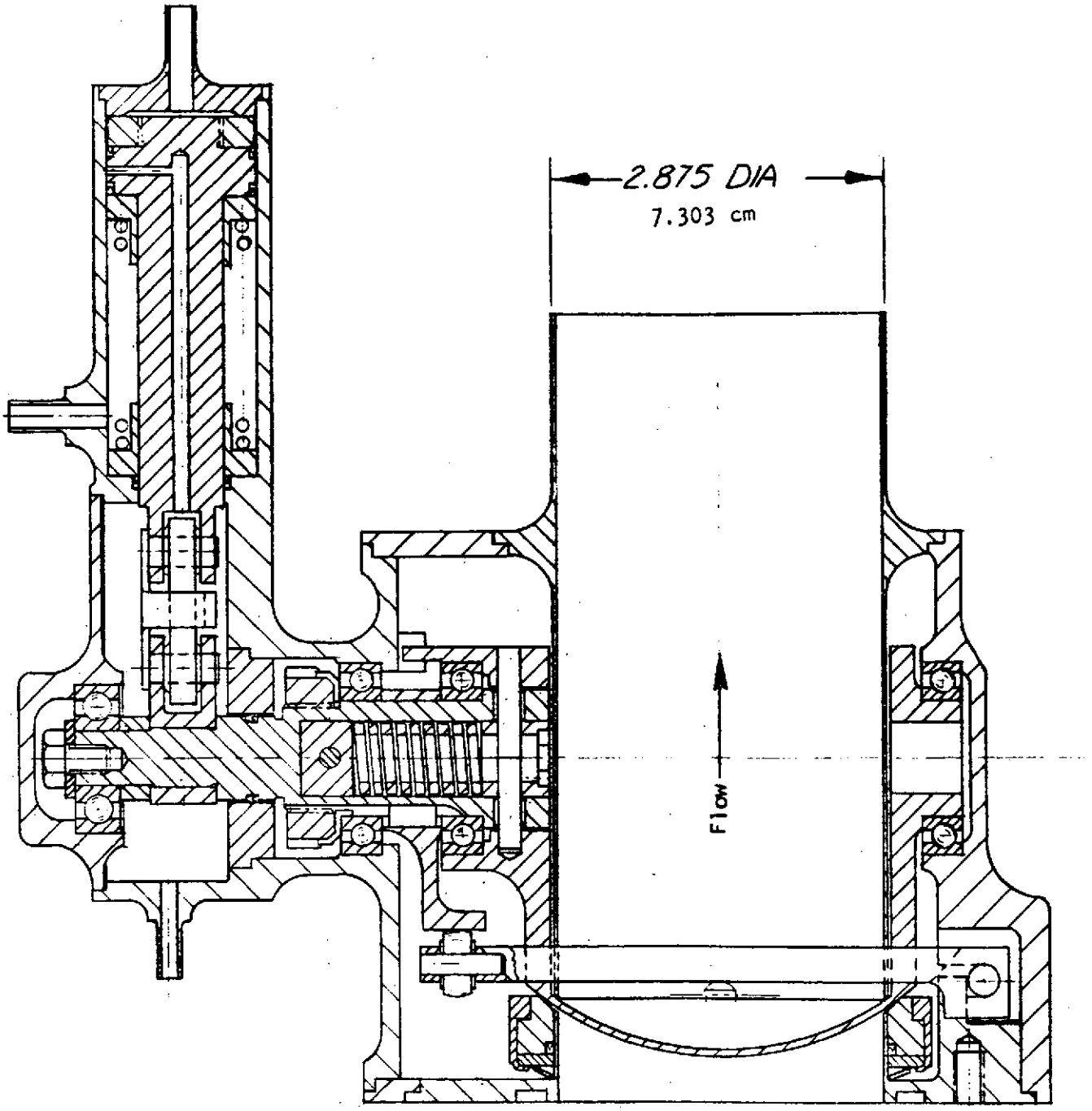

Figure 7-12. Main Propellant Valve

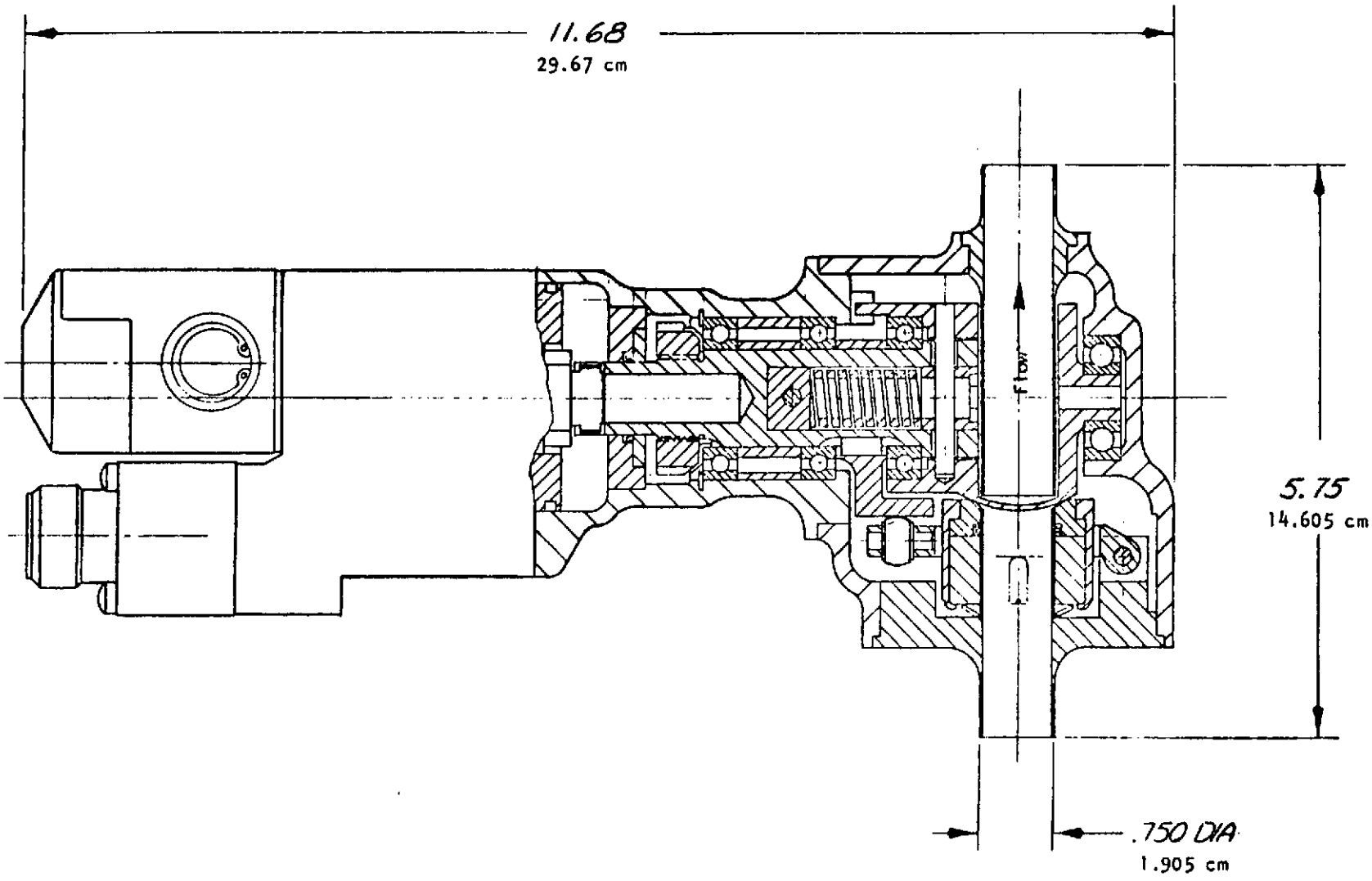

Figure 7-13. Control Valve

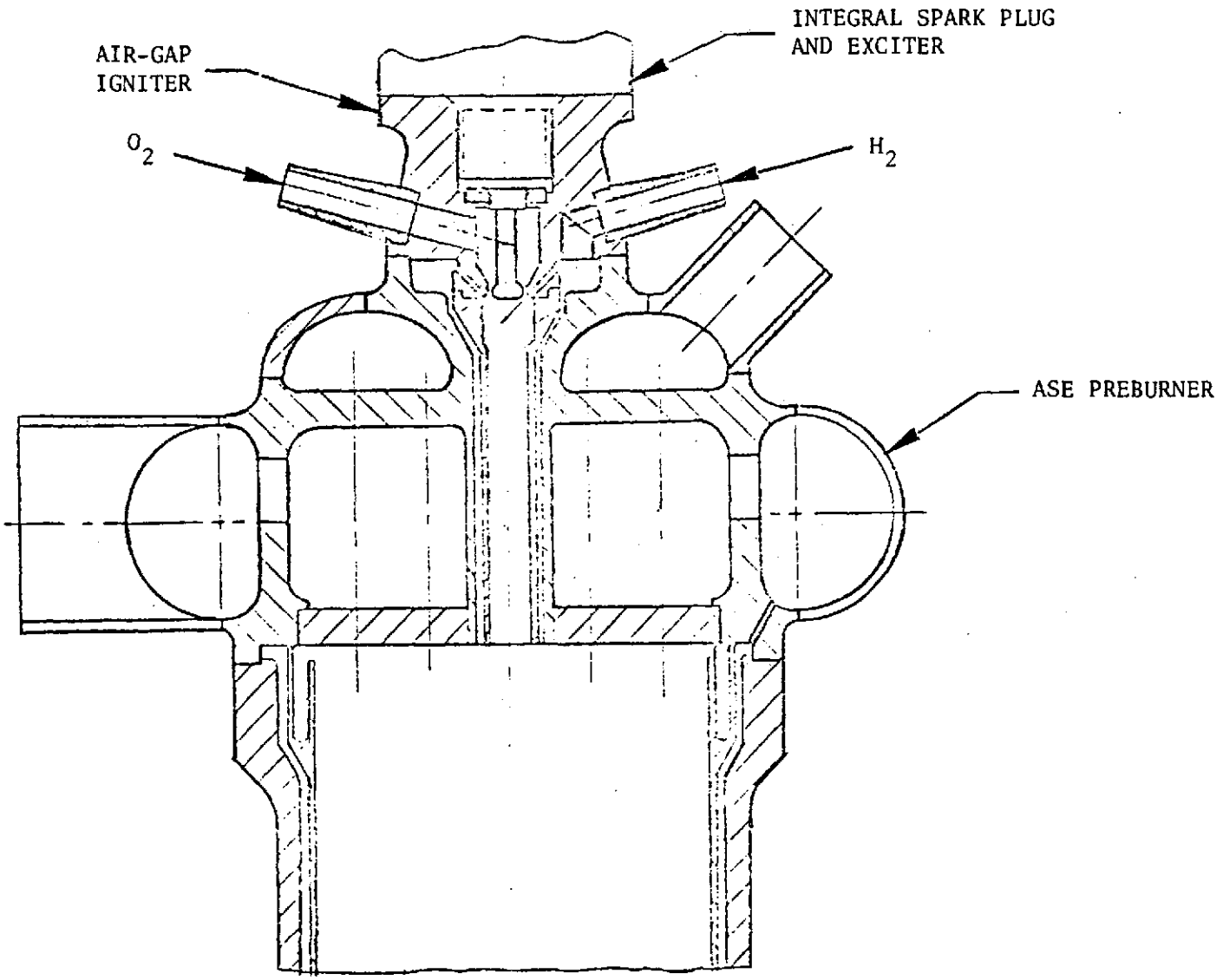

Figure 7-14. ASE Preburner Air-Gap Igniter

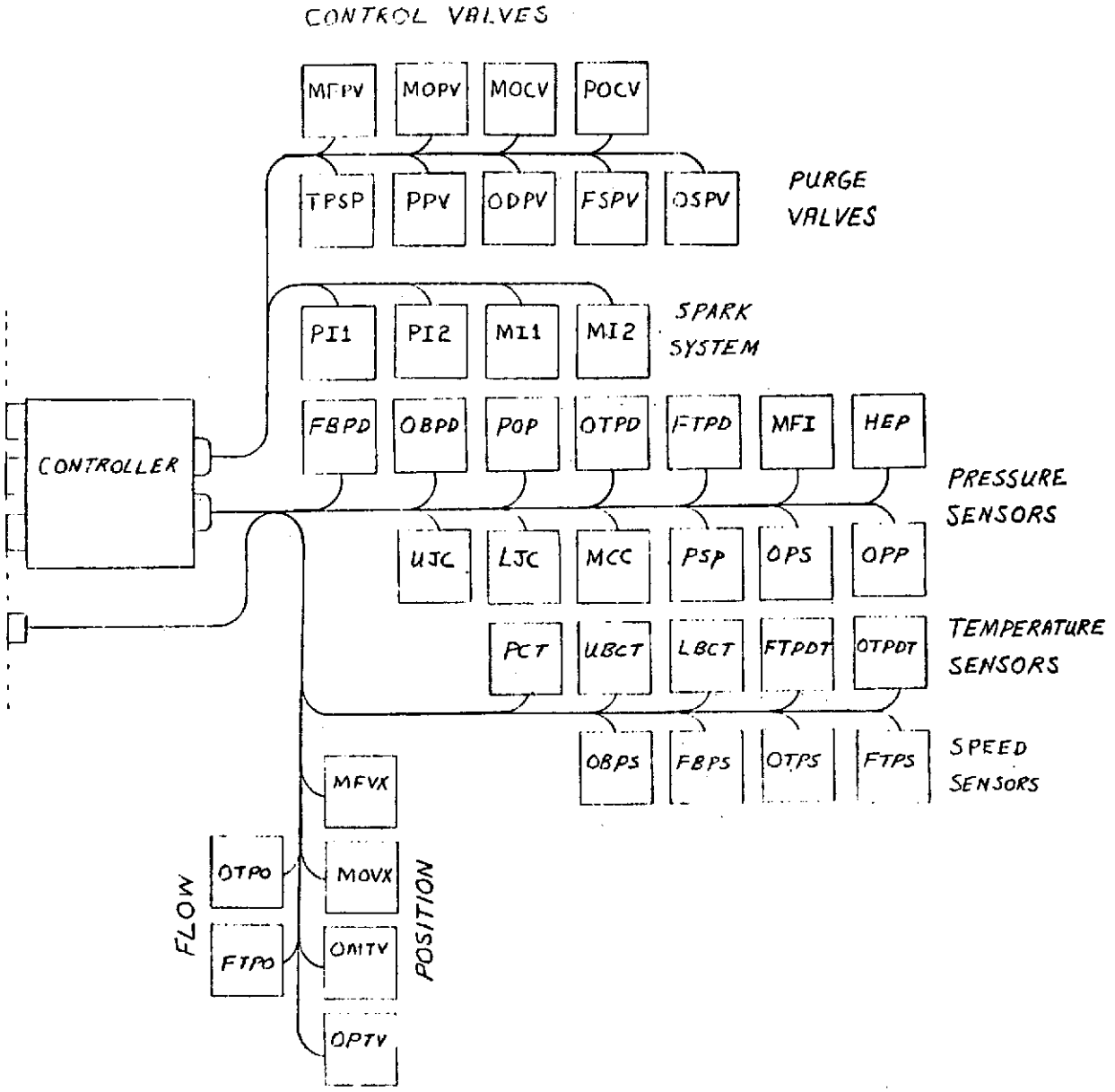

Figure 7-15. Engine Electrical System Block Diagram

Page intentionally left blank

TABLE 7-2. ENGINE INSTRUMENTATION REQUIREMENTS

Pressures	Instrument Type	Function 1	2	3	4	5	6	Abbreviation
Fuel Boost Pump Discharge	RC7003 *	X			X			FBPDP
Ox Boost Pump Discharge	RC7001	X			X			OBPDP
Preburner Outlet	RC7001				X		X	POP
Fuel Turbopump Discharge	RC7001	X		X	X		X	FTPD
Ox Turbopump Discharge	RC7003 *	X		X	X		X	OTPD
Main Fuel/Gas Injection	RC7001				X			MFI
Upper/Lower Jacket Coolant Discharge Pres.	RC7003 *				X			UJC/LJC
Main Combustion Chamber	RC7001		X		X		X	MCC
Pneumatic System	RC7001				X	X	X	PSP
Oxidizer Pumps-Seals (purge)	RC7001				X	X	X	OPS
Oxidizer Purge System	RC7001				X	X	X	OPP
Heat Exchanger	RC7001						X	HEP
Temperatures								
Preburner Chamber	RC7004	X	X		X		X	PCT
Upper/Lower Bulk Coolant Temp.	RC7003 *				X		X	UBCT/LBCT
Fuel Turbopump Discharge	RC7003 *				X			FTPDT
Ox. T/P Discharge	RC7003 *			X	X			OTPDT
Flowrates								
Ox. Turbopump Outlet	RC7005	X	X	X			X	OTPO
Fuel Turbopump Outlet	RC7005	X	X	X			X	FTPO
Speeds								
Ox. & Fuel Boost Pumps	RC7005				X		X	OBP/FBP
Ox. & Fuel Turbopumps	RC7005				X		X	OTP/FTP
Valve Positions								
Main Fuel Valve	POT	X			X	X	X	MFVX
Main Oxidizer Valve	POT	X			X	X	X	MOVX
Oxidizer Throttle Valve (Main)	LVDT	X	X	X	X	X	X	OMTM
Oxidizer T.V. (Preburner)	LVDT	X	X	X	X	X	X	OPTV

Functions

1. Engine Start and Cutoff Control
2. Engine Thrust Control
3. Mixture Ratio Control
4. Engine Monitor/Checkout
5. Engine Ready
6. Engine Limit Control

* Integral Pressure/Temperature Elements

TABLE 7-3. ABBREVIATIONS

MFPV - Main Fuel Pilot Valve

MOPV - Main Oxidizer Pilot Valve

MOCV - Main Oxidizer Control Valve

POCV - Preburner Oxidizer Control Valve

PPV - Preburner Purge Valve

ODPV - Oxidizer Dome Purge Valve

FSPV - Fuel System Purge Valve

OSPV - Oxidizer System Purge Valve

PI 1 - Preburner Igniter No. 1

PI 2 - Preburner Igniter No. 2

MI 1 - Main Igniter No. 1

MI 2 - Main Igniter No. 2

TPSP - Turbopump Seal Purge

CONCLUSIONS

The study conducted to select an optimum engine configuration from a number of alternative concepts has resulted in the selection of a high-performance, lightweight system. The engine is designed to provide a nominal specific impulse of 473.4 seconds with an engine weight of 152.86 kg (337 pounds) for the fixed nozzle configuration. The retractable nozzle concept results in a total engine weight of 174.18 kg (384 pounds), while allowing retraction of the nozzle to afford a 128.27-cm (50.5-inch) overall engine stowed length. The engine design consists of GH_2 turbine-driven boost pumps, single preburner, split-flow regenerative-cooled thrust chamber (to ϵ = 100:1) and dump-cooled nozzle (ϵ = 100:1 to 400:1). The engine is designed to start with saturated propellants under tank-head/pumped-idle conditions and operate in mainstage with engine inlet NPSH values of 5.97 joule/kg (2 feet) LO_2 and 44.8 joule/kg (15 feet) LH_2, respectively.

The engine design selected provides a basis for proper focusing of component research and a system suitable for study of component interactions and engine dynamics. The design fully meets the requirements for engine design and operation specified in the contract Work Statement.

APPENDIX A

GROUND RULES FOR ADVANCED SPACE ENGINE PRELIMINARY DESIGN

GENERAL

Components that are subject to a low cycle fatigue mode of failure will be designed for a minimum of 300 cycles times a safety factor of 4.

Components that are subject to a fracture mode of failure will be designed for a minimum of 300 cycles times a safety factor of 4.

Components that are subject to a high cycle fatigue mode of failure will be designed within the allowable stress range diagram (based on the material endurance limit). If stress range material property data are not available, modified Goodman diagrams, constructed as shown below, shall be utilized:

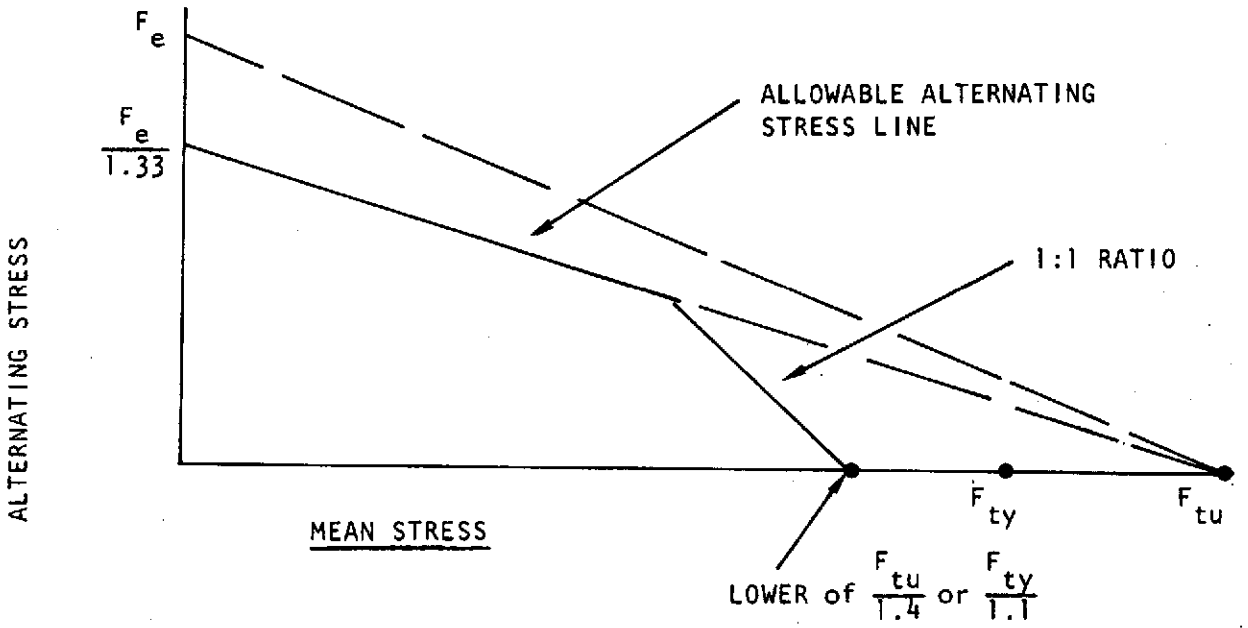

F_e = Material Endurance Limit
F^{ty} = Material Yield Strength (0.2 percent offset)
F_{tu} = Material Ultimate Strength

Effective stress will be based on the Mises-Hencky constant energy of distortion theory.

Unless otherwise noted under component ground rules specified herein, the following minimum factors of safety will be utilized.

Factor of Safety (0.2 percent yield) = 1.1 x Limit Load
Factor of Safety (Ultimate) = 1.4 x Limit Load
Limit Load: The maximum predicted load or pressure at the most critical operating condition

Components subject to pressure loading shall be designed to the following minimum proof and burst pressures:

Proof Pressure = 1.2 x Limit Pressure
Burst Pressure = 1.5 x Limit Pressure

INDUCER

Inducer inlet NPSH will not be less than the following:

LH_2, NPSH = 1.3 $cm^2/2g$
LOX, NPSH = 2.3 $cm^2/2g$

IMPELLER

Inducers and/or impellers utilized in the high-pressure pumps will be designed for operation above incipient cavitation.

Impeller burst speed will be at least 20 percent above the maximum operating speed.

Impeller effective stress at 5 percent above the maximum operating speed will not exceed the allowable 0.2 percent yield stress. (Does not apply to areas in which local yielding is permitted.)

TURBINE

Blade root steady-state stress will not exceed the allowable 1 percent 10-hour creep stress.

Stress state at the blade root, as defined by the steady-state stress and an assumed vibratory stress equal to the gas bending stress, will be within the allowable stress range diagram or modified Goodman diagram.

No blade natural frequencies will be within ±15 percent of known sources of excitation at steady-state operating speeds.

Disk burst speed will be at least 20 percent above the maximum operating speed.

Disk maximum effective stress at 5 percent above the maximum operating speed will not exceed the allowable 0.2 percent yield stress. (Does not apply to areas in which local yielding is permitted.)

BEARINGS

Turbopump designs will utilize rolling elements bearings. Maximum DN:

	LOX	LH_2	GH_2
Roller	$1.5x10^6$	$2.0x10^6$	$0.5x10^6$
Ball	$1.5x10^6$	$2.0x10^6$	$1.2x10^6$

B_{10} life $\geq$ 100 hours

Material:

Rolling Elements	440 C
Races	440 C

SEALS

Turbopump designs will utilize conventional type seals. Face contact seal maximum PV, FV, and P_fV Factors*:

	LOX	LH_2	GH_2	H_2+H_2O
PV Factor	25,000 (525,380)	50,000 (1,050,761)	20,000 (420,304)	10,000 (210,152)
FV Factor	2,000 (106,257)	4,000 (213,515)	1.500 (80,069)	800 (42,703)
P_fV Factor	60,000 ($1.261x10^8$)	200,000 ($4.203x10^8$)	50,000 ($1.051x10^8$)	20,000 ($4.203x10^7$)

*PV = unit load times rubbing velocity (lb/in.^{2} x ft/sec; N/cm-s)
FV = face load per unit length times rubbing velocity (lb/in. x ft/sec; N-s)
P_fV = fluid pressure differential times rubbing velocity (psig x ft/sec; N/m-s)

GEARS

Pitch line velocity (maximum	20,000 fpm (101.6 m/s)
Hertz stress (maximum	60,000 psi ($4.137x10^8$ N/m^2)
Material	AMS 6260

CRITICAL SPEED

Rotor bending frequency will be at least 25 percent above the rotor maximum operating speed.

A minimum margin of 20 percent will be maintained between rotor rigid body critical speeds and rotor steady-state operating speeds at full thrust and the 6:1 throttled thrust condition. Rigid body critical speeds within the

throttled-to-full thrust range will be permitted only if deemed necessary by both the contractor Program Manager and the NASA Project Engineer.

THRUST CHAMBER

High heat flux portion of chamber will be of nontubular construction. It will be of milled construction with dimensional limits of:

Minimum slot width = 0.030 in. (0.0762 cm)
Maximum slot depth/width = 4 to 1 in. (10.16 to 0.54 cm)

Minimum web thickness - 0.030 in. (0.0762 cm)
Minimum wall thickness = 0.025 in. (0.0635 cm)

Lightweight construction (tubular with high-strength, high-temperature alloys), starting at lowest feasible expansion ratio, will be used.

APPENDIX B

TECHNOLOGY DESIGN BASE

The Advanced Space Engine (ASE) Preliminary Design effort currently in progress is directed toward providing a design base for investigating the technology required for achieving a high-performance propulsion system capable of fulfilling orbital maneuvering stage requirements. The design of the engine will be conducted utilizing materials and material properties consistent with current technology. This appendix identifies prospective materials, stress level data, and fatigue life analysis methods in fulfillment of the ASE Preliminary Design contract (NAS3-16751) milestone. In addition, the NASA ground rules establishing the minimum acceptable criteria to be utilized during the design process are included in Appendix A.

Presented herein are the materials, stress level data, and thermal fatigue life analysis approach to be used in the design of the engine.

MATERIALS AND STRESS LEVELS

The materials selected for key component applications and the related stress level data to be utilized in the stress analyses to be conducted are presented in Table B-1. The selection of these materials is based on past experience, current similar applications, and known desirable properties. In addition to the required stress and environmental considerations, particular emphasis is being placed on avoiding problems unique to high-performance systems such as hydrogen embrittlement, effects of large thermal gradients, etc., by proper selection of materials and processes and the institution of adequate design margins to ensure high structural reliability. The stress level data presented consists of yield and ultimate stress values and the percent elongation for the materials at the expected operating temperature for each specific component. These data represent currently established material properties. The final stress levels have been established for each component based on final material selection and definition of operating conditions.

THERMAL FATIGUE ANALYSIS

Thermal fatigue analysis consists of assessing the accumulation of damage to components as thermal cycles occur during normal operation. The length of time under load as well as repetitions of load are evaluated.

Cyclic influence is evaluated by using the materials fatigue properties. Length of time under load is evaluated by using the materials stress-rupture properties. Damage to the component is expressed in terms of the fractional part of its materials capability that is utilized to satisfy the service requirements.

The formulation of a life equation is dependent on safety factor policy and failure definition. A safety factor of 4 and typical material properties are used in the life equation and failure is said to have occurred when a crack

TABLE B-1. ADVANCED SPACE ENGINE COMPONENT MATERIALS AND STRESS LEVEL DATA

Component	Material	Temperature F(K)	Material Properties		
			σ_{ty}, psi (N/m^2)	σ_{tu}, psi (N/m^2)	ε, %
Thrust Chamber					
Liner	NARloy-Z	70/1000 (294/811)	20,000/10,000 ($1.379x10^8/6.89x10^7$)	40,000/15,000 ($2.758x10^8/1.034x10^8$)	42/40
Jacket	INCO 718	-370/70 (50/294)	180,000/150,000 ($1.24x10^9/1.034x10^9$)	213,000/180,000 ($1.450x10^9/1.241x10^9$)	7.5/12
Shell	INCO 718	70 (294)	150,000 ($1.034x10^9$)	175,000 ($1.207x10^9$)	12
Inlet Manifold	INCO 718	-370 (50)	180,000 ($1.24x10^9$)	213,000 ($1.469x10^9$)	7.5
Exit Manifold	INCO 718	70 (294)	150,000 ($1.034x10^9$)	180,000 ($1.241x10^9$)	12
Exit Manifold Rings	INCO 625	70 (294)	55,000 ($3.79x10^8$)	115,000 $7.929x10^8$	30
Nozzle					
Tubes	A-286	-380/500 (44.4/533)	128,000/83,000 ($8.83x10^8/5.72x10^8$	193,000/126,000 ($1.331x10^9/8.687x10^8$)	14/25
Jacket	INCO 718	-110/70 (194/294)	156,000/150,000 ($1.076x10^9/1.034x10^9$)	187,000/180,000 ($1.290x10^9/1.241x10^9$)	12.3/12
Inlet Manifold	INCO 718	-380 (44.4)	181,000 ($1.248x10^9$)	214,000 $(1.475x10^9$	7.5
Exit Manifold	INCO 718	-70 (217)	154,000 ($1.062x10^9$)	186,000 ($1.282x10^9$)	12
Rings Support	CRES 347	70 (294)	30,000 ($2.068x10^8$)	75,000 ($5.171x10^8$)	40
Nozzle Extension					
Tubes	A-286	-350/1000 (50/811)	127,000/76,500 ($8.756x10^8/5.274x10^8$)	190,000/114,500 ($1.310x10^9/7.894x10^8$)	15/15
Structure	INCO 718	70 (294)	150,000 ($1.034x10^9$)	180,000 ($1.241x10^9$)	12
Inlet Manifold	INCO 718	-380 (44.4	181,000 ($1.248x10^9$)	214,000 ($1.475x10^9$)	7.5
Preburner					
Injector Body	INCO 625	-270/1500 (106/1089)	71,000/30,000 ($4.895x10^8/2.068x10^8$)	140,000/47,000 ($9.653x10^8/3.241x10^8$)	38/60
Oxidizer Posts	304L	-270 (106)	28,000 ($1.931x10^8$)	164,000 ($1.131x10^9$)	35
Combustor	INCO 625	1400 (1033)	35,000 ($2.413x10^8$)	63,000 ($4.344x10^8$)	50
Oxidizer Inlet	INCO 625	-275 (1028)	71,000 ($4.895x10^8$)	140,000 ($9.653x10^8$)	38
Fuel Inlet	INCO 625	70 (294)	55,000 ($3.792x10^8$)	115,000 $7.929x10^8$	30
Exit Manifold	Haynes 188	-1400 (522)	34,500 ($2.379x10^8$)	84,000 ($5.792x10^8$)	28
Injector Main					
Oxidizer Posts	Haynes 188	-280 (100)	89,000 ($6.136x10^8$)	160,000 ($1.103x10^9$)	40
Sleeve	A-286	1300 (978)	55,000 ($3.792x10^8$)	67,000 ($4.61x10^8$)	26
Body	INCO 718	70 (294)	150,000 ($1.034x10^9$)	180,000 ($1.241x10^9$)	12
Manifold	INCO 718	70 (294)	150,000 ($1.034x10^9$)	180,000 ($1.241x10^9$)	12
FacePlate	321 CRES (Rigimesh)	160 (344)	12,900 ($8.894x10^7$)	26,200 ($1.806x10^8$)	36
Hot-Gas Manifold	INCO 625	1300 (978)	36,000 ($2.482x10^8$)	75,000 ($5.171x10^8$)	37
Pump Housing					
High-Pressure Fuel Turbopump	INCO 718	-420 (22)	184,000 ($1.269x10^9$)	218,000 ($1.503x10^9$)	8
High-Pressure Oxidizer Turbopump	INCO 718	-300 (89)	170,000 ($1.172x10^9$)	204,000 ($1.407x10^9$)	7.5
Low-Pressure Fuel Turbopump	Tens-50	-420 (22)	42,000 ($2.896x10^8$)	51,000 ($3.516x10^8$)	2
Low-Pressure Oxidizer Turbopump	Tens-50	-300 (89)	40,000 ($2.758x10^8$)	48,000 ($3.309x10^8$)	2.5
Pump Impeller	Cast				
High-Pressure Fuel Turbopump	Ti	-420 (22)	125,000 ($8.618x10^8$)	145,000 ($9.997x10^8$)	9
High-Pressure Oxidizer Turbopump	INCO 718	-300 (89)	170,000 ($1.172x10^9$)	204,000 ($1.407x10^9$)	7.5

TABLE B-1. (Concluded)

Component	Material	Temperature F(K)	Material Properties		
			σ_{ty}, psi (N/m^2)	σ_{tu}, psi (N/m^2)	ε,%
Turbine Manifold					
High-Pressure Fuel Turbopump	Rene 41	1500 (1089)	96,000 ($6.619x10^8$)	110,000 ($7.584x10^8$)	14
High-Pressure Oxidizer Turbopump	Rene	1500 (1089)	96,000 ($6.619x10^8$)	110,000 ($7.584x10^8$)	14
Low-Pressure Fuel Turbopump	Tens-50	60 (289)	36,000 ($2.482x10^8$)	46,000 ($3.172x10^8$)	4
Low-Pressure Oxidizer Turbopump	Tens-50	60 (289)	36,000 ($2.482x10^8$	46,000 ($3.172x10^8$	4
Turbine Nozzle					
High-Pressure Fuel Turbopump	Rene 41	1500 (1089)	96,000 ($6.618x10^8$)	110,000 ($7.584x10^8$)	14
High-Pressure Oxidizer Turbopump	Rene 41	1500 (1089)	96,000 ($6.619x10^8$)	110,000 ($7.584x10^8$)	14
Low-Pressure Fuel Turbopump	Tens-50	70 (294)	36,000 ($2.482x10^8$)	46,000 ($3.172x10^8$)	4
Low-Pressure Oxidizer Turbopump	Tens-50	70 (294)	36,000 ($2.482x10^8$)	46,000 ($3.172x10^8$)	4
Turbine Shaft, Disk and Blades					
High-Pressure Fuel Turbopump	Mod. Astr.	1400 (1033)	117,000 ($8.067x10^8$)	145,000 ($9.997x10^8$)	15
High-Pressure Oxidizer Turbopump	Mod. Astr.	1400 (1033)	117,000 ($8.067x10^8$	145,000 ($9.997x10^8$)	15
Low-Pressure Fuel Turbopump	A-286	70 (294)	95,000 ($6.550x10^8$)	140,000 ($9.653x10^8$)	12
Low-Pressure Oxidizer Turbopump	A-286	70 (294)	95,000 ($6.550x10^8$)	140,000 ($9.653x10^8$)	12
Inducer					
High-Pressure Oxidizer Turbopump	K-Monel	-300 (89)	109,500 ($7.550x10^8$)	160,000 ($1.103x10^9$)	30
Low-Pressure Fuel Turbopump	Ti	-420 (22)	125,000 ($8.618x10^8$)	145,000 ($9.997x10^8$)	9
Low-Pressure Oxidizer Turbopump	K-Monel	-300 (89)	109,500 ($7.550x10^8$)	160,000 ($1.103x10^9$)	30
System Main Ducting					
Preburner High-Pressure Turbines	Haynes 188	1400 (1033)	34,500 ($2.379x10^8$)	84,000 ($5.792x10^8$)	28
Thrust Chamber/Low-Pressure Turbines	Haynes 188	70 (294)	58,000 ($3.999x10^8$)	128,000 ($8.825x10^8$)	46
Low-Pressure Turbine/Preburner Fuel	Haynes 188	70 (294)	58,000 ($3.999x10^8$)	128,000 ($8.825x10^8$)	46
Oxidizer High-Pressure Pump/Injector	Haynes 188	-270 (106)	88,000 ($6.067x10^8$)	165,000 ($1.138x10^9$)	40
Pneumatic Lines	321 SS	70 (294)	30,000 ($2.068x10^8$	75,000 ($5.171x10^8$)	40
Valves					
Main Fuel Valve	INCO 718	420 (489)	142,000 ($9.791x10^8$)	170,000 ($1.172x10^9$)	12
Main Oxidizer Valve	INCO 718	-300 (89)	170,000 ($1.172x10^9$)	204,000 ($1.407x10^9$)	7.5
Oxidizer Control Valves	INCO-718 Cast	-300 (89)	170,000 ($1.172x10^9$)	162,000 ($1.117x10^9$)	7.5
Antiflood Valve	INCO 718	-300 (89)	176,000 ($1.213x10^9$)	205,000 ($1.413x10^9$)	12
Pneumatic Solenoid Body	321 SS	70 (249	30,000 ($2.068x10^8$)	75,000 ($5.171x10^8$)	40
Gimbal Bearing	INCO 718	70 (249)	150,000 ($1.034x10^9$)	180,000 ($1.241x10^8$)	12

appears. (A safety factor of 4, along with typical low-cycle fatigue data reduced by two on-cycles, was used to design the ASE thrust chamber.)

This definition of failure for the hot wall of a thrust chamber, for example, does not ordinarily result in functional failure because it will usually continue to operate normally for many cycles and extensive operating time after a leaking crack appears. Therefore, the consequences of cracking must be evaluted in each case relative to functional requirements.

Fatigue Properties

The property of concern is the materials thermal fatigue capability. This may be evaluated in various ways:

1. Universal slopes equation
2. Isothermal fatigue test data
3. Thermal fatigue test data
4. Hardware operating data

Fatigue data for the materials to be used in most critical components of the ASE is available at Rocketdyne. For example, isothermal fatigue tests have been conducted at Rocketdyne for candidate thrust chamber liner materials, NARloy-Z and zirconium copper. Figures B-1 and B-2 are plots of the typical thermal fatigue capability of these materials in the range of temperatures from 294 to 922 K (70 to 1200 F). In any case, where fatigue data are not available, the Universal Slopes equation will be used to evaluate thermal fatigue properties.

Stress Rupture Properties

Stress rupture data are available for the materials being considered for this program. Stress rupture testing also has been conducted at Rocketdyne for the NARloy-Z and zirconium copper liner materials. Both materials were in the condition of being heat treated and aged with no subsequent cold work. This is expected to be the condition of these materials when used in a thrust chamber wall. The data are plotted in Fig. B-3 and B-4 and are considered as the typical stress rupture capability. The Larson-Miller equation* was used to extend the range of test data where required.

Material Damage Fractions

Material damage is expressed in terms of fractions which relate material capability to service requirements. Fatigue damage fraction is:

$$\phi_f = \frac{n}{N_f}$$

*"A Time-Temperature Relationship for Rupture and Creep Stresses," by F. R. Larson and James Miller, Transactions of the ASME, July 1952, pp. 765-775.

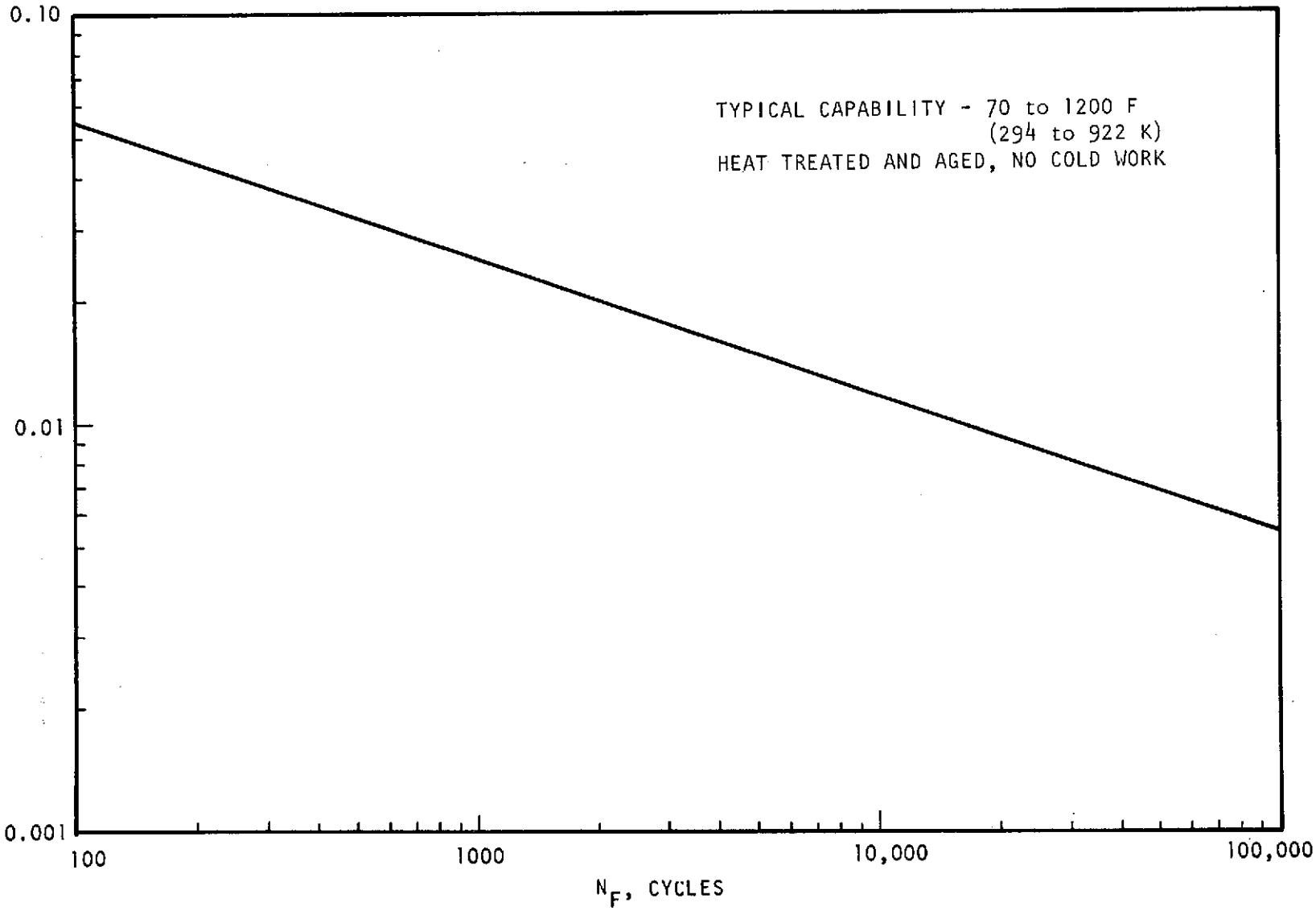

Figure B-1. NARloy-Z Thermal Fatigue Life

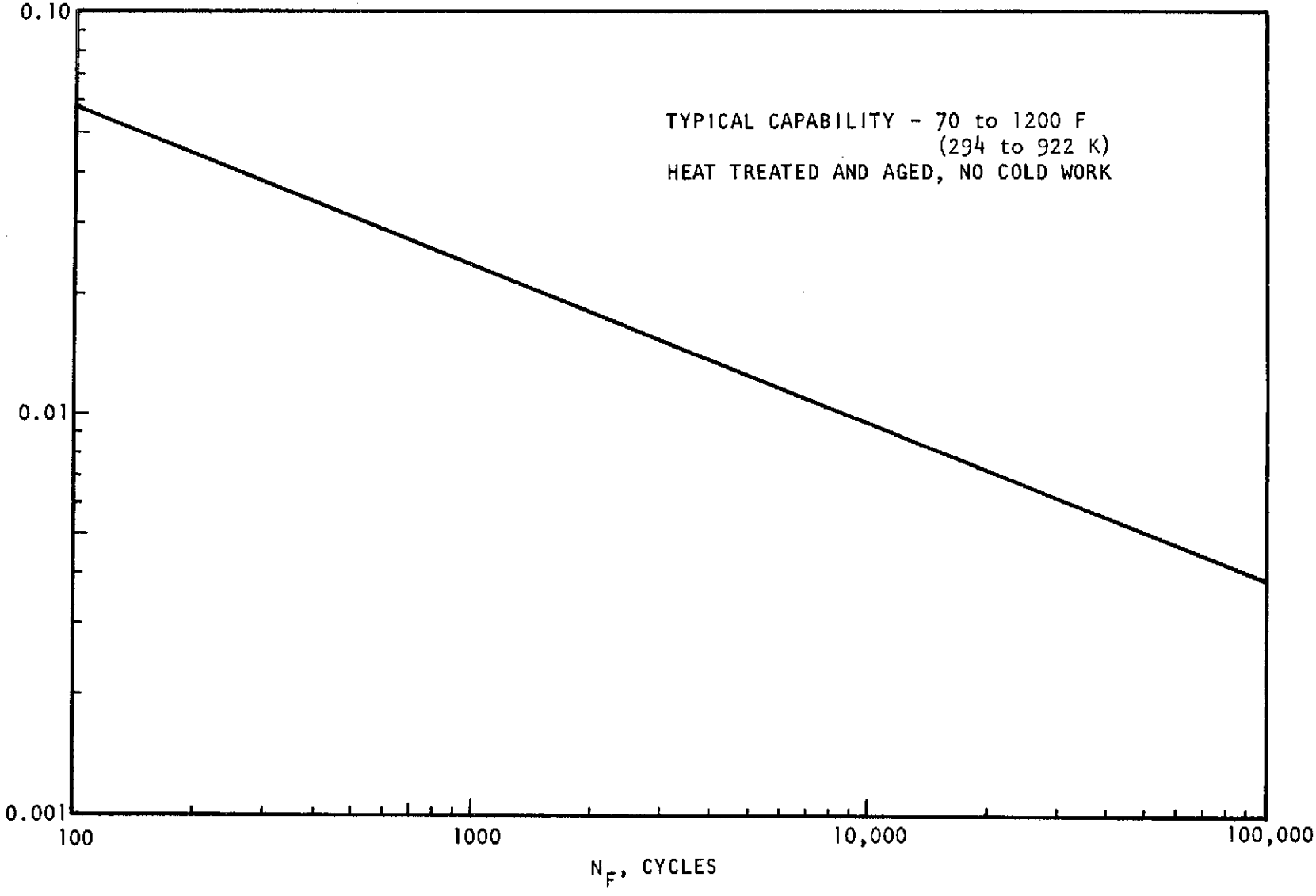

Figure B-2. Zirconium Copper Thermal Fatigue Life

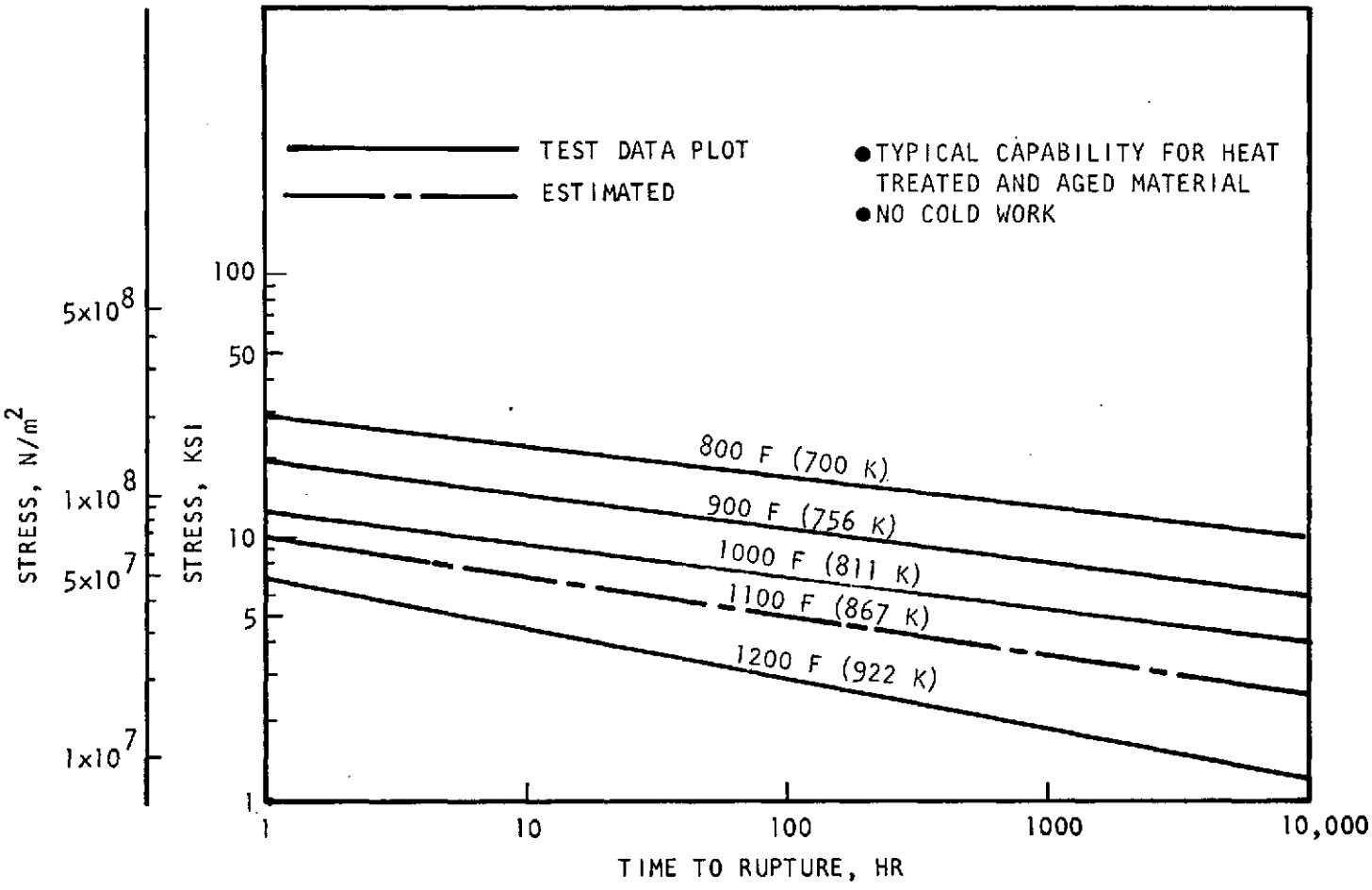

Figure B-3. NARloy-Z Stress Rupture

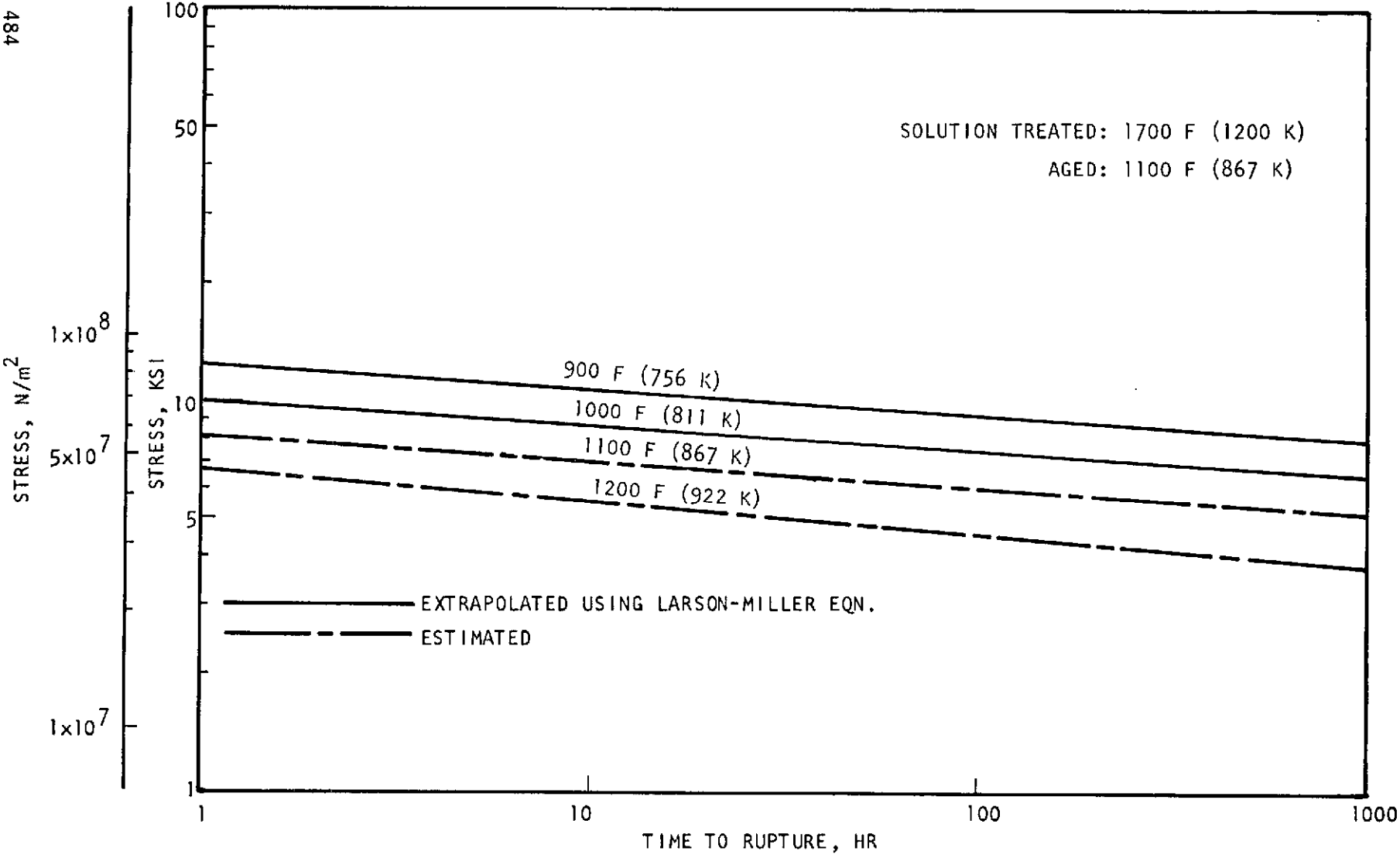

Figure B-4. Zirconium-Copper Stress Rupture

where

n = number of cycles of loading applied

N_f = number of cycles of loading to cause fatigue failure

Creep damage fraction is:

$$\phi_c = \frac{t}{T_r}$$

where

t = number of hours load is applied

T_r = number of hours to produce rupture under the applied load and temperature

Life Equation

The life equation is:

$$4\phi_f + 4\phi_c = 1$$

This equation includes a safety factor of 4. It is theorized that the total material damage is $(\phi_f + \phi_c)$. Therefore, when $(\phi_f + \phi_c) = 1$, failure would result.

The life equation described above will be used for all design and materials in this program.

Stress and Strain Analysis

Analysis methods suited to the stress and strain conditions will be used for the design study. Computer stress and strain analysis will be used where feasible Structural computations may be separated into three categories:

1. Stress calculations for basic structural criteria
2. Stress calculation for determination of creep damage fraction, ϕ
3. Cyclic strain range calculation for determination of fatigue damage fraction, ϕ_f

The criteria used in evaluating the stress and strain of the various components are the same in all cases. The means by which the individual component carries loads and distributes strains must be evaluated in its analysis. To illustrate, consider the structural elements that form the thrust chamber regeneratively cooled tubes.

Basic Structural Criteria. The following analysis is used for tubes:

$$\sigma = \frac{PR}{t}$$

$$\sigma \leq \frac{F_{tu}}{1.5}$$

$$\phi \leq \frac{F_{ty}}{1.2}$$

where

σ = average hoop stresses

p = coolant pressure

R = tube inside radius

t = 90 percent of nominal tube wall thickness

F_{tu} = minimum guaranteed ultimate tensile strength of material at the average steady-state operating temperature through the hot wall

T_{ty} = minimum guaranteed yield tensile strength of material at the average steady-state operating temperature through the hot wall

Creep Damage Fraction. The following analysis is used for tubes:

$$\sigma = \frac{\Delta PRK}{t}$$

$$\phi_c = \frac{t}{T_r}$$

where

σ = tube outer diameter hoop stress

ΔP = coolant pressure minus hot-gas pressure

R = tube inside radius

K = thick wall tube factor for converting average hoop stress to outer surface stress

t = 90 percent of nominal tube wall thickness

T_r = hours to rupture when stress of σ and temperature equal the hot-gas face temperature

t = hours of firing time

Cyclic Strain Range Calculation. The following analysis is used for tubes:

$$\varepsilon_{ai} = \alpha_j \, (T_{ji}-70) - \alpha_w \, (T_{wi}-70)$$

$$\varepsilon_{as} = \alpha_j \, (T_{js}-70) - \alpha_w \, (T_{ws}-70)$$

$$\varepsilon_{atot} = \varepsilon_{as} - \varepsilon_{ai}$$

$$\varepsilon_c = \frac{\alpha_w (T_{wc} - T_{ws})}{2}$$

$$\varepsilon_e = 1.155 \sqrt{\varepsilon_{atot}^2 + \varepsilon_{atot}\,\varepsilon_c + \varepsilon_c^2}$$

where

ε_{ai} = initial hot-gas surface axial strain
ε_{as} = steady-state operating hot-gas surface axial strain
ε_{atot} = hot-gas surface axial strain range
ε_c = hot-gas surface circumferential strain range
ε_e = equivalent uniaxial strain range
α_j = jacket material coefficient of thermal expansion
α_w = tube material coefficient of thermal expansion
T_{ji} = initial temperature (F) of jacket
T_{wi} = initial temperature (F) of hot-gas surface
T_{js} = steady-state operating temperature (F) of jacket
T_{ws} = steady-state operating temperature (F) of hot-gas suface
T_{wc} = hot-gas wall coolant side temperature (F)

Fatigue Damage Fraction. The equivalent uniaxial cyclic strain range is used to enter the fatigue plot to find the number of cycles to cause fatigue failure, N_f. The fatigue damage fraction is then calculated as:

$$\phi_f = \frac{n}{N_f}$$

where n is the design requirement for number of cycles. In the event that cycles of a different type occur, each type of cycle is analyzed separately and a damage fraction calculated for each. The total fatigue damage, ϕ_f, is then:

$$\phi_f = \sum \frac{n_1}{N_{f1}} + \ldots + \frac{N_n}{N_{fn}}$$

APPENDIX C

REFERENCES

1. AFRPL-TR-72-27, Vol. I and II, Orbit-to-Orbit Shuttle Engine Design Study Final Report Draft (F04611-71-C-0039), USAF Edwards Air Force Base, California, February 1972.
2. AFRPL-TR-72-45, Books 1-4, Orbit-to-Orbit Shuttle Engine Design Study Final Report (F04611-71-C0040), USAF, Edwards Air Force Base, California, May 1972.
3. AFRPL-TR-72-4, Vol. II, 25,000-Pound-Thrust Bell Engine Configuration Design and Analysis (F04611-67-C-0016), USAF, Edwards Air Force Base, California, December 1971.
4. Coultas, T. A. and R. C. Kesselring, "Extension of the Priem Theory and Its Use in Simulation of Instability on the Computer," CPIA Publication No. 105, May 1966.
5. Oberg, C. L., T. L. Wong, and W. M. Ford: Final Report: Evaluation of Acoustic Cavities for Combustion Stabilization, NASA CR-115087, Rocketdyne Division, Rockwell International Corporation, Canoga Park, California, July 1971.
6. McMillion, R. L. and J. A. Nestlerode, "Design Criterion for Acoustic Absorbers," CPIA Publication No. 220, Vol. I, November 1971.
7. R-9258, Advanced Hydrogen Oxygen Chamber Design Analysis, NASA CR-121213, Contract NAS3-16774, Rocketdyne Division, Rockwell International, Canoga Park, California, November 1973.
8. Rupe, J. H., The Liquid Phase Mixing of a Pair of Impinging Streams, Progress Report No. 20-195, Jet Propulsion Laboratory, Pasadena, California, 6 August 1953.
9. R-8928P-1, Integrated Thruster Assembly Investigation, Rocketdyne Division, Rockwell International Corporation, Canoga Park, California, 3 April 1972.

APPENDIX D

BIBLIOGRAPHY

Hoshide, R. K., C. E. Nielson, Final Report, Study of Blade Clearance Effects on Centrifugal Pumps, NASA CR-120815, R-8806, Rocketdyne Division, Rockwell International, Canoga Park, California, November 1972.

King, J. A., Design of Inducer for Two-Phase Operation, Final Report, R-8832, Rocketdyne Division, Rockwell International, Canoga Park, California, January 1972.

King, J. A. and E. C. Farrel, Final Report, The Transient Performance of a Hydraulic-Turbine-Driven Inducer: Computer Predictions and Test Verification," NASA CR-72518, R-7747, Rocketdyne Division, Rockwell International, Canoga Park, California, February 1969.

King, J. A., Low-Speed Inducers for a Rocket Engine Feed System, Final Report, Report No. R-8272, Rocketdyne Division, Rockwell International, Canoga Park, California, June 1970.

King, J. A., Low-Speed Inducers for Cryogenic Upper Stages, Milestone Report, ASR 73-25, Rocketdyne Division, Rockwell International, Canoga Park, California, 19 January 1973.

Kesselring, R. C., "Stability Sealing Using a Modular Injection Concept," CPIA Publication No. 192, Vol. II, December 1969.

Lindley, B. K. and A. R. Martinson, An Evaluation of a Hubless Inducer and a Full Flow Hydraulic Turbine-Driven Inducer Boost Pump, NASA CR-72995, NASA Lewis Research Center, October 1971.

Peterson, R. E., Stress Concentration Design Factors, 1953.

Pollack, M. N.: SSME Preburner, Plan of Action, Injector Element Mixing Tests, SSME 72-2109, Rocketdyne Division, Rockwell International, Canoga Park, California, 19 December 1972.

MDC G2818, Vol. I, Space Tug Point Design Study (SA-2465 to NAS7-101), February 1972.

MDC G2818, Vol. II, Space Tug Point Design Study (SA-2465 to NAS7-101), February 1972.

SD72-SA-0032, Vol. III, Part 1, Space Tug Point Design Study Final Report (SA-2190 to NAS7-200), February 1972.

SD72-SA-0032, Vol. III, Part 2, Space Tug Point Design Study Final Report (SA-2190 to NAS7-200), February 1972.

R-8402, Advanced Turbopump Program, Final Report, Contract SNPC-72, Rocketdyne Division, Rockwell International, Canoga Park, California, 26 January 1971.

R-9022, Final Report Advanced Turbopump Technology Program, Contract SNPC-77, Rocketdyne Division, Rockwell International, Canoga Park, California, 23 June 1972.

ASR72-295, Computer Program for Calculation of Analytical Engine Dynamics, Steady-State Optimization and Design, NAS3-16687, Rocketdyne Division, Rockwell International, Canoga Park, California.

Page intentionally left blank

APPENDIX E

DISTRIBUTION LIST (CONTRACT NAS3-16751)

	Copies
National Aeronatuics and Space Administration Lewis Research Center 21000 Brookpark Road Cleveland, Ohip 44135	
Attn: Contracting Officer MS 500-313	1
E. A. Bourke MS 500-205	5
Technical Utilization Office MS 3-16	1
Technical Report Control Office MS 5-5	1
AFSC Liaison Office MS 501-3	2
Library MS 60-3	2
Office of Reliability and Quality Assurance MS 500-211	1
N. T. Musial MS 500-113	1
D. D. Scheer, Project Manager MS 500-203	12
E. M. Krawczonek MS 500-209	1
Director, Manned Space Technology, RS Office of Aeronautics and Space Technology NASA Headquarters Washington, DC 20546	1
Director Space Prop. and Power, RP Office of Aeronautics and Space Technology NASA Headquarters Washington, DC 20546	2

	Copies
Director, Launch Vehicles and Propulsion, SV Office of Space Science NASA Headquarters Washington, DC 20546	1
Director, Materials and Structures Division, RW Office of Aeronautics and Space Technology NASA Headquarters Washington, DC 20546	1
Director, Advanced Missions, MT Office of Manned Space Flight NASA Headquarters Washington, DC 20546 Attn: J. C. Malament, MTG	1
Director, Physics and Astronomy Programs, SC Office of Space Science NASA Headquarters Washington, DC 20546	1
Director, Planetary Programs, SL Office of Space Science NASA Headquarters Washington, DC 20546	1
Office of Aeronautics and Space Technology, R NASA Headquarters Washington, DC 20546	1
Attn: F. W. Stephenson, RPI	1
NASA Scientific and Technical Information Facility P.O. Box 33 College Park, Maryland 20740 Attn: NASA Representative	10
National Aeronautics and Space Administration Goddard Space Flight Center Greenbelt, Maryland 20771 Attn: Library	1

	Copies
National Aeronautics and Space Administration John F. Kennedy Space Center Cocoa Beach, Florida 32931	4
Attn: Library R. B. Grigsby LL-MLV-3 W. S. Brosier LL-OPN-2 R. Engel SP-B	
National Aeronautics and Space Administration Langley Research Center Langley Station Hampton, Virginia 23365	1
Attn: Library	
I. O. Mac Conoehie MS 411	1
National Aeronautics and Space Administration Johnson Space Center Houston, Texas 77001	5
Attn: Library C. W. Yodzis R. W. Polifka J. C. Hooper, III J. G. Thibadaux	
National Aeronautics and Space Administration George C. Marshall Space Flight Center Huntsville, Alabama 35912	8
Attn: Library A. G. Orillion T. W. Barret J. L. Sanders J. Thomson F. W. Braams S. Saucier H. G. Paul	

	Copies
Jet Propulsion Laboratory 4800 Oak Grove Drive Pasadena, California 91103 Attn: Library	1
Defense Documentation Center Cameron Station Building 5 5010 Duke Street Alexandria, Virginia 22314 Attn: TISIA	1
National Aeronautics and Space Administration Ames Research Center Moffett Field, California 94035 Attn: Library	1
National Aeronautics and Space Administration Flight Research Center P.O. Box 273 Edwards, California 93523 Attn: Library	1
Director, Technology Utilization Division Office of Technology Utilization NASA Headquarters Washington, DC 20546	1
Office of the Director of Defense Research and Engineering Washington, DC 20301 Attn: Office of Assistant Director (Chemical Technology)	1
RTD (RTNP) Bolling Air Force Base Washington, DC 20332	1
Arnold Engineering Development Center Air Force Systems Command Tullahoma, Tennessee 37389 Attn: Library	

	Copies
Advanced Research Projects Agency Washington, DC 20525 Attn: Library	1
Aeronautical Systems Division Air Force Systems Command Wright-Patterson Air Force Base Dayton, Ohio Attn: Library	1
Air Force Missile Test Center Patrick Air Force Base, Florida Attn: Library	1
Air Force Systems Command Andrews Air Force Base Washington, DC 20332 Attn: Library	1
Air Force Rocket Propulsion Laboratory (RPR) Edwards, California 93523 Attn: Library R. L. Wiswell LKDS W. W. Wells KLDS	3
Air Force Rocket Propulsion Laboratory (RPM) Edwards, California 93523 Attn: Library	1
Air Force FTC (FTAT-2) Edwards Air Force Base, California 93523 Attn: Library	
Air Force Office of Scientific Research Washington, DC 20333 Attn: Library	1

	Copies
Space and Missile Systems Organization Air Force Unit Post Office Los Angeles, California 90045 Attn: Technical Data Center Captain W. Moll, Jr. XRZE	2
Office of Research Analyses (OAR) Holloman Air Force Base, New Mexico 88330 Attn: Library RRRD	1
U. S. Air Force Washington, DC Attn: Library	1
Commanding Officer U. S. Army Research Office (Durham) Box CM, Duke Skation Durham, North Carolina 27706 Attn: Library	1
U. S. Army Missile Command Redstone Scientific Information Center Redstone Aosenal, Alabama 35808 Attn: Document Section	1
Bureau of Naval Weapons Department of the Navy Washington, DC Attn: Library	1
Commander U. S. Naval Missile Center Point Mugu, California 93041 Attn: Technical Library	1
Commander U. S. Naval Weapons Center China Lake, California 93557 Attn: Library	1

	Copies
Commanding Officer Naval Research Branch Office 1030 E. Green Street Pasadena, California 91101 Attn: Library	1
Director (Code 6180) U. S. Naval Research Laboratory Washington, DC 20390 Attn: Library	1
Picatinny Arsenal Dover, New Jersey 07801 Attn: Library	1
Air Force Aero Propulsion Laboratory Research and Technology Division Air Force Systems Command United States Air Force Wright-Patterson AFB, Ohio 45433 Attn: APRP (Library)	1
Space Division Aerojet-General Corporation 9200 East Flair Drive El Monte, California 91734 Attn: Library	1
Aerojet Liquid Rocket Comapny P.O. Box 15847 Sacramento, California 95813 Attn: Technical Library 2484-2015A	1
Aerospace Corporation 2400 E. El Segundo Blvd. Los Angeles, California 90045 Attn: Library-Documents V. H. Monteil	2

	Copies
Astropower Laboratory McDonnell-Douglas Aircraft Company 2121 Paularino Newport Beach, California 92163 Attn: Library	1
Bell Aerosystems, Inc. Box 1 Buffalo, New York 14240 Attn: Library	1
Boeing Company Space Division P.O. Box 868 SCattle, Washington 98124 Attn: Library	1
Chemical Propulsion Information Agency Applied Physics Laboratory 8621 Georgia Avenue Silver Spring, Maryland 20910	1
Chrysler Corporation Missile Division P.O. Box 2628 Detroit, Michigan Attn: Library	1
Chrysler Corporation Space Division P.O. Box 29200 New Orleans, Louisiana 70129 Attn: Library	1
Curtiss-Wright Corporation Wright Aeronautical Division Woodridge, New Jersey Attn: Library	1
Fairchild Stratos Corporation Aircraft Missiles Division Hagerstown, Maryland Attn: Library	1

	Copies
Republic Aviation Fairchild Hiller Corporation Farmington, Long Island New York	1
General Dynamics/Convair P.O. Box 1128 San Diego, California 92112 Attn: Library C. F. Peters	2
Missiles and Space Systems Center General Electric Company Valley Forge Space Technology Center P.O. Box 8555 Philadelphia, Pa. 19101 Attn: Library	1
General Electric Company Flight Propulsion Laboratory Department Cincinnati, Ohio Attn: Library	1
Grumman Aircraft Engineering Corporation Bethpage, Long Island, New York Attn: Library	1
Kidde Aerospace Division Walter Kidde and Company, Inc. 567 Main Street Belleville, New Jersey 07109	1
Ling-Temco-Vought Corporation P.O. Box 5907 Dallas, Texas 75222 Attn: Library	1
Lockheed Missiles and Space Company P.O. Box 504 Sunnyvale, California 94087 Attn: Library	1

	Copies
Lockheed Propulsion Company P.O. Box 111 Redlands, California 92374 Attn: Library	1
Marquardt Corporation 16555 Saticoy Street Box 2013 - South Annex Van Nuys, California 91409	1
Denver Division Martin-Marietta Corporation P.O. Box 179 Denver, Colorado 80201 Attn: Library	1
Orlando Division Martin-Marietta Corporation Box 5827 Orlando, Florida Attn: Library	1
Western Division McDonnell-Douglas Astronautics 5301 Bolsa Ave. Huntington Beach, California 92647 Attn: Library L. Q. Westmoreland	2
McDonnell Douglas Aircraft Corporation P.O. Box 516 Lambert Field, Missouri 63166 Attn: Library	1
Rocketdyne Division Rockwell International 6633 Canoga Avenue Canoga Park, California 91304 Attn: Library Department 596-306	1

	Copies
Space and Information Systems Division Rockwell International 12214 Lakewood Blvd. Downey, California Attn: Library	
Rocket Research Corporation Willow Road at 116th Street Redmond, Washington 98052 Attn: Library	1
United Aircraft Corporation United Technology Center P.O. Box 358 Sunnyvale, California 94038 Attn: Library	1
Thiokol Chemical Corporation Redstone Division Huntsville, Alabama Attn: Library	1
TRW Systems Inc. 1 Space Park Redondo Beach, CMlifornia 90278 Attn: Technical Library Document Acquisitions A. H. Zimmerman	2
TRW TAPCO Division 23555 Euclid Avenue Cleveland, Ohio	1
United Aircraft Corporation Corporation Library 400 Main Street East Hardford, Connecticut 06108 Attn: Library	1

	Copies
United Aircraft Corporation Pratt and Whitney Division Florida Research and Development Center P.O. Box 2691 West Palm Beach, Florida 33402 Attn: Library	1